Terms and Conditions of Use of Digitised Theses from Trinity College Library Dublin

Copyright statement

All material supplied by Trinity College Library is protected by copyright (under the Copyright and Related Rights Act, 2000 as amended) and other relevant Intellectual Property Rights. By accessing and using a Digitised Thesis from Trinity College Library you acknowledge that all Intellectual Property Rights in any Works supplied are the sole and exclusive property of the copyright and/or other IPR holder. Specific copyright holders may not be explicitly identified. Use of materials from other sources within a thesis should not be construed as a claim over them.

A non-exclusive, non-transferable licence is hereby granted to those using or reproducing, in whole or in part, the material for valid purposes, providing the copyright owners are acknowledged using the normal conventions. Where specific permission to use material is required, this is identified and such permission must be sought from the copyright holder or agency cited.

Liability statement

By using a Digitised Thesis, I accept that Trinity College Dublin bears no legal responsibility for the accuracy, legality or comprehensiveness of materials contained within the thesis, and that Trinity College Dublin accepts no liability for indirect, consequential, or incidental, damages or losses arising from use of the thesis for whatever reason. Information located in a thesis may be subject to specific use constraints, details of which may not be explicitly described. It is the responsibility of potential and actual users to be aware of such constraints and to abide by them. By making use of material from a digitised thesis, you accept these copyright and disclaimer provisions. Where it is brought to the attention of Trinity College Library that there may be a breach of copyright or other restraint, it is the policy to withdraw or take down access to a thesis while the issue is being resolved.

Access Agreement

By using a Digitised Thesis from Trinity College Library you are bound by the following Terms & Conditions. Please read them carefully.

I have read and I understand the following statement: All material supplied via a Digitised Thesis from Trinity College Library is protected by copyright and other intellectual property rights, and duplication or sale of all or part of any of a thesis is not permitted, except that material may be duplicated by you for your research use or for educational purposes in electronic or print form providing the copyright owners are acknowledged using the normal conventions. You must obtain permission for any other use. Electronic or print copies may not be offered, whether for sale or otherwise to anyone. This copy has been supplied on the understanding that it is copyright material and that no quotation from the thesis may be published without proper acknowledgement.

An investigation of the molecular signalling events which occur in cannabinoid-mediated neuronal apoptosis

by

Aoife Gowran

Thesis submitted for the degree of Doctor of Philosophy at the University of Dublin, Trinity College

Trinity College Institute of Neuroscience
Department of Physiology
School of Medicine
Trinity College
Dublin 2
Ireland

Declaration

This thesis is submitted by the understated for the degree of Doctor of Philosophy at the University of Dublin, Trinity College and has not been submitted to any other university as an exercise for a degree. I declare that this thesis is entirely my own work and I give permission to the library to lend or copy this thesis upon request.

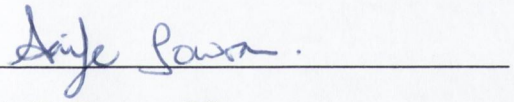

Aoife Gowran, BSc

I Abstract

The plant-derived cannabinoid Δ^9-Tetrahydrocannabinol, is the predominant psychoactive moiety of cannabis and exerts a variety of psychological and physiological effects in humans. Previous investigations in this laboratory have shown that Δ^9-Tetrahydrocannabinol (5 μM) induces apoptosis in cortical neurones *via* signalling through the cannabinoid receptor type 1. The phosphorylation of the tumour suppressor protein, p53 at serine residue 15 is a critical step in stabilising p53 and promoting p53-induced apoptosis. I report that Δ^9-Tetrahydrocannabinol activates p53 by inducing the phosphorylation of serine residue 15, which was mediated by the stress activated protein kinase, c-jun N terminal kinase 1. Furthermore, Δ^9-Tetrahydrocannabinol induced the translocation of phosphorylated-p53^{ser15} to the lysosomal membrane; an event that coincided with Δ^9-Tetrahydrocannabinol-induced lysosomal membrane destabilisation. Δ^9-Tetrahydrocannabinol also induced the selective translocation of cathepsin-D, a lysosomal protease which was required for Δ^9-Tetrahydrocannabinol-induced caspase-3 activation and DNA fragmentation. Depleting neurones of p53 using small interfering RNA inhibited Δ^9-Tetrahydrocannabinol-induced lysosomal membrane destabilisation and DNA fragmentation, indicating that p53 signalling is pivotal in Δ^9-Tetrahydrocannabinol-induced lysosomal branch of neuronal apoptosis. Additional evidence for the proclivity of Δ^9-Tetrahydrocannabinol to regulate p53 signalling was demonstrated by the alterations observed in the p53 post translational modifying proteins, murine double minute 2 and small ubiquitin modifier 1. The observed changes in these p53 regulatory proteins could potentially increase the activity of p53, thus promoting Δ^9-Tetrahydrocannabinol-induced p53-dependent neuronal apoptosis. I also present evidence that the endocannabinoids, anandamide (20 μM) and 2-arachidonoylglycerol (20 μM) have the proclivity to induce neuronal apoptosis *in vitro*, involving similar mechanisms to those activated by Δ^9-Tetrahydrocannabinol. Conversely, a low concentration of 2-arachidonoylglycerol (0.01 μM) provided neuroprotection against glutamate-induced excitotoxicity. These results indicate that endocannabinoids have pleiotropic effects in cultured cortical neurones and can exert both neurotoxic and neuroprotective effects. This thesis also shows that

there is an inter-relationship between neuronal maturity and Δ^9-Tetrahydrocannabinol *in vivo* neurotoxicity. Briefly, Δ^9-Tetrahydrocannabinol (1 mg/Kg) induced the release of cathepsin-D from the lysosomes, caspase-3 activation and DNA fragmentation in the neonatal, but not in the adult, rat cerebral cortex. These results indicate that Δ^9-Tetrahydrocannabinol induces a similar neurotoxic response *in vivo* and can be considered to offer a molecular mechanism for the deleterious effect that maternal use of cannabis may have on the developing cerebral cortex.

II Acknowledgements

First and foremost I would like to thank my supervisor Professor Veronica Campbell. When I think back to the day on which you offered me a PhD position it kind of didn't sink in for a long time. So it was now time for me to sink my teeth into something which at the time I knew hardly anything about but judging from your enthusiasm for the project I knew that I would have no regrets. I just want to thank Veronica for her guidance, patience, understanding and for encouragement when I thought I couldn't do things, your natural optimism is the perfect anecdote to my personal pessimism. Also, thank you for giving me the opportunity to work on something completely unique, which I have always dreamed of doing. I look forward to my future work in your laboratory and I have no doubt that VAC lab has a bright future ahead.

I would also like to thank Dr Tom Connor, Professor Marina Lynch, and Professor Kingston Mills for use of additional laboratory equipment. I would also like to acknowledge Science Foundation Ireland for providing funding for this work.

There are so many other people who I have worked with over the last 3 years, I just hope I don't forget anyone. I would like to thank past members of VAC lab Dr Róisín McCormack, Dr Eric Farrell and Dr Eric Downer thanks for answering my endless questions, especially Eric D who has always given me helpful advice on all things cannabinoids. Special thanks to current VAC lab members, Janis, Manoj and Baby. Janis, thanks for not laughing too much when I potter around the lab when I really should leave. We will definitely have to get Colonel Brandon a Miss Marianne when I get back, looking forward to more talk of books and other things over coffee. An extra special thanks goes to Emma Kearney my fellow write up buddy and fellow 'wonky donkey' we kick the hard way's ass! Thanks for all the encouragement and for letting me crash at your place. Last but not least I would like to thank all the students that have done their projects in the VAC lab, especially Catherine Keogh, Orla Marron, Simon Bull, Nora La Roche, Niamh Walsh, Claire Doyle, Carrie Murphy and also Damien and Declan who I probably still call by the wrong names. Each student has

probably given me more knowledge than I could ever possibly have given to him or her.

Thank you to all members of the physiology staff especially Quentin, Ann, Lesley, Alice, Aidan, Doreen, David and Kieran.

I would like to thank my friends and soon to be doctors Máire and Anne-Maire. Both of you know what it is like to do something like this, so thanks for understanding that from time to time thesis work comes before play. Also thank you to Sandra and Gavin for their support. I also want to thank Dr Nikki Carrol and all the rest of the Vit chicks I will look forward to many more nights out with you all. I would also like to thank Elizabeth for her support and advice on all matter of things. Finally, I would like to thank my family who have supported me in many ways during the course of my PhD and I would like to dedicate this thesis to the memory of my Nana, Claire and my niece, Megan. Losing the two of you was the hardest thing I have had to deal with, but I am definitely a stronger person now and maybe, just maybe, a little more optimistic.

III Abbreviations

AC	Adenylyl cyclase
AEA	Anandamide (N-arachidonoylethanolamide)
AFC	Ac-DEVD-7-amino-4-trifluoromethylcoumarin
2-AG	2-arachidonoylglycerol
ANOVA	Analysis of variance
AMT	Anandamide membrane transporter
AO	Acridine orange
APAF-1	Apoptosis protease activating factor 1
APS	Ammonium persulphate
ARA-C	Cytosine-arabino-furanoside
BODIPY FL	Boron dipyrromethene difluoride fluorophore
BSA	Bovine serum albumin
cAMP	Cyclic adenosine monophosphate
CB	Cannabinoid
CBN	Cannabinol
CDN	Cannabidiol
CBV	Cannabivarin
CDi	Cathepsin-D inhibitor
CHO	Chinese hamster ovary
CLi	Cathepsin L inhibitor
CZP	Capsazepine
CNS	Central nervous system
DAB	Diaminobenzidine
DEVD	Aspartic-glutamic-valine-aspartic residue
JNKi	JNK1 inhibitor
DMSO	Dimethyl sulphoxide
DNA	Deoxyribonucleic acid
DNAse	Deoxyribonuclease
dNTP	Deoxynucleotidetriphosphate

DTT	Dithiothreitol
ECL	Enhanced chemiluminescence
EDTA	Ethylenediamine-tetra-acetic acid
ERK	Extracellular signal related kinase
EtOH	Ethanol
FAAH	Fatty acid amidehydrolase
FITC	Flourescein isothiocyanate
GABA	γ amino butyric acid
G protein	GTP-binding protein
GTP	Guanosine triphosphate
H_2O_2	Hydrogen peroxide
hr	Hour
HRP	Horse radish peroxidase
$5HT_3$	5-Hydroxytryptamine (serotonin)
IgG	Immunoglobulin G
IU	International unit
JNK	c-Jun N-terminal kinase
kDa	Kilo Dalton
LMP	Lysosomal membrane permeabilisation
LPS	Lipopolysaccaride
LTP	Long term potentiation
MAPK	Mitogen-activated protein kinase
MCA	7-methoxycoumarin-4-acetyl acid
Mdm2	Murine double minute 2 protein
Min	Minute
mRNA	Messenger ribonucleic acid
nACh	Nicotinic acetylcholine
NAD	Nicotinamide adenine dinucleotide
NBM	Neurobasal medium
NGF	Nerve growth factor
NH_2	Amino terminal

NMDA	N-methyl-D-aspartate
O/N	Overnight
PAGE	Polyacrylamide gel electrophoresis
PBS	Phosphate-buffered saline
PC12	Phaeochromocytoma cell line
PCR	Polymerase chain reaction
Pif-α	Pifithrin-α
PKB	Protein kinase B
PKC	Protein kinase C
PMSF	Phenylmethylsulphonyl fluoride
POC-R	Perfusion open/closed cultivation system
PTX	Pertusis toxin
RER	Rough endoplasmic reticulum
RNA	Ribonucleic acid
RNase	Ribonuclease
ROS	Reactive oxygen species
RT	Room temperature
SDS	Sodium dodecyl sulphate
SDS-PAGE	SDS-polyacrylamide gel electrophoresis
Ser	Serine
SEM	Standard error of mean
siRNA	Small interfering RNA
SNP	Single nucleotide polymorphism
SUMO	Small ubiquitin relatated modifying protein
SyK	Spleen tyrosine kinase
SyKi	Spleen tyrosine kinase inhibitor (sulfonamide)
TASK-1	TWIK-related Acid-Sensitive K+ channel type 1
TBS	Tris-buffered saline
TBS-T	TBS-Tween
TdT	Terminal deoxynucleotidyl transferase
TEMED	N,N,N-N-tetramethylenediamine

Δ^9-THC	Delta-9-Tetrahydrocannabinol
Tris-HCl	Trizma-hydrochloride
$TRPV_1/VR_1$	Transient receptor potential vanilloid type1
TUNEL	TdT-mediated-UTP-end nick labelling
Tyr	Tyrosine
Ub	Ubiquitin
UBL	Ubiquitin like protein
UTR	Untranslated region
UV	Ultraviolet light
vCon	Vehicle control
VEGF	Vascular endothelial growth factor

IV List of tables

V List of figures

VI Table of contents

Chapter 2

Materials and Methods

Chapter 3

An investigation of the early signalling events in Δ^9-THC-induced neuronal apoptosis

Chapter 4

The role of the lysosomal system in Δ^9-THC-induced neuronal apoptosis

Chapter 5

An investigation into the effect of endocannabinoids on neuronal viability

Chapter 6

The effect of development on Δ^9-THC-induced apoptosis in the rat cerebral cortex - An *in vivo* study

Chapter 1

Introduction

1.1 Cannabis - a brief history

The hemp plant (*cannabis sativa*) first characterised by von Linne in 1753, is a fast growing annual which has characteristic finely branched leaves with saw tooth edges (Clarke, 1981). *Cannabis sativa* probably originated in Central Asia, however, it has been cultivated around the world as a versatile economically beneficial crop producing food, medicinal products, canvas fabric and rope (Iversen, 2000; Robinson, 1996). Currently the plant is thought of mainly in the context of its psychoactive properties and is now grown for its Δ^9-Tetrahydrocannabinol content, the main psychoactive component of cannabis, and not for its fibre content (Iversen, 2000). The psychoactive chemicals are found in most parts of the cannabis plant with the highest concentrations found in the sticky resin produced by glands at the base of the fine hairs that coat the leaves and particularly the bracts of the female flower head. The seeds contain no psychoactive chemicals, but like all seeds they have a high nutritional content (Iversen, 2000).

Cannabis preparations have been used for medicinal, recreational and ceremonial purposes in many human cultures for thousands of years. It was Napoleon's retreating army that spread the recreational use of cannabis as a psychoactive drug to a naïve Europe. Although cannabis was cultivated in Europe and America at this time, its psychoactive properties were largely unknown, possibly due to the low psychoactive chemical properties of plant strains grown for fibre production. The Irishman Sir William B. O'Shaugnessey carried out the first experimental characterisation of the drug and advocated the medicinal use of cannabis in Europe. O'Shaugnessey (1842) observed that cannabis was non-toxic, even at high doses and acted as an analgesic, a muscle relaxant and an anticonvulsant. The medicinal use of cannabis became popular for a time and was used to treat insomnia, neuralgia, migraine and dysmenorrhoea. However, the use of cannabis waned due to technical difficulties obtaining consistent preparations and the increased availability of opium, which at the time was considered a more reliable and effective drug. Whilst the medicinal use of cannabis was not sustained, the recreational use of the drug increased during the early 19th Century. However, this was confined to a small number of artisans. Authors such as Ludlow ('The Hasheesh Eater', 1857), Baudelaire ('Les Paradis Artificiels', 1860), and

Strindberg ('Son of a Servant', 1909) recounted their experiences with hashish in grand literary style and provide descriptive accounts of the subjective effects of cannabis. Since the use of cannabis as a recreational drug was increasing steadily, its prohibition quickly ensued and was followed by what has been described by some as the 'demonisation' of the drug. During the period between *c.* 1950 to *c.* 1970 the medicinal use of cannabis was halted and virtually all research interest in the field was terminated (Iversen, 2000). Despite this tincture of cannabis remained on the British pharmacopoeia until 1973. However, since then there has been advances in several fields such as pharmaceutical purification, synthetic chemistry and molecular biology which has led to a steady growth in research into this multipurpose plant and the effects that its active compounds have on physiological systems.

1.2 Cannabis - current trends

Despite its illegal nature, cannabis is the World's most used recreational drug. Since the middle of the 20th Century, cannabis use has become steadily more prevalent especially in young people (Ashton, 2001). There is a considerable population, which includes 1% of schoolchildren, who smoke cannabis daily or several (5 - 15) times a day and who may be chronically intoxicated due to the slow elimination of cannabis from the body (Robertson *et al.*, 1996). Throughout Europe, America and Australia public debate has centred on the possible legalisation of cannabis use, at least for therapeutic purposes. The best evidence on the affects of liberalising cannabis policy comes from The Netherlands. To satisfy international treaties, the Dutch law states that cannabis is illegal, however, in 1976 The Netherlands formally adopted a policy of non-enforcement of the cannabis laws. Therefore, the cannabis regime in The Netherlands lies somewhere between depenalisation of cannabis possession and complete legalisation. This harm minimization policy seems to work well with the Dutch tradition of "gedoogbeleid" which is the formal, systematic application of discretion (MacCoun and Reuter, 1997 and 2001). MacCoun and Reuter also report that it is not decriminalisation of cannabis but the legalisation and subsequent commercialisation that may be responsible for increases in cannabis use. A cross-sectional comparison of

all drug use surveys carried out from 1970 to 1996 was carried out by MacCoun and Reuter (2001) and has shown that rates (lifetime prevalence) of cannabis use in The Netherlands are similar to those in the USA but higher than in neighbouring countries. The situation in The Netherlands regarding the 'gateway' association, where it is believed that the use of cannabis leads to the use of other drugs is less clear. However, a regime that tolerates home cultivation of small quantities (as in Alaska and South Australia) might be more effective in reducing the 'gateway' association than the Dutch commercialised supply of cannabis (MacCoun and Reuter, 1997, 2001). The research of MacCoun and Reuter, in addition to others in the field highlight the complexities (both policy and non-policy based) that are involved in the debate over the legalisation of cannabis.

A general population survey commissioned by the National Advisory Committee on Drugs (NACD) in The Republic of Ireland made several findings on the prevalence rates for the use of key illegal drugs in Irish people aged 15 - 64. The survey found that the use of cannabis was more prevalent in male respondents and also in younger respondents. The lifetime prevalence rate for those aged 15 to 34 was 24%, which is more than double the rate for those aged 35 to 64, having a prevalence rate of just 11%. Males (life time prevalence; 22%) were found to use cannabis more than females (12%) and this was found across all age groups. The NACD survey also found that 22% of current users have used cannabis on a daily or almost daily basis. This trend is more prevalent in males (27%) than in females (11%) and in younger (23%) rather than older respondents (21%; NACD, 2004). The use of cannabis by young adults is of particular concern due to cannabis being viewed by many as a potential risk factor in precipitating the onset of psychosis and schizophrenia in susceptible individuals (Emrich *et al.,* 1997; Moore *et al.*, 2007). Cannabis resin incorporated into a cigarette was the most commonly used (68%) form of cannabis. Ingesting Δ^9-Tetrahydrocannabinol by smoking a cigarette containing cannabis plant material or cannabis resin is the most efficient way to administer Δ^9-Tetrahydrocannabinol. Another less efficient method of administering Δ^9-Tetrahydrocannabinol is by consuming food or alcoholic beverages containing the fat-soluble psychoactive

compounds of cannabis. The NACD survey found that consumption of cannabis in food was higher in females (5%) than in males (3%).

1.3 The effects of cannabis consumption

Many factors impinge on the behavioural effects of cannabis such as the amount of active compound in the preparation, route of administration and subject expectations (Ameri, 1999). The numerous pharmacological actions of cannabis are complex and affect almost every system of the body; they include a unique combination of some effects associated with alcohol, tranquillizers, opioids and hallucinogens *e.g.*, an initial sense of euphoria followed by a period of sedation (Ashton, 1998). These subjective effects of cannabis peaks 20 minutes after smoking and slowly dissipates over 3 - 4 hours (Chiang and Barnett, 1984). At low doses cannabis produces a mixture of stimulatory and depressant effects but at high doses cannabis exerts mainly depressive effects. Acute effects of cannabis consumption are associated with impaired functioning in a variety of cognitive and performance tasks, including impaired memory, altered time sense and decrements in tasks such as reaction time, learning perception, motor co-ordination and attention (Block *et al.*, 1992; Chait and Perry, 1994; Heishman *et al.*, 1997; Court, 1998). These effects can persist for up to 24 hours post consumption (Heishman *et al.*, 1990; Yesavage *et al.*, 1985). Some of the behavioural effects of cannabis have been linked to alterations in the functional activity of the cerebral cortex (Jentsch *et al.*, 1997). This is supported by evidence that cannabis exposure causes deficits in tasks dependent on working memory (Mathew *et al.*, 1997; Jentsch *et al.*, 1997).

Cannabis consumption, like alcohol, has been linked to an increased risk of road traffic accidents and their co-abuse has been reported to have an additive effect on cognitive impairment (O'Kane *et al.*, 2002; Perez-Reyes *et al.*, 1988; Ramaekers *et al.*, 2004). Apart from its actions in the CNS cannabis affects many other body systems, including the cardiovascular, respiratory, gastro-intestinal, immune, endocrine and reproductive systems, all of which may carry health hazards, especially with chronic use (Ashton, 1999). The prevalence of recreational cannabis use has increased markedly

over the past decade; this widespread use carries health risks to the individual and to the wider community (Ashton, 1999). However, the use of cannabis to alleviate symptoms of AIDS, multiple sclerosis and nausea due to chemotherapy *etc.*, has highlighted the potential use of the active compounds in cannabis, termed cannabinoids, in the treatment of these conditions. The use of cannabis and synthetic cannabis analogues as therapeutic agents requires detailed investigations into the exact physiological effects of cannabis.

1.4 Δ^9-Tetrahydrocannabinol

The cannabis plant contains some 400 chemical compounds of which more than 60 are termed cannabinoids (Ashton, 1999). The main cannabinoids found in the cannabis plant are: Δ^9-Tetrahydrocannabinol, Δ^8-Tetrahydrocannabinol, cannabidiol (CBD), cannabinol (CBN), Δ^9-Tetrahydrocannabivarin (Δ^9-THCV) amongst many other cannabinoid types (Pertwee, 2006). Δ^9-Tetrahydrocannabinol (Δ^9-THC) is the main psychoactive component in cannabis although there are other less potent psychoactive compounds in cannabis *e.g.*, CBN (Mechoulam and Gaoni 1965; Paton and Pertwee, 1972). The structure and stereochemistry of Δ^9-THC was elucidated in 1964 by Mechoulam and Gaoni (Figure 1.1). At least four molecular moieties of the Δ^9-THC structure contribute to its cannabimimetic activity. The phenolic hydroxyl is necessary for cannabinoid activity. Increases in side chain length can increase potency. The Southern aliphatic hydroxyl and Northern aliphatic hydroxyl both effect activity (Mechoulam *et al.*, 1987). Δ^9-THC is an extremely lipophillic molecule and passes the blood brain barrier to reach its site of action within seconds of inhaling cannabis smoke (Agurell *et al.*, 1986). Being highly fat-soluble, Δ^9-THC accumulates in fatty tissues from where it is slowly released back into other body compartments, including the brain (Ashton, 1999). Phyto-cannabinoids are differentially distributed within the brain with higher concentrations observed in the frontal cerebral cortex, hippocampus and cerebellum (McIsaac *et al.*, 1971). The sequestering of Δ^9-THC in fatty tissues and its re-release into the blood stream and the brain accounts for the long tissue half-life of Δ^9-THC (Maykut, 1985). The complete elimination of a single dose from the body may

take up to 30 days. Δ^9-THC and other cannabinoids are metabolised in the liver forming more than 20 metabolites some of which are also psychoactive *e.g.*, 11-Hydroxy-Δ^9-Tetrahydrocannabinol.

The Δ^9-THC content of cannabis varies with the strain of plant used and preparation type (Table 1.1). The average Δ^9-THC content in a cannabis cigarette in the 1970s was 10 mg however a modern cannabis cigarette may contain more than 60 - 150 mg (Ashton, 1999). In addition, the emergence of more potent genetically engineered plant strains infers that modern cannabis may contain even more Δ^9-THC than previously observed. Therefore, current cannabis smokers may be exposed to higher Δ^9-THC concentrations than smokers in the 1960s and 1970s which may have currently unknown consequences. The Δ^9-THC content of cannabis also varies with the geographical location of cultivation. Cannabis cultivated in the tropics has a Δ^9-THC to cannabidiol (CBD; a non-psychoactive cannabinoid compound) ratio of 10:1, whilst plants cultivated in more northern latitudes have less Δ^9-THC to cannabidiol ratio (1:2; Clarke, 1981).

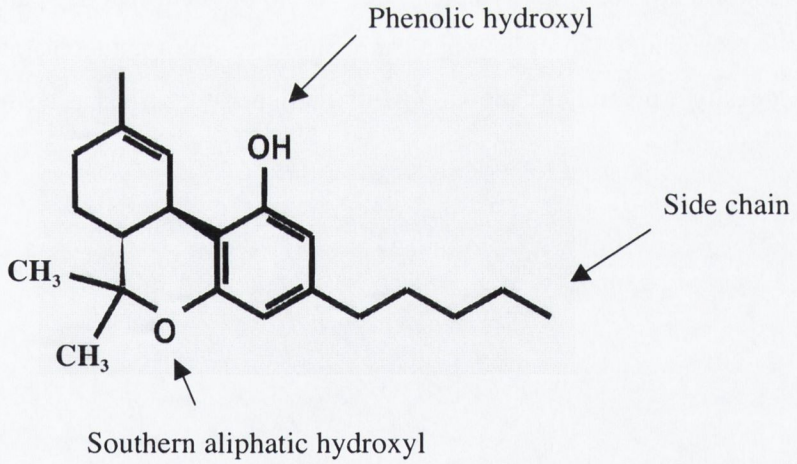

Figure 1.1: The key structural elements of Δ^9-THC.

(Adapted from Iversen, 2000).

Since the elucidation of the structure of Δ^9-THC many hundreds of chemical analogues have been synthesised *e.g.,* WIN 55212-2, HU-210, CP 55940 (D'Ambra *et al.*, 1992; Mechoulam *et al.*, 1988; Johnson and Melvin, 1987). Development of these synthetic cannabinoid analogues has aided the dissection of the molecular actions of cannabis. Synthetic cannabinoids may also be utilised as therapeutic remedies for a number of pathophysiological conditions such as, Multiple Sclerosis (MS), Alzheimer's and Parkinson's disease. However, at present, only a few cannabis-based compounds are licensed for medicinal use. Dronabinol, the generic name for Δ^9-THC, is mixed with sesame oil and is marketed under the name of Marinol®, which is licensed for use as an appetite stimulant to counteract AIDS wasting syndrome and as an antiemetic for cancer patients undergoing chemotherapy. Nabilone (Cesamet®) is a potent synthetic Δ^9-THC analogue, with slightly less undesirable psychoactive effects, is primarily used to alleviate nausea and vomiting associated with cancer chemotherapy and also acts as an appetite stimulant. Sativex™ is another cannabinoid-based medicine containing a mixture of Δ^9-THC and cannabidiol, a non-psychoactive phyto-cannabinoid, and is prescribed for the symptomatic relief of neuropathic pain in adults with MS. Rimonabant (Acomplia®) is a cannabinoid receptor antagonist, which is used as an anti-obesity drug and has shown potential in laboratory trials as a smoking cessation aide.

Preparation type	Source	Approx. Δ^9-THC content
Cannabis (herbal)	Cigarette of dried leaves/flowers *etc.*, from plants cultivated in the 1960s and 1970s	1 - 3% Δ^9-THC (10 mg/cigarette)
	Modern cannabis cigarette using more potent material or plant strains (sinsemilla, skunk, white widow *et al.*)	6 - 20% Δ^9-THC (60 - 150 mg/cigarette)
Cannabis resin (Hashish)	Resin secreted in the flower heads	10 - 20% Δ^9-THC
Hashish oil	Product of extraction by organic solvents	15 - 30% Δ^9-THC (sometimes up to 65%)

Table 1.1: Δ^9-THC concentrations in different preparations of cannabis.
(Adapted from Ashton, 1999).

1.5 Cannabinoid receptors

The identification of Δ^9-THC was not immediately followed by the full understanding of its molecular mechanism of action. Initially, due to the lipophillic nature and the central depressant effects of Δ^9-THC, cannabinoids were thought to mediate their actions through the disruption of membrane ordering (Paton and Pertwee, 1972). The revelation of the strict structural requirements for the pharmacological activity of Δ^9-THC provided early evidence for the existence of a specific cannabinoid receptor. Sensitivity to pertussis toxin (PTX) also provided evidence that Δ^9-THC acts through a $G_{i/o}$ protein-coupled cannabinoid receptor mechanism (Howlett *et al.*, 1986). These speculations were resolved when it was discovered that cannabinoids inhibit the enzyme adenylyl cyclase resulting in a decrease in cyclic adenosine monophosphate (cAMP), therefore indicating the actions of cannabinoids are mediated through a cell surface G protein-coupled receptor (Howlett *et al.*, 1989). Profound cAMP inhibition by the binding of guanine nucleotides suggested that the cannabinoid receptor is closely linked with the second messenger system of which cAMP is an important component (Herkenham *et al.*, 1990). Advances in synthetic chemistry, pharmacology research and molecular biology since the isolation of Δ^9-THC in the 1960s, culminated in the cloning of cannabinoid receptors in the early 1990s. To date, only two cannabinoid receptors have been cloned, CB_1 and CB_2, although there are other putative cannabinoid receptors (Matsuda *et al.*, 1990; Munro *et al.*, 1993; Mackie and Stella, 2006). Cannabinoid receptors consist of an extracellular N-terminal and intracellular C-terminal, intersected by a 7 α helical hydrophobic transmembrane region. These basic structural features are hallmarks of G protein-coupled receptors.

1.5.1 Cannabinoid receptor types

Confirmation of the existence of a specific cannabinoid binding receptor came with the cloning in 1990 of the CB_1 receptor from a rat cerebral cortex cDNA library by a probe derived from a member of G protein-coupled receptors (Matsuda *et al.*, 1990). This was quickly followed by the identification of the human cannabinoid receptor homologue (hCB_1; Gerard *et al.*, 1991). Furthermore, a second human cannabinoid-binding receptor, the cannabinoid receptor type 2 (hCB_2), was isolated by its homology

to other G protein-coupled receptors, using a polymerase chain reaction (PCR) assay in HL60 promyelocytic leukaemic cells (Munro *et al.*, 1993). Rat CB_2 receptor was cloned and characterised from a rat spleen cDNA library by Brown *et al.*, (2002). Despite hCB_1 and hCB_2 sharing only 44% overall structural homology (68% homology within the transmembrane domains), both receptors demonstrate similar binding affinity for Δ^9-THC (Munro *et al.*, 1993; Adams and Martin, 1996). There are considerable differences in the size of both receptors; CB_1 has an apparent molecular weight of 64 kDa (after post translational modification in the rough endoplasmic reticulum and Golgi), whilst the molecular weight of CB_2 is *c.* 40 kDa. This discrepancy is due to CB_1 possessing a large (166 amino acid) extracellular N-terminal domain. Furthermore, altering the N-terminal domain of the CB_1 receptor can lead to increased stability and targeting to the cell surface which could possibly be a site suitable for modulation which would consequently affect ligand availability and specificity (Andersson *et al.*, 2003).

Two splice variants of the hCB_1 receptor with distinct ligand binding and activation properties have been identified, the first isolated from a human lung cDNA library deemed hCB_1A and a second discovered during cloning of hCB_1A (hCB_1B; Shire *et al.*, 1995; Ryberg *et al.*, 2005). Single nucleotide polymorphism (SNP) and other genetic variations in the human cannabinoid receptor gene ($hCNR_1$) and in other endocannabinoid system regulatory genes *e.g.,* FAAH, have been reported to be associated with various human disorders (Zhang *et al.*, 2004; Onaivi *et al.*, 2002). Hoenicka *et al.*, 2007, have shown that there is a relationship between the co-morbidity of alcoholism and antisocial behaviour with variations found in the 3'UTR of $hCNR_1$ and the C385A SNP found in FAAH. Russo *et al.*, 2007 found that the A3813G SNP in $hCNR_1$ was significantly associated with increased anthropometric data in two independent groups of Caucasian European adult males. Four SNPs in the $hCNR_1$ were found to modulate striatal responses to facial stimuli, which could implicate that CNR1 genotype, could affect conditions involving deficits in social reward processing such as autism (Chakrabarti *et al.*, 2006). Interestingly, SNPs found in the $hCNR_2$ gene have been identified and are associated with osteoporosis and autoimmunity (Karsak *et al.*, 2005; Sipe *et al.*, 2005).

Several studies showing unusual pharmacological profiles of cannabinoid ligands and receptors have strengthened the hypothesis that there are more undiscovered cannabinoid receptors (Fride *et al.*, 2003, Begg *et al.*, 2005, Breivogel *et al.*, 2001). Early reports linking the orphan G protein-coupled receptor, GPR55 with cannabinoids came from patents and meeting abstracts, which are not subject to the peer review process. (Brown and Wise, 2001; Dromota *et al.*, 2004; Brown *et al.*, 2005; Sjögren *et al.*, 2005). Recently Ryberg *et al.*, (2007) have published (in a peer reviewed journal) the cloning and sequencing of human, mouse and rat GPR55. Ryberg and co-workers (2007) also reported that the receptor was activated (EC_{50} values in the low nM concentrations) by several CB_1/CB_2 receptor agonists *e.g.*, Δ^9-THC, HU-210, CP55940, AEA, 2-AG and also the CB_1 selective noladin ether. Future peer reviewed work originating from meeting abstracts will with no doubt lead the way to answering the unknown aspects of GPR55's role in cannabinoid pharmacology (reviewed in Pertwee, 2007).

The abnormal-cannabidiol receptor is another putative novel cannabinoid receptor, which has not been characterised molecularly. This G protein-coupled receptor is present in the endothelium of the rat mesenteric artery and its activation by ligands such as abnormal cannabidiol, anandamide and virodhamine has been shown to induce vasorelaxation and the activation of glial cell migration (reviewed in Pertwee, 2005). The synthetic cannabinoid ligands, CP 55940 and cannabinoid receptor antagonists, SR141716A and LY320135 inhibit noradrenaline release in cardiovascular synaptic nerve endings *via* novel pre-synaptic imidazoline-like receptors (Gothert *et al.*, 1999; Molderings *et al.*, 1999). The activation of peroxisome proliferator-activated receptors (PPARs), post-synaptic muscarinic receptors and the adenosine A_1 receptors by cannabinoid ligands and antagonists have also been reported, which may represent several new therapeutic avenues for a diverse set of conditions (Burstein, 2005; Christopoulos and Wilson, 2001; Savinainen *et al.*, 2003). Furthermore, anandamide can act as a conditional activator of Transient receptor potential vanilloid type 1 ($TRPV_1$) during periods of inflammation where inflammatory mediators convert anandamide to a potent activator of $TRPV_1$, which is not observed in the normal physiological state (Movsesyan *et al.*, 2004; Singh-Tahim *et al.*, 2005). Cannabinoid

receptor homo- and hetero-dimerisation can also result in alternative cannabinoid signalling (Wagner-Miller *et al., 2002;* Mackie, 2005). So far hetero-dimerisation of the CB_1 receptor with D_2 dopamine, adenosine A_{2A}, 5-HT_2 receptors and the receptor tyrosine kinase TrkB have been demonstrated (Kearn *et al.*, 2004; Carriba *et al.*, 2007; Cheer *et al.*, 1999; Berghuis *et al.*, 2005). Genetic diversity, such as splice variants, SNPs, homo- and hetero-dimerisation of cannabinoid receptors and the existence of more cannabinoid receptor types and atypical cannabinoid receptor signalling represent an exciting area for the modification of cannabinoid signalling.

1.5.2 Cannabinoid receptor distribution

Cannabinoid receptors are among the most abundant G protein-coupled receptors in the brain, with densities similar to levels of γ-amino butyric acid (GABA) receptors and glutamate-gated ion channels (Howlett *et al.*, 2004). The distribution of cannabinoid receptors within the CNS was first described by Herkenham *et al.*, in a study using quantitative *in vitro* receptor autoradiography with tritium labelled CP 55940 as an agonist (Herkenham *et al.*, 1991, 1990). Figure 1.3 shows that the distribution of cannabinoid receptors is highly heterogeneous with the highest receptor densities (dark areas) present in the basal ganglia, the globus pallidus, the hippocampus, particularly within the dentate gyrus and the molecular layer of the cerebellum. The paucity of CB_1 receptors in the brainstem, which mediates respiratory and cardiovascular functions, may account for the lack of toxicity associated with Δ^9-THC and other cannabinoid ligands (Herkenham *et al.*, 1991, 1990).

Cannabinoid receptor distribution in the cerebral cortex can be best ascertained within the more elaborate human cerebral cortex. The highest densities are found in association with the limbic cortices, with lower levels within the primary sensory and motor regions, suggesting an important role in motivational (limbic) and cognitive (association) information processing (Glass *et al.*, 1997; Biegon and Kerman, 2001; Howlett *et al.*, 2004). Thus, the effects of cannabinoids on memory and cognition are consistent with receptor localisation in the hippocampus and cerebral cortex (Adams and Martin, 1996). There is also evidence for the presence of cannabinoid receptors in regions associated with mediating the brain reward system *e.g.*, nucleus accumbens,

which suggests an association with dopaminergic neurones and the modulation of neurotransmission (Katona *et al.*, 2001). Although it has been assumed in the past that CB_1 receptors occur exclusively in the brain, there is also evidence for peripheral localisation. Levels comparable with CB_2 are found in the spleen and tonsils and at very low levels in adrenal gland, heart, uterus, ovary, testis and pre-synaptically on sympathetic nerve terminals (Galiègue *et al.*, 1995; Gerard *et al.*, 1991; Ishac *et al.*, 1996). Biegon and Kerman (2001) have found that CB_1 receptor distribution varies during development with a relatively low and regionally selective expression rate in the human postnatal brain. Receptor densities in the globus pallidus pars medialis of foetal brains were comparable to those observed in adult brains. Lower densities were observed in the caudate and putamen. This discrepancy may explain the relatively mild and selective nature of postnatal deficits observed in infants exposed to cannabinoids *in utero* (Biegon and Kerman, 2001).

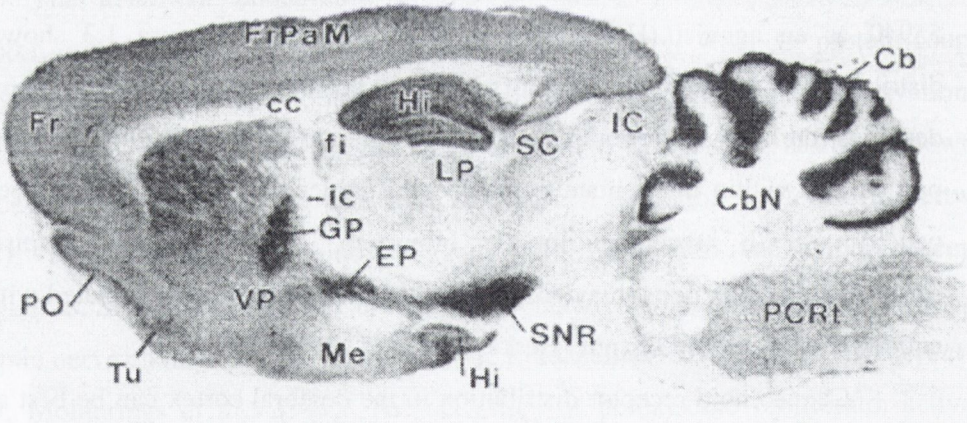

Figure 1.2: Cannabinoid receptor distribution in the rat brain.

Cb (cerebellum), GP (globus pallidus), Hi (hippocampus), Fr (frontal cortex). (Adapted from Herkenham *et al.*, 1991).

Conversely CB_2 is found mainly in the periphery where it is predominantly expressed in the spleen, tonsils and immune cells (Munro *et al.*, 1993; Schatz *et al.*, 1997; Galiègue *et al.*, 1995). The localisation of CB_2 in immune tissues is believed to

be responsible for the immunosuppressive properties of cannabis (Ameri, 1998; Kaminski *et al.*, 1994). CB_2 receptors are also expressed in the brainstem, which have shown to be functionally coupled to the inhibition of emesis (van Sickle *et al.*, 2005). The CB_2 receptor has also been identified in several areas of the rat brain such as the cerebellum, striatum, amygdala, substatia nigra, cerebral cortex and the periaqueductal gray (Gong *et al.*, 2006; Onaivi *et al.*, 2006). Furthermore, CB_2 expression has been found on neuronal and glial processes in the rat brain (Gong *et al.*, 2006). This newly identified multifocal expression of CB_2 suggests that this receptor may play an important role in endocannabinoid signalling in the CNS. The CB_2 receptor is mainly confined to glial cells and has been implicated in the control of neural survival and can mediate neuroprotection through their anti-inflammatory actions (Nunez *et al.*, 2004; Fernandez-Ruiz *et al.*, 2007; Ehrhart *et al.*, 2005). In the Alzheimer's disease (AD) brain and in animal models of AD-like pathology, CB_2 receptors are up regulated within the active microglia present in those brain regions where senile plaques are abundant (Benito *et al.*, 2003; Ramirez *et al.*, 2005). The up regulation of CB_2 in such pathological situations may be an attempt to reduce neuroinflammation since CB_2 receptor activation *in vitro* reduces the production of pro-inflammatory molecules by microglia (Facchinetti *et al.*, 2003). Furthermore, CB_2 receptor ligands are now subject to intense investigation due to their potential use as anti-inflammatory mediators in the CNS and may alleviate the symptoms of neurodegenerative diseases (Ashton, 2007).

1.6 Endogenous cannabinoids

The precedent set by morphine and the enkephalines - *i.e.,* that mammalian tissues produce endogenous ligands in addition to a specific set of receptors through which they mediate their effects - led the path to the discovery of cannabinoid receptors and their endogenous ligands, the endocannabinoids. Numerous bioactive lipids with cannabinoid receptor binding capabilities have been extracted from animal tissues and these include: N-arachidonoylethanolamine (anandamide; AEA), 2-arachidonoylglycerol (2-AG), ether-linked 2-arachidonoylglycerol (noladin ether), and virodhamine (Devane *et al.,* 1992; Mechoulam *et al.*, 1995; Sugiura *et al.,* 1995; Hanus

et al., 2001; Porter *et al.*, 2002). Additionally the following lipid signalling molecules have been identified as having cannabimimetic activities: N-arachidonoyl dopamine, N-arachidonoyl glycine, N-arachidonoyl serine, and others among the N-acyl ethanolamine and 2-acyl glycerol families (Bisogno *et al.*, 2000; Sheskin *et al.*, 1997; Milman *et al.*, 2006; for review see Bradshaw, 2007). Both AEA and 2-AG are the so-called 'true' endogenous cannabinoids as they potently bind and functionally activate one or both cannabinoid receptor types (CB_1 and CB_2; see section 1.6). Consequently, they are the most characterised endocannabinoids. The cannabinoid signalling system, which includes the endogenous ligands and the proteins for their synthesis and inactivation, has a role in many physiological systems (Rodríguez de Fonseca *et al.*, 2005). Endocannabinoids are critical regulators of early developmental activity and are important in CNS circuit development and synaptogenesis (Bernard *et al.*, 2005; Harkany *et al.*, 2007; Berghuis *et al.*, 2007). Furthermore, the endocannabinoid system regulates the perception and modulation of pain, food-intake and energy metabolism, fear and anxiety, and has a critical role in learning and memory (Rice *et al.*, 2002; Finn *et al.*, 2004; Pagotto and Pasquali, 2006; Balerio *et al.*, 2006; Chevaleyre *et al.*, 2006). The ability of endocannabinoids to act as retrograde messengers, enabling the modulation of neurotransmitter release from afferent pre-synaptic terminals, has been shown to play an important role in short-term and long term synaptic plasticity (Wilson and Nicoll, 2002). Depolarization-induced suppression of excitation/inhibition (DSE/I) brought about by the actions of endocannabinoids is believed to affect memory, cognition and pain (Diana and Marty, 2004).

Anandamide, AEA

2-Arachidonoylglycerol, 2-AG

Noladin ether

Virodhamine

Figure 1.3: Chemical structures of the endocannabinoids

(Adapted from Bisogno *et al.*, 2005).

1.6.1 Anandamide

The name anandamide comes from the Sanskrit word for 'internal bliss' and amide the designation for the chemical bonding that distinguishes anandamide from the exogenous cannabinoid receptor agonists (Ameri, 1998). Anandamide (AEA) was isolated from porcine brain extracts by Devane *et al.*, in 1992 and was the first endocannabinoid to be discovered. AEA is the amide between arachidonic acid and ethanolamine and displays properties expected of an endogenous cannabinoid *e.g.*, competes for cannabinoid receptor binding, suppresses the electrically induced twitch response of mouse vas deferens, and induces hypothermia, analgesia, and inhibits long term potentiation (Bisogno *et al.*, 2005; Devane *et al.*, 1992; Terranova *et al.*, 1995). These effects occur rapidly but have a short duration of action due to the rapid enzymatic degradation and are 4 - 20 fold less potent than Δ^9-THC in producing these pharmacological effects. AEA has shown to be widely distributed in the brain and the periphery with the highest levels correlating with areas of high cannabinoid receptor density *e.g.*, cerebellum and spleen (Felder *et al.*, 1996, 1993a). Small amounts are also found in the heart, thalamus and skin, with only trace levels detected in serum and cerebrospinal fluid. In the brain AEA levels are in the order of pmol/g tissue, which is comparable to other neurotransmitters such as dopamine and serotonin, but are 10-fold lower than those for GABA and glutamate (Sugiura *et al.*, 2002; Ameri, 1998). AEA displays pharmacological and biochemical properties of a cannabinoid agonist for both cannabinoid receptor types however, the significant levels of AEA found in the heart and thalamus, known for their paucity of $CB_{1/2}$ expression, may suggest that a novel cannabinoid receptor type could exist for AEA (Felder *et al.*, 1993).

Biochemical assays show that AEA has definite cannabimimetic effects. The binding of AEA to cannabinoid receptors causes the inhibition of andenylyl cyclase (AC) in both neuroblastoma cells and Chinese hamster ovary (CHO) cells with a maximal inhibition of AC lower than that evoked by synthetic cannabinoid agonists, indicating a lower efficacy of AEA (Felder *et al.*, 1995, 1993b; Vogel *et al.*, 1993). Furthermore, AEA inhibits N-type calcium currents although with less efficacy than Δ^9-THC or the synthetic cannabinoid WIN 55212-2. AEA also inhibits L-type Ca^{2+} channels as a result of its conversion to arachidonic acid (Mackie *et al.*, 1993; Shimasue

et al., 1996). The above studies suggest that AEA displays the properties of a partial CB_1 receptor agonist, the consequence of which is a lower magnitude of effect, even at saturating concentrations (Mackie *et al.*, 1993). It has been shown that AEA produces effects which are not mediated by cannabinoid receptors *e.g.*, the induction of neuronal apoptosis independent of cannabinoid, NMDA and TRPV1 receptors, NF-KB inhibition and the allosteric modulation of glycine receptors (Movsesyan *et al.*, 2004; Sancho *et al.*, 2003; Hejazi *et al.*, 2006; for review see Maccarrone and Finazzi-Agró, 2003). Furthermore, AEA inhibits gap-junction conductance in striatal astrocytes, which may infer that AEA has a role in the control of intercellular communications by regulating gap-junction permeability (Venance *et al.*, 1995).

Soon after the discovery of AEA, enzymatic pathways responsible for its biosynthesis and degradation were elucidated. The generation of AEA in response to a stimulant was first described by Di Marzo *et al.*, (1994) in rat brain neurones stimulated with ionomycin. Stimulation of cells with various agents causes the generation of AEA such as, Δ^9-THC-stimulated N18TG2 cells, lipopolysaccaride (LPS)-stimulated RAW264.7 mouse macrophages and in the simultaneous activation of the NMDA and acetylcholine receptor in rat cortical neurones (Burstein and Hunter, 1995; Pestonjamasp and Burstein, 1998; Stella and Piomelli, 2001). There are currently 2 pathways, which have been proposed to be the major route for the synthesis of AEA. Firstly, synthesis from free arachidonic acid and ethanolamine by fatty acid amide hydrolase (FAAH) acting in reverse was first described by Deutsch and Chin, 1993. However, several factors question the involvement of this pathway in the physiological generation of AEA *e.g.*, differences in the fatty acid profile of the N-acyl moiety of N-acylethanolamine compared to the free fatty acids in the same tissues and the amount of substrates which would be required are not observed in tissue (Sugiura, 2007). Secondly, synthesis from its pre-existing membrane precursor, N-arachidonoyl phosphatidylethanolamine (NAPE) by a (NAPE)-specific phospholipase D (NAPE-PLD) has also been reported by Schmid *et al.*, in 1996. Another AEA synthetic pathway was observed in macrophages exposed to the bacterial endotoxin LPS by Liu and colleagues (2006). This pathway involves the synthesis of AEA from NAPE through the actions of phospholipase C and a tyrosine phosphatase, PTPN22. In addition, AEA

can also be synthesised by the actions of alpha/beta-hydrolase-4 on NArPE, forming glycerol-phospho-AEA, which can then be converted to AEA by an as yet unknown phosphodiesterase (Simon and Cravatt, 2006). The existence of these alternative biosynthetic pathways may indicate that the specific route of AEA synthesis may depend on the type of cells and stimuli involved.

The cellular uptake and degradation of AEA is also a matter of controversy at present. Facilitated transport, FAAH gated passive diffusion and intracellular sequestration have all been proposed (Di Marzo *et al.*, 1994; Deutsch *et al.*, 2001; Hillard and Jarrahian, 2000). However, it is presently thought that in general AEA is inactivated through cellular reuptake and enzymatic degradation mechanisms, involving at least two enzymes, fatty acid amide hydrolase (FAAH) and the unidentified putative AEA protein transporter (AMT; Starowicz *et al.*, 2007). FAAH is a widely distributed membrane-bound serine hydrolase and was cloned from rat liver plasma membranes in 1996 (Tsou *et al.*, 1998; Hillard *et al.*, 1995; Ueda *et al.*, 1995; Cravatt *et al.*, 1996). The post-synaptic location of FAAH indicates that degradation of AEA is mainly a post-synaptic process (Starowicz *et al.*, 2007). FAAH can also limit the ability of AEA to act on its intracellular target, $TRPV_1$, this coupled with a strong colocalisation between the two, strongly supports the idea that AEA is a true endovanilloid (De Petrocellis *et al.*, 2001; Starowicz *et al.*, 2007; Cristino *et al.*, 2006). In contrast to FAAH, the existence of a putative protein transporter for AEA, the AMT, is still a matter of great controversy and debate. Although AEA can passively diffuse through lipid membranes, an accelerated diffusion has been observed in neurones and glia, indicating that there are additional unidentified facilitators for AEA transport across membranes (Di Marzo *et al.*, 1994; Beltramo *et al.*, 1997; Hillard *et al.*, 1997). It has been suggested that the most likely scenario for AEA transport occurs through multiple pathways involving passive diffusion aided by specific membrane proteins (Ehehalt *et al.*, 2006; Fowler and Thors, 2007).

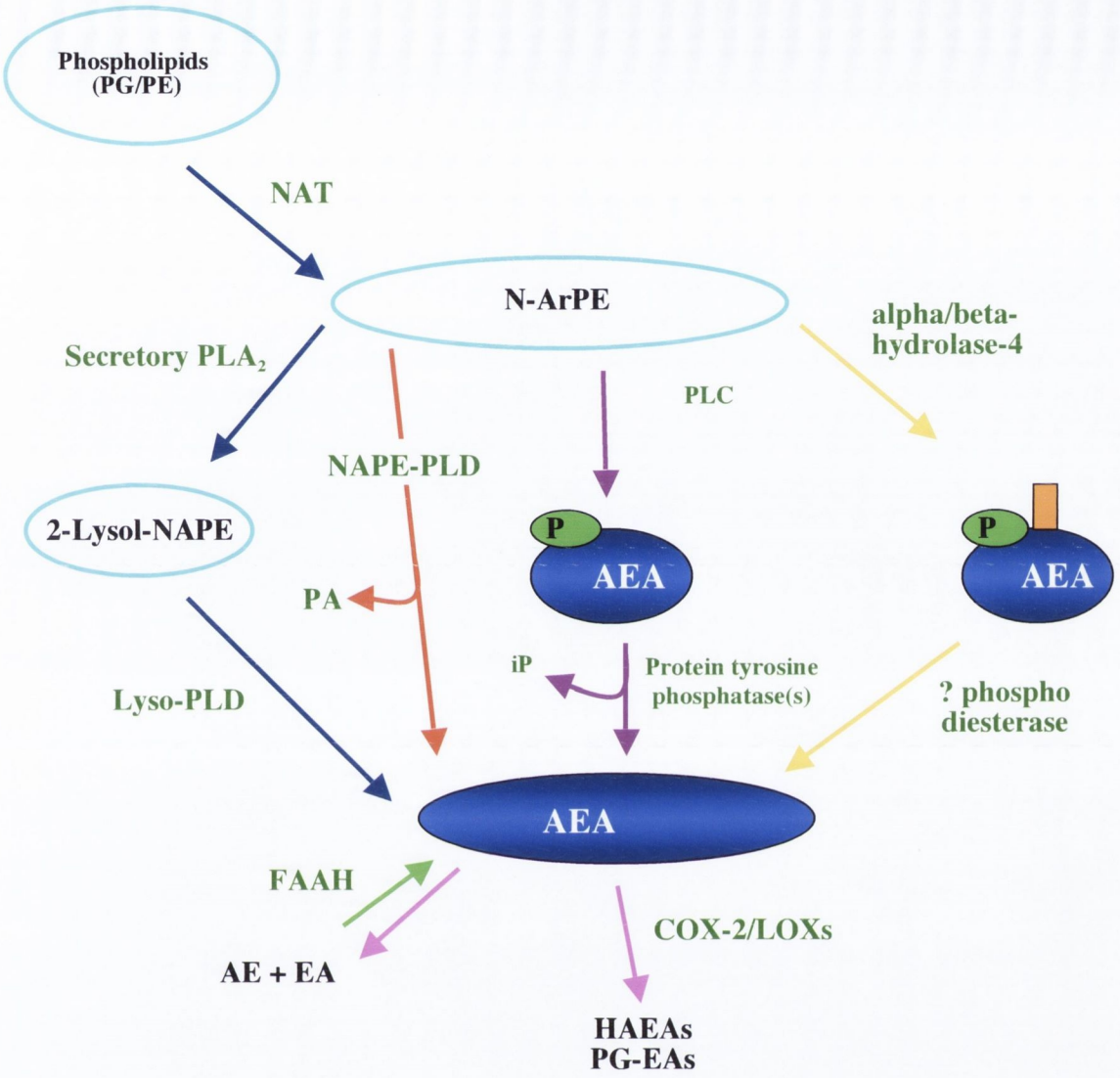

Figure 1.4: The key metabolic enzymes involved in anandamide synthesis and degradation.

A fatty arachidonic acid chain is transferred by N-acyltyltransferase (NAT) from phospholipids such as, phosphoglycerides (PG) and phosphatidylethanolamine (PE) to form N-arachidonylethanolamine (N-ArPE; red arrows). This intermediate is then hydrolysed by phospholipase D (PLD) to yield anandamide (AEA) and phosphatidic acid (PA). In addition, alternative pathways for AEA formation from N-ArPE are shown. The energy-independent condensation of ethanolamine (EA) and arachidonic acid (AA) by the reverse action of fatty acid amide hydrolase (FAAH) has also been postulated (green arrow). Another alternative pathway which involves the conversion of NAPE into 2-lysol-NAPEs by the action of secretory phospholipase A_2 ($sPLA_2$) which is then converted to N-acyl-ethanolmides (including AEA) by a selective lyso-PLD (navy arrows). Recent studeies have suggested parallel pathways for AEA synthesis, where AEA is generated from NAPE in a two-step process involving various enzymes (purple and yellow arrows). Degradation pathways (pink arrows), AEA is rapidly cleaved by FAAH to yield AA and EA. Alternatively, lipoxygenases (LOXs) and cyclooxygenase-2 (COX-2) can metabolise AEA, generating hydroxyl derivatives of AEA (HAEAs) and prostaglandin-ethanolamides (PG-EAs), respectively.

In 1995, 2 separate laboratories independently discovered the arachidonic acid derivative, 2-arachidonoylglycerol (2-AG; Mechoulam *et al.*, 1995; Sugiura *et al.*, 1995). Bisogno *et al.,* (1997) demonstrated the generation of 2-AG as an endogenous cannabinoid receptor ligand in N18TG2 cells stimulated with ionomycin. 2-AG generation was also shown to occur in both electrically stimulated rat hippocampal slices and in ionomycin-stimulated neurones (Stella *et al.*, 1997). The presence of Ca^{2+}, NMDA, ethanol, and LPS can stimulate the production of 2-AG (Kondo *et al.*, 1998; Stella and Piomelli 2001; Basavarajappa *et al.*, 2000; Di Marzo *et al.*, 1999). Levels of 2-AG in the rat brain are in the order of nmol/g tissue, which is significantly more than those observed for AEA (Sugiura *et al.*, 1995). 2-AG induces cannabimimetic actions such as binding to cannabinoid receptors, inhibition of adenylyl cyclase and the twitch response in murine vas deferens, hypothermia and analgesia (Mechoulam *et al.*, 1995). 2-AG inhibits voltage gated Ca^{2+} channels, depolarisation induced Ca^{2+} influx and neurotransmitter release, and activates inwardly rectifying K^+ channels (Oz *et al.*, 2004; Sugiura *et al.*, 1996; D'Amico *et al.*, 2004; Guo *et al.*, 2004). Signalling proteins such as p42/p44 mitogen-activating protein (MAP) kinase, p38 MAP kinase and c-jun N-terminal kinase (JNK) are activated by 2-AG (Kobayashi *et al.*, 2001; Derkinderen *et al.*, 2001a; Rueda *et al.*, 2000).

Akin to the synthesis of AEA, there are also multiple pathways for the generation of 2-AG. Synthesis of 2-AG most commonly occurs as a result of the hydrolysis of phosphatidylinositol (PI) involving the enzymatic actions of phospholipase C (PLC) and diacylglycerol lipase (DAGL) or the actions of phospholipase A_1 (PLA_1) and PLC (Sugiura *et al.*, 2006). However, other biosynthetic pathways have been postulated to occur in discrete areas of the brain *e.g.*, Tsutsumi and colleagues (1994), have identified a distinct lyso PI-specific phospholipase C (PLC*) which is only active in synaptosomes (also Oka *et al.*, 2007). Nakane *et al.*, (2002) have shown that in rat brain homogenate 2-AG is synthesised from 2-arachidonoyl lysophosphaticdic acid (LPA) by the actions of a phosphatase and suggest that LPA may act as a substrate for the generation of 2-AG during certain conditions in the brain. Experiments performed by Sugiura and co-workers (2007) have suggested that the mechanism responsible for the generation of 2-AG in the brain differs from that

occurring in inflamed tissues. They argue that it is unlikely that inositol phospholipids act as the sole source of 2-AG, and so, other phospholipids *e.g.*, phosphatidic acid (PA) also act as precursors for the generation of 2-AG during periods of inflammation (Sugiura, 2007).

2-AG uptake is a saturable process, independent of Na^{2+} and energy, which is sensitive to inhibition of FAAH with AM 404 (Beltramo and Piomelli, 2000). Bisogno *et al.*, (2001) demonstrated that 2-AG uptake was inhibited in rat C6 glioma cells by AM 404 and linvanil. Hajos *et al.*, have also described a temperature and AM 404 sensitive mechanism for 2-AG uptake in rat hippocampal and primary cultured cortical neurones (Hajos *et al.*, 2004). Interestingly, Hajos and colleagues also demonstrated that AEA prevented the uptake of 2-AG. Some investigators have interpreted these attributes as evidence for the existence of a transporter for endocannabinoids, namely the putative AEA membrane transporter (AMT). However, such a transporter has not been definitively characterised and so more research is needed to identify the uptake mechanism of endocannabinoids. If such transporter(s) exist, they potentially represent a unique point of control, which can be targeted by drugs designed to augment endocannabinoid signalling.

Researchers have focussed on FAAH and Monoacylglycerol lipase (MGL) as enzymes, which rapidly hydrolyse 2-AG to yield arachidonic acid and glycerol in many cell types. Goparaju *et al.*, (1999) demonstrated that 2-AG was hydrolysed by MGL-like activity in the cytosol and particulate fractions of the porcine brain. Dinh et al., cloned MGL from a rat brain cDNA library, in 2002. In addition, FAAH can also hydrolyse 2-AG to arachidonic acid and glycerol (Di Marzo *et al.*, 1998a; Goparaju *et al.*, 1998). Increased levels of 2-AG in mice repeatedly treated with FAAH inhibitors have been reported, however, levels of 2-AG were unchanged in $FAAH^{-/-}$ mice compared to $FAAH^{+/+}$ mice (de Lago *et al.*, 2005; Pacher *et al.*, 2005). Gulyás *et al.*, 2004 have shown that FAAH and MGL have different *loci* in the hippocampus, cerebellum and amygdala. Interestingly MGL is expressed in pre-synaptic terminals and inhibiting its actions has been shown to enhance retrograde signalling from pyramidal neurones to GABAergic terminals in the rat hippocampus (Gulyás *et al.*, 2004; Dinh *et al.*, 2002). This has prompted the suggestion that MGL activity is more prevalent than

FAAH activity in the brain (Dinh *et al.*, 2002; Jhaveri *et al.*, 2006). 2-AG also acts as a substrate for COX-2 and lipoxygenases (LOXs) *in vitro* (Kozak and Marnett, 2002). The resultant oxygenated derivatives of 2-AG are metabolically stable with long tissue half-lives and have diverse biological activities such as, the mobilisation of Ca^{2+}, PPAR-α activation and the ability to act as a pro-drug which can be transferred to a remote tissue where it is metabolised by a resident hydrolase to release bioactive eicosanoids (Kozak *et al.*, 2002; Nirodi *et al.*, 2004; Kozak *et al.*, 2002; Kozak and Marnett, 2002).

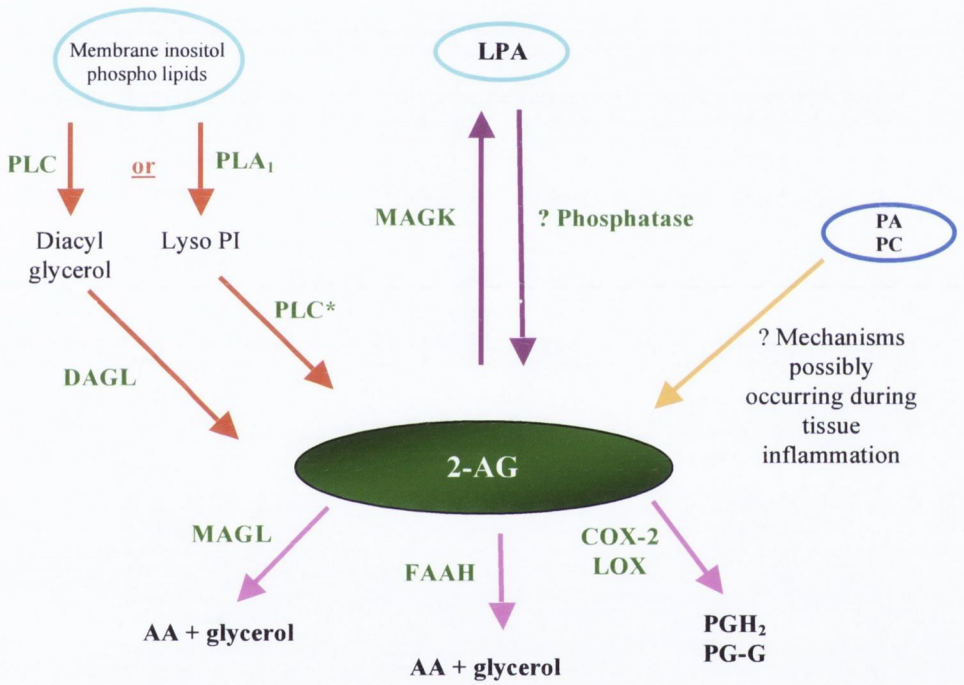

Figure 1.5: The key metabolic enzymes involved in 2-arachidonoylglycerol synthesis and degradation.

2-AG can be formed from arachidonic acid (AA)-containing membrane phospholipids trough the action of phospholipase C (PLC) and diacylglycerol lipase (DAGL) or through the actions of phospholipase A_1 (PLA_1) and a lyso-specific phospholipase C (PLC*; red arrows). Another synthetic and degradative pathway for 2-AG involves the actions of monoacyl glycerol kinase (MAGK) and of an as yet unidentified phosphatase on 2-arachidonoyl lysophosphatidic acid (LPA; purple arrows). Phosphatidic acid (PA) and phosphatidylcholine (PC) can also be used to form 2-AG indicating that several other types of diacyl glycerophospholipids other than inositol phospholipids serve as a precursor molecules in the synthesis of 2-AG. Monoacyl glycerol lipase (MAGL) is the most ubiquitous mechanism for 2-AG degradation. In addition, FAAH can also degrade 2-AG generating AA and glycerol. The enzymatic oxengenation of 2-AG is an additional catabolic pathway for 2-AG and results in the generation of PGH_2 glycerol esters (PG-G) and other oxygenated derivatives.

1.7 Cannabinoid signal transduction mechanisms

Cannabinoid receptors couple to multiple signal transduction pathways including G protein-coupling, andenylyl cyclase (AC), mitogen-activated protein (MAP) kinase, ion channels, intracellular Ca^{2+} concentration and other signalling systems. Most cannabinoid effects are sensitive to pertusis toxin (PTX) implicating cannabinoid receptor coupling to a $G_{\alpha i/o}$ protein (Demuth *et al.*, 2006). The proximal intracellular C-terminal domain of the cannabinoid receptor is critical for G protein coupling and the distal C-terminal domain modulates the magnitude and kinetics of signal transduction (Nie and Lewis, 2001). There is also evidence that CB_1 receptors can couple to $G_{\alpha s}$ leading to the stimulation rather than the inhibition of AC (Jarrahian *et al.*, 2004). The PTX-sensitive inhibition of AC by micromolar concentrations of Δ^9-THC in neuroblastoma cells was the first characterised CB_1 receptor signal transduction response (Howlett and Fleming, 1984, Howlett *et al.*, 1986). The functional inhibition of AC leads to a reduction in cytosolic cAMP levels, which causes the inactivation of protein kinase A (PKA) phosphorylation pathway. Cannabinoid-mediated inhibition of cAMP has been demonstrated in slices of rat hippocampus, striatum, cerebral cortex and cerebellum (Bidaut-Russell *et al.*, 1990). Modulation of the intracellular cAMP concentration and PKA phosphorylation, can result in major changes in cellular activity such the expression of synaptic plasticity-related genes such as extracellular signal regulated kinase (ERK) and focal adhesion kinase (FAK; Derkinderen *et al.*, 2003, 2001b, 1996). The MAP kinase pathway is a key signalling mechanism that regulates many cellular functions such as cell growth, transformation and apoptosis *via* the phosphorylation of various cytoplasmic and nuclear substrate proteins. CB_1 receptor activation by the synthetic cannabinoids, CP 55940 and HU-210 have been shown to link positively to p42/p44 MAP kinase and ERK, in CHO and human astrocytoma cells respectively (Bouaboula *et al.*, 1995, Galve-Roperh *et al.*, 2002). *In vivo* acute administration of Δ^9-THC induces a progressive and transient activation of MAP kinase and ERK in rat dorsal striatum and nucleus accumbens and also in murine hippocampus, and cerebellum (Valjent *et al.*, 2001; Derkinderen *et al.*, 2003a; Rubino *et al.*, 2004). AEA and 2-AG have also been shown to stimulate p38 MAP kinase in rat and murine hippocampus (Derkinderen *et al.*, 2001). The exact mechanisms for the

induction of MAP kinase by CB_1 receptors have not been fully elucidated, but cannabinoid receptors are not believed to act as tyrosine kinase-coupled receptors as the structure of CB_1 receptors and their sensitivity to PTX makes this unlikely (Demuth *et al.*, 2006). Increased glucose and phospholipid metabolism and glycogen synthesis through the activation of MAP kinase by Δ^9-THC and HU-210 has been reported in primary rat astrocyte cultures (Sanchez *et al.*, 1998). This effect has been proposed to involve the activation of phosphoinositol 3 kinase (PI3K) or the release of ceramide. Bouaboula *et al.*, have demonstrated that activation of the CB_1 and the CB_2 receptor induces the activation of MAP kinase which leads to a dose- and time-dependent increase in the expression of the immediate early gene *krox*-24 in the U373 human astrocytoma cell line and the HL60 human promyelocytic leukaemia cell line, and CHO cells (Bouaboula *et al.*, 1996; Bouaboula *et al.*, 1995). In mouse hippocampus, Δ^9-THC induces the expression of *krox*-24, brain derived neurotrophin factor (BDNF) and c-Fos protein also in a MAP kinase dependant manner (Derkinderen *et al.*, 2003). BDNF and *krox*-24 are known to be important for synaptic plasticity suggesting that gene regulation by MAP kinase is an important physiological mechanism by which cannabinoids can modulate synaptic plasticity (Demuth *et al.*, 2006). AEA has been shown to increase c-Fos protein and down regulate *Trk* nerve growth factor receptors in the rat brain (Patel *et al.*, 1998; Melck *et al.*, 2000).

Cannabinoids modulate voltage-dependant ion channels (inhibition of primarily N- and P/Q-type Ca^{2+} channels and the activation of inwardly-rectifying and A-type K^+ channels) mediated through the interaction of G protein $\beta\gamma$ subunits with ion channels (Mackie *et al.*, 1993, Hampson *et al.*, 1998, Deadwyler *et al.*, 1995). However, inhibition of K^+, M and K currents has also been reported (Schweitzer, 2000; Hampson *et al.*, 2000). Furthermore, there is evidence that cannabinoids modulate ion-channel function directly *e.g.*, on TASK-1 channels (Maingret *et al.*, 2001). The modulation of voltage-dependent ion channels is thought to underlie the cannabinoid-induced depression of synaptic transmission in the brain and, in turn, reduce both excitatory and inhibitory neurotransmitter release (Nicholson *et al.*, 2003). Ca^{2+} concentration is increased by 2-AG and WIN 55212-2 in NG108-15 cells in a PTX and SR 141716A-sensitive manner, a PLC inhibitor blocked this response suggesting an IP_3-mediated

release of Ca^{2+} from internal stores (Sugiura *et al.*, 1996). Methanandamide, WIN 55212-2 and HU-210 have all shown the ability to enhance Ca^{2+} release from IP_3-sensitive stores in response to depolarisation induced by high K^+ or NMDA receptor stimulation (Netzeband *et al.*, 1999).

A number of investigations have demonstrated that cannabinoids can modulate the activity of other receptor types, which produces unorthodox cannabinoid signal transduction pathways. It is conceivable that some effects of cannabinoids, which are insensitive to cannabinoid receptor antagonism, may occur *via* synergistic receptor interaction (Demuth *et al.*, 2006). Pharmacological interactions between the cannabinoid and the opioid systems have been suggested, mainly concerning antinociception, hypothermia and hypotension (Bloom and Dewey, 1978; Lee et al., 2006a). Smith *et al.*, (1998) found that subcutaneous administration of Δ^9-THC enhanced the antinociceptive potency of the opioid agonist morphine in the mouse tail-flick test. Maione *et al.*, (2006) found that FAAH inhibition and 2-AG induced $TRPV_1$-mediated analgesia in a descending pain pathway in rodents. Other cannabinoid receptor-independent signal transduction pathways exist such as the inhibition of serotonin 5-HT_3 receptors, nACh receptors and the activation of NMDA receptors (Godlewski *et al.*, 2003; Oz *et al.*, 2004; Hampson *et al.*, 1998).

1.8 Apoptosis

The term apoptosis describes a process characterised by distinct morphological changes such as condensation and cleavage of DNA into oligonucleosomal fragments, shrinkage of cytoplasm, membrane blebbing and packaging of cellular contents into membrane bound apoptotic bodies for deletion by phagocytic cells. Another feature of the apoptotic process is the presentation of epitopes such as the expression of cell surface death receptors and the loss of phosphatidylserine asymmetry in the plasma membrane which marks the cell as a phagocytic target. In contrast to necrosis, apoptosis is an ordered process that does not trigger a pronounced inflammatory response, due in part to the maintenance of an intact plasma membrane (Blatt and Glick, 2001). To bring about the destruction of a cell apoptosis relies on the strict regulation of biochemical

events such as intracellular signal transduction, ordered enzyme cascades and gene transcription (Kerr, 2002; see Figure 1.6). Apoptosis is most commonly identified using methods that detect modulations in these key biochemical events. Apoptosis is the pre-eminent form of pathophysiological cell death, whilst necrosis is relevant only in circumstances of gross injury such as blunt trauma, toxin exposure or loss of blood supply (Raffray and Cohen, 1997; Blatt and Glick, 2001). This theory can be expanded to regard apoptosis as an ordered gradual response to a specific message received from intracellular or extracellular signalling and necrosis as a non-specialised immediate response to a major non-specific injury (Wyllie *et al.*, 1987; Raffray and Cohen, 1997).

1.8.1 Neuronal apoptosis

The death of unnecessary cells by apoptosis is a common feature of normal embryonic nervous system development and continues on into late adulthood. Disruption of this developmental apoptosis can lead to changes in neural stem cell proliferation rates and the balance between neurogenesis and gliogenesis, which can manifest as a multitude of neurocognitive and physical impairments (Boya and De Le Rosa, 2006). Approximately 50% of the total number of neurones formed die by apoptosis during normal foetal development in rats, mice and humans (Lo *et al.*, 1995). There is evidence that surviving post-mitotic neurones hold the apoptotic death program at a relatively high state of readiness during post-developmental life due to their limited capacity for self-renewal and repair (Wyllie *et al.*, 1987; Morrison *et al.*, 2003). Neural progenitor cells rely on a supply of information from neurotrophins and a number of other intermediary mediators such as cell-cell contacts and intercellular communication to modulate anti-apoptotic and pro-apoptotic signals. Integration of these mediators allows the control of cell lineage, location and fate of neural progenitors. Neurotrophin interaction with receptor tyrosine kinases provides survival signals, as well as promoting differentiation and neurite extension *e.g.*, nerve growth factor, brain derived neurotrophic factor (BDNF), and neurotrophins 3 and 4/5. Disturbance or modulation of this information supply can produce apoptosis by default and is observed in many pathological conditions (Raffray and Cohen, 1997). In several mouse model of Alzheimer's disease neurogenesis is reduced and factors that enhance neurogenesis *e.g.*,

up regulated BDNF can enhance neurogenesis and may improve animal performance in cognitive tasks (Dong *et al.*, 2004; Lee *et al.*, 2000). Therefore targeting neurogenesis is receiving interest as a means to mitigate the symptoms of AD. In this regard it is notable that the cannabinoid system also regulates neurogenesis and has been reported to govern TrkB receptor-dependent signalling pathways to modulate selective interneuronal migration and specification during embryonic neurogenesis (Berghuis *et al.*, 2005; Galve-Roperh *et al.*, 2007). Furthermore, it is unlikely that apoptosis proceeds in a linear cascade of events in complex neuronal network systems. Rather it is more likely that neuronal cell death proceeds *via* multiple intricately connected pathways, which culminate in the physical destruction and deletion of cells with out negatively impacting on the surrounding cells.

1.8.2 Caspase signalling

Despite the diversity in pro-apoptotic signalling cascades, most cell death pathways ultimately converge with the activation of caspases (Blatt and Glick, 2001). Caspases are specialised proteases that are essential for the physical execution of apoptosis. The role of caspases in apoptosis first became evident when a cell death-related gene, *ced*-3, which is essential for apoptosis in *Caenorhabditis elegans*, was found to be homologous to the mammalian caspases (Yuan *et al.*, 1993). They are distinct from other proteases due to their requirement for a cysteine residue for catalysis and an aspartic acid residue for specificity. Caspases are synthesised as a single polypeptide chain, which must undergo cleavage and dimerisation for full enzymatic activity (Earnshaw *et al.*, 1999; Krammer, 1999). There are at least 14 different caspases identified in mammalian tissues (Nuñez *et al.*, 1998). Most caspases can be grouped into 3 different categories based on substrate specificity. Group I, caspases involved in inflammatory processes (caspases 1, 4 and 5), group II, signalling caspases since they can activate other caspases initiating an activation cascade (caspases 6, 8, 9 and 10), group III, effector caspases since activation of these lead to cell death (caspases 2, 3, and 7; Garcia-Calvo *et al.*, 1998; Casciola-Rosen *et al.*, 1996). Caspases are responsible for cleaving numerous cellular targets, including structural elements, nuclear proteins and signalling proteins *e.g.*, actin, DNA repair enzymes and

phospholipase A (Krammer, 1999). Apoptosis is usually accompanied by the activation of caspase-3, which is one of the most extensively studied caspase (Janicke *et al.*, 1998). In healthy cells, including neurones, caspase-3 exists as a pro-enzyme (32 kDa) and is processed upon cell stress by caspase-9 to an active heterodimeric form (17 kDa and 12 kDa; Slee *et al.*, 1999). The most common mechanism of caspase-3 activation involves the release of cytochrome-c from the mitochondria into the cytosol (Reed, 1997). In the cytosol, cytochrome-c can activate Apaf-1, which oligomerises to form a caspase activating complex known as the Apaf-1 apoptosome. The initiator protein caspase-9 is then recruited to the Apaf-1 apoptosome to form a holoenzyme complex, which then activates pro-caspase-3 (Cain, 2003; Figure 1.6). However, there are many more mechanisms, which activate caspase-3. The ligation of Fas-associated death domain (FADD) leads to the activation of caspase-8, which can cleave pro-caspase-3 to its active form (Schmitz *et al.*, 2000). Additionally, the lysosomal proteases cathepsin-L and cathepsin-D and the serine protease granzyme B, can directly cleave caspase-3 to its heterodimeric active form (Ishisaka *et al.*, 1999; Kågedal *et al.*, 2001a; Heinrich *et al.*, 2004; Lord *et al.*, 2003). Once activated, caspase-3 is capable of autocatalysis as well as regulating other signalling proteins such as, PKCδ, MEKK and the mitochondrial associated proteins Bcl_2 and Bax (Datta *et al.*, 1996; Shiah *et al.*, 2001). Once activated, caspase-3 is directly involved in the sustained induction of DNA damage and the disruption of DNA repair mechanisms, such as the inactivation of poly (ADP-ribose) polymerase (PARP), which culminate in the rapid and irreversible distruction of the cell (Janicke *et al.*, 1998; Decker and Muller, 2002).

1.8.3 Involvement of lysosomal signalling in apoptosis

Death domains, caspases and mitochondria have been the major focus of apoptosis research. However, other cellular components have recently been implicated in apoptotic signalling, such as the lysosomes (Brunk *et al.*, 2001). Lysosomes are small highly acidic membrane-bound organelles containing many proteolytic enzymes and are the main site for the intracellular degradation of long-lived proteins (Dunn, 1994). Lysosomes also function in digestion of cell waste, tissue remodelling, lysis of invaders and the autolytic replenishment of amino acids and glucose which are needed for *de*

novo protein synthesis (Yamashima *et al.*, 1998). Considering the many functions of lysosomes it is not surprising that more than 80 hydrolytic enzymes are found in lysosomes *e.g.*, amylases, lipases and proteases (Ditaranto-Desimone, 2003; Adler *et al.*, 1989). The acidic pH of the lysosomes is maintained by the activity of a H-ATPase pump in the lysosomal membrane which pumps H^+ ions from the cytosol to the interior of the lysosome (Geisow, 1982). In addition to maintaining normal cytosolic pH, lysosomes also function as intracellular Ca^+ regulators (He *et al.*, 2002). Several other highly glycosylated proteins are present on the lysosomal membrane *e.g.*, lysosomal associated membrane proteins (LAMPs), lysosomal integral membrane proteins (LIMPs) and lysosomal acid phosphatase (LAP). These proteins have multiple functions such as, retention of degradative enzymes, maintenance of the acidic environment and some yet to be identified functions.

De Duve (1970) was the first to link lysosomal membrane disruption and leakage of its degradative enzymes with cell death. Until recently lysosomes have been associated predominantly with necrotic cell death rather than with apoptosis. There are several reasons to link lysosomes directly to the initiation of apoptosis. Research using lysosomotropic detergents and other lysosomal damaging agents has reported apoptotic cell morphology and a number of other hallmarks of apoptosis (Wilson *et al.*, 1987; Zdolsek *et al.*, 1993a; Brunk *et al.*, 2001b). Indeed, Brunk *et al.*, (2001a) suggest that lysosomal rupture, even partial lysosomal membrane destabilisation, might be an early event in apoptosis upstream from the loss of mitochondrial membrane potential. Lysosomal membrane destabilisation (LMD; Figure 1.6) can be induced by a multitude of initiating factors including the production of ROS, sphingosine, the action of phospholipase A_2, depletion of lysosomal associated heat shock protein-70 (HSP70), induction of p53 mediated apoptosis and the association of Bax with the lysosomal membrane (Zdolsek *et al.*, 1993b; Kågedal *et al.*, 2001b; Zhao *et al.*, 2001; Nylandsted *et al.*, 2004; Yuan *et al.*, 2002; Kågedal *et al.*, 2005). LMD can cause the release of ROS and lysosomal proteases such as cathepsins into the cytosol (Chwieralski *et al.*, 2006). Cathepsins are proteases, which under physiological conditions are localised intralysosomally. In response to certain signals, cathepsins can be released from the lysosomes into the cytosol where they have been shown to trigger apoptotic cell death

via numerous pathways (Chwieralski *et al.*, 2006). Cathepsins have an optimal activity at acidic pH, however, recent studies have demonstrated that cathepsins can function at neutral pH for up to several hours (Turk *et al.*, 1993). Furthermore, Beaujouin and co-workers observed no differences in the ability of catalytically active or inactive cathepsin-D to induce apoptosis (Beaujouin *et al.*, 2006). This indicates that the presence of cathepsin-D in the cytosol alone is enough to trigger apoptosis. Laurent-Matha *et al.*, (2005) have shown that cathepsin-D is necessary for invasive fibroblast growth, a process that was independent of cathepsin-D proteolytic activity. Cathepsins, amongst other lysosomal enzymes, can act on the mitochondria, promoting release of cytochrome-c and ROS in addition to the activation of caspase-3 (Johansson *et al.*, 2003a; Zhao *et al.*, 2003; Ishisaka *et al.*, 1999; see Figure 1.6). Findings from Yuan *et al.*, (2002) indicate that p53-induced apoptosis involves a lysosomal-mitochondrial pathway in which early lysosomal destabilisation plays an initiating role upstream of mitochondrial dysfunction. It appears that lysosomal signalling functions in apoptosis *via* multiple molecular pathways, which often integrate with traditional mediators of apoptosis *e.g.*, mitochondrial membrane destabilisation and caspase activation.

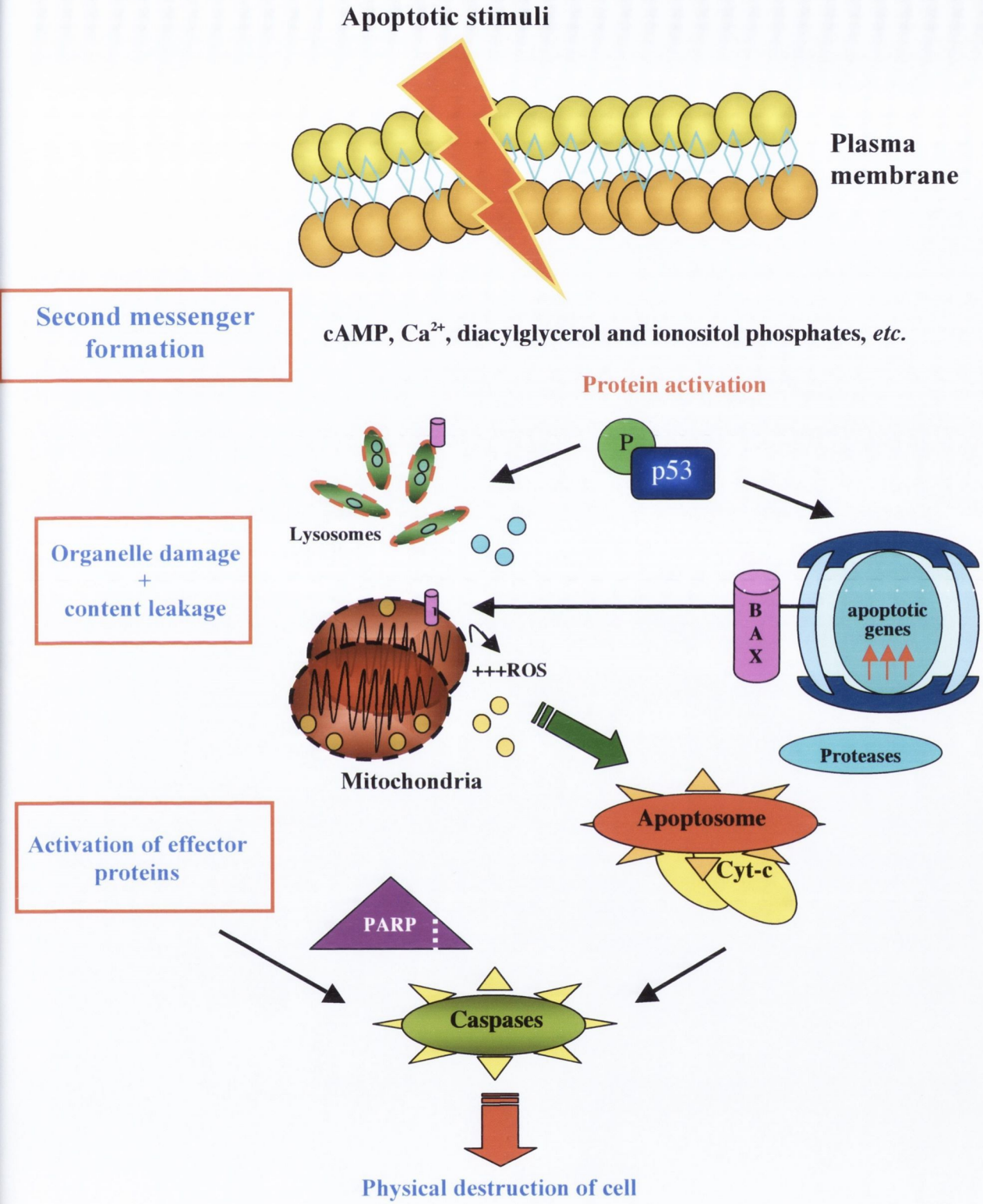

Figure 1.6: The main signalling pathways in apoptosis.

1.9 Spleen tyrosine kinase (SyK)

Spleen tyrosine kinase (SyK) is a member of an autonomous family of non-receptor tyrosine kinases, which contain two adjacent Src homology 2 (SH_2) domains and a kinase domain but unlike Src-family kinases, SyK lacks an SH_3 domain (Sada *et al.*, 2001). Other members include zeta activating protein (ZAP)-70, the Src family and the Tec family (Turner *et al.*, 2000). Activation of SyK occurs through the binding of tandem SH_2 domains to immunoreceptor tyrosine-based activation motifs (ITAMs). SyK is similar to JNK as it activates certain pathways by phosphorylation in addition to autophosphorylation. Activated SyK is critical for the phosphorylation of tyrosine residues in multiple proteins involved in the regulation of important pathways leading from a receptor, such as Ca^{2+} mobilisation and MAPK cascades (Coopman and Mueller, 2006). SyK was first recognised as a 40 kDa proteolytic fragment derived from a p72 tyrosine kinase present in spleen, thymus and lung (Zioncheck *et al.*, 1988). The SyK gene was first cloned from porcine spleen and encodes a 72 kDa protein, which is highly susceptible to proteolysis (Taniguchi *et al.*, 1991). Until recently SyK has almost exclusively been studied in haematopoietic cells such B and T lymphocytes, natural killer cells, mast cells, macrophages and platelets (Coopman and Mueller, 2006). SyK functions in the downstream signalling of activated immunoreceptors containing ITAMs *e.g.*, B cell receptors (BCR) and T cell receptors (TCR). Once activated SyK can initiate the phosphorylation of specific enzyme substrates and adapter proteins which play a role in co-ordinating a series of cellular responses such as, proliferation, differentiation and phagocytosis (Coopman and Mueller, 2006; Yanagi *et al.*, 2001). It is interesting to note that SyK expression negatively affects cell activities such as 3-D cell outgrowth, migration, tumour metastasis and proliferation potential, and the secretion of many chemoattractant factors (Coopman *et al.*, 2000; Mahabeleshwar and Kundu, 2003; Hoeller *et al.*, 2005; Li *et al.*, 2005). Furthermore, SyK is recruited to the brain scaffold protein, Tamalin, which forms a multi protein assembly including metabotropic glutamate receptors and other post-synaptic proteins (Hirose *et al.*, 2004). SyK is also expressed in human primary Fc receptor activated microglia and has been implicated in neurone-like differentiation, ERK activation and supernumerary neurite formation in P19 cells (Song *et al.*, 2004; Tsujimura *et al.*, 2001). Interestingly, SyK

activation has been shown to be responsible for lysosomal changes in BCR-induced cell death involving fusion of BCR carrying endosomes to lysosomes (He *et al.*, 2005).

1.10 Tumour suppressor protein 53 (p53)

Tumour suppressor protein 53 (p53) is a transcription factor that has a critical role in preventing uncontrolled cell division. The p53 protein can activate stress-mediated G1 cell-cycle arrest to facilitate DNA repair, or if this is impossible p53 promotes cell death (Levine, 1997). This is dependent on the type of cell and the nature of the stimulus incurred by the cell (Evan and Littlewood, 1998). The p53 protein is short lived with a half-life of only 10 - 30 minutes and is constitutively expressed at low levels in most cell types including neurones (Culmsee and Mattson, 2005). However, upon activation by cell stress stimuli, p53 becomes activated which enables its accumulation and prolongs its half-life. Various stress stimuli can lead to the activation of p53 *e.g.*, cytotoxic drugs, heat shock, ionising radiation, cellular Ca^{2+} overload, hypoxia and oxidative stress (Blatt and Glick, 2001). The pro-apoptotic actions of p53 are largely mediated through the transactivation of specific target genes, blocking the expression of selected genes, interference with other transcription factors or through other transcription independent pathways (Culmsee and Mattson, 2005). p53 acts as a sequence-specific activator of $P21^{WAF1/CIP-1}$ protein, which blocks cell proliferation by regulating cyclin-dependent kinases (Zörnig *et al.*, 2001). The pro-apoptotic Bax protein is transcriptionally induced by p53 after DNA damage and can mediate cell death by inserting itself into the outer mitochondrial membrane (OMM; Miyashita and Reed, 1995). The insertion of Bax causes the disruption of the OMM and release of mitochondrial contents such as cytochrome-c, Smac/Diablo, endonuclease G, Htr2/Omi and apoptosis-inducing factor (AIF), which leads to the activation of pro-apoptotic signalling cascades (Le Bras *et al.*, 2006; Saelens *et al.*, 2004). However, in $Bax^{-/-}$ mice the pro-apoptotic p53 function is not affected, signifying that there are alternative scenarios for p53-mediated cell death (Moroy and Zörnig, 1996). Indeed, p53 is known to activate the transcription of the Fas receptor (CD95), c-fos, BH3-only protein PUMA and Noxa, and p53-regulated apoptosis-inducing protein 1 ($p53AIP_1$), all of which

prime the cell for apoptosis (Bennett *et al.*, 1998; Elkeles *et al.*, 1999; Jeffers *et al.*, 2003; Oda *et al.*, 2000; Wesierska-Gadek *et al.*, 2005). In response to ROS production, p53 can block the Nrf2-induced activation of antioxidant genes such as those responsible for generation and metabolism of glutathione (Faraonio *et al.*, 2006). Conversely, p53 can also induce apoptosis independent of transcriptional regulation *e.g.*, by direct signalling at the mitochondria and lysosomes, direct protein-protein interactions and increased cell surface redistribution of cell death receptors (Marchenko *et al.*, 2000; Yuan *et al.*, 2002; Chipuk and Green, 2003; Bennett *et al.*, 1998). The pleotropic nature of p53-mediated apoptosis signifies the importance of this protein in apoptotic signalling. The final route by which apoptosis is mediated by p53 most likely depends on the cell type and the nature of death stimulus received (Zörnig *et al.*, 2001).

1.10.1 Post translational modification of p53

Due to the critical nature of the p53 protein in deciding cell fate, it is not surprising that p53 activity is a highly regulated protein. Regulation of p53 occurs at many levels *e.g.*, control of mRNA levels (transcriptional), alterations in p53 protein half-life and functional activity, and post translational modifications. Regulation by post translational modification allows different cell types to rapidly activate a unique set of responses to diverse cell stress stimuli (for reviews see Lavin and Gueven, 2006; Giaccia and Kastan, 1998). Post translational modifications by phosphorylation, acetylation, methylation and ubiquitination are carried out mainly in the N- and C-termini by a number of proteins *e.g.*, JNK has been shown to induce the activation of p53 by phosphorylation at serine 15 in the N-terminal as a result of treatment with glutamate, Δ^9-THC and by blocking NF-KB activity (Chen *et al.*, 2003; Downer *et al.*, 2007a; Zerbini *et al.*, 2005). Furthermore, phosphorylation of p53 on serine 15 in response to genotoxic stress has been shown to reduce the ability of p53 to bind to its negative regulator Mdm2, thus leading to an accumulation of active p53 (Shieh *et al.*, 1997; Banin *et al.*, 1998). In addition, serine residues 20, 33 and 46 are phosphorylated and serine residues 376 and 378 undergo dephosphorylation in response to cell stress (Lavin and Gueven, 2006). Once phosphorylated, the stability of the p53 protein is increased, allowing it to act as a transcription factor to up regulate many p53 responsive

genes *e.g.*, Mdm2 and the pro-apoptotic Bcl-2 family member, Bax. Transactivation of pro-apoptotic genes, such as Bax, leads to further down stream signalling which culminates in the activation of proteins responsible for initiating the physical destruction of the cell.

Alterations in proteins which bind post translationally to p53 can also have an effect not only on p53 activity but also its degradation, its cellular location, its homo-dimerisation potential and its sequence-specific DNA binding ability. Degradation of p53 is regulated by the interaction with the Murine double minute protein (Mdm2). Mdm2 functions both as an ubiquitin ligase, to label p53 for degradation at the proteosome and as a post translational modifier that blocks the p53 transactivation domain, thus making interaction with p53 target genes impossible (Ashcroft *et al.*, 2000; Oren, 1999; Momand *et al.*, 2000). Apoptosis-inducing signals readily induce the stabilisation of the p53 protein, which results in an accumulation of the activated protein in stressed cells. Stabilisation is likely to reflect mechanisms that allow p53 to become resistant to Mdm2-mediated degradation (Ashcroft *et al.*, 2000). *In vitro* studies using DNA-damaging agents have shown that phosphorylation within the N-terminus of p53, particularly at serines 15, 20 and 37, causes a reduction in the interaction between p53 and Mdm2 (Shieh *et al.*, 1997; Unger *et al.*, 1999). However, the observation that a phosphorylation deficient p53 mutant can still be stabilised in response to DNA-damaging agents suggests that there are phosphorylation-independent pathways leading to the stabilisation of p53 (Blattner *et al.*, 1999). In order to transactivate its target genes, p53 must be translocated to the nucleus. A number of protein modifiers can bind to p53 and affect its cellular location *e.g.*, association with Mdm2 causes translocation from the nucleus to the cytosol and association with Bax induces translocation to the mitochondria (Roth *et al.*, 1998; Chipuk *et al.*, 2003). Association with the small ubiquitin-related modifier (SUMO) protein has also been shown to affect the transactivation potential of p53 (Gostissa *et al.*, 1999; Rodriguez *et al.*, 1999). Interestingly, the modulation of p53 by SUMO can decrease the strength of the interaction between p53 and Mdm2, thus promoting its nuclear export (Carter *et al.*, 2007).

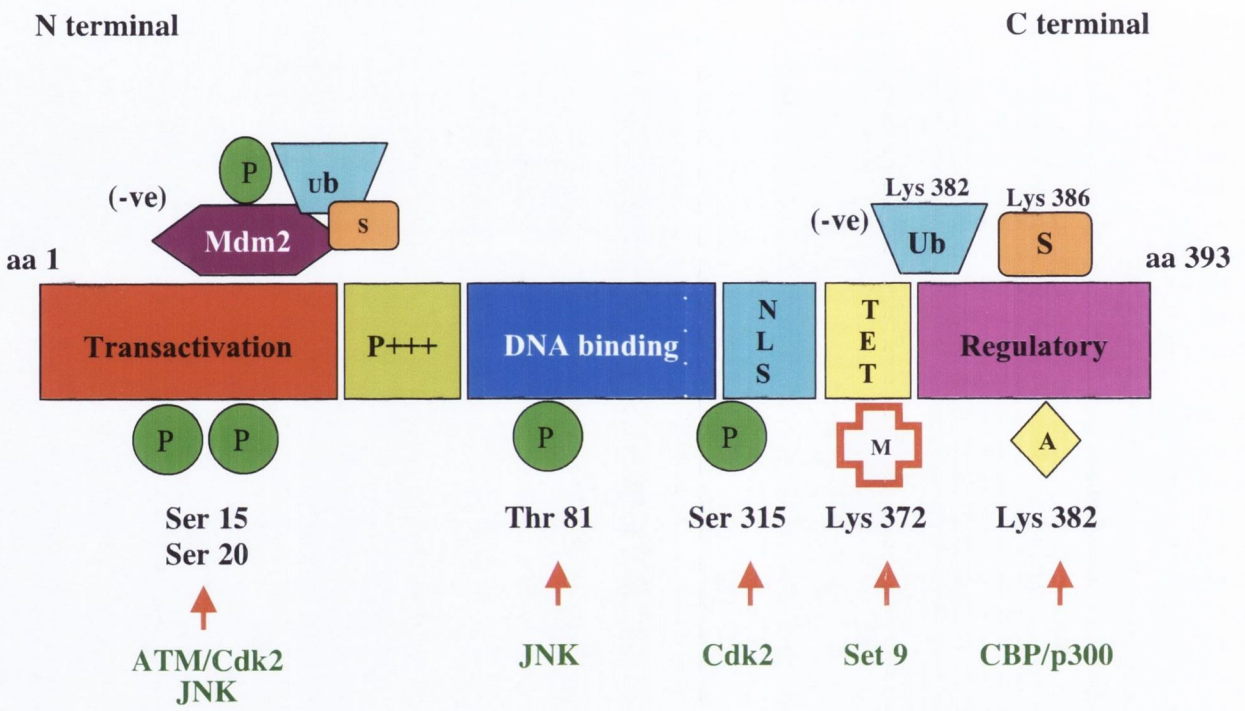

Figure 1.7: Post translational modifications to p53.

The bar represents the 393 amino acid (aa) p53 polypeptide; regions associated with transactivation, sequence specific DNA binding domain, nuclear localisation signalling (NLS), tetramerisation (TET) are represented in addition to the proline rich domain (P+++), and the DNA-mediated negative regulation of specific DNA binding domain (regulatory). The amino acid position of selected phosphorylation (P), methylation (M) and acetylation (A) are shown in addition to the enzyme (green text) responsible for the modification. The proteins that interact with p53 post translationally are shown in the upper part of the schematic representation of p53, Mdm2, which can also be itself modified by ubiquitin (Ub) and SUMO (S). Both Mdm2 and ubiquitin are negative regulators of p53 and hence decrease the p53 response.

1.10.2 Modification of p53 with Small ubiquitin-related modifier (SUMO)

Small Ubiquitin-related MOdifier (SUMO) is a member of the ubiquitin-related protein family, which consists of Nedd8 and Apg12 among others. These proteins are highly conserved, found in all eukaryotes, are essential for viability and are implicated in a large number of processes including nuclear transport, cell cycle control, DNA repair, signal transduction and regulation of ubiquitin-dependent degradation (Matunis *et al., 1996;* Johnson and Blobel, 1999; Hardeland *et al.,* 2002; Rui *et al.,* 2002; Desterro *et al.,* 1998). Mammalian cells contain at least 3 genes encoding 3 distinct and ubiquitously expressed SUMO proteins (SUMO-1, -2 -3) which share varying degrees of similarity with each other, SUMO-2 and -3 being the most similar sharing 87% sequence identity with each other compared to only 47% for SUMO-1 (Melchior, 2000). Despite sharing only 18% sequence similarity, the folded structure of the C-terminal domain of SUMOs are virtually super imposable to ubiquitin except the presence of a N-terminal extension on SUMO (Bayer *et al.*, 1998; Vijay-Kumar *et al.*, 1987). Ubiquitin is a low molecular weight protein, which is covalently attached to substrate proteins by a 3-step multi-enzyme pathway. Labelling a protein with ubiquitin targets the protein for degradation *via* the proteosome. The reversible covalent attachment of SUMO to a specific lysine residue (positioned in the consensus sequence ψKXE) of the substrate protein is controlled by an enzyme pathway analogous to the ubiquitin pathway (Johnson, 2004). SUMOylation involves a SUMO E1 activating enzyme (the heterodimer Aos1/Uba2), a SUMO E2 conjugating enzyme (Ubc9) and a SUMO E3 ligase, which binds to the substrate protein and Ubc9 and promotes the transfer of SUMO to the substrate protein. There are specific isopeptidases called SUMO/sentrin-specific proteases (SENPs), which remove SUMO from proteins, thus making the modification reversible whilst also providing a source of free unconjugated SUMO. SENPs also act as C-terminal hydrolases by processing the immature form of SUMO to its mature form, which exposes the di-glycine motif that is necessary for conjugation to the substrate protein (Melchior and Hengst, 2002; Matunis *et al.*, 1996, Hoege *et al.*, 2002). In contrast to ubiquitination, SUMOylation does not label proteins for degradation but rather effects the proteins molecular interactions (Melchior, 2000;

Melchior and Hengst, 2002). SUMOylation of a protein appears to alter the proteins interactions with other macromolecules *e.g.*, interactions with other proteins or DNA. SUMOylation often has a positive effect on protein-protein interactions and promotes the assembly of several multi-protein complexes that are involved in gene transcription (Johnson, 2004). In certain circumstances, the SUMOylation of proteins can also act as an antagonist of ubiquitin thus generating a protein that is resistant to degradation (Desterro *et al.*, 1998). The post translational modification of a protein by SUMO provides a highly diverse set of subtle transient repercussions that seem to be target specific.

p53 was one of the first proteins for which SUMOylation was demonstrated, however, the physiological relevance of this post translational modification remains enigmatic (Melcoir and Hengst, 2002). SUMO-1 binds to the C-terminus of p53 at lysine 368, which lies within the SUMO conjugation motif present on p53 (Melcoir and Hengst, 2002). Post translational modification of p53 with SUMO-1 has been reported to increase the transactivation of p53 responsive genes (Gostissa *et al.*, 1999; Rodriguez *et al.*, 1999). These reports, showing a positive effect on p53 activity after SUMOylation, utilised reporter assays which relied on the over expression of SUMO-1 and Ubc9. Since SUMO-1 has a large number of potential targets, over expression of SUMO-1 and Ubc9 could potentially influence many events of transcription including reporter constructs (Melchoir 2000). Indeed, it has also been shown that SUMOylation of p53 has no effect on its transcriptional activity and that the co-expression of p53 and SUMO with enzymes that catalyse SUMOylation can repress p53 activity (Kwek *et al.*, 2001; Schmidt and Müller, 2002). Furthermore, the levels of SUMOylated p53 are marginal even with over expression of SUMO-1 and/or Ubc9 (a SUMO E2 enzyme), which puts the physiological significance of this modification into question. However, the low steady state levels of SUMOylated p53 can be interpreted as the modification being a dynamic process necessary for transient interactions or processes, such as, p53 import or export from the nucleus and the release from protein/protein or protein/DNA complexes (Melchoir 2000; Melchoir and Hengst 2002). In addition, Müller and co-workers (2000) found that inhibition of serine/threonine phosphatases dramatically reduced the ability of p53 to be SUMOylated suggesting that phosphorylation acts to

antagonise SUMOylation. Indeed, Lin *et al.*, (2004) have shown that the phosphorylation of serine 20 in p53 as a consequence of exposure to DNA damaging agents strongly reduced the SUMOylation of p53.

1.10.3 Modification of p53 with Murine double minute 2 (Mdm2)

The murine double minute 2 gene is one of three genes (Mdm 1, 2 and 3) located in extrachromosomal nuclear bodies called double minutes. The Mdm genes were originally found to be over expressed by amplification in the spontaneously transformed mouse BALB/c cell line, 3T3-DM (Cahilly-Snyder *et al.*, 1987; Fakharzadeh *et al.*, 1991). The transformation potential of Mdm2 is as a result of the ability of Mdm2 to inhibit p53-mediated transactivation (Momand *et al.*, 1992). Mdm2 null mice are early embryonic lethal, dying before implantation, due to the loss of the ability to regulate p53 activity since it has been shown that the concomitant deletion of p53 reverses this lethality (Jones *et al.*, 1995; Montes de Oca Luna *et al.*, 1995). Mdm2 functions as an ubiquitin ligase enzyme and is the enzyme responsible for the monomeric ubiquitination of p53 on multiple lysine residues in addition to self-ubiquitination (Lai *et al.*, 2001; Fang *et al.*, 2000; Honda and Yasuda, 2000). Monomeric ubiquitination is involved in receptor endocytosis, transcription, DNA repair and caspase recruitment, while poly ubiquitination is generally involved in protein degradation (Lee and Peter, 2003). It is now believed that Mdm2 functions as a critical titrator of p53 activity and loss of Mdm2 results in an active p53 (Iwakuma and Lozano, 2003). p53 acts as a transcription factor at the Mdm2 gene promoter, thus p53 transcriptionally up regulates Mdm2 expression. Due to the ability of Mdm2 to inhibit p53 activity a negative feedback loop is formed which provides a tight regulatory mechanism for controlling the function of p53 in cell cycle progression and apoptosis. Several post translational modifications of both p53 and Mdm2 can effect this interaction. The phosphorylation of either p53 or Mdm2 by various kinases has been shown to weaken the interaction between the two proteins (Unger *et al.*, 1999; Shieh *et al.*, 1997; Zhang and Prives, 2001). Interestingly Carter *et al.*, (2007) have shown that SUMOylation of p53 promotes the detachment of Mdm2 from p53 and that this increases its cytosolic degradation or for a cytosol based pro-apoptotic function.

Furthermore, deSUMOylation of Mdm2 by the SUMO-specific protease SUSP4 increased Mdm2 self-ubiquitination resulting in p53 stabilisation (Lee et al., 2006b).

1.10.4 p53 and neuronal apoptosis

Degeneration and death of specific populations of neurones has been implicated in mediating the symptoms associated with conditions such as, Parkinson's disease (PD), Alzheimer's disease (AD), ischaemic stroke, traumatic brain injury and amyotrophic lateral sclerosis (ALS). Evidence for a pivotal function of p53 in neuronal death associated with neurodegenerative diseases, such as those above, is provided by data from *in vitro* and *in vivo* models which show increased p53 levels in dying neurones (Morrison *et al.*, 2003). Due to their post-mitotic state most neurones have a limited repair and self-renewal capacity, hence p53 activation in neurones is associated with an apoptotic rather than a repair and recovery fate (Raffray and Cohen, 2001). In many types of post-mitotic neurones, p53 may mediate apoptosis induced by a range of insults including DNA damage, hypoxia, withdrawal of trophic support, hypoglycaemia and oxidative stress (Morrison *et al.*, 2003; Johansson *et al.*, 2003b). *In vivo* studies have demonstrated that treatment with NMDA, the NMDA agonist quinolinic acid, and kanic acid all induce p53-dependant excitotoxic neuronal death (Li *et al.*, 2002; Qin *et al.*, 1999; Nakai *et al.*, 2000). In addition, we have shown that p53 is activated in neurones exposed to Aβ and Δ^9-THC *in vitro* (Fogarty *et al.*, 2003; Downer *et al.*, 2007a). Furthermore, increased p53 immunoreactivity is associated with many *in vivo* animal models of epilepsy, AD and PD (Tan *et al.*, 2002; De La Monte *et al.*, 2007; Bretaud *et al.*, 2007). In addition, the inhibition of p53 *e.g.*, by pharmacological inhibition or down regulation by siRNA or antisense can protect neurones against the excitotoxic insults, which is a common feature of neurodegenerative disease (Culmsee *et al.*, 2001; Lakkaraju *et al.*, 2001; Xiang *et al.*, 1996). Pifithrin-α, a pharmacological inhibitor of p53 is neuroprotective in both progressive neuronal death and excitotoxic neuronal death associated with chronic neurodegenerative diseases and acute brain insults respectively (Duan *et al.*, 2002; Leker *et al.*, 2004). Work carried out by Culmsee (2003) and Zhu (2002) and their co-workers, have demonstrated in models of stroke and brain trauma, that pifithrin-α treatment preserves brain function in a

clinically relevant therapeutic time window *i.e.,* post insult. Additionally depletion of the p53 protein with siRNA prevents apoptosis induced by Δ^9-THC in cultured cortical neurones (Downer *et al.*, 2007a). Surprisingly, in addition to its role in neuronal apoptosis, p53 is also involved in neurite outgrowth and axonal regeneration, a process which involves the post translational acetylation of p53 at lysine 320 and transactivation of Coronin 1b and Rab 13 genes which are proteins required for neurite outgrowth (Di Giovanni *et al.*, 2006). Furthermore, p53 induced by MEKK-JNK signalling is essential for developmental neurone death (Aloyz *et al.*, 1998). Overall, p53 is modulated in a number of neurodegenerative diseases and in relevant cell culture and animal models of neuronal death and neurodegeneration, thus the inhibition of p53 represents a novel therapeutic strategy with substantial reasoning.

1.13 Cannabinoids and neural cell fate

The ability of cannabinoids to promote both cell death and cell survival in parallel is one of the most intriguing aspects of cannabinoid action (Sarne and Keren, 2004). This 'dualism of action' makes cannabinoids ideal candidate drugs for the treatment of brain tumours and the treatment of neurodegenerative diseases. There is a large volume of evidence, which indicate that cannabinoids may protect neurones from toxic insults both *in vitro* and *in vivo* (Marsicano *et al.*, 2002; Iuvone *et al.*, 2004; Panikashvili *et al.*, 2001; Van Der Stelt *et al.*, 2001). There is mounting *in vitro* and *in vivo* data to suggest that cannabinoids have neuroprotective effects following brain injury (Mechoulam *et al.*, 2002). Indeed, the formation of endocannabinoids is enhanced after brain injury and there is evidence that these compounds reduce the secondary damage incurred after the initial injury (Hansen *et al.*, 2001; Panikashvili *et al.*, 2001). However, cannabinoid-induced neurotoxicity, through the activation of pro-apoptotic signalling mechanisms, has been reported in primary neurones and in transformed neural cells (Chan *et al.*, 1998; Campbell, 2001; Downer *et al.,* 2007a, 2003, 2001; Sánchez *et al.*, 1998; Jacobsson *et al.*, 2001; Maccarrone *et al.*, 2000; Sarker and Maruyama, 2003).

1.13.1 Cannabinoids and neuroprotection

The majority of neurodegenerative diseases are associated with excessive glutamatergic transmission, oxidative stress and/or inflammatory changes that lead to activation of the apoptotic cascade and subsequent neuronal demise. Cannabinoids confer neuroprotection both *in vivo* and *in vitro* and in a number of paradigms of neurodegeneration (Guzmán *et al.*, 2002). The molecular mechanisms underlying this neuroprotection involve both CB receptor-dependent and receptor-independent events. In addition, cannabinoids reduce excessive glutamatergic synaptic activity and induce anti-oxidant effects during neuronal stress. Endogenous cannabinoids can protect cultured cortical neurones from oxygen and glucose deprivation independently of CB_1 and CB_2 receptor activation (Nagayama *et al.*, 1999; Sinor *et al.*, 2000). Δ^9-THC and cannabidiol can both decrease glutamate toxicity in rat cortical neuronal cultures in a manner that is not blocked by CB_1 receptor antagonists (Hampson *et al.*, 1998b). Cannabidiol, as a result of its anti-oxidative and anti-apoptotic properties, also protects cultured rat PC12 cells from toxic β-amyloid-induced neurotoxicity that is independent of the CB_1 receptor (Iuvone *et al.*, 2004). In contrast, several reports showing cannabinoids to exert their neuroprotective properties *via* the activation of the CB_1 receptor in mouse spinal neurones, cultured hippocampal neurones and primary cerebellar cell cultures (Abood *et al.*, 2001; Shen and Thayer, 1998; Marisicanno *et al.*, 2002). Neuronal damage can increase the production of endocannabinoids and cells lacking CB_1 receptors are more vulnerable to damage (Stella *et al.*, 1997; Marsicano *et al.*, 2003). These studies indicate that neural cannabinoid tone influences neuronal survival and suggest that augmentation of the cannabinoid system may offer protection against the deleterious consequences of pathogenic molecules such as Aβ, α-synuclein and other neurotoxic protein aggregates. The dysregulation of intracellular Ca^{2+} homeostasis and excessive activation of the NMDA subtype of glutamate receptor, leading to excitotoxicity, are features of neurodegeneration (Smith *et al.*, 2005; Sonkusare *et al.*, 2005). Thus, strategies that reduce Ca^{2+} influx and limit excitotoxicity may confer neuroprotection. The non-psychotrophic cannabinoid, HU-211 can act as a stereoselective inhibitor of the NMDA receptor and is reported to protect rat forebrain and cortical neuronal cultures from NMDA-induced neurotoxicity *via* its negative

affects on the receptor (Nadler *et al.*, 1993; Eshhar *et al.*, 1993). Cannabinoids have also shown neuroprotective affects during *in vivo* experiments involving the induction of brain damage as a result of ischaemia, injection of ouabain, closed head injury and the focal administration of ceramide (Nagayama *et al.*, 1999; van der Stelt *et al.*, 2001; Panikashvili *et al.*, 2001; Gómez del Pulgar *et al.*, 2002). A variety of mechanisms have been suggested to be responsible for the neuroprotective properties of cannabinoids *e.g.*, scavenging of ROS species, inhibition of caspase-3 processing and inhibition of voltage sensitive Ca^{2+} channels, which prevents ca^{2+} overload in the cell (Hampson *et al.*, 1998b; Marisicanno *et al.*, 2002; Iuvone *et al.*, 2004; Shen and Thayer, 1998). Taken together, these experimental findings suggest that cannabinoids may have potential therapeutic value to reverse cellular changes that contribute to neurodegeneration and also to promote brain repair. Cannabinoids are also capable of increasing BDNF to confer protection against excitotoxicity (Khaspekov *et al.*, 2004). In non-neuronal cells the induction of nerve growth factor is also facilitated by cannabinoids, acting through the PI3K/PKB pathway and activation of the CB_1 receptor by the endocannabinoid, 2-AG, can also couple to an axonal growth response, whilst CB_1 receptor antagonists inhibit axonal growth (Sanchez *et al.*, 2003a; Williams *et al.*, 2003).

Another exciting mechanism that could account for the ability of cannabinoids to confer neuroprotection may be related to their regulation of neurogenesis, which can take place in the dentate gyrus of the hippocampus and the sub ventricular zone (Grote and Hannan, 2007; Galve-Roperh *et al.*, 2007). Adult neurogenesis is defective in mice lacking CB_1 receptors and the synthetic cannabinoid, WIN 55212-2, stimulates adult neurogenesis by opposing the anti-neurogenic effect of nitric oxide (NO; Jin *et al.*, 2004; Kim *et al.*, 2006). Also the CB_1 agonist HU-210 has anxiolytic and antidepressant effects, which may be a functional consequence of enhanced neurogenesis (Jiang *et al.*, 2005). CB_2 receptor activation also stimulates neural progenitor proliferation *in vitro* and *in vivo* and targeting neurogenesis *via* the CB_2 receptor would avoid undesired psychoactive side effects (Palazuelos *et al.*, 2006). CB_2 receptors have been implicated in the control of neural survival and are up regulated in inflamed tissue *e.g.*, on the active microglia present in those brain regions where senile plaques are present in AD

brains (Fernandez-Ruiz *et al.*, 2007; Benito *et al.*, 2003; Ramirez *et al.*, 2005). The up regulation of CB_2 in such pathological situations may be an attempt to reduce neuroinflammation since CB_2 receptor activation *in vitro* reduces the microglial production of pro-inflammatory molecules (Facchinetti *et al.*, 2003). Such control in the production of inflammatory mediators may be due to a direct impact on activity of transcription factors, such as NF-KB (Panikashvili *et al.*, 2005; Esposito *et al.*, 2006). Thus, the neuroprotective mechanisms of cannabinoids are likely to include a down regulation in activity of the transcription factors that are pertinent to induction of the pro-inflammatory cytokines that serve as key players in neurodegenerative disease, whilst also stimulating the production of anti-inflammatory species such as IL-1ra (Molina-Holgado *et al.*, 2003). The manipulation of such inflammatory pathways may be exploited for the treatment of neurodegenerative disease such as AD. CB_2 agonists do offer the advantage of being devoid of psychoactivity, however it is important to recognise that they may have other side effects such as immune suppression, which would be undesirable in an elderly population (Pertwee, 2005).

It is also worth considering how the aforementioned properties of cannabinoids may be beneficial in ameliorating the symptoms of other diseases in which neuroinflammation, oxidative stress and neurodegeneration are key features, such as MS and Parkinson's disease. Benito *et al.,* (2007) have reported that components of the cannabinoid system are upregulated in MS plaques, suggesting that endocannabinoids either have a role in the pathogenesis of MS or may be up regulated as a consequence of the pathology. MS is associated with excitotoxicity and neuroinflammation and these represent features of the disease that cannabinoids may be able to circumvent (Pitt *et al.*, 2000; Smith *et al.*, 2000; Ziemssen, 2005). In encephalomyelitis virus-induced demyelinating disease, an animal model of MS, the mixed cannabinoid agonist HU-210 reduces axonal damage and improves motor function as a consequence of a concomitant activation of the CB_1 receptor in neurones and CB_2 in astrocytes (Docagne *et al.*, 2007). Other studies in animal models of MS have demonstrated a role for the CB_2 receptor in enhancing T cell apoptosis and suppressing microglial activation, whilst the CB_1 receptor is associated with neuroprotection (Sanchez *et al.*, 2006; Ehrhart *et al.*, 2005; Pryce *et al*, 2007; Mestre *et al.*, 2006). Such neuroprotective and anti-oxidant

properties of cannabinoids also underlie their ability to reverse the motor deficits in animal models of Parkinson's disease and lend support of a potential role for cannabinoid-based therapies to mitigate the symptoms of a range of neurodegenerative conditions (Lastres-Becker *et al.*, 2005; Garcia-Arencibia *et al.*, 2007).

Thus, the neuroprotective effects of cannabinoids may involve short-term adaptation to neuronal stress, such as limiting excitotoxicity as well as longer-term adaptations, such as enhancing neurogenesis. Whether these effects will be beneficial in the treatment of neurodegeneration in the future is an exciting topic that undoubtedly warrants further investigation.

1.13.2 Cannabinoids and neurotoxicity

Although the bulk of experimental evidence indicates that cannabinoids may protect neurones from toxic insults, there is increasing evidence from *in vitro* and *in vivo* studies involving animals and humans that suggests cannabinoids can also have a more sinister affect. The following section describes experiments, which demonstrate the neurotoxic profile of cannabinoids and highlights the complexities associated with cannabinoids and the control of survival/death signals in brain cells.

Δ^9-THC (1 μM) induces apoptosis independent of the CB_1 receptor in a C6.9 subclone glioma cell line as determined by DNA fragmentation and loss of plasma membrane asymmetry (Sánchez *et al.*, 1998). Galve-Roperh *et al.*, (2000) have shown this effect in Wistar rats with malignant gliomas, this effect involves sustained ceramide production and ERK activation. Δ^9-THC (1 - 10 μM) induces apoptosis in primary hippocampal neurones in a dose dependant manner and involves increased intracellular Ca^+, generation of free radicals and DNA fragmentation (Chan *et al.*, 1998). Furthermore, Δ^9-THC (5 μM) induces apoptosis in cortical neurones via CB_1 involving translocation of cytochrome-c to the cytosol and activation of caspase-3 as well as activation of JNK_1 and p53 stress activated proteins (Campbell, 2001; Downer *et al.*, 2007a, 2003, 2001). AEA (0.1 - 10 μM) induces apoptotic body formation and DNA fragmentation in CHP100 neuroblastoma cells *via* $TRPV_1$ (Maccarrone *et al.*, 2000). Sarker and colleagues (2000) have also shown AEA (10 μM) to induce apoptosis in PC12 cells *via* superoxide production and caspase-3 activity. Blázquez and co-workers

(2004) have also shown cytostatic effects in gliomas, involving the SR 141716A-sensitive inhibition of pro-tumour angiogenesis vascular endothelial growth factor (VEGF) signalling, after *in vivo* and *in vitro* cannabinoid administration. AEA (10 - 50 μM) induced apoptosis in primary neuronal cultures *via* calpain activation, which was independent of CB_1, CB_2, $TRPV_1$ and NMDA receptors (Movsesyan *et al.*, 2004). Unlike AEA, 2-AG does not seem to induce neuronal cell death (Maccarone and Finazzi-Agro, 2003). However, one exception has been reported in rat glioma C6 cells, where the antiproliferative effect of 2-AG was comparable to that of AEA (Jaccobsson *et al.*, 2001). Kim *et al.*, (2005) have shown that there is functional cross talk between the $TRPV_1$ and CB_1 receptors, at the low micro molar range, in AEA and HU-210 induced degeneration of mesencephalic dopaminergic neurones both *in vivo* and *in vitro*.

As mentioned earlier (section 1.1) cannabinoids cause alterations in cognitive processes, specifically in learning and memory. These memory effects are thought to be due to alterations in synaptic functioning. Indeed, exogenous and endogenous cannabinoids have been shown to influence long term potentiation (LTP) *via* depolarisation-induced suppression of inhibition (DSI) and depolarisation-induced suppression of excitation (DSE) which in turn effects the release of GABA and glutamate (Wilson and Nicoll, 2001 and Diana and Marty, 2004). However, cell death in the CNS is also known to cause significant cognitive dysfunction, it is therefore conceivable that the effects of cannabis on cognitive processes are attributable to cannabinoid-induced neurotoxicity (Raffray and Cohen, 1997; Morrison and Hof, 2007). Indeed, chronic exposure to Δ^9-THC produces morphological changes in brain structures that are indicative of toxicity, such as decreased mean neuronal volume and synaptic density in the hippocampal CA3 region, dendritic degradation in CA1 of the hippocampus and retraction from pyramidal cells (Scallet *et al.*, 1987, 1991; Lawston *et al.*, 2000). Furthermore, some authors have suggested exposure to ultra-low levels of Δ^9-THC (0.001 mg/Kg) produces cognitive impairment (Sarne and Keren, 2004). This hypothesis has recently been demonstrated *in vivo* and has been attributed to the opposing effects that low and high doses of Δ^9-THC has on Ca^{2+} entry to the cell; high doses inducing the inhibition of Ca^{2+} entry, therefore providing neuroprotection and low

doses potentiating the entry of Ca^{2+} into cells consequently leading to neurotoxicity (Tselnicker *et al.*, 2007). Conversely, no histopathological alterations in the brain were found in rats treated orally with up to 50 mg/Kg/day Δ^9-THC for 2 years and in rats treated with 1 mg/Kg/day Δ^9-THC intracranially for 7 days (Chan *et al.*, 1996; Galve-Roperh *et al.*, 2000).

Recently, functional magnetic resonance imaging (fMRI) has demonstrated a reduction in white matter in the left parietal lobe and reduced grey matter in the parahippocampal gyrus in a group of heavy cannabis users (Matochik *et al.*, 2005). Reductions in frontal white matter have also been reported in a group of poly-substance drug abusers (Schlaepfer *et al.*, 2006). These studies did not identify any mechanisms responsible for the structural changes, however, neurotoxicity was alluded to *e.g.*, inhibition of myelination. These studies were carried out on heavy cannabis and poly-substance abusers and so must be interpreted with caution since a fMRI study has shown that frequent users of cannabis can compensate for subtle cognitive deficits by using larger or additional brain areas which questions the physiological relevance of the changes in brain parameters observed in other studies (Jager *et al.*, 2006; Kanayama *et al.*, 2004). Furthermore, Tzilos and colleagues (2005) have found that cannabis does not cause any changes in hippocampal morphology in a group of long-term cannabis users.

Overall, the neurotoxic and neuroprotective effects of cannabinoids are likely to depend on a variety of influences such as the nature of the insult, the cell type, the stage of development and the particular type of cannabinoid under investigation amongst many other influences. Whilst the effect of chronic cannabis use on neuronal viability remains to be fully resolved, it is evident that both synthetic and endogenous cannabinoids have the proclivity to confer neuroprotection against a range of insults that are pertinent in excitoxicity, neuroinflammation, oxidative damage and other pathology associated with neurodegenerative diseases, such as Alzheimer's, Parkinsons and Multiple sclerosis. Future therapeutic strategies to ameliorate the symptoms of neurodegenerative diseases may target the endocannabinoid system, hence the possibility of cannabinoids possessing neurotoxic properties requires an urgent review of these opposing properties.

1.14 Aims

The main aims of this thesis were:

- To delineate the biochemical pathways induced by Δ^9-THC in cerebral cortical neurones which results in the demise of neurones.
- To further examine the role of p53 and its interacting proteins in the Δ^9-THC-signalling cascade in cultured cortical neurones.
- To establish whether Δ^9-THC impacts on the lysosomal system and if so to elucidate the underlying mechanisms by which lysosomes participate in the apoptotic pathway induced by Δ^9-THC.
- To investigate the proclivity of the endocannabinoids, anandamide and 2-arachidonoylglycerol to induce apoptosis in cultured cortical neurones.
- To ascertain if the *in vivo* apoptotic actions of Δ^9-THC on the rat cerebral cortex are reliant on age.

Chapter 2

Materials and methods

2.1 Cell culture

2.1.1 Aseptic technique

Successful cell culture relies on the maintenance of a sterile work environment and the practice of good anti-microbial technique. These principles prevent microbial infection of areas that are in contact with the cell culture. The following aseptic procedures were strictly adhered to for all cell culture procedures.

2.1.2 Sterilisation of glassware, plastics and dissection instruments

All glassware, pipette tips, double de-ionised water (ddH_2O) and microfuge tubes (Sarstedt, Leister, UK) were sealed with autoclave tape (Sigma-Aldrich, Dorset, UK), and autoclaved at 145°C for 30 minutes with 30 psi pressure (Systec 3850 MIV, Unitech, Dublin, Ireland) before being doused in 70% alcohol and placed in a laminar flow hood (Astec-Microflow laminar flow workstation, Florida, USA). Prior to use, all dissection instruments were sonicated (VWR International) for 5 minutes, and oven baked (Sanyo-Gallenkamp Hotbox Oven, Model #OHG050, Loughborough, UK) at 200°C overnight, to ensure sterility.

2.1.3 Sterility of work environment

All cell culture work was carried out in a laminar flow hood (Astec-Microflow laminar flow workstation, Florida, USA). The sterile environment in the flow hood is maintained by the downward flow of air filtered through HEPA (high efficiency particle air) filters at the top of the flow hood. This constant airflow creates a barrier in front of the open portion of the hood, thus preventing the entry of external airborne contaminants into the laminar flow hood. These filters were allowed to run for a minimum of 15 minutes prior to starting any cell manipulations. Before use, the laminar flow hood was doused in 70% ethanol, and accessible areas were wiped down. Disposable latex powder-free gloves (sprayed with 70% ethanol) were worn at all times, and changed at regular intervals to avoid contamination. Whilst cell manipulations were carried out in the laminar flow hood, movements were kept to a

minimum in order to prevent fluctuations in the protective air barrier at the front of the hood. After each day the hood was exposed to ultraviolet (UV) light overnight. All bench areas were wiped down with 70% ethanol before and after any cell manipulations were performed. The entire culture room suite was thoroughly cleaned every week, and the whole room exposed to an overhead source of UV light, for a minimum of 24 hours.

2.1.4 Reagents and medium formulation

All supplements (Glutamax, Invitrogen, Paisley, UK) were sterile filtered into plain, unsupplemented media, using 0.2 μm cellulose acetate syringe filters (Pall Corporation, Michigan, USA) attached to a sterile syringe (B.Braun Medical Ltd., Melsungen, Germany). Neurobasal medium (NBM; Invitrogen, Paisley, UK) supplemented with heat inactivated horse serum (10%), penicillin (100 U/ml), streptomycin (100 U/ml) and glutamine (2 mM) was only used in the laminar flow hood, to ensure sterility. Complete supplemented NBM was used to extinction or was disposed of after 2 weeks sterile storage at 4°C.

2.1.5 Waste disposal

All hazardous material (lab plastic, sharps, gloves and carcasses) was separated into appropriate UN-approved primary packaging, and sent to the hazardous material facility (Trinity College Dublin) where it was disposed of in accordance with Irish and EU legislative requirements.

2.2 Primary culture of cerebral cortical neurones

The culture of primary cortical neurones is an *in vitro* technique, which requires dissection of the brain, removal of the cerebral cortex and dissociation of the cortical tissue to obtain a population of cerebral cortical neurones. Primary neuronal cell cultures are regarded as superior to cell line models as they represent a non-transformed unaltered genotype and hence have a more faithful phenotype.

2.2.1 Preparation of sterile coverslips

To ensure sterility, 13 mm diameter glass coverslips (VWR International, Leuven, Belgium) were soaked in 70% ethanol, with constant rotation at 4°C, for 24 hours, followed by an overnight exposure to UV light in the laminar flow hood. On the day of neuronal preparation the sterilized coverslips were coated with poly-L-lysine (60 μg/ml in sterile ddH_2O; Sigma-Aldrich, Dorset UK) in a final volume of 25 ml, for 1 hour at 37°C to provide a suitable surface to which dissociated neurones would adhere. Coated coverslips were then air-dried in the laminar flow hood and placed in sterile 24-well plates (Sarstedt, Leister, UK) until required for use.

2.2.2 Animals

Postnatal 1-day old Wistar rats (specified-pathogen free) were born at the BioResources Unit (Trinity College, Dublin 2, Ireland). Parent animals were maintained under a 12 hour light/dark cycle at an ambient temperature of 22 - 23°C. On day of parturition, pups were removed from the litter cage, and placed in a ventilated box containing suitable clean bedding. The animals were then taken to the Trinity College Institute of Neuroscience, and kept in the culture room suite until dissection.

2.2.3 Dissection

Primary cerebral cortical neurones were established from postnatal 1-day old Wistar rats. Dissection of one rat brain yielded a preparation of a single 24-well plate. Rats were decapitated using a large sterile scissors, and the skull exposed by cutting the skin in a straight line from the neck to the tip of the nose with a smaller sterile scissors. The skull was removed by cutting on either side of it with a small sterile scissors, ensuring that the inside point of the scissors remained against the skull at all times. A sterile forceps was used to lift back the skull and expose the brain. The cerebral cortices were removed with a curved forceps and placed in a sterile Petri dish (Sarstedt, Leister, UK) containing sterile Phosphate Buffered Saline (PBS; 100 mM NaCl, 80 mM Na_2HPO_4, 20 mM NaH_2PO_4, pH 7.4). Any meninges were carefully removed using a fine forceps, and cortices were chopped into 3 - 4 mm pieces with a sterile disposable scalpel (Schwann-Mann, Sheffield, UK).

2.2.4 Dissociation procedure

Cortical tissue was incubated with 2 ml sterile PBS containing trypsin (0.3% (w/v); Sigma-Aldrich, Dorset, UK) in a humidified chamber (5% CO_2; 95% air) for 25 minutes at 37°C. Trypsin digestion of connective tissue was followed by trituration (x5) of the dissociated neurones in sterile PBS containing soyabean trypsin inhibitor (0.1% (w/v); Sigma-Aldrich, Dorset, UK), DNAse (0.2 mg/ml; Sigma-Aldrich, Dorset, UK) and $MgSO_4$ (0.1 M; Sigma-Aldrich, Dorset, UK). The cell suspension was gently filtered through a sterile 40 μm nylon mesh filter (Becton Dickonson Labware Europe, France) to remove tissue clumps, and centrifuged (Model 2-16K, Sigma-Aldrich, Dorset, UK) at 2 000 x g for 3 minutes at 20°C. The pellet was resuspended in NBM (Invitrogen, Paisley, UK), supplemented with heat inactivated horse serum (10%; Gibco BRL, Maryland, USA) penicillin (100 U/ml; Gibco BRL, Maryland, USA), streptomycin (100 U/ml; Gibco BRL, Maryland, USA) and glutamine (2 mM; Glutamax, Gibco BRL, Maryland, USA). B27 (1% (v/v); Gibco BRL, Maryland, USA) was also added to NBM for its neuroprotective antioxidant properties (Huang *et al.*, 2000).

2.2.5 Plating of resuspended neurones

Resuspended neurones in supplemented NBM+B27 were placed on the centre of each coverslip, at a density of 0.25 x 10^6, and allowed to adhere for 2 hours in a humidified incubator containing 5% CO_2; 95% air at 37°C (Binder CO_2 incubator, series CB, Binder GmbH, Tuttlingen, Germany). Cells were then flooded with 400 μl of pre-warmed supplemented NBM+B27. Cells were incubated for 3 days *in vitro*. Media was replaced with supplemented NBM containing 5 ng/ml cytosine-arabino-furanoside (ARA-C; Sigma-Aldrich, Dorset, UK) to prevent proliferation of non-neuronal cells and maintain the purity of the cortical neuronal culture. This ensured that microglia and astrocyte contamination was less than 5% in culture preparations. Media containing ARA-C was removed after 24 hours and replaced with supplemented NBM (400 μl/well). Cells were grown in culture for up to 5 days post ARA-C treatment, with media replaced every 3 days depending on treatment conditions. Cultured neurones were monitored daily by light microscopy (Nikon TMS, Nikon Instech Co., Ltd.,

Kanagawa, Japan) to ensure cultures looked healthy, and lacked bacterial or fungal infection. Sample images of cultured cortical neurones at the (i) initial stage of plating, (ii) 2 days *in vitro* and (iii) 4 days *in vitro* are depicted in Figure 2.1.

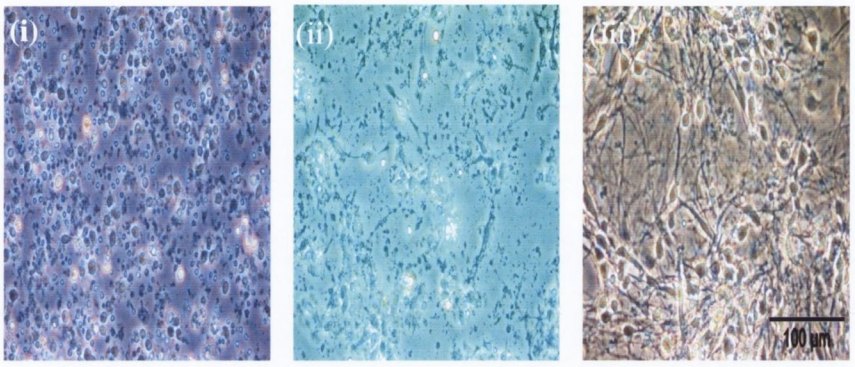

Figure 2.1 Time-dependent changes in cultured neuronal morphology.

(i) Neurones display rounded cell soma and an absence of neurites after initial plating. After 4 days *in vitro* (iii), cells have developed pear-shaped cell bodies and an extensive neurite network, representative of a mature neurone. Scale bar is 100 μm.

2.2.6 Culturing cortical neurones for Acridine Orange uptake experiments

Cortical neurones were cultured as in section 2.2.2 - 2.2.5 with the following exceptions. Cells were plated at a cell density of 2.1 x 10^5 on sterile, poly-L-lysine coated glass-bottomed chambers (Nunc Lab Tek™, Biosciences, Erembodegem, Belgium).

2.3 Cell treatments

2.3.1 Δ^9-Tetrahydrocannabinol (Δ^9-THC)

Δ^9-THC was obtained from Sigma-Aldrich Company Ltd., (Dorset, UK) and held under licence (Misuse of drugs act 1977, 1984, Department of Health and Children Ireland, licence number 151229-1-2004) in the Trinity College Institute of Neuroscience. The drug dissolved in ethanol was stored securely at -20°C as an 80 mM stock solution. For culture use, the stock drug was diluted to the final concentration in pre-warmed supplemented NBM, and 0.006% ethanol (v/v) was used as a vehicle control.

2.3.2 Anandamide (AEA)

Arachidonic acid N-(hydroxyethyl)amide (anandamide; AEA) was obtained from Sigma-Aldrich Company Ltd., (Dorset, UK). The drug was dissolved in methanol and stored as a 10 mM stock solution at -20°C. For culture use, the stock drug was diluted to final concentration in pre-warmed NBM, and 0.02% methanol (v/v) was used as a vehicle control.

2.3.3 2-Arachidonoylglycerol (2-AG)

Arachidonoylglycerol (2-AG) was purchased from Sigma-Aldrich Company Ltd., (Dorset, UK). The drug was dissolved in acetonitrile solution and stored as a 20 mM stock solution at -20°C. For culture use, the stock drug was diluted to final concentration in pre-warmed NBM, and 0.02% acetonitrile (v/v) was used as a vehicle control.

2.3.4 CB_1 cannabinoid receptor inhibitor

The selective CB_1 receptor antagonist, N-piperidin-1-yl)-5-(4-idophenyl)-1-(2,4 dichlorophenyl)-4-methyl-l H-pyrazole-3-carboxamide (AM 251; Gately *et al.*, 1996; Tocris Cookson Ltd., Bristol, UK) was stored as a 10 mM stock solution in dimethylsulfoxide (DMSO; Sigma-Aldrich, Dorset, UK), and diluted to a final

concentration of 10 μM in warm culture media for addition-to cultures. Neurones were pre-incubated with AM 251 for 30 minutes before treating. AM 251 is a structural analogue of SR 141716A, a compound considered to be the prototypical CB_1 antagonist (Rinaldi-Carmona *et al.*, 1994). It is a selective, high-affinity inhibitor, and has a 306-fold selectivity for the CB_1 over the CB_2 receptor (Lan *et al.*, 1999).

2.3.5 p53 inhibitor

The p53 inhibitor, pifithrin-α (pif-α; Calbiochem International, Darmstadt, Germany) was made up as a stock solution of 1 mM in DMSO, and was used at a final concentration of 100 nM. Cells were exposed to the p53 inhibitor for 60 minutes prior to drug treatment. This inhibitor is a cell permeable, highly lipophillic molecule that efficiently inhibits the transactivation of p53-responsive genes and reversibly blocks p53-mediated apoptosis (Culmsee *et al.*, 2001).

2.3.6 Cathepsin-L inhibitor

Cathepsin-L inhibitor, 1-Z-FF-FMK (CLi; Calbiochem, Nottingham, UK) was made up as a stock solution of 20 mM stock solution in DMSO, and was diluted in pre-warmed NBM to a final concentration of 10 μM. Cells were exposed to CLi for 30 minutes prior to drug treatment. This inhibitor is a cell-permeable, potent and irreversible inhibitor of cathepsin-L (Ravanko *et al.*, 2004).

2.3.7 Cathepsin-D inhibitor

The cathepsin-D inhibitor octapeptide, H-Gly-Glu-Gly-Phe-Leu-Gly-D-Phe-Leu-OH (CDi; Bachem, Merseyside, UK) is a competitive inhibitor of cathepsin-D (Gubensek *al.*, 1976). CDi was stored at -20°C as a 5 mM stock solution in DMSO, and used at a final concentration of 10 μM. Cells were pre-treated with CDi for 30 minutes before cannabinoid drug treatment.

2.3.8 JNK1 inhibitor

The JNK1 inhibitor, D-JNK-1, (JNKi) was obtained from Alexis Biochemicals (Lausanne, Switzerland) as a 1 mM stock dissolved in sterile PBS and was stored at -20°C. The stock was diluted in pre-warmed NBM to a final concentration of 10 μM. Cells were exposed to JNKi for 30 minutes prior to drug treatment. JNKi is a protease resistant peptide, which inhibits the interaction between JNK1, and its substrates resulting in a JNK1 knock out phenotype. The D-stereoisomer is preferable over the L-stereoisomer in neuronal applications due to its high resistance to proteolytic degradation (Bonny *et al.*, 2001; Borsello *et al.*, 2003).

2.3.9 VR_1 vanilloid receptor antagonist

The VR_1 antagonist, Capsazepine (CZP; *N*-[2-(4-Chlorophenyl)ethyl]-1,3,4,5-tetrahydro-7,8-dihydroxy-2*H*-2-benzazepine-2-carbothioamide; Tocris Cookson Ltd., Bristol, UK) was made up as a stock solution of 10 mM in DMSO, and stored at -20°C. The stock was diluted in pre-warmed NBM to a final concentration of 10 μM. Cells were exposed to CZP for 30 minutes prior to drug treatment. CZP is a selective vanilloid receptor antagonist (Dickenson and Dray, 1991).

2.3.10 SyK inhibitor

SyK inhibitor, Sulfonamide (SyKi; Calbiochem International, Darmstadt, Germany) was made up as a 5 μM stock solution in DMSO and stored at -20°C. The stock was diluted in pre-warmed NBM to a final concentration of 50 nM. Cells were exposed to SyKi for 30 minutes prior to drug treatment. SyK is a potent cell-permeable inhibitor of SyK (Lai, *et al.*, 2003).

2.3.11 *In vitro model* of excitoxicity - treatment with glutamate

Exposure to glutamate at micro molar concentrations has been shown to induce excitoxicity culminating in neuronal apoptosis (Bösel *et al.*, 2005; Almeida *et al.*, 2005). Cultured cortical neurones were exposed to 50 μM L-glutamate (monosodium salt; dissolved in ddH_2O; Sigma-Aldrich, Dorset, UK) in supplemented NBM for 1 hour. 2-AG (0.01 μM) was added either 1 hour before glutamate treatment (pre-),

during glutamate treatment (co-) or after glutamate treatment (post-). Control cells were incubated with vehicle (0.02% acetonitrile) alone for 2 hours. Cell viability was assessed following treatment by TUNEL analysis.

2.3.12 *In vivo* drug administration

The following animal experiments were performed under a license granted by the Minister for Health and Children (Ireland) under the Cruelty to Animals Act 1876, incorporating the European Community Directive, 86/609/EC.

All animals (adolescents; 3 months-old, adults; 4 - 9 months-old) used were from an inbred strain of the male Wistar rat obtained from the Bioresources unit, Trinity College Dublin. Animals were housed 4 to a cage under standard laboratory conditions in the Department of Physiology, Trinity College Dublin. An ambient temperature of 20 - 23°C and a 12-hour light/dark cycle was maintained. All animals were assessed for health and well-being on a daily basis, and had free access to water and standard laboratory food (Red Mills, Kilkenny, Ireland). To reduce stress, animals were exposed to frequent non-experimental handling at least 3-days prior to experiments being performed. Neonatal animals (5 - 7 days-old) were brought from the Bioresources unit directly to Trinity College Institute of Neuroscience and experimental procedures were performed immediately.

Animal weights were measured and recorded. An intraperitoneal (i.p.) injection of urethane (1.5 g/Kg; 33% w/v) was used to anaesthetise animals; the absence of a pedal reflex was used to confirm deep anaesthesia. Animals were kept warm whilst awaiting procedures and during the length of the experiment. Anaesthetised rats were injected subcutaneously (s.c.) with 0.9% saline containing 5% ethanol and 5% Cremophor EL (vehicle control, vCon; Sigma-Aldrich, Dorset, UK) or 1 - 30 mg/Kg Δ^9-THC dissolved in 0.9% saline containing 5% ethanol and 5% Cremophor (Sigma-Aldrich, Dorset, UK). To block the CB_1 receptor, an injection of AM 251 (10 mg/Kg i.p.) was given 1-hour prior to vehicle or Δ^9-THC treatment. All animals were treated with Δ^9-THC or vehicle for 2 - 3 hours before being sacrificed by decapitation. After decapitation, the brains were rapidly removed, and dissected on ice into their two hemispheres.

For cryostat sectioning the left hemisphere was covered in OCT compound (R.A. Lamb, Sussex, UK), snap frozen in liquid nitrogen onto cork discs for sectioning and stored at -80°C. Glass slides were coated with subbing solution (0.5% gelatine (w/v), 0.05% chrome alum (w/v; Sigma-Aldrich, Dorset, UK) in dH_2O for 10 seconds at 60°C and allowed to dry overnight at room temperature. This provided a suitable surface to which sections could adhere. On day of the experiment the half brain was equilibrated to -20°C for 20 - 30 minutes. Saggital sections (10 μm) were cut, stained with methylene green for 2 minutes and viewed by light microscopy (Nikon Labophot, Nikon Instech Co., Ltd., Kanagawa, Japan) for detection of the hippocampus. For each animal, 21 sections (10 μm) were cut onto 7 subbed slides (3 sections per slide), allowed to dry for 10 minutes and stored at -20°C until required.

For preparation of slices for freezing the cerebral cortex and hippocampus were dissected from the right hemisphere, and the tissue was chopped bidirectionally to a thickness of 350 μm using a McIlwain tissue chopper (Mickle Laboratory Engineering Co., Surrey, UK), and placed in 4 microfuge tubes containing 1 ml Krebs-calcium (136 mM NaCl, 2.54 mM KCl, 1.18 mM KH_2PO_4, 1.18 mM $MgSO_4.7H_2O$, 16 mM $NaHCO_3$, 10 mM glucose, 2 mM $CaCl_2$, pH 7.4). Slices were allowed to settle and were rinsed twice with Krebs-calcium containing 10% DMSO, and stored at -80°C until required for biochemical analysis.

2.4 Protein quantification

2.4.1 Bradford assay

Protein concentration from *in vitro* cell culture samples was assessed according to the Bradford method (Bradford, 1976). Standards were prepared from a stock solution of 1000 μg/ml bovine serum albumin (BSA; Sigma-Aldrich, Dorset, UK). This stock solution was serially diluted with ddH_2O to prepare a range of standards from 3.125 μg/ml to 1000 μg/ml. A blank of ddH_2O was also included. Standards (10 μl) and samples (10 μl) were plated in triplicate into a 96-well plate (Sarstedt, Wexford, Ireland). Bio-Rad dye reagent concentrate (1:5 dilution in dH_2O, 200 μl; Bio-Rad,

Hertfordshire, UK) was added to standards and samples and incubated for 5 minutes at RT. The absorbance was assessed at 600 nm using a 96/98-well plate reader (EIA Multiwell reader, Sigma-Aldrich, Dorset, UK). The protein concentration of samples was calculated from a regression line plotted (Prism 4) from the absorbencies of the BSA standards.

2.4.2 Bicinchoninic Acid (BCA) assay

Protein concentration from *in vivo* tissue samples was assessed using the BCA™ protein assay kit (Pierce, Leiden, The Netherlands) which was used due to its compatibility with detergents in the lysis buffer used for tissue harvesting and for its broad working range (20 - 2000 μg/ml). Standards were prepared from a stock solution of 2000 μg/ml bovine serum albumin. This stock solution was serially diluted with ddH_2O to prepare a range of standards from 25 μg/ml to 2000 μg/ml. A blank of ddH_2O was also included. Standards (25 μl) and samples (25 μl) were plated into a 96-well plate (Sarstedt, Wexford, Ireland) in triplicate. The BCA assay relies on the detection of the cuprous cation (Cu^{+1}) released during the biuret reaction. The purpled-coloured reaction product is formed by the chelation of two molecules of BCA with one cuprous ion. The absorbance of the reaction product was measured at 570 nm using a 96/98-well plate reader (EIA Multiwell reader, Sigma-Aldrich, Dorset, UK). The protein concentration of samples was calculated from a regression line plotted (Prism 4) from the absorbencies of the BSA standards.

2.5 Sodium Dodecyl Sulphate-Polyacrylamide Gel Electrophoresis (SDS-PAGE)

2.5.1 Preparation of cell culture protein

To analyse expression of protein, neuronal cultures were washed in PBS, and harvested by scraping coverslips in lysis buffer (25 mM HEPES, 5 mM $MgCl_2$, 5 mM dithiothreitol, 5 mM EDTA, 2 mM PMSF, 10 μg/ml leupeptin, 6.25 μg/ml pepstatin, 10

μg/ml aprotinin, pH 7.4) on ice using the rubber insert of a 1 ml syringe (B.Braun Medical Ltd., Melsungen, Germany). Lysates were sonicated (2 seconds) in ice-cold lysis buffer (Soniprep 150, Sanyo Europe Ltd.). The total protein concentration of each sample was determined using the Bradford method (see section 2.4.1). Samples were standardised so that they contained 300 μg/ml total protein. 4X SDS sample buffer (150 mM Tris-HCl pH 7.4, 10% w/v glycerol, 4% w/v SDS, 5% v/v β-mercaptoethanol, 0.002% w/v bromophenol blue) was added to each sample. Samples were boiled for 5 minutes using a heating block (Stuart SBH1300, Carl Stuart, Dublin, Ireland) and were stored at -20°C until required.

2.5.2 Preparation of tissue section protein

To analyse expression of protein, tissue sections were washed in Krebs-calcium before homogenizing in tissue ice-cold lysis buffer (10 mM Tris-HCl pH 7.4, 50 mM NaCl, 10 mM $Na_4P_2O_7.10H_2O$, 50 mM NaF, 1% IGEPAL, 1 mM Na_3VO_4, 1 mM PMSF and protease inhibitor cocktail) using a polytron tissue disruptor (Kinetatica AG, Littau, Switzerland). The total protein concentration of each sample was determined using the BCA assay (see section 2.4.2). Samples were standardised so that they contained 500 μg/ml total protein. 4X SDS sample buffer (150 mM Tris-HCl pH 7.4, 10% w/v glycerol, 4% w/v SDS, 5% v/v β-mercaptoethanol, 0.002% w/v bromophenol blue) was added to each sample. Samples were boiled for 5 minutes using a heating block (Stuart SBH1300, Carl Stuart, Dublin, Ireland) and stored at -20°C until required.

2.5.3 Gel electrophoresis

Polyacrylamide separating gels (1 mm thick), with a monomer concentration of 7.5%, 10% or 12% overlaid with a 4% stacking gel, were cast by setting them between two 10 cm wide glass plates (Sigma-Aldrich, Dorset, UK), which were mounted on an electrophoresis unit (Sigma Techware, Dorset, UK) using spring clamps. The upper and lower reservoirs were flooded with electrode-running buffer (25 mM Tris-base, 200 mM glycine, 0.1% SDS (w/v)). Samples were loaded into the wells and proteins were separated by the application of a 32 mA current to the gel apparatus. Pre-stained molecular weight standards (5 μl; Bio-Rad, Hertfordshire, UK) were used to confirm

the molecular weight of protein bands. The migration of bromophenol blue (Sigma-Aldrich, Dorset, UK) was monitored, and the current was switched off when the dye band reached the bottom of the gel (20 - 30 minutes).

2.5.4 Semi-dry electrophoretic blotting of proteins

The gel was removed from the apparatus and placed on top of a sheet of nitrocellulose blotting paper (0.45 μm pore size; Sigma-Aldrich, Dorset, UK), which had been cut to the approximate size of the gel and soaked in ice-cold transfer buffer (25 mM Tris-base pH8.3, 192 mM glycine, 20% methanol (v/v), 0.05% SDS (w/v)). A sandwich was made by placing one piece of filter paper (Standard grade No. 3, Whatman, Kent, UK) on top of the gel and one piece beneath the nitrocellulose paper. This sandwich was soaked in transfer buffer and placed on the platinum-coated titanium electrode (anode) of a semi-dry blotter (Sigma-Aldrich, Dorset, UK). The lid of the blotter (stainless steal cathode) was moistened with transfer buffer, placed on top of the sandwich and sealed. The uncovered portion of the anode was shielded with a mylar cut-out (Sigma-Aldrich, Dorset, UK), ensuring that all applied current passed through the sandwich. A constant current of 225 mA was applied for 75 minutes.

2.6 Western immunoblotting

The following describes the general protocol used to identify proteins of interest, which was carried out directly following transfer of proteins to the nitrocellulose membrane. The specific details for every protein assessed by western immunoblot in this thesis are presented in table 2.1.

2.6.1 General protocol for western immunoblot

The nitrocellulose blotting paper was blocked for non-specific antibody binding and this was washed off (wash 1) with tris-buffered saline (TBS; 20 mM Tris-HCl pH 7.8, 150 mM NaCl) containing 0.05% (v/v) Tween (TBS-T). The membrane was incubated with a primary antibody raised against the appropriate protein. The primary

antibody was washed off (wash 2) with TBS-T and incubated with a secondary antibody conjugated to horseradish peroxidase (HRP; Sigma-Aldrich, Dorset, UK). The secondary antibody was washed off (wash 3) TBS-T and the membrane was incubated with a chemiluminescent detection solution (Supersignal (s/s) Ultra, Pierce, Leiden, The Netherlands). The membrane was then exposed to 5 x 7 inch photographic film (Hyperfilm®; Amersham, Buckinghamshire, UK) and developed using an Agfa film processor (Agfa-Gevart Group, Dublin, Ireland).

2.6.2 β actin expression

Following western immunoblotting, the membrane was stripped with antibody-stripping solution (1:10 dilution in dH_2O; Reblot Plus Strong antibody stripping solution; Chemicon, California, USA) and re-probed for total β actin expression to confirm equal loading of protein. The protocol outlined in section 2.6 was followed using the specific parameters for the β actin protein that are outlined in table 2.1.

2.6.3 Densitometry

In all cases quantification of protein bands exposed on-to photographic film was achieved by densitometric analysis using the GelDoc-It imaging system and Lab works image acquisition and analysis software (UVP Bioimaging systems, Cambridge, UK). In all cases ratios of phosphorylated target protein/target protein or target protein/total β actin were quoted using arbitrary units.

Protein Target (source)	Protein Band size (kDa)	Supplier	Block % in TBS-T	Wash details	Antibody dilution % BSA/milk (w/v) in TBS-T	Developing details
Total-p53 (gt)	53	Santa Cruz Biotech.	5% o/n@4°C	1) 2 x 10 min 2) 3 x 20 min 3) 6 x 10 min	**1^0** 1:500 0.1% BSA **o/n@4°C** **2^0** 1:800 0.1% BSA 1hr@RT	s/s 5 min exp. 1 min
Phosphorylated p53 (ser ^{15}; rbt)	53	Cell signaling tech.	5% o/n@4°C	1) 2 x 10 min 2) 3 x 15 min 3) 6 x 10 min	**1^0** 1:400 0.2% BSAo/n@4°C **2^0** 1:1000 0.2% BSA 1hr@RT	s/s 3 min exp. 3 sec
Total-SyK (rbt)	80	Santa Cruz Biotech.	5% o/n@4°C	1) 2 x 10 min 2) 3 x 15 min 3) 4 x 15 min	**1^0** 1:200 0.1% BSA **o/n@4°C** **2^0** 1:500 0.1% BSA 1hr@RT	s/s 3 min exp. 30 sec
Phosphorylated SyK (tyr ^{323}; rbt)	72	Cell signaling tech.	5% o/n@4°C	1) 3 x 10 min 2) 4 x 15 min 3) 4 x 15 min	**1^0** 1:1000 0.1% BSA o/n@4°C **2^0** 1:1000 0.1% BSA 1hr@RT	s/s 3 min exp. 3 sec
SUMO-1 (rbt)	17	Abcam	5% o/n@4°C	1) 2 x 10 min 2) 4 x 15 min 3) 4 x 15 min	**1^0** 1:500 0.1% BSA **o/n@4°C** **2^0** 1:800 0.1% BSA 1hr@RT	s/s 5 min exp. 30 sec
Mdm2 (rbt)	90	Abcam	5% o/n@4°C	1) 2 x 10 min 2) 4 x 15 min 3) 4 x 15 min	**1^0** 1:200 0.2% milk o/n@4°C **2^0** 1:500 0.2% milk 1hr@RT	s/s 3 min exp. 3 sec
Cathepsin-D (rbt)	~52 (pro) 34 (active)	Calbiochem	5% o/n@4°C	1) 2 x 10 min 2) 4 x 15 min 3) 4 x 15 min	**1^0** 1:500 0.5% milk o/n@4°C **2^0** 1:1000 0.5% milk 1hr@RT	s/s 5 min exp. 1 min
β actin (rbt)	46	Abcam	5% o/n@4°C	1) 2 x 10 min 2) 4 x 15 min 3) 4 x 15 min	**1^0** 1:5000 0.1% BSA o/n@4°C **2^0** 1:1000 0.1% BSA 1hr@RT	s/s 3 min exp. 5 sec

Table 2.1 Western blot protocol details.

2.7 Terminal deoxynucleotidyltransferase-mediated UTP nick end labelling (TUNEL)

To determine apoptotic cell death in neuronal cultures, DNA fragmentation was monitored using TUNEL staining according to the manufacturer's instructions (DeadEnd Colorimetric/Fluorometric Apoptosis Detection System; Promega Corporation, Wisconsin, USA). The use of fluorometric TUNEL was used in some cases where fluorometric determination of DNA fragmentation was deemed necessary. TUNEL staining measures the fragmented DNA of apoptotic cells by catalytically incorporating biotin (for colorimetric) or fluorescein (for fluorometric)-12-dUTP at 3'-OH DNA ends using the Terminal Deoxynucleotidyl Transferase enzyme (TdT). Biotin chains were detected using horseradish-peroxidase-labeled streptavidin (HRP-Streptavidin) followed by detection using hydrogen peroxide and the stable chromogen, diaminobenzidine (DAB). Using this procedure, apoptotic nuclei are stained dark brown when viewed under light microscopy. Fluorescein chains were directly visualised by fluorescence microscopy using appropriate excitation wavelength and filter sets (see Table 2.3).

2.7.1 Colorimetric TUNEL

Following treatment, cells were washed once in ice-cold PBS and fixed with paraformaldehyde (4%; w/v; Sigma Aldrich, Dorset, UK) for 30 minutes at RT. Cells were then washed twice with ice-cold PBS and stored at 4°C until required. Cells were permeabilised with Triton-X100 (0.2%; v/v) for 5 minutes at RT. The permeabilisation solution was washed off for 5 minutes 2 times in PBS, cells were then re-fixed in 4% paraformaldehyde (w/v) for 5 minutes. The cells were incubated in equilibration buffer (200 mM $K(CH_3)_2$ As O_2, 25 mM Tris-HCl, 0.2 mM DTT, 0.25 mg/ml BSA, 2.5 mM $CoCl_2$) for 10 - 15 minutes. A reaction buffer (biotinylated nucleotide mix (10 mM Tris-HCl pH 7.6, 1 mM EDTA), Terminal deoxynucleotidyl Transferase (TdT) enzyme in equilibration buffer) was applied for 60 minutes at 37°C to incorporate biotinylated nucleotides at the 3'-OH ends of fragmented DNA. To stop the reaction, cells were incubated with SCC (0.15 M NaCl, 0.17 M Na $H(C_3H_5\ O(COO)_3)$) for 15 minutes, cells were washed for 5 minutes 3 times in PBS. Endogenous peroxidases were blocked

using 0.3% H_2O_2 (v/v) for 3 minutes (Sigma-Aldrich, Dorset UK). Cells were washed for 5 minutes 3 times in PBS. HRP-labelled streptavidin was bound to the biotinylated nucleotides (1:100 dilution in PBS) for 40 minutes at RT. Apoptotic cells (TUNEL positive) were detected using a DAB solution. This solution stains the nuclei of TUNEL positive cells dark brown after 10 minutes. The cells were washed in several changes of dH_2O, counter-stained with methyl green for 5 minutes, and finally dehydrated from alcohol to xylene. Coverslips were then mounted on-to glass slides using DPX permanent mountant (BDH Laboratory Supplies, Dorset, UK). The neurones were viewed under light microscopy (Nikon Labophot, Nikon Instech Co., Ltd., Kanagawa, Japan) at x40 magnification. Cells displaying TUNEL positive nuclei were counted and expressed as a percentage of the total number of cells examined (>500 cells/coverslip).

2.7.2 Fluorometric TUNEL

Cells or 10 μm frozen tissue sections were permeabilised with Triton-X100 (0.2%; v/v) and proteinase K (1 μg/ml) for 5 minutes at RT. Cells/sections were washed for two 5 minute washes. Cells/sections were then refixed in 4% paraformaldehyde (w/v) for 5 minutes at RT. The cells/sections were incubated in equilibration buffer (200 mM $K(CH_3)_2$ As O_2,, 25 mM Tris-HCl 0.2 mM DTT, 0.25 mg/ml BSA, 2.5 mM $CoCl_2$) for 10 - 15 minutes. A reaction buffer (fluorescein-12-dUTP (10 mM Tris-HCl pH 7.6, 1 mM EDTA), Terminal deoxynucleotidyl Transferase (TdT) enzyme in equilibration buffer) was applied for 60 minutes at 37°C to incorporate fluorescein labelled nucleotides at the 3'-OH ends of fragmented DNA. To stop the reaction cells/sections were incubated with SCC (0.15 M NaCl, 0.17 M Na $H(C_3H_5\ O(COO)_3)$) for 15 minutes and cells/sections were washed for 5 minutes 3 times in PBS. Cells were mounted on-to glass slides using vectashield containing the counter-stain propidium iodide (Vector Laboratories, Peterborough, UK) and coverslips were sealed using clear nail varnish. Tissue sections were counter-stained with Hoecsht dye and mounted on-to glass coverslips using fluorescent mounting medium (Vector Laboratories, Peterborough, UK). Samples were stored in the dark at 4°C until needed for analysis. Incorporated fluorescein was visualised concomitantly with the counter-stain

fluorophore with a confocal microscope (Zeiss, LSM-510-META, Karl Zeiss, UK) using appropriate excitation wavelengths and filter sets (see Table 2.3).

2.8 Fluorescence immunocytochemistry

The following describes the general protocol used to identify proteins of interest, which was carried out following *in vitro* cell treatments. The specific details for every protein assessed by fluorescent immunocytochemistry in this thesis are presented in table 2.2.

2.8.1 General protocol for fluorescence immunocytochemistry

Cells were fixed with 4% paraformaldehyde (30 min at RT), permeabilised with 0.2% Triton-X100 (5 min at RT), and non-reactive sites were blocked (2 hr at RT) in blocking buffer (PBS containing animal serum; Vector laboratories, Peterborough, UK). Cell manipulations were carried out in a light protected humidified environment from this point. The blocking buffer was washed off (wash 1) with PBS and cells were incubated with primary antibody raised against the protein of interest. The primary antibody was washed off (wash 2) with PBS and cells were incubated with an appropriate biotinylated secondary antibody (Vector Laboratories, Peterborough, UK). The secondary antibody was washed off (wash 3) and cells were incubated with Alexa 488. The cells were then washed (wash 4) in PBS. In some cases (for p-SyK and Mdm2) nuclei were counterstained with Hoechst stain (Hoechst 33258, Invitrogen, Paisley, UK). The coverslips were mounted onto glass slides using Vectashield® fluorescent mounting media (Vector Laboratories, Peterborough, UK). The edge of each coverslip was sealed with clear nail varnish and slides were stored in the dark at 4°C until needed for analysis. The incorporated fluorophores were examined with a confocal microscope (Zeiss, LSM-510-META, Karl Zeiss, UK) using appropriate excitation wavelengths and filter sets (see Table 2.3).

2.8.2 Cathepsin-D

Pepstatin A (isovaleryl-$_L$-valyl-4-amino-3-hydroxy-6-methylheptanoyl-$_L$-alanyl-4-amino-3-hydroxy-6-methylheptanoic acid), a potent and selective inhibitor of cathepsin-D, covalently conjugated with the Boron dipyrromethene difluoride (BODIPY) fluorophore was used to label cathepsin-D in live cultured cortical neurones. Fluorescently tagged enzyme inhibitors, such as BODIPY FL-pepstatin A, are valuable tools in understanding the distribution, interactions and localisation of a protein (Chen *et al.,* 2000). The BODIPY fluorophore is both photostable and pH-insensitive; both important qualities in a fluorophore. In live cells, BODIPY FL-pepstatin A is internalised and transported to the lysosomes were it selectively binds cathepsin-D at pH 4.5. These properties make BODIPY FL-pepstatin A an ideal tool for the study of the localisation, secretion and trafficking of cathepsin-D.

Prior to drug treatment cells were incubated with NBM containing BODIPY FL-pepstatin A (1 μM; Molecular Probes, Inc., Oregan, USA) for 1 hour at 37°C in order to label cathepsin-D. From this point on cells were manipulated in a light protected environment. Cells were treated as desired and were washed in pre-warmed PBS and fixed with 4% paraformaldehyde. Coverslips were mounted on-to glass slides using flourescent mounting medium (Vectashield®; Vector Laboratories, Peterborough, UK). The edge of each coverslip was sealed with nail varnish and slides were stored in the dark at 4°C until needed for analysis. The incorporated fluorophore was examined with a confocal microscope (Zeiss, LSM-510-META, Karl Zeiss, UK) using appropriate excitation wavelength and filter sets (see Table 2.3).

2.9 Colocalisation analysis

2.9.1 Phospho-p53^{ser15} / SUMO-1

Following treatment, cells were fixed with 4% paraformaldehyde, permeabilised with 0.2% Triton-X100, and non-reactive sites were blocked in blocking buffer (PBS containing 5% goat serum (v/v); Vector Laboratories, Peterborough, UK) for 2 hours at RT. Cell manipulations were carried out in a light protected humidified environment

from this point. Coverslips were washed for 5 minutes before being incubated with the first primary antibody, rabbit anti-phospho $p53^{ser15}$ (1:100 dilution in PBS containing 10% goat serum) overnight at 4°C. Cells were washed for 5 minutes 3 times in PBS. The first secondary antibody, goat anti-rabbit IgG conjugated to biotin (1:200 in PBS containing 10% goat serum; Sigma-Aldrich, Dorset, UK) was incubated for 1 hour at RT. Cells were washed for 5 minutes 3 times in PBS, and incubated with ExtrAvidin®-R-Phycoerythrin conjugate (1:50 dilution in dH_2O; Sigma-Aldrich, Dorset, UK) for 40 minutes at RT. The cells were washed for 8 minutes 5 times with dH_2O. Cells were once more blocked in blocking buffer (PBS containing 5% goat serum (v/v); Vector Laboratories, Peterborough, UK) for 2 hours at RT and washed for 5 minutes 2 times in PBS. The second primary antibody, mouse anti-SUMO-1 antibody was incubated overnight at 4°C (1:100 dilution in PBS containing 10% goat serum (v/v); Santa Cruz Biotechnology Inc., California, USA). Coverslips were washed for 5 minutes 3 times in PBS. Cells were incubated with the second secondary antibody (goat anti-mouse conjugated to biotin; 1:200 dilution in PBS containing 10% goat serum; Vector Laboratories, Peterborough, UK) for 1 hour at RT. Cells were washed for 5 minutes 3 times in PBS, and incubated with ExtrAvidin® FITC (1:50 dilution in dH_2O; Sigma-Aldrich, Dorset, UK) for 40 minutes at RT. Cells were washed for 5 minutes 8 times in dH_2O before mounting on-to glass slides using fluorescent mounting medium (Vectashield®; Vector Laboratories, Peterborough, UK). The edge of each coverslip was sealed with nail varnish and slides were stored in the dark at 4°C until needed for analysis. The incorporated fluorophores were examined with a confocal microscope (Zeiss, LSM-510-META, Karl Zeiss, UK) using appropriate excitation wavelengths and filter sets (see Table 2.3).

2.9.2 Phospho-$p53^{ser15}$ / Lysotracker

Prior to drug treatment cells were incubated with NBM containing Lyso Tracker™ (700 nM; Invitrogen, Paisley, UK) for 25 minutes at 37°C in order to label lysosomes. Cell manipulations were carried out in a light protected humidified environment from this point. Cells were treated as desired, washed in pre-warmed PBS, fixed with 4% paraformaldehyde, permeabilised with 0.2% Triton-X100, and non-

reactive sites were blocked in blocking buffer (PBS containing 10% goat serum (v/v); Vector Laboratories, Peterborough, UK) for 2 hours at RT. Coverslips were washed for 5 minutes before being incubated with primary antibody, rabbit anti-phospho $p53^{ser15}$ (1:100 dilution in PBS containing 10% goat serum) overnight at 4°C. Cells were washed for 5 minutes 3 times in PBS. The secondary antibody goat anti-rabbit IgG conjugated to biotin (1:200 in PBS containing 10% goat serum; Sigma-Aldrich, Dorset, UK) was incubated for 1 hour at RT. Cells were washed for 5 minutes 3 times in PBS and then incubated with Alexa 488 (1:1000 dilution in dH_2O; Invitrogen, Paisley, UK) in 10% goat serum (v/v) for 30 minutes at RT. The cells were washed for 5 minutes 12 times with dH_2O. Cells were mounted on-to glass slides using fluorescent mounting medium (Vectashield®; Vector Laboratories, Peterborough, UK). The edge of each coverslip was sealed with nail varnish and stored in the dark at 4°C until needed for analysis. The incorporated fluorophores were examined with a confocal microscope (Zeiss, LSM-510-META, Karl Zeiss, UK) using appropriate excitation wavelengths and filter sets (see Table 2.3).

2.9.3 Phospho-SyK^{tyr323} / Lysotracker

Prior to drug treatment cells were incubated with NBM containing Lyso Tracker™ (700 nM; Invitrogen, Paisley, UK) for 25 minutes at 37°C in order to label lysosomes. Cell manipulations were carried out in a light protected humidified environment from this point. Cells were treated as desired, washed in pre-warmed PBS, fixed with 4% paraformaldehyde, permeabilised with 0.2% Triton-X100, and non-reactive sites were blocked in blocking buffer (PBS containing 20% goat serum (v/v); Vector Laboratories, Peterborough, UK) for 2 hours at RT. Coverslips were washed for 5 minutes before being incubated with primary antibody, rabbit anti-phospho SyK^{tyr323} (1:500 dilution in PBS containing 10% goat serum) overnight at 4°C. Cells were washed for 5 minutes 3 times in PBS. The secondary antibody goat anti-rabbit IgG conjugated to biotin (1:200 in PBS containing 20% goat serum; Sigma-Aldrich, Dorset, UK) was incubated for 1 hour at RT. Cells were washed for 5 minutes 3 times in PBS and then incubated with Alexa 488 (1:1000 dilution in dH_2O; Invitrogen, Paisley, UK) in 20% goat serum (v/v) for 30 minutes at RT. The cells were washed for 5 minutes 12

times with dH_2O. Cells were mounted on-to glass slides using fluorescent mounting medium (Vectashield®; Vector Laboratories, Peterborough, UK). The edge of each coverslip was sealed with nail varnish and slides were stored in the dark at 4°C until needed for analysis. The incorporated fluorophores were examined with a confocal microscope (Zeiss, LSM-510-META, Karl Zeiss, UK) using appropriate excitation wavelengths and filter sets (see Table 2.3).

2.9.4 Cathepsin-D/ Lysotracker

Prior to BODIPY FL-pepstatin A treatment, cells were incubated with NBM containing Lyso Tracker™ (700 nM; Invitrogen, Paisley, UK) for 25 minutes at 37°C in order to label lysosomes. Cell manipulations were carried out in a light protected humidified environment from this point. Cells were then incubated with NBM containing BODIPY FL-pepstatin A (1 μM; Molecular Probes, Inc., Oregan, USA) for 1 hour at 37°C. Cells were washed in pre-warmed PBS and fixed with 4% paraformaldehyde. Coverslips were mounted on-to glass slides using fluorescent mounting medium (Vectashield®; Vector Laboratories, Peterborough, UK). The edge of each coverslip was sealed with nail varnish and slides were stored in the dark at 4°C until needed for analysis. The incorporated fluorophores were examined with a confocal microscope (Zeiss, LSM-510-META, Karl Zeiss, UK) using appropriate excitation wavelengths and filter sets (see Table 2.3).

Fluorophore	Peak excitation/emission wavelength (nm)	Beam splitters
Acridine orange	488/505 and 633	HFT 488 Lambda scan 499 - 670
Alexa Fluor 488™	488/520	HFT 488 LP 505
Bodipy FL	504/513	HFT 488 Lambda scan 499 - 553
Fluorescein (FITC)	488/520	HFT 488 BP 505 - 530
Hoechst 33258	345/487	HFT UV/488/543/633 LP 456 - 499
Lyso Tracker™ Red	577/590	HFT 488/543 NFT 545 LP 560
Phycoerytrin R (PE)	565/578	HFT 488/543 NFT 545 BP 560 - 615
Propidium iodide	535/615	HFT 488/543 BP 560-615

Table 2.3 List of confocal microscope configurations.

Protein Target (source)	Supplier	Block % in TBS-T	Wash details	Antibody dilution % Block (v/v) in PBS	Alexa 488
SUMO-1 (mse)	Santa Cruz Biotech.	20% goat serum 2 hr @ RT	1) 2 x 5 min 2) 3 x 5 min 3) 3 x 5 min 4) 5 x 8 min	1^0 1:50 10% Block o/n@4°C 2^0 1:100 10% Block 1hr@RT	1:500 5% Block 30 min @ RT
Phosphorylated SyK (tyr ^{323}; rbt)	Cell signaling tech.	5% goat serum o/n@4°C	1) 2 x 5 min 2) 3 x 5 min 3) 3 x 5 min 4) 5 x 8 min	1^0 1:500 20% Block o/n@4°C 2^0 1:200 20% Block 1hr@RT	1:1000 20% Block 30 min @ RT
Total-p53 (gt)	Santa Cruz Biotech.	10% 2 hr @ RT	1) 2 x 5 min 2) 3 x 5 min 3) 3 x 5 min 4) 5 x 8 min	1^0 1:100 10% Block o/n@4°C 2^0 1:200 10% Block 1hr@RT	1:1000 30 min @ RT
Phoshorylated p53 (ser^{15}; rbt)	Cell signaling tech.	5% goat serum o/n@4°C	1) 2 x 5 min 2) 3 x 5 min 3) 3 x 5 min 4) 5 x 8 min	1^0 1:100 10% Block o/n@4°C 2^0 1:200 10% Block 1hr@RT	1:1000 30 min @ RT
Caspase-3 (rbt)	Promega	30% goat serum o/n@4°C	1) 2 x 5 min 2) 4 x 5 min 3) 4 x 5 min 4) 12 x 5 min	1^0 1:1000 30% Block o/n@4°C 2^0 1:1500 30% Block 1hr@RT	1:1000 30% Block 20 min @ RT

Table 2.2 Immunocytochemistry protocol details.

2.10 Immunoprecipitation

Immunoprecipitation is a procedure, which usually involves a protein interacting with an antibody, removal of the protein-antibody complex followed by examination of the protein for quantification or other characteristics such as molecular weight and isoelectric point.

2.10.1 Total-p53/SUMO-1

Following treatment cells were harvested into ice-cold lysis buffer (0.15 M Tris-HCl pH 6.7, 5% SDS, 30% glycerol; as detailed by Hilgarth and Sarge (2005), using the rubber insert of a 1 ml syringe (B.Braun Medical Ltd., Melsungen, Germany). Samples were diluted 1:3 with PBS containing 0.5% Nonidet P-40 and complete protease inhibitor cocktail (Roche, Penzberg, Germany) and centrifuged for 5 minutes at 10 000 x g at 4°C. Total protein was determined using the BCA assay and samples were equalised to 600 μg/ml. The samples were pre-cleared with 50 μl of TrueBlot™ anti-goat IgG beads (eBiosciences, California, USA) for 30 minutes on ice. Samples were centrifuged for 5 minutes at 10 000 x g and the supernatant removed. The remainder of the supernatant was incubated with 5 μg of a polyclonal goat anti-total p53 antibody (N19; Santa Cruz Biotechnology Inc., California, USA) and rotated at 4°C for 1 hour to allow protein-antibody interaction. Samples were centrifuged at 10 000 x g at 4°C for 1 minute, and the supernatant was discarded. The anti-goat IgG beads were washed in lysis buffer (50 mM Tris-HCl pH 8.0, 150 mM NaCl, 1% NP-40) 4 times collecting the beads and discarding the supernatant after each wash. After the last wash reducing sample buffer (25 mM Tris-Base pH 6.5, 50 mM DTT, 6% SDS, 10% glycerol, 0.05% bromophenol blue) was added to the bead pellet. Samples were vortexed, and heated to 90°C for 10 minutes. Samples were centrifuged at 10 000 x g for 3 minutes at 4°C, and supernatant was stored in a separate tube at -20°C until needed. Samples were separated on a 12% SDS gel and proteins were transferred to a nitrocellulose membrane (see section 2.5.2 and 2.53). Following this, the membrane was blocked in 5% non-fat milk in buffer A (25 mM Tris-HCl pH 7.3, 0.15 M NaCl, 0.1% Tween-20) overnight at 4°C with gentle agitation. The membrane was rinsed briefly before incubating with goat anti-SUMO-1 (1:400 in 0.5% milk in buffer A; Abcam Ltd., Cambridge, UK) for 2

hours at RT. The membrane was then washed for 15 minutes 4 times in TBS-T. The secondary antibody (goat anti-rabbit IgG-HRP, 1:400 dilution in TBS-T containing 0.1% BSA (w/v); Sigma-Aldrich, Dorset, UK) was incubated for 1 hour at RT and the membrane washed for 15 minutes 4 times in TBS-T. Supersignal (Pierce, Leiden, The Netherlands) was added to the membrane, incubated for 3 minutes and the membrane exposed to photographic film for 3 seconds in the dark prior to being developed.

2.11 Enzyme activity analysis

2.11.1 Measurement of caspase-3 activity

Cleavage of the caspase-3 substrate (Ac-DEVD-7-amino-4-trifluoromethylcoumarin peptide (AFC); Alexis Corporation, Nottingham, UK) to its fluorescent product was used to determine the activity of caspase-3. Following treatment cells were washed in ice-cold PBS and cells were harvested by scraping coverslips in lysis buffer (25 mM HEPES, 5 mM $MgCl_2$, 5 mM dithiothreitol, 5 mM EDTA, 2 mM PMSF, 10 μg/ml leupeptin, 6.25 μg/ml pepstatin, 10 μg/ml aprotinin, pH 7.4) on ice using the rubber insert of a 1 ml syringe (B.Braun Medical Ltd., Melsungen, Germany). Lysates were sonicated for 2 seconds (Soniprep 150, Sanyo Europe Ltd.). Samples (50 μl) were incubated with the DEVD peptide (10 μM; 4 μl) and incubation buffer (46 μl; 50 mM HEPES, 10 mM dithiothreitol, 20% glycerol (v/v), pH7.4) or as an internal control incubation buffer alone for 1 hour at 37°C. Fluorescence was assessed (excitation, 400 nm; emission, 505 nm) using a spectrofluorimeter (Fluroscan Ascent FL plate reader; Labsystems, Vantaa, Finland).

2.11.2 Measurement of cathepsin-L activity

Cleavage of the cathepsin-L substrate (Z-Phe-Arg- amino-4-trifluoromethylcoumarin peptide (AFC); Alexis Biochemicals, Nottingham, UK) to its fluorescent product was used to determine the activity of cathepsin-L. The peptide is a substrate for both cathepsin-L and cathepsin-B so to ensure cathepsin-L specificity of the assay the pH of the incubation buffer was set at pH 5 (Kamboj et al., 1993).

Following treatment cells were washed in ice-cold PBS. Cells were harvested by scraping coverslips in urea buffer (20 mM NaOAc, 4 mM EDTA, 8 mM DTT, 4 M Urea; pH 5) on ice using the rubber insert of a 1 ml syringe (B.Braun Medical Ltd., Melsungen, Germany). Lysates were sonicated for 2 seconds (Soniprep 150, Sanyo Europe Ltd.). Samples (90 μl) were incubated with the Z-Phe-Arg-AFC peptide (150 μM; 10 μl), or for internal control samples, urea buffer (100 μl) for 1 hour at 37°C. Fluorescence was assessed (excitation, 400 nm; emission, 505 nm) using a spectrofluorimeter (Fluroscan Ascent FL plate reader; Labsystems, Vantaa, Finland).

2.11.3 Measurement of cathepsin-D activity

An InnoZyme™ Cathepsin D Immunocapture activity kit (Calbiochem International, Darmstadt, Germany) was used following the manufacturer's protocol to perform this assay. 96-well plates were pre-coated with a monoclonal anti-cathepsin-D to capture cathepsin-D from standards and samples. Captured cathepsin-D from the cytosolic fraction of samples was detected using an internally quenched fluorescent cathepsin-D substrate peptide, Mca-Gly-Lys-Pro-Ile-Leu-Phe-Arg-Leu-Lys-(Dnp)-D-Arg-NH_2. Release of the fluorescent product, Mca-Gly-Lys-Pro-Ile-Leu-Phe was determined fluorometrically at excitation 328 nm and emission 393 nm using a spectrofluorimeter (Spectramax Gemini and Softmax Pro 4.8 software, Molecular Devices, California, USA). Sample cathepsin-D activity was read from a standard curve of cathepsin-D activity using affinity purified cathepsin-D enzyme; standards ranged from 3.125 ng/ml to 50 ng/ml. Cathepsin-D activity was expressed as units per mg protein per minute.

2.12 Lysosomal integrity assay – acridine orange relocation

Acridine orange (AO; Molecular Probes, Leiden, The Netherlands) was used to investigate the membrane integrity of lysosomes. The degree of AO release from lysosomes to the cytosol was monitored by confocal microscopy. AO is a fluorogenic organic weak base, which freely diffuses into cells and across the membranes of cellular organelles. In acidic membrane-bound compartments such as lysosomes AO

becomes protonated, which traps the AO within the compartment, hence AO concentration increases in these discrete compartments. This accumulation produces a change in the fluorescence emission of the dye, from a peak emission of 525 nm to 633 nm due to the concentration-dependent stacking of the dye molecules. Figure 2.2 shows the characteristic staining profile of AO; one can observe a green diffuse staining (525 nm; cytosol, nucleus and other non-acidic cellular components) and punctate staining (633 nm; lysosomes and late endosomes). This metachromatic characteristic can be utilised to determine the stability of acidic membrane-bound organelles. In the event of lysosomal destabilisation the punctate orange staining (633 nm emission) dissipates in rapid discrete events, the AO returning to the incubation medium. To label lysosomes cultured cortical neurones were incubated with AO (5 μg/ml) for 10 minutes at 37°C, neurones were then exposed to the desired drug treatments. After treatment the drug containing media was replaced with supplemented NBM. Neurones were analysed with a laser scanning confocal microscope using the Lambda mode (LSM 510 META, Zeiss, Heidelberg, Germany). Following imaging linear un-mixing of the emission spectra from a population of cells was performed using LSM Image Examiner Software 4. Emission at 633 nm was used as an indicator of lysosomal membrane integrity. High 633 nm emission indicated intact lysosomal membranes and low 633 nm emission indicated unstable lysosomal membranes.

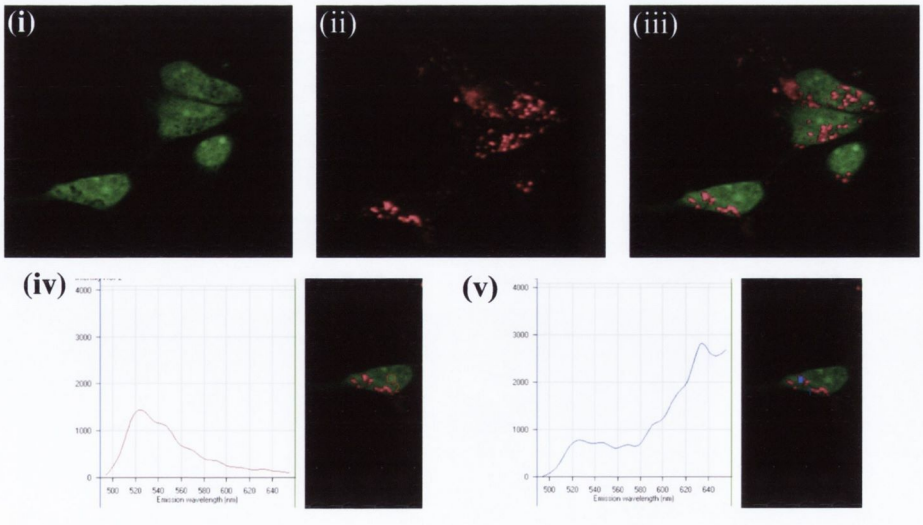

Figure 2.2 Metachromatic characteristics of Acridine orange and linear un-mixing of emission spectra.
The two distinct emissions of AO (i and ii) and an overlay image (iii). Emission spectra graphs showing the intensity of the fluorescence at 525 nm (iv) and 633 nm (v).

2.13 Gene knock out using small interfering RNA (siRNA)

Small interfering RNA (siRNAs) are the functional intermediates in the RNA interference pathway (RNAi; Figure 2.3). The RNAi pathway is a mechanism that is important in the defence against viral invasion, transposon expansion and post transcriptional regulation. The RNAi pathway is extremely potent and is conserved through evolution. This novel defence pathway was first described in 1990 whilst investigating plant and fungal genetics (Jorgensen, 1990). Since that time major progress has ensued which culminated in 2006 when a Nobel Prize was awarded to Craig Mello and Andrew Fire for their work involving specific mRNA degradation triggered by long double-stranded RNAs (dsRNAs) in *Caenorhabditis elegans* (Fire *et al.*, 1998). The founders of this new methodology observed that exposure to only a few molecules of dsRNA induced sequence specific reduction of the target mRNA.

The RNAi pathway is initiated when a cell encounters a long dsRNA transcribed from an invading virus or from an endogenous aetiology such as a mobilised transposon, an inappropriately transcribed sequence or a non-coding microRNA (miRNA). The cytoplasmic, RNase III-like protein, Dicer, cleaves the dsRNA molecules into small RNA duplexes (19 - 25 bp), which have classic 3' dinucleotide overhangs. These small interferring RNA duplexes (siRNAs) are incorporated into a protein complex called RNA-induced Silencing Complex (RISC). The two strands are unwound by an ATP-dependent helicase activity, thus enabling the 'guide' RNA strand to independently target complimentary mRNA. Once target recognition occurs RISC mediates either the site-specific cleavage of mRNA in the region of the siRNA-mRNA duplex or through a miRNA-like mechanism of translational repression. The final mechanism carried out is dependent on the degree of complementarity between guide and target mRNA. The resultant gene silencing is more potent in the site-specific cleavage mechanism, since RISC uncouples when the mRNA is cleaved, thus allowing the siRNA programmed RISC to re-survey the pool of mRNA for more complimentary sequences. It is this aspect of the RNAi pathway, which makes the gene silencing results so potent and long lasting.

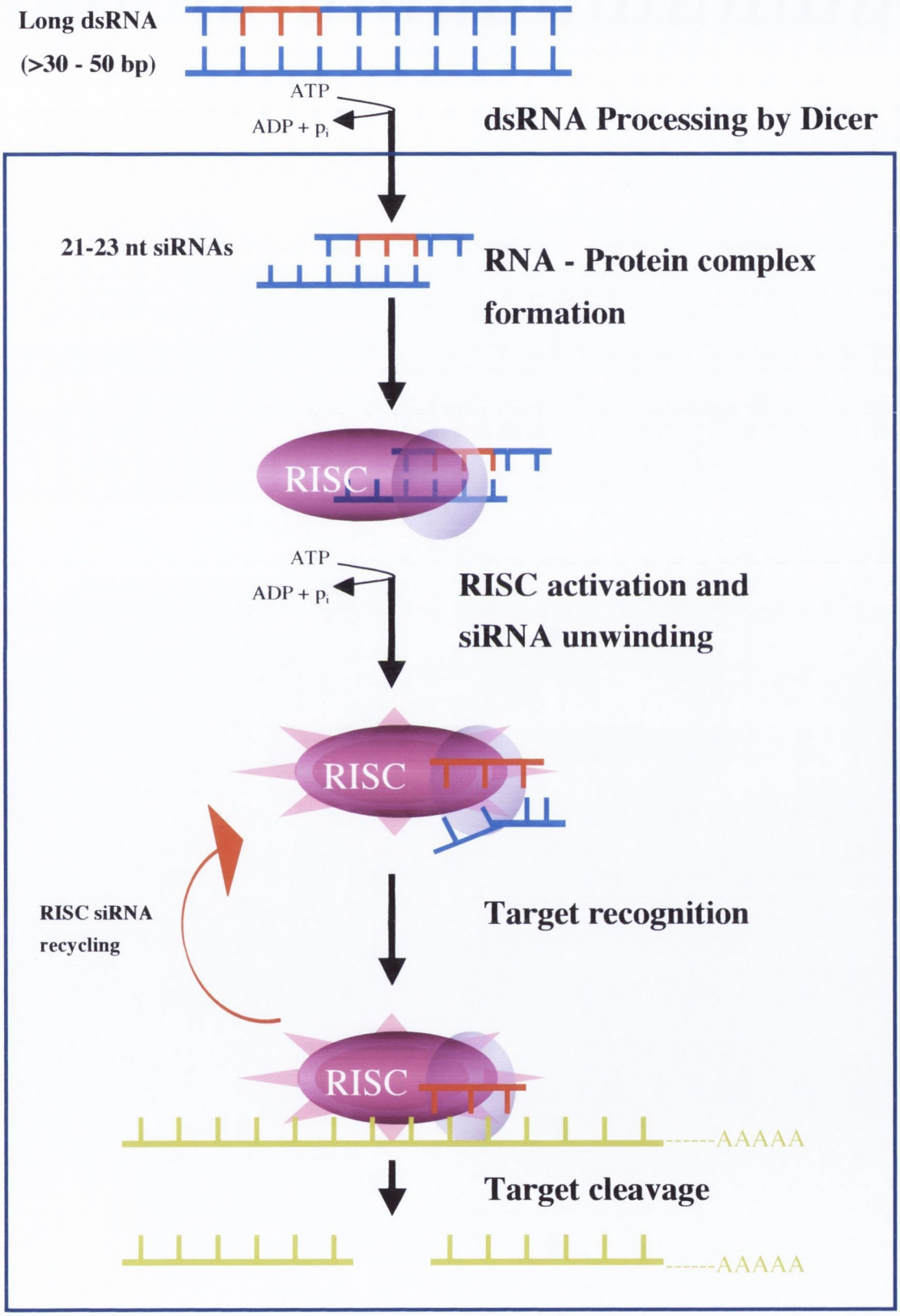

Figure 2.3 The RNA interference pathway.

The induction of the RNAi pathway relies on the use of long dsRNA strands to activate Dicer, which generates siRNA. However, exposure of mammalian cells to long dsRNA causes the induction of the interferon response, which can lead to inhibition of general protein synthesis and cell death (Baglioni *et al.,* 1979). It is for this reason that short, synthetic duplexes, which mimic the naturally occurring 19-25 bp siRNA must be used to achieve gene silencing *via* the RNAi pathway in mammalian cells (boxed region in Figure 2.3; Elbashir *et al.,* 2001; Caplen *et al.,* 2001). The use of pools of multiple numbers of unique siRNAs (all targeting the same gene) increases both specificity (by reducing off-target silencing) and potency (by increasing target recognition).

2.13.1 Depletion of p53 protein using siRNA *in vitro*

Custom ON-TARGET Plus Smart pool small interfering RNA (siRNA) containing a mixture of 4 SMART selection designed siRNAs targeting rat p53 (Gen Bank™ accession number NM_030989; p53 siRNA) was purchased from Dharmacon (Lafayette, Colorado, USA). Primary cortical neurones were transfected with p53 siRNA (100 nM) using Dharmacon transfection lipid number 3. A control siRNA duplex containing at least 4 mismatches to any rat gene (ON-TARGET Plus siControl Non-Targeting siRNA; Con siRNA) was used in parallel experiments. Optimal transfection efficiency and conditions were determined by using FAM labelled non-specific siRNA (SiGlo green; Dharmacon, Lafayette, Colorado, USA) Effective p53 knockdown was analysed using immunohistochemistry and western immunoblot.

2.14 Statistical analysis

All statistical analysis was carried out using Prism 4 (GraphPad Prism, California, USA). Data were expressed as means ± standard error of the mean (SEM). Statistical analysis was performed by use of a one or two ANOVA. If significant changes were observed, the data was further analysed using a Newmann-Keuls *post hoc* test. A p value of less than 0.05 was considered statistically significant. The exact p values were quoted where possible, to allow a wider interpretation of the experiment. When making comparisons between two groups a suitable t test was carried out. When

using standard curves a minimum r squared value of >0.98 was set to ensure the accuracy of each standard curve.

Chapter 3

An investigation of the early signalling events in Δ^9-THC-induced neuronal apoptosis

3.1 Introduction

The tumour suppressor protein p53 has been called the 'guardian of the genome' since it has a central role in causing cell cycle arrest or apoptosis in response to a variety of cell stressors (lane, 1992; Levine, 1997). In unstressed cells, p53 is present in a latent state and is maintained at low levels through targeted degradation mainly by the association with its negative regulator Mdm2 (Appella and Anderson, 2001). However, during periods of cell stress such as calcium overload, oxidative stress, nutrient deprivation *etc.*, p53 becomes activated which causes levels to rise due to resistance to Mdm2 mediated degradation. This activation occurs largely through post translational alterations rather than changes in p53 gene expression levels (Oren, 1999). This is particularly relevant in post mitotic cells such as neurones where the activation of p53 following cell stress needs to occur quickly and to result in the induction of apoptosis rather than a slow process involving cell cycle arrest and DNA repair which could cause a delayed and ineffective response to neuronal stress. A role for p53 has been demonstrated for neuronal apoptosis induced by Aβ, excitotoxicity and oxidative stress (Fogarty *et al.*, 2003; Culmsee *et al.*, 2001; Shibata *et al.*, 2006).

Human p53 is post translationally modified with different modifiers on at least 18 sites, which is responsible for titrating the biological activity of p53 (Appella and Anderson, 2000). Despite the pleotrophic nature of these modifiers, it has been shown that phosphorylation plays an important role in the regulation of p53 induced growth arrest and apoptosis (Herr and Debatin, 2001). Several kinases that detect various cell stress signals can initiate a unique set of signalling pathways, which culminate in the activation of p53 by phosphorylation (Appella and Anderson, 2000). For example JNK has been shown to induce the phosphorylation of p53 at serine 15 and threonine 81 after exposure to Δ^9-THC and UV irradiation respectively (Downer *et al.*, 2007a; Buschmann *et al.*, 2001). Furthermore, phosphorylation of p53 on serine 15 in response to genotoxic stress has been shown to reduce the ability of p53 to bind to its negative regulator, Mdm2, thus leading to an accumulation of active p53 (Shieh *et al.*, 1997; Banin *et al.*, 1998). In addition, serine residues 20, 33 and 46 are phosphorylated, whilst serine residues 376 and 378 undergo dephosphorylaion in response to cell stress (Lavin and Gueven, 2006). Once phosphorylated or dephoshorylated, the stability of the p53

protein is increased, allowing it to act as a transcription factor to up regulate many p53 responsive genes *e.g.,* Mdm2 and the pro-apoptotic Bcl-2 family member, Bax. Transactivation of pro-apoptotic genes such as Bax leads to further down stream signalling which culminates in the activation of proteins responsible for the initiation of the physical destruction of the cell.

Stabilisation of p53 can be achieved by other forms of post translational modification *e.g.,* acetylation, ubiquitination and modification of p53 with p53 interacting proteins such as SUMO and Mdm2. The pattern of proteins that are SUMOylated or labelled (by Mdm2) with an ubiquitin degradation tag can change in response to certain changes in the cell cycle or in growth conditions. Post translational modification of p53 with SUMO-1 has been reported to increase the transactivation of p53 responsive genes (Gostissa *et al.*, 1999; Rodriguez *et al.*, 1999). However, it has also been shown that SUMOylation of p53 has no effect on its transcriptional activity and that the co-expression of p53 and SUMO-1 with enzymes responsible for SUMOylating proteins repress p53 activity (Kwek *et al.*, 2001; Schmidt and Muller, 2002). As p53 is a transcription factor for the Mdm2 gene the Mdm2 protein is up regulated when p53 is expressed. Therefore cell stress causes a paradoxical activation of p53 while simultaneously increasing Mdm2 expression, which subsequently increases the degradation of p53 by Mdm2 mediated ubiquitination. Therefore, a challenge has been to explain how the abundant Mdm2 is prevented from inhibiting p53, thus ensuring that p53 can execute an appropriate stress response (Stommel and Wahl, 2005). This question is resolved by the existence of two p53 response elements in the Mdm2 gene, which are responsible for producing two different length Mdm2 proteins, with different p53 binding abilities. The longer length Mdm2 protein (p90Mdm2) contains the entire p53-binding site and inhibits p53 function. However, the shorter Mdm2 protein (p76Mdm2) has lost half of the p53 binding site and cannot bind p53 (Perry, 2004). The p76Mdm2 protein acts as a dominant-negative inhibitor of p90Mdm2, which causes the stabilisation of p53 (Perry *et al.*, 2000). Although Mdm2 can inhibit p53 by directly interfering with the ability of p53 to induce gene expression the main function of Mdm2 is to act as an ubiquitin ligase for p53. Labelling p53 with an ubiquitin tag causes the degradation of p53 by 26 S proteosome. In addition,

ubiquitination of p53 by Mdm2 promotes the translocation of p53 from the nucleus to the cytoplasm (Carter *et al.*, 2007). Furthermore, Mdm2 has the ability to ubiquitinate itself and can also be modified by SUMO. Interaction of Mdm2 with SUMO or deSUMOylating isopeptidases causes p53 activation due to decreased levels of Mdm2 caused by the up regulation of its self-ubiquitination. Therefore, the association of Mdm2 with SUMO induces a shift away from p53 ubiquitination and degradation to p53 activation (Chen and Chen, 2003; Lee *et al.*, 2006b). SUMOylation of a protein adds approximately 20 kDa to the molecular weight of the substrate protein, which can be easily detected by immunoprecipitation followed by western immunoblot analysis (Johnson, 2004). Regulation of p53 stability and activity involving interactions with and between SUMO and Mdm2 and their modifying proteins is a complex issue, which has not yet been definitively characterised. It is likely that different cell stressors activate a unique affect on p53 modifying proteins and that there are multiple proteins that control p53 activity.

The role of the protein tyrosine kinase, SyK, in cannabinoid-mediated neurotoxicity was also a focus for investigation. SyK mediates a diverse set of cellular responses such as cell proliferation, differentiation and phagocytosis (Yanagi *et al.*, 2001). SyK has a widespread expression pattern in cells such as haematopoietic cells, fibroblasts, epithelial cells, hepatocytes and neurones (Yanagi *et al.*, 2001). The involvement of SyK in the fusion of B cell receptor-carrying endosomes to lysosomes in the immature B cell line DT40 is of particular interest to our investigation into the effects of cannabinoids on the lysosomal system (He *et al.*, 2005; see thesis chapter 4). In addition, the finding that SyK is required for the LPS-induced c-Jun N-terminal kinase activation is of interest since previous work from our laboratory has shown that Δ^9-THC modulates the expression of JNK (Yamada *et al.*, 2001; Downer *et al.*, 2003).

The experimental work carried out in this chapter aimed to establish a role for JNK1 in the Δ^9-THC-induced increase in p53 phosphorylated at serine 15. The rationale behind this is based on our previous results showing that Δ^9-THC induces pro-apoptotic signalling molecules involving JNK signalling, and that p53, which we have also shown to be involved in the Δ^9-THC-induced apoptotic cascade, is a substrate for regulation by JNK. To investigate this, p53 expression was examined in cells treated with Δ^9-THC in

the presence or absence of a JNK1 inhibitor. In addition, to investigate the events, which occur, downstream of p53 in Δ^9-THC-treated neurones, p53 specific siRNA was used to deplete p53 protein expression and the role of p53 in Δ^9-THC-mediated induction of DNA fragmentation was assessed in these cells. Furthermore, the effect of Δ^9-THC on the p53 interacting proteins, SUMO-1 and Mdm2 was assessed by western immunoblot, immunocytochemistry and immunoprecipitation. Since Δ^9-THC activates a plethora of signalling kinases, the proclivity of Δ^9-THC to induce the activation of a novel kinase, SyK was examined in this chapter. The role of p53 in Δ^9-THC-induced phospho-SyK^{tyr323} expression and DNA fragmentation was also assessed.

3.2.1 Δ^9-THC induces DNA fragmentation in cultured cortical neurones.

We have previously demonstrated that Δ^9-THC-induces DNA fragmentation in cultured cortical neurones (Campbell 2001, Downer *et al.*, 2001). In order to corroborate this observation, another independent assessment of Δ^9-THC neurotoxicity was undertaken. Cultured cortical neurones were exposed to Δ^9-THC (5 μM) for 15 minutes and 2 hours, cells were fixed and the level of DNA fragmentation was assessed using TUNEL (Figure 3.1). In vehicle (0.006% ethanol) treated neurones, no significant incidence of DNA fragmentation was observed (20 ± 6% TUNEL positive cells) and treatment with Δ^9-THC (5 μM) for 15 minutes also had no significant effect on DNA fragmentation (16 ± 2% TUNEL positive cells; Figure 3.1A). However, cells exposed to Δ^9-THC (5 μM) for 2 hours displayed a significant increase in the number of cells displaying fragmented DNA (55 ± 8% TUNEL positive cells; $p<0.001$, vs. vehicle, and Δ^9-THC (15 minutes), Student Newman Keuls, n=6). This finding endorses the previous findings of our laboratory.

Figure 3.1: Δ^9-THC induces DNA fragmentation in cultured cortical neurones

Neurones were treated with vehicle or Δ^9-THC (5 μM) for 15 min and 2 hr, fixed and DNA fragmentation was assessed by TUNEL staining.

A: Δ^9-THC induced a significant increase in DNA fragmentation after exposure to Δ^9-THC (5 μM) for 2 hr. Results are means ± SEM, ***$p<0.001$, vs., vehicle, +++$p<0.001$, vs., THC (15 min; 5 μM), Student Newman Keuls, n=6.

B: Representative images of TUNEL stained neurones treated with (i) vehicle and (ii) Δ^9-THC for 2 hr. Arrows indicate TUNEL positive cells.

A

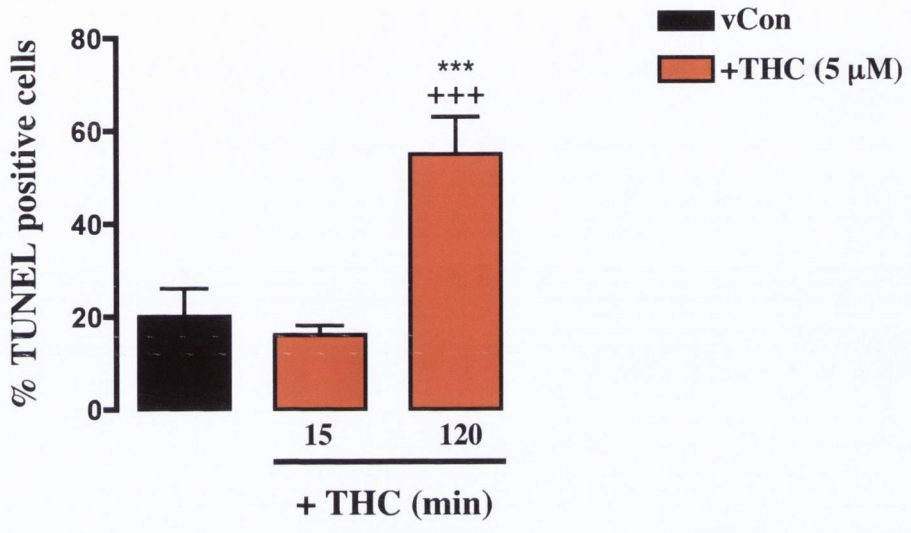
vCon
+THC (5 μM)
% TUNEL positive cells
80
60
40
20
0
***
+++
15
120
+ THC (min)

B

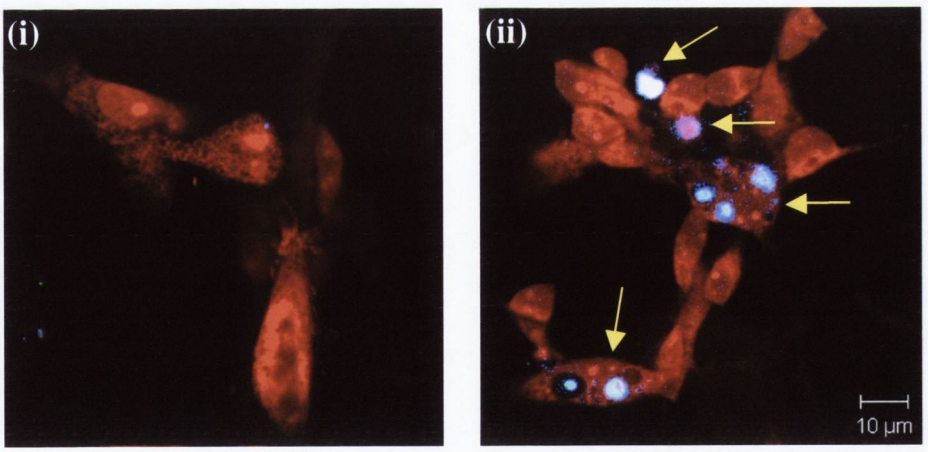
(i)
(ii)
10 μm

3.2.2 Δ^9-THC-induced increase in phospho-p53^{ser15} protein expression is dependent on JNK1

The tumour suppressor protein p53 is an important signalling molecule in the regulation of G1 cell cycle arrest or alternatively to induce apoptosis (Levine, 1997). We have found previously found that Δ^9-THC induces a rapid phosphorylation, and thus activation, of p53 (p-p53^{ser15}; Downer *et al.*, 2007a). The stress activated protein kinase, c-jun N-terminal kinase (JNK) is known to phosphorylate p53 at various sites including serine 15 (ser 15; Blatt and Glick, 2001). Previous results from this laboratory have indicated that JNK signalling is pertinent in Δ^9-THC-induced apoptosis (Downer *et al.*, 2003). To assess the role of JNK1 in coupling Δ^9-THC to p53 activation, cortical neurones were pre-treated with the selective JNK1 inhibitor JNKi (10 μM) for 30 minutes prior to Δ^9-THC (5 μM) exposure for 5 minutes. Pre-treatment with JNKi prevented the Δ^9-THC-induced increase in p53 phosphorylation at serine residue 15 after 5 minutes Δ^9-THC exposure ($p=0.0001$, ANOVA, $n=6$; Figure 3.2). In cortical neurones treated with ethanol vehicle for 5 minutes p53 phosphorylation at serine residue 15:total-p53 (p-p53^{ser15}:t-p53) expression was 3.42 ± 0.44 arbitrary units (mean ± SEM) and this was significantly increased following Δ^9-THC treatment to 7.64 ± 0.71 ($p<0.001$, Student Newman Keuls, $n=6$). While pre-treatment with JNKi alone had no effect on the level of p-p53^{ser15}:t-p53 expression (3.70 ± 0.48), it prevented the Δ^9-THC-induced increase in p-p53^{ser15}:t-p53 expression (2.94 ± 0.37) indicating that the phosphorylation of p53 induced by Δ^9-THC is dependent on JNK1 (Figure 3.2A). Sample confocal images demonstrating the JNK1-dependent increase in p-p53^{ser15} expression following Δ^9-THC treatment are shown in Figure 3.2B.

Figure 3.2: The Δ^9-THC-induced increase in phospho-p53^{ser15} protein expression is dependent on JNK1

Cultured cortical neurones were pre-incubated with JNK1 inhibitor, JNKi (10 μM) for 30 minutes prior to Δ^9-THC (5 μM) treatment for 5 minutes. Cell protein was harvested and analysed for phospho-p53^{ser15} (p-p53^{ser15}) and total-p53 (t-p53) expression using western immunoblot (panel A). In addition some cells were fixed after treatment and phospho-p53^{ser15} was labelled using immunocytochemistry (panel B).

A: Δ^9-THC (5 μM, 5 min) evoked a significant increase in p-p53^{ser15}:t-p53 expression. Pre-incubation with JNKi prior to Δ^9-THC exposure abolished the Δ^9-THC-induced p-p53^{ser15}:t-p53 expression observed at 5 min. Results are expressed as means ± SEM, ***p,<0.001, vs., vehicle, Student Neman Keuls, n=6.

B: Representative images of fluorescently labelled p-p53^{ser15} in vehicle (i), Δ^9-THC (ii), (iii) JNKi alone and (iv) Δ^9-THC + JNKi-treated cultures.

A

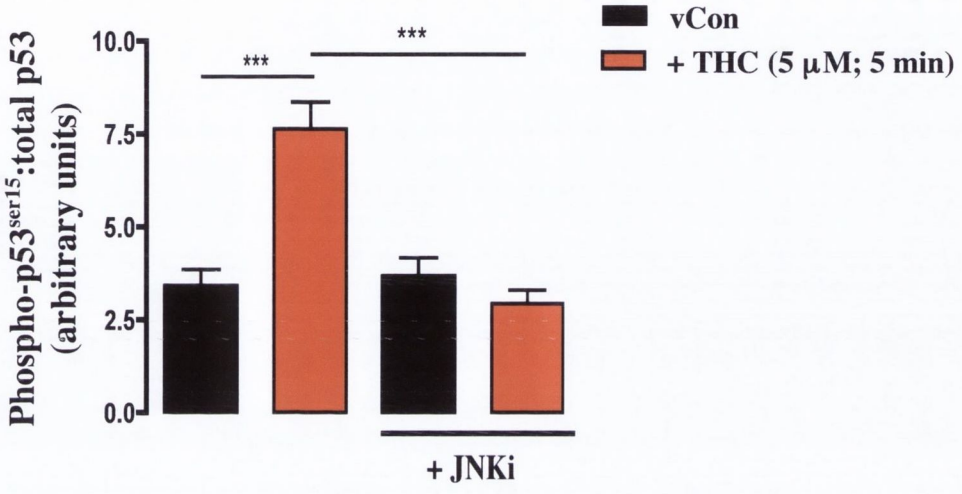
vCon
+ THC (5 μM; 5 min)
Phospho-p53ser15:total p53 (arbitrary units)
10.0
7.5
5.0
2.5
0.0
***
***
+ JNKi

B

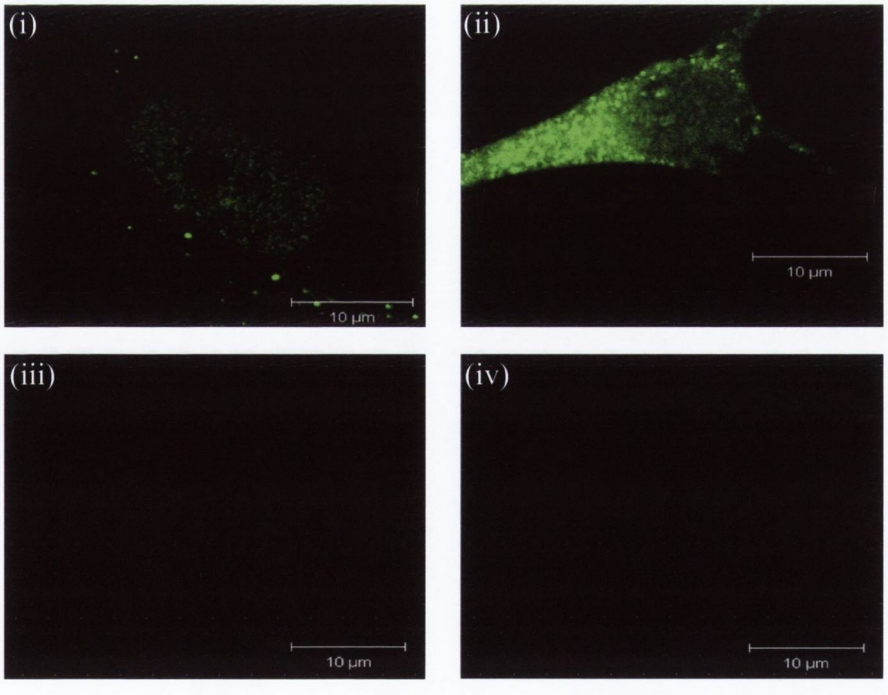
(i)
10 μm
(ii)
10 μm
(iii)
10 μm
(iv)
10 μm

3.2.3 Δ^9-THC induces an increase in SUMO-1 expression in a time dependent manner

The Small Ubiquitin-like MOdifier protein-1 (SUMO-1) has been shown to be a post translational modifier of p53 (Johnson, 2004). The addition of SUMO-1, or SUMOylation of p53 affects its stability and transactivation potential (Carter *et al.*, 2007; Gostissa *et al.*, 1998). Since Δ^9-THC-induced a post translational modification of p53, by phosphorylation of serine 15, it was determined if SUMO-1 was regulated by Δ^9-THC. SUMO-1 expression was assessed following treatment with Δ^9-THC (5 μM) for 5 - 30 minutes (Figure 3.3A). Following Δ^9-THC treatment for 5 minutes, SUMO-1 expression was 104.90 ± 17.07 arbitrary units (mean ± SEM), comparable to that found in cells treated with vehicle (81.27 ± 12.39). However, SUMO-1 expression was significantly increased to 134.70 ± 17.49 when neurones were treated with 5 μM Δ^9-THC for 15 minutes ($p<0.05$ vs. vehicle, Student's t-test, n=4 independent observations). This effect was maintained after 30 minutes treatment with Δ^9-THC (126.20 ± 11.17; $p<0.05$ vs. vehicle, Student's t-test, n=4). A sample western immunoblot demonstrating the Δ^9-THC-induced increase in SUMO-1 expression following Δ^9-THC treatment is shown in Figure 3.3B. Sample confocal images demonstrating the time dependent increase in SUMO-1 expression following Δ^9-THC treatment are shown in Figure 3.3C.

Figure 3.3: Δ^9-THC induces an increase in SUMO-1 expression in a time dependent manner

Cultured cortical neurones were treated with Δ^9-THC (5 μM) for 5 - 30 minutes, cell protein was harvested and analysed for the expression levels of SUMO-1 using western immunoblot and immunocytochemistry.

A: Δ^9-THC significantly increased SUMO-1 expression at 15 and 30 min but not at 5 min. Results are expressed as mean ± SEM for 4 independent observations, *$p<0.05$ vs., vehicle, Student's t-test, n=4.

B: A sample western immunoblot demonstrating the increase in SUMO-1 protein expression at 15 (lane 3) and 30 min (lane 4) of Δ^9-THC treatment compared to vehicle-treated (lane 1) and 5 min (lane 2) Δ^9-THC-treatment. β actin expression was monitored to ensure equal protein loading.

C: Representative confocal images of SUMO-1 expression in cultured cortical neurones treated with vehicle (i), and Δ^9-THC (5 μM) for 5 min (ii), 15 min (iii) and 30 min (iv).

A

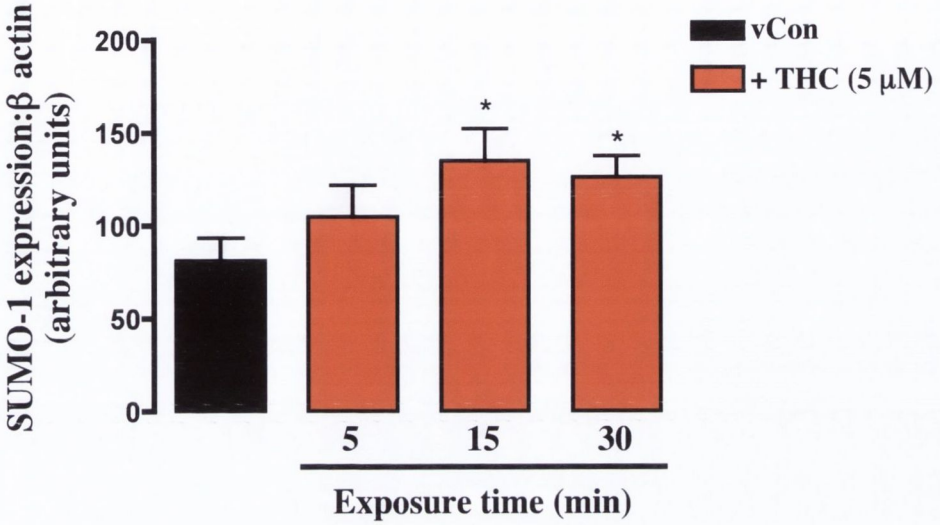
SUMO-1 expression:β actin
(arbitrary units)
200
150
100
50
0
vCon
+ THC (5 μM)
*
*
5
15
30
Exposure time (min)

B

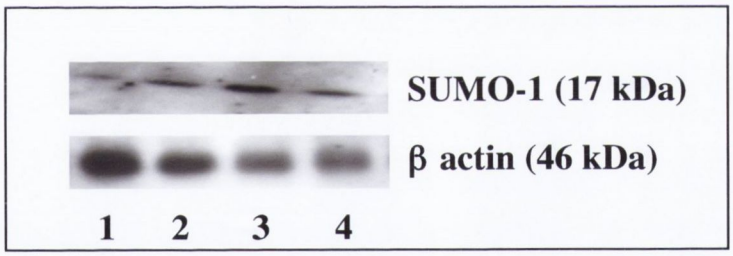
SUMO-1 (17 kDa)
β actin (46 kDa)
1
2
3
4

C

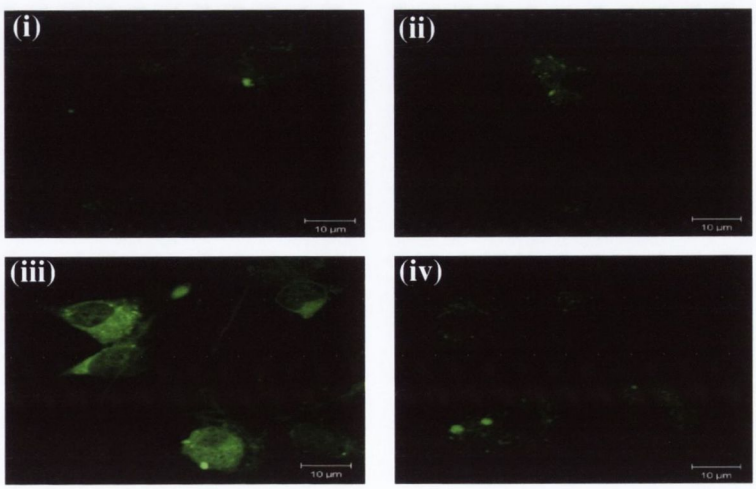
(i)
(ii)
(iii)
(iv)

3.2.4 The effect of Δ^9-THC on p53-SUMO-1 colocalisation

The majority of SUMO-1 exists in a protein bound form, changes in the extra- and intra-cellular environment *e.g.,* oxidative and osmotic stress *etc.,* can lead to alterations in the levels of certain SUMO-1 conjugated protein and can cause an increase in 'free' unconjugated SUMO-1 (Melchior, 2000; Everett *et al.*, 1999). Thus, colocalisation analysis by immunoprecipitation and immunocytochemistry was carried out to determine if the increase in SUMO-1 expression was associated with a Δ^9-THC-induced alteration of the SUMOylation status of p53. In this study, the SUMOylation status of p53 was determined by immunoprecipitation of p53 from cell cultures treated with Δ^9-THC (5 μM) for 15 minutes in the presence or absence of the CB_1 receptor antagonist, AM 251 (10 μM; 30 minute pre-treatment). Figure 3.4A depicts the Δ^9-THC-induced decrease in SUMOylated p53 level *via* the CB_1 receptor ($p=0.0032$, ANOVA, n=6). Δ^9-THC treatment for 15 minutes induced a significant decrease in SUMOylated p53 levels from 2551.40 ± 311.62 arbitrary units (mean ± SEM) in vehicle-treated neurones, to 1291.70 ± 144.72 following a 15 minute exposure to Δ^9-THC ($p<0.05$ vs., vehicle, Student Newman Keuls, n=6). AM 251 treatment alone had no effect on SUMOylated p53 levels (2901.70 ± 294.67), however it prevented the Δ^9-THC-induced decrease in SUMOylated p53 expression (2307.30 ± 305.83, $p<0.05$ vs., Δ^9-THC, Student Newman Keuls, n=6). This indicates that Δ^9-THC induces a decrease in SUMOylated p53 levels *via* the CB_1 receptor. Figure 3.4B depicts a sample immunoblot demonstrating the CB_1-dependent decrease in SUMOylated p53 levels induced by Δ^9-THC. The effect of Δ^9-THC on SUMOylated p53 levels was also assessed by immunocytochemistry in fixed cell cultures (Figure 3.4C). SUMO-1 and phospho-p53 were labelled with RPE and fluorescein fluorophores respectively. Cells were viewed by confocal microscopy and colocalisation was determined by the overlap of the two fluorophores. In vehicle-treated neurones, the majority of p53 was present in a SUMOylated form (i). However, in cultures treated with Δ^9-THC for 15 minutes (ii) displayed a decrease in the amount of SUMOylated p53 (Figure 3.4C).

Figure 3.4: The effect of Δ^9-THC on p53-SUMO-1 colocalisation

Cultured cortical neurones were exposed to Δ^9-THC (5 μM) or vehicle for 15 min in the presence or absence of AM 251 (10 μM 30 min pre-treatment). Following treatment, total p53 was immunoprecipitated from cell lysates and the level of SUMO-1 expression in the precipitated p53 was analysed by western immunoblot using an anti-SUMO-1 antibody. SUMO-1-p53 colocalisation was also assessed in fixed neurones treated with either vehicle or Δ^9-THC (5 μM, 15 min) by immunocytochemistry.

A: Pre-incubation of cortical neurones with AM 251 prior to Δ^9-THC exposure abolished the Δ^9-THC-induced decrease in SUMOylated p53 expression observed at 15 min. Results are expressed as means ± SEM, *$p<0.05$ Student Newman Keuls, n=6).

B: A sample western immunoblot demonstrating the decrease in SUMOylated p53 expression after 15 min of Δ^9-THC-treatment (lane 2) compared to SUMOylated p53 expression in control neurones (lane 1). While AM 251 had no effect on SUMOylated p53 expression (lane 3), it abolished the ability of Δ^9-THC to decrease the SUMOylated p53 expression (lane 4).

C: Overlay confocal images of p53 and SUMO-1 stained neurones treated with vehicle (i) or Δ^9-THC 5 μM for 15 min (ii). Colocalised pixels are represented in white.

A

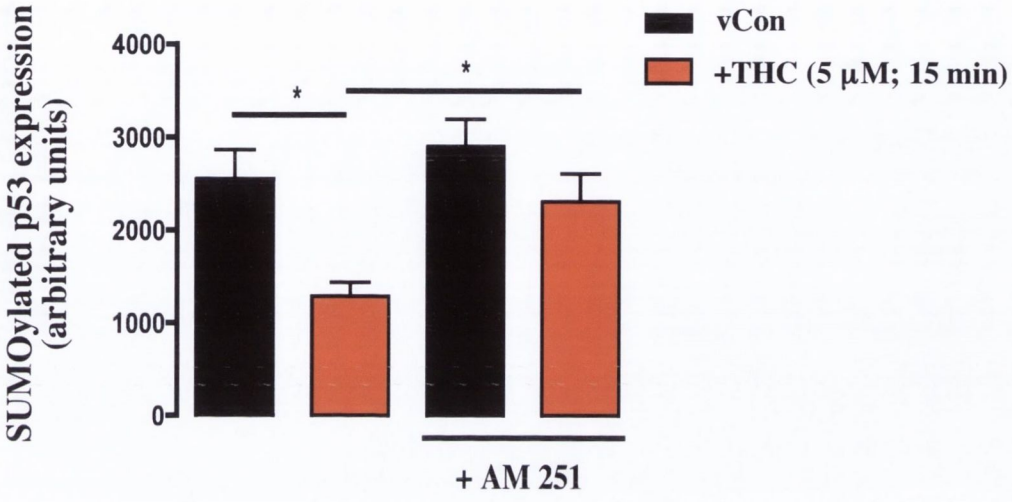
SUMOylated p53 expression
(arbitrary units)
4000
3000
2000
1000
0
*
*
vCon
+THC (5 μM; 15 min)
+ AM 251

B

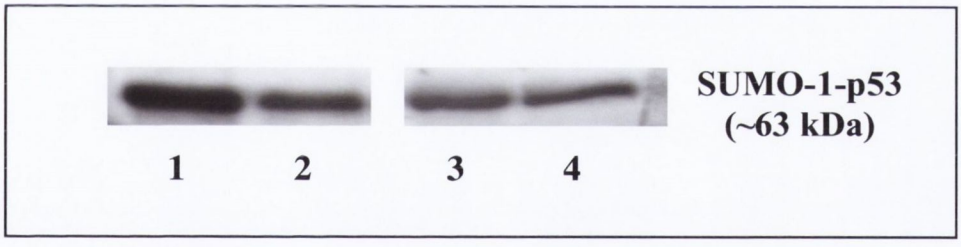
SUMO-1-p53
(~63 kDa)
1
2
3
4

C

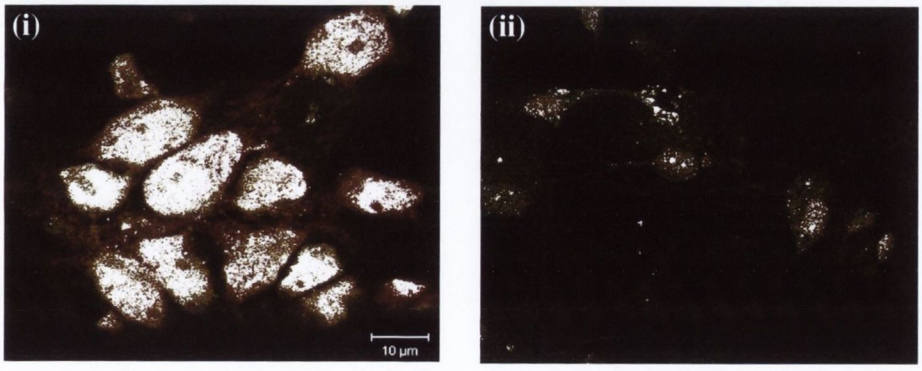
(i)
10 μm
(ii)

3.2.5 The effect of Δ^9-THC on Mdm2 expression

The activation of p53 induces the transcription of the Mdm2 gene. Since Mdm2 is a negative regulator of p53 an auto-regulatory feedback loop is formed which is responsible for the tight control of p53. There are two p53 response elements in the Mdm2 gene, which upon p53 activation generates either; a full-length p90Mdm2 protein or a p76Mdm2 protein depending on which promoter transcription is initiated at (Iwakuma and Lozano, 2003). The p90Mdm2 protein contains the entire p53 binding site and inhibits p53 function whilst the p76Mdm2 protein has lost half of the p53 interaction site and cannot bind p53 (Perry, 2004). Mdm2 can also be cleaved by caspase-like enzyme activity during apoptosis and in non-apoptotic cells generating a 60 kD fragment (p60Mdm2; Pochampally *et al.*, 1999, 1998). To further establish the role of Δ^9-THC in post translational modification of p53, the effect of Δ^9-THC on Mdm2 was assessed using western immunoblot. Cultured cortical neurones were exposed to Δ^9-THC (5 μM) for various time points (5 - 120 minutes) and expression levels of Mdm2, induced by p53 activation, were assessed. Figure 3.5 depicts the Δ^9-THC-induced expression of the Mdm2 protein ($p<0.0001$, ANOVA, $n=6$). Following Δ^9-THC treatment for 5 minutes, Mdm2 expression was 0.56 ± 0.06 arbitrary units (mean ± SEM) which was significantly higher to that found in cells treated with vehicle (0.33 ± 0.03; $p<0.001$ vs., vehicle, Student Newman Keuls, $n=6$). However, the induction of Mdm2 protein was not maintained at subsequent time points (15 - 120 minutes; Figure 3.5B lanes 2 - 6). This result provides additional corroborating evidence that Δ^9-THC regulates the p53 protein. A sample immunoblot demonstrating the induction of the Mdm2 protein after 5 minutes of Δ^9-THC treatment is shown in Figure 3.5B. β actin expression was monitored to ensure equal protein loading. Sample confocal images demonstrating the transient increase in Mdm2 expression following Δ^9-THC treatment are shown in Figure 3.5C.

Figure 3.5: The effect of Δ^9-THC on Mdm2 expression

A: A significant increase in the Mdm2 protein was found following treatment with Δ^9-THC for 5 min. Treatment with Δ^9-THC at other time points (15 - 120 min) did not induce the expression of this form of Mdm2. Results are expressed as mean ± SEM for 6 observations, ***$p<0.001$ vs., vehicle, Student Newman Keuls, n=6.

B: A sample western immunoblot demonstrating the induction of the Mdm2 (arrow ≈ 72 kDa) protein expression at 5 min of Δ^9-THC treatment (lane 2). Lane 1 represents vehicle-treated neurones, neurones treated with Δ^9-THC for 15 min (lane 3), 30 min (lane 4), 60 min (lane 5) and neurones treated with Δ^9-THC for 120 min (lane 6). The p60Mdm2 cleavage product and C terminal fragment are also visable on blot.

C: Representitive images of fluorescently labelled Mdm2 in neurones treated with vehicle (i), and neurones exposed to Δ^9-THC for 5 (ii), 15 (iii) and 30 min (iv). Nuclei are stained with Hoechst dye (blue).

A

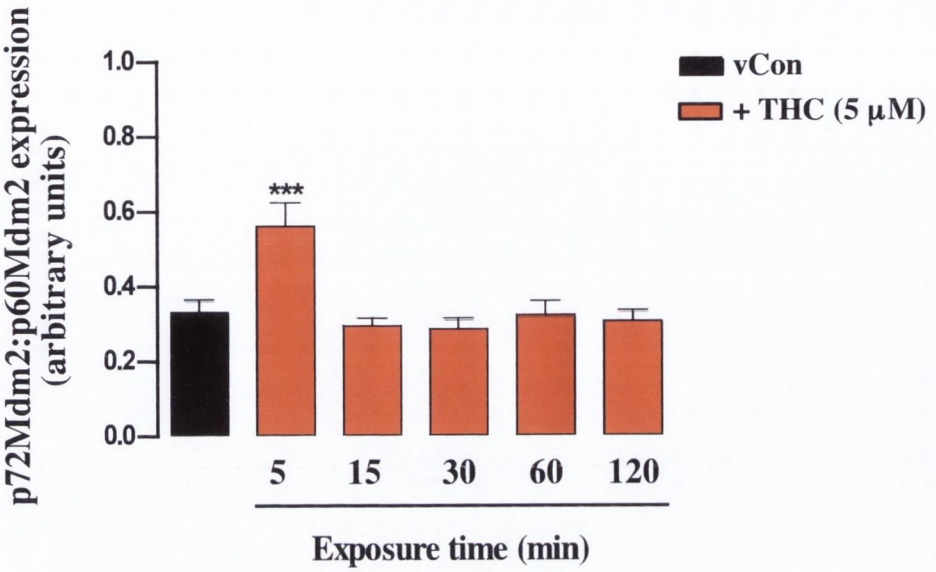
p72Mdm2:p60Mdm2 expression
(arbitrary units)
1.0
0.8
0.6
0.4
0.2
0.0
***
vCon
+ THC (5 μM)
5
15
30
60
120
Exposure time (min)

B

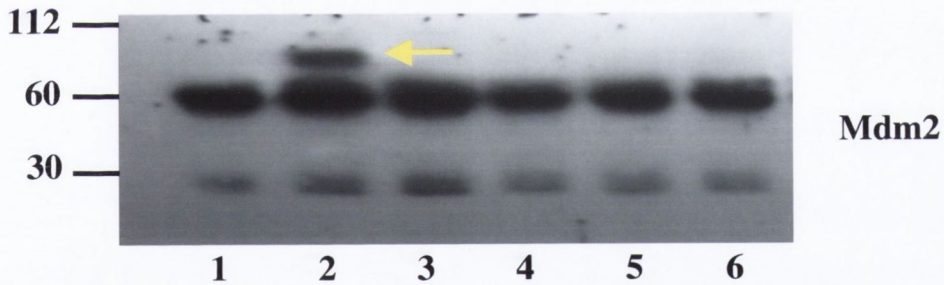
112
60
30
Mdm2
1
2
3
4
5
6

C

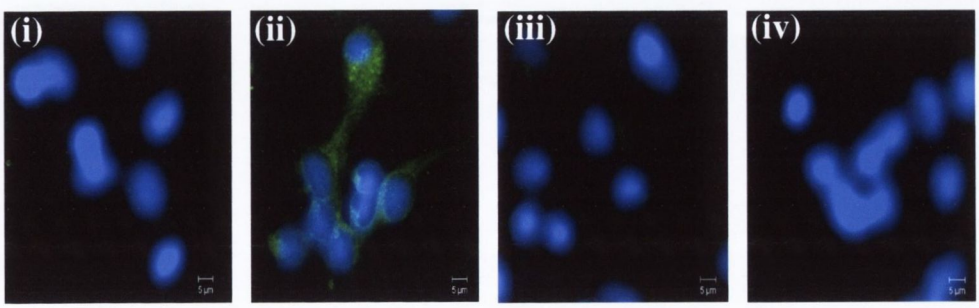
(i)
(ii)
(iii)
(iv)

3.2.6 Transfection efficiency optimisation

In these experiments siRNA mediated knock down of p53 in cultured cortical neurones was used to investigate the role of the tumour suppressor in Δ^9-THC-induced neuronal apoptosis. siRNA induces a naturally occurring defence pathway which culminates in the degradation of a specific protein's mRNA. RNA interference (RNAi) has become an invaluable tool for the application of both transient and stable gene repression during *in vitro* studies. RNAi is also advantageous since it negates the need for the time-consuming production of knockout animals. Custom ON-TARGET Plus Smart pool of small interfering RNA (siRNA), designed by Dharmacon to contain a mixture of 4 siRNAs targeting rat p53 (Gen Bank™ accession number NM_030989; p53 siRNA), was used to downregulate p53 gene expression. A control siRNA duplex containing at least 4 mismatches to any rat gene (ON-TARGET Plus siControl Non-Targeting siRNA; Con siRNA) was used in parallel experiments. To identify the optimum transfection lipid and monitor the uptake pattern of siRNA, neurones were incubated in fluorescein-labelled control siRNA (100 nM) for 24 and 48 hours using 4 different transfection lipids (Dharmacon transfection lipid 1, 2, 3 or 4). It was found that a 24 hour treatment was sufficient to deliver siGlo to the perinuclear area (Figure 3.6A). After 48 hours incubation (Figure 3.6B) increased uptake of siGlo was observed partitioning into both cytoplasmic and nuclear compartments. Transfection lipid number 3 provided the most intense fluorescent signal at both 24 and 48 hours, signifying that it was the optimal transfection reagent for our cultured neuronal preparations (Figure 3.6A and B (iii)). To determine the effectiveness of the p53 siRNA, p53 expression was assessed by immunocytochemistry and western immunoblot. In cortical neurones transfected with transfection lipid 3 and p53 siRNA for 48 hours, no increase in the level of p53 was detected after exposure to Δ^9-THC (5 μM) for 5 minutes ($p<0.05$ vs., con siRNA and Δ^9-THC (5 μM; 5 min), Student's t-test, n=3 observations; Figure 3.7A). Western immunoblot analysis corroborated the downregulation of the p53 gene (Figure 3.7B).

Figure 3.6: Transfection efficiency optimisation

Cultured cortical neurones were pre-incubated with transfection lipid 1, 2, 3 or 4 in the presence of fluorescein-labelled non coding siRNA (siGlo; 100 nM) for 24 and 48 hours at 37°C. Treated cells were fixed and incorporated siGlo was assessed using confocal microscopy.

A: Incubation of cortical neurones with transfection lipid number 1 (i), number 2 (ii), number 3 (iii) and number 4 (iv) for 24 hours. Efficent siGlo uptake was observed in neurones transfected with lipid 3 for 24 hours.

B: Incubation of cortical neurones with transfection lipid number 1 (i), number 2 (ii), number 3 (iii) and number 4 (iv) for 48 hours. After 48 hours transfection nuclear localisation of siGlo was observed. Arrows indicate intense nuclear uptake.

A

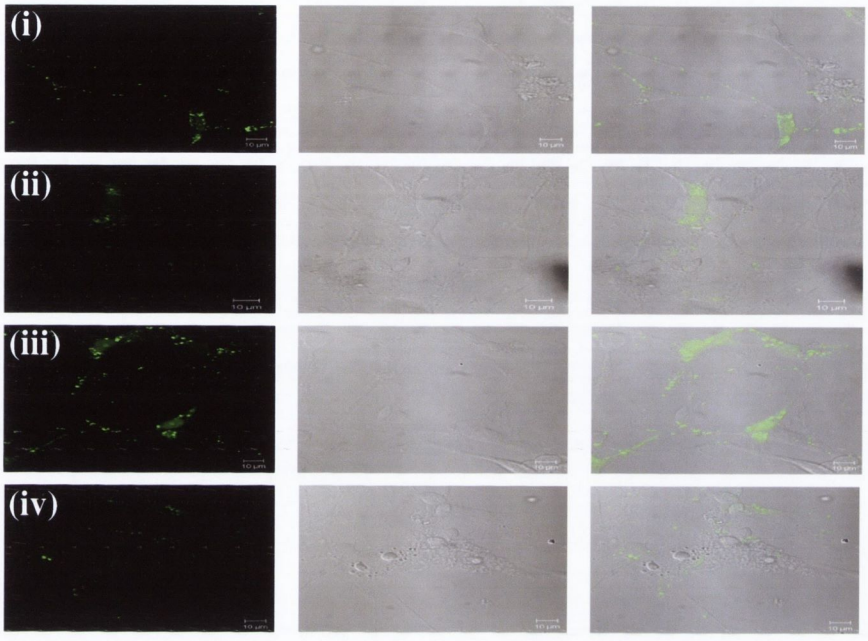

B

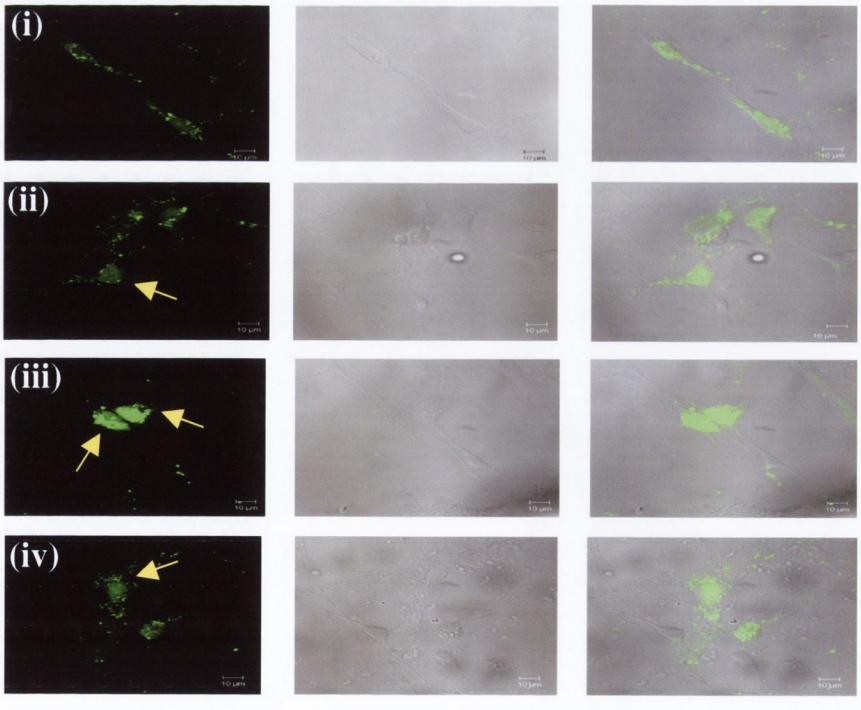

Figure 3.7: The successful depletion of p53 protein with siRNA

Cultured cortical neurones were pre-incubated with transfection lipid 3 in the presence of con siRNA or p53 siRNA (100 nM) for 48 hours at 37°C. Neurones were then exposed to Δ^9-THC (5 μM) for 5 min, fixed and total-p53 expression was determined using immunocytochemistry (panel A). Total-p53 expression was assessed by western immunoblot (panel B).

A: Δ^9-THC induced p53 protein expression in neurones transfected with con siRNA (i) but not in neurones transfected with p53-siRNA (ii). Results are expressed as means ± SEM, *$p<0.05$, vs., con siRNA and Δ^9-THC, Student's t test, n=3 observations. Arrows indicate cells showing an increase in p53 expression.

B: A sample immunoblot demonstrating that p53 siRNA treatment for 48 hr (lane 2) reduced p53 protein expression as compared to con siRNA-treated neurones (lane 1).

A

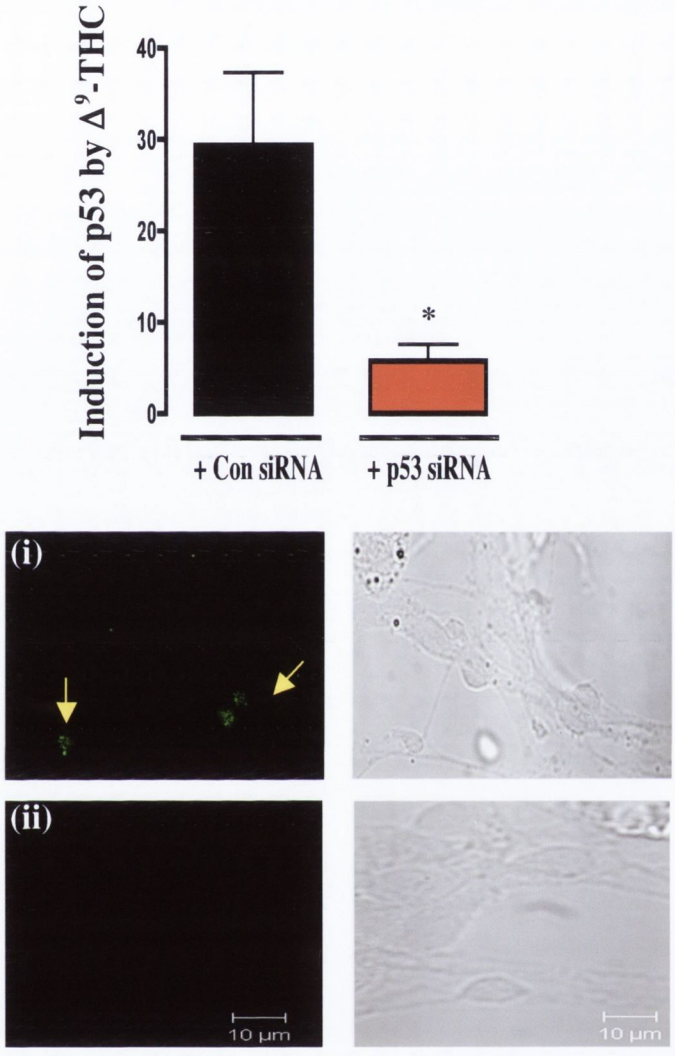
Induction of p53 by Δ9-THC
40
30
20
10
0
*
+ Con siRNA
+ p53 siRNA
(i)
(ii)
10 μm
10 μm

B

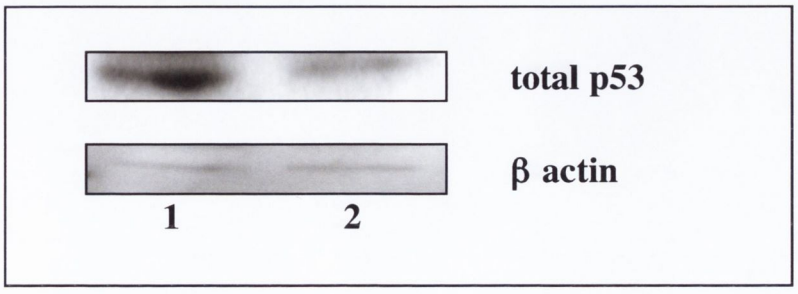
total p53
β actin
1
2

3.2.7 p53 down-regulation by p53 specific siRNA prevents Δ^9-THC-induced DNA fragmentation

Fragmentation of nuclear material into oligonucleosomal moieties is a hallmark of apoptosis and can be assessed by a variety of techniques. Δ^9-THC-induced apoptosis reaches maximal levels after 2 - 3 hours post-treatment (Campbell, 2001; Downer *et al.*, 2001) therefore this time point was used to determine the role of p53 in Δ^9-THC-induced DNA fragmentation. In this study, the TUNEL (see methods section 2.7) technique was used to assess the levels of fragmented DNA in cultured cortical neurones following siRNA-mediated depletion of p53. Figure 3.8 demonstrates that p53 siRNA significantly reduces Δ^9-THC-induced DNA fragmentation ($p=0.0001$, ANOVA, n=6). In vehicle-treated cells, 8.70 ± 0.58% (mean ± SEM) of cells displayed fragmented DNA (TUNEL positive) and this was significantly increased to 34.11 ± 1.55% in cells treated with Δ^9-THC (5 μM) for 2 hours ($p<0.001$, Student Newman Keuls, n=6). Exposure of cells to p53 siRNA (100 nM) for 48 hours prior to Δ^9-THC (5 μM) treatment prevented the Δ^9-THC-induced increase in TUNEL staining (9.49 ± 1.37% TUNEL positive cells). In cells pre-treated with con siRNA (100 nM) the Δ^9-THC-induced increase in DNA fragmentation was retained (39.52 ± 4.09% TUNEL positive cells, $p<0.001$ vs., vehicle in the presence of Con siRNA Student Newman Keuls, n=6). These results demonstrate that depletion of p53 by siRNA prevents Δ^9-THC-induced DNA fragmentation. These data are also consistent with our previous studies using a pharmacological inhibitor of p53, pifithrin-α (100 nM), to block Δ^9-THC-induced apoptosis (Downer *et al.*, 2007a).

Figure 3.8: p53 down-regulation by p53 specific siRNA prevents Δ^9-THC-induced DNA fragmentation

Cultured cortical neurones were pre-incubated with transfection lipid 3 in the presence of con siRNA or p53 siRNA (100 nM) for 48 hours at 37°C. Neurones were treated with vCon or Δ^9-THC (5 μM) for 2 hours, fixed and DNA fragmentation assessed by TUNEL. Fluorescein (apoptotic cells) and propidium iodide (all cells) overlay images are shown.

A: Pre-incubation of neurones with p53 siRNA prior to Δ^9-THC exposure abolished the Δ^9-THC-induced increase in DNA fragmentation. Results are expressed as mean ± SEM, ***p<0.001 vs., vehicle, &&& vs. vehicle in the presence of Con siRNA, +++p<0.001 vs., Δ^9-THC in the presence of Con siRNA, Student Newman Keuls, n=6.

B: Representative images of neurones treated with (i) vehicle and (ii) Δ^9-THC in the presence of con siRNA, and neurones treated with (iii) vehicle and (iv) Δ^9-THC in the presence of p53 siRNA. Arrows indicate cells displaying fragmented DNA.

A

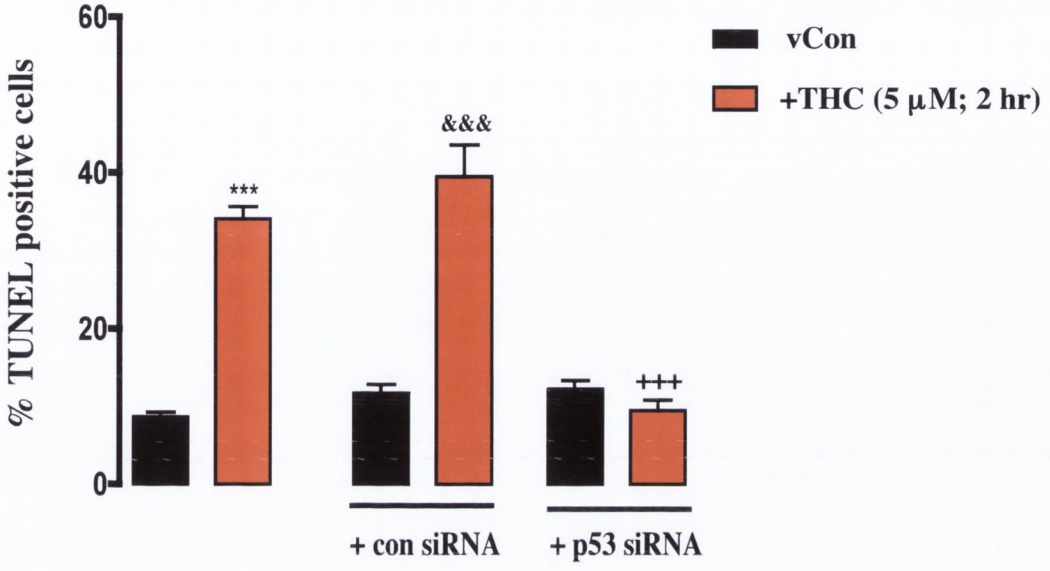
% TUNEL positive cells
60
40
20
0
***
&&&
+++
vCon
+THC (5 μM; 2 hr)
+ con siRNA
+ p53 siRNA

B

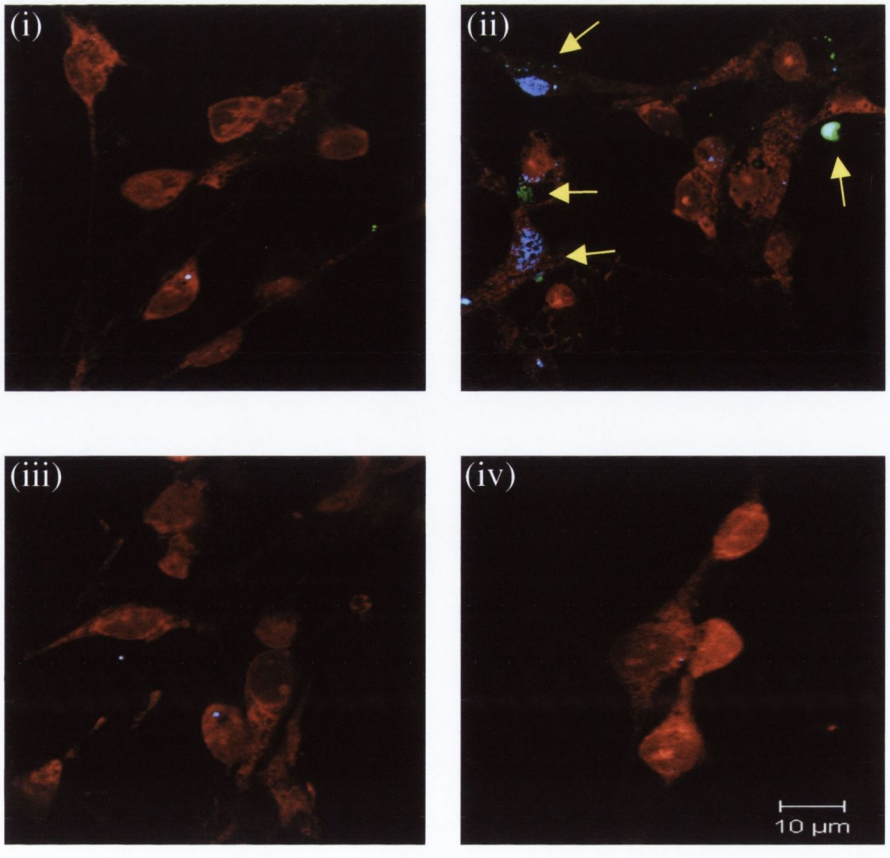
(i)
(ii)
(iii)
(iv)
10 μm

3.2.8 Δ^9-THC induces an increase in phospho-SyK^{tyr323} expression through the CB_1 receptor

The role of the non-receptor protein tyrosine kinase, SyK in cannabinoid-mediated neurotoxicity was examined in this study. SyK has a widespread expression pattern in cells such as, haematopoietic cells, fibroblasts, epithelial cells, hepatocytes and neuronal cells (Yanagi *et al.*, 2001). Previous results from our laboratory have found that cultured cortical neurones do express SyK at early time points of apoptosis induced by $A\beta_{1\text{-}42}$. SyK mediates a diverse set of cellular responses such as, cell proliferation, differentiation and phagocytosis (Coopman and Mueller, 2006; Yanagi *et al.*, 2001). The involvement of SyK in the fusion of B cell receptor-carrying endosomes to lysosomes in the immature B cell line DT40 (He *et al.*, 2005) is of particular interest to our investigation into the effects of cannabinoids on the lysosomal system (see chapter 4). In addition, the finding that SyK is required for the LPS-induced c-Jun N-terminal kinase activation is of interest since previous work from our laboratory has shown Δ^9-THC modulates the expression of JNK (Arndt *et al.*, 2004; Downer *et al.*, 2003).

To investigate the effect of Δ^9-THC on phospho-SyK^{tyr323} expression, cultured cortical neurones were exposed to Δ^9-THC (5 μM) for 15 minutes and phospho-SyK^{tyr323} (p-SyK^{tyr323}) expression assessed by western immunoblot (Figure 3.9A). In vehicle-treated neurones, p-SyK^{tyr323} expression was 105.00 ± 14.84 arbitrary units which was significantly increased to 357.00 ± 133.10 ($p<0.05$, vs., vehicle, Mann-Whitney t test, n=8-13). While treatment with AM 251 (10 μM) alone had no effect on p-SyK^{tyr323} expression (113.30 ± 16.90) the Δ^9-THC-induced increase in p-SyK^{tyr323} was abolished when cells were pre-treated with AM 251 prior to Δ^9-THC exposure (86.83 ± 26.42; $p<0.05$ vs., Δ^9-THC, Mann-Whitney t test, n=8-13). p-SyK^{tyr323} immunoreactivity was also detected by immunocytochemistry and followed the same expression pattern (Figure 3.9B).

Figure 3.9: Δ^9-THC induces an increase in phospho-SyK^{tyr323} expression through the CB_1 receptor

Cultured cortical neurones were pre-incubated with AM 251 (10 μM) for 30 minutes prior to Δ^9-THC (5 μM) treatment for 15 minutes. Cell protein was harvested and analysed for phospho-SyK^{tyr323} (p-SyK^{tyr323}) expression using western immunoblot (panel A). In addition some cells were fixed after treatment and p-SyK^{tyr323} was labelled using immunocytochemistry (panel B).

A: Pre-incubation of neurones with AM 251 prior to Δ^9-THC exposure abolished the Δ^9-THC-induced increase in p-SyK^{tyr323} expression observed at 15 min. Inset: a sample western immunoblot showing that Δ^9-THC treatment for 5 minutes increases p-SyK^{tyr323} expression (lane 2) as compared to control neurones (lane 1). Exposure of cells to AM 251 alone had no effect on p-SyK^{tyr323} expression (lane 3). The increase in p-SyK^{tyr323} expression was prevented by AM 251 pre-treatment (lane 4). Results are expressed as mean ± SEM, *$p<0.05$ vs., vehicle, +$p<0.05$ vs., Δ^9-THC, Mann Whitney test, n=8-13.

B: Sample immunofluorescent images of p-SyK^{tyr323} immunoreactivity in (i) vehicle, (ii) Δ^9-THC, (iii) AM 251 and (iv) AM 251 and Δ^9-THC-treated neurones.

A

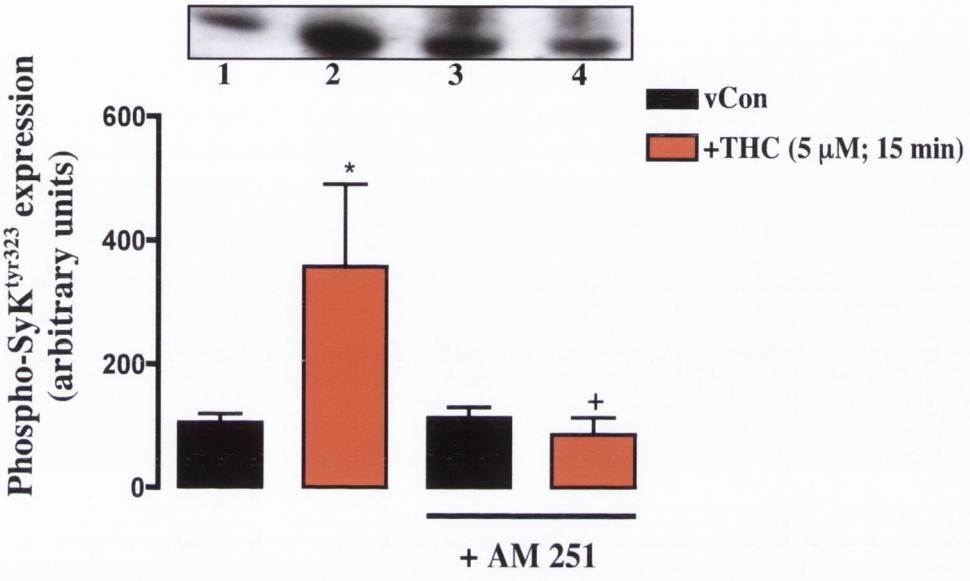
1
2
3
4
vCon
+THC (5 μM; 15 min)
Phospho-SyK^{tyr323} expression
(arbitrary units)
600
400
200
0
*
+
+ AM 251

B

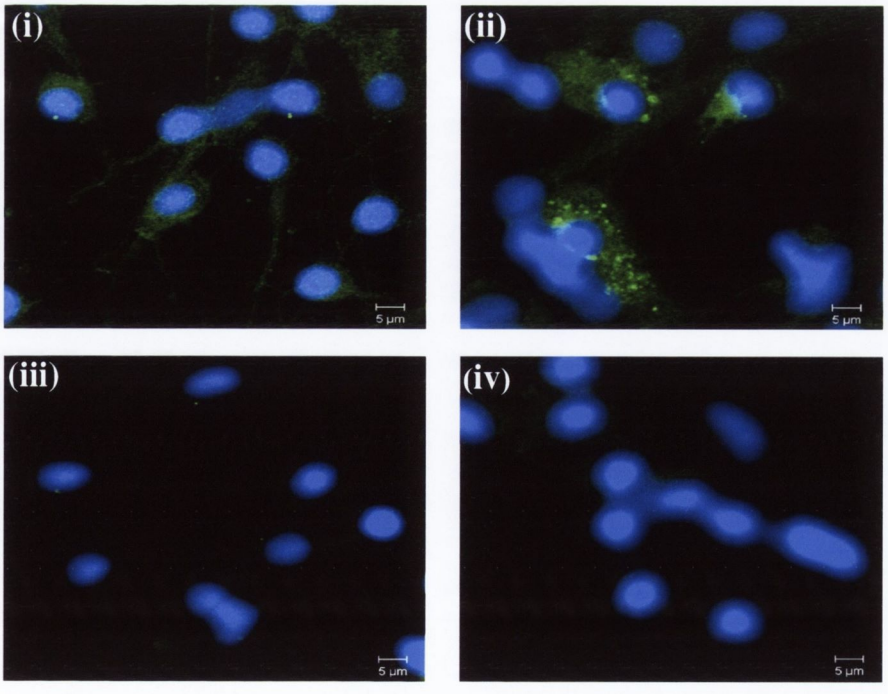
(i)
(ii)
(iii)
(iv)
5 μm

3.2.8 Δ^9-THC induces an increase in phospho-SyK^{tyr323} expression through the CB_1 receptor

The role of the non-receptor protein tyrosine kinase, SyK in cannabinoid-mediated neurotoxicity was examined in this study. SyK has a widespread expression pattern in cells such as, haematopoietic cells, fibroblasts, epithelial cells, hepatocytes and neuronal cells (Yanagi *et al.*, 2001). Previous results from our laboratory have found that cultured cortical neurones do express SyK at early time points of apoptosis induced by $A\beta_{1\text{-}42}$. SyK mediates a diverse set of cellular responses such as, cell proliferation, differentiation and phagocytosis (Coopman and Mueller, 2006; Yanagi *et al.*, 2001). The involvement of SyK in the fusion of B cell receptor-carrying endosomes to lysosomes in the immature B cell line DT40 (He *et al.*, 2005) is of particular interest to our investigation into the effects of cannabinoids on the lysosomal system (see chapter 4). In addition, the finding that SyK is required for the LPS-induced c-Jun N-terminal kinase activation is of interest since previous work from our laboratory has shown Δ^9-THC modulates the expression of JNK (Arndt *et al.*, 2004; Downer *et al.*, 2003).

To investigate the effect of Δ^9-THC on phospho-SyK^{tyr323} expression, cultured cortical neurones were exposed to Δ^9-THC (5 μM) for 15 minutes and phospho-SyK^{tyr323} (p-SyK^{tyr323}) expression assessed by western immunoblot (Figure 3.9A). In vehicle-treated neurones, p-SyK^{tyr323} expression was 105.00 ± 14.84 arbitrary units which was significantly increased to 357.00 ± 133.10 ($p<0.05$, vs., vehicle, Mann-Whitney t test, n=8-13). While treatment with AM 251 (10 μM) alone had no effect on p-SyK^{tyr323} expression (113.30 ± 16.90) the Δ^9-THC-induced increase in p-SyK^{tyr323} was abolished when cells were pre-treated with AM 251 prior to Δ^9-THC exposure (86.83 ± 26.42; $p<0.05$ vs., Δ^9-THC, Mann-Whitney t test, n=8-13). p-SyK^{tyr323} immunoreactivity was also detected by immunocytochemistry and followed the same expression pattern (Figure 3.9B).

Figure 3.9: Δ^9-THC induces an increase in phospho-SyK^{tyr323} expression through the CB_1 receptor

Cultured cortical neurones were pre-incubated with AM 251 (10 μM) for 30 minutes prior to Δ^9-THC (5 μM) treatment for 15 minutes. Cell protein was harvested and analysed for phospho-SyK^{tyr323} (p-SyK^{tyr323}) expression using western immunoblot (panel A). In addition some cells were fixed after treatment and p-SyK^{tyr323} was labelled using immunocytochemistry (panel B).

A: Pre-incubation of neurones with AM 251 prior to Δ^9-THC exposure abolished the Δ^9-THC-induced increase in p-SyK^{tyr323} expression observed at 15 min. Inset: a sample western immunoblot showing that Δ^9-THC treatment for 5 minutes increases p-SyK^{tyr323} expression (lane 2) as compared to control neurones (lane 1). Exposure of cells to AM 251 alone had no effect on p-SyK^{tyr323} expression (lane 3). The increase in p-SyK^{tyr323} expression was prevented by AM 251 pre-treatment (lane 4). Results are expressed as mean ± SEM, *$p<0.05$ vs., vehicle, +$p<0.05$ vs., Δ^9-THC, Mann Whitney test, n=8-13.

B: Sample immunofluorescent images of p-SyK^{tyr323} immunoreactivity in (i) vehicle, (ii) Δ^9-THC, (iii) AM 251 and (iv) AM 251 and Δ^9-THC-treated neurones.

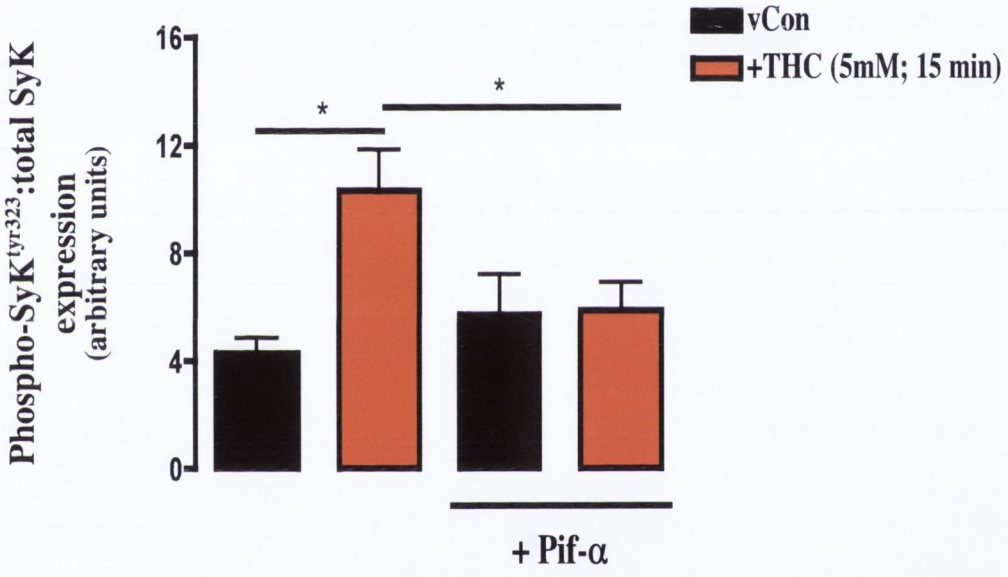
vCon
+THC (5mM; 15 min)
Phospho-SyK^{tyr323}:total SyK expression (arbitrary units)
16
12
8
4
0
*
*
+ Pif-α

3.2.10 Δ^9-THC-induced DNA fragmentation is dependent on SyK activity

Since SyK activity was increased by Δ^9-THC *via* p53 it was decided that an investigation into whether SyK activity was required for the induction of DNA fragmentation, which is an end stage marker of Δ^9-THC-induced apoptosis. In this study, the TUNEL (see methods section 2.7) technique was used to assess levels of DNA fragmentation in cultured cortical neurones following the pharmacological inhibition of SyK. Figure 3.11 shows the SyK dependent nature of Δ^9-THC-induced DNA fragmentation ($p=0.0022$, ANOVA, n=6 observations). In vehicle-treated cells, 20 ± 6% (mean ± SEM) of cells displayed fragmented DNA (TUNEL positive) and this was significantly increased to 55 ± 8% in cells treated with Δ^9-THC (5 μM) for 2 hours ($p<0.01$, Student Newman Keuls, n=6 observations). While treatment with SyKi (50 nM) had no effect on neuronal viability (34 ± 15% TUNEL positive), it prevented the Δ^9-THC-induced increase in TUNEL staining (15 ± 7% TUNEL positive cells). These results demonstrate that Δ^9-THC-induced DNA fragmentation is dependent on SyK activity. Sample images of TUNEL stained neurones are shown in Figure 3.11B.

Figure 3.11: Δ^9-THC-induced DNA fragmentation is dependent on SyK activity

Neurones were treated with SyKi (50 nM) for 60 minutes prior to exposure to Δ^9-THC (5 μM) for 2 hours, fixed and fragmented DNA was assessed using the TUNEL technique.

A: Pre-incubation of neurones with SyKi prior to Δ^9-THC exposure abolished the Δ^9-THC-induced increase in DNA fragmentation observed at 2 hours. Results are expressed as means ± SEM, **$p<0.01$, n=6 observations.

B: Representative images of TUNEL stained neurones demonstrating Δ^9-THC-induced DNA fragmentation in (i) vehicle, (ii) Δ^9-THC, (iii) SyKi alone and (iv) neurones treated with Δ^9-THC in the presence of SyKi. Arrows indicate cells displaying fragmented DNA. Scale bar is 10 μm.

A

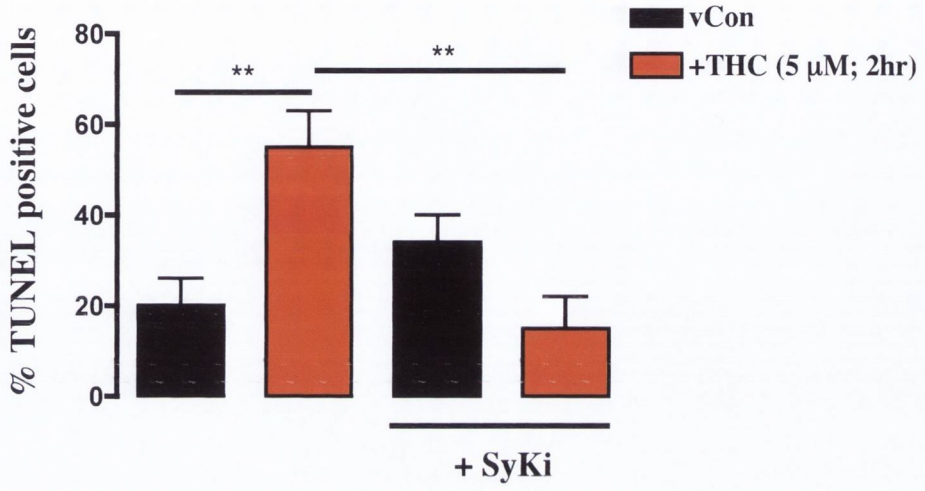
% TUNEL positive cells
80
60
40
20
0
**
**
vCon
+THC (5 μM; 2hr)
+ SyKi

B

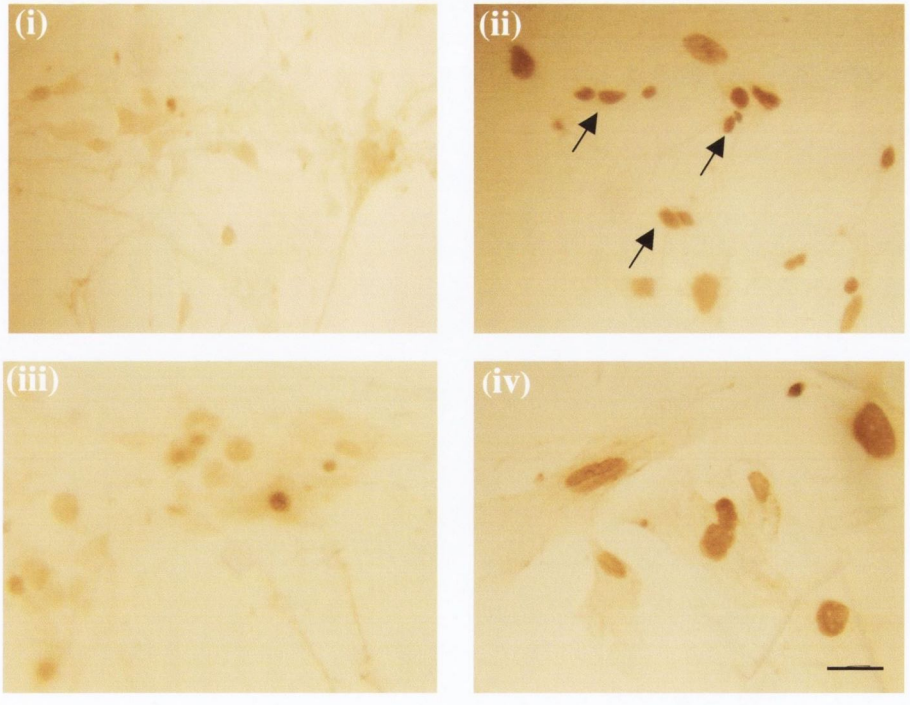
(i)
(ii)
(iii)
(iv)

3.3 Discussion

The aim of this study was to corroborate the neurotoxic effects of Δ^9-THC *in vitro* and to further characterise the role of specific signal transduction moieties that are involved in the neurotoxic pathway which we have previously shown to be induced by Δ^9-THC (Campbell, 2001; Downer *et al.*, 2003, 2001). *In vitro* Δ^9-THC neurotoxicity was examined using primary cerebral cortical neurones to characterise signal transduction mechanisms contributing to toxicity. In accordance to our previous findings, Δ^9-THC induced DNA fragmentation in the nucleus of cultured neurones, reflecting an apoptotic response to Δ^9-THC. The Δ^9-THC-induced DNA fragmentation reached a significant level after 2 hours Δ^9-THC exposure, however, no significant changes were observed after 15 minutes exposure. Δ^9-THC was found to induce the phosphorylation of the tumour suppressor protein, p53 at serine 15 (Downer *et al.*, 2007a). The ability of Δ^9-THC to induce the activation of p53 was blocked by a specific inhibitor of JNK1, D-JNK-1 (JNKi), indicating that this stress-activated protein kinase is essential for both the activation of p53 and the induction of Δ^9-THC-induced neurotoxicity. Furthermore, Δ^9-THC significantly increased the level of unconjugated SUMO-1 protein in the cytosol in a time-dependent manner with a maximal response observed after 15 minutes Δ^9-THC treatment. Following additional colocalisation experiments, Δ^9-THC induced the removal of SUMO from p53. The CB_1 receptor antagonist, AM 251, abated the effect of Δ^9-THC on the SUMOylation status of p53 as shown by p53 immunoprecipitation. Δ^9-THC induced an increase in the expression of the p53-responsive protein, Mdm2, after 5 minutes exposure to Δ^9-THC, which coincides with the increase in p-p53^{ser15}. A siRNA approach was used to further delineate the contribution of p53 in Δ^9-THC-induced neuronal death. To enhance the cellular uptake, siRNA complexes were pre-incubated with 4 different transfection lipids. In order to assess which transfection lipid delivered the most siRNA to neurones, FAM-labelled siRNA were pre-incubated with each transfection lipid and fluorescence in the nucleus was used to measure transfection efficiency. Dharmacon lipid number 3 displayed the most uptake of fluorescently labelled siRNAs to the nucleus and so it was the transfection lipid used in all further experiments. Treatment of neurones with specific siRNAs targeted towards rat p53 mRNA effectively reduced the expression of

the p53 protein as assessed by immunocytochemistry and western immunoblot. The siRNA-mediated reduction of p53 protein expression prevented Δ^9-THC-induced DNA fragmentation. This corroborates our previous findings that showed the pharmacological inhibition of p53, using pifithrin-α prevented Δ^9-THC-induced DNA fragmentation (Downer *et al.*, 2007a). In addition to these findings, a new signalling kinase, SyK, was regulated by Δ^9-THC *via* the CB_1 receptor. Treatment of neurones with pifithrin-α, a pharmacological inhibitor of p53 activity blocked the activation of SyK and an inhibitor of SyK activity, sulfonamide, prevented Δ^9-THC-induced DNA fragmentation. The use of these inhibitors indicate that the activity of both p53 and SyK is required for the downstream signalling of Δ^9-THC neurotoxicity. Data herein suggest that CB_1 receptor activation by Δ^9-THC induces a series of signalling cascades where p53 and SyK play a central role, hence they may be pertinent in mediating the neurotoxic properties of Δ^9-THC.

Apoptosis, or programmed cell death, is a normal physiological process, which a cell actively takes part in its own destruction without triggering an inflammatory response (Kerr *et al.*, 1972). This process is characterised by distinct morphological and biochemical changes to the cell, including the fragmentation of DNA and the activation of pro-apoptotic proteins. The proclivity of Δ^9-THC to induce DNA fragmentation was assessed by the fluorometric TUNEL technique. This technique provides a quantitative assessment of cell death in cultured cells and tissue sections. In addition, the TUNEL technique also allows the examination of cells for the morphological signs of apoptosis such as, membrane blebbing, cell shrinkage and the formation of nuclear bodies. The induction of DNA fragmentation was observed following treatment with Δ^9-THC for 2 hours, which is in line with our previous observations and coincides with the time frame of the induction of cannabis' psychoactive effects (Downer *et al.*, 2001; Chiang and Barnett, 1984). These observations corroborate our previous conclusion that the duration of cannabinoid exposure determines the level and appearance of neurotoxicity. This rapid initiation of Δ^9-THC-induced neurotoxicity is comparable to that observed in primary hippocampal cultures and dendritic cells derived from murine bone marrow (Chan *et al.*, 1998; Do *et al.*, 2004). However, Sánchez *et al.*, (1998) have shown that

treatment with Δ^9-THC for 4 - 5 days induced apoptosis in transformed C6.9 glioma cell line, however they failed to see this in primary cells.

We have previously shown that Δ^9-THC regulates both JNK and p53 in cultured cortical neurones (Downer *et al.*, 2003, 2007a). Several kinases have the ability to phosphorylate and stabilise p53 *e.g.,* casein kinases, and members of the MAP kinase family, such as, p38 MAPK, ERK, and JNK (Blatt and Glick, 2001). Furthermore, several papers indicate that JNK acts upstream of p53 and induces the phosphorylation on multiple separate amino acid residues in response to a diverse set of cell stress stimuli (for review see Wu, 2004). There is evidence that p53 becomes phosphorylated on serine 15 following cellular stress and that this disrupts the interaction of p53 with its negative regulatory protein, Mdm2 (Shieh *et al.*, 1997). The Δ^9-THC-induced increase in p53 phosphorylation was blocked with JNKi, this coupled with our previous findings regarding the early activation of JNK1 by Δ^9-THC, lead us to propose that the upstream activation of the JNK1 signalling pathway couples Δ^9-THC to the activation of p53 in this *in vitro* system.

The mechanism of p53-induced apoptosis has been extensively studied and involves many different proteins including SUMO and Mdm2. The modification with SUMO or SUMOylation has been linked to pathways associated with a diverse set of cellular functions *e.g.,* intracellular trafficking, cell cycle control, DNA repair and replication, RNA metabolism and cell signalling (Hay, 2005). Although nuclear proteins were the first proteins that were found to be SUMOylated, both cytoplasmic and plasma membrane associated proteins are modified by SUMO (Boddy *et al.*, 1996; Desterro *et al.*, 1998; Okura *et al.*, 1996). p53 can be post translationally modified by at least two ubiquitin like (UBL) proteins, SUMO-1 and NEDD8 (Watson and Irwin, 2006). The first report that p53 was a target of SUMO-1 conjugation came from a report that human Ubc9, the SUMO E2 transferring enzyme, associates with p53 in yeast (Shen *et al.*, 1996). The association of p53 with SUMO-1 has been linked to the regulation of the transcriptional activity, intracellular location and the apoptotic potential of p53 (Gostissa *et al.*, 1999; Rodriguez *et al.*, 1999; Carter *et al.*, 2007; Müller *et al.*, 2000). However, since these initial reports there have been conflicting reports as to the functional effects of this p53 modification, hence no consensus as

regards p53 SUMOylation has been reached (for reviews see Melchior and Hengst, 2002; Watson and Irwin, 2006). In addition, some authors have questioned the physiological relevance of SUMOylation since most SUMO targets, including p53, are modified at very low steady state levels and that there is a limited pool of 'free' unconjugated SUMO-1 available for use (Bossis and Melchior, 2006; Johnson, 2004). However, the role of p53 SUMOylation is perhaps a more subtle modification that may be acting in conjunction to other post translational modifications *e.g.,* phosphorylation, acetylation and even the interaction between p53 interacting proteins such as, Mdm2. The phosphorylation of a protein can act as a positive or negative signal for the SUMOylation of a protein *e.g.,* the phosphorylation of PML nuclear body, a protein involved in the repression of gene expression and apoptotic pathways, induces the deconjugation of SUMO-1 at the beginning of mitosis (Everett *et al.*, 1999). Interestingly, the phosphorylation of both c-Jun and p53 induces a deSUMOylation of the respective protein (Muller *et al.,* 2000; Lin *et al.*, 2004). The findings of Lin *et al.*, are of particular interest, due to their observations that phosphorylation on serine 20 induced by checkpoint kinase 2 (cdk2) in response to DNA damage was responsible for the deSUMOylation of the p53 protein. These results, coupled with our observations on the effect of Δ^9-THC on the SUMOylation status of p53, indicate that the phosphorylation of certain proteins during periods of cell stress can cause the protein to become deSUMOylated. Whether phosphorylation inhibits the access of SUMO conjugating enzymes or recruits SUMO deconjugating enzymes remains unknown. However, loss of these enzymes causes G_2/M cell cycle block in yeast and early embryonic death in mice, which indicate that they are fundamental proteins required for life, a similarity shared with many kinases and phosphatases (Bossis and Melchior, 2006; Li and Hochstrasser, 1999; Nacerddine *et al.*, 2005). These observations have prompted some authors to go as far as comparing SUMOylation with phosphorylation, at least in regards to the frequency of occurrence and the large number of potential substrates (Marx, 2005; Bossis and Melchior, 2007). Interestingly, the SUMO regulatory system is modified by stresses, with different cell stressors such as high oxidative stress, heat and osmotic shock, resulting in specific alterations of SUMO regulatory enzymes (Manza *et al.*, 2004; Zhou *et al.*, 2004). Furthermore, these

stressors increase the conjugation of SUMO-2/3 but not SUMO-1 to substrate proteins, however this could be simply due to the large pool of free SUMO-2 and -3 compared to the small pool of free SUMO-1 that is present under normal physiological conditions (Saitoh and Hinchey, 2000). Manza *et al.*, (2004) have shown that stress induces a near complete shift of SUMO-1, -2 and -3 to a different set of protein targets, including proteins that function as chaperones and components of cellular stress responses. Taken together, these findings indicate that the SUMOylation status of a protein and the activity of the SUMOylation regulatory enzymes are important in the control of cell fate and proliferation. This makes our results concerning the effect of Δ^9-THC on the free SUMO protein pool and the SUMOylation status of p53 all the more interesting and relevant in the endeavour to establish the neurotoxic signalling pathway of Δ^9-THC in cultured cortical neurones.

p53 acts as a transcription factor for Mdm2, thus when activated, p53 transcriptionally up regulates Mdm2 protein expression. Due to the ability of Mdm2 to inhibit p53 activity, a negative feedback loop is formed which provides a tight regulatory mechanism, which controls the function of p53 in cell cycle progression and apoptosis. Mdm2 functions as a critical titrator of p53 activity and loss of Mdm2 results in an active p53 that is resistant to degradation (Iwakuma and Lozano, 2003). Δ^9-THC induced an increase in the expression of the Mdm2 protein after 5 minutes exposure. This occurred at the same time that Δ^9-THC-induces the activation of p53, which may indicate that p53 may be responsible for the up regulation of Mdm2. The Mdm2 gene has two separate p53 response elements, which generate 2 different length Mdm2 proteins, the p90Mdm2 which is capable of binding and labelling p53 for degradation and the p76Mdm2 which has lost its p53 binding site and so cannot act as a p53 repressor (Perry, 2004). The expression of p90Mdm2 is thought to facilitate the return of p53 to normal levels and Perry *et al.*, (2000) have suggested that p76Mdm2 interferes with the ability of p90Mdm2 to stimulate the degradation of p53. The calculated molecular weight of the unknown full length Mdm2 band induced by Δ^9-THC treatment for 5 minutes was 72 kDa. Therefore, given that there are small differences in molecular weights of proteins between different species, we propose that Δ^9-THC induces this p53 inhibiting form of Mdm2. The 60 kDa band observed is most

likely a p60Mdm2 protein produced by the action of a caspase-like enzyme(s), which is normally expressed at high levels during normal culture conditions (Pochampally *et al.*, 1999). The 30 kDa band represents the C terminal degradative fragment (Pochampally *et al.*, 1999, 1998).

The ability of Δ^9-THC to induce changes in both SUMO and Mdm2 provides additional evidence that p53 signalling is pertinent in the Δ^9-THC-induced apoptotic pathway in our culture system. To corroborate our previous finding that the pharmacological inhibition of p53 prevented Δ^9-THC-induced DNA fragmentation, we used siRNA to deplete the p53 protein in neuronal cultures and then assessed the proclivity of Δ^9-THC to induce DNA fragmentation. Treatment with p53 specific siRNA successfully inhibited Δ^9-THC-induced apoptosis as assessed by the TUNEL technique (Downer *et al.*, 2007a). This signifies the importance of p53 as a signalling molecule in Δ^9-THC-induced neurotoxicity. This is the first report that has linked p53 activity to the neurotoxicity of Δ^9-THC in cultured cortical neurones. Cannabinoids have been shown to evoke apoptosis in a variety of cell types including gliomas, leukaemic cells and colorectal carcinomas and manipulation of this apoptotic cascade may have therapeutic value in the treatment of cancers (Velasco *et al.*, 2004; Powles *et al.*, 2005; Patsos *et al.*, 2005). However, the cannabinoid-mediated apoptosis of leukaemic cells is p53-independent the role of p53 in the anti-tumoural effect of cannabinoids requires further investigation. Cannabinoid-induced neuronal death may contribute to the role of cannabinoids in brain development, hence the p53-dependent apoptotic pathway reported here may provide a molecular mechanism for endocannabinoid-mediated physiological cell death that is necessary for appropriate development of the brain (Fernandez-Ruiz *et al.*, 2004).

The activation of tyrosine kinases, both receptor and non-receptor types, is an initiating step involved in the regulation of many cell signalling cascades which regulate proliferation, differentiation and inflammatory processes. The non-receptor protein tyrosine kinase, SyK can act downstream of Src kinases and serves as a signal amplifier and as a mediator in the assembly of multiprotein signalling complexes (Chan *et al.*, 1994). SyK has been almost exclusively studied in haematopoietic cells where it is involved in the proximal downstream signalling of activated immunoreceptors *e.g.*,

BCR and TCR (Sada *et al.*, 2001). The phosphorylation of SyK induces its activation, which leads to the binding or phosphorylation of adaptor proteins, which can then partake in various cell-signalling processes (Ding *et al.*, 2000). In this study, exposure of neurones to Δ^9-THC for 15 minutes provoked an increase of SyK phosphorylated on tyrosine 323 (p-SyK^{tyr323}) as shown by western immunoblot and immunocytochemistry. This was abrogated by the CB_1 receptor antagonist AM 251 indicating that this signalling kinase is regulated through the CB_1 receptor. This is the first report, that we know of regarding the activation of SyK through the ligation of the cannabinnoid receptor by Δ^9-THC. The activation of SyK was also blocked by the pharmacological inhibition of p53 activity. This indicates that p53 maybe one of the molecular signalling proteins involved in the SyK signalling pathway. It has been reported that cellular stressors *e.g.,* Aβ, ionising radiation, UV irradiation, H_2O_2, LPS and genotoxic agents activate the SyK family (Combs *et al.*, 1999; Kharbanda *et al.*, 1994; Hardwick and Sefton, 1995; Brumell *et al.*, 1996; Arndt *et al.*, 2004; Zou *et al.*, 2004). The activation of SyK leads to the initiation of a number of diverse signalling cascades depending on the cell type and stimulus involved. Phosphorylation of SyK has been linked to the activation of caspase-3 in immune cells but the exact molecular mechanisms involved were not investigated (Zhou *et al.*, 2006). We have found that blocking the activity of SyK with sulfonamide (SyKi), a pharmacological inhibitor of SyK, effectively prevented Δ^9-THC-induced DNA fragmentation, indicating that the activity of this protein tyrosine kinase is indispensable in the Δ^9-THC-induced apoptotic signalling cascade, which we have described previously (Downer *et al.*, 2001). The aetiology for the activation of SyK remains to be fully elucidated, however the activation of SyK in non-immune cells such as neurones, has been reported to be dependent on immunoreceptor tyrosine activation motif (ITAM)-like signalling and the direct association with phosphotyrosine phosphatases or protein kinases (Kitano *et al.*, 2002; Hecht and Zick, 1992; Sidorenko *et al.*, 1995). It is interesting to note that the metabotropic glutamate receptor-associated scaffolding protein, Tamalin, recruits SyK which can then activate downstream protein tyrosine kinases which in turn activate phospholipase C-γ (Hirose *et al.*, 2004). Ligation of cannabinoid receptors leads to the recruitment and activation of a diverse set of adaptor proteins including Src kinases

which can activate the transcription of protein scaffolding proteins (He *et al.*, 2005). Indeed, He and co-workers (2005) suggest that the activity of small GTPases and protein kinases such as Src and JNK regulate Stat3, a transcriptional regulator, to mediate CB_1 receptor-$G_{i/o}$-induced neurite outgrowth in Neuro-2A cells. There are many other reports that link Src activity to cannabinoid receptor activation and so it is conceivable that SyK maybe activated downstream of cannabinoid receptor ligation (Derkinderen *et al.*, 2001b; Lee *et al.*, 2003b). The role of SyK in inducing apoptosis is not yet clear with both pro- and anti-apoptotic functions being reported in the literature (Combs *et al.*, 2001; Qin *et al.*, 1997). These functions may be of relevance to our observations that Δ^9-THC regulates SyK signalling and that SyK activity is required for the induction of Δ^9-THC-induced neurotoxicity and Δ^9-THC may modulate neuronal differentiation and survival *via* SyK signalling.

In conclusion, the results presented here demonstrate the diverse signalling cascades that are involved in Δ^9-THC-induced neuronal apoptosis. They show that Δ^9-THC induces DNA fragmentation and the phosphorylation of the pro-apoptotic protein, p53 *via* the protein kinase JNK1. Δ^9-THC also regulated other post translational modifiers of p53 *i.e.,* SUMO-1 and Mdm2 in a time-dependent manner. The regulation of these modifying proteins could facilitate p53-inudced apoptosis by increasing p53 stability and possibly by effecting its cellular location. The siRNA-mediated depletion of p53 abrogated the proclivity of Δ^9-THC to induce DNA fragmentation, thus definitively showing the role of p53 in the apoptotic-signalling cascade induced by Δ^9-THC. The results also show the involvement of a new signalling molecule, SyK in Δ^9-THC-induced neuronal death. The identification of these novel signalling pathways may represent control points, which can be targeted by drugs to harness the influence that cannabinoids have on cell fate.

Summary schematic

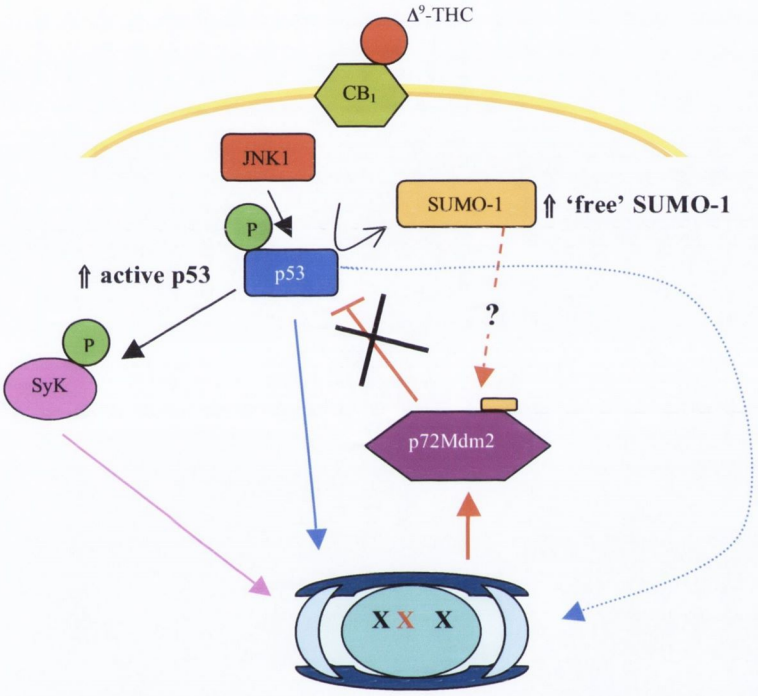

Chapter 4

The role of the lysosomal system in Δ^9-THC-induced neuronal apoptosis

4.1 Introduction

Apoptosis is an active form of cell death that plays an essential role in brain development and ensures the survival of the correct numbers of neuronal and glial populations (Kerr *et al.*, 1972; Boya and de la Rosa, 2006). However, excessive or the inappropriate activation of this cell death pathway can lead to neurodegenerative disease and has been implicated in eliciting behavioural deficits (Mattson, 2000; Nijhawan *et al.*, 2000; Harris *et al.*, 2003). The intrinsic apoptotic pathway involves the translocation of mitochondrial proteins *e.g.,* cytochrome c, into the cytosol followed by the activation of caspase cascades that culminates in the physical degradation of the cell. Indeed, we have previously shown that exposure of cultured cortical neurones to Δ^9-THC causes cytochrome release and caspase-3 activation followed by the demise of the cell (Campbell, 2000; Downer *et al.*, 2001). Modulation of intracellular organelles is a common phenomenon during apoptosis. However, whilst most studies focus on the mitochondrial regulation of apoptosis, several reports have indicated that the lysosomes play a role in early apoptotic events (Turk *et al.*, 2002; Kågedal *et al.*, 2005). For many years lysosomes and their degradative proteases were thought to be involved in necrotic and autophagic cell death or in non-specific intracellular protein degradation respectively. However, today these concepts are outdated and the term 'the lysosomal pathway of apoptosis' is now accepted terminology (Guicciardi *et al.*, 2004). The lysosomal pathway of apoptosis describes the induction of lysosomal membrane destabilisation with subsequent release of proteolytic enzymes into the cytosol, and their active contribution to the cell death signalling pathways (Guicciardi *et al.*, 2004). One of the key factors in determining the type of cell death (apoptosis or necrosis) evoked by lysosomal membrane destabilisation is the magnitude of membrane destabilisation and the amount of proteolytic enzymes released into the cytosol (Li *et al.*, 2000). Necrotic cell death is associated with the total destruction of the organelle coupled with the uncontrolled release of high concentrations of lysosomal enzymes, whilst the partial degradation of the lysosomal membrane coupled with the controlled release of selective proteases triggers apoptotic cell death (Bursch, 2001; Turk *et al.*, 2002). In both instances the amount of degradative enzymes released into the cytosol is sufficient to overcome the native inhibitors present normally in the cell *e.g.,* the

cystatins, which are present to protect the cell against the spontaneous leakage of lysosomal contents, which is a normal cellular process (Berg *et al.*, 1995; Claus *et al.*, 1998). Once released into the cytosol lysosomal enzymes can contribute directly to the cell death cascade by the direct cleavage of key cellular substrates *e.g.*, caspase-3, or by acting in consort with caspases in the death pathway (Leist and Jaattela, 2001).

The lysosomal proteolytic enzymes, also called cathepsins, represent the largest group of degradative enzymes in lysosomes. There are at least 13 cathepsins, which have been identified in mammals (Chwieralski *et al.*, 2006). Lysosomal enzymes including cathepsins B, L, and cathepsin-D (the only aspartic proteases in the cathepsin family) can be translocated from the lysosomal lumen to the cytosol in response to a variety of signals *e.g.*, TNF receptor ligation, p53 activation, oxidative stress and exposure to the second messenger sphingosine (Guicciardi *et al.*, 2000; Yuan *et al.*, 2002; Nilsson *et al.*, 1997; Kågedal *et al.*, 2001). Furthermore, cathepsin D has been shown to induce the insertion of the pro-apoptotic Bcl_2 family member, Bax into the lysosomal membrane, causing membrane destabilisation and leakage of cathepsin-D into the cytosol (Kågedal *et al.*, 2005). The work carried out by Kågedal and colleagues has also identified that cathepsin-D activated p53 and caspase-3 which is remarkably similar to the mechanism of action we propose for the induction of Δ^9-THC-induced neurotoxicity *in vitro* and *in vivo* (Kågedal *et al.*, 2001; Downer *et al.*, 2007a and b). In addition, a further report showing p53 induces apoptosis *via* a lysosomal-mitochondrial pathway that is initiated by lysosomal destabilisation is of particular interest given the central role that we have shown p53 to have in our *in vitro* Δ^9-THC-induced neurotoxic system (Yuan *et al.*, 2002).

The engagement of several receptors, including G protein-coupled receptors, leads to receptor endocytosis, which culminates in the receptor being either recycled to the cell membrane or trafficked to the lysosomes for degradation (Grampp *et al.*, 2007). This internalisation process involves the phosphorylation by a G protein-receptor kinase (GRK) and recruitment of an arrestin protein (Gainetdinov *et al.*, 2004). It has been recently established that SyK is an important protein involved in immunoreceptor internalisation followed by lysosomal targeting and degradation, and is required for the propagation of downstream signalling (He *et al.*, 2005a; Bonnerot *et al.*, 1998). These

findings are of interest to our investigations considering we have shown that Δ^9-THC regulates SyK *via* the CB_1 receptor (chapter 3). Indeed, the CB_1 receptor can be targeted to the lysosomes after agonist-induced internalisation and has also been shown to recruit Src protein tyrosine kinases, which are up stream regulators of SyK (Sarnataro *et al.*, 2005; He *et al.*, 2005b).

The aim of this study was to firstly investigate whether Δ^9-THC impacts on the stability of the lysosomal membrane, which was assessed by the relocation of acridine orange, and the level of cathepsin enzyme activity in cytosolic fractions. Given that there is evidence for a role of p53 and SyK in the functioning of lysosomes, it was determined if these proteins, which we have previously shown to be regulated by Δ^9-THC, are involved in lysosomal signalling in our *in vitro* Δ^9-THC-induced apoptotic pathway. The association of phospho-$p53^{ser15}$ and phospho-SyK^{tyr323} with the lysosomal membrane was investigated by immunocytochemistry using phospho-specific antibodies and the specific lysosomal marker, LysoTracker Red™. In addition, the role of cathepsins in the propagation of further downstream Δ^9-THC-induced apoptotic markers *e.g.*, caspase-3 activity and DNA fragmentation, was also assessed.

4.2.1 Δ^9-THC induces lysosomal destabilisation in a time-dependent manner

Lysosomal membrane destabilisation can occur as a result of many cell stressors and has a role in early apoptotic signalling (Brunk *et al.*, 2001; Turk *et al.*, 2002). Acridine Orange (AO) relocation (Methods 2.12) is a method used to investigate the integrity of the lysosomal membrane. AO can diffuse through cellular membranes including subcellular membrane enclosed compartments such as, lysosomes, mitochondria and nuclei. However, in acidic membrane-bound compartments *e.g.*, lysosomes, AO becomes protonated. In a protonated state, AO cannot pass back through membranes and so accumulates in these acidic membrane-bound compartments. Due to its metachromatic propeties, AO also differentially labels cellular compartments. Highly concentrated AO has a peak emission of 633 nm (pink, punctate acidic compartment staining) whereas a lower concentration of AO displays a peak emission of 525 nm (green, diffuse cytoplasmic staining).

Relocation of AO from lysosomes was assessed using confocal microscopy using the 488 nm Argon laser to excite AO and the META analysis function to collected emissions over the wavelength range of 499.7 - 670.7 nm. Figure 4.1 depicts the time course of Δ^9-THC-induced lysosomal instability ($p=0.0067$, ANOVA, $n=4$). Cortical neurones were treated with AO (5 μg/ml) for 10 minutes prior to incubation with Δ^9-THC (5 μM) for 15 - 120 minutes. Following Δ^9-THC treatment for 15 minutes, AO emission at 633 nm was 45 ± 6 fluorescent intensity units (mean ± SEM, Figure 4.1A) which was significantly lower to that found in cells treated with vehicle (203 ± 43; $p<0.01$, vs., vehicle, Student Newman Keuls, $n=4$). This indicates that the lysosomal membrane was no longer able to retain AO at high concentrations which results in a decrease in 633 nm emission. The induction of lysosomal instability was maintained at 30, 60 and 120 minutes (58 ±10, 109 ± 45 and 54 ± 2, respectively; $p<0.05$ and $p<0.01$, vs., vehicle, Student Newman Keuls, $n=4$). Representative images of AO stained cortical neurones demonstrating the induction of lysosomal membrane instability are shown in Figure 4.1B.

Figure 4.1: Δ^9-THC induces lysosomal destabilisation in a time-dependent manner

Cortical neurones were exposed to AO (5 μg/ml) for 10 min prior to incubation with Δ^9-THC (5 μM) for 15 - 120 min. Relocation of AO from the lysosomes to the cytosol was assessed. Highly concentrated AO displayed a pink fluorescence and was localised in discrete punctate compartments within the cell. Lower concentrations of AO displayed a green fluorescence and had a diffuse staining pattern.

A: Highly concentrated AO found in intact lysosomes emits at 633 nm. By measuring the mean fluorescent intensity at this wavelength we can monitor the integrity of the lysosomal membrane. Δ^9-THC (5 μM) significantly reduces the mean fluorescence intensity at 633 nm at 15, 30, 60 and 120 min. Results are means ± SEM, *$p<0.05$, **$p<0.01$, vs., vehicle, Student Newman Keuls, n=4.

B: Confocal images of AO staining of (i) vehicle-treated neurones, and neurones treated with Δ^9-THC (5 μM) for 15 (ii), 30 (iii), 60 (iv), and 120 min (v).

A

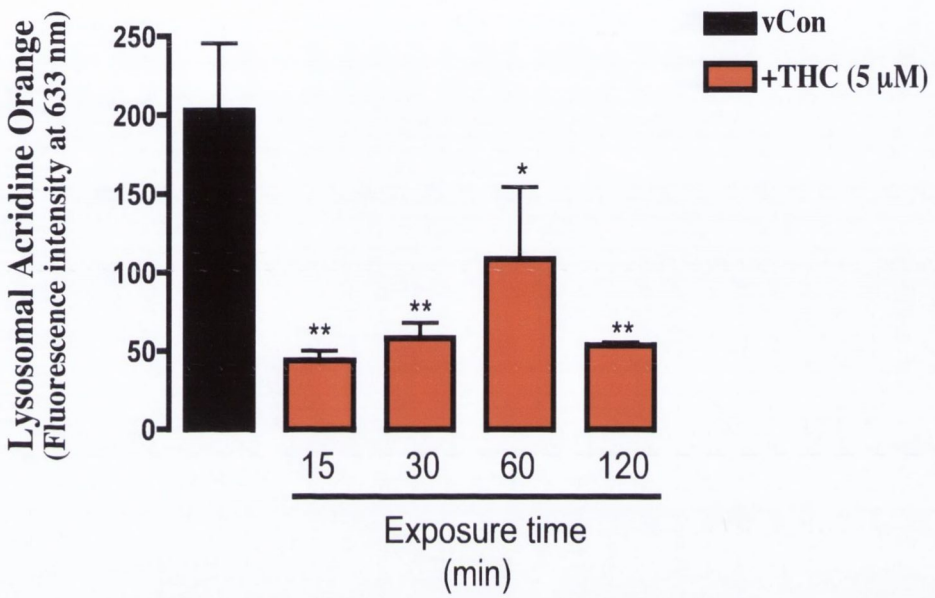
Lysosomal Acridine Orange
(Fluorescence intensity at 633 nm)
250
200
150
100
50
0
vCon
+THC (5 μM)
**
**
*
**
15
30
60
120
Exposure time
(min)

B

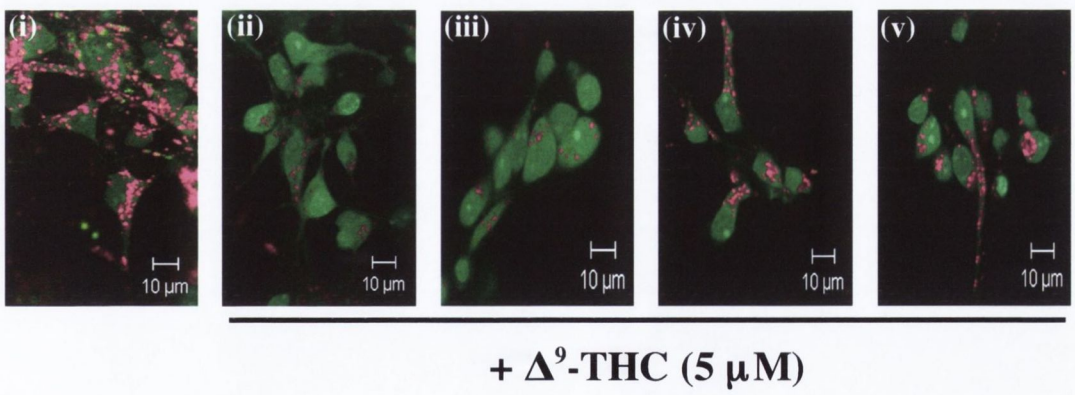
(i)
(ii)
(iii)
(iv)
(v)
10 μm
10 μm
10 μm
10 μm
10 μm
+ Δ9-THC (5 μM)

4.2.2 Δ^9-THC induces lysosomal destabilisation in a dose-dependent manner

In this study cortical neurones were treated with AO (5 μg/ml) for 10 minutes prior to incubation with Δ^9-THC (0.05 - 50 μM) for 15 minutes. Relocation of AO from lysosomes was assessed using confocal microscopy using the 488 nm Argon laser to excite AO and the META analysis function to collected emissions over the wavelength range of 499.7 - 670.7 nm. Figure 4.2 depicts the dose response of Δ^9-THC-induced lysosomal instability ($p=0.0018$, ANOVA, n=4). Following exposure to 0.05 μM Δ^9-THC for 15 minutes, AO emission at 633 nm was 141 ± 11 fluorescence intensity units (mean ± SEM, Figure 4.2A) which was comparable to that found in cells treated with vehicle (188 ± 47). A significant reduction in fluorescence intensity at 633 nm, indicative of lysosomal rupture, was observed after exposure to 0.5, 5 and 50 μM Δ^9-THC (83 ± 15, 45 ± 6 and 45 ± 9 respectively; $p<0.05$ and $p<0.01$ vs., vehicle, Student Newman Keuls, n=4). In addition, exposure to 5 and 50 μM Δ^9-THC significantly decreased 633 nm emission compared to 0.05 μM Δ9-THC ($p<0.05$, vs., 0.05 μM Δ^9-THC, Student Newman Keuls, n=4). Representative images of AO stained cortical neurones after 15 minutes exposure to 0.05 - 50 μM Δ^9-THC (ii) - (v) compared to cells treated with vehicle alone (i) are shown in Figure 4.2B.

Figure 4.2: Δ^9-THC induces lysosomal destabilisation in a dose-dependent manner

Cortical neurones were exposed to AO (5 μg/ml) for 10 min prior to incubation with 0.05 - 50 μM Δ^9-THC for 15 min. Relocation of AO from the lysosomes to the cytosol was assessed and mean fluorescence intensity at 633 nm was used to monitor lysosomal membrane stability.

A: The mean fluorescence intensity at 633 nm is significantly reduced following exposure to 0.5, 5 and 50 μM Δ^9-THC for 15 min. Results are expressed as means ± SEM, *$p<0.05$, **$p<0.01$ vs., vehicle, +$p<0.05$ vs., 0.05 μM Δ^9-THC, Student Newman Keuls, n=4).

B: Confocal images of AO staining of (i) vehicle-treated neurones, and neurones treated with 0.05 (ii), 0.5 (iii), 5 (iv), and 50 μM (v) Δ^9-THC for 15 min.

A

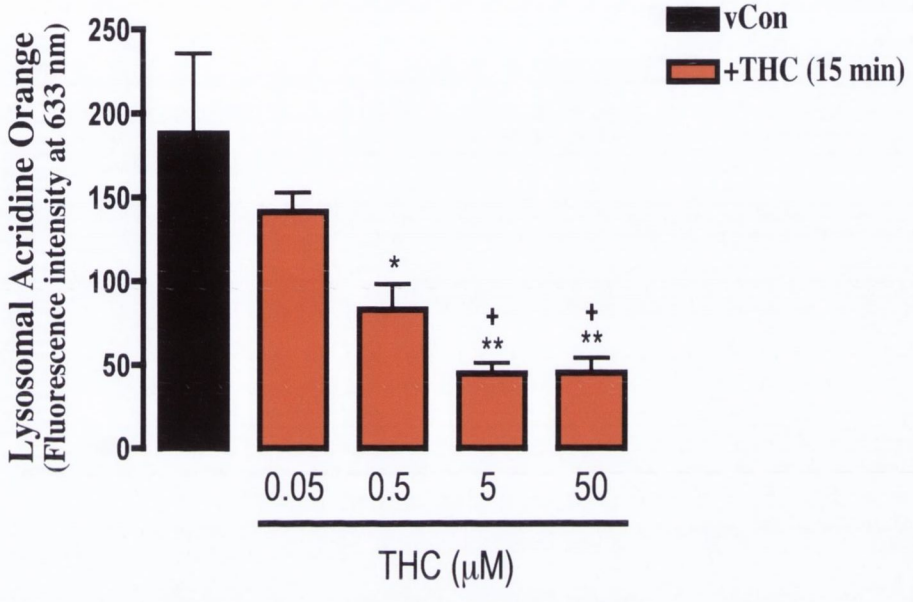
vCon
+THC (15 min)
Lysosomal Acridine Orange
(Fluorescence intensity at 633 nm)
250
200
150
100
50
0
*
+
**
+
**
0.05
0.5
5
50
THC (μM)

B

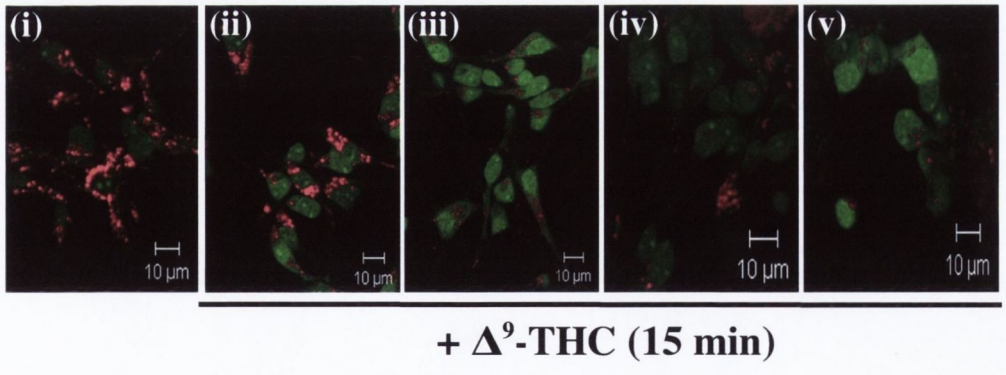
(i)
(ii)
(iii)
(iv)
(v)
10 μm
10 μm
10 μm
10 μm
10 μm
+ Δ9-THC (15 min)

4.2.3 Δ^9-THC-induced lysosomal destabilisation is dependent on the CB_1 receptor

Cortical neurones were treated with AO (5 μg/ml) for 10 minutes prior to incubation with Δ^9-THC (5 μM) for 15 minutes in the presence or absence of the CB_1 receptor antagonist AM 251 (30 minute pre-treatment). Relocation of AO from lysosomes was assessed using confocal microscopy using the 488 nm Argon laser to excite AO and the META analysis function to collected emissions over the wavelength range of 499.7 - 670.7 nm. Figure 4.3 demonstrates that Δ^9-THC-induced lysosomal membrane instability is CB_1 dependent ($p=0.0040$, ANOVA, n=4). Following Δ^9-THC treatment for 15 minutes, AO emission at 633 nm was 39.84 ± 2.96 fluorescence intensity units (mean ± SEM, Figure 4.3A) which was significantly lower to that found in cells treated with vehicle (121.6 ± 19.71; $p<0.01$, vs., vehicle, Student Newman Keuls, n=4). While incubation with AM 251 alone had no effect on lysosomal membrane stability (131.00 ± 15.67), Δ^9-THC failed to induce lysosomal instability in the presence of AM 251 (107.90 ± 15.68; $p<0.01$, vs., Δ^9-THC, Student Newman Keuls, n=4). Figure 4.3B shows representative images of AO stained cortical neurones demonstrating the CB_1-dependent induction of lysosomal membrane instability.

Figure 4.3: Δ^9-THC-induced lysosomal destabilisation is dependent on the CB_1 receptor

Cortical neurones were exposed to AO (5 μg/ml) for 10 min prior to incubation with Δ^9-THC (5 μM) for 15 min in the presence or absence of AM 251 (30 min pre-treatment). Relocation of AO from the lysosomes to the cytosol was assessed and the mean fluorescence intensity at 633 nm was monitored as an indicator of lysosomal membrane stability.

A: Δ^9-THC (5 μM) reduces the mean fluorescence intensity at 633 nm at 15 min, pre-treatment with AM 251 (10 μM) abolished the Δ^9-THC-induced reduction in 633 nm emission. Results shown are means ± SEM, **p<0.01, Student Newman Keuls, n=4.

B: Confocal images of AO staining of neurones treated with vehicle (i), Δ^9-THC for 15 min (ii), AM 251 alone (iii), AM 251 and Δ^9-THC (5 μM) for 15 min (iv). Arrows indicate cells containing destabilised lysosomes.

A

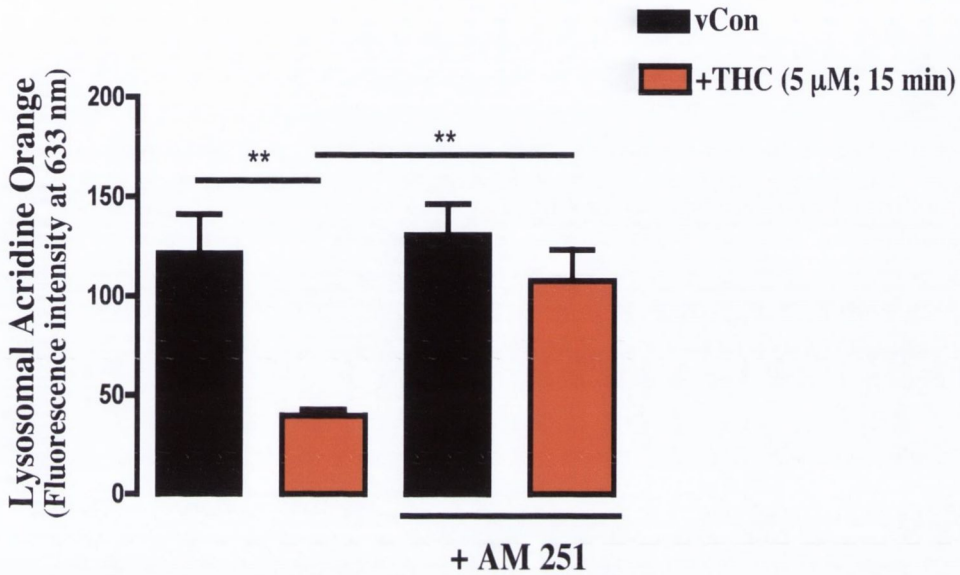
vCon
+THC (5 μM; 15 min)
Lysosomal Acridine Orange
(Fluorescence intensity at 633 nm)
200
150
100
50
0
**
**
+ AM 251

B

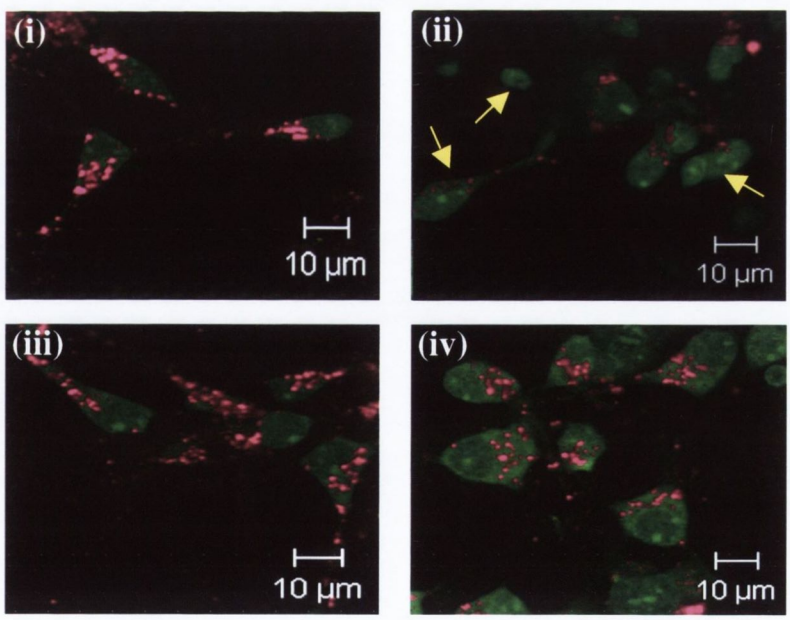
(i)
10 μm
(ii)
10 μm
(iii)
10 μm
(iv)
10 μm

4.2.4 Δ^9-THC induces p53 to colocalise with the lysosomes

It has been shown that phosphorylated p53 (at serine 15) can colocalise with the lysosomal membrane causing alterations in lysosomal morphology and ultimately to the demise of the cell *via* a lysosomal-mediated cell-death pathway (Yuan *et al.*, 2002). In this study, the effect of Δ^9-THC on the cellular distribution of phospho-p53^{ser15} was assessed in relation to its association with the specific lysosomal marker, LysoTracker™ Red. Cultured cortical neurones were incubated with LysoTracker™ Red (700 nM) prior to incubation with Δ^9-THC (5 μM) for 15 minutes. Phospho-p53^{ser15} expression was detected by immunocytochemistry using a polyclonal antibody that only labels p53 when phosphorylated on serine 15. Following staining, cells were visualised by confocal microscopy. Exposure to Δ^9-THC induced an increase in phospho-p53^{ser15} (Alexa 488) expression in the nucleus, which is indicative of a pro-apoptotic response where activated p53 translocates to the nucleus in order to transactivate p53 responsive genes. In addition to increased p53 in the nucleus, Δ^9-THC-induced a significant proportion of activated p53 to colocalise with the lysosomes (LysoTracker™ Red; Figure 4.3A). In cells treated with Δ^9-THC (5 μM) for 15 minutes the intensity of colocalised pixels was 348 ± 37 mean fluorescence intensity units which was significantly greater than that observed in cells exposed to vehicle (139 ± 31; p=0.0159, vs., vehicle, Mann Whitney test, n=4 observations). Figure 4.3B shows representative confocal images of cells treated with vehicle (i) and Δ^9-THC (ii). Colocalised pixels are represented in purple and blue. Figure 4.3C shows a representative line analysis depicting the green and red channel fluorescent emission that occurred along the arrow in image (i). The line analysis graph (Figure 4.3C (ii)) accurately shows the colocalisation (blue highlighted peaks) between phospho-p53^{ser15} (Alexa 488; green line) and the lysosomes (LysoTracker™ Red; red line).

Figure 4.4: Δ^9-THC induces p53 to colocalise with the lysosomes

Confocal microscopy was used to visualise the distribution of phospsho-p53^{ser15} within cortical neurones following treatment with Δ^9-THC (5 μM; 15 min). Cells were double labelled with the lysosomal specific marker LysoTracker™ Red, and an Alexa 488-labelled phospho-p53^{ser15} antibody.

A: Confocal analysis shows that Δ^9-THC (5 μM; 15 min) exposure increases the colocalisation of phospho-p53^{ser15} with LysoTracker™ Red (*p=0.0159, Mann Whitney test, n=4 observations).

B: Confocal images of neurones treated with (i) vehicle and (ii) Δ^9-THC (5 μM; 15 min). Phospho-p53^{ser15} (green channel), Lysosomes (red channel) and overlay images are presented. Inset: close up of a lysosome (zoom 6 (a) and 9 (b).

C: A line analysis graph (ii) confirming the colocalisation between phospho-p53^{ser15} (green line) with and lysosomes (red line) which occurs following Δ^9-THC treatment.

A

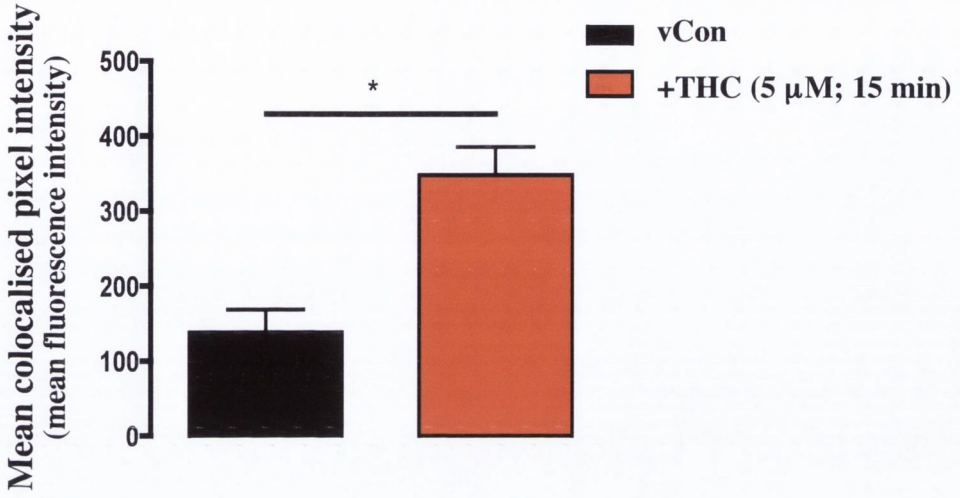
Mean colocalised pixel intensity
(mean fluorescence intensity)
500
400
300
200
100
0
*
vCon
+THC (5 μM; 15 min)

B

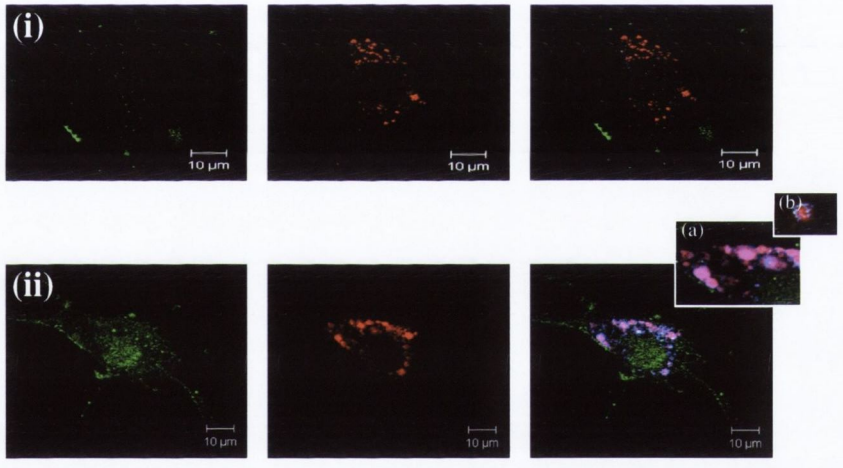
(i)
(ii)
10 μm
(a)
(b)

C

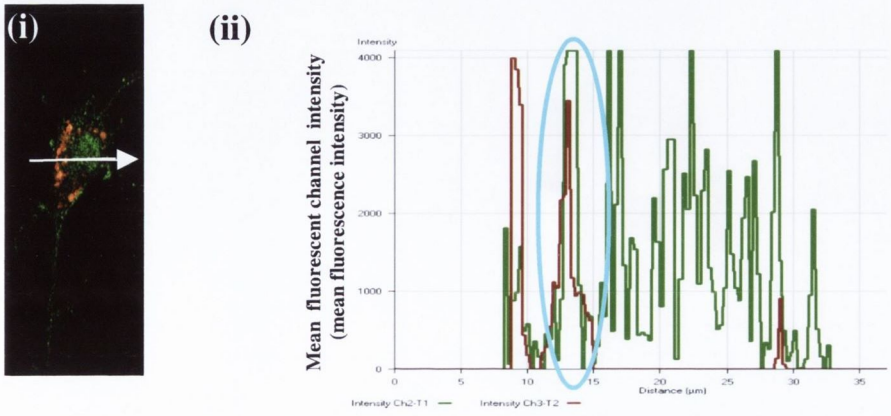
(i)
(ii)
Mean fluorescent channel intensity
(mean fluorescence intensity)
Intensity
4000
3000
2000
1000
0
0
5
10
15
20
25
30
35
Distance (μm)
Intensity Ch2-T1
Intensity Ch3-T2

4.2.5 Δ^9-THC-induced lysosomal instability is dependent on p53 activity

Since Δ^9-THC causes the colocalisation of phospho-p53^{ser15} with lysosomes, the role of p53 in Δ^9-THC-induced lysosomal membrane instability was assessed in this study. Two distinct techniques were used to assess the role of p53 in Δ^9-THC-induced lysosomal membrane instability, they were: (i) the pharmacological inhibition of p53 activation and transactivation and (ii) the depletion of p53 protein by siRNA. Cortical neurones were treated with AO (5 μg/ml) for 10 minutes prior to incubation with Δ^9-THC (5 μM) for 15 minutes in the presence or absence of pifithrin-α (Pif-α; 100 nM, 1 hour pre-treatment; Figure 4.5A), or siRNA specifically targeting p53 (p53 siRNA; 100 nM, 48 hour pre-treatment; Figure 4.5B). Relocation of AO from lysosomes was assessed using confocal microscopy using the META analysis function (excitation 488 nm, emission range 499.7 - 670.7 nm).

Figure 4.5A shows the Δ^9-THC-induced lysosomal membrane instability is abolished by the pharmacological inhibition of p53 activation and transactivation with pifithrin-α ($p=0.0056$, ANOVA, $n=4$). Following Δ^9-THC treatment for 15 minutes, AO emission at 633 nm was 39.41 ± 2.56 fluorescence intensity units (mean ± SEM, Figure 4.5A) which was significantly lower to that found in cells treated with vehicle (118.40 ± 20.82; $p<0.01$, vs., vehicle, Student Newman Keuls, $n=4$). While incubation with pifithrin-α alone had no effect on lysosomal membrane stability (130.00 ± 21.34), Δ^9-THC failed to induce lysosomal instability in the presence of pifithrin-α (93.81 ± 5.38; $p<0.05$, vs., Δ^9-THC, Student Newman Keuls, $n=4$). Figure 4.5B shows the Δ^9-THC-induced lysosomal membrane instability is abolished by the depletion of p53 protein with p53 specific siRNA ($p=0.0001$, ANOVA, $n=4$). Following Δ^9-THC treatment for 15 minutes, AO emission at 633 nm was 59.60 ± 5.64 fluorescence intensity units (mean ± SEM, Figure 4.5B) which was significantly lower to that found in cells treated with vehicle (104.70 ± 3.44; $p<0.001$, vs., vehicle, Student Newman Keuls, $n=6$). Incubation with either control non-targeting (Con siRNA) or p53-targeting siRNA (p53 siRNA) alone did not affect lysosomal membrane stability (118.70 ± 6.27 and 111.50 ± 6.93 respectively). However, in the presence of p53 siRNA, Δ^9-THC failed to induce lysosomal membrane instability (104.30 ± 5.86; $p<0.001$, vs., Con siRNA + Δ^9-THC, Student Newman Keuls, $n=6$).

Figure 4.5: Δ^9-THC-induced lysosomal instability is dependent on p53 activity

Cortical neurones were exposed to AO (5 μg/ml) for 10 min prior to incubation with pif-α (100 nM, 1 hr pre-treatment; panel A) or with siRNA (100 nM, 48 hr pre-treatment; panel B). Neurones were then treated with Δ^9-THC (5 μM) for 15 min and the emission at 633 nm was assessed.

A: Δ^9-THC induced lysosomal destabilisation as indicated by a significant reduction in fluorescence intensity at 633 nm and is abolished by pre-treatment with pif-α (100 nM). Results are means ± SEM, *p<0.05, **p<0.01, Student Newman Keuls, n=4. Inset: Confocal images of neurones treated with (i) vehicle, (ii) Δ^9-THC, (iii) pif-α alone and (iv) pif-α and Δ^9-THC.

B: Δ^9-THC-induced lysosomal destabilisation as indicated by a significant reduction in fluorescence intensity at 633 nm, is also abolished by pre-treatment with p53 siRNA (100 nM). Results are means ± SEM, ***p<0.001, Student Newman Keuls, n=6. Inset: Confocal images of neurones treated with (i) Con siRNA and vehicle, (ii) Con siRNA and Δ^9-THC, (iii) p53 siRNA and vehicle, (iv) p53 siRNA and Δ^9-THC.

A

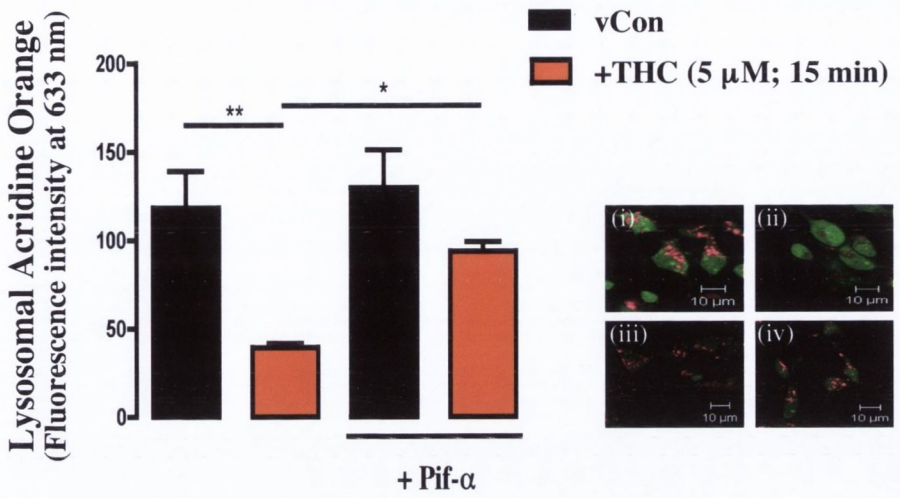
Lysosomal Acridine Orange
(Fluorescence intensity at 633 nm)
200
150
100
50
0
**
*
vCon
+THC (5 μM; 15 min)
+ Pif-α
(i)
(ii)
(iii)
(iv)
10 μm

B

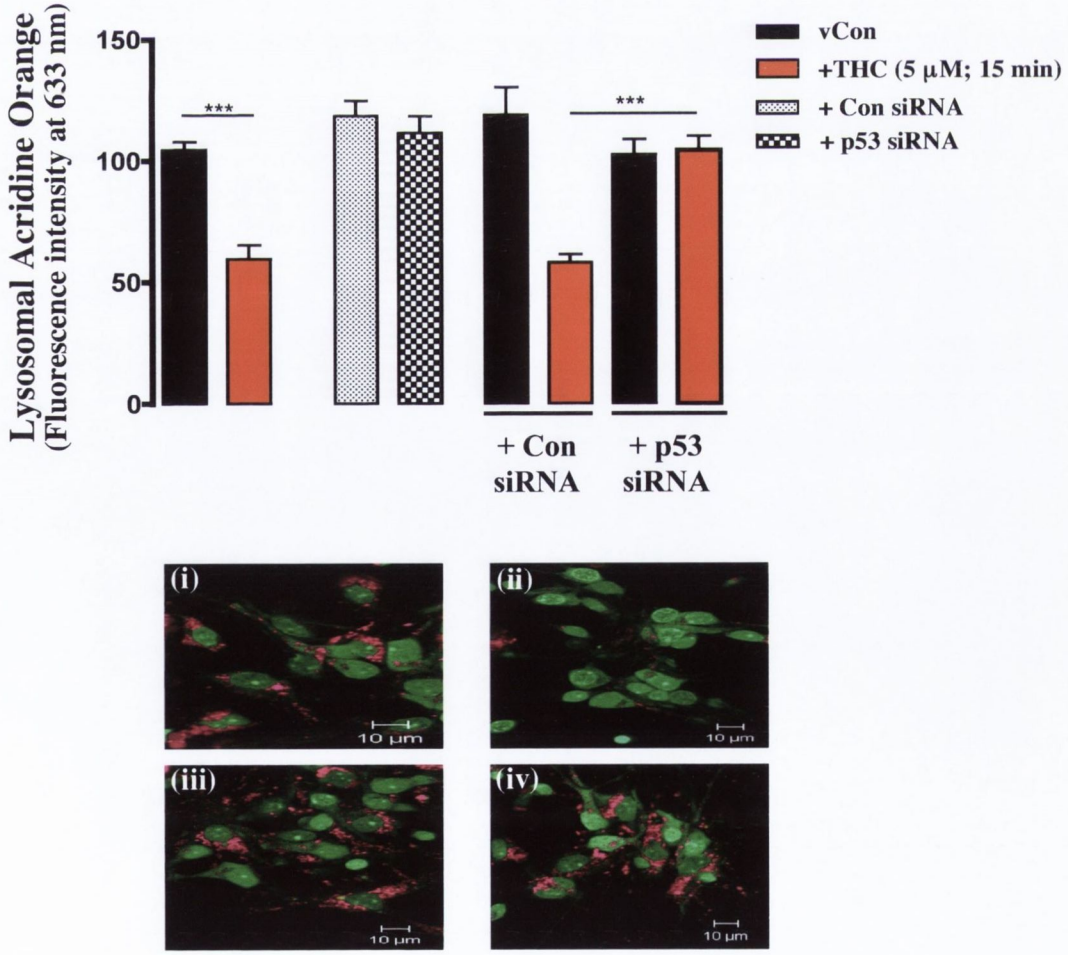
Lysosomal Acridine Orange
(Fluorescence intensity at 633 nm)
150
100
50
0
***
***
vCon
+THC (5 μM; 15 min)
+ Con siRNA
+ p53 siRNA
+ Con siRNA
+ p53 siRNA
(i)
(ii)
(iii)
(iv)
10 μm

4.2.6 The effect of Δ^9-THC on SyK colocalisation with the lysosomes

Since Δ^9-THC regulates the expression of SyK, a protein important for the normal function of lysosomes, its role in Δ^9-THC-induced destabilisation of the lysosomal membrane was investigated. In this study, the effect of Δ^9-THC on the cellular distribution of phospho-SyK^{tyr323} was assessed in regards to its association with the specific lysosomal marker, LysoTracker^{TM} Red. Cultured cortical neurones were incubated with LysoTracker^{TM} Red (700 nM) prior to incubation with Δ^9-THC (5 μM) for 15 minutes. Phospho-SyK^{tyr323} expression was detected by immunocytochemistry using a polyclonal antibody that only labels SyK when phosphorylated on tyrosine 323. Following labelling, cells were visualised by confocal microscopy. Exposure to Δ^9-THC did not promote the association of p-SyK with lysosomes. Thus, in cells treated with Δ^9-THC (5 μM) for 15 minutes the intensity of colocalised LysoTracker^{TM} and Alexa 488 (p-SyK) pixels was 1239 ± 169 mean fluorescence intensity units which was not significantly greater than that observed in cells exposed to vehicle (979 ± 166; p=0.3150, vs., vehicle, Student's t test, n=4 observations). Figure 4.6B shows representative confocal images of cells treated with vehicle (i) and Δ^9-THC (ii). Colocalised pixels are represented in purple and blue.

Figure 4.6: The effect of Δ^9-THC on SyK colocalisation with the lysosomes

Confocal microscopy was used to visualise the distribution of phospho-SyK^{tyr323} within cortical neurones following treatment with Δ^9-THC (5 μM; 15 min). Cells were double labelled with the lysosomal specific marker LysoTracker™ Red, and an Alexa 488-labelled phospho-SyK^{tyr323} antibody.

A: Confocal analysis shows Δ^9-THC (5 μM; 15 min) exposure has no significant effect on the colocalisation of phospho-SyK^{tyr323} with LysoTracker™ Red ($p=0.3150$, vs., vehicle, Student's t test, n=4 observations).

B: Confocal images of neurones treated with (i) vehicle and (ii) Δ^9-THC (5 μM; 15 min). Phospho-SyK^{tyr323} (green channel), Lysosomes (red channel) and overlay images are presented. Inset: close up of lysosomes (zoom 6).

A

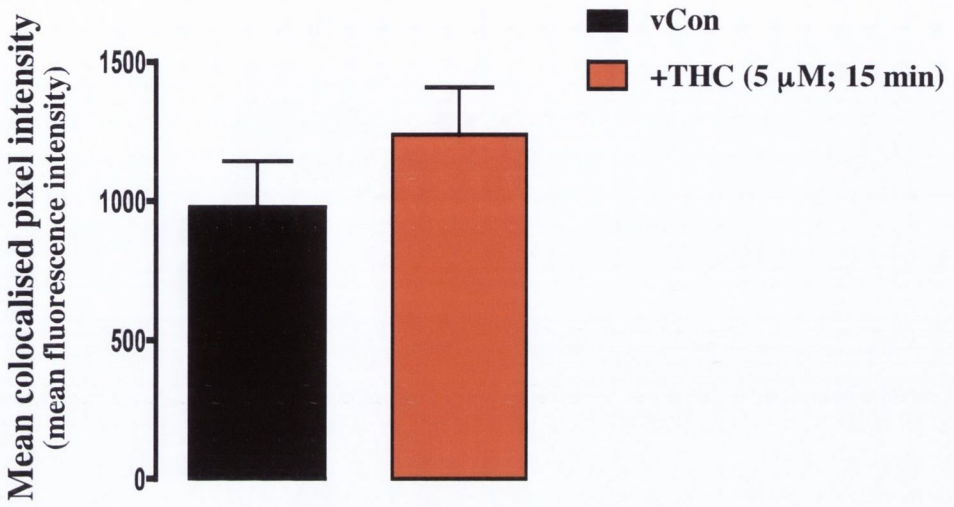
Mean colocalised pixel intensity
(mean fluorescence intensity)
1500
1000
500
0
vCon
+THC (5 μM; 15 min)

B

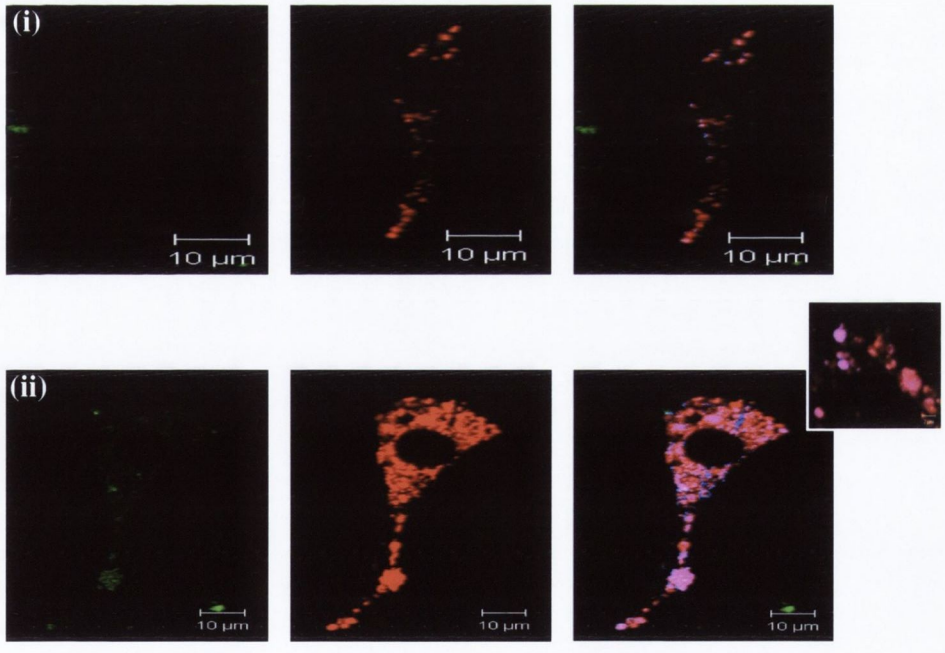
(i)
10 μm
10 μm
10 μm
(ii)
10 μm
10 μm
10 μm

4.2.7 Δ^9-THC-induced lysosomal destabilisation is dependent on SyK activity

Cortical neurones were treated with AO (5 μg/ml) for 10 minutes prior to incubation with Δ^9-THC (5 μM) for 15 minutes in the presence or absence of the SyK inhibitor, SyKi (50 nM; 60 minute pre-treatment). Relocation of AO from lysosomes was assessed using confocal microscopy using the 488 nm Argon laser to excite AO and the META analysis function to collected emissions over the wavelength range of 499.7 - 670.7 nm. Figure 4.7 demonstrates that Δ^9-THC-induced lysosomal destabilisation is dependent on SyK activity ($p=0.0008$, ANOVA, $n=4$). Following Δ^9-THC treatment for 15 minutes, AO emission at 633 nm was 39.46 ± 2.61 fluorescence intensity units (mean ± SEM, Figure 4.7A) which was significantly lower to that found in cells treated with vehicle (117.80 ± 20.97; $p<0.01$, vs., vehicle, Student Newman Keuls, $n=4$). While incubation with SyKi alone had no effect on lysosomal membrane stability (117.10 ± 6.41), Δ^9-THC failed to induce lysosomal instability in the presence of SyKi (119.40 ± 7.13; $p<0.01$, vs., Δ^9-THC, Student Newman Keuls, $n=4$). Figure 4.7B shows representative images of AO stained cortical neurones demonstrating the SyK-dependent induction of lysosomal membrane instability.

Figure 4.7: Δ^9-THC-induced lysosomal destabilisation is dependent on SyK activity

Cortical neurones were exposed to AO (5 μg/ml) for 10 min prior to incubation with SyKi (50 nM, 1 hr pre-treatment), neurones were treated with Δ^9-THC (5 μM) for 15 min and the emission at 633 nm was assessed.

A: Δ^9-THC-induced lysosomal destabilisation is abolished by pre-treatment with SyKi (50 nM). Results are means ± SEM, **p<0.01, Student Newman Keuls, n=4.

B: Confocal images of AO stained neurones treated with (i) vehicle, (ii) Δ^9-THC, (iii) SyKi alone and (iv) SyKi and Δ^9-THC.

A

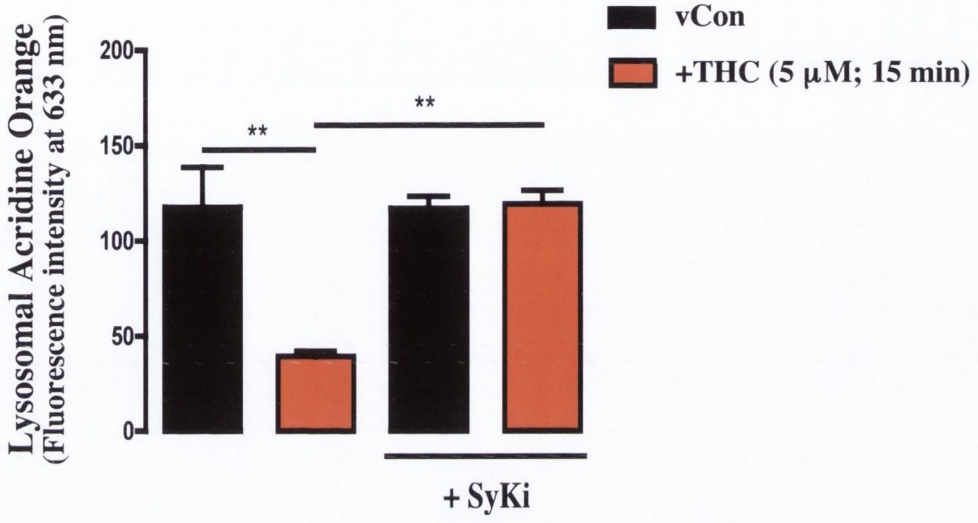
Lysosomal Acridine Orange
(Fluorescence intensity at 633 nm)
200
150
100
50
0
**
**
vCon
+THC (5 μM; 15 min)
+ SyKi

B

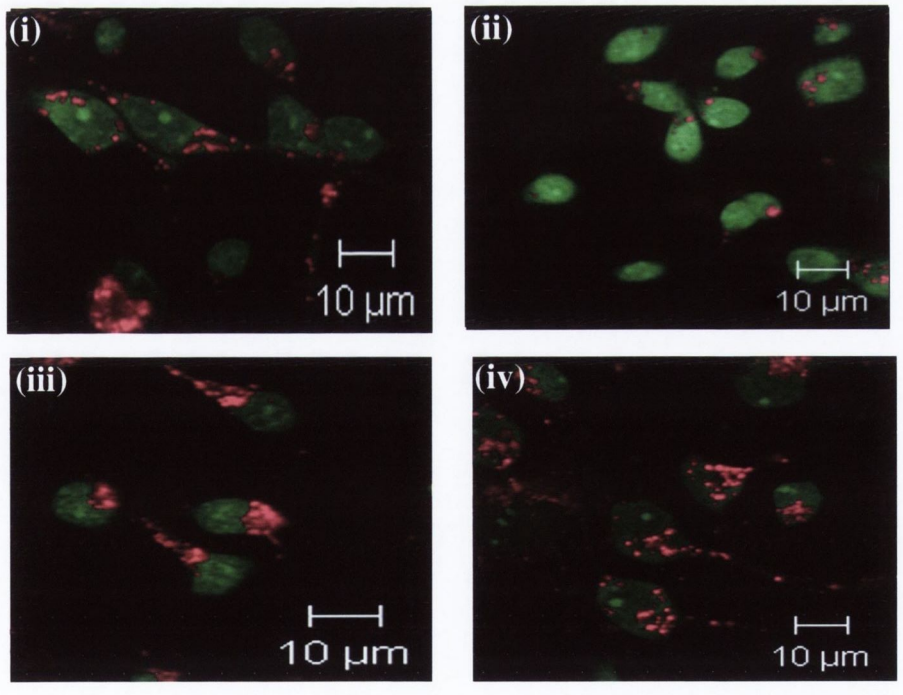
(i)
10 μm
(ii)
10 μm
(iii)
10 μm
(iv)
10 μm

4.2.8 The effect of Δ^9-THC on cathepsin-L activity

The disruption of the lysosomal membrane can result in the release of cathepsins which are known to induce apoptosis (Turk *et al.*, 2002). We investigated whether cathepsin-L was translocated to the cytosol after treatment with Δ^9-THC (5 μM) for 1 hour. Cathepsin-L activity was assessed in cytosolic fractions collected from cultured cortical neurones treated with Δ^9-THC by the cleavage of a fluorogenic cathepsin-L substrate. Figure 4.8 demonstrates that following exposure to Δ^9-THC (5 μM) for 1 hour there was no appreciable effect on cathepsin-L activity. In cells treated with Δ^9-THC (5 μM) for 1 hour cathepsin-L activity was 821.9 ± 82.4 ρmoles AFC produced per mg protein per minute which was comparable to cells treated with vehicle (905.4 ± 51.9; p=0.4079, Student's t test, n=7). This result shows that cathepsin-L activity is not up regulated in the cytosol by Δ^9-THC within the time periods studied.

Figure 4.8: The effect of Δ^9-THC on cathepsin-L activity

Cultured cortical neurones were treated with Δ^9-THC (5 μM) for 1 hr. Cathepsin-L activity was assayed in cytosolic fractions by the cleavage of a fluorogenic cathepsin-L substrate. Δ^9-THC had no significant effect on cathepsin-L activity. Results are expressed as ρmoles AFC produced per mg protein per min and are means ± SEM, p=0.4079, vs., vehicle, Student's t test, n=7.

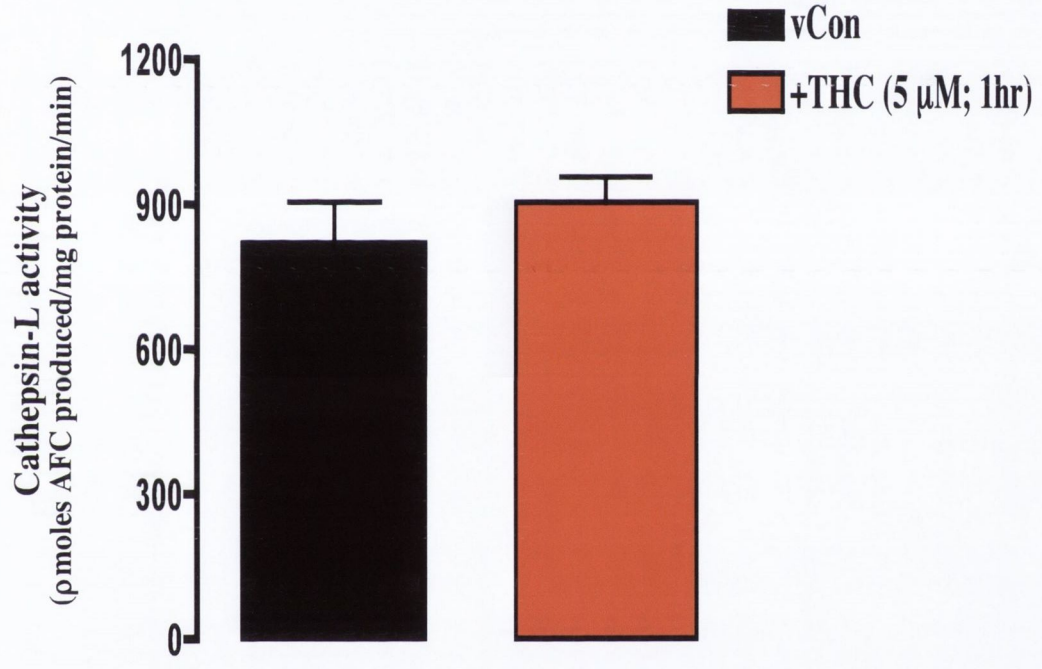
vCon
+THC (5 μM; 1hr)
Cathepsin-L activity
(ρmoles AFC produced/mg protein/min)
1200
900
600
300
0

4.2.9 Δ^9-THC-induced DNA fragmentation is dependent on cathepsin-L activity

DNA fragmentation was assessed by TUNEL staining in cultured cortical neurones following exposure to Δ^9-THC (5 μM) for 2 hours in the presence or absence of a cell permeable inhibitor of cathepsin-L (CLi; 30 minute pre-treatment). Figure 4.9 depicts the cathepsin-L-dependent nature of Δ^9-THC-induced DNA fragmentation ($p<0.0001$, ANOVA, n=6-9 observations). In vehicle-treated cells, 9.4 ± 0.7% (mean ± SEM) of cells displayed fragmented DNA in the nucleus (TUNEL positive). This was significantly increased to 21.0 ± 1.3% in cells treated with Δ^9-THC for 2 hours ($p<0.001$, vs., vehicle, Student Newman Keuls, n=6-9 observations; Figure 4.9A). While treatment of cells with CLi alone for 30 minutes had no effect on neuronal viability (11.9 ± 0.7% neurones with fragmented DNA), it prevented the Δ^9-THC-induced increase in DNA fragmentation (10.7 ± 1.0%; $p<0.001$, vs., Δ^9-THC, Student Newman Keuls, n=6-9 observations). This finding suggests that cathepsin-L is involved in Δ^9-THC-induced DNA fragmentation. Representative images of TUNEL stained neurones are shown in Figure 4.9B.

Figure 4.9: Δ^9-THC-induced DNA fragmentation is dependent on cathepsin-L activity

Cortical neurones were treated with CLi (10 μM) for 30 minutes prior to exposure to Δ^9-THC (5 μM) for 2 hours. Cell viability was assessed using the TUNEL technique.

A: Δ^9-THC significantly increased the percentage of TUNEL positive cells. CLi abolished the Δ^9-THC-induced increase in DNA fragmentation. Results are displayed as mean ± SEM, ***p<0.001, Student Newman Keuls, n=6-9 observations.

B: Sample images of TUNEL stained neurones treated with (i) vehicle, (ii) Δ^9-THC, (iii) CLi alone and (iv) Δ^9-THC in the presence of CLi. Arrows indicate TUNEL positive neurones. Scale bar is 10 μm.

A

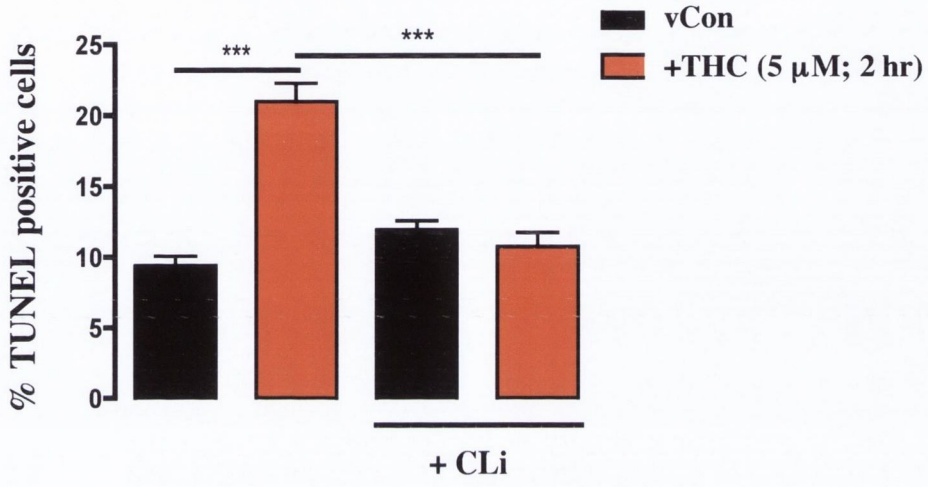
% TUNEL positive cells
25
20
15
10
5
0
***
***
vCon
+THC (5 μM; 2 hr)
+ CLi

B

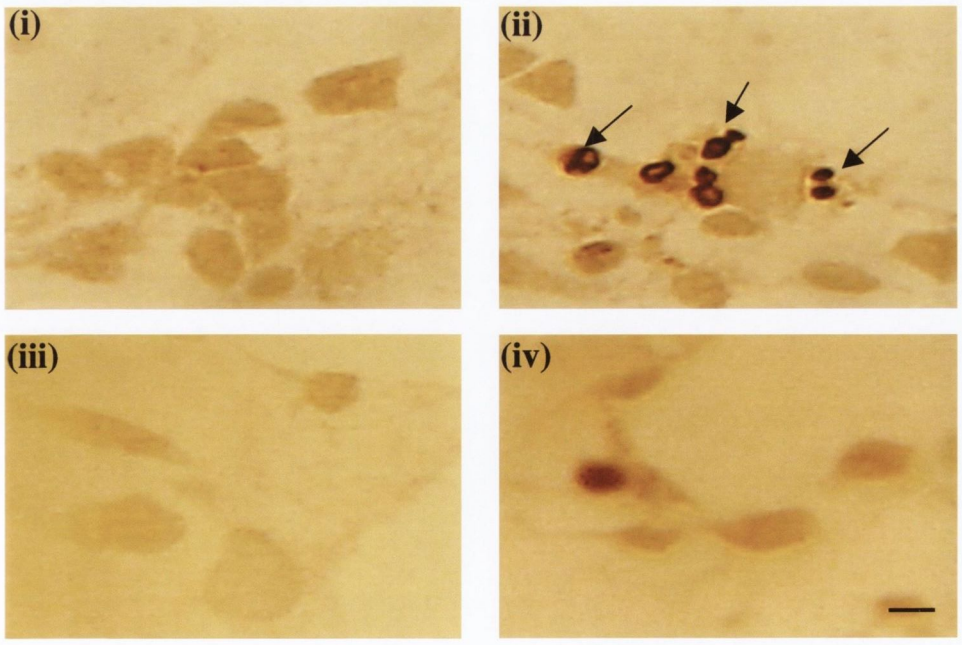
(i)
(ii)
(iii)
(iv)

4.2.10 Δ^9-THC causes the release of cathepsin-D into the cytosol

It has been widely documented that cell stress can cause the selective partial release of small amounts of lysosomal proteolytic enzymes into the cytosol (Gicciardi *et al.*, 2004). Furthermore, Δ^9-THC has been shown to induce the release of cathepsin-D in macrophages (Matveyeva *et al.*, 2000). For this reason the effect of Δ^9-THC on cathepsin-D location was assessed in cultured cortical neurones. Cathepsin-D activity was assessed in cytosolic fractions collected from cultured cortical neurones treated with Δ^9-THC (5 μM) for 1 hour in the presence or absence of the CB_1 antagonist, AM 251 (10 μM, 30 minute pre-treatment) by an immunocapture-based assay. Figure 4.8 demonstrates that following exposure to Δ^9-THC (5 μM) for 1 hour there was a significant increase in the level of cathepsin-D in cytosolic fractions from cells treated with Δ^9-THC ($p=0.0119$, ANOVA, $n=6$). In cells treated with Δ^9-THC (5 μM) for 1 hour cathepsin-D activity was 15.16 ± 4.28 nmoles MCA produced per mg protein per minute which was significantly higher than that observed in cells treated with vehicle (3.31 ± 1.60; $p<0.05$, vs., vehicle, Student Newman Keuls, $n=6$). While treatment with AM 251 alone had no effect on cathepsin-D activity (7.95 ± 1.49), Δ^9-THC failed to induce an increase in cathepsin-D activity in the presence of AM 251 (4.49 ± 0.34; $p<0.05$, vs., Δ^9-THC, Student Newman Keuls, $n=6$).

In addition, cathepsin-D distribution in neuronal cultures was assessed by confocal microscopy using fluorescently tagged pepstatin A (BODIPY FL-pepstatin A). Neurones were incubated with BODIPY FL-pepstatin A (1 μM) for 1 hour at 37°C to allow the labelling of cathepsin-D prior to exposure to Δ^9-THC or vehicle for 1 hour. BODIPY FL-pepstatin A displayed a punctate staining pattern in cells treated with vehicle (Figure 4.10B, (i)) indicating that cathepsin-D was located in lysosomes. However, in neurones exposed to Δ^9-THC (Figure 4.10B, (ii)), a more diffuse staining pattern was observed indicating that cathepsin-D was not restricted to the lysosomes. These results suggest that cathepsin-D is specifically released from lysosomes into the cytosol in cultured cortical neurones following Δ^9-THC exposure. Figure 4.10C shows that BODIPY FL-pepstatin A colocalises with lysosomes.

Figure 4.10: Δ^9-THC causes the release of cathepsin-D into the cytosol

A: Cultured cortical neurones were treated with Δ^9-THC (5 μM) for 1 hr. Cathepsin-D activity was assayed in cytosolic fractions by an immunocapture-based assay. Δ^9-THC significantly increased cathepsin-D activity which was abolished by pre-treatment with the CB_1 receptor antagonist AM 251. Results are expressed as nmoles MCA produced per mg protein per min and are means ± SEM, *$p<0.05$, Student Newman Keuls, n=7.

B: Cortical neurones were pre-treated with BODIPY FL-pepstatin A (1 μM; 1 hr pre-treatment) and exposed to vehicle (i) or 5 μM Δ^9-THC (ii) for 1 hr. Distribution of BODIPY FL-pepstatin A was assessed using confocal microscopy. A diffuse staining pattern was observed in Δ^9-THC-treated neurones compared to vehicle-treated neurones.

C: Confocal images of neurones treated with BODIPY FL-pepstatin A (1 μM; 1 hr pre-treatment) and incubated with LysoTracker™ (700 nM) for 25 min at 37°C. BODIPY FL-pepstatin A (green channel), Lysosomes (red channel) and overlay images are presented. BODIPY FL-pepstatin A colocalises with the lysosomes (yellow).

A

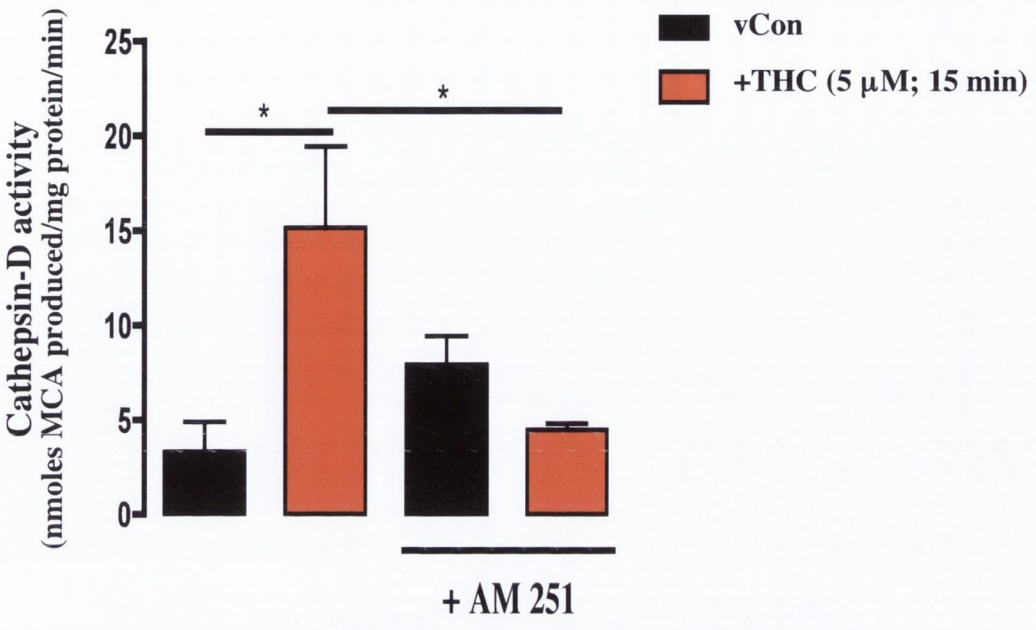
vCon
+THC (5 µM; 15 min)
Cathepsin-D activity
(nmoles MCA produced/mg protein/min)
25
20
15
10
5
0
*
*
+ AM 251

B

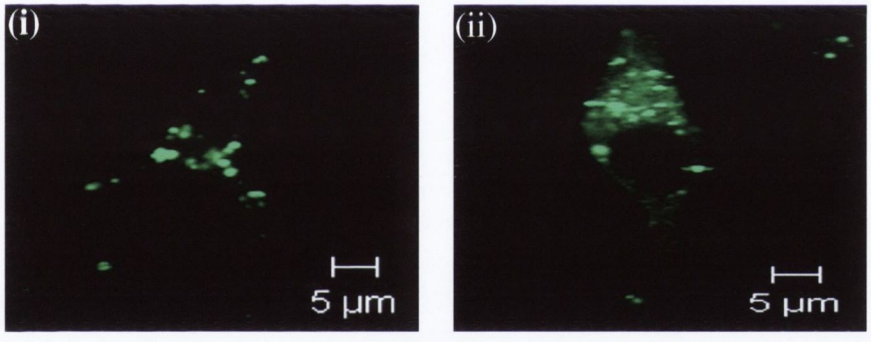
(i)
5 µm
(ii)
5 µm

C

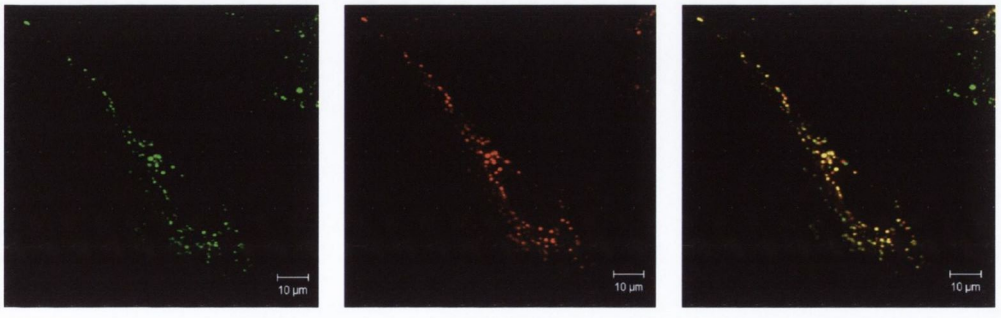
10 µm
10 µm
10 µm

4.2.11 Δ^9-THC-induced cathepsin-D release is dependent on p53 activity

In this study cathepsin-D activity was assessed in cytosolic fractions collected from cultured cortical neurones treated with Δ^9-THC (5 μM) for 1 hour in the presence or absence of the p53 inhibitor, pifithrin-α (100 nM, 60 minute pre-treatment) using an immunocapture-based assay. Figure 4.11 demonstrates that following exposure to Δ^9-THC (5 μM) for 1 hour there was a significant increase in the level of cathepsin-D in cytosolic fractions from cells treated with Δ^9-THC, which was abrogated by pifithrin-α ($p=0.0008$, ANOVA, n=6). In cells treated with Δ^9-THC (5 μM) for 1 hour cathepsin-D activity was 8.31 ± 2.28 nmoles MCA produced per mg protein per minute which was significantly more than cells treated with vehicle (1.96 ± 0.72; $p<0.01$, vs., vehicle, Student Newman Keuls, n=6). While treatment with pifithrin-α alone had no effect on cathepsin-D activity (1.20 ± 0.23) it prevented the Δ^9-THC-induced increase in cathepsin-D activity (0.98 ± 0.23; $p<0.01$, vs., Δ^9-THC, Student Newman Keuls, n=6). This result indicates that p53 is involved in the Δ^9-THC-induced relocation of cathepsin-D in cortical neurones.

Figure 4.11: Δ^9-THC-induced cathepsin-D release is dependent on p53 activity

Cultured cortical neurones were treated with Δ^9-THC (5 μM) for 1 hr. Cathepsin-D activity was assayed in cytosolic fractions using an immunocapture-based assay. Δ^9-THC significantly increased cathepsin-D activity and this was abolished by pifithrin-α. Results are expressed as nmoles MCA produced per mg protein per min and are means ± SEM, **p=0.01, Student Newman Keuls, n=6.

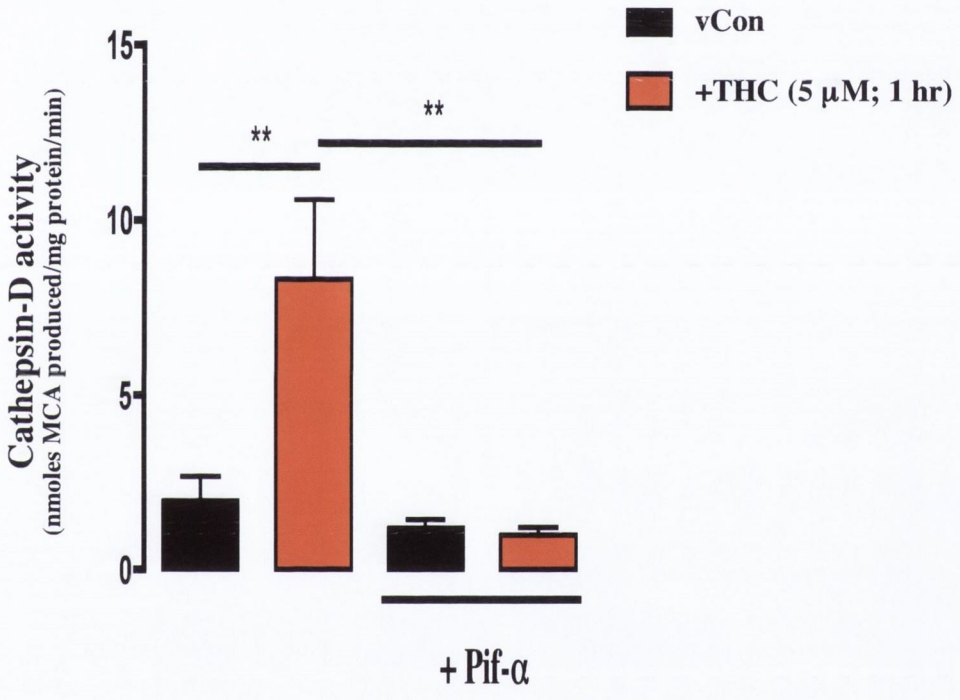
vCon
+THC (5 μM; 1 hr)
Cathepsin-D activity
(nmoles MCA produced/mg protein/min)
15
10
5
0
**
**
+ Pif-α

4.2.12 Δ^9-THC-induced caspase-3 activity is dependent on cathepsin-D activity

It has been previously shown that cathepsin-D can cause caspase-3 activation (Heinrich *et al.*, 2004). Therefore we investigated the role of cathepsin-D in the Δ^9-THC-induced increase in caspase-3 activity. Caspase-3 activity was assessed in cytosolic fractions collected from cultured cortical neurones treated with Δ^9-THC (5 μM) for 2 hours in the presence or absence of a cathepsin-D inhibitor (CDi; 10 μM, 30 minute pre-treatment) by cleavage of a fluorogenic substrate. Figure 4.12A demonstrates that following exposure to Δ^9-THC (5 μM) for 2 hours there was a significant increase in caspase-3 activity in the cytosolic fraction of cells treated with Δ^9-THC which was abolished by inhibition of cathepsin-D activity ($p<0.0001$, ANOVA, n=6-7). In cells treated with Δ^9-THC (5 μM) for 1 hour caspase-3 activity was 128 ± 27% greater than in cells treated with vehicle ($p<0.001$, vs., vehicle, Student Newman Keuls, n=6-7). Treatment with CDi in the presence of Δ^9-THC significantly decreased the level of caspase-3 activity (10 ± 19% greater than control values; $p<0.001$, vs., Δ^9-THC, Student Newman Keuls, n=6-7). These results indicate that cathepsin-D activity is necessary for the Δ^9-THC-induced increase in caspase-3 activity. Fluorescent images of the CDi-dependent increase in active caspase-3 immunoreactivity in neurones treated with Δ^9-THC are shown in Figure 4.12B.

Figure 4.12: Δ^9-THC-induced caspase-3 activity is dependent on cathepsin-D activity

A: Cultured cortical neurones were treated with Δ^9-THC (5 μM) for 2 hr and total protein was harvested. Caspase-3 activity was assayed by the cleavage of the fluorogenic caspase-3 substrate (DEVD-AFC). The Δ^9-THC-induced increase in caspase-3 activity was abolished by the inhibition of cathepsin-D (CDi; 10 μM). Results are shown as % of control, means ± SEM, ***p<0.001, Student Newman Keuls, n=6.

B: Cultured cortical neurones were treated with Δ^9-THC (5 μM) for 2 hr, fixed and caspase-3 expression was assessed by immunocytochemistry using an antibody that specifically recognises the active form of caspase-3. Sample confocal images of neurones treated with vehicle (i), Δ^9-THC (ii), CDi alone (iii) and CDi and Δ^9-THC (iv). DIC images are also represented. Arrows indicate cells expressing active caspase-3.

A

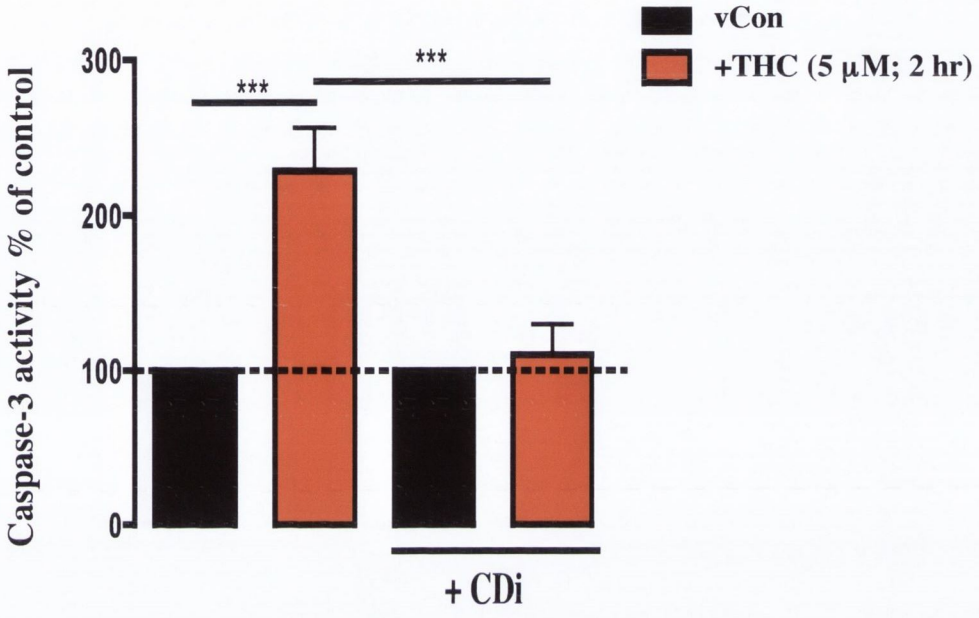
vCon
+THC (5 μM; 2 hr)
Caspase-3 activity % of control
300
200
100
0
***
***
+ CDi

B

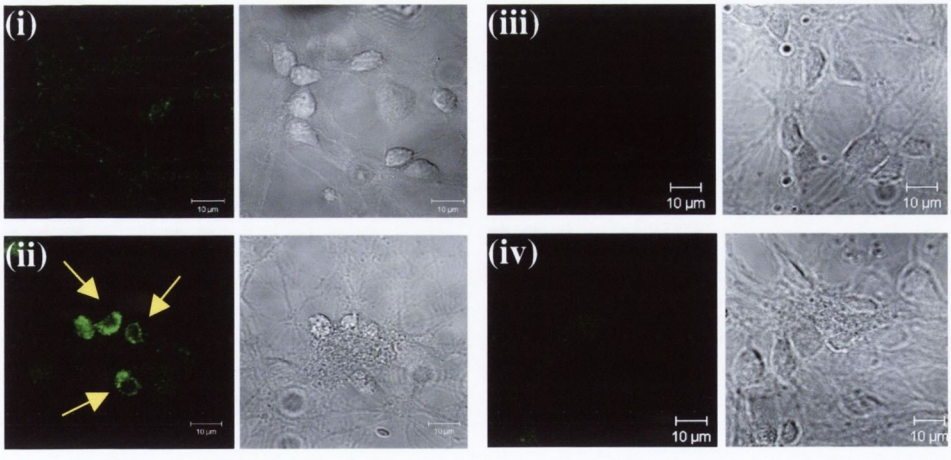
(i)
(ii)
(iii)
(iv)
10 μm

4.2.13 Δ^9-THC-induced DNA fragmentation is dependent on cathepsin-D activity

DNA fragmentation was assessed by TUNEL staining in cultured cortical neurones following exposure to Δ^9-THC (5 μM) for 2 hours in the presence or absence of a cell permeable inhibitor of cathepsin-D (CDi; 30 minute pre-treatment). Figure 4.13 demonstrates that Δ^9-THC-induced DNA fragmentation is dependent on cathepsin-D activity ($p<0.0001$, ANOVA, n=6 observations). In vehicle-treated cells, 16.15 ± 2.24% (mean ± SEM) of cells displayed fragmented DNA in the nucleus (TUNEL positive). This was significantly increased to 58.79 ± 3.18% in cells treated with Δ^9-THC for 2 hours ($p<0.001$, vs., vehicle, Students Newman Keuls, n=6 observations). Pre-treatment of cells with CDi prevented the Δ^9-THC-induced increase in DNA fragmentation (25.31 ± 3.26%; $p<0.001$, vs., Δ^9-THC, Student Newman Keuls, n=6 observations). This finding suggests that cathepsin-D is involved in Δ^9-THC-induced DNA fragmentation. Representative images of TUNEL stained neurones are shown in Figure 4.13B.

Figure 4.13: Δ^9-THC-induced DNA fragmentation is dependent on cathepsin-D activity

Cortical neurones were treated with CDi (10 μM) for 30 minutes prior to exposure to Δ^9-THC (5 μM) for 2 hours. Cell viability was assessed using the TUNEL technique.

A: Δ^9-THC significantly increased the percentage of TUNEL positive cells. CDi abolished the Δ^9-THC-induced increase in DNA fragmentation. Results are displayed as mean ± SEM, ***p<0.001, Students Newman Keuls, n=6 observations.

B: Sample images TUNEL stained neurones treated with (i) vehicle, (ii) Δ^9-THC, (iii) CDi alone and (iv) Δ^9-THC in the presence of CDi. Arrows indicate TUNEL positive neurones.

A

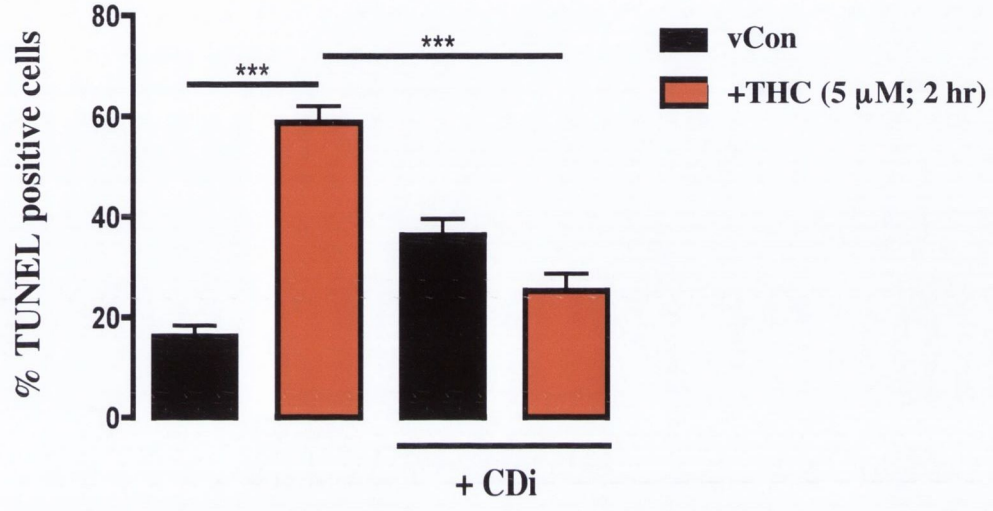
% TUNEL positive cells
80
60
40
20
0
***
***
vCon
+THC (5 μM; 2 hr)
+ CDi

B

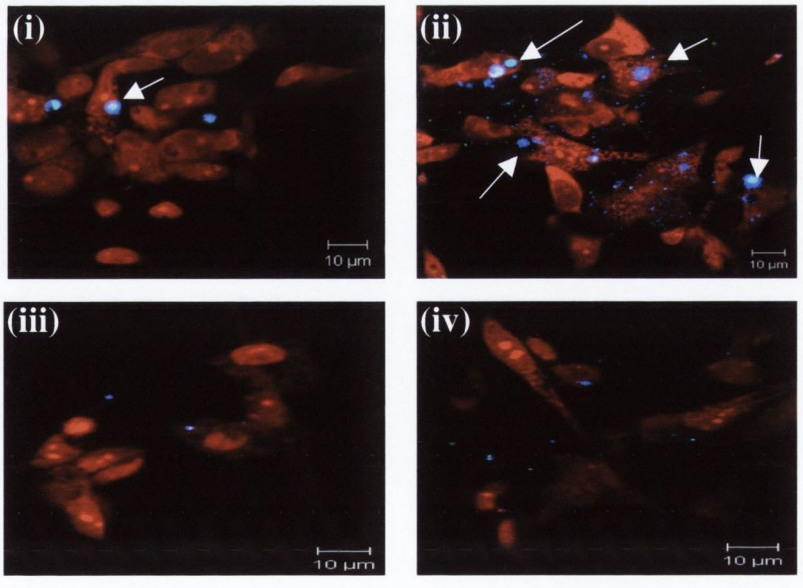
(i)
(ii)
(iii)
(iv)
10 μm
10 μm
10 μm
10 μm

4.3 Discussion

Experimental work in this chapter investigated the role of lysosomal signalling in Δ^9-THC-induced neuronal apoptosis. The data provides evidence for Δ^9-THC promoting lysosomal membrane destabilisation in a time- and dose-dependent manner mediated through the CB_1 receptor. The results also suggest that Δ^9-THC causes the translocation of phospho-p53^{ser15} to the lysosomes indicating that this pro-apoptotic signalling protein is involved in the lysosomal-mediated initiation of apoptosis. Furthermore, the proclivity of Δ^9-THC to promote the induction of lysosomal instability was dependent on p53 activity since both pharmacological inhibition of p53 activity and siRNA mediated p53 protein depletion prevented Δ^9-THC-induced lysosomal membrane instability. Inhibiting the activity of SyK also prevented the ability of Δ^9-THC to induce the disruption of the lysosomal membrane, however, a significant colocalisation of SyK with lysosomes was not observed. This may indicate that SyK signals to other, as yet unidentified, signalling proteins to evoke Δ^9-THC-induced lysosomal membrane instability. In addition, the release of cathepsins from lysosomes was assessed as another marker for destabilised lysosomal membranes. Δ^9-THC-induced a significant release of cathepsin-D but not cathepsin-L. This selective release of cathepsin-D, coupled with the fact that no obvious morphological signs of cell death were observed at the time of maximal lysosomal membrane destabilisation (15 minutes), indicates that the effect of Δ^9-THC on the lysosome is a specific process subject to rigorous control through the activation of at least two signalling proteins. The role of cathepsins in the activation of downstream apoptotic signalling events was also subject to investigation in this study. Inhibition of cathepsin catalytic activity, using small peptide inhibitors, prevented Δ^9-THC-induced caspase-3 activation and DNA fragmentation. Overall, these data provide evidence for a lysosomal branch of the apoptotic program in neuronal cell death caused by exposure to Δ^9-THC.

Lysosomes, originally thought to be stable organelles, are now emerging as early pro-apoptotic signalling organelles. The leakage of the proteolytic contents of lysosomes, as a result of a destabilisation of the lysosomal membrane, can activate cell death signalling cascades both directly and indirectly. It is for this reason that the role of lysosomes in the apoptotic cascade is compared to the leakage of mitochondrial

proteins from the mitochondria, which is a well-established feature of apoptosis. The integrity of the lysosomal membrane and the maintenance of a lysosomal-cytosolic pH gradient were assessed using the acridine orange (AO) relocation technique. In this approach cells are incubated with a fluorogenic organic weak base, which diffuses through the cell membrane and accumulates in the lysosomes due to the acidic environment in the lysosomes. The accumulation of AO in the lysosomes creates a shift in the fluorescent emission profile of AO. In concentrated form *i.e.,* concentrations found in the lysosomes, AO emission peak is 633 nm, however lower concentrations of AO (concentrations found in the nucleus and cytosol) display an emission peak at 520 nm. Thus, measuring the emission at 633 nm can assess the integrity of the lysosomal membrane and/or change in lysosomal pH; decreased 633 nm implicates that the lysosomal membrane has been compromised. Several groups have reported that the leakage of AO from lysosomes to the cytosol is an accurate representation of decreased lysosomal membrane integrity (Yuan *et al.*, 2002; Li *et al.*, 2002).

The results of the study indicate that in vehicle-treated cells AO fluorescence exhibited a punctate distribution with a high level of fluorescence at 633 nm emission, reflective of intact lysosomes. However, cells exposed to Δ^9-THC displayed a significant decrease in 633 nm emission indicating that the lysosomal membrane was compromised and was no longer able to retain high levels of AO. The lysosomal membrane destabilisation induced by Δ^9-THC was rapidly induced within 15 minutes of drug treatment. This indicates that lysosomal destabilisation occurs early in the time line of our apoptotic cascade, which culminates after 2 - 3 hours of drug treatment. This observation is in accordance with several reports, which suggest that lysosomal membrane instability occurs shortly after exposure to an insult and acts as an initiator of the mitochondrial pathway of apoptosis (Antunes *et al.*, 2001; Yuan *et al.*, 2002; Bidère *et al.*, 2003; Cirman *et al.*, 2004). Indeed, Terman *et al.*, (2006) have put forward a hypothesis for the presence of a 'lysosomal-mitochondrial axis', which proposes that crosstalk between the lysosome and mitochondria exists in long lived post mitotic cells, such as neurones and cardiac myocytes, and is important for mediating apoptosis in these cells. Furthermore, additional lysosomal rupture as a consequence of transient oxidative stress originating from the mitochondria caused by the negative action of

lysosomal enzymes on the mitochondrial membrane creates an amplifying loop system, which accelerates the apoptotic process. In neuronal cells, which are particularly sensitive to cell stressors, lysosomal membrane destabilisation is induced by exposure to hypoxia, Aβ and 6-Hydroxydopamine (Islekel *et al.*, 1999; Li *et al.*, 2003; Boland *et al.*, 2004; Lee *et al.*, 2007). Post mitotic cells like neurones have extremely concentrated levels of proteolytic enzymes present in their lysosomes (up to 1mM for cathepsins alone), which is due to lack of cell division which normally dilutes the concentration of the contents of lysosomes (Mason, 1996). It is believed that this is the reason why leakage of proteolytic enzymes as a consequence of lysosomal membrane destabilisation activates an apoptotic response in many post mitotic cells. Interestingly, early reports in the literature describing the lytic effect of Δ^9-THC on isolated liver lysosomes and subsequent release of acid hydrolases would indicate that Δ^9-THC, which is highly lipophillic, may directly influence lysosomal permeability in some cell types (Raz *et al.*, 1973; Britton and Mellors, 1974; Irvin and Mellors, 1975).

The mechanism of p53-induced apoptosis has been extensively studied and involves the activation of the mitochondrial/caspase pathway of apoptosis and regulates the transcription of pro-apoptotic genes. Since Δ^9-THC induced an early activation of the p53 protein, it was pertinent to investigate the role of p53 in Δ^9-THC-induced lysosomal membrane instability. The p53 protein was largely associated with the nucleus where it is likely to participate in the transcription of apoptotic genes (Green and Chipuk, 2006). However, a substantial proportion of p53 immunoreactivity colocalised with the lysosomal marker LysoTracker Red™, indicating the association of p53 with the lysosomal compartment early in the cell death cascade. To assess whether p53 regulates lysosomal integrity we used the reversible p53 inhibitor, pifithrin-α, which prevents p53 transactivation and phosphorylation, as well as siRNA-mediated depletion of p53. Using both experimental approaches the Δ^9-THC-induced permeabilisation of lysosomes was prevented, providing evidence for a role of p53 in controlling lysosomal permeability. However, the exact molecular mechanism for p53-dependent Δ^9-THC-induced lysosomal membrane destabilisation have yet to be elucidated, but interaction with Bax followed by insertion into the lysosomal membrane is one possibility that has been demonstrated (Kågedal *et al.*, 2001a). This is interesting,

as a previous result from our laboratory has shown that Δ^9-THC increases the upregulation of Bax in the cytosol (Downer *et al.*, 2001). Another potential signalling molecule pertinent in the regulation of lysosomal dynamics is intracellular sphinogosine, which is also regulated by cannabinoids and is necessary for the induction of apoptosis in glioma cells (Kågedal *et al.*, 2001b; Galve-Roperh *et al.*, 2000). We have recently demonstrated that *in vivo* administration of Δ^9-THC increases the cytosolic expression and activity of cathepsin-D and the results presented herein demonstrate that p53-mediated regulation of lysosomal integrity may be a key factor in this event (Downer *et al.*, 2007b).

Since Δ^9-THC-induced apoptosis was regulated by the tyrosine kinase SyK, it was decided to investigate the role of this protein in mediating Δ^9-THC-induced lysosomal membrane destabilisation. Inhibiting the activity of SyK prevented Δ^9-THC-induced lysosomal membrane destabilisation, however, no significant colocalisation between SyK and the lysosomes was observed. These results indicate that SyK has an important role in Δ^9-THC-induced lysosomal permeabilisation, which is likely to involve signalling upstream of the lysosomes and not through direct activity at the lysosomal membrane. A recent study by He and colleagues (2005) showed that after BCR-cross linking lysosomal membrane permeability and the concomitant release of lysosomal enzymes was absent in SyK deficient cells and that BCR-induced apoptosis was as a result of SyK activity. In that study SyK was found to associate with the BCR-carrying endosomes, which may explain why no significant colocalisation with the lysosomes was found in our experiments. Whilst our results do not point to a direct association between SyK and the lysosomes the inhibition of Δ^9-THC-induced lysosomal membrane destabilisation by using an SyK inhibitor is an interesting finding which should be investigated further.

The release of degradative lysosomal enzymes *e.g.,* cathepsins, is a natural consequence of lysosomal membrane destabilisation. Cathepsins are thought to play a significant role in apoptosis and their release from the lysosomal compartment is induced by a number of cell stressors *e.g.,* oxidative stress, p53 activation, exposure to Aβ (Roberg and Ollinger, 1998; Yuan *et al.*, 2002; Boland *et al.*, 2004). There may also be a direct activation of caspases by lysosomal cathepsins (Vancompernolle *et al.*,

1998). Furthermore, cathepsin-D, both in its mature or inactive form, can impact on an as yet unidentified substrate(s) to induce apoptosis (Schestkowa *et al.*, 2007). Hence we investigated the role of cathepsins in Δ^9-THC-induced apoptosis in cultured cortical neurones. Δ^9-THC-induced the specific release of cathepsin-D as cathepsin-L release was not observed. However, inhibition of cathepsin-L did prevent Δ^9-THC-induced DNA fragmentation, which would indicate that cathepsin-L might have a role in the apoptotic response induced by Δ^9-THC. Interestingly, cathepsin-L activity has been linked with activating cathepsin-D and it is common to observe an increase in cathepsin-D in parallel to a decrease in cathepsin-L activity. This observation is believed to be as a result of the main role of cathepsin-L being the regulation of intralysosomal homeostasis of protease content and has prompted some researchers to suggest that cathepsin-L plays a crucial role in the activation of cathepsin-D activity (Wille *et al.*, 2004). These observations may explain why cathepsin-L inhibition prevented Δ^9-THC-induced apoptosis in the absence of its relocation in our experiments. The ability of Δ^9-THC to regulate cathepsin-D was examined using an immunocapture-based assay for cathepsin-D activity and immunocytochemistry using a cathepsin-D specific fluorescent probe, BODIPY FL-pepstatin A (methods section 2.8.6). Δ^9-THC-induced an increase in cathepsin-D activity after 1 hour drug treatment which was mediated through the CB_1 receptor. Matveyeva *et al.*, (2000) have demonstrated that Δ^9-THC increases cathepsin-D activity *via* the CB_2 receptor which may contribute to deficits in antigen-dependent processing. The subcellular distribution of cathepsin-D was also altered by Δ^9-THC treatment. After Δ^9-THC treatment the distribution of fluorescently labelled cathepsin-D was extremely diffuse in appearance compared to the punctate appearance observed in vehicle-treated cells, indicating that cathepsin-D was no longer confined in the lysosomes. Colocalisation analysis using the lysosomal specific marker, LysoTracker Red™, confirmed the lysosomal localisation of fluorescent labelled cathepsin-D. The redistribution of cathepsin-D to the cytosol correlated with an increase in cathepsin-D activity. The alteration in the subcellular distribution of cathepsin-D was also observed in a mesencephalic dopaminergic neuronal cell line, N27 cells, treated with methamphetamine (Kanthasamy *et al.*, 2006). Kanthasamy and co-workers (2006) observed that untreated cells displayed a granular

cathepsin-D staining pattern, whilst cells treated with methamphetamine showed an increased level of cathepsin-D staining and displayed a globular pattern. The observations of Kanthasamy *et al.*, (2006) are indicative of a disruption of the lysosomal membrane followed by the release of cathepsin-D which has been shown to activate the apoptotic pathway.

Since we have shown that p53 is involved in regulating Δ^9-THC-induced lysosomal membrane destabilisation, the role of p53 in the release of cathepsin-D from the lysosomal lumen was investigated. Pharmacological inhibition of p53 with pifithrin-α abrogated the Δ^9-THC-induced release of cathepsin-D into the cytosol indicating that p53 activity is required for the release of lysosomal proteases upon Δ^9-THC-induced membrane instability. Therefore, it is interesting to note that p53 acts as a transcriptional up regulator of cathepsin-D. Furthermore, experiments carried out by Kågedal *et al.*, (2001a) showed that the induction of oxidative stress caused an increase in the p53 protein, which caused an increase in cathepsin-D activity and translocation of cathepsin-D to the nucleus, all of which preceded the activation of caspase-3. This report is extremely relevant since further studies carried out in our laboratory show that cathepsin-D activity is necessary for Δ^9-THC-induced increase in caspase-3 activity and the induction of apoptosis. A link between cathepsin-D and caspase-3 has been reported to occur during apoptosis *via* a Bid- and Bax-signalling pathway (Johansson *et al.*, 2003; Kågedal *et al.*, 2005). Our recent *in vivo* studies have demonstrated that administration of Δ^9-THC increases the cytosolic expression and activity of cathepsin-D in the cerebral cortex as part of the apoptotic cascade and the results presented herein would indicate that p53-mediated regulation of lysosomal integrity is a key factor in this neurotoxic event (Downer *et al.*, 2007b). In this regard it is notable that cathepsin-D gene expression outlines the regions of physiological cell death during embryonic development and the aberrant engagement of this apoptotic pathway by exogenous phytocannabinoids during *in utero* cannabis exposure may cause the disruption of the finely tuned endocannabinoid-mediated brain developmental processes (Zuzarte-Luis *et al.*, 2007; Harkany *et al.*, 2007).

Overall, these data indicate a novel role for pro-apoptotic lysosomal signalling in Δ^9-THC-induced neuronal apoptosis involving the tumour suppressor protein, p53.

Given the interest in the ability of cannabinoids to regulate cell fate, this pathway may be important for the anti-tumoural properties of cannabinoids, as well as being involved in the control of neural cell viability.

Summary schematic

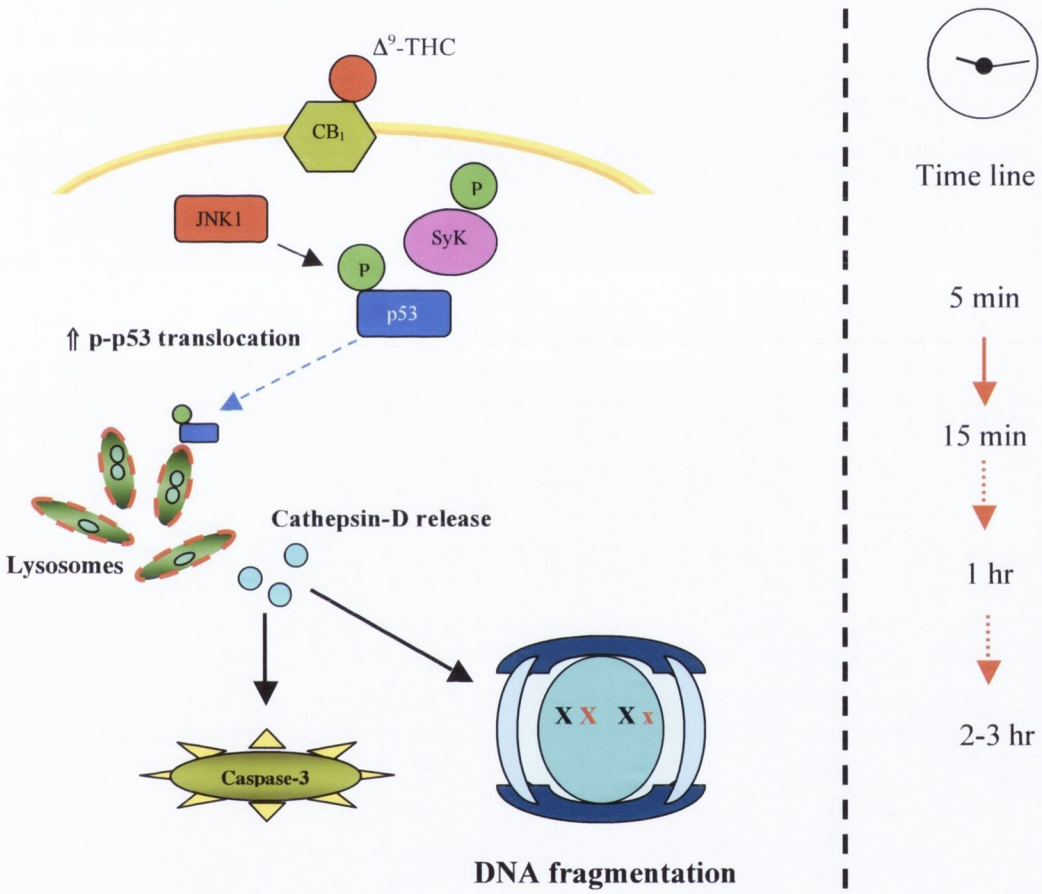

Chapter 5

An investigation into the effect of endocannabinoids on neuronal viability

5.1 Introduction

Many investigations have shown anandamide (AEA) to be cytotoxic *in vivo* and *in vitro* in cells such as human breast carcinomas, primary neuronal cultures, CHP100 neuroblastoma, PC12 cells, C6 gliomas, epithelial tumours, uterine cervix cancer cells, keratinocytes, and osteosarcoma cells (De Petrocellis *et al.*, 1998; Movsesyan *et al.*, 2004; Maccarrone *et al.*, 2000; Sarker *et al.*, 2000; Jacobsson *et al.*, 2001; Bifulco *et al.*, 2001; Contassot *et al.*, 2004; Telek *et al.*, 2007; Hsu *et al.*, 2007). Furthermore, there is evidence that the immunosuppressive effects of AEA are associated with the inhibition of proliferation and the induction of apoptosis in lymphocytes (Schwarz *et al.*, 2000). Given this, and since we have shown that Δ^9-THC induces a neurotoxic effect in cultured cortical neurones, the effect of the main endogenous cannabinoid ligands, AEA and 2-AG, on the viability of cultured cortical neurones was investigated in this chapter.

The pro-apoptotic activity of AEA in different cells is mediated through the activation of different receptors, which in turn trigger a variety of signalling mechanisms downstream of the ligated receptors. The transient receptor potential vanilloid subtype 1 (TRPV1 or VR_1) is a non-selective cation channel activated by vanilloids such as capsaicin (Caterina and Julius, 2001). In addition, anandamide, arachidonoyl-dopamine and products of lipoxygenases can also activate VR_1 (Di Marzo *et al.*, 2001; Huang *et al.*, 2002; Hwang *et al.*, 2000). Activation of VR_1 excites sensory neurones, causes pain and the accumulation of intracellular Ca^{2+} which can lead to mitochondrial disruption and oxidative cell damage (Shin *et al.*, 2003). Indeed, activation of VR_1 by AEA has been shown to induce increases in Ca^{2+} which led to the release of cytochrome c and caspase-3 activation in dopaminergic neurones (Kim *et al.*, 2005). Maccarrone and co-workers (2000) have demonstrated that AEA-induced apoptotic body formation and DNA fragmentation in neuronal CHP100 neuroblastoma cells through a pathway involving activation of VR_1, rises in intracellular calcium, mitochondrial uncoupling and cytochrome c release. Caspase-3 activation in addition to the condensation and fragmentation of DNA has been shown to be a result of AEA-induced superoxide anion formation in PC12 cells, however, a receptor was not identified for mediating these pro-apoptotic signals (Sarker *et al.*, 2000). The *in vivo* pro-apoptotic effect of AEA *via* VR_1 has been confirmed in neonatal rats treated with

AEA (1 mg/Kg s.c. for up to 20 weeks post partum), which resulted in the selective mitochondrial damage of VR_1 expressing B-type sensory neurones of the rat trigeminal ganglion. These mitochondrial effects were of a permanent and progressive manner and first observed after 1 week of treatment (Szöke *et al.*, 2002). Conversely, AEA has been shown to induce neurotoxicity independently of VR_1, CB_1, CB_2 and the NMDA receptor in primary cortical neurones and cerebellar granule cells (Movesesyan *et al.*, 2004). Key pro-apoptotic determinates were found to be activated in that study, such as, intracellular Ca^{2+}, mitochondrial damage and activation of caspase-3. However, due to an observed concomitant activation of calpain and the selective inhibition of neurotoxicity by calpain inhibitors, Movesesyan *et al.*, concluded that calpain activation acting upstream of caspase pathways play a role in AEA-induced neuronal death. These findings are consistent with other reports showing the lack of effects of CB_1, CB_2 or VR_1 antagonists on AEA-induced cell death in cell lines (Sarker and Maruyama, 2003). One possible explanation for the unresolved mechanism of action for AEA-induced toxicity may be the differing binding site location, intracellular for VR_1 and extracellular for CB_1 and CB_2. Indeed, the oxidative metabolites generated during the catabolism of AEA may be critical in controlling its pro-apoptotic potential since these metabolites can modulate the effect of AEA on VR_1 receptors (Maccarrone *et al.*, 2003; De Petrocellis *et al.*, 2001). Therefore further studies hold the answer regarding the relative contribution that AEA synthesis, degradation and alternative receptor binding patterns has on the decision between cell survival and death (Maccarrone and Finazzi-Agró, 2003).

Concentrations of 2-AG are the highest amongst the endocannabinoids and 2-AG invokes different responses such as proliferation, growth arrest, decreased cell contractility, cell death and anti-inflammatory pathways in various cell types (Rueda *et al.*, 2000; Sarker *et al.*, 2003; Berdyshev, *et al.*, 2001; Derkinderen *et al.*, 2003). It has been recently demonstrated that 2-AG induces apoptosis in activated hepatic fibrogenic stellate cells, but not in hepatocytes. This suggests that 2-AG through its pro-apoptotic effects has an anti-fibrogenic role in the liver, which could be of therapeutic use in the treatment of liver fibrosis (Siegmund and Brenner, 2005; Siegmund *et al.*, 2007). In addition, the anti-proliferative potency of 2-AG in rat glioma C6 cells is similar to that

of AEA (Jacobsson *et al.*, 2001). Recent work by Sang and colleagues (2007) have also demonstrated that 2-AG metabolites generated by COX-2, potentiated excitatory glutamatergic synaptic transmission and produced neurotoxicity in a CB_1 independent manner which was mediated *via* ERK, p38 MAPK, IP_3 and NF-KB signal transduction pathways. However, 2-AG is unable to modulate survival in CHP100 or human lymphoma U937 cells (Maccarrone *et al.*, 2000).

Cannabinoids differ with respect to their neuroprotective capacity and it has been suggested that 2-AG, AEA and Δ^9-THC use different mechanisms to exert neuroprotection on different cell types in the CNS and/or invading monocytes and activated T-cells after cerebral injury (Kreutz *et al.*, 2007). A number of studies have demonstrated that AEA and 2-AG, in addition to classical and synthetic cannabinoids can suppress the excitation of neuronal cells *in vitro* (Suguira *et al.*, 2006). However, the results of Hansen and colleagues (2001) show that AEA and not 2-AG is produced by strong neurodegenerative stimuli *e.g.,* NMDA excitoxicity and traumatic brain injury. Stimulation of the CB_1 receptor dampens the destructive impact of brain insults by lowering the release of glutamate, therefore, cannabinoids exhibit neuroprotective actions in cultured neuronal cells exposed to stress (Shen *et al.*, 1998; Sinor *et al.*, 2000; Nagayama *et al.*, 1999). However, reports showing cannabinoid-induced neuroprotection is not prevented by CB_1 blockade and that cannabinoids, AEA in particular, possess alternative receptor binding capabilities, which indicates that the mechanism of neuroprotection provided by AEA and 2-AG is not clear cut (Sinor *et al.*, 2000; Nagayama *et al.*, 1999; McAllister and Glass, 2002).

Given that there is an apparent dualism in the effects of endocannabinoids on cell survival and that previous findings from our laboratory show a neurotoxic profile for Δ^9-THC in cultured cortical neurones, this chapter aimed to assess the effect of two endocannabinoids, AEA and 2-AG, on the viability of cultured cortical neurones. In addition, the potential role of each endocannabinoid in the signal transduction pathways that we have shown to be regulated by Δ^9-THC was analysed. The presence of apoptotic markers such as, DNA fragmentation, caspase-3 activation and p53 phosphorylation were analysed in cultured cortical neurones exposed to AEA or 2-AG, as assessed by TUNEL staining, biochemical assay, immunocytochemistry and western immunoblot.

Furthermore, the potential neuroprotective influence of 2-AG was investigated by assessing the proclivity of 2-AG to prevent glutamate-induced DNA damage in cultured cortical neurones.

5.2.1 AEA-induced DNA fragmentation is independent of CB_1 and VR_1

To determine whether the endogenous cannabinoid, anandamide (AEA), is neurotoxic we assessed its ability to induce DNA fragmentation in cultured rat cortical neurones. DNA fragmentation was assessed by TUNEL staining following exposure to AEA (0.1 - 200 μM) for 2 hours (Figure 5.1A). AEA induced DNA fragmentation in a dose-dependent manner ($p<0.0001$, ANOVA, n=4-7 observations). In vehicle-treated cells, 6.99 ± 0.67% (mean ± SEM) of cells displayed fragmented DNA in the nucleus (TUNEL positive). This was comparable to cells treated with 0.1 and 5 μM AEA for 2 hours (10.26 ± 0.68% and 13.95 ± 1.85%, respectively). However, treatment of cells with 20, 100 and 200 μM AEA induced a significant increase in DNA fragmentation (21.06 ± 2.20%, 23.78 ± 3.37% and 36.53 ± 4.14%, respectively; $p<0.001$, vs., vehicle, Student Newman Keuls, n=4-7 observations). This finding demonstrates that AEA induces apoptosis in cultured cortical neurones in a dose-dependent manner.

To investigate the receptor involved in mediating AEA-induced DNA fragmentation cultured cortical neurones were TUNEL stained following exposure to AEA (0.1 - 200 μM) for 2 hours in the presence of the CB_1 receptor antagonist, AM 251 (10 μM, 30 minute pre-treatment; Figure 5.1B). AEA induced DNA fragmentation in a CB_1 receptor independent manner ($p<0.0001$, ANOVA, n=4-7 observations). In cells treated with vehicle in the presence of AM 251, 8.13 ± 0.56% (mean ± SEM) were TUNEL positive, which was comparable to cells treated with 0.1 μM AEA for 2 hours in the presence of AM 251 (9.06 ± 0.99%). The number of cells displaying fragmented DNA was significantly increased in neurones treated with 5 μM AEA in the presence of AM 251 for 2 hours (16.47 ± 1.12%, $p<0.05$, vs., AM 251 and vehicle, Student Newman Keuls, n=4-7 observations). This response was also maintained in neurones treated with 20, 100, and 200 μM AEA in the presence of AM 251 for 2 hours (26.05 ± 2.28%, 34.60 ± 4.91% and 31.23 ± 2.49%, respectively, $p<0.001$, vs., AM 251 and vehicle, Student Newman Keuls, n=4-7 observations; Figure 5.1B). This finding suggests that AEA induced DNA fragmentation is not mediated through the CB_1 receptor. Representative images of TUNEL stained neurones are shown in Figure 5.1E.

To determine if AEA-induced DNA fragmentation was mediated *via* the VR_1 receptor cultured cortical neurones were TUNEL stained following exposure to AEA (0.1 - 200 μM) for 2 hours in the presence of the VR_1 receptor antagonist, capsazepine (CZP; 10 μM, 30 minute pre-treatment). Figure 5.1C demonstrates that the AEA induced DNA fragmentation occurs in a VR_1 receptor independent manner ($p<0.0001$, ANOVA, n=4 observations). In cells treated with vehicle in the presence of CZP, 7.07 ± 0.67% (mean ± SEM) were TUNEL positive, which was comparable to cells treated with 0.1 μM AEA in the presence of CZP for 2 hours (11.22 ± 2.39%). The number of cells displaying fragmented DNA was significantly increased in neurones treated with 5 μM AEA in the presence of CZP for 2 hours (14.42 ± 0.65%, $p<0.05$, vs., vehicle, Student Newman Keuls, n=4 observations). This was also maintained in neurones treated with 20, 100, and 200 μM AEA in the presence of CZP for 2 hours (23.19 ± 1.23%, 34.05 ± 4.70% and 41.80 ± 5.57% respectively, $p<0.001$, vs., vehicle, Student Newman Keuls, n=4 observations; Figure 5.1C). This finding suggests that AEA-induced DNA fragmentation is not mediated through the VR_1 receptor.

When data were collated significant differences were found between the inhibitor groups which indicated that the neurotoxic profile of AEA depended on the type of available receptor present at the time of exposure to drug (Figure 5.1D). Figure 5.1E displays TUNEL stained neurones treated with various concentrations of AEA.

Figure 5.1: AEA-induced DNA fragmentation is independent of CB_1 and VR_1

A: Primary cortical neurones were treated with AEA (0.1 - 200 μM) for 2 hours, cells were fixed and analysed for DNA fragmentation using TUNEL. A significant increase in DNA fragmentation (TUNEL +ve neurones) was found following treatment with AEA at concentrations of 20, 100 and 200 μM. Results are expressed as mean ± SEM, ***p<0.001, vs., vehicle, Student Newman Keuls, n=4-7 observations.

B: Cell viability was assessed by the TUNEL assay in cultured cortical neurones treated with AEA (0.1 - 200 μM; 2 hr) in the presence of the CB_1 receptor antagonist AM 251 (10 μM; 30 min pre-treatment). AEA-induced DNA fragmentation was not prevented by AM 251. Results are expressed as means ± SEM, *p<0.05, ***p<0.001, vs., vehicle, Student Newman Keuls, n=4-7.

C: Cell viability was assessed by the TUNEL assay in cultured cortical neurones treated with AEA (0.1 - 200 μM; 2 hr) in the presence of the VR_1 receptor antagonist, CZP (10 μM; 30 min pre-treatment). AEA-induced DNA fragmentation was not prevented by CZP. Results are expressed as mean ± SEM, *p<0.05, ***p<0.001, vs., vehicle, Student Newman Keuls, n=4 observations.

D: Significant differences were observed between AEA (200 μM) in the presence of AM 251 compared to between AEA (200 μM) in the presence of CZP (*p<0.05, Student Newman Keuls, n=4-7 observations). In addition there was a significant difference between AEA (100 μM) compared to AEA (100 μM) in the presence of both AM 251 and CZP (+ and &, respectively, p<0.05, Student Newman Keuls, n=4-7).

E: Light microscopy images of TUNEL stained neurones treated with (i) vehicle, (ii) AEA (100 μM), (iii) AM 251 alone and (iv) AEA (100 μM) in the presence of AM 251. Arrows indicate TUNEL-positive cells. Scale bar is 10 μm.

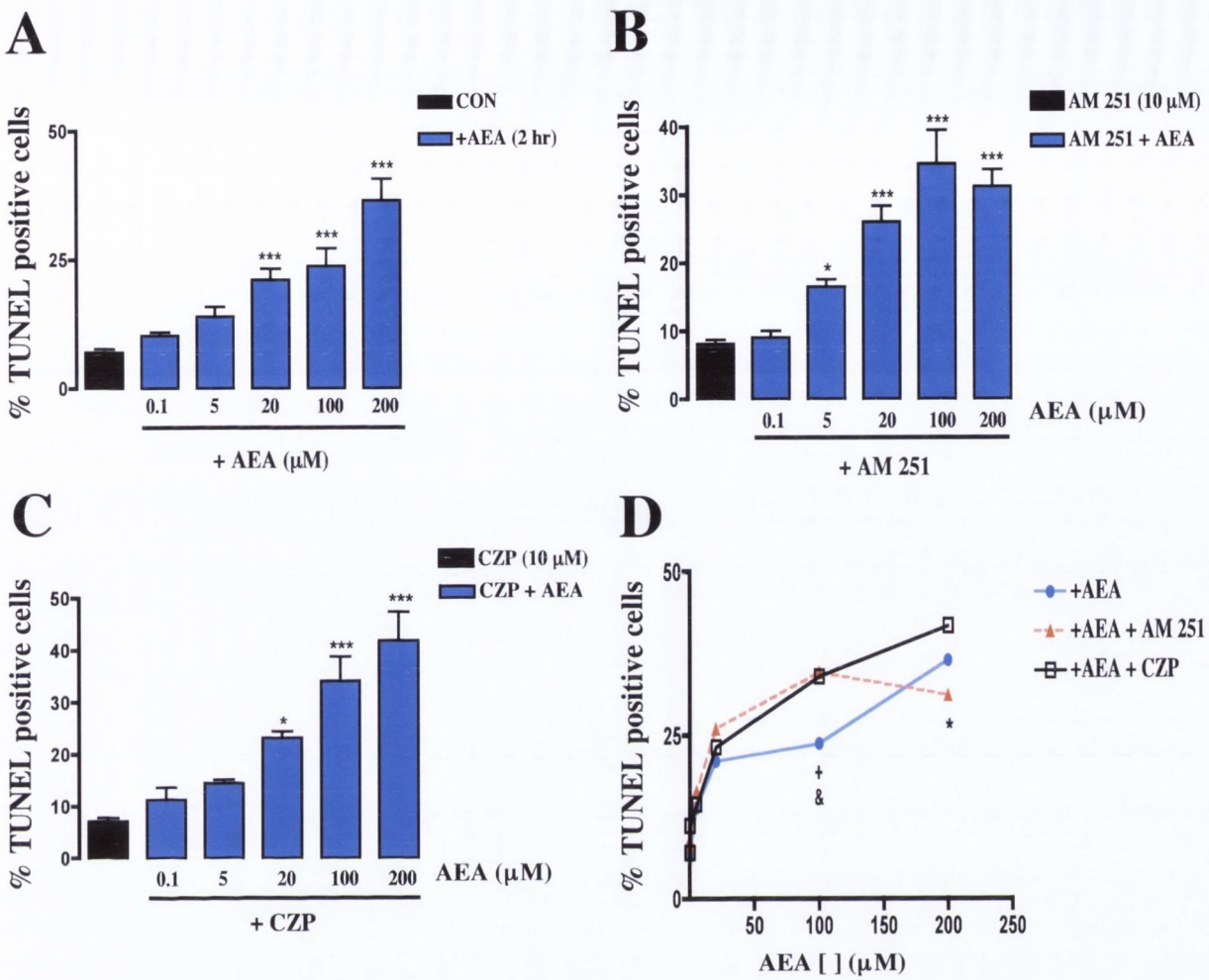
A
% TUNEL positive cells
CON
+AEA (2 hr)
0.1
5
20
100
200
+ AEA (μM)
B
% TUNEL positive cells
AM 251 (10 μM)
AM 251 + AEA
AEA (μM)
+ AM 251
C
% TUNEL positive cells
CZP (10 μM)
CZP + AEA
AEA (μM)
+ CZP
D
% TUNEL positive cells
+AEA
+AEA + AM 251
+AEA + CZP
AEA [ ] (μM)

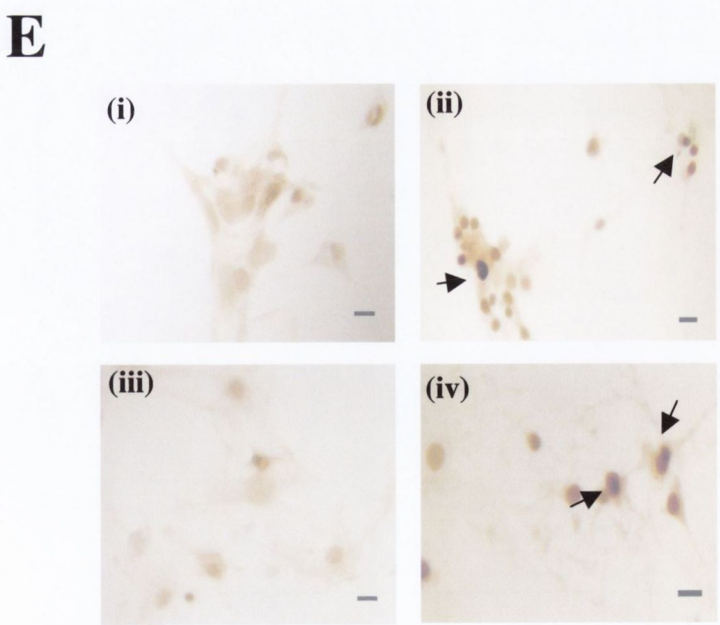
E
(i)
(ii)
(iii)
(iv)

5.2.2 The effect of AEA on caspase-3 activity

Furthermore, we investigated the neurotoxicity of AEA by assessing the effect of AEA on caspase-3 activity. Cytosolic fractions were collected from cultured cortical neurones treated with AEA (20 μM) for 2 hours in the presence or absence of the CB_1 receptor antagonist (AM 251; 10 μM, 30 minute pre-treatment) and caspase-3 activity was determined by the cleavage of a fluorogenic substrate. Figure 5.2 demonstrates that following exposure to AEA (20 μM) for 2 hours there was a significant increase in caspase-3 activity in cytosolic fractions from cells treated with AEA, which was not abolished by inhibition of the CB_1 receptor ($p=0.0049$, ANOVA, n=8-9). In cells treated with AEA (20 μM) for 2 hours caspase-3 activity was 4.00 ± 1.10 nmoles AFC produced per mg protein per minute which was significantly more than cells treated with vehicle (0.86 ± 0.65; $p<0.05$, vs., vehicle, Student Newman Keuls, n=8-9). While treatment with AM 251 alone had no effect on caspase-3 activity (0.45 ± 0.33) it did not prevent the AEA-induced increase in caspase-3 activity (3.60 ± 1.00; $p<0.05$, vs., AM 251, Student Newman Keuls, n=8-9). This result indicates that caspase-3 is involved in the AEA-induced increase in caspase-3 activity in cortical neurones.

Figure 5.2: The effect of AEA on caspase-3 activity

Cultured cortical neurones were treated with AEA (20 μM) for 2 hr and total protein was harvested. Caspase-3 activity was assayed by cleavage of the fluorogenic caspase-3 substrate (DEVD-AFC). The AEA-induced increase in caspase-3 activity was not abolished by AM 251. Results shown are means ± SEM, *$p<0.05$, Student Newman Keuls, n=6.

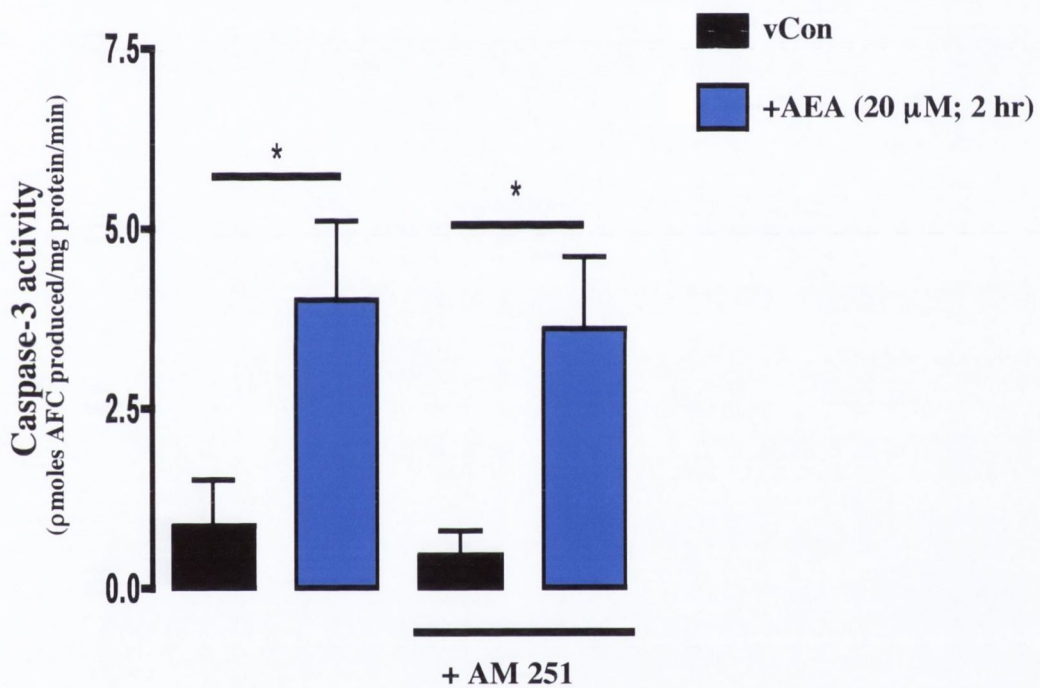
vCon
+AEA (20 μM; 2 hr)
Caspase-3 activity
(ρmoles AFC produced/mg protein/min)
7.5
5.0
2.5
0.0
*
*
+ AM 251

5.2.3 AEA-induced DNA fragmentation is dependent on p53 activity

DNA fragmentation was assessed by TUNEL staining cultured cortical neurones following exposure to AEA (20 μM) for 2 hours in the presence or absence of pifithrin-α (Pif-α; 100 nM, 60 minute pre-treatment). Figure 5.5 demonstrates that the AEA-induced DNA fragmentation occurs in a p53-dependent manner ($p<0.0001$, ANOVA, n=6 observations). AEA exposure significantly increased the percentage of cells displaying fragmented DNA in the nucleus (TUNEL positive) from 12.88 ± 1.01% (mean ± SEM) in vehicle-treated neurones to 48.34 ± 4.18% ($p<0.001$, vs., vehicle, Student Newman Keuls, n=6 observations). While treatment with pifithrin-α alone had no effect on neuronal viability (13.27 ± 0.70%), it prevented the AEA-induced increase in DNA fragmentation (13.09 ± 1.45% TUNEL positive cells; $p<0.001$, vs., THC, Student Newman Keuls, n=6 observations, Figure 5.3A). This finding suggests that AEA-induced DNA fragmentation is mediated by p53 signalling. Representative images of TUNEL stained neurones are shown in Figure 5.3B.

Figure 5.3: AEA induced DNA fragmentation is dependent on p53 activity

A: Assessment of DNA fragmentation was performed after treatment of neurones with AEA (20 μM) in the presence or absence of the p53 inhibitor, pifithrin-α (Pif-α; 100 nM, 60 min pre-treatment). AEA significantly increased the percentage of neurones displaying fragmented DNA. Pifithrin-α abolished the AEA-induced increase in DNA fragmentation. Results are expressed as mean ± SEM, ***$p<0.001$, Student Newman Keuls, n=6 observations.

B: Sample images of cells treated with (i) vehicle, (ii) AEA (20 μM), (iii) pifithrin-α and (iv) AEA (20 μM) in the presence of pifithrin-α. Arrows indicate TUNEL positive cells.

A

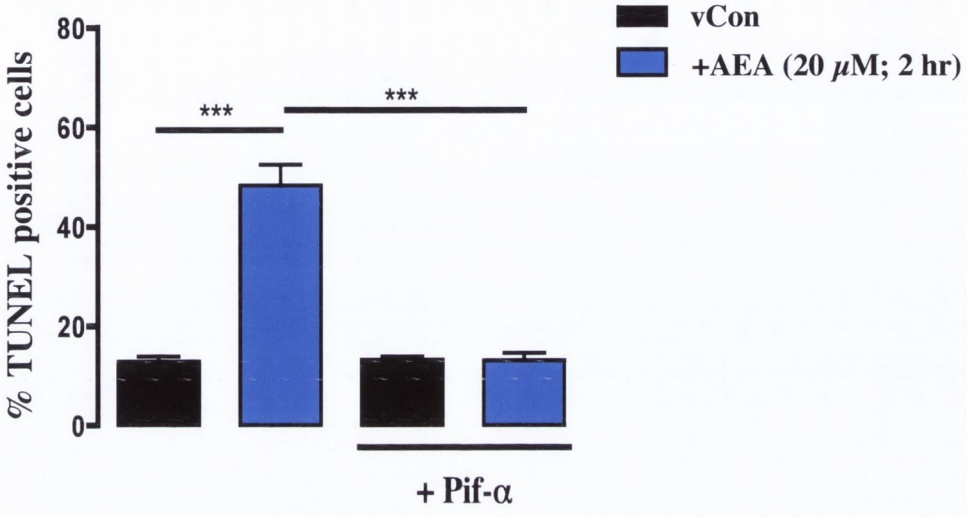
vCon
+AEA (20 μM; 2 hr)
% TUNEL positive cells
80
60
40
20
0
***
***
+ Pif-α

B

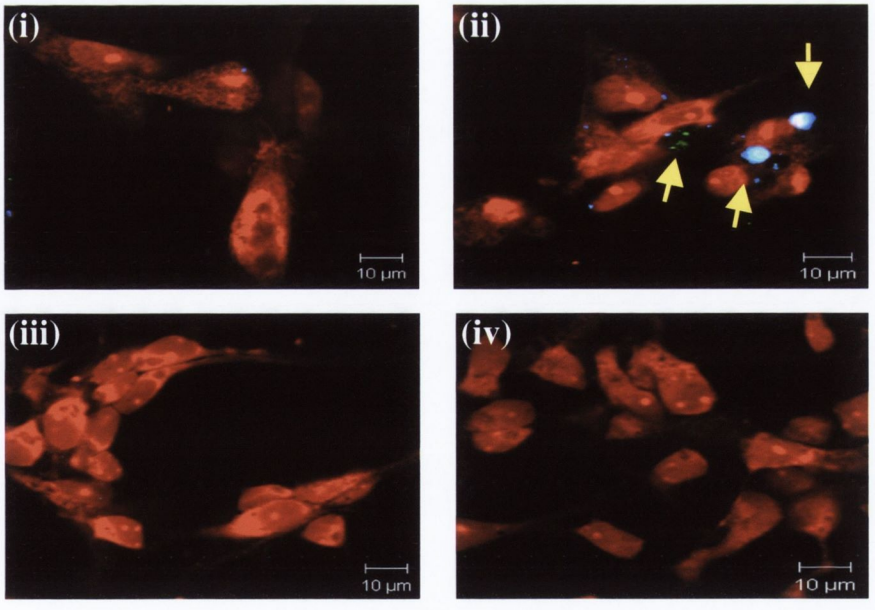
(i)
10 μm
(ii)
10 μm
(iii)
10 μm
(iv)
10 μm

5.2.4 The effect of AEA on phospho-p53^{ser15} expression

Since AEA-induced DNA fragmentation is dependent upon p53 activity, we assessed the effect of AEA on phospho-p53^{ser15} (p--p53^{ser15}) and total p53 (t-p53) expression levels. Cultured cortical neurones were exposed to AEA (0.02 and 20 μM) for 5 minutes. Expression levels of t-p53 and p-p53^{ser15} were measured by western immunoblot and bandwidths were quantified using densitometry. Figure 5.4A shows the effect of AEA on p-p53^{ser15}:t-p53 expression ($p=0.2020$, ANOVA, $n=4$). In cells exposed to vehicle for 5 minutes, p-p53^{ser15}:t-p53 expression was 2.16 ± 0.25 (mean arbitrary units ± SEM) which was not significantly affected by treatment with 0.02 and 20 μM AEA for 5 minutes (3.71 ± 0.93 and 2.82 ± 0.15; $p=0.1579$ and $p= 0.0657$ respectively). This finding suggests that there is a trend towards an AEA-induced increase in p-p53^{ser15}:t-p53 expression. Representative western immunoblots demonstrating p-p53^{ser15}, t-p53 and β actin expression in neurones treated with vehicle (lane 1), 0.02 and 20 μM AEA (lane 3 and 4, respectively) are shown in Figure 5.4B.

Figure 5.4: The effect of AEA on phospho-p53^{ser15} expression

A: Cultured cortical neurones were treated with 0.02 and 20 μM AEA for 5 min. Cells were harvested and p-p53^{ser15}:t-p53 expression was assessed by western immunoblot and immunocytochemistry. There was a trend towards an increase in p-p53^{ser15}:t-p53 expression, however this was non-significant (n=4). Inset: sample confocal images showing p-p53^{ser15} expression in cells treated with vehicle (i), 0.02 and 20 μM AEA for 5 min, (ii) and (iii), respectively.

B: Representative immunoblots of p-p53^{ser15}, t-p53 and β actin. Lane 1 vehicle treated neurones, and neurones exposed to 0.02 μM AEA (lane 2) and 20 μM AEA (lane 3).

A

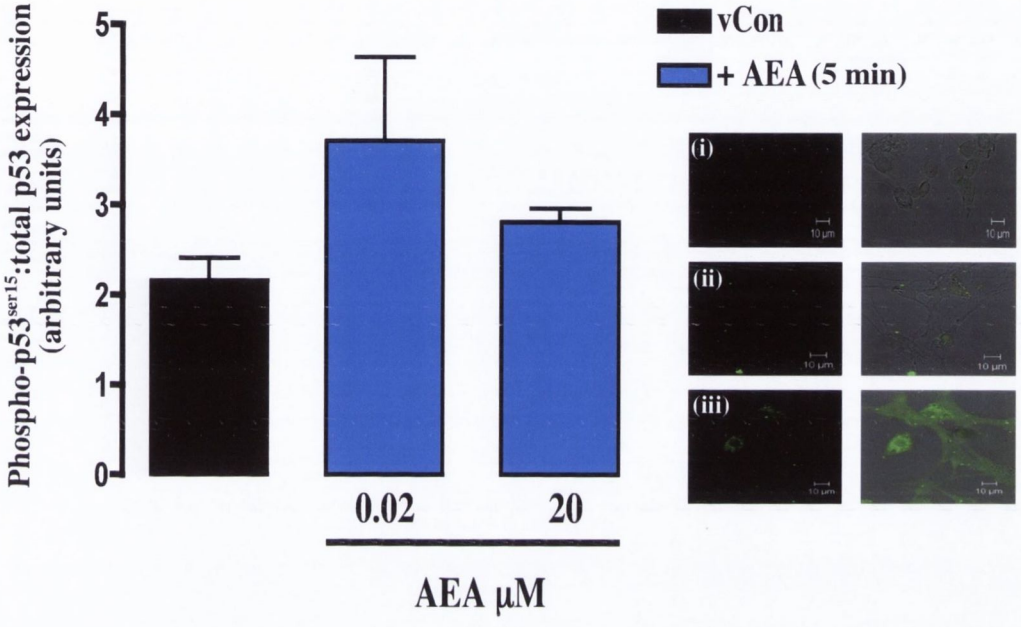
Phospho-p53ser15:total p53 expression
(arbitrary units)
5
4
3
2
1
0
vCon
+ AEA (5 min)
(i)
(ii)
(iii)
10 µm
0.02
20
AEA µM

B

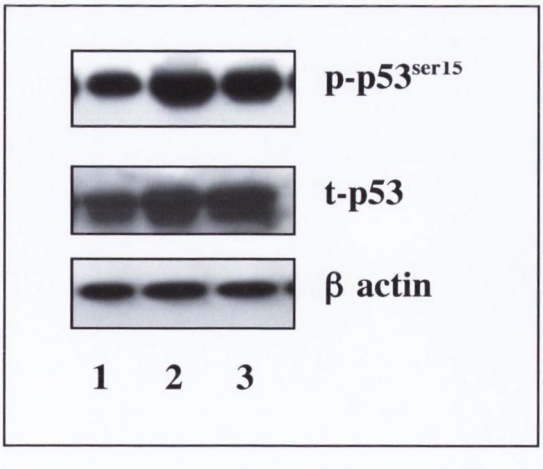
p-p53ser15
t-p53
β actin
1
2
3

5.2.5 AEA induces lysosomal destabilisation in a dose-dependent manner

Since Δ^9-THC-induced neuronal apoptosis involved the disruption of the lysosomal membrane it was decided to determine if AEA affected the stability of the lysosome. In this study cortical neurones were treated with AO (5 μg/ml) for 10 minutes prior to incubation with AEA (0.02 - 40 μM) for 15 minutes. Relocation of AO from lysosomes was assessed using confocal microscopy using the 488 nm Argon laser to excite AO and the META analysis function to collected emissions over the wavelength range of 499.7 - 670.7 nm. Figure 5.5 demonstrates that AEA-induces a significant decrease in 633 nm emission in a dose-dependent manner ($p=0.0112$, ANOVA, n=4), which is indicative of lysosomal membrane instability. Following exposure to 0.02 μM AEA for 15 minutes, AO emission at 633 nm was 140 ± 5 fluorescence intensity units (mean ± SEM, Figure 5.5A) which was comparable to that found in cells treated with vehicle (185 ± 49). A significant reduction in fluorescence intensity at 633 nm was observed after exposure to 0.2, 20 and 40 μM AEA (78 ± 31, 50 ± 15 and 54 ± 5, respectively; $p<0.05$, vs., vehicle, Student Newman Keuls, n=4), reflective of leakage of AO from the lysosomes as a consequence of lysosomal rupture. Representative images of AO stained cortical neurones are shown in Figure 5.5B.

Figure 5.5: AEA induces lysosomal destabilisation in a dose-dependent manner

Cortical neurones were exposed to AO (5 μg/ml) for 10 min prior to incubation with 0.02 - 40 μM AEA for 15 min. Relocation of AO from the lysosomes to the cytosol was assessed and mean fluorescence intensity at 633 nm was monitored.

A: The mean fluorescence intensity at 633 nm is significantly reduced following exposure to 0.2, 20 and 40 μM AEA for 15 min. Results shown are means ± SEM, *$p<0.05$, vs., vehicle, Student Newman Keuls, n=4.

B: Confocal images of AO staining of (i) vehicle-treated neurones, and neurones treated with 0.02 (ii), 0.2 (iii), 20 (iv), and (v) 40 μM AEA for 15 minutes.

A

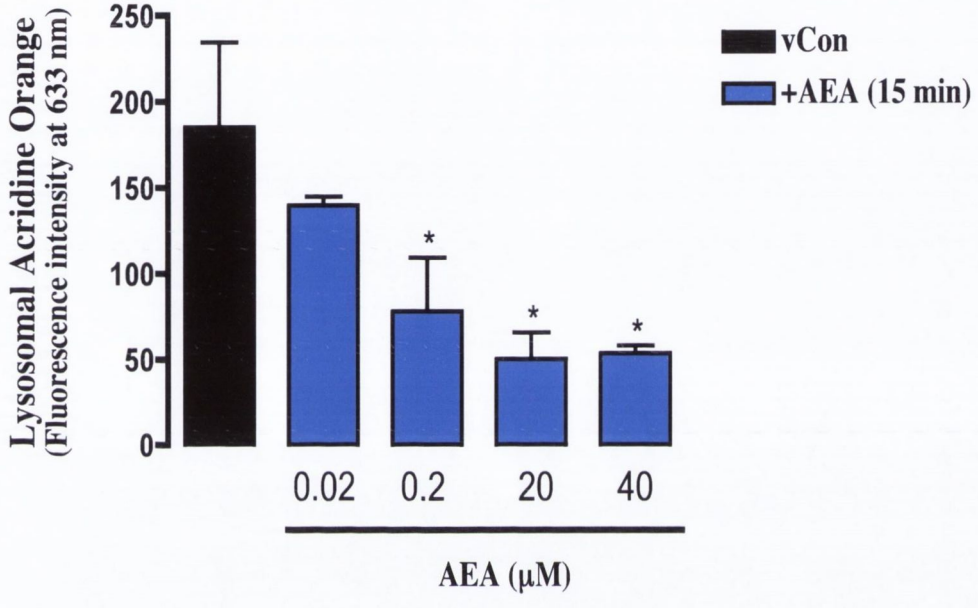
Lysosomal Acridine Orange
(Fluorescence intensity at 633 nm)
250
200
150
100
50
0
vCon
+AEA (15 min)
*
*
*
0.02
0.2
20
40
AEA (μM)

B

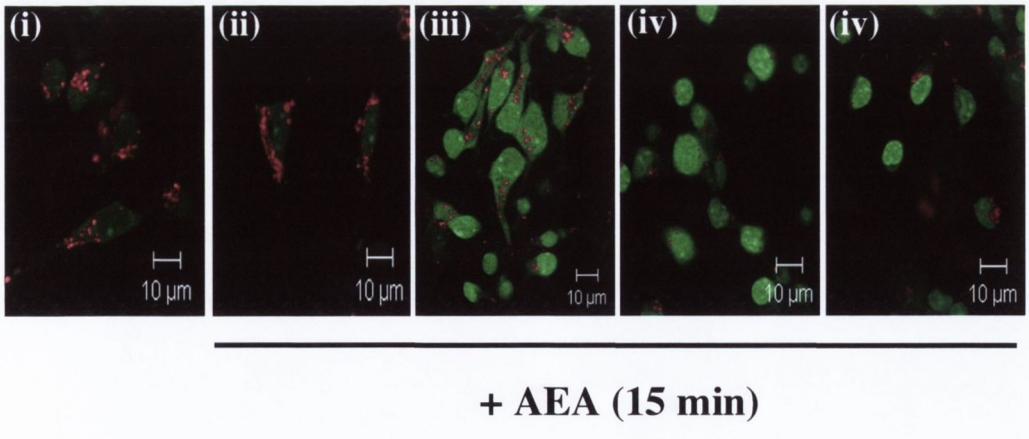
(i)
(ii)
(iii)
(iv)
(iv)
10 μm
10 μm
10 μm
10 μm
10 μm
+ AEA (15 min)

5.2.6 AEA induces lysosomal destabilisation in a time-dependent manner

Cortical neurones were treated with AO (5 μg/ml) for 10 minutes prior to incubation with AEA (20 μM) for 15 - 120 minutes. Relocation of AO from lysosomes was assessed using confocal microscopy using the META analysis function (excitation 488 nm, emission wavelength range 499.7 - 670.7 nm). Figure 5.6 demonstrates that AEA-induces a significant decrease in 633 nm emission in a time-dependent manner ($p=0.0044$, ANOVA, n=4). Following AEA treatment for 15 minutes, AO emission at 633 nm was 49 ± 16 fluorescence intensity units (mean ± SEM, Figure 5.6A) which was significantly lower to that found in cells treated with vehicle (207 ± 40; $p<0.01$, Student Newman Keuls, n=4). This indicates that the lysosomal membrane was no longer able to retain AO at high concentrations which results in a decrease in 633 nm emission. The induction of lysosomal instability was maintained at 30 and 120 minutes (45 ± 4 and 39 ± 4, respectively; $p<0.01$, Student Newman Keuls, n=4) but not after 60 minutes (118 ± 50) of AEA treatment. Representative images of AO stained cortical neurones demonstrating the induction of lysosomal membrane instability are shown in Figure 5.6B.

Figure 5.6: AEA induces lysosomal destabilisation in a time-dependent manner

Cortical neurones were exposed to AO (5 μg/ml) for 10 min prior to incubation with AEA (20 μM) for 15 - 120 min. Relocation of AO from the lysosomes to the cytosol was assessed by monitoring 633 nm fluorescence intensity.

A: AEA (20 μM) significantly reduced the mean fluorescence intensity at 633 nm at 15, 30 and 120 min, **p<0.01, Student Newman Keuls, vs., vehicle, n=4.

B: Confocal images of AO staining of (i) vehicle-treated neurones, and neurones treated with AEA (20 μM) for 15 (ii), 30 (iii), 60 (iv), and 120 min (v).

A

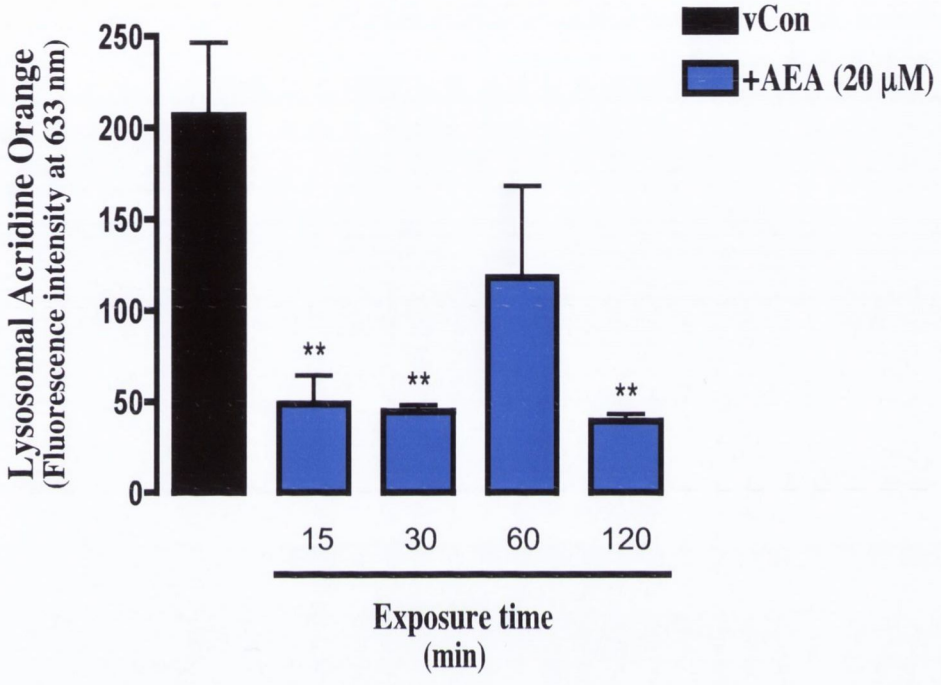
vCon
+AEA (20 μM)
Lysosomal Acridine Orange
(Fluorescence intensity at 633 nm)
250
200
150
100
50
0
**
**
**
15
30
60
120
Exposure time
(min)

B

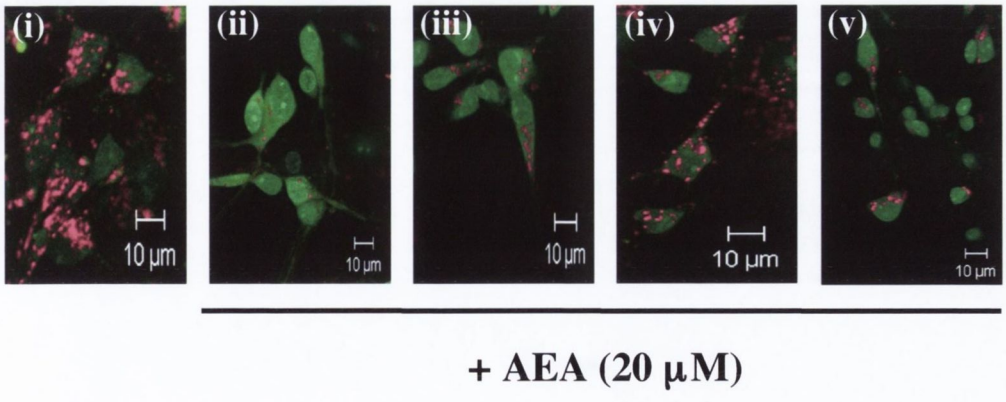
(i)
10 μm
(ii)
10 μm
(iii)
10 μm
(iv)
10 μm
(v)
10 μm
+ AEA (20 μM)

5.2.7 AEA-induced lysosomal destabilisation is independent of the CB_1 receptor

Cortical neurones were treated with AO (5 μg/ml) for 10 minutes prior to incubation with AEA (20 μM) for 15 minutes in the presence or absence of the CB_1 receptor antagonist, AM 251 (10 μM, 30 minute pre-treatment). Relocation of AO from lysosomes was assessed using confocal microscopy using the META analysis function (excitation 488 nm, emission wavelength range 499.7 - 670.7 nm). Figure 5.7 demonstrates the CB_1 dependent decrease in lysosomal membrane stability ($p<0.0001$, ANOVA, n=4). Following AEA treatment for 15 minutes, AO emission at 633 nm was 34 ± 3 fluorescence intensity units (mean ± SEM) which was significantly lower to that found in cells treated with vehicle (95 ± 4; $p<0.001$, vs., vehicle, Student Newman Keuls, n=4), reflective of leakage of AO from the lysosomes as a consequence of lysosomal rupture. While incubation with AM 251 alone had no effect on the fluorescence intensity at 633 nm (106 ± 3) it failed to abolish the AEA-induced decrease in 633 nm fluorescence intensity (49 ± 5; $p<0.001$, vs., AM 251, Student Newman Keuls. n=4; Figure 5.7A). Figure 5.7B shows representative images of AO stained cortical neurones demonstrating the CB_1 dependent induction of AEA-induced lysosomal membrane instability.

Figure 5.7: AEA-induced lysosomal destabilisation is independent of the CB_1 receptor

Cortical neurones were exposed to AO (5 μg/ml) for 10 min prior to incubation with AEA (20 μM) for 15 min in the presence or absence of AM 251 (10 μM, 30 min pre-treatment). Relocation of AO from lysosomes to the cytosol was assessed and the mean fluorescence intensity at 633 nm was monitored as an indicator of lysosomal membrane stability.

A: AEA (20 μM) reduces the mean fluorescence intensity at 633 nm at 15 min, pre-treatment with AM 251 (10 μM) did not prevent the AEA-induced reduction in 633 nm emission. Results shown are means ± SEM, ***$p<0.001$, Student Newman Keuls, n=4.

B: Confocal images of AO staining of neurones treated with vehicle (i), AEA (20 μM) for 15 min (ii), AM 251 alone (iii), AM 251 and AEA (20 μM) for 15 min (iv).

A

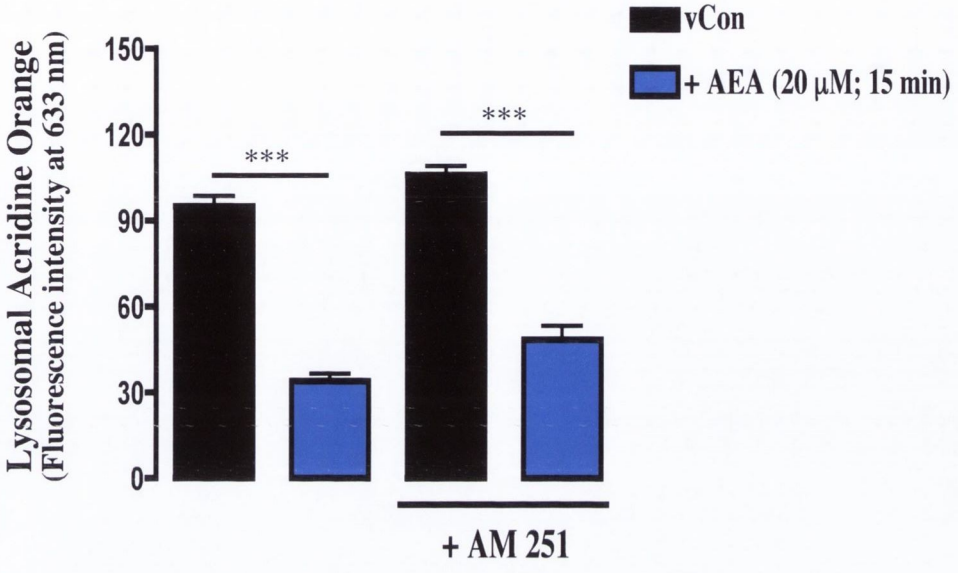
vCon
+ AEA (20 μM; 15 min)
Lysosomal Acridine Orange
(Fluorescence intensity at 633 nm)
150
120
90
60
30
0
***
***
+ AM 251

B

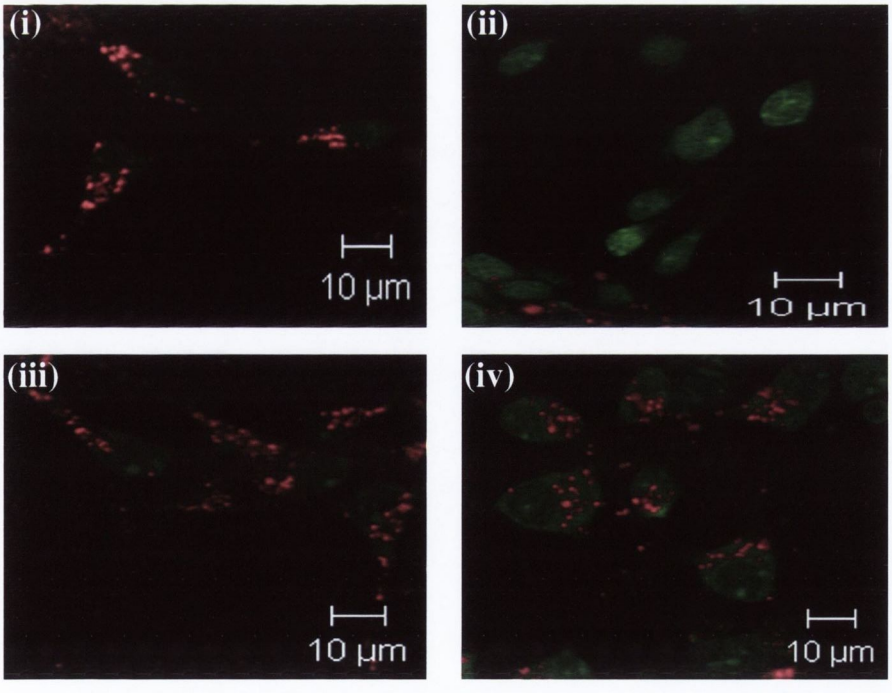
(i)
10 μm
(ii)
10 μm
(iii)
10 μm
(iv)
10 μm

5.2.8 AEA-induced lysosomal destabilisation is dependent on p53 activity

The role of phospho-p53^{ser15} in AEA-induced lysosomal membrane instability was assessed in this study. Cortical neurones were treated with AO (5 μg/ml) for 10 minutes prior to incubation with AEA (20 μM) for 15 minutes in the presence or absence of the pharmacological inhibitor of p53, pifithrin-α (Pif-α; 100 nM, 1 hr pre-treatment). Relocation of AO from lysosomes was assessed using confocal microscopy using the 488 nm Argon laser to excite AO and the META analysis function to collected emissions over the wavelength range of 499.7 - 670.7 nm. Figure 5.7A shows that the AEA induced a decrease in fluorescence intensity at 633 nm, which was abolished by the pharmacological inhibition of p53 activity ($p=0.0014$, ANOVA, n=4). Following AEA treatment for 15 minutes, AO emission at 633 nm was 33 ± 2 fluorescent intensity units (mean ± SEM) which was significantly lower to that found in cells treated with vehicle (98 ± 5; $p<0.01$, vs., vehicle, Student Newman Keuls, n=4), indicative of an instability in the lysosomal membrane. While incubation with pifithrin-α alone had no effect on 633 nm fluorescence intensity (117 ± 22), it prevented AEA-induced decrease in 633 nm fluorescence intensity (91 ± 5; $p<0.01$, vs., AEA, Student Newman Keuls, n=4; Figure 5.10A). This indicates that p53 is required for AEA-induced lysosomal membrane destabilisation. Figure 5.7B shows AO stained neurones demonstrating the p53-dependent nature of AEA-induced lysosomal membrane instability.

Figure 5.7: AEA-induced lysosomal destabilisation is dependent on p53 activity

Cortical neurones were exposed to AO (5 μg/ml) for 10 min prior to incubation with Pif-α (100 nM, 1 hr pre-treatment). Neurones were then treated with AEA (20 μM) for 15 min and the fluorescence emission at 633 nm was assessed.

A: The AEA induced lysosomal destabilisation, as indicated by a significant reduction in fluorescence intensity at 633 nm, is abolished by pre-treatment with Pif-α (100 nM). Results shown are means ± SEM, **$p<0.01$, Student Newman Keuls, n=4.

B: Confocal images of AO stained neurones treated with (i) vehicle, (ii) AEA (20 μM) for 15 min, (iii) Pif-α alone and (iv) Pif-α and AEA (20 μM) for 15 min.

A

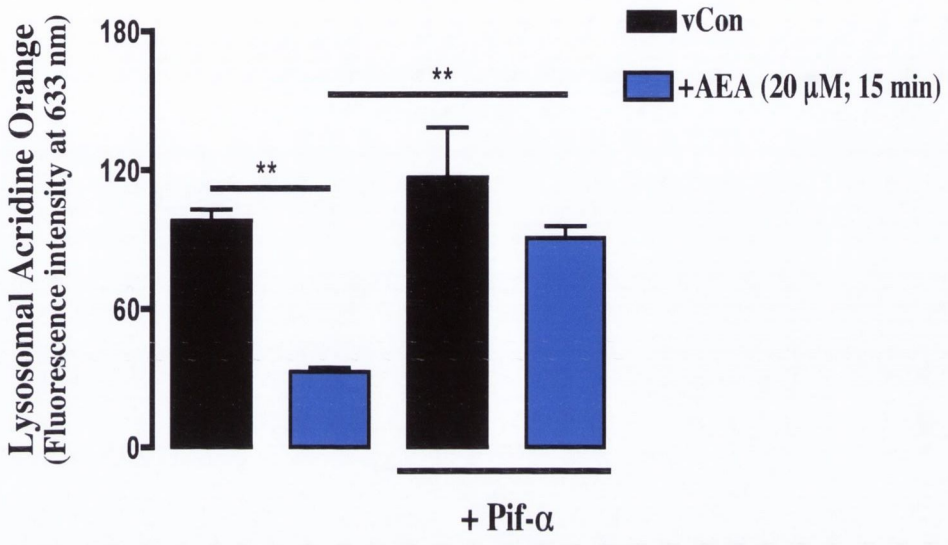
Lysosomal Acridine Orange
(Fluorescence intensity at 633 nm)
180
120
60
0
**
**
vCon
+AEA (20 μM; 15 min)
+ Pif-α

B

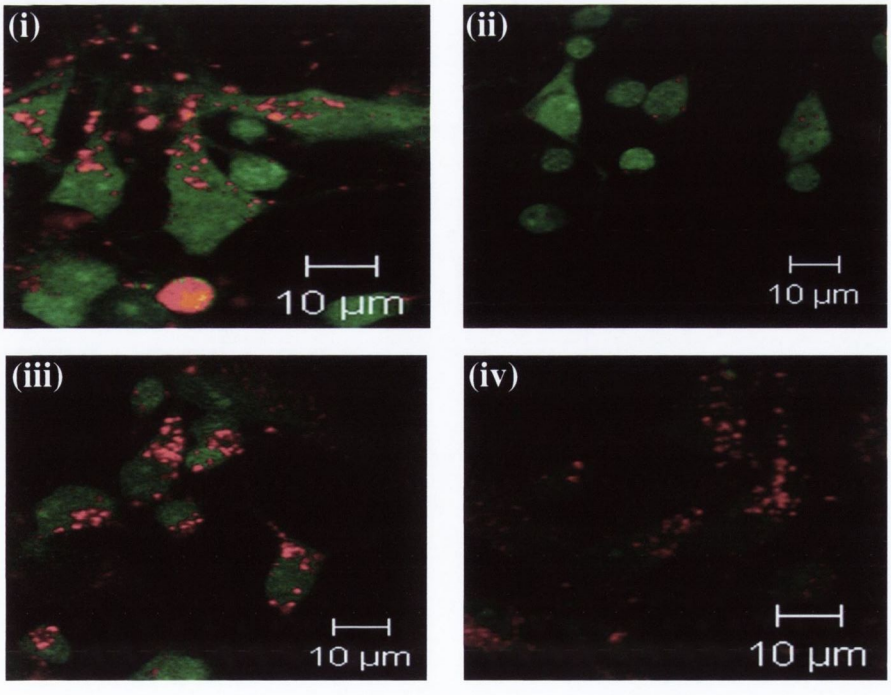
(i)
10 μm
(ii)
10 μm
(iii)
10 μm
(iv)
10 μm

5.2.9 AEA-induced lysosomal destabilisation is dependent on SyK activity

Cortical neurones were treated with AO (5 μg/ml) for 10 minutes prior to incubation with AEA (20 μM) for 15 minutes in the presence or absence of a SyK inhibitor (SyKi; 50 nM, 60 minute pre-treatment). Relocation of AO from lysosomes was assessed using confocal microscopy using the 488 nm Argon laser to excite AO and the META analysis function to collected emissions over the wavelength range of 499.7 - 670.7 nm. Figure 5.9 demonstrated the SyK-dependent nature of AEA-induced lysosomal destabilisation ($p=0.0004$, ANOVA, $n=4$). Following AEA treatment for 15 minutes, AO emission at 633 nm was 34 ± 2 fluorescent intensity units (mean ± SEM) which was significantly lower to that found in cells treated with vehicle (80 ± 17; $p<0.01$, vs., vehicle, Student Newman Keuls, $n=4$; Figure 5.9A). While incubation with SyKi alone had no effect on 633 nm fluorescence intensity (114 ± 8), AEA failed to induce a decrease in 633 nm fluorescence intensity in the presence of SyKi (106 ± 6; $p<0.001$, vs., AEA, Student Newman Keuls, $n=4$) indicating that SyK activity is required for AEA-induced destabilisation of the lysosomal membrane. Figure 5.9B shows the SyK-dependent nature of AEA-induced lysosomal membrane instability as indicated by a significant reduction in fluorescence intensity at 633 nm.

Figure 5.9: AEA-induced lysosomal destabilisation is dependent on SyK activity

Cortical neurones were exposed to AO (5 μg/ml) for 10 min prior to incubation with SyKi (50 nM, 1 hr pre-treatment), neurones were then treated with AEA (20 μM) for 15 min and the emission at 633 nm was assessed.

A: AEA-induced lysosomal destabilisation, as indicated by a significant reduction in fluorescence intensity at 633 nm, is abolished by pre-treatment with SyKi (50 nM). Results shown are means ± SEM, **p<0.01, ***p<0.001, Student Newman Keuls, n=4.

B: Confocal images of AO staining of neurones treated with vehicle (i), AEA (20 μM) for 15 min (ii), SyKi alone (iii), SyKi and AEA (20 μM) for 15 min (iv).

A

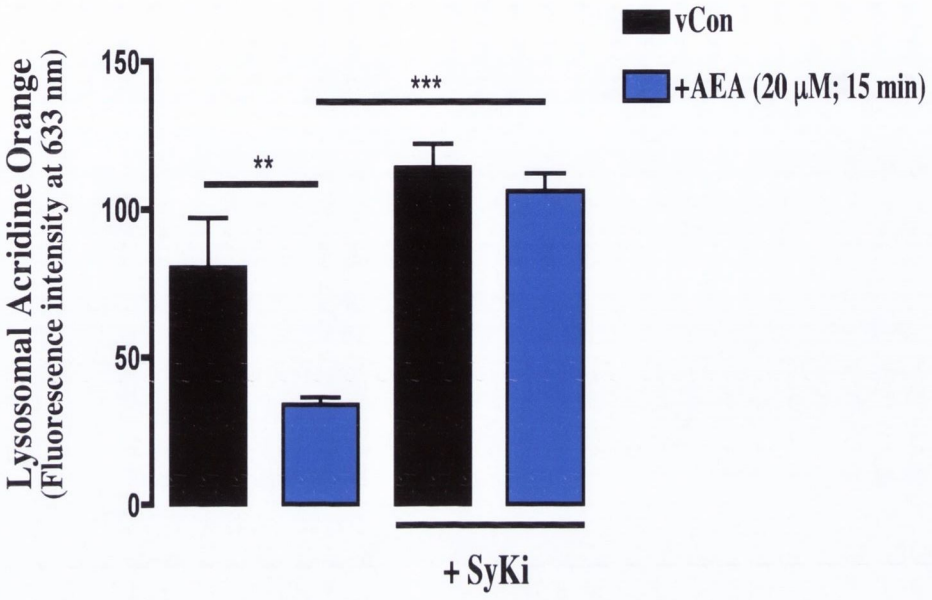
vCon
+AEA (20 μM; 15 min)
Lysosomal Acridine Orange
(Fluorescence intensity at 633 nm)
150
100
50
0
**
***
+ SyKi

B

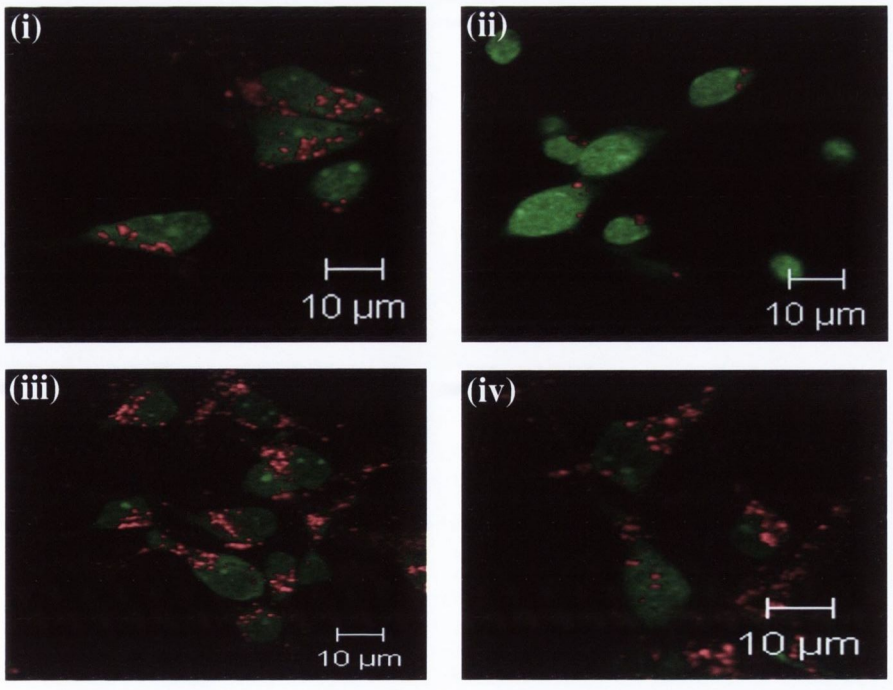
(i)
10 μm
(ii)
10 μm
(iii)
10 μm
(iv)
10 μm

5.2.10 AEA-induced caspase-3 activity is dependent on cathepsin-D activity

The disruption of the lysosomal membrane can result in the release of cathepsins which are known to induce apoptosis (Turk *et al.*, 2002). Since we observed that Δ^9-THC-induced an increase in caspase-3 activity, which was dependent on cathepsin-D activity, the role of cathepsin-D in AEA-induced caspase-3 activity was assessed. Cytosolic fractions were collected from cultured cortical neurones treated with AEA (20 μM) for 2 hours in the presence or absence of a cathepsin-D inhibitor (CDi; 10 μM, 30 minute pre-treatment). Caspase-3 activity was determined by cleavage of a fluorogenic caspase-3 substrate (DEVD-AFC). Figure 5.10 demonstrates that exposure to AEA (20 μM) for 2 hours evoked a significant increase in caspase-3 activity which was abolished by inhibition of cathepsin-D activity ($p=0.0078$, ANOVA, $n=6$). In cells treated with AEA (20 μM) for 2 hours caspase-3 activity was 105 ± 49% greater than in cells treated with vehicle ($p<0.05$, vs., vehicle, Student Newman Keuls, $n=6$). Treatment with AEA in the presence of CDi significantly decreased the level of caspase-3 activity (30 ± 15% less than cells treated with CDi alone; $p<0.01$, vs., AEA, Student Newman Keuls, $n=6$). These results indicate that cathepsin-D activity is necessary for the AEA-induced increase in caspase-3 activity.

Figure 5.10: AEA-induced caspase-3 activity is dependent on cathepsin-D activity

Cultured cortical neurones were treated with AEA (20 μM) for 2 hr and total protein was harvested. Caspase-3 activity was assayed by cleavage of the fluorogenic caspase-3 substrate (DEVD-AFC). The AEA-induced increase in caspase-3 activity was abolished by the inhibition of cathepsin-D. Results shown are means ± SEM, *p<0.05, **p<0.01, Student Newman Keuls, n=6.

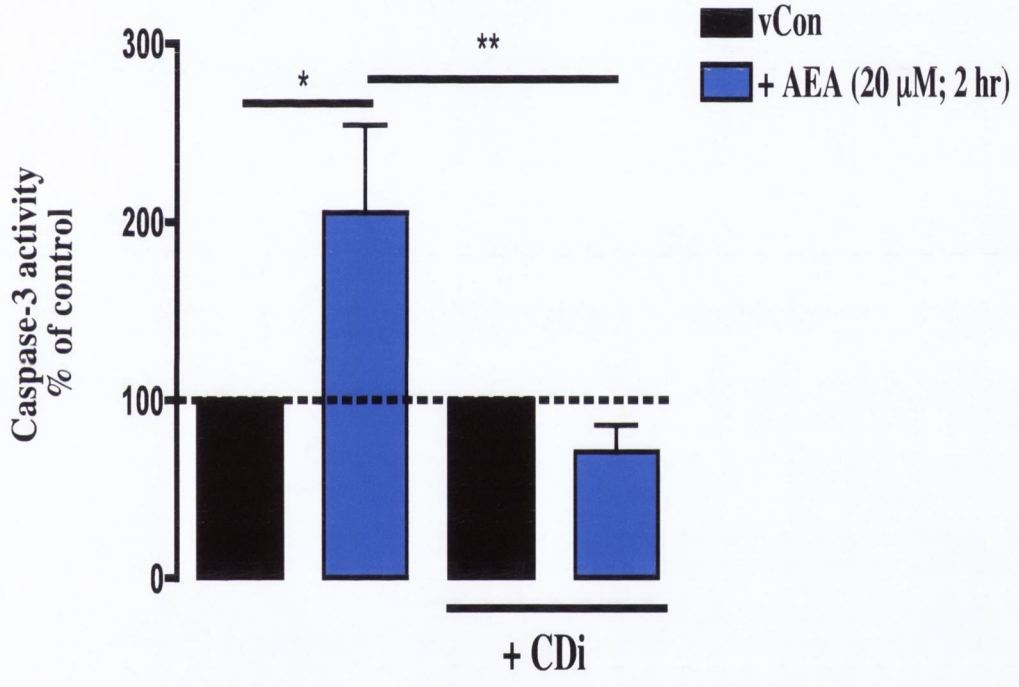
vCon
+ AEA (20 μM; 2 hr)
Caspase-3 activity
% of control
300
200
100
0
*
**
+ CDi

5.2.11 AEA-induced DNA fragmentation is dependent on cathepsin-D activity

DNA fragmentation was assessed by TUNEL staining in cultured cortical neurones following exposure to AEA (20 μM) for 2 hours in the presence or absence of a cell permeable inhibitor of cathepsin-D (CDi; 30 minute pre-treatment). Figure 5.11 demonstrates that AEA-induced DNA fragmentation is dependent on cathepsin-D activity ($p<0.0001$, ANOVA, n=6 observations). In vehicle-treated cells, 15.82 ± 2.10% (mean ± SEM) of cells displayed fragmented DNA in the nucleus (TUNEL positive). This was significantly increased to 52.59 ± 3.18% in cells treated with AEA for 2 hours ($p<0.001$, vs., vehicle, Student Newman Keuls, n=6 observations; Figure 5.11A). Treatment of cells with CDi prevented the AEA-induced increase in DNA fragmentation (28.40 ± 1.51%; $p<0.001$, vs., AEA, Student Newman Keuls, n=6 observations). This finding suggests that cathepsin-D is involved in AEA-induced DNA fragmentation. Representative images of TUNEL stained neurones are shown in Figure 5.11B.

Figure 5.11: AEA-induced DNA fragmentation is dependent on cathepsin-D activity

Cortical neurones were treated with AEA (20 μM) for 2 hr in the presence or absence of a cathepsin-D inhibitor (CDi; 10 μM, 30 min pre-treatment). Cell viability was assessed using the TUNEL technique.

A: AEA significantly increased the percentage of TUNEL positive cells. CDi abolished the AEA-induced increase in DNA fragmentation. Results are displayed as means ± SEM, ***p<0.001, Student Newman Keuls, n=6 observations.

B: Sample images of (i) vehicle-treated cells, and cells treated with (ii) AEA (20 μM) for 2 hr, (iii) CDi alone and (iv) AEA (20 μM) for 2 hr in the presence of CDi. Arrows indicate TUNEL positive neurones.

A

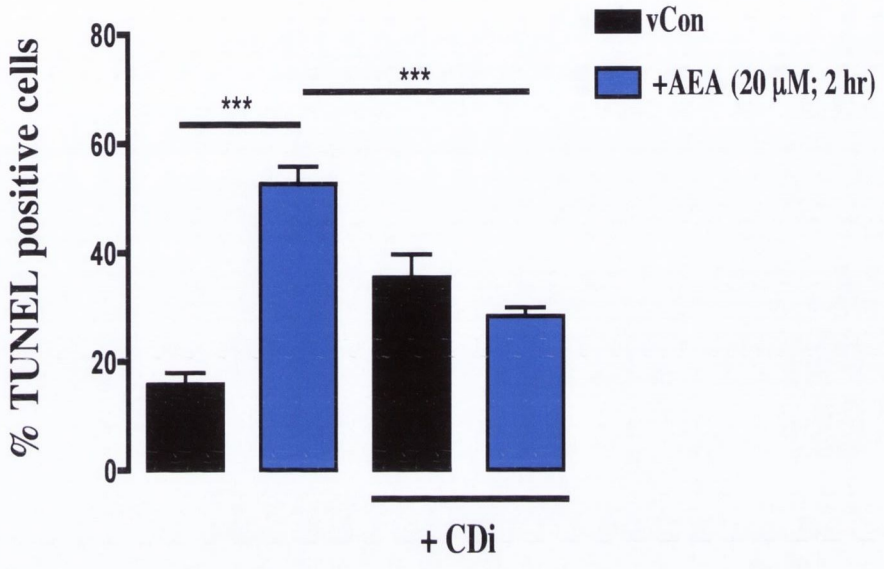
vCon
+AEA (20 µM; 2 hr)
% TUNEL positive cells
80
60
40
20
0
***
***
+ CDi

B

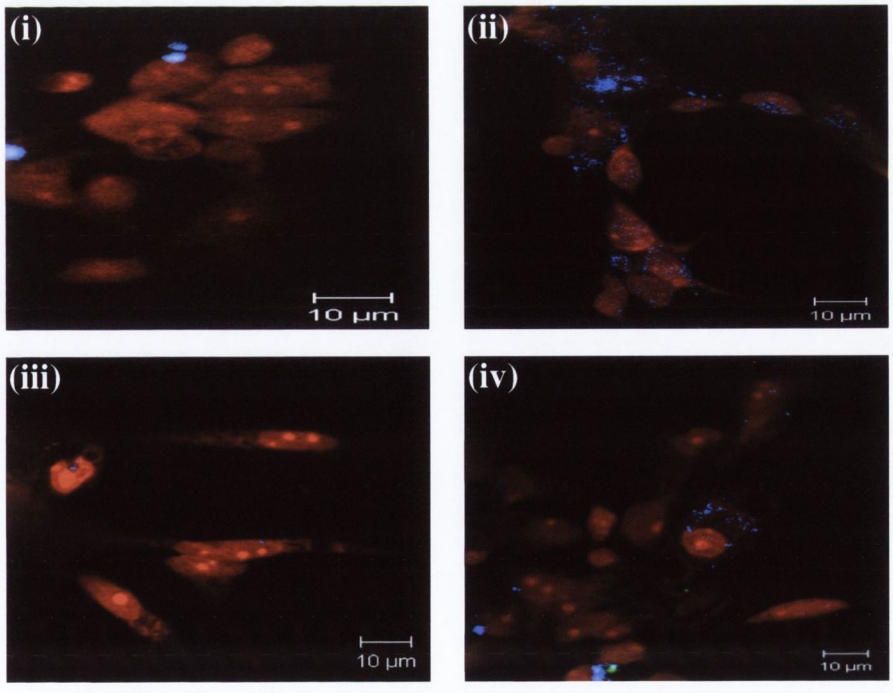
(i)
10 µm
(ii)
10 µm
(iii)
10 µm
(iv)
10 µm

5.2.12 2-AG induces DNA fragmentation in a dose dependent manner

To determine whether the endogenous cannabinoid 2-arachidonoylglycerol (2-AG) is neurotoxic to neurones we assessed its ability to induce DNA fragmentation in cultured rat cortical neurones. DNA fragmentation was assessed by TUNEL staining following exposure to 2-AG (0.02 - 20 μM) for 2 hours. Figure 5.12 shows tht 2-AG induces DNA fragmentation only at a high concentration ($p=0.0403$, ANOVA, $n=6$ observations). In vehicle-treated cells, 10 ± 2% (mean ± SEM) of cells displayed fragmented DNA in the nucleus (TUNEL positive). This was comparable to cells treated with 0.02, 0.2 and 2 μM 2-AG for 2 hours (19 ± 11%, 28 ± 5%, and 20 ± 4%, respectively). However, treatment of cells with 20 μM 2-AG induced a significant increase in DNA fragmentation (41 ± 8%; $p<0.05$, vs., vehicle, Student Newman Keuls, $n=6$ observations). This finding demonstrates that 2-AG induces apoptosis in cultured cortical neurones only at high concentrations. Figure 5.12B depicts sample images of TUNEL stained neurones treated with 2-AG.

Figure 5.12: 2-AG induces DNA fragmentation in a dose dependent manner

A: Assessment of the number of TUNEL positive cells was made after treatment of neurones with 2-AG (0.02 - 20 μM) for 2 hr. 2-AG significantly increased the percentage of TUNEL positive cells following exposure to 20 μM 2-AG for 2 hr. Results are displayed as means ± SEM, *$p<0.05$, Student Newman Keuls, n=6 observations.

B: Sample images of TUNEL stained neurones treated with 0.02 μM (i), 0.2 μM (ii), 2 μM (iii) and 20 μM 2-AG (iv) for 2 hr. Arrows indicate TUNEL positive neurones. Scale bar is 10 μm.

A

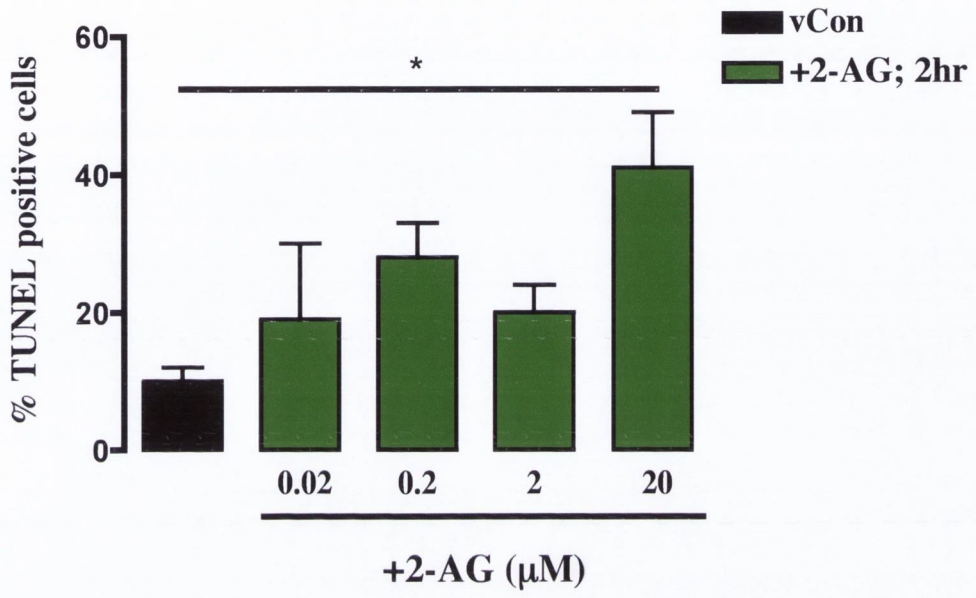
vCon
+2-AG; 2hr
% TUNEL positive cells
60
40
20
0
*
0.02
0.2
2
20
+2-AG (μM)

B

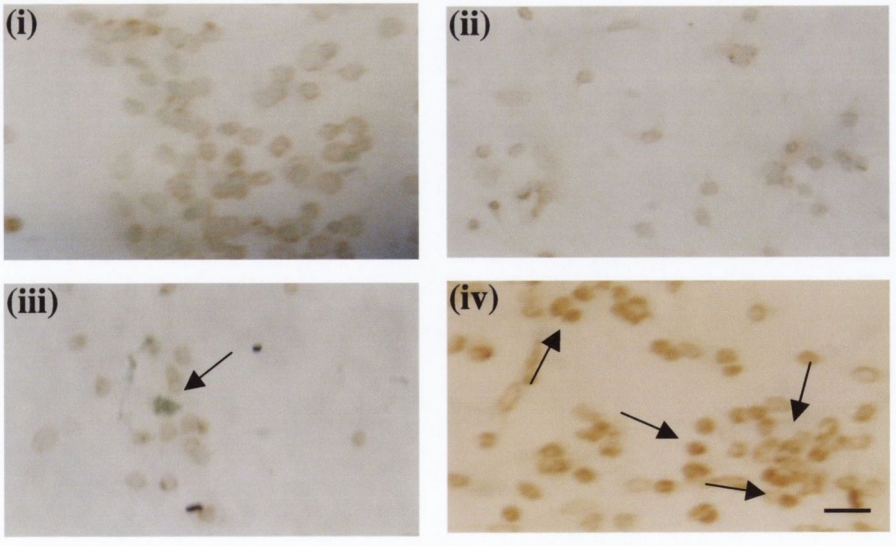
(i)
(ii)
(iii)
(iv)

5.2.13 The effect of CB_1 receptor inhibition on 2-AG-induced DNA fragmentation

DNA fragmentation was assessed by TUNEL staining in cultured cortical neurones following exposure to 2-AG (20 μM) for 2 hours in the presence of the CB_1 receptor antagonist, AM 251 (10 μM, 30 minute pre-treatment). Figure 5.13 demonstrates the CB_1 receptor-dependent nature of 2-AG-induced DNA fragmentation ($p<0.0001$, ANOVA, n=6 observations). In cells treated with 2-AG (20 μM) for 2 hours, 41 ± 8% (mean ± SEM) of cells displayed fragmented DNA in the nucleus (TUNEL positive) which was significantly higher than cells treated with vehicle (10 ± 5%; $p<0.001$, vs., vehicle, Student Newman Keuls, n=6 observations). While treatment with AM 251 alone did not affect the level of DNA fragmentation (8 ± 5%) it prevented the 2-AG-induced DNA fragmentation (3 ± 0.1%; $p<0.001$, vs., 2-AG, Student Newman Keuls, n=6 observations; Figure 5.15). This finding suggests that 2-AG-induced DNA fragmentation is mediated through the CB_1 receptor.

Figure 5.13: The effect of CB_1 receptor inhibition on 2-AG-induced DNA fragmentation

Cell viability was assessed by the TUNEL assay in cultured cortical neurones treated with 2-AG (20 μM; 2 hr) in the presence or absence of the CB_1 receptor antagonist, AM 251 (10 μM, 30 min pre-treatment). 2-AG-induced DNA fragmentation was prevented by AM 251. Results are expressed as means ± SEM, ***p<0.001, Student Newman Keuls, n=6 observations.

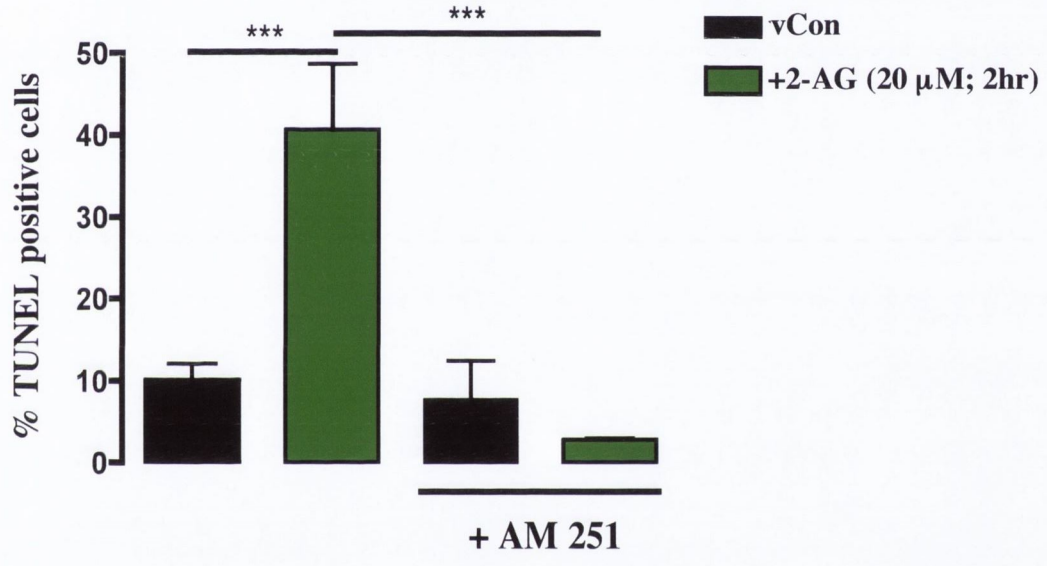
***
***
vCon
+2-AG (20 μM; 2hr)
% TUNEL positive cells
50
40
30
20
10
0
+ AM 251

5.2.14 The effect of 2-AG on caspase-3 activity

To determine the effect of 2-AG on caspase-3 activity, cytosolic fractions were collected from cultured cortical neurones treated with 2-AG (20 μM) for 2 hours. The activity of caspase-3 was determined by the cleavage of a fluorogenic caspase-3 substrate (DEVD-AFC). Figure 5.14 demonstrates that following exposure to 2-AG (20 μM) for 2 hours there was no increase in caspase-3 activity ($p=0.1905$, student's t test, $n=4$). In cells treated with 2-AG (20 μM) for 2 hours caspase-3 activity was 239 ± 9 ρmoles AFC produced per mg protein per minute which was comparable to cells treated with vehicle (253 ± 3). These results indicate that 2-AG does not increase caspase-3 activity.

Figure 5.14: The effect of 2-AG on caspase-3 activity

Treatment of primary cortical neurones with 2-AG (20 μM) for 2 hours had no effect on caspase-3 activity as assessed by the cleavage of the fluorogenic caspase-3 substrate (DEVD-AFC). Results are expressed as mean ± SEM for 4 independent observations.

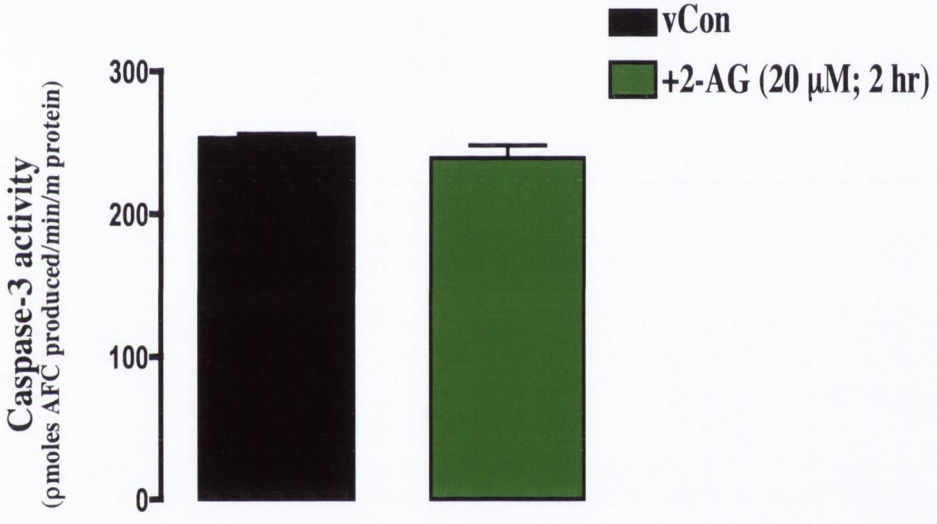
vCon
+2-AG (20 μM; 2 hr)
Caspase-3 activity
(ρmoles AFC produced/min/m protein)
300
200
100
0

5.2.15 The effect of 2-AG on phospho-p53^{ser15} expression

In this study we assessed the effect of 2-AG on phospho-p53^{ser15} (p-p53^{ser15}) expression levels. Cultured cortical neurones were exposed to 2-AG (0.02 and 20 μM) for 5 minutes. Expression levels of total cellular p53 (t-p53) and p-p53^{ser15} were measured by western immunoblot and bandwidths were quantified using densitometry (Figure 5.15A). 2-AG-induced a non-significant increase in p-p53^{ser15}:t-p53 expression ($p=0.1909$, ANOVA, $n=4$). In cells exposed to vehicle for 5 minutes, p-p53^{ser15}:t-p53 expression was 2.74 ± 0.48 arbitrary units which was not significantly increased following treatment with 0.02 and 20 μM 2-AG for 5 minutes (3.78 ± 0.48 and 4.52 ± 0.86; $p=0.1756$ and $p=0.1204$ respectively vs., vehicle, Student's t test, $n=4$). This finding suggests that there is a trend towards a 2-AG-induced increase in p-p53^{ser15}:t-p53 expression. Representative western immunoblots demonstrating t-p53, p-p53^{ser15} and β actin expression are shown in Figure 5.15B.

Figure 5.15: The effect of 2-AG on phospho-p53^{ser15} expression

A: Cultured cortical neurones were treated with 0.02 and 20 μM 2-AG for 5 min. Cells were harvested and phospho-p53^{ser15} (p-p53^{ser15}), total-p53 (t-p53) expression was assessed by western immunoblot. There was a trend towards an increase in p-p53^{ser15}:t-p53 expression, however, this was non-significant.

B: Representative immunoblots of p-p53^{ser15}, t-p53 and β actin. Lane 1 vehicle treated neurones, and neurones exposed to 0.02 μM 2-AG (lane 2), 20 μM 2-AG (lane 3) for 5 min.

A

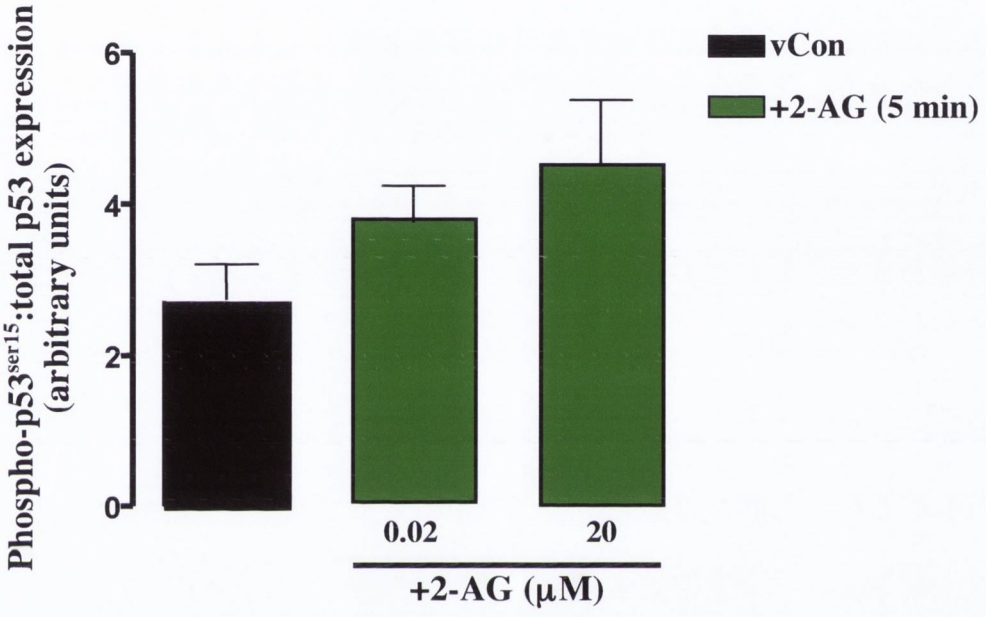
Phospho-p53ser15:total p53 expression
(arbitrary units)
6
4
2
0
vCon
+2-AG (5 min)
0.02
20
+2-AG (μM)

B

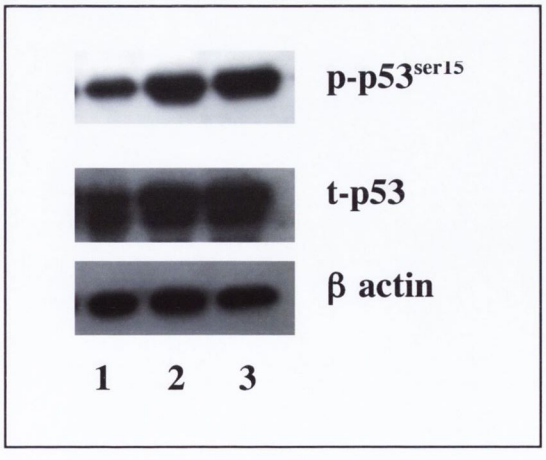
p-p53ser15
t-p53
β actin
1
2
3

5.2.16 2-AG (0.01 μM) prevents glutamate-induced DNA fragmentation

Since low concentrations of 2-AG did not induce signs of neurotoxicity we investigated whether 2-AG could be neuroprotective at low concentrations. To determine whether 2-AG provides neuroprotection against neurotoxic insults, cortical neurones were exposed to a pre-, post- and co-treatment of 2-AG (0.01 μM) with a neurotoxic glutamate insult (50 μM, 1 hour treatment), neurotoxicity was then assessed using the TUNEL technique. Figure 5.16A demonstrates that glutamate-induced neurotoxicity is prevented by a low dose of 2-AG ($p=0.0011$, ANOVA, n=6 observations). In control cells the % of cells with fragmented DNA was 8 ± 5% which was significantly increased to 25 ± 6% after treatment with glutamate (50 μM) for 1 hour ($p<0.01$, vs., vehicle, Student Newman Keuls, n=6 observations). However, in cells pre-treated with 2-AG for 1 hour before the addition of glutamate, a significant decrease in DNA fragmentation was observed (5 ± 2%; $p<0.01$, vs., glutamate, Student Newman Keuls, n=6 observations). A significant decrease was also observed in cells treated with 2-AG (0.01 μM) post glutamate treatment (7 ± 1%; $p<0.01$, vs., glutamate, Student Newman Keuls, n=6 observations). Furthermore, the treatment of 2-AG and glutamate together (co-treatment) for 1 hour produced a significant decrease in DNA fragmentation (2 ± 0.6%, $p<0.01$, vs., glutamate, Student Newman Keuls, n=6 observations). These results suggest that a low dose of 2-AG provides neuroprotection against glutamate-induced neurotoxicity. Figure 5.16B shows sample images of TUNEL stained neurones, arrows indicate TUNEL positive cells.

Figure 5.16: 2-AG (0.01 μM) prevents glutamate-induced DNA fragmentation

A: Assessment of DNA fragmentation was performed after treatment of neurones with glutamate (50 μM; 1 hr) alone, and a pre-, post- or co-treatment of 2-AG (0.01 μM). Glutamate significantly increased the percentage of neurones displaying fragmented DNA. 2-AG abolished the glutamate-induced increase in DNA fragmentation. Results are expressed as means ± SEM, **p<0.01, vs. vehicle, ++p<0.01, vs., glutamate, Student Newman Keuls, n=5 observations.

B: Representative images of cells treated with (i) vehicle, (ii) glutamate (50 μM; 1 hr), (iii) 0.01 μM 2-AG pre-glutamate treament, (iv) 0.01 μM 2-AG post-glutamate treatment and (v) co-treatment. Arrows indicate TUNEL positive cells. Scale bar is 10 μm.

A

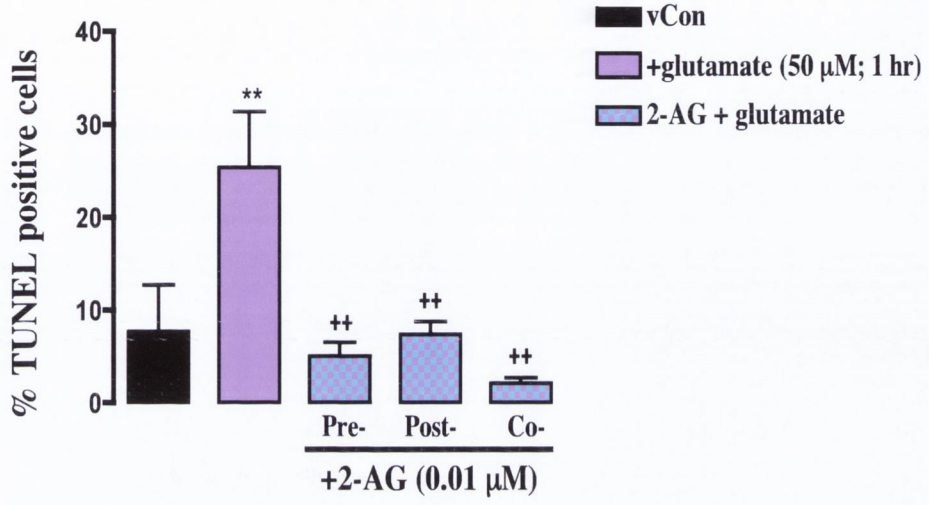
% TUNEL positive cells
40
30
20
10
0
**
++
++
++
Pre-
Post-
Co-
+2-AG (0.01 μM)
vCon
+glutamate (50 μM; 1 hr)
2-AG + glutamate

B

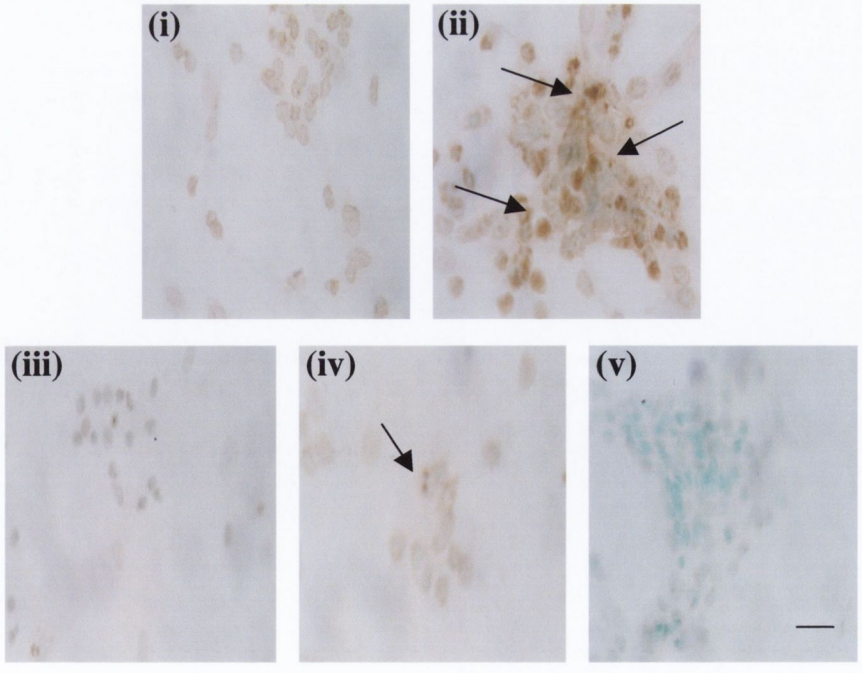
(i)
(ii)
(iii)
(iv)
(v)

5.3 Discussion

The aim of this aspect of the study was to determine whether the endocannabinoids, AEA and 2-AG, exerted a neurotoxic response in cultured cortical neurones and to identify which apoptotic signalling pathways were regulated by these endocannabinoids. Since we have previously shown that Δ^9-THC regulates pro-apoptotic markers, such as activation of the p53 protein, induction of lysosomal instability, caspase-3 activation and DNA fragmentation, these apoptotic markers were assessed in cultured cortical neurones exposed to exogenously applied endocannabinoids AEA and 2-AG. The results indicate that both AEA and 2-AG at high concentrations induce hallmarks of apoptosis *e.g.*, caspase-3 activation (AEA only) and DNA fragmentation (AEA and 2-AG). The ability of AEA to induce DNA fragmentation was not blocked by AM 251 or by the VR_1 antagonist, capsazepine (CZP), indicating that AEA-induced neurotoxicity is not mediated through the CB_1 or VR_1 receptors in cortical neurones. In addition, AEA was found to induce an increase in caspase-3 activity in a CB_1 independent manner. Furthermore, AEA also had a negative impact on the stability of lysosomes and induced a destabilisation of the lysosomal membrane in a dose- and time-dependent manner, akin to the observations with Δ^9-THC which are discussed in chapter 4. The proclivity of AEA to impact on the lysosomal system was not abated by CB_1 antagonism with AM 251, however, the negative impact of AEA on lysosomal stability was blocked by the pharmacological inhibition of p53 and SyK, indicating that AEA regulates similar signalling pathways to Δ^9-THC albeit *via* an as yet unidentified receptor system. However, AEA did not cause a significant increase in active p53 (phospho-p53^{ser15}). The AEA-induced caspase-3 activity and DNA fragmentation was prevented by cathepsin-D inhibition, indicating that lysosomal disruption caused the release of cathepsin-D, which then enabled its involvement in the apoptotic pathway. 2-AG also caused the CB_1-dependent induction of DNA fragmentation at high concentrations, however, a concomitant increase in caspase-3 activity was not observed. Furthermore, 2-AG did not cause the activation of the tumour suppressor protein, p53 and capase-3. Given the difference in the proclivity of 2-AG to induce capsase-3 activity (compared to AEA), the ability of a low concentration of 2-AG to provide protection to neurones exposed to an excitotoxic

glutamate treatment was also assessed using the TUNEL technique. Glutamate excitotoxicity was prevented by a pre-, post- and co-treatment with 0.01 μM 2-AG, indicating that a low concentration of 2-AG provides neuroprotection against glutamate-induced excitoxicity.

AEA induced a dose dependent increase in fragmented DNA in cultured cortical neurones, however the concentrations used are higher than that required for receptor activation. Since AEA levels have been reported to be up regulated during brain injury, our *in vitro* model can only be considered to represent levels of AEA that occur during pathophysiological situations, such as intracerebral NMDA injection, mild concussive head trauma and NMDA receptor blockade (Hansen *et al.*, 2001). The proclivity of AEA to induce DNA fragmentation in cultured cortical neurones was not prevented by blocking the CB_1 or VR_1 receptors. This finding is in agreement with Movsesyan *et al.*, (2004), who also found that the inhibition of CB_1, CB_2 VR_1 or NMDA receptors also failed to prevent AEA-induced apoptosis in primary neuronal cultures. Sarker and Maruyama (2003) also found similar results in PC12 cells exposed to 10 μM AEA. Interestingly, Sarker and Maruyama showed that plasma membrane cholesterol depletion prevented AEA-induced apoptosis. Plasma membrane cholesterol depletion causes changes in the lipid raft domains that are present in plasma membranes and contain a sub set of cellular proteins including receptors (Simons and Ikonen, 1997). Altering the content of lipid rafts with cholesterol depleting agents has been shown to affect signal transduction from cell surface receptors and also with the ability to induce apoptosis (Moran and Miceli, 1998; Gajate and Mollinedo, 2001). These observations may provide a mechanism of action for AEA-induced apoptosis observed in our culture system. In our experiments, in addition to inducing DNA fragmentation, AEA also caused the activation of caspase-3, another apoptotic hallmark, this was independent of the CB_1 receptor, which is also in agreement with the studies carried out by Sarker and Maruyama (2003) and Movsesyan and co-workers (2004).

There was a difference in the proclivity of AEA to induce DNA fragmentation between the two types of receptor antagonism utilised. The CB_1 antagonist prevented AEA-induced DNA fragmentation up to 5 μM AEA, however blockade of VR_1 abrogated AEA-induced DNA damage up to 20 μM which is 4 times more than that the

threshold concentration observed for AM 251. This indicated that signalling through the CB_1, which possibly occurs when VR_1 is blocked with CZP, couples strongly to the apoptotic pathway. These differences may be associated with the receptor coupling efficiency or alternatively as a result of the intracellular activation of VR_1 by various endocannabinoid metabolites. Overall, inhibition of the CB_1 receptor potentiated, instead of reducing the induction of DNA fragmentation (as seen when VR_1 was blocked). However, considering the failure of both receptor antagonists to prevent AEA-induced apoptosis, it must be concluded that a different binding site or regulatory processes must be involved *e.g.*, GPR 55, the non CB_1/CB_2 receptor or the involvement of lipid rafts in the regulation of cannabinoid receptors.

Although a receptor was not identified as the mediator for AEA-induced apoptosis, the activation of similar pro-apoptotic signalling molecules to those observed to be induced by Δ^9-THC were up regulated as a result of AEA treatment *e.g.*, destabilisation of the lysosomal membrane resulting in the release of proteases that had the ability to potentiate the apoptotic cascade. The negative impact that AEA had on the lysosomal membrane was abrogated by inhibition of p53, however, only a trend towards an increase in active p53 expression was observed following AEA treatment for 5 minutes. Furthermore, the inhibition of p53 activity successfully abrogated AEA-induced DNA fragmentation, which implies that p53 signalling is a central factor in AEA-induced neuronal death. To our knowledge, this is the first time that AEA has been linked to p53 activity. In addition, the inhibition of SyK signalling also prevented AEA-induced destabilisation of the lysosomal membrane. These results, although highly speculative, may suggest that AEA-induced apoptosis follows a similar signalling pathway to Δ^9-THC-induced apoptosis, albeit mediated through a different, as yet unidentified receptor mechanism.

In comparison to AEA, 2-AG produced a less potent increase in fragmented DNA. Interestingly, CB_1 antagonism did prevent the 2-AG (20 μM)-induced DNA fragmentation, indicating that the CB_1 receptor mediates 2-AG-induced neuronal apoptosis. However, 2-AG at the same concentration failed to induce a significant increase in caspase-3 activity, which highlights the weak nature of 2-AG-induced apoptosis. Alternatively it may indicate the activation of a caspase-independent form of

cell death *e.g.*, calpain-dependent cell death. 2-AG failed to induce an activation of the tumour suppressor p53 as only a trend towards an increase was observed.

Considering the failure of 2-AG to induce a consistent, robust pro-apoptotic response in cultured cortical neurones, it was decided to assess the ability of a very low concentration of 2-AG (0.01 μM) to prevent glutamate-induced excitotoxicity. The application of exogenous glutamate resulted in a robust apoptotic response in our culture system, which was prevented by 2-AG irrespective of the timing of application (pre-, post- or co-treatment with glutamate). These results indicate that 2-AG at a low concentration strongly inhibits glutamatergic excitoxicity. Excitotoxicity underlies many neurodegenerative diseases and drugs that attenuate glutamatergic synaptic transmission show promise as palliative agents for neurodegeneration (Boast *et al.*, 1988; Park *et al.*, 1988). Neuronal damage results in the up regulation of endocannabinoid production and an up regulation of components within the endocannabinoid system is a common feature in neurodegenerative diseased brains (Stella *et al.*, 1997; Micale *et al.*, 2007). Cannabinoids, 2-AG in particular, have been shown to reduce glutamatergic activity and the modulation of the endocannabinoid system has been shown to provide neuroprotection (Gilbert *et al.*, 2007; Panikashvili *et al.*, 2001). 2-AG is increased during Aβ-induced hippocampal degeneration, gliosis and cognitive decline; this may reflect an attempt of the endocannabinoid system to provide neuroprotection from Aβ-induced damage (van der Stelt *et al.*, 2006). Furthermore, in that study when endocannabinoid uptake was inhibited by VDM-11, the Aβ-induced neurotoxicity and memory impairment was reversed, although this was dependent upon early administration of the reuptake inhibitor. Those findings suggest that robust and early pharmacological enhancement of brain endocannabinoid levels may protect against the deleterious consequences of Aβ. Other endocannabinoids, such as AEA and noladin ether, have been found to reduce Aβ neurotoxicity *in vitro* via activation of the CB_1 receptor and engagement with the extracellular-regulated kinase pathway (Milton, 2002). Thus, endocannabinoids can reverse the negative consequences of exposure to Aβ and such findings suggest that drugs designed to augment endocannabinoid tone, including inhibitors of endocannabinoid uptake and metabolism, may have potential in the treatment of AD. However, the study by van der Stelt *et al.*, (2003) advices caution

regarding the timing of endocannabinoid up regulation by pharmacological intervention in relation to the time-course of development of the disease pathology, since administration of VDM-11 later in the pathological cascade actually induced a negative effect on the memory retention ability of rodents. These results coupled with our initial findings will provide a platform upon which our continuing research into the role of endocannabinoids in neuroprotection and aging will continue.

Summary schematic

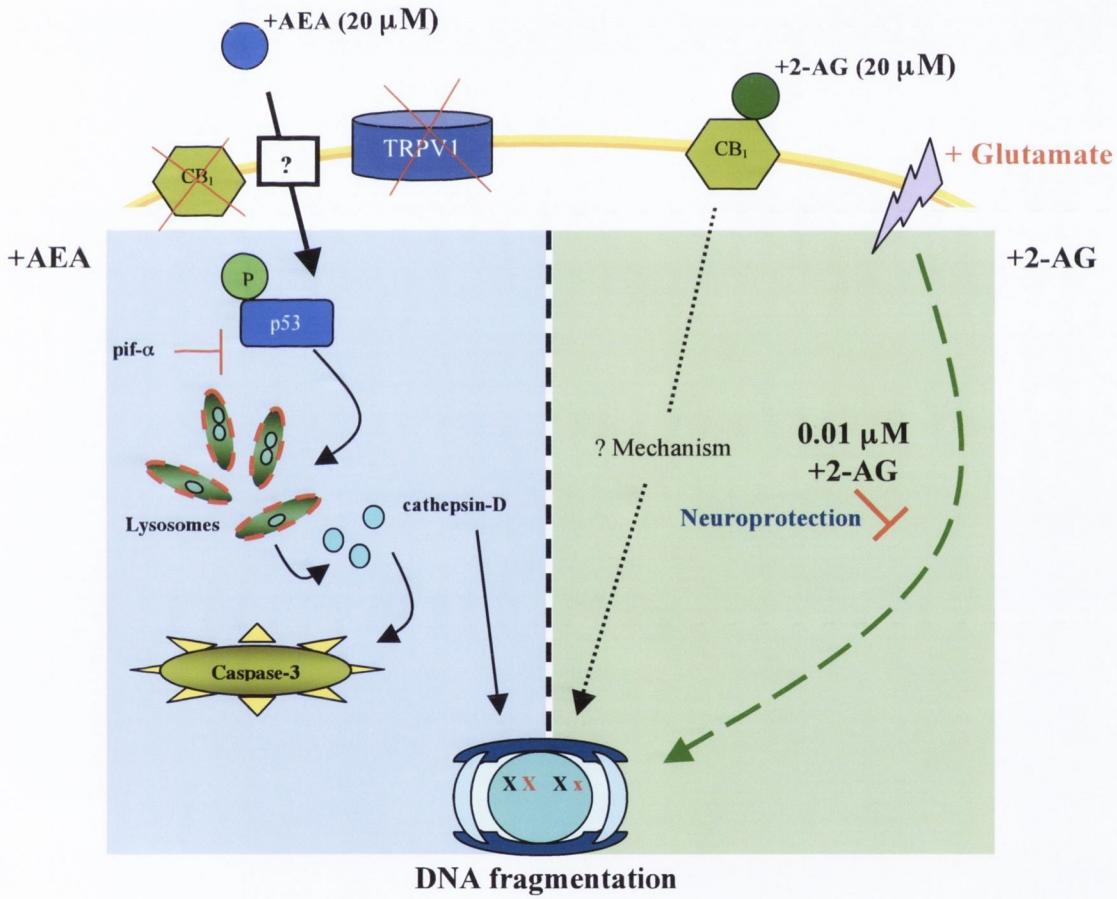

Chapter 6

The effect of development on Δ^9-THC-induced apoptosis in the cerebral rat cortex - An in vivo study

6.1 Introduction

The CB_1 receptor is expressed in the foetal and early postnatal brain, however, its expression pattern varies during development (Fernández-Ruiz *et al.*, 2000; Berrendero *et al.*, 1999; Rodríguez de Fonseca *et al.*, 1993). These findings, coupled with the involvement of the endocannabinoid system in virtually all stages of reproduction, are consistent with a role for the cannabinoid system in controlling events pertinent in neural development (Harkany *et al.*, 2007). Indeed, endocannabinoids are important in the proliferation and fate specification of neural progenitors, and in the migration, lineage segregation, differentiation and survival of neurones in the developing foetal brain (Galve-Roperh *et al.*, 2006; Berghuis *et al.*, 2005, 2007; Harkany *et al.*, 2007). Δ^9-THC crosses the placenta during pregnancy and it has been reported that foetal Δ^9-THC plasma concentrations are approximately 10% of those found in the dams that received treatment with Δ^9-THC administered *via* gastric intubation (Hutchings *et al.*, 1989). In addition, the administration of cannabinoids to pregnant dams, before or during organogenesis, produces abnormalities in the dopaminergic neurotransmitter system that is indicative of neurotoxicity (Fernández-Ruiz *et al.*, 1996, 1994, 1992). Furthermore, the *in utero* exposure to Δ^9-THC has a negative effect on foetal growth and causes impaired developmental plasticity (Hurd *et al.*, 2005; Bernard *et al.*, 2005). Longitudinal studies have demonstrated that the prenatal exposure to cannabis in humans is associated with deficits in executive function and visuospatial working memory that persist into adulthood (Huizink and Mulder, 2006; Smith *et al.*, 2006; Fried *et al.*, 2003; Fried and Smith, 2001; Faden and Graubard 2000). Δ^9-THC exposure causes the down-regulation and desensitisation of the CB_1 receptor in a region specific manner which may be responsible for the rather subtle cognitive impairments seen in children exposed prenatally to cannabis (Zhuang *et al.*, 1998; Sim *et al.*, 1996).

The ability of cannabinoids to modulate other neurotransmitter signalling pathways has been reported in many animal studies, specifically glutamatergic signalling. Mereu *et al.*, (2003), have found that glutamatergic signalling is reduced as a result of the exposure to CB_1 receptor agonists during gestation. Furthermore, prenatal cannabis treatment modulates the glutamatergic system by decreasing the expression of

AMPA glutamate receptor subunits and glutamate transporters (Suarez *et al.*, 2004a, 2004b). Suarez and co-workers (2002) also found that cannabis prevented the production of glutamine, the precursor of glutamate, in glia. Thus, whilst a neurodevelopmental role for endocannabinoids is becoming clear, the aberrant activation of such pathways by exogenous phytocannabinoids or prescribed endocannabinoid system altering drugs may have undesired consequences on the developing brain which must be investigated further.

As detailed in the previous chapter the potential of cannabinoids to elicit neurotoxicity is controversial (Sarne and Mechoulam, 2005). However, morphological differences, indicative of neurotoxicity, were found in human subjects who chronically used cannabis (Schlaepfer *et al.*, 2006; Matochick *et al.*, 2005). Some of the deleterious effects of cannabis may be related to alterations in pathways involved in the control of neurogenesis, synaptogenesis and neuronal wiring, impaired myelination or possibly by aberrant neuronal death (Harkany *et al.*, 2007; Schlaepfer *et al.*, 2006). Previous findings obtained by this group also suggest that the neonatal brain is more susceptible to the neurotoxic effects of Δ^9-THC (Downer *et al.*, 2007a).

Given the dualism in the literature of neuroprotective versus neurotoxic effects of Δ^9-THC, the aim of this study was to examine the proclivity of Δ^9-THC to couple to the biochemical hallmarks of apoptosis in the neonatal, adolescent and adult rat cerebral cortex. The present study also aimed to identify if Δ^9-THC had a negative impact on the lysosomal system, akin to our *in vitro* findings. Specifically, neonatal, adolescent and adult animals received subcutaneous injections of Δ^9-THC (1 - 30 mg/Kg, s.c.) and were maintained for 3 hours, a time point at which Δ^9-THC induces a significant level of apoptosis in cultured cortical neurones. Rats were then sacrificed and the proclivity of Δ^9-THC to induce caspase-3 activation and DNA fragmentation was assessed. In addition, the expression of phospho-p53^{ser15} was determined by western immunoblot. Finally, the contribution of the lysosomal branch of apoptosis was determined by assessing cathepsin-D expression levels and activity in cytosolic fractions obtained from cerebral cortical tissue taken from rats treated with a subcutaneous dose of Δ^9-THC (1 - 30 mg/Kg).

6.2.1 Δ^9-THC induces DNA fragmentation in neonatal but not adult cerebral cortex

We have previously shown that Δ^9-THC-induces neurotoxicity in the neonatal, but not in the adult, cerebral cortex after an acute subcutaneous injection (s.c.) of Δ^9-THC (1 - 30 mg/Kg; Downer *et al.*, 2007b). In this study we examined the ability of Δ^9-THC to induce DNA fragmentation in the rat cerebral cortex at 2 stages of development: neonatal (5 - 7 days old) and adults (> 4 months old). Animals received subcutaneous injections of 1 mg/Kg Δ^9-THC in vehicle (5% absolute alcohol, 5% Cemophor EL and 90% sterile saline) for 3 hours. A control group of animals received injections of vehicle alone for 3 hours. Following treatment, cryostat sections were prepared and the level of DNA fragmentation was determined using the TUNEL technique (Figure 6.1). Neonatal rats treated with Δ^9-THC for 3 hours showed a higher level of DNA fragmentation (n=4; Figure 6.1A). There was a moderate increase in the level of DNA fragmentation in adults exposed to Δ^9-THC for 3 hours (Figure 6.1B). This suggests that the apoptotic actions of Δ^9-THC in the cerebral cortex are dependent on neuronal maturity, with the neonatal cortex being more susceptible to the neurotoxic effects of Δ^9-THC. This also corroborates our *in vitro* observations concerning the neurotoxic profile of Δ^9-THC. Representative images of cryostat sections of the cerebral cortex stained for DNA fragmentation using the TUNEL technique are shown in Figure 6.1.

Figure 6.1: Δ^9-THC induces DNA fragmentation in neonatal but not adult cerebral cortex

Neonatal (5 - 7-days old) and adult (> 4 months old) rats received subcutaneous injections of 1 mg/Kg Δ^9-THC in vehicle or vehicle alone for 3 hr and cryostat sections were prepared. The level of DNA fragmentation was determined in the cerebral cortex using the TUNEL technique. Cells with fragmented DNA stained green and the Hoechst stain labelled nuclei blue.

A: Exposure of neonatal animals to Δ^9-THC (ii) increased the number of cells in the cerebral cortex displaying fragmented DNA (TUNEL-positive) relative to vehicle-treated animals (i). Fragmented DNA (green), Hoechst (blue) and overlay images are presented. Scale bar is 50 μm.

B: Vehicle-treated (i) and Δ^9-THC-treated (ii) adult rats displayed only moderate levels of DNA fragmentation in the cerebral cortex. Fragmented DNA (green), Hoechst (blue) and overlay images are presented. Scale bar is 50 μm.

A

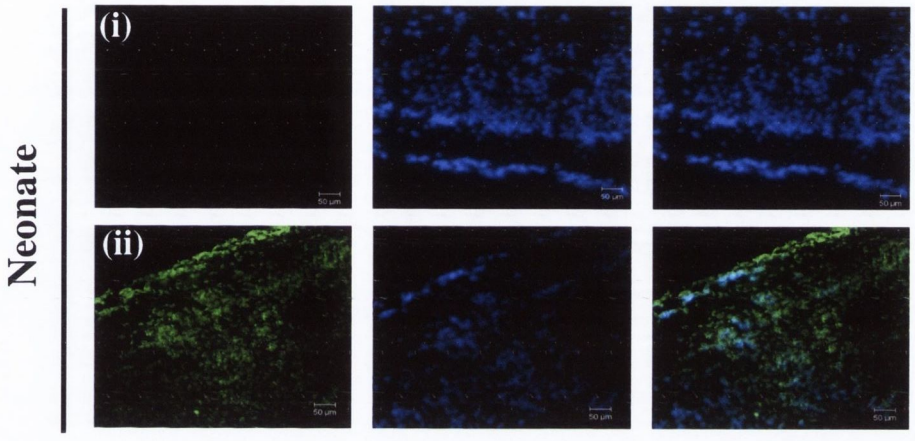

B

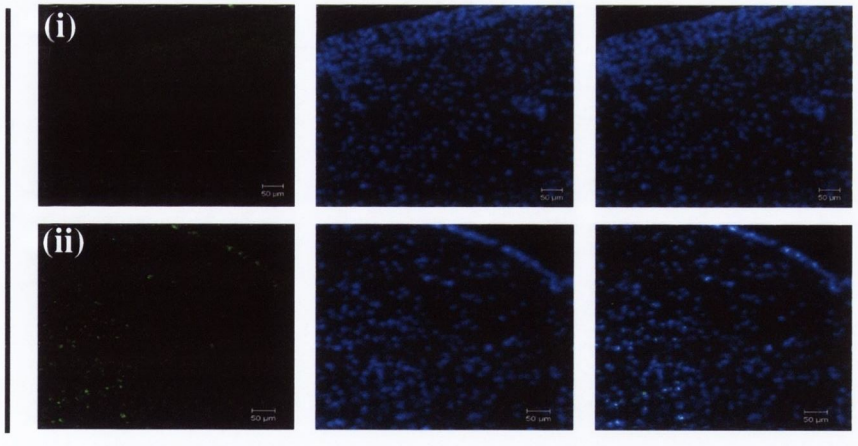

6.2.2 The effect of Δ^9-THC exposure on caspase-3 activity at different stages of development

To determine if Δ^9-THC regulates caspase-3 *in vivo* and to assess the contribution of brain development to Δ^9-THC-induced caspase-3 activation, neonatal (5 - 7-days old), adolescent (3 months old) and adult (8 - 9 months old) rats received subcutaneous injections of Δ^9-THC (1 mg/Kg) in vehicle (5% absolute alcohol, 5% Cremophore EL and 90% sterile saline) or vehicle alone for 3 hours. Following treatment, cortical slices were prepared, homogenised in lysis buffer and caspase-3 activity determined by monitoring the cleavage of the fluorogenic caspase-3 substrate, DEVD-AFC (Figure 6.2).

Figure 6.2A demonstrates that in vehicle-treated neonatal rats, caspase-3 activity was 4.67 ± 0.98 ρmoles AFC produced per mg protein per minute (mean ± SEM), this was significantly increased to 22.98 ± 8.47 ρmoles AFC produced per mg protein per minute in neonatal rats exposed to Δ^9-THC (1 mg/Kg) for 3 hours (p=0.0260, Mann Whitney test, n=6). Figure 6.2B demonstrates that in vehicle-treated adolescent rats, caspase-3 activity was 0.28 ± 0.05 ρmoles AFC produced per mg protein per minute (mean ± SEM). However, an increase in caspase-3 activity was not observed in adolescent rats exposed to Δ^9-THC (1 mg/Kg) for 3 hours (0.37 ± 0.046 ρmoles AFC produced per mg protein per minute; p=0.4452, vs., vehicle treated adolescents, Mann Whitney test, n=6). Figure 6.2C demonstrates that in vehicle-treated adult rats, caspase-3 activity was 0.11 ± 0.02 ρmoles AFC produced per mg protein per minute (mean ± SEM) which was not significantly different to the levels observed in adult rats exposed to Δ^9-THC (1 mg/Kg) for 3 hours (0.14 ± 0.04 ρmoles AFC produced per mg protein per minute; p=0.8182, Mann Whitney test, n=6). These findings indicate that Δ^9-THC induces caspase-3 activation in the neonatal cerebral cortex *in vivo* and not at later stages of development.

Figure 6.2: The effect of Δ^9-THC exposure on caspase-3 activity at different stages of development

Neonatal (5 - 7-days old), adolescent (3 months old) and adult (8 - 9 months old) Wistar rats were exposed to Δ^9-THC (1 mg/Kg s.c.) for 3 hr. Cerebral cortices were removed and homogenised on ice. Caspase-3 activity in tissue cytosolic fractions was determined by monitoring the cleavage of the fluorgenic caspase-3 substrate (DEVD-AFC).

A: Treatment of neonatal rats with Δ^9-THC significantly increased caspase-3 activity. Results are expressed as the means ± SEM, *$p<0.05$, vs., vehicle, Mann Whitney test, n=6). Inset: western immunoblot demonstrating the increase in active caspase-3 in neonates treated with vehicle (lane 1) and Δ^9-THC (lane 2).

B: Treatment of adolescent rats with Δ^9-THC had no effect on caspase-3 activity. Results are expressed as the means ± SEM, p=0.4452, Mann Whitney test, n=6).

C: Treatment of adult rats with Δ^9-THC had no effect on caspase-3 activity. Results are expressed as the means ± SEM, p=0.8182, Mann Whitney test, n=6).

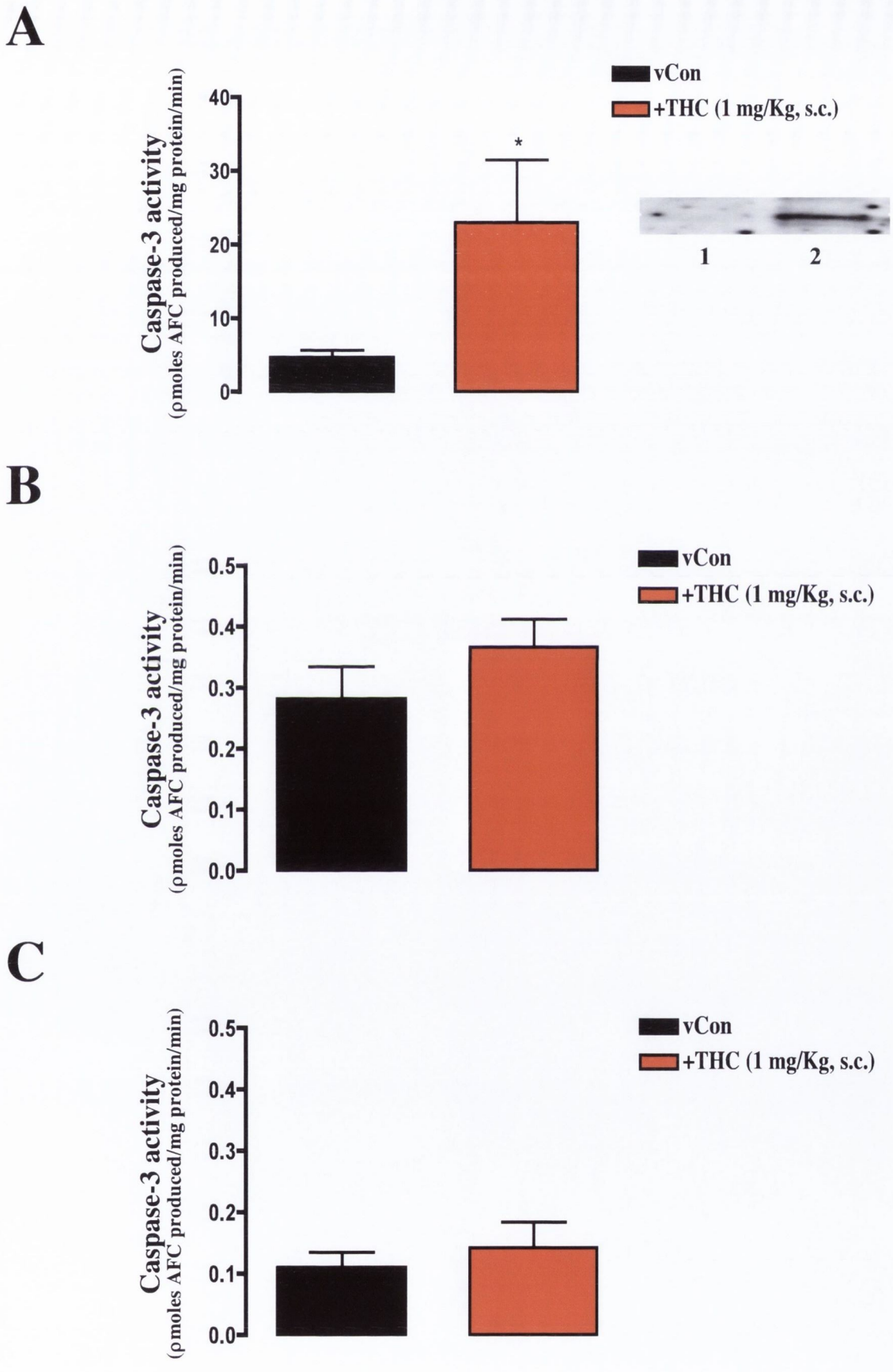
A
vCon
+THC (1 mg/Kg, s.c.)
Caspase-3 activity
(ρmoles AFC produced/mg protein/min)
40
30
20
10
0
*
1
2
B
vCon
+THC (1 mg/Kg, s.c.)
Caspase-3 activity
(ρmoles AFC produced/mg protein/min)
0.5
0.4
0.3
0.2
0.1
0.0
C
vCon
+THC (1 mg/Kg, s.c.)
Caspase-3 activity
(ρmoles AFC produced/mg protein/min)
0.5
0.4
0.3
0.2
0.1
0.0

6.2.3 The effect of Δ^9-THC on phospho-p53^{ser15} expression in the developing rat cerebral cortex

The Δ^9-THC-induced apoptosis of cultured cortical neurones involves an increase in the activation of the tumour suppressor protein, p53 (Downer *et al.*, 2007a). To determine if Δ^9-THC regulates p53 activation *in vivo*, neonatal (5 - 7-days old), adolescent (3 months old) and adult (8 - 9 months old) rats received subcutaneous injections of Δ^9-THC (1 mg/Kg s.c.) in vehicle (5% absolute alcohol, 5% Cremophore EL and 90% sterile saline) or vehicle alone for 3 hours. Following treatment, cortical slices were prepared, homogenised in lysis buffer and phospho-p53^{ser15} (p-p53^{ser15}) expression determined by western immunoblot using an antibody that recognises p53 only when phosphorylated on serine 15. There was a trend towards an increase in p-p53^{ser15} expression in the neonatal cerebral cortex, but not significantly so. Figure 6.3A demonstrates that p-p53^{ser15} expression in the cerebral cortex of vehicle-treated neonatal rats was 0.10 ± 0.04 (arbitrary units; mean ± SEM) and Δ^9-THC treatment did not significantly affect p-p53^{ser15} expression (0.17 ± 0.04; vs., vehicle, p=0.2154, Student's t test, n=6). In adolescents treated with vehicle, p-p53^{ser15} expression was 0.40 ± 0.18 (mean ± SEM) and Δ^9-THC treatment did not significantly affect p-p53^{ser15} expression (0.26 ± 0.12;p=0.5258, vs., vehicle, student's t test, n=6). In adults treated with vehicle p-p53^{ser15} expression was 0.04 ± 0.02 (mean ± SEM), Δ^9-THC treatment did not significantly affect p-p53^{ser15} expression (0.06 ± 0.02; p=0.4727, vs., vehicle, student's t test, n=6). Sample immunoblots demonstrating the effect of Δ^9-THC on p-p53^{ser15} expression in neonatal, adolescent and adult cerebral cortices *in vivo* are shown in Figure 6.3B.

Figure 6.3: The effect of Δ^9-THC on phospho-p53^{ser15} expression in the developing rat cerebral cortex

Neonatal (5 - 7-days old), adolescent (3 months old) and adult (8 - 9 months old) Wistar rats were exposed to Δ^9-THC (1 mg/Kg s.c.) for 3 hr. Cerebral cortices were removed and homogenised on ice. Phospho-p53^{ser15} (p-p53^{ser15}) expression was assessed by western immunoblot.

A: Δ^9-THC (1 mg/Kg) induced no significant increase in p-p53^{ser15} expression in the neonatal, adolescent or adult cerebral cortex. Results are expressed as mean ± SEM, n=6.

B: Representative western immunoblot showing the developmental p-p53^{ser15} expression pattern. β actin confirms equal loading of protein.

A

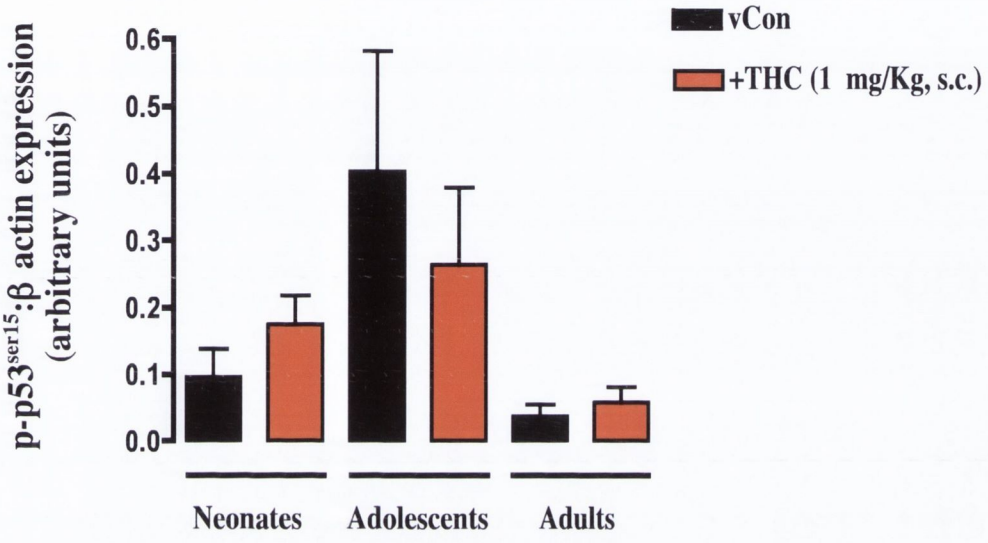
vCon
+THC (1 mg/Kg, s.c.)
p-p53ser15:β actin expression (arbitrary units)
0.6
0.5
0.4
0.3
0.2
0.1
0.0
Neonates
Adolescents
Adults

B

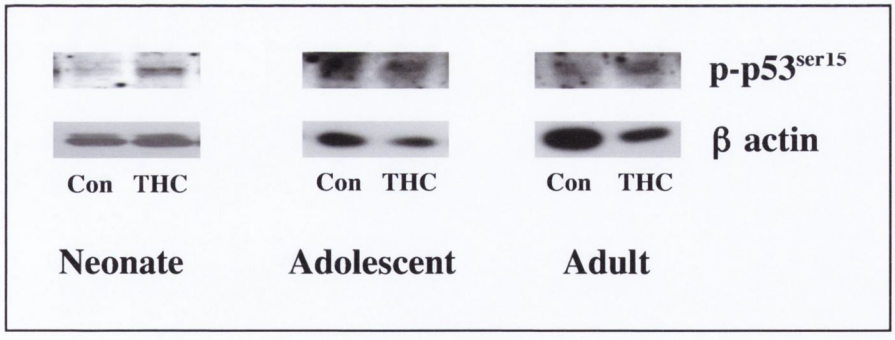
p-p53ser15
β actin
Con THC
Con THC
Con THC
Neonate
Adolescent
Adult

6.2.4 Δ^9 THC-induces an increase in cathepsin-D activity in neonatal but not adult cerebral cortex

Since we observed that Δ^9-THC had a negative impact on the lysosome *in vitro*, this study aimed to determine if Δ^9-THC affects the lysosomal system *in vivo*, and if this was affected by age. Neonatal (5 - 7-days old) and adult (> 4 months old) rats received a subcutaneous injection of Δ^9-THC (1 and 30 mg/Kg s.c.) in vehicle (5% absolute alcohol, 5% Cremophore EL and 90% sterile saline) or vehicle alone for 3 hours. Following treatment, cortical slices were prepared, homogenised in lysis buffer and cathepsin-D activity determined by an immunocapture-based assay. Figure 6.4 demonstrates that cathepsin-D activity is significantly increased by Δ^9-THC in the cerebral cortex of neonatal but not adult rats (Age_{effect} $p<0.0001$, 2-way ANOVA, n=4 - 6). In figure 6.4A, cathepsin-D activity in the cerebral cortex of vehicle-treated neonatal rats was 0.31 ± 0.06 nmoles MCA produced per mg protein per minute (mean ± SEM), treatment with Δ^9-THC (1 mg/Kg) significantly increased cathepsin-D activity in the neonatal cerebral cortex (0.78 ± 0.16; $p<0.05$, vs., vehicle, Student Newman Keuls, n=4 - 6). Cathepsin-D activity was further increased to 1.45 ± 0.22 nmoles MCA produced per mg protein per minute following administration of the higher dose of Δ^9-THC (30 mg/Kg) for 3 hours ($p<0.001$, vs., vehicle, $p<0.01$, vs., 1 mg/Kg, Students Newman Keuls, n=4 - 6). In figure 6.4B, cathepsin-D activity in the cerebral cortex of vehicle-treated adult rats was 0.35 ± 0.05 (nmoles MCA produced per mg protein per minute; mean ± SEM) and treatment with Δ^9-THC (1 mg/Kg) significantly decreased cathepsin-D activity in the adult cerebral cortex (0.18 ± 0.02; $p<0.05$, vs., vehicle, Student Newman Keuls, n=4 - 6). Cathepsin-D activity was further significantly decreased to 0.19 ± 0.03 nmoles MCA produced per mg protein per minute ($p<0.05$, vs., vehicle, Student Newman Keuls, n=4 - 6) when rats were administered the higher Δ^9-THC dose of 30 mg/Kg.

Figure 6.4: Δ^9-THC induces an increase in cathepsin-D activity in neonatal but not adult cerebral cortex

Neonatal (5 - 7-days old) and adult (> 4 months old) Wistar rats were exposed to Δ^9-THC (1 and 30 mg/Kg s.c.) for 3 hr. Cerebral cortices were then removed and homogenised on ice. Cathepsin-D activity in tissue cytosolic fractions was determined using an immunocapture-based assay.

A: Δ^9-THC (1 and 30 mg/Kg, s.c.) induced a significant increase in cathepsin-D activity in the neonatal cerebral cortex. Results are expressed as means ± SEM, * $p<0.05$, *** $p<0.001$, vs., vehicle, ++$p<0.01$, vs., 1 mg/Kg Δ^9-THC, Student Newman Keuls, n=4 - 6.

B: Δ^9-THC (1 and 30 mg/Kg s.c.) induced a significant decrease in cathepsin-D activity in the adult cerebral cortex. Results are expressed as mean ± SEM, * $p<0.05$, vs., vehicle, Student Newman Keuls, n=4 - 6.

2-way ANOVA: Age_{effect} $F(1, 23)=34.25$; $p<0.0001$, $Drug\ treatment_{effect}$ $F(2, 23)=7.86$; $p=0.0025$, $Interaction_{effect}$ $F(2, 23)=13.23$; $p=0.0001$.

A

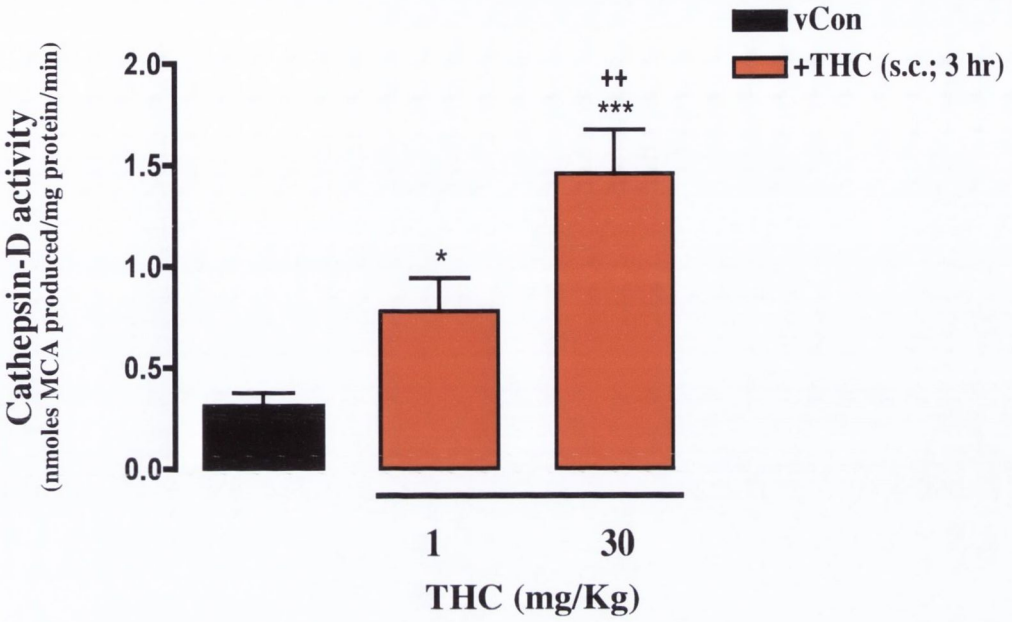
vCon
+THC (s.c.; 3 hr)
Cathepsin-D activity
(nmoles MCA produced/mg protein/min)
2.0
1.5
1.0
0.5
0.0
*
++
***
1
30
THC (mg/Kg)

B

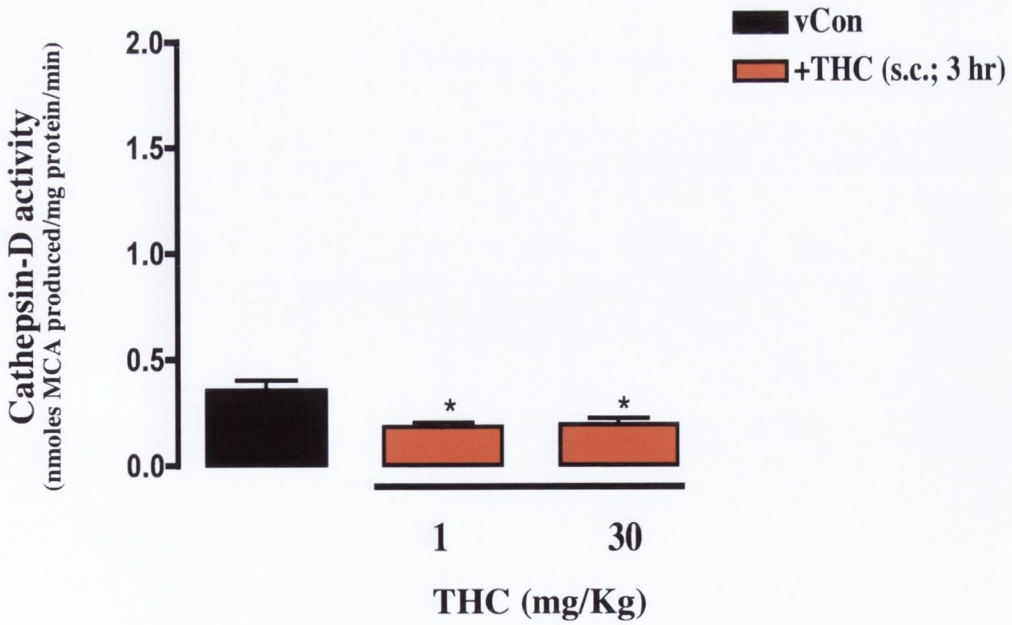
vCon
+THC (s.c.; 3 hr)
Cathepsin-D activity
(nmoles MCA produced/mg protein/min)
2.0
1.5
1.0
0.5
0.0
*
*
1
30
THC (mg/Kg)

6.2.5 Δ^9-THC-induces the release of the active form of cathepsin-D from the lysosomes in neonatal but not adult cerebral cortex

To determine if Δ^9-THC causes the release of the active form of cathepsin-D (34 kDa) *in vivo*, neonatal (5 - 7-days old), and adult (> 4 months old) rats received a subcutaneous injection of Δ^9-THC (10 mg/Kg, s.c.) in vehicle (5% absolute alcohol, 5% Cremophore EL and 90% sterile saline) or vehicle alone for 3 hours. Following treatment, cortical slices were prepared, homogenised in lysis buffer and cathepsin-D expression determined by western immunoblot. A significant increase in expression of the active and pro-form of cathepsin-D (34 and 52 kDa, respectively) was observed in cerebral cortices isolated from neonates but not adults treated with Δ^9-THC (10 mg/Kg, s.c.) for 3 hours (Age_{effect} $p<0.0001$, 2-way ANOVA; Figure 6.5). Figure 6.5A demonstrates that the expression level of the active form of cathepsin-D (34 kDa) in the cerebral cortex of vehicle-treated neonatal rats was 0.10 ± 0.03 arbitrary units (mean ± SEM) and Δ^9-THC treatment significantly increased cathepsin-D (34 kDa) expression (0.60 ± 0.19; $p<0.05$, vs., vehicle, Student Newman Keuls, n=6). In adults treated with vehicle, cathepsin-D (34 kDa) expression was 0.17 ± 0.03 arbitrary units (mean ± SEM), which was not changed after treatment with Δ^9-THC (0.14 ± 0.05).

Figure 6.5B demonstrates that the expression level of the pro-form of cathepsin-D (52 kDa) in the cerebral cortex of vehicle-treated neonatal rats was 0.38 ± 0.11 arbitrary units (mean ± SEM) and Δ^9-THC treatment significantly increased cathepsin-D (52 kDa) expression (1.68 ± 0.35; $p<0.01$, vs., vehicle, Student Newman Keuls, n=6). In adults treated with vehicle, cathepsin-D (52 kDa) expression was 0.98 ± 0.29 (mean ± SEM), which was not changed after treatment with Δ^9-THC (0.43 ± 0.08). Sample immunoblots demonstrating the effect of Δ^9-THC on cathepsin-D expression in neonatal and adult cerebral cortices *in vivo* are shown in Figure 6.5C.

Figure 6.5: Δ^9-THC-induces the release of cathepsin-D from the lysosomes in neonatal but not adult cerebral cortex

Neonatal (5 - 7-days old) and adult (> 4 months old) Wistar rats were exposed to Δ^9-THC (10 mg/Kg, s.c.) for 3 hr. cerebral cortices were then removed and homogenised on ice. Cathepsin-D expression was assessed by western immunoblot.

A: Δ^9-THC (10 mg/Kg, s.c.) induced a significant increase in the expression of the active form of cathepsin-D (34 kDa) in neonatal, but not in adult cerebral cortex. Results are expressed as means ± SEM, * $p<0.05$, Student Newman Keuls, n=6.

B: Δ^9-THC (10 mg/Kg, s.c.) induced a significant increase in the expression of the pro-form of cathepsin-D (52 kDa) in neonatal, but not in adult cerebral cortex. Results are expressed as means ± SEM, ** $p<0.01$, Student Newman Keuls, n=6.

C: Representative western immunoblot showing the Δ^9-THC-induced release of cathepsin-D from the lysosomes in neonates but not in adults. Neonates treated with vehicle (lane 1) and Δ^9-THC (lane 2), and adults treated with vehicle (lane 3) and Δ^9-THC (lane 4). Arrow indicates the active form of cathepsin-D. β actin confirms equal loading of protein.

A

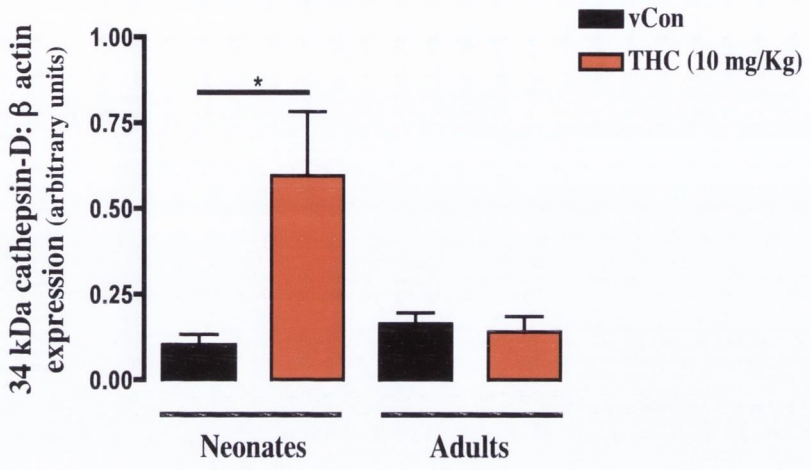
vCon
THC (10 mg/Kg)
34 kDa cathepsin-D: β actin expression (arbitrary units)
1.00
0.75
0.50
0.25
0.00
*
Neonates
Adults

B

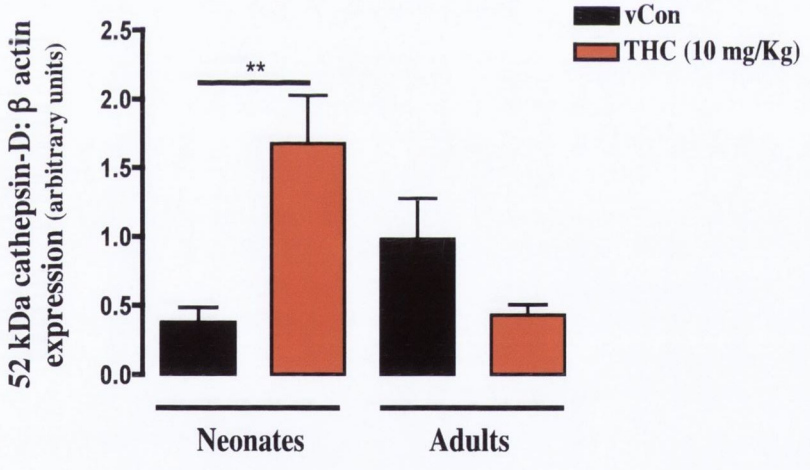
vCon
THC (10 mg/Kg)
52 kDa cathepsin-D: β actin expression (arbitrary units)
2.5
2.0
1.5
1.0
0.5
0.0
**
Neonates
Adults

C

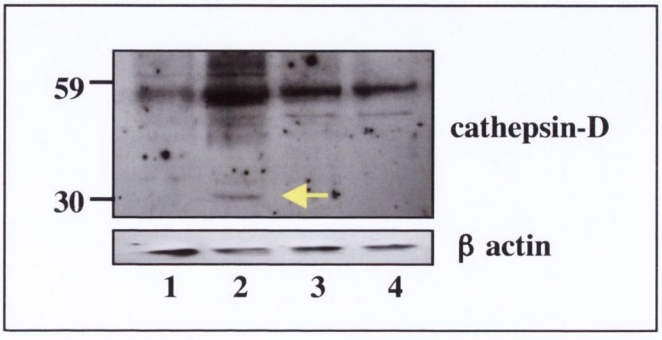
59
30
cathepsin-D
β actin
1
2
3
4

6.3 Discussion

The aim of this study was to examine the relationship between the stage of brain development and the potential for Δ^9-THC to couple to the activation of an apoptotic response, namely the activation of p53, caspase-3, and the cleavage of DNA; hallmarks of apoptosis that have been previously been found to be involved in mediating the pro-apoptotic effect of Δ^9-THC in cultured cortical neurones (Campbell, 2001; Downer *et al.*, 2007a, 2003, 2001). In this *in vivo* study, Δ^9-THC induced the activation of caspase-3 activity in cerebral cortices isolated from neonatal rats. However, this apoptotic response was not observed in adolescent or adult rats exposed to Δ^9-THC. These results indicate that neonatal rat cerebral cortices are more vulnerable to the neurotoxic effects of Δ^9-THC than the cerebral cortices of adolescent or adult rats. A similar profile was observed in the other pro-apoptotic parameters investigated *i.e.,* cathepsin-D activity and DNA fragmentation. Despite the increase in CB_1 receptor expression in the adult cerebral cortex compared to the neonatal cerebral cortex (Downer *et al.*, 2007b), the activation of the apoptotic pathway by Δ^9-THC is less robust in the adult rat cerebral cortex. Unfortunately, results obtained from the adolescent group and from the study on the effect of Δ^9-THC exposure on p53 expression at different developmental stages were not clear-cut and so no definitive findings could be reached regarding the susceptibility of the adolescent cerebral cortex to the neurotoxic effect of Δ^9-THC. This could possibly have occurred due to the fact that age comparisons between rats and humans are notoriously difficult and are not directly comparable (Quinn, 2005). Therefore, only a more in-depth investigation using more developmental time points could accurately identify differences in pro-apoptotic hallmarks during the development of the rat cerebral cortex. In addition to age, the exposure time of 3 hours may have been inappropriate to assess differences in apoptotic markers, given that we have previously observed a distinct time-line for the activation of specific apoptotic signalling molecules *in vitro e.g.,* p53 is activated after 5 minutes Δ^9-THC exposure, whilst caspase-3 activity is first increased after 1 hour Δ^9-THC exposure (Campbell, 2001; Downer *et al.*, 2007a, 2001). Therefore, to observe these dynamic changes, future experiments should incorporate multiple exposure time-points and possibly the inclusion of a chronic treatment group. Despite this, we did observe a neurotoxic

response in the neonatal cerebral cortex following Δ^9-THC exposure. If one considers that the rat neonatal brain is a model of the developing human brain during the third trimester of pregnancy, and the fact that a proportion of ingested Δ^9-THC can cross the placenta, our data suggests that the immature cerebral cortex *in utero* may be more vulnerable to Δ^9-THC-induced neurotoxicity at this critical phase in brain development. Despite this, it must also be noted that deleterious effects, as a result of cannabis exposure, has been observed in adults (Matochick *et al.*, 2005). However, since neurogenesis is known to continue into adulthood *e.g.,* in the hippocampus, and that cannabinoids have the ability to effect neuronal progenitors in a number of different ways, these results may indicate that exogenous phytocannabinoids may prevent or disturb *de novo* neurogenesis or effect other mechanisms occurring in the adult brain (Maćkowiak *et al.*, 2004; Harkany *et al.*, 2007).

In this study we have also identified that the peripheral administration of Δ^9-THC increases the cytosolic expression and activity of the lysosomal protease, cathepsin-D in the neonatal rat cerebral cortex. As detailed in chapter 4 of this thesis, lysosomal permeabilisation is an upstream event in apoptosis and leads to the release of lysosomal cathepsin enzymes into the cytosol, which in turn can participate in the apoptotic cascade (Kågedal *et al.*, 2005; Schestkowa *et al.*, 2007). This pathway is implicated in the physiological cell death that occurs during embryonic development (Zuarte-Luis *et al.*, 2007). It is interesting to speculate that when the immature brain is exposed to Δ^9-THC following maternal use of cannabis, aberrant activation of the cathepsin pathway may evoke excessive neuronal apoptosis that may contribute, in part, to the cognitive deficits observed later on in early adulthood. Additionally, if the *in utero* exposure to Δ^9-THC causes an alteration in the cannabinoid signalling system, this may result in the aberrant activation of apoptosis due to a lack of survival signals from neurotrophins *etc.,* to immature neurones or neural progenitors. Conversely, we found that adults treated with Δ^9-THC displayed a significant decrease in cathepsin-D compared to control animals, indicating that perhaps in adult animals Δ^9-THC may have neuroprotective properties. This observation is extremely interesting since Sato *et al.*, (2006), have shown that cathepsin-D was selectively and linearly increased during aging in the cerebral cortex and hippocampus. Increased cathepsin-D activity has been

found in a number of laboratories, however cathepsin-D deficiency results in neurodegeneration (Nakamura *et al.*, 1989; Kenessey *et al.*, 1989; Nakanishi *et al.*, 1994; Koike *et al.*, 2000). Furthermore, cathepsin-D is known to breakdown neurofilaments and tau which are cytoskeleton components of neurones (Nixon and Marotte, 1984; Bednarski and Lynch, 1996). Therefore cathepsin-D may slowly digest cytoskeleton components in neurones, which may be responsible for morphological changes and functional loss of neurones in the immature and aged brain (Jung *et al.*, 1999). However, if cathepsin-D disrupts neurofibrillary tau tangles which are hallmarks of neurodegeneration, our observations showing Δ^9-THC induces a decrease in cathepsin-D in the adult cerebral cortex may suggest that cannabinoids may be useful therapeutic tools which may be able to modulate this feature of neurodegeneration and could be of relevance for the treatment of Alzheimer's disease.

The affect of Δ^9-THC on the lysosomes was first observed in studies carried out in the 1970s. Raz *et al.*, (1973) observed that both Δ^9-THC and cannabidiol caused an increase in acid phosphatase in lysosomal fractions taken from rat livers which was indicative of a disruption of the lysosomal membrane. Similarly, Britton and Mellors (1974) also observed the lytic effect of Δ^9-THC on rat liver lysosomes during their *in vitro* investigations. In 1975 the lysosomal-uptake kinetics of Δ^9-THC were reported, Δ^9-THC was rapidly taken up (within minutes) into liver lysosomes akin to the rapid appearance of cannabinoids in the CNS (Irvin and Mellors, 1975). Davies and co-workers (1979) observed increases in the volume densities of mitochondria, lysosomes, lipid inclusions and decreases in cytoplasmic volume in alveolar macrophages isolated from rats exposed to the smoke from tobacco containing cigarettes. These observations are indicative of an apoptotic response, however, in an additional animal group exposed to cigarettes containing cannabis, changes in lipid inclusions and a reduction in the volume of the cytoplasm were the only altered parameters. At that time the stabilisation and rupture of organelle membranes by other fat soluble compounds *e.g.,* vitamins D, E and K, and steroids, were well documented and this alteration was believed to be as a result of the unspecific membrane-modifying properties of these compounds. However, the molecular complexities involved in CB receptor-mediated signalling to lysosomes were not known at this stage and so the negative impact which Δ^9-THC has on

lysosomes was interpreted as an unspecific affect caused by the membrane-modifying properties that Δ^9-THC possesses and not a co-ordinated event.

In recent years, it has been shown that the CB_1 receptor associates with lysosomes and that cannabinoids can regulate the lysosomal system through the CB_2 receptor. Matveyeva *et al.*, (2000) have reported that Δ^9-THC increases cathepsin-D activity, but not other thiol cathepsins, *via* the CB_2 receptor in cultured macrophage hybridomas and this was linked to an antigen-dependent processing defect in Δ^9-THC-exposed macrophages. Sarnataro and colleagues (2005) observed that a substantial proportion of the CB_1 receptor is present in lysosomes in a human breast cancer cell line which was dependent on the presence of cholesterol in plasma membrane lipid rafts. The compartmentalisation of several receptors and their ligands has been reported to be responsible for regulating cellular responses to effectors and so it is necessary to elucidate cannabinoid receptor trafficking mechanisms in order to fully understand the physiological response to cannabinoids. Therefore, perhaps our observations concerning the age-dependent effect of Δ^9-THC on the lysosomal system *in vivo* may represent a difference in subcellular cannabinoid receptor trafficking, possibly as a result of differences in membrane fluidity between neonates and adult animals. Interestingly, Sarnataro *et al.*, (2005) found that when lipid rafts were perturbed by cholesterol depletion, CB_1 receptor resided in the cytoplasm suggesting that the intracellular localisation pathway followed by the CB_1 receptor is dependent on the integrity of lipid rafts. Furthermore, the association of aging with increased levels of plasma membrane lipid peroxidation which results in increased plasma membrane rigidity, could be a mechanism which anchors cannabinoid receptors to the cell surface, leaving the lysosomal system and the level of hydrolytic enzymes present in the cytosol unchanged.

A number of *in vitro* and *in vivo* experiments have described differential effects of cannabinoids on cell viability (Chan *et al.*, 1998; Galve-Roperh *et al.*, 2000; Sinor *et al.*, 2000; van der Stelt *et al.*, 2001; Downer *et al.*, 2007a,b). This study has demonstrated that the proclivity of Δ^9-THC to couple to the apoptotic pathway is more robust in the neonatal rat cerebral cortex, compared to the adult cerebral cortex. The finding that the immature rat brain is more vulnerable to the toxicity of Δ^9-THC may

underlie the cognitive deficits that occur following gestational exposure to cannabis in humans and the data informs the growing debate regarding the teratogenic potential of cannabis (Smith *et al.*, 2006; Fried and Smith, 2001).

Summary schematic

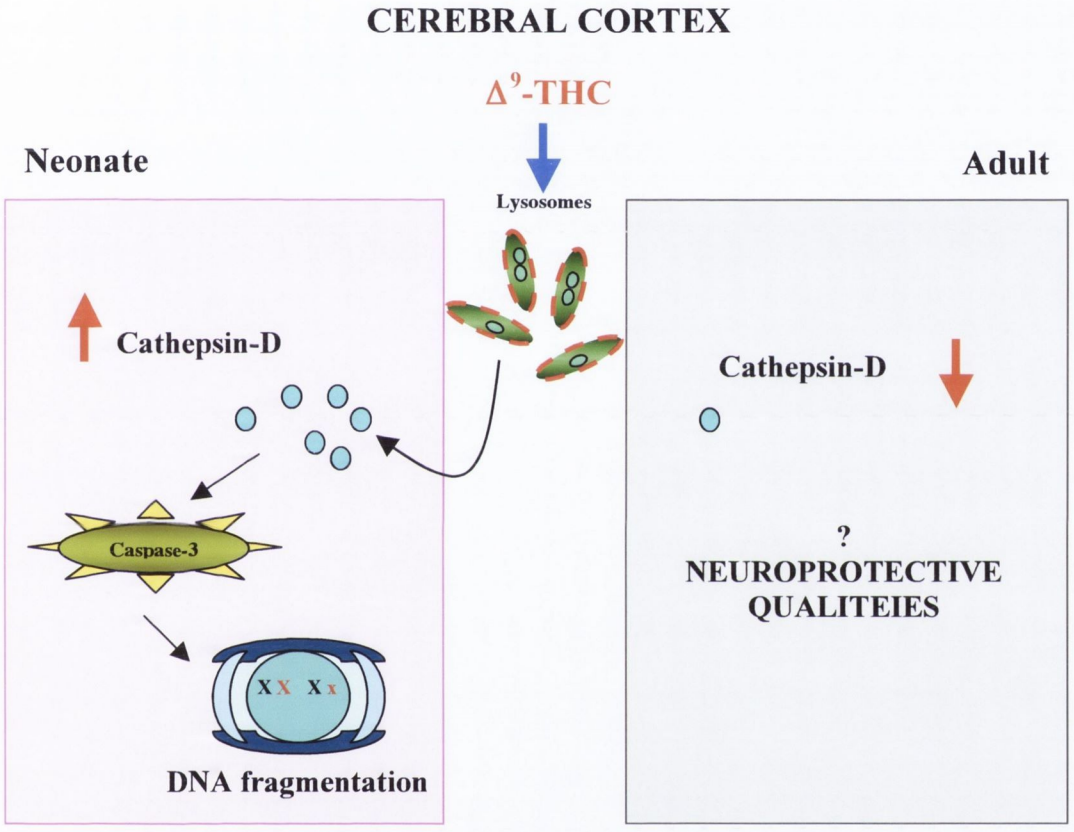

Chapter 7

Final discussion

7.1 General discussion

The binding of cannabinoids such as Δ^9-THC, endocannabinoids, and synthetic agonists and antagonists to specific G protein-coupled cannabinoid receptors, is accepted to exert a broad spectrum of effects on the CNS as well as on peripheral sites (Di Marzo *et al.*, 1998; Porter and Felder. 2001). In recent years, scientific research into the plethora of cannabinoid-mediated effects have yielded vast amounts of information which has filled the gaps in our knowledge of the cannabinoid system, whilst also creating new avenues of research through the revelation that the cannabinoid system is involved in many physiological and pathological processes. However, to evaluate the pharmacological and toxicological profile of cannabis, which contains many chemically active compounds, the scientific community has focussed on the effect of Δ^9-THC to evaluate the molecular mechanisms activated as a consequence of exposure to cannabis. Recently, there has been a growing interest in the role of cannabinoids in the control of the neuronal survival/death decision, which has particularly focussed on finding new therapeutic options for cancer and neurodegenerative diseases *e.g.,* cannabidiol. However, in addition to these areas, the role of cannabinoids in the maturation of complex neuronal networks and the sculpting of the immature CNS has been the focus of several investigations. Some lines of investigation have aimed to identify the effects that *in utero* exposure to cannabinoids (phytocannabinoids or prescribed medication containing cannabimimetic moieties) has on the cannabinoid-regulated CNS developmental processes. The overall aim of this thesis was to try and identify signalling mechanisms that mediate Δ^9-THC-induced neurotoxicity *in vitro*, whilst also attempting to establish if these signalling mechanisms occur *in vivo*. We also sought to examine the effects of brain development on the Δ^9-THC-induced appearance of neurotoxicity.

7.1.1 Summary of thesis findings

Since our laboratory has previously identified some of the molecular targets modulated by Δ^9-THC, namely, p53, JNK, Bax, cytochrome-c and caspase-3 (Campbell, 2001; Downer *et al.*, 2007b, 2003, 2001), the current study aimed to

identify, (i) the signalling mechanism responsible for p53 activation, (ii) the signalling consequences of p53 activation, and (iii) novel molecular signalling pathways regulated by Δ^9-THC. The next aspect of this study was to determine if the endocannabinoids, AEA and 2-AG, elicited a neurotoxic response, similar to that of Δ^9-THC in our *in vitro* culture system. Finally, this thesis aimed to determine whether Δ^9-THC invokes a neurotoxic response in an age-dependent manner by examining the ability of Δ^9-THC to induce apoptotic markers in the neonatal, adolescent and adult cerebral cortex.

Briefly, this thesis found that p53 was activated by the kinase activity of JNK1. Δ^9-THC also induced the transcription of the p53 responsive gene Mdm2, which was an additional indicator of p53 activation. The p53 post translational modifier protein, SUMO-1 was also positively regulated by Δ^9-THC and this coincided with the activation and deSUMOylation of p53 which may indicate that the SUMOylation status of p53 may have consequences for p53 function. Δ^9-THC induced an activation of SyK *via* p53 and SyK activity is required for the induction of Δ^9-THC-induced DNA fragmentation. This is the first time that Δ^9-THC has been reported to regulate SyK and identifies a novel aspect of cannabinoid signalling in the brain. The lysosomal system was also found to be pertinent in mediating Δ^9-THC-induced apoptosis and involved the destabilisation of the lysosomal membrane followed by the cathepsin-dependent activation of caspase-3 and DNA fragmentation. Despite the early findings that Δ^9-THC has a negative impact on lysosomal integrity in peripheral tissues and cells, this is the first time that Δ^9-THC -induced lysosomal membrane destabilisation has been observed in the CNS. Interestingly, data from the investigation of the neurotoxic potential of endocannabinoids, AEA and 2-AG, showed that both endocannabinoids evoked an apoptotic response in cultured cortical neurones which involved caspase-3 activity (not observed in the case of 2-AG) and DNA fragmentation. In addition, AEA induced a dose- and time-dependent destabilisation of the lysosomal membrane, which was dependent on p53 and SyK activity, akin to Δ^9-THC negative effect on lysosomal membrane stability. In contrast to the CB_1-mediated lysosomal membrane destabilisation induced by Δ^9-THC, CB_1 receptor antagonism did not prevent AEA-

induced lysosomal membrane destabilisation. Furthermore, a low concentration of 2-AG (0.01 μM) displayed a less robust activation of the apoptotic cascade and provided significant neuroprotection against glutamate excitoxicity. The investigation of the effects of development response to Δ^9-THC yielded interesting results. The results indicated that the immature brain was more vulnerable to the neurotoxic effects of Δ^9-THC, as assessed by measuring caspase-3 activity and the amount of fragmented DNA in the cerebral cortex of neonatal rats exposed to Δ^9-THC. Developmental differences in the response of neonatal and adult animals to Δ^9-THC at the level of the lysosomal system were also observed, such as, the release and activation of cathepsin-D. Overall, the data presented in this thesis indicates that cannabinoids have the proclivity to induce apoptosis in cultured cortical neurones. *In vivo,* Δ^9-THC specifically induces apoptotic markers in the immature rat cerebral cortex, which provides evidence for an inter-relationship between neuronal maturity and Δ^9-THC apoptotic signal transduction.

7.1.2 p53/ SUMO/Mdm2

Cells undergoing terminal differentiation express very low levels of p53 compared to neuronal precursors and the activation of p53 in these post-mitotic cells has been proposed to activate an apoptotic, rather than a rest and repair response (Rogel *et al.*, 1985; Raffray and Cohen, 2001). It has also been shown that p53 can regulate neural cell differentiation, which is of interest to our laboratory given our findings that the developing cerebral cortex is more prone to the toxic effects of Δ^9-THC *in vivo.* Our findings support an essential role for p53 in Δ^9-THC-induced neuronal apoptosis *in vitro.* If one views our *in vitro* neuronal cultures as a representation of cells present during the developing embryonic human neocortex, then our findings may provide a molecular rationale for the reported cannabis-related developmental impairments. Eizenberg and co-workers (1996) observed a change in the cellular distribution of p53 between differentiated and undifferentiated neurones. These studies found that early in the differentiation process, p53 accumulates in the nucleus, where it may activate genes involved in cell differentiation. However, once the differentiation process begins, p53 levels rise before being exported to the cytoplasm when it is no longer needed for

transactivation of target genes. Interestingly, it has also been observed that p53 contributes to oligodendrocyte differentiation (Tokumoto *et al.*, 2001; Billon *et al.*, 2004). Considering the important role that the cannabinoid system has both on neural progenitor proliferation and specification, the studies mentioned above, in conjunction with our findings, highlight the need for further study into the regulation of p53 by cannabinoids and its consequences for CNS development. Conversely it has been reported that proteins normally involved in cell cycle and cell death can take on another function as promoters of neurite regeneration and, axon outgrowth and regeneration which occurs during CNS or peripheral nerve injury (Benowitz and Routtenberg, 1997; Hughes *et al.*, 1999; Emery *et al.*, 2003). Indeed, both c-jun and p53 have been implicated in axonal regeneration and neurite out growth (Raivch *et al.*, 2004; Di Giovanni *et al.*, 2006). Overall, these studies suggest that the p53 protein has pleiotropic functions in the CNS, modulation of which could be exploited as a neuroprotective therapeutic strategy in both the developing and mature/aging CNS given the potential of cannabinoids to control these opposing p53 functions.

In addition to the activation of p53, we also observed that several other signalling proteins were regulated by Δ^9-THC, namely, the p53 responsive protein Mdm2, the post translational modifier protein SUMO-1 and SyK. These observations as far as we can determine are newly identified cannabinoid-regulated signalling mechanisms. Our findings regarding the induction of the Mdm2 protein provides corroborating evidence that Δ^9-THC regulates p53 signalling. In addition, the observation that only the shorter Mdm2 protein, which is incapable of degrading p53, was transcribed provides additional evidence that exposure of neurones to Δ^9-THC increases p53 stabilisation, which has a pro-apoptotic effect function (Downer *et al.*, 2007a). Since the post translational modification status of Mdm2 has a bearing on its subcellular location and its ability to act as a p53 ubiquitin ligase, it would be interesting to investigate whether Δ^9-THC induces changes in the SUMOylation and phosphorylation status of the Mdm2 protein and to assess if any of these modifications are linked to disturbing or hindering the ability of Mdm2 to regulate p53. Although cannabis has been traditionally associated with the relief of pain and nausea that cancer patients experience, the diverse pharmacological activities of cannabimimetic

compounds as modulators of tumour growth, angiogenesis and metastasis have prompted investigation into the therapeutic use of cannabinoids as cancer therapies. Therefore, the proclivity for Δ^9-THC to regulate cell cycle regulatory proteins such has p53 and Mdm2 could indicate that cannabinoid compounds may provide a novel therapeutic strategy for the treatment of tumours that are resistant to standard chemotherapeutic strategies (Michiue *et al.*, 2005; Dudkina and Lindsley, 2007).

The observation that Δ^9-THC alters the process of SUMOylation is exciting considering that a recent report has suggested that in neurones, SUMOylation permits a rapid and reversible modification of receptor membrane localisation and synaptic function (Martin *et al.*, 2007). Additionally, SUMOylation has been implicated in the pathogenesis of several neurodegenerative diseases, such as Parkinson's disease, Alzheimer's disease, amyotrophic lateral sclerosis, neuronal intranuclear inclusion disease, multiple system atrophy, Huntington's disease and other related polyglutamine disorders by impacting on pathways such as oxidative stress, protein aggregation and proteasome-mediated degradation (Hattori and Mizuno, 2004; Dorval *et al.*, 2007; Gibb *et al.*, 2007; Takahashi-Fujigasaki *et al.*, 2006; Lieberman, 2004; Dorval and Fraser, 2007). Current studies have yet to give conclusive evidence as to the precise involvement of the SUMO pathway in the pathogenesis of neurodegenerative diseases and so represents a novel area for future studies (Lieberman, 2004). It would be interesting to investigate the ability of the endocannabinoid system to regulate SUMO regulatory processes in the normal and degenerating brain since global shifts in protein SUMOylation in response to oxidative stress have been reported (Manza *et al.*, 2004). Our findings related to the proclivity of Δ^9-THC to increase the levels of unconjugated SUMO-1 and to induce the deSUMOylation of p53 are novel, however, further experiments should be carried out in order to gain a deeper understanding of the cellular consequences of Δ^9-THC-induced changes on SUMO and to determine the role of SUMOylation status in the neurotoxic response to cannabinoids. It may be particularly interesting to investigate the role of the cannabinoid system in regulating the levels of unconjugated SUMO-1, in addition to investigating if the SUMOylation status of other Δ^9-THC-regulated proteins *e.g.*, JNK and Mdm2. Given that SUMO-2 and -3 are associated with cell stress it may be pertinent to investigate if cannabinoids offer

neuroprotection by affecting the conjugation of proteins with these stress-activated forms of SUMO (Saitoh and Hinchey, 2000). Gibb *et al.*, (2007) have found that the SUMOylation of a C-terminal fragment of the astroglial glutamate transporter EAAT2, causes the redirection of the transporter to the nucleus which may be responsible for the transcriptional regulation of genes affecting astrocyte physiology. Taking the findings of Gibb *et al.*, (2007) and further reports that receptor SUMOylation can modulate synaptic function (Coussen and Choquet, 2007; Martin *et al.*, 2007) an investigation into the potential for CB receptors to undergo SUMOylation would be both challenging and interesting considering that the availability and targeting of CB receptors is an important mechanism for controlling the functions of endocannabinoids within the CNS. Since SUMO is involved in many processes and is essential for normal growth and development (Hay, 2007; Johnson, 2004), it may be pertinent for us to examine if there are any developmental changes in the SUMO regulatory system and if these may be modulated by cannabinoids.

7.1.3 Lysosomes

Lysosomal destabilisation and the subsequent release of hydrolytic enzymes has been linked with apoptotic cell death and developmental programmed cell death (Terman *et al.*, 2006; Zuarte-Luis *et al.*, 2007). In addition the fact that tumour invasion and metastasis are associated with altered lysosomal trafficking and increased expression of specific cathepsins implies that cancer cells are already sensitised to death pathways involving lysosomal membrane permeabilisation and release of proteolytic enzymes. Thus, lysomotrophic agents are seen as potential targets for cancer therapy which exploits this "Achilles heel" (Fehrenbacher and Jäättelä, 2005; Tardy *et al.*, 2006; Gocheva and Joyce, 2007). The results of our experiments investigating the effects of Δ^9-THC on the lysosomal system may be of interest to the wider disciplines of cannabinoid research such as, the anti-tumour potential of cannabinoids, cannabinoid receptor cycling and cannabinoid system functions in the developing CNS.

Additionally, there is growing evidence that rapid and local pH transients as a result of the activation/inhibition of Na^+/H^+ exchangers (NHEs) may alter neuronal excitability and a wide variety of neuronal signalling events are pH-dependent *e.g.*,

voltage- and ligand-gated ion channels, transmitter uptake through transporters, intracellular signal transduction, and intracellular communication *via* gap junctions (Di Marzo *et al.*, 1998). Interestingly, G protein-coupled receptors, including CB_1, have been shown to activate NHEs and leading to changes in cytosolic pH, cell volume and cell spreading capabilities (Noel and Pouyssegur, 1995; Garnovskaya *et al.*, 1997; Bouaboula *et al.*, 1999). Indeed, CP 55940 activates a plasma membrane localised Na^+/H^+ exchanger, NHE-1, causing the alkalisation of the cytosol in CB_1 receptor over expressing CHO cells and in the U373MG astrocytoma cell line which endogenously expresses the CB_1 receptor (Bouaboula *et al.*, 1999). To date five NHE isoforms have been identified and possess different subcellular locations and tissue distribution patterns. It is tempting to speculate that the NHE exchangers located on lysosomes may be responsible for the effects of Δ^9-THC on lysosomes observed in our *in vivo* and *in vitro* studies. Furthermore, McGuiness and colleagues (2006) have shown that the disruption of lysosomes in the axons of hippocampal pyramidal cells provides an intracellular store of Ca^{2+}, which results in the frequency of spontaneous neurotransmitter release. Cannabinoids have been shown to cause intracellular Ca^{2+} increases *via* the activation of Ca^{2+} pumps in the endoplasmic reticulum and the activation of IP_3 sensitive intracellular Ca^{2+} stores (Lauckner *et al.*, 2005; Netzeband *et al.*, 1999). Thus, it would be interesting to find out if cannabinoids induce a destabilisation of the lysosomal membrane, akin to the observations of McGuiness *et al.*, (2006), in order to access additional Ca^{2+} stores needed for neurotransmission and if this was the mechanism which explains our *in vitro* and *in vivo* findings showing Δ^9-THC induces the destabilisation of the lysosomal membrane. To assess the effect of Δ^9-THC on lysosomal Ca^{2+} stores, the combination of labelling lysosomes with LysoTracker™ and monitoring fluctuations in calcium by real-time fluorometric calcium imaging could be performed on neuronal cultures or synaptosomes. The dysregulation of intracellular Ca^{2+} homeostasis and activation of the NMDA subtype of glutamate receptor, leading to excitoxicity, are features of neurodegenerative diseases such as Alzheimer's disease (Smith *et al.*, 2005; Sonkusare *et al.*, 2005). Thus strategies that reduce Ca^{2+} influx and limit excitoxicity may confer neuroprotection. Endocannabinoid up regulation is observed in a number of neurotoxic paradigms that

are associated with elevated intracellular Ca^{2+} concentration and are believed to be an attempt of the cell to provide feedback inhibition of excitotoxicity (Hasen *et al.*, 2001; Di Marzo *et al.*, 1994; Stella *et al.*, 1997). Indeed, cannabidiol, the principle non-psychoactive component found in cannabis has potent antioxidant properties that offer neuroprotection against glutamate toxicity and has been proposed to be of therapeutic use for neurodegenerative diseases (Hampson *et al.*, 1998b; Russo and Guy, 2006; Campbell and Gowran, 2007).

7.1.4 Development

The endocannabinoid system is active from pre-conception through to birth and continues to play specific roles in many of processes which occur throughout life *e.g.*, fertility, conception, embryo implantation, pregnancy maintenance, foetal growth, foetal CNS development, labour, feeding, developmental changes during puberty and protection from neurodegenerative diseases during old age (Schuel *et al.*, 2002; Wang *et al.*, 2006; Maccarrone *et al.*, 2002; Davitian *et al.*, 2006; Harkany *et al.*, 2007; Dennedy *et al.*, 2004; Fride *et al.*, 2005; Field and Tyrey, 1990; Campbell and Gowran, 2007). Cannabis use during pregnancy results in the transfer of Δ^9-THC through the placenta to the developing foetus and causes many negative effects to the growing foetus (Hutchings *et al.*, 1987, 1989). At present, the effects of prenatal exposure on the developing foetal nervous system is growing at a fast pace and many potential hypothesis have been proposed to be responsible for the long lasting cognitive, motor and social deficits observed in children who are prenatally exposed to cannabis (Fried *et al.*, 2003; Huizink and Mulder, 2006; Richardson *et al.*, 1995). Given the importance of the endocannabinoid system in development, our findings regarding the vulnerability of the neonatal cerebral cortex to the neurotoxic effects of cannabis provides a highly valuable and relevant molecular mechanism for the induction of the neuronal deficits seen in offspring exposed to cannabis during pregnancy.

Chronic users of cannabis display signs of cognitive impairment, however, there are studies that provided evidence for and against this theory (Bolla *et al.*, 2005; Fried *et al.*, 2005). A possible explanation for these contradictory findings may be that the age at which drug use began effects the likelihood of cognitive impairment (Murray *et*

al., 2007). The fact that the first two decades of brain development have the most influence on the functioning of the mature CNS and is the most vulnerable period of CNS development highlights the negative potential which cannabis use has during adolescence (Toga *et al.*, 2006). Several studies have observed that exposure to Δ^9-THC during adolescence elicits cognitive deficits in both humans and rats. Ehrenreich *et al.*, (1999) have reported that adults who used cannabis before, but not after, the age of 16 performed poorly in a task that required focused attention. Pope and co-workers (2003) corroborated this when they found that long-term heavy cannabis users who stopped using cannabis at 17 years of age scored lower verbal IQ scores compared to cannabis users who started after 17 years of age. A number of animal studies, using animals aged between 28 to 32 days old, have shown similar negative cognitive effects following adolescent exposure to CB_1 receptor agonists *e.g.,* decreased spatial and non-spatial learning ability, deficits in working memory and increased anxiety (Cha *et al.*, 2006; Schneider and Kooch, 2003; O'Shea *et al.*, 2004). Although our results showed a heightened sensitivity of the neonatal cerebral cortex to the neurotoxic effects of Δ^9-THC, which correlates with the cognitive deficits seen in offspring prenatally exposed to cannabis, our results regarding the response of an adolescent group to an acute dose of Δ^9-THC failed to yield conclusive findings to support a neurotoxic mechanism responsible for the deficits observed in the behavioural studies mentioned above. The reason for the failure to draw a casual conclusion regarding the neurotoxic potential of Δ^9-THC in adolescents pertains to the fact that the animals used in this study were too old (3 - 4 months old) and were more representative of a middle-aged rat rather than an adolescent. Hence, further experimentation using a broader age range of rat is more likely to cover the critical pre-pubescent period. Furthermore, we did not observe any signs of toxicity in adult rats (4 - 9 months old) exposed to Δ^9-THC. This may be of importance considering that cannabinoids are currently being investigated as potential neuroprotective agents for age-related conditions such as Alzheimer's Disease. Finally, with the current reintroduction of cannabinoid-based medicine for the treatment and management of a number of diseases, the fact that most of the pre-clinical trials for these therapeutic agents were carried out in adult animals raises the urgent need for a

full investigation of the pharmacology and neurotoxicity of these new therapeutic agents in a wide range of developmental time points.

7.1.5 Final comments

Since its discovery more than 4,000 years ago, cannabis use has the proclivity to polarise opinions, ranging from idolisation to demonisation. It falls to the scientific community involved in cannabinoid research to try and bridge the gap between the protagonists who idolise 'cannabis culture' and the prohibitionists who demonise cannabis (Murray *et al.*, 2007). Scientists aim to do this by drawing the attention of both groups to the realities of our current knowledge concerning cannabis - *i.e.*, the exploitation of the beneficial properties of cannabinoids represents a realistic and powerful therapeutic tool for the treatment of many diseases, whilst also acknowledging the negative effects of cannabis misuse such as cognitive deficits, the increased risk of psychotic illnesses and the focus of this study, neurotoxicity.

7.2 Recommendations for future work

- The experiments utilising siRNA to deplete p53 in cultured neurones should be assessed *in vivo*.
- The post translational status of other proteins that we have previously shown to be regulated by Δ^9-THC should be assessed *e.g.*, SUMOylation/Phosphorylation of Mdm2 and JNK1. Although we have demonstrated that Δ^9-THC impacts on the SUMO-1 regulatory system, it would be interesting to find out if Δ^9-THC effects the levels or substrates of SUMO-2 or -3, since they are associated with stress situations. Additionally inhibitors of deSUMOylating enzymes, which are now available, should be used to establish if the Δ^9-THC-induced deSUMOylation is a mandatory event in neuronal apoptosis induced by Δ^9-THC.

- The role of CB_1 receptor internalisation and subcellular trafficking could be investigated, possibly focusing on the lysosomal compartment and the association with Δ^9-THC-regulated signalling proteins such as, p53, SyK and SUMO-1.
- Real-time monitoring of Δ^9-THC-induced lysosomal membrane destabilisation would give important data regarding the exact timing of the Δ^9-THC-mediated lysosomal events. Changes in cytosolic pH following Δ^9-THC treatment would provide further evidence that a destabilisation of the lysosomal membrane occurred.
- We have clearly demonstrated that AEA is neurotoxic to neuronal cultures, yet the receptor signalling responsible (if any) was not identified. Future experiments could utilise MCD which blocks the action of lipid rafts to assess if these are responsible for our observations. Alternatively we could assess the effect of using a FAAH inhibitor to determine if the AMT or AEA metabolites acting on the intracellular side of TRPV1 could be responsible for the neurotoxic profile of AEA.
- 2-AG showed neuroprotective potential against glutamate-induced toxicity therefore we could assess the proclivity to provide neuroprotection against Aβ and other neuronal stressors such as hypoxia.
- A neurotoxic profile was observed following the acute administration of Δ^9-THC in the neonatal, but not in the adult, cerebral cortex, however these *in vivo* experiments could be expanded by doing the following:
    - Use a wider range of developmental ages and doses of Δ^9-THC.
    - Establish if these effects are mediated by the CB_1 receptor.
    - Identify if SUMO-1, Mdm2 or SyK are regulated by Δ^9-THC *in vivo*.
    - Perform a chronic treatment study including animals exposed to cannabinoids *in utero*.

- Link the biochemical markers of neurotoxicity with structural alterations in the brain by using MRI.
- Assess the effect of Δ^9-THC in other areas of the rat brain.
- Use of p53 siRNA or p53 knockout animals to assess the role of p53 *in vivo*.

VII References

ABOOD, M.E., RIZVI, G., SALLAPUDI, N. & MCALLISTER, S.D. (2001). Activation of the CB1 cannabinoid receptor protects cultured mouse spinal neurons against excitotoxicity. *Neurosci Lett*, **309,** 197-201.

ADAMS, I.B. & MARTIN, B.R. (1996). Cannabis: pharmacology and toxicology in animals and humans. *Addiction*, **91,** 1585-614.

ADLER, A.J. (1989). Selective presence of acid hydrolases in the interphotoreceptor matrix. *Exp Eye Res*, **49,** 1067-77.

AGURELL, S., HALLDIN, M., LINDGREN, J.E., OHLSSON, A., WIDMAN, M., GILLESPIE, H. & HOLLISTER, L. (1986). Pharmacokinetics and metabolism of delta 1-tetrahydrocannabinol and other cannabinoids with emphasis on man. *Pharmacol Rev*, **38,** 21-43.

ALMEIDA, R.D., MANADAS, B.J., MELO, C.V., GOMES, J.R., MENDES, C.S., GRAOS, M.M., CARVALHO, R.F., CARVALHO, A.P. & DUARTE, C.B. (2005). Neuroprotection by BDNF against glutamate-induced apoptotic cell death is mediated by ERK and PI3-kinase pathways. *Cell Death Differ*, **12,** 1329-43.

ALOYZ, R.S., BAMJI, S.X., POZNIAK, C.D., TOMA, J.G., ATWAL, J., KAPLAN, D.R. & MILLER, F.D. (1998). p53 is essential for developmental neuron death as regulated by the TrkA and p75 neurotrophin receptors. *J Cell Biol*, **143,** 1691-703.

AMERI, A. (1999). The effects of cannabinoids on the brain. *Prog Neurobiol*, **58,** 315-48.

ANDERSSON, H., D'ANTONA, A.M., KENDALL, D.A., VON HEIJNE, G. & CHIN, C.N. (2003). Membrane assembly of the cannabinoid receptor 1: impact of a long N-terminal tail. *Mol Pharmacol*, **64,** 570-7.

ANTUNES, F., CADENAS, E. & BRUNK, U.T. (2001). Apoptosis induced by exposure to a low steady-state concentration of H2O2 is a consequence of lysosomal rupture. *Biochem J*, **356,** 549-55.

APPELLA, E. & ANDERSON, C.W. (2001). Post-translational modifications and activation of p53 by genotoxic stresses. *Eur J Biochem*, **268,** 2764-72.

ARNDT, P.G., SUZUKI, N., AVDI, N.J., MALCOLM, K.C. & WORTHEN, G.S. (2004). Lipopolysaccharide-induced c-Jun NH2-terminal kinase activation in human neutrophils: role of phosphatidylinositol 3-Kinase and Syk-mediated pathways.

J Biol Chem, **279,** 10883-91.

ASHCROFT, M., TAYA, Y. & VOUSDEN, K.H. (2000). Stress signals utilize multiple pathways to stabilize p53. *Mol Cell Biol*, **20,** 3224-33.

ASHTON, C. (1998). Cannabis: Clinical and pharmacological Aspects. In *Department of health report for the advisory council on the misuse of drugs*.

ASHTON, C.H. (1999). Adverse effects of cannabis and cannabinoids. *Br J Anaesth*, **83,** 637-49.

ASHTON, C.H. (2001). Pharmacology and effects of cannabis: a brief review. *Br J Psychiatry*, **178,** 101-6.

ASHTON, J.C. (2007). Cannabinoids for the treatment of inflammation. *Curr Opin Investig Drugs*, **8,** 373-84.

BAGLIONI, C. (1979). Interferon-induced enzymatic actvities and their role in the antiviral state. *Cell*, **17,** 255-264.

BAKER, D., PRYCE, G., DAVIES, W.L. & HILEY, C.R. (2006). In silico patent searching reveals a new cannabinoid receptor. *Trends Pharmacol Sci*, **27,** 1-4.

BALERIO, G.N., ASO, E. & MALDONADO, R. (2006). Role of the cannabinoid system in the effects induced by nicotine on anxiety-like behaviour in mice. *Psychopharmacology (Berl)*, **184,** 504-13.

BANIN, S., MOYAL, L., SHIEH, S., TAYA, Y., ANDERSON, C.W., CHESSA, L., SMORODINSKY, N.I., PRIVES, C., REISS, Y., SHILOH, Y. & ZIV, Y. (1998). Enhanced phosphorylation of p53 by ATM in response to DNA damage. *Science*, **281,** 1674-7.

BASAVARAJAPPA, B.S., SAITO, M., COOPER, T.B. & HUNGUND, B.L. (2000). Stimulation of cannabinoid receptor agonist 2-arachidonylglycerol by chronic ethanol and its modulation by specific neuromodulators in cerebellar granule neurons. *Biochim Biophys Acta*, **1535,** 78-86.

BAUDELAIRE, C. (1860). *Les Paradis Artificiels*: Citadel.

BAYER, P., ARNDT, A., METZGER, S., MAHAJAN, R., MELCHIOR, F., JAENICKE, R. & BECKER, J. (1998). Structure determination of the small ubiquitin-related modifier SUMO-1. *J Mol Biol*, **280,** 275-86.

BEAUJOUIN, M., BAGHDIGUIAN, S., GLONDU-LASSIS, M., BERCHEM, G. & LIAUDET-

COOPMAN, E. (2006). Overexpression of both catalytically active and -inactive cathepsin D by cancer cells enhances apoptosis-dependent chemo-sensitivity. *Oncogene*, **25,** 1967-73.

BEGG, M., PACHER, P., BATKAI, S., OSEI-HYIAMAN, D., OFFERTALER, L., MO, F.M., LIU, J. & KUNOS, G. (2005). Evidence for novel cannabinoid receptors. *Pharmacol Ther*, **106,** 133-45.

BELTRAMO, M. & PIOMELLI, D. (2000). Carrier-mediated transport and enzymatic hydrolysis of the endogenous cannabinoid 2-arachidonylglycerol. *Neuroreport*, **11,** 1231-5.

BELTRAMO, M., STELLA, N., CALIGNANO, A., LIN, S.Y., MAKRIYANNIS, A. & PIOMELLI, D. (1997). Functional role of high-affinity anandamide transport, as revealed by selective inhibition. *Science*, **277,** 1094-7.

BENITO, C., NUNEZ, E., TOLON, R.M., CARRIER, E.J., RABANO, A., HILLARD, C.J. & ROMERO, J. (2003). Cannabinoid CB2 receptors and fatty acid amide hydrolase are selectively overexpressed in neuritic plaque-associated glia in Alzheimer's disease brains. *J Neurosci*, **23,** 11136-41.

BENITO, C., ROMERO, J.P., TOLON, R.M., CLEMENTE, D., DOCAGNE, F., HILLARD, C.J., GUAZA, C. & ROMERO, J. (2007). Cannabinoid CB1 and CB2 receptors and fatty acid amide hydrolase are specific markers of plaque cell subtypes in human multiple sclerosis. *J Neurosci*, **27,** 2396-402.

BENNETT, M., MACDONALD, K., CHAN, S.W., LUZIO, J.P., SIMARI, R. & WEISSBERG, P. (1998). Cell surface trafficking of Fas: a rapid mechanism of p53-mediated apoptosis. *Science*, **282,** 290-3.

BENOWITZ, L.I. & ROUTTENBERG, A. (1997). GAP-43: an intrinsic determinant of neuronal development and plasticity. *Trends Neurosci*, **20,** 84-91.

BERDYSHEV, E.V. (2000). Cannabinoid receptors and the regulation of immune response. *Chem Phys Lipids*, **108,** 169-90.

BERG, T., GJOEN, T. & BAKKE, O. (1995). Physiological functions of endosomal proteolysis. *Biochem J*, **307 (Pt 2),** 313-26.

BERGHUIS, P., DOBSZAY, M.B., WANG, X., SPANO, S., LEDDA, F., SOUSA, K.M., SCHULTE, G., ERNFORS, P., MACKIE, K., PARATCHA, G., HURD, Y.L. & HARKANY, T. (2005).

Endocannabinoids regulate interneuron migration and morphogenesis by transactivating the TrkB receptor. *Proc Natl Acad Sci U S A*, **102,** 19115-20.

BERGHUIS, P., RAJNICEK, A.M., MOROZOV, Y.M., ROSS, R.A., MULDER, J., URBAN, G.M., MONORY, K., MARSICANO, G., MATTEOLI, M., CANTY, A., IRVING, A.J., KATONA, I., YANAGAWA, Y., RAKIC, P., LUTZ, B., MACKIE, K. & HARKANY, T. (2007). Hardwiring the brain: endocannabinoids shape neuronal connectivity. *Science*, **316,** 1212-6.

BERNARD, C., MILH, M., MOROZOV, Y.M., BEN-ARI, Y., FREUND, T.F. & GOZLAN, H. (2005). Altering cannabinoid signaling during development disrupts neuronal activity. *Proc Natl Acad Sci U S A*, **102,** 9388-93.

BERRENDERO, F., SEPE, N., RAMOS, J.A., DI MARZO, V. & FERNANDEZ-RUIZ, J.J. (1999). Analysis of cannabinoid receptor binding and mRNA expression and endogenous cannabinoid contents in the developing rat brain during late gestation and early postnatal period. *Synapse*, **33,** 181-91.

BIDAUT-RUSSELL, M., DEVANE, W.A. & HOWLETT, A.C. (1990). Cannabinoid receptors and modulation of cyclic AMP accumulation in the rat brain. *J Neurochem*, **55,** 21-6.

BIDERE, N., LORENZO, H.K., CARMONA, S., LAFORGE, M., HARPER, F., DUMONT, C. & SENIK, A. (2003). Cathepsin D triggers Bax activation, resulting in selective apoptosis-inducing factor (AIF) relocation in T lymphocytes entering the early commitment phase to apoptosis. *J Biol Chem*, **278,** 31401-11.

BIEGON, A. & KERMAN, I.A. (2001). Autoradiographic study of pre- and postnatal distribution of cannabinoid receptors in human brain. *Neuroimage*, **14,** 1463-8.

BIFULCO, M., LAEZZA, C., PORTELLA, G., VITALE, M., ORLANDO, P., DE PETROCELLIS, L. & DI MARZO, V. (2001). Control by the endogenous cannabinoid system of ras oncogene-dependent tumor growth. *Faseb J*, **15,** 2745-7.

BILLON, N., TERRINONI, A., JOLICOEUR, C., MCCARTHY, A., RICHARDSON, W.D., MELINO, G. & RAFF, M. (2004). Roles for p53 and p73 during oligodendrocyte development. *Development*, **131,** 1211-20.

BISOGNO, T., LIGRESTI, A. & DI MARZO, V. (2005). The endocannabinoid signalling system: biochemical aspects. *Pharmacol Biochem Behav*, **81,** 224-38.

BISOGNO, T., MACCARRONE, M., DE PETROCELLIS, L., JARRAHIAN, A., FINAZZI-AGRO, A., HILLARD, C. & DI MARZO, V. (2001). The uptake by cells of 2-arachidonoylglycerol, an endogenous agonist of cannabinoid receptors. *Eur J Biochem*, **268,** 1982-9.

BISOGNO, T., MELCK, D., BOBROV, M., GRETSKAYA, N.M., BEZUGLOV, V.V., DE PETROCELLIS, L. & DI MARZO, V. (2000). N-acyl-dopamines: novel synthetic CB(1) cannabinoid-receptor ligands and inhibitors of anandamide inactivation with cannabimimetic activity in vitro and in vivo. *Biochem J*, **351 Pt 3,** 817-24.

BISOGNO, T., SEPE, N., MELCK, D., MAURELLI, S., DE PETROCELLIS, L. & DI MARZO, V. (1997). Biosynthesis, release and degradation of the novel endogenous cannabimimetic metabolite 2-arachidonoylglycerol in mouse neuroblastoma cells. *Biochem J*, **322 (Pt 2),** 671-7.

BLATT, N.B. & GLICK, G.D. (2001). Signaling pathways and effector mechanisms pre-programmed cell death. *Bioorg Med Chem*, **9,** 1371-84.

BLATTNER, C., TOBIASCH, E., LITFEN, M., RAHMSDORF, H.J. & HERRLICH, P. (1999). DNA damage induced p53 stabilization: no indication for an involvement of p53 phosphorylation. *Oncogene*, **18,** 1723-32.

BLAZQUEZ, C., GONZALEZ-FERIA, L., ALVAREZ, L., HARO, A., CASANOVA, M.L. & GUZMAN, M. (2004). Cannabinoids inhibit the vascular endothelial growth factor pathway in gliomas. *Cancer Res*, **64,** 5617-23.

BLOCK, R.I., FARINPOUR, R. & BRAVERMAN, K. (1992). Acute effects of marijuana on cognition: relationships to chronic effects and smoking techniques. *Pharmacol Biochem Behav*, **43,** 907-17.

BLOOM, A.S. & DEWEY, W.L. (1978). A comparison of some pharmacological actions of morphine and delta9-tetrahydrocannabinol in the mouse. *Psychopharmacology (Berl)*, **57,** 243-8.

BOAST, C.A., GERHARDT, S.C., PASTOR, G., LEHMANN, J., ETIENNE, P.E. & LIEBMAN, J.M. (1988). The N-methyl-D-aspartate antagonists CGS 19755 and CPP reduce ischemic brain damage in gerbils. *Brain Res*, **442,** 345-8.

BODDY, M.N., HOWE, K., ETKIN, L.D., SOLOMON, E. & FREEMONT, P.S. (1996). PIC 1, a novel ubiquitin-like protein which interacts with the PML component of a

multiprotein complex that is disrupted in acute promyelocytic leukaemia. *Oncogene*, **13,** 971-82.

BOLAND, B. & CAMPBELL, V. (2004). Abeta-mediated activation of the apoptotic cascade in cultured cortical neurones: a role for cathepsin-L. *Neurobiol Aging*, **25,** 83-91.

BONNEROT, C., BRIKEN, V., BRACHET, V., LANKAR, D., CASSARD, S., JABRI, B. & AMIGORENA, S. (1998). syk protein tyrosine kinase regulates Fc receptor gamma-chain-mediated transport to lysosomes. *Embo J*, **17,** 4606-16.

BONNY, C., OBERSON, A., NEGRI, S., SAUSER, C. & SCHORDERET, D.F. (2001). Cell-permeable peptide inhibitors of JNK: novel blockers of beta-cell death. *Diabetes*, **50,** 77-82.

BORSELLO, T., CLARKE, P.G., HIRT, L., VERCELLI, A., REPICI, M., SCHORDERET, D.F., BOGOUSSLAVSKY, J. & BONNY, C. (2003). A peptide inhibitor of c-Jun N-terminal kinase protects against excitotoxicity and cerebral ischemia. *Nat Med*, **9,** 1180-6.

BOSEL, J., GANDOR, F., HARMS, C., SYNOWITZ, M., HARMS, U., DJOUFACK, P.C., MEGOW, D., DIRNAGL, U., HORTNAGL, H., FINK, K.B. & ENDRES, M. (2005). Neuroprotective effects of atorvastatin against glutamate-induced excitotoxicity in primary cortical neurones. *J Neurochem*, **92,** 1386-98.

BOSSIS, G. & MELCHIOR, F. (2006). SUMO: regulating the regulator. *Cell Div*, **1,** 13.

BOUABOULA, M., BIANCHINI, L., MCKENZIE, F.R., POUYSSEGUR, J. & CASELLAS, P. (1999). Cannabinoid receptor CB1 activates the Na+/H+ exchanger NHE-1 isoform via Gi-mediated mitogen activated protein kinase signaling transduction pathways. *FEBS Lett*, **449,** 61-5.

BOUABOULA, M., POINOT-CHAZEL, C., BOURRIE, B., CANAT, X., CALANDRA, B., RINALDI-CARMONA, M., LE FUR, G. & CASELLAS, P. (1995). Activation of mitogen-activated protein kinases by stimulation of the central cannabinoid receptor CB1. *Biochem J*, **312 (Pt 2),** 637-41.

BOUABOULA, M., POINOT-CHAZEL, C., MARCHAND, J., CANAT, X., BOURRIE, B., RINALDI-CARMONA, M., CALANDRA, B., LE FUR, G. & CASELLAS, P. (1996). Signaling pathway associated with stimulation of CB2 peripheral cannabinoid receptor.

Involvement of both mitogen-activated protein kinase and induction of Krox-24 expression. *Eur J Biochem*, **237,** 704-11.

BOYA, P. & DE LA ROSA, E.J. (2005). Cell death in early neural life. *Birth Defects Res C Embryo Today*, **75,** 281-93.

BRADFORD, M. (1976). A rapid and sensitive method for the quantitation of microgram quantities of protein utilizing the principle of protein-dye binding. *Anal Biochem*, **7,** 248-254.

BRADSHAW, H. (2007). Other cannabimimetic lipid signalling molecules. In *Cannabinoids and the brain*. ed. K_ofalvi, A.: Springer-Verlag.

BREIVOGEL, C.S., GRIFFIN, G., DI MARZO, V. & MARTIN, B.R. (2001). Evidence for a new G protein-coupled cannabinoid receptor in mouse brain. *Mol Pharmacol*, **60,** 155-63.

BRETAUD, S., ALLEN, C., INGHAM, P.W. & BANDMANN, O. (2007). p53-dependent neuronal cell death in a DJ-1-deficient zebrafish model of Parkinson's disease. *J Neurochem*, **100,** 1626-35.

BRITTON, R.S. & MELLORS, A. (1974). Lysis of rat liver lysosomes in vitro by delta9-tetrahydrocannabinol. *Biochem Pharmacol*, **23,** 1342-4.

BROWN AJ, UENO S, SUEN K, DOWELL SJ & A, W. (2005). Molecular indentification of GPR55 as a third G protein-coupled receptor responsive to cannabinoid ligands. In *Symposium on the cannabinoids* pp. p 16 Burlington, Vermont, USA.: International Cannabinoid Research Society.

BROWN AJ & WISE A (2001). Indentification of modulators of GPR55 activity. Patent number, *WO/2001/086305*.
http://www.wipo.int/pctdb/en/wo.jsp?wo=2001086305

BROWN, S.M., WAGER-MILLER, J. & MACKIE, K. (2002). Cloning and molecular characterization of the rat CB2 cannabinoid receptor. *Biochim Biophys Acta*, **1576,** 255-64.

BRUMELL, J.H., BURKHARDT, A.L., BOLEN, J.B. & GRINSTEIN, S. (1996). Endogenous reactive oxygen intermediates activate tyrosine kinases in human neutrophils. *J Biol Chem*, **271,** 1455-61.

BRUNK, U.T. (2000). Lysosomotropic detergents induce time- and dose-dependent

apoptosis/necrosis in cultured cells. *Redox Rep*, **5,** 87-8.

BRUNK, U.T., NEUZIL, J. & EATON, J.W. (2001). Lysosomal involvement in apoptosis. *Redox Rep*, **6,** 91-7.

BURSCH, W. (2001). The autophagosomal-lysosomal compartment in programmed cell death. *Cell Death Differ*, **8,** 569-81.

BURSTEIN, S. (2005). PPAR-gamma: a nuclear receptor with affinity for cannabinoids. *Life Sci*, **77,** 1674-84.

BURSTEIN, S.H. & HUNTER, S.A. (1995). Stimulation of anandamide biosynthesis in N-18TG2 neuroblastoma cells by delta 9-tetrahydrocannabinol (THC). *Biochem Pharmacol*, **49,** 855-8.

BUSCHMANN, T., POTAPOVA, O., BAR-SHIRA, A., IVANOV, V.N., FUCHS, S.Y., HENDERSON, S., FRIED, V.A., MINAMOTO, T., ALARCON-VARGAS, D., PINCUS, M.R., GAARDE, W.A., HOLBROOK, N.J., SHILOH, Y. & RONAI, Z. (2001). Jun NH2-terminal kinase phosphorylation of p53 on Thr-81 is important for p53 stabilization and transcriptional activities in response to stress. *Mol Cell Biol*, **21,** 2743-54.

CAHILLY-SNYDER, L., YANG-FENG, T., FRANCKE, U. & GEORGE, D.L. (1987). Molecular analysis and chromosomal mapping of amplified genes isolated from a transformed mouse 3T3 cell line. *Somat Cell Mol Genet*, **13,** 235-44.

CAIN, K. (2003). Chemical-induced apoptosis: formation of the Apaf-1 apoptosome. *Drug Metab Rev*, **35,** 337-63.

CAMPBELL, V.A. (2001). Tetrahydrocannabinol-induced apoptosis of cultured cortical neurones is associated with cytochrome c release and caspase-3 activation. *Neuropharmacology*, **40,** 702-9.

CAMPBELL, V.A. & GOWRAN, A. (2007). Alzheimer's disease; taking the edge off with cannabinoids? *Br J Pharmacol*.

CAPLEN, N.J., PARRISH, S., IMANI, F., FIRE, A. & MORGAN, R.A. (2001). Specific inhibition of gene expression by small double-stranded RNAs in invertebrate and vertebrate systems. *Proc Natl Acad Sci U S A*, **98,** 9742-7.

CARRIBA, P., ORTIZ, O., PATKAR, K., JUSTINOVA, Z., STROIK, J., THEMANN, A., MULLER, C., WOODS, A.S., HOPE, B.T., CIRUELA, F., CASADO, V., CANELA, E.I., LLUIS, C., GOLDBERG, S.R., MORATALLA, R., FRANCO, R. & FERRE, S. (2007). Striatal

Adenosine A(2A) and Cannabinoid CB(1) Receptors Form Functional Heteromeric Complexes that Mediate the Motor Effects of Cannabinoids. *Neuropsychopharmacology*.

CARTER, S., BISCHOF, O., DEJEAN, A. & VOUSDEN, K.H. (2007). C-terminal modifications regulate MDM2 dissociation and nuclear export of p53. *Nat Cell Biol*, **9,** 428-35.

CASCIOLA-ROSEN, L., NICHOLSON, D.W., CHONG, T., ROWAN, K.R., THORNBERRY, N.A., MILLER, D.K. & ROSEN, A. (1996). Apopain/CPP32 cleaves proteins that are essential for cellular repair: a fundamental principle of apoptotic death. *J Exp Med*, **183,** 1957-64.

CATERINA, M.J. & JULIUS, D. (2001). The vanilloid receptor: a molecular gateway to the pain pathway. *Annu Rev Neurosci*, **24,** 487-517.

CHAIT, L.D. & PERRY, J.L. (1994). Acute and residual effects of alcohol and marijuana, alone and in combination, on mood and performance. *Psychopharmacology (Berl)*, **115,** 340-9.

CHAKRABARTI, B., KENT, L., SUCKLING, J., BULLMORE, E. & BARON-COHEN, S. (2006). Variations in the human cannabinoid receptor (CNR1) gene modulate striatal responses to happy faces. *Eur J Neurosci*, **23,** 1944-8.

CHAN, G.C., HINDS, T.R., IMPEY, S. & STORM, D.R. (1998). Hippocampal neurotoxicity of Delta9-tetrahydrocannabinol. *J Neurosci*, **18,** 5322-32.

CHAN, P.C., SILLS, R.C., BRAUN, A.G., HASEMAN, J.K. & BUCHER, J.R. (1996). Toxicity and carcinogenicity of delta 9-tetrahydrocannabinol in Fischer rats and B6C3F1 mice. *Fundam Appl Toxicol*, **30,** 109-17.

CHAN, T.A., CHU, C.A., RAUEN, K.A., KROIHER, M., TATAREWICZ, S.M. & STEELE, R.E. (1994). Identification of a gene encoding a novel protein-tyrosine kinase containing SH2 domains and ankyrin-like repeats. *Oncogene*, **9,** 1253-9.

CHEER, J.F., CADOGAN, A.K., MARSDEN, C.A., FONE, K.C. & KENDALL, D.A. (1999). Modification of 5-HT2 receptor mediated behaviour in the rat by oleamide and the role of cannabinoid receptors. *Neuropharmacology*, **38,** 533-41.

CHEN, C.S., CHEN, W.N., ZHOU, M., ARTTAMANGKUL, S. & HAUGLAND, R.P. (2000). Probing the cathepsin D using a BODIPY FL-pepstatin A: applications in

fluorescence polarization and microscopy. *J Biochem Biophys Methods*, **42,** 137-51.

CHEN, L. & CHEN, J. (2003). MDM2-ARF complex regulates p53 sumoylation. *Oncogene*, **22,** 5348-57.

CHEN, R.W., QIN, Z.H., REN, M., KANAI, H., CHALECKA-FRANASZEK, E., LEEDS, P. & CHUANG, D.M. (2003). Regulation of c-Jun N-terminal kinase, p38 kinase and AP-1 DNA binding in cultured brain neurons: roles in glutamate excitotoxicity and lithium neuroprotection. *J Neurochem*, **84,** 566-75.

CHEVALEYRE, V., TAKAHASHI, K.A. & CASTILLO, P.E. (2006). Endocannabinoid-mediated synaptic plasticity in the CNS. *Annu Rev Neurosci*, **29,** 37-76.

CHIANG, C.W. & BARNETT, G. (1984). Marijuana effect and delta-9-tetrahydrocannabinol plasma level. *Clin Pharmacol Ther*, **36,** 234-8.

CHIPUK, J.E. & GREEN, D.R. (2003). p53's believe it or not: lessons on transcription-independent death. *J Clin Immunol*, **23,** 355-61.

CHIPUK, J.E., MAURER, U., GREEN, D.R. & SCHULER, M. (2003). Pharmacologic activation of p53 elicits Bax-dependent apoptosis in the absence of transcription. *Cancer Cell*, **4,** 371-81.

CHRISTOPOULOS, A. & WILSON, K. (2001). Interaction of anandamide with the M(1) and M(4) muscarinic acetylcholine receptors. *Brain Res*, **915,** 70-8.

CHWIERALSKI, C.E., WELTE, T. & BUHLING, F. (2006). Cathepsin-regulated apoptosis. *Apoptosis*, **11,** 143-9.

CIRMAN, T., ORESIC, K., MAZOVEC, G.D., TURK, V., REED, J.C., MYERS, R.M., SALVESEN, G.S. & TURK, B. (2004). Selective disruption of lysosomes in HeLa cells triggers apoptosis mediated by cleavage of Bid by multiple papain-like lysosomal cathepsins. *J Biol Chem*, **279,** 3578-87.

CLARKE, R. (1981). *Marijuana botany*. Berkeley, CA: Ronin publishing.

CLAUS, V., JAHRAUS, A., TJELLE, T., BERG, T., KIRSCHKE, H., FAULSTICH, H. & GRIFFITHS, G. (1998). Lysosomal enzyme trafficking between phagosomes, endosomes, and lysosomes in J774 macrophages. Enrichment of cathepsin H in early endosomes. *J Biol Chem*, **273,** 9842-51.

COMBS, C.K., JOHNSON, D.E., CANNADY, S.B., LEHMAN, T.M. & LANDRETH, G.E. (1999).

Identification of microglial signal transduction pathways mediating a neurotoxic response to amyloidogenic fragments of beta-amyloid and prion proteins. *J Neurosci*, **19,** 928-39.

COMBS, C.K., KARLO, J.C., KAO, S.C. & LANDRETH, G.E. (2001). beta-Amyloid stimulation of microglia and monocytes results in TNFalpha-dependent expression of inducible nitric oxide synthase and neuronal apoptosis. *J Neurosci*, **21,** 1179-88.

CONTASSOT, E., TENAN, M., SCHNURIGER, V., PELTE, M.F. & DIETRICH, P.Y. (2004). Arachidonyl ethanolamide induces apoptosis of uterine cervix cancer cells via aberrantly expressed vanilloid receptor-1. *Gynecol Oncol*, **93,** 182-8.

COOPMAN, P.J., DO, M.T., BARTH, M., BOWDEN, E.T., HAYES, A.J., BASYUK, E., BLANCATO, J.K., VEZZA, P.R., MCLESKEY, S.W., MANGEAT, P.H. & MUELLER, S.C. (2000). The Syk tyrosine kinase suppresses malignant growth of human breast cancer cells. *Nature*, **406,** 742-7.

COOPMAN, P.J. & MUELLER, S.C. (2006). The Syk tyrosine kinase: a new negative regulator in tumor growth and progression. *Cancer Lett*, **241,** 159-73.

COURT, J.M. (1998). Cannabis and brain function. *J Paediatr Child Health*, **34,** 1-5.

COUSSEN, F. & CHOQUET, D. (2007). Neuroscience: wrestling with SUMO. *Nature*, **447,** 271-2.

CRAVATT, B.F., GIANG, D.K., MAYFIELD, S.P., BOGER, D.L., LERNER, R.A. & GILULA, N.B. (1996). Molecular characterization of an enzyme that degrades neuromodulatory fatty-acid amides. *Nature*, **384,** 83-7.

CRISTINO, L., DE PETROCELLIS, L., PRYCE, G., BAKER, D., GUGLIELMOTTI, V. & DI MARZO, V. (2006). Immunohistochemical localization of cannabinoid type 1 and vanilloid transient receptor potential vanilloid type 1 receptors in the mouse brain. *Neuroscience*, **139,** 1405-15.

CULMSEE, C. & MATTSON, M.P. (2005). p53 in neuronal apoptosis. *Biochem Biophys Res Commun*, **331,** 761-77.

CULMSEE, C., SIEWE, J., JUNKER, V., RETIOUNSKAIA, M., SCHWARZ, S., CAMANDOLA, S., EL-METAINY, S., BEHNKE, H., MATTSON, M.P. & KRIEGLSTEIN, J. (2003). Reciprocal inhibition of p53 and nuclear factor-kappaB transcriptional activities determines

cell survival or death in neurons. *J Neurosci*, **23,** 8586-95.

CULMSEE, C., ZHU, X., YU, Q.S., CHAN, S.L., CAMANDOLA, S., GUO, Z., GREIG, N.H. & MATTSON, M.P. (2001). A synthetic inhibitor of p53 protects neurons against death induced by ischemic and excitotoxic insults, and amyloid beta-peptide. *J Neurochem*, **77,** 220-8.

D'AMBRA, T.E., ESTEP, K.G., BELL, M.R., EISSENSTAT, M.A., JOSEF, K.A., WARD, S.J., HAYCOCK, D.A., BAIZMAN, E.R., CASIANO, F.M., BEGLIN, N.C. & ET AL. (1992). Conformationally restrained analogues of pravadoline: nanomolar potent, enantioselective, (aminoalkyl)indole agonists of the cannabinoid receptor. *J Med Chem*, **35,** 124-35.

D'AMICO, M., CANNIZZARO, C., PREZIOSI, P. & MARTIRE, M. (2004). Inhibition by anandamide and synthetic cannabimimetics of the release of [3H]D-aspartate and [3H]GABA from synaptosomes isolated from the rat hippocampus. *Neurochem Res*, **29,** 1553-61.

DATTA, R., BANACH, D., KOJIMA, H., TALANIAN, R.V., ALNEMRI, E.S., WONG, W.W. & KUFE, D.W. (1996). Activation of the CPP32 protease in apoptosis induced by 1-beta-D-arabinofuranosylcytosine and other DNA-damaging agents. *Blood*, **88,** 1936-43.

DAVIES, P., SORNBERGER, G.C. & HUBER, G.L. (1979). Effects of experimental marijuana and tobacco smoke inhalation on alveolar macrophages. A comparative stereologic study. *Lab Invest*, **41,** 220-3.

DAVITIAN, C., UZAN, M., TIGAIZIN, A., DUCARME, G., DAUPHIN, H. & PONCELET, C. (2006). [Maternal cannabis use and intra-uterine growth restriction]. *Gynecol Obstet Fertil*, **34,** 632-7.

DE DUVE, C. (1970). The role of lysosomes in cellular pathology. *Triangle*, **9,** 200-8.

DE LA MONTE, S.M., TONG, M., LESTER-COLL, N., PLATER, M., JR. & WANDS, J.R. (2006). Therapeutic rescue of neurodegeneration in experimental type 3 diabetes: relevance to Alzheimer's disease. *J Alzheimers Dis*, **10,** 89-109.

DE LAGO, E., PETROSINO, S., VALENTI, M., MORERA, E., ORTEGA-GUTIERREZ, S., FERNANDEZ-RUIZ, J. & DI MARZO, V. (2005). Effect of repeated systemic administration of selective inhibitors of endocannabinoid inactivation on rat

brain endocannabinoid levels. *Biochem Pharmacol*, **70,** 446-52.

DE PETROCELLIS, L., BISOGNO, T., MACCARRONE, M., DAVIS, J.B., FINAZZI-AGRO, A. & DI MARZO, V. (2001). The activity of anandamide at vanilloid VR1 receptors requires facilitated transport across the cell membrane and is limited by intracellular metabolism. *J Biol Chem*, **276,** 12856-63.

DE PETROCELLIS, L., MELCK, D., PALMISANO, A., BISOGNO, T., LAEZZA, C., BIFULCO, M. & DI MARZO, V. (1998). The endogenous cannabinoid anandamide inhibits human breast cancer cell proliferation. *Proc Natl Acad Sci U S A*, **95,** 8375-80.

DEADWYLER, S.A., HAMPSON, R.E., MU, J., WHYTE, A. & CHILDERS, S. (1995). Cannabinoids modulate voltage sensitive potassium A-current in hippocampal neurons via a cAMP-dependent process. *J Pharmacol Exp Ther*, **273,** 734-43.

DECKER, P. & MULLER, S. (2002). Modulating poly (ADP-ribose) polymerase activity: potential for the prevention and therapy of pathogenic situations involving DNA damage and oxidative stress. *Curr Pharm Biotechnol*, **3,** 275-83.

DEMUTH, D.G. & MOLLEMAN, A. (2006). Cannabinoid signalling. *Life Sci*, **78,** 549-63.

DENNEDY, M.C., FRIEL, A.M., HOULIHAN, D.D., BRODERICK, V.M., SMITH, T. & MORRISON, J.J. (2004). Cannabinoids and the human uterus during pregnancy. *Am J Obstet Gynecol*, **190,** 2-9; discussion 3A.

DERKINDEREN, P., LEDENT, C., PARMENTIER, M. & GIRAULT, J.A. (2001). Cannabinoids activate p38 mitogen-activated protein kinases through CB1 receptors in hippocampus. *J Neurochem*, **77,** 957-60.

DERKINDEREN, P., TOUTANT, M., BURGAYA, F., LE BERT, M., SICILIANO, J.C., DE FRANCISCIS, V., GELMAN, M. & GIRAULT, J.A. (1996). Regulation of a neuronal form of focal adhesion kinase by anandamide. *Science*, **273,** 1719-22.

DERKINDEREN, P., TOUTANT, M., KADARE, G., LEDENT, C., PARMENTIER, M. & GIRAULT, J.A. (2001). Dual role of Fyn in the regulation of FAK+6,7 by cannabinoids in hippocampus. *J Biol Chem*, **276,** 38289-96.

DERKINDEREN, P., VALJENT, E., TOUTANT, M., CORVOL, J.C., ENSLEN, H., LEDENT, C., TRZASKOS, J., CABOCHE, J. & GIRAULT, J.A. (2003). Regulation of extracellular signal-regulated kinase by cannabinoids in hippocampus. *J Neurosci*, **23,** 2371-82.

DESTERRO, J.M., RODRIGUEZ, M.S. & HAY, R.T. (1998). SUMO-1 modification of IkappaBalpha inhibits NF-kappaB activation. *Mol Cell*, **2,** 233-9.

DESTERRO, J.M., RODRIGUEZ, M.S. & HAY, R.T. (1998). SUMO-1 modification of IkappaBalpha inhibits NF-kappaB activation. *Mol Cell*, **2,** 233-9.

DEUTSCH, D.G. & CHIN, S.A. (1993). Enzymatic synthesis and degradation of anandamide, a cannabinoid receptor agonist. *Biochem Pharmacol*, **46,** 791-6.

DEUTSCH, D.G., GLASER, S.T., HOWELL, J.M., KUNZ, J.S., PUFFENBARGER, R.A., HILLARD, C.J. & ABUMRAD, N. (2001). The cellular uptake of anandamide is coupled to its breakdown by fatty-acid amide hydrolase. *J Biol Chem*, **276,** 6967-73.

DEVANE, W.A., HANUS, L., BREUER, A., PERTWEE, R.G., STEVENSON, L.A., GRIFFIN, G., GIBSON, D., MANDELBAUM, A., ETINGER, A. & MECHOULAM, R. (1992). Isolation and structure of a brain constituent that binds to the cannabinoid receptor. *Science*, **258,** 1946-9.

DI GIOVANNI, S., KNIGHTS, C.D., RAO, M., YAKOVLEV, A., BEERS, J., CATANIA, J., AVANTAGGIATI, M.L. & FADEN, A.I. (2006). The tumor suppressor protein p53 is required for neurite outgrowth and axon regeneration. *Embo J*, **25,** 4084-96.

DI MARZO, V. (1998). 'Endocannabinoids' and other fatty acid derivatives with cannabimimetic properties: biochemistry and possible physiopathological relevance. *Biochim Biophys Acta*, **1392,** 153-75.

DI MARZO, V., BISOGNO, T. & DE PETROCELLIS, L. (2001). Anandamide: some like it hot. *Trends Pharmacol Sci*, **22,** 346-9.

DI MARZO, V., BISOGNO, T., DE PETROCELLIS, L., MELCK, D., ORLANDO, P., WAGNER, J.A. & KUNOS, G. (1999). Biosynthesis and inactivation of the endocannabinoid 2-arachidonoylglycerol in circulating and tumoral macrophages. *Eur J Biochem*, **264,** 258-67.

DI MARZO, V., BISOGNO, T., SUGIURA, T., MELCK, D. & DE PETROCELLIS, L. (1998). The novel endogenous cannabinoid 2-arachidonoylglycerol is inactivated by neuronal- and basophil-like cells: connections with anandamide. *Biochem J*, **331 (Pt 1),** 15-9.

DI MARZO, V., FONTANA, A., CADAS, H., SCHINELLI, S., CIMINO, G., SCHWARTZ, J.C. & PIOMELLI, D. (1994). Formation and inactivation of endogenous cannabinoid

anandamide in central neurons. *Nature*, **372,** 686-91.

DIANA, M.A. & MARTY, A. (2004). Endocannabinoid-mediated short-term synaptic plasticity: depolarization-induced suppression of inhibition (DSI) and depolarization-induced suppression of excitation (DSE). *Br J Pharmacol*, **142,** 9-19.

DICKENSON, A.H. & DRAY, A. (1991). Selective antagonism of capsaicin by capsazepine: evidence for a spinal receptor site in capsaicin-induced antinociception. *Br J Pharmacol*, **104,** 1045-9.

DING, J., TAKANO, T., GAO, S., HAN, W., NODA, C., YANAGI, S. & YAMAMURA, H. (2000). Syk is required for the activation of Akt survival pathway in B cells exposed to oxidative stress. *J Biol Chem*, **275,** 30873-7.

DINH, T.P., CARPENTER, D., LESLIE, F.M., FREUND, T.F., KATONA, I., SENSI, S.L., KATHURIA, S. & PIOMELLI, D. (2002). Brain monoglyceride lipase participating in endocannabinoid inactivation. *Proc Natl Acad Sci U S A*, **99,** 10819-24.

DINH, T.P., FREUND, T.F. & PIOMELLI, D. (2002). A role for monoglyceride lipase in 2-arachidonoylglycerol inactivation. *Chem Phys Lipids*, **121,** 149-58.

DITARANTO-DESIMONE, K., SAITO, M., TEKIRIAN, T.L., SAITO, M., BERG, M., DUBOWCHIK, G., SOREGHAN, B., THOMAS, S., MARKS, N. & YANG, A.J. (2003). Neuronal endosomal/lysosomal membrane destabilization activates caspases and induces abnormal accumulation of the lipid secondary messenger ceramide. *Brain Res Bull*, **59,** 523-31.

DO, Y., MCKALLIP, R.J., NAGARKATTI, M. & NAGARKATTI, P.S. (2004). Activation through cannabinoid receptors 1 and 2 on dendritic cells triggers NF-kappaB-dependent apoptosis: novel role for endogenous and exogenous cannabinoids in immunoregulation. *J Immunol*, **173,** 2373-82.

DOCAGNE, F., MUNETON, V., CLEMENTE, D., ALI, C., LORIA, F., CORREA, F., HERNANGOMEZ, M., MESTRE, L., VIVIEN, D. & GUAZA, C. (2007). Excitotoxicity in a chronic model of multiple sclerosis: Neuroprotective effects of cannabinoids through CB1 and CB2 receptor activation. *Mol Cell Neurosci*, **34,** 551-61.

DONG, H., GOICO, B., MARTIN, M., CSERNANSKY, C.A., BERTCHUME, A. & CSERNANSKY, J.G. (2004). Modulation of hippocampal cell proliferation, memory, and

amyloid plaque deposition in APPsw (Tg2576) mutant mice by isolation stress. *Neuroscience*, **127,** 601-9.

DORVAL, V. & FRASER, P.E. (2007). SUMO on the road to neurodegeneration. *Biochim Biophys Acta*, **1773,** 694-706.

DORVAL, V., MAZZELLA, M.J., MATHEWS, P.M., HAY, R.T. & FRASER, P.E. (2007). Modulation of Abeta generation by small ubiquitin-like modifiers does not require conjugation to target proteins. *Biochem J*, **404,** 309-16.

DOWNER, E., BOLAND, B., FOGARTY, M. & CAMPBELL, V. (2001). Delta 9-tetrahydrocannabinol induces the apoptotic pathway in cultured cortical neurones via activation of the CB1 receptor. *Neuroreport*, **12,** 3973-8.

DOWNER, E.J., FOGARTY, M.P. & CAMPBELL, V.A. (2003). Tetrahydrocannabinol-induced neurotoxicity depends on CB1 receptor-mediated c-Jun N-terminal kinase activation in cultured cortical neurons. *Br J Pharmacol*, **140,** 547-57.

DOWNER, E.J., GOWRAN, A. & CAMPBELL, V.A. (2007). A comparison of the apoptotic effect of Delta(9)-tetrahydrocannabinol in the neonatal and adult rat cerebral cortex. *Brain Res.*

DOWNER, E.J., GOWRAN, A., MURPHY, A.C. & CAMPBELL, V.A. (2007). The tumour suppressor protein, p53, is involved in the activation of the apoptotic cascade by Delta9-tetrahydrocannabinol in cultured cortical neurons. *Eur J Pharmacol*, **564,** 57-65.

DROMOTA T, GREASLEY P & T, G. (2004). Screening assays for cannabinoid-lingand type modulators of GPR55. Patent number, WO/2004/074844. http://www.wipo.int/pctdb/en/wo.jsp?wo=200407844

DUAN, W., ZHU, X., LADENHEIM, B., YU, Q.S., GUO, Z., OYLER, J., CUTLER, R.G., CADET, J.L., GREIG, N.H. & MATTSON, M.P. (2002). p53 inhibitors preserve dopamine neurons and motor function in experimental parkinsonism. *Ann Neurol*, **52,** 597-606.

DUDKINA, A.S. & LINDSLEY, C.W. (2007). Small molecule protein-protein inhibitors for the p53-MDM2 interaction. *Curr Top Med Chem*, **7,** 952-60.

DUNN, W.A., JR. (1994). Autophagy and related mechanisms of lysosome-mediated protein degradation. *Trends Cell Biol*, **4,** 139-43.

EARNSHAW, W.C., MARTINS, L.M. & KAUFMANN, S.H. (1999). Mammalian caspases: structure, activation, substrates, and functions during apoptosis. *Annu Rev Biochem*, **68,** 383-424.

EHEHALT, R., FULLEKRUG, J., POHL, J., RING, A., HERRMANN, T. & STREMMEL, W. (2006). Translocation of long chain fatty acids across the plasma membrane--lipid rafts and fatty acid transport proteins. *Mol Cell Biochem*, **284,** 135-40.

EHRHART, J., OBREGON, D., MORI, T., HOU, H., SUN, N., BAI, Y., KLEIN, T., FERNANDEZ, F., TAN, J. & SHYTLE, R.D. (2005). Stimulation of cannabinoid receptor 2 (CB2) suppresses microglial activation. *J Neuroinflammation*, **2,** 29.

EIZENBERG, O., FABER-ELMAN, A., GOTTLIEB, E., OREN, M., ROTTER, V. & SCHWARTZ, M. (1996). p53 plays a regulatory role in differentiation and apoptosis of central nervous system-associated cells. *Mol Cell Biol*, **16,** 5178-85.

ELBASHIR, S.M., HARBORTH, J., LENDECKEL, W., YALCIN, A., WEBER, K. & TUSCHL, T. (2001). Duplexes of 21-nucleotide RNAs mediate RNA interference in cultured mammalian cells. *Nature*, **411,** 494-8.

ELKELES, A., JUVEN-GERSHON, T., ISRAELI, D., WILDER, S., ZALCENSTEIN, A. & OREN, M. (1999). The c-fos proto-oncogene is a target for transactivation by the p53 tumor suppressor. *Mol Cell Biol*, **19,** 2594-600.

EMERY, D.L., ROYO, N.C., FISCHER, I., SAATMAN, K.E. & MCINTOSH, T.K. (2003). Plasticity following injury to the adult central nervous system: is recapitulation of a developmental state worth promoting? *J Neurotrauma*, **20,** 1271-92.

EMRICH, H.M., LEWEKE, F.M. & SCHNEIDER, U. (1997). Towards a cannabinoid hypothesis of schizophrenia: cognitive impairments due to dysregulation of the endogenous cannabinoid system. *Pharmacol Biochem Behav*, **56,** 803-7.

ENOKIDO, Y., ARAKI, T., TANAKA, K., AIZAWA, S. & HATANAKA, H. (1996). Involvement of p53 in DNA strand break-induced apoptosis in postmitotic CNS neurons. *Eur J Neurosci*, **8,** 1812-21.

ESHHAR, N., STRIEM, S. & BIEGON, A. (1993). HU-211, a non-psychotropic cannabinoid, rescues cortical neurones from excitatory amino acid toxicity in culture. *Neuroreport*, **5,** 237-40.

ESPOSITO, G., DE FILIPPIS, D., MAIURI, M.C., DE STEFANO, D., CARNUCCIO, R. & IUVONE, T.

(2006). Cannabidiol inhibits inducible nitric oxide synthase protein expression and nitric oxide production in beta-amyloid stimulated PC12 neurons through p38 MAP kinase and NF-kappaB involvement. *Neurosci Lett*, **399,** 91-5.

EVAN, G. & LITTLEWOOD, T. (1998). A matter of life and cell death. *Science*, **281,** 1317-22.

EVERETT, R.D., LOMONTE, P., STERNSDORF, T., VAN DRIEL, R. & ORR, A. (1999). Cell cycle regulation of PML modification and ND10 composition. *J Cell Sci*, **112 (Pt 24),** 4581-8.

FACCHINETTI, F., DEL GIUDICE, E., FUREGATO, S., PASSAROTTO, M. & LEON, A. (2003). Cannabinoids ablate release of TNFalpha in rat microglial cells stimulated with lypopolysaccharide. *Glia*, **41,** 161-8.

FADEN, V.B. & GRAUBARD, B.I. (2000). Maternal substance use during pregnancy and developmental outcome at age three. *J Subst Abuse*, **12,** 329-40.

FAKHARZADEH, S.S., TRUSKO, S.P. & GEORGE, D.L. (1991). Tumorigenic potential associated with enhanced expression of a gene that is amplified in a mouse tumor cell line. *Embo J*, **10,** 1565-9.

FANG, S., JENSEN, J.P., LUDWIG, R.L., VOUSDEN, K.H. & WEISSMAN, A.M. (2000). Mdm2 is a RING finger-dependent ubiquitin protein ligase for itself and p53. *J Biol Chem*, **275,** 8945-51.

FARAONIO, R., VERGARA, P., DI MARZO, D., PIERANTONI, M.G., NAPOLITANO, M., RUSSO, T. & CIMINO, F. (2006). p53 suppresses the Nrf2-dependent transcription of antioxidant response genes. *J Biol Chem*, **281,** 39776-84.

FEHRENBACHER, N. & JAATTELA, M. (2005). Lysosomes as targets for cancer therapy. *Cancer Res*, **65,** 2993-5.

FELDER, C.C., BRILEY, E.M., AXELROD, J., SIMPSON, J.T., MACKIE, K. & DEVANE, W.A. (1993). Anandamide, an endogenous cannabimimetic eicosanoid, binds to the cloned human cannabinoid receptor and stimulates receptor-mediated signal transduction. *Proc Natl Acad Sci U S A*, **90,** 7656-60.

FELDER, C.C., BRILEY, E.M., AXELROD, J., SIMPSON, J.T., MACKIE, K. & DEVANE, W.A. (1993). Anandamide, an endogenous cannabimimetic eicosanoid, binds to the cloned human cannabinoid receptor and stimulates receptor-mediated signal

transduction. *Proc Natl Acad Sci U S A*, **90,** 7656-60.

FELDER, C.C., JOYCE, K.E., BRILEY, E.M., MANSOURI, J., MACKIE, K., BLOND, O., LAI, Y., MA, A.L. & MITCHELL, R.L. (1995). Comparison of the pharmacology and signal transduction of the human cannabinoid CB1 and CB2 receptors. *Mol Pharmacol*, **48,** 443-50.

FELDER, C.C., NIELSEN, A., BRILEY, E.M., PALKOVITS, M., PRILLER, J., AXELROD, J., NGUYEN, D.N., RICHARDSON, J.M., RIGGIN, R.M., KOPPEL, G.A., PAUL, S.M. & BECKER, G.W. (1996). Isolation and measurement of the endogenous cannabinoid receptor agonist, anandamide, in brain and peripheral tissues of human and rat. *FEBS Lett*, **393,** 231-5.

FERNANDEZ-RUIZ, J., BERRENDERO, F., HERNANDEZ, M.L. & RAMOS, J.A. (2000). The endogenous cannabinoid system and brain development. *Trends Neurosci*, **23,** 14-20.

FERNANDEZ-RUIZ, J., ROMERO, J., VELASCO, G., TOLON, R.M., RAMOS, J.A. & GUZMAN, M. (2007). Cannabinoid CB2 receptor: a new target for controlling neural cell survival? *Trends Pharmacol Sci*, **28,** 39-45.

FERNANDEZ-RUIZ, J.J., RAMOS, J.A., GARCIA-PALOMERO, E., GARCIA-GIL, L. & ROMERO, J. (1996). *Dopaminergic neurons as neurochemical substrates of neurobehavioural effects of marihuana: developmental and adult studies*: CYM Press.

FERNANDEZ-RUIZ, J.R.M.C.A.B.J. (1994). *Ontogenic and adult changes in the activity of the hypothalamic and extrahypothalamic dopaminergic neurons after perinatal cannabinoid exposure.*: Farranad Press.

FERNANDEZ-RUIZ, J.R.M.N.F.R.D.F.J. (1992). *Maternal cannabinoid exposure and brain development: changes in the ontogeny of dopaminergic neurons*: CRC Press.

FERNáNDEZ-RUIZ, R.J.N.M.R.D.F.F.J. (1992). *Maternal cannabinoid exposure and brain development: changes in the ontogeny of dopaminergic neurons.* : CRC Press.

FIELD, E. & TYREY, L. (1990). Delayed sexual maturation during prepubertal cannabinoid treatment: importance of the timing of treatment. *J Pharmacol Exp Ther*, **254,** 171-5.

FINN, D.P., JHAVERI, M.D., BECKETT, S.R., KENDALL, D.A., MARSDEN, C.A. & CHAPMAN,

V. (2004). Cannabinoids modulate ultrasound-induced aversive responses in rats. *Psychopharmacology (Berl)*, **172,** 41-51.

FIRE, A., XU, S., MONTGOMERY, M.K., KOSTAS, S.A., DRIVER, S.E. & MELLO, C.C. (1998). Potent and specific genetic interference by double-stranded RNA in Caenorhabditis elegans. *Nature*, **391,** 806-11.

FOGARTY, M.P., DOWNER, E.J. & CAMPBELL, V. (2003). A role for c-Jun N-terminal kinase 1 (JNK1), but not JNK2, in the beta-amyloid-mediated stabilization of protein p53 and induction of the apoptotic cascade in cultured cortical neurons. *Biochem J*, **371,** 789-98.

FOWLER, L.T.J. (2007). Removal of endocannabinoids by the body - mechanisms and therapeutic possibilities. In *Cannabinoids and the brain.* ed. Kofalvi, A.: Springer-Verlag.

FREUND, T.F., KATONA, I. & PIOMELLI, D. (2003). Role of endogenous cannabinoids in synaptic signaling. *Physiol Rev*, **83,** 1017-66.

FRIDE, E., BREGMAN, T. & KIRKHAM, T.C. (2005). Endocannabinoids and food intake: newborn suckling and appetite regulation in adulthood. *Exp Biol Med (Maywood)*, **230,** 225-34.

FRIDE, E., FOOX, A., ROSENBERG, E., FAIGENBOIM, M., COHEN, V., BARDA, L., BLAU, H. & MECHOULAM, R. (2003). Milk intake and survival in newborn cannabinoid CB1 receptor knockout mice: evidence for a "CB3" receptor. *Eur J Pharmacol*, **461,** 27-34.

FRIED, P.A. & SMITH, A.M. (2001). A literature review of the consequences of prenatal marihuana exposure. An emerging theme of a deficiency in aspects of executive function. *Neurotoxicol Teratol*, **23,** 1-11.

FRIED, P.A., WATKINSON, B. & GRAY, R. (2003). Differential effects on cognitive functioning in 13- to 16-year-olds prenatally exposed to cigarettes and marihuana. *Neurotoxicol Teratol*, **25,** 427-36.

GAINETDINOV, R.R., PREMONT, R.T., BOHN, L.M., LEFKOWITZ, R.J. & CARON, M.G. (2004). Desensitization of G protein-coupled receptors and neuronal functions. *Annu Rev Neurosci*, **27,** 107-44.

GAJATE, C. & MOLLINEDO, F. (2001). The antitumor ether lipid ET-18-OCH(3) induces

apoptosis through translocation and capping of Fas/CD95 into membrane rafts in human leukemic cells. *Blood*, **98,** 3860-3.

GALIEGUE, S., MARY, S., MARCHAND, J., DUSSOSSOY, D., CARRIERE, D., CARAYON, P., BOUABOULA, M., SHIRE, D., LE FUR, G. & CASELLAS, P. (1995). Expression of central and peripheral cannabinoid receptors in human immune tissues and leukocyte subpopulations. *Eur J Biochem*, **232,** 54-61.

GALVE-ROPERH, I., AGUADO, T., PALAZUELOS, J. & GUZMAN, M. (2007). The endocannabinoid system and neurogenesis in health and disease. *Neuroscientist*, **13,** 109-14.

GALVE-ROPERH, I., AGUADO, T., RUEDA, D., VELASCO, G. & GUZMAN, M. (2006). Endocannabinoids: a new family of lipid mediators involved in the regulation of neural cell development. *Curr Pharm Des*, **12,** 2319-25.

GALVE-ROPERH, I., RUEDA, D., GOMEZ DEL PULGAR, T., VELASCO, G. & GUZMAN, M. (2002). Mechanism of extracellular signal-regulated kinase activation by the CB(1) cannabinoid receptor. *Mol Pharmacol*, **62,** 1385-92.

GALVE-ROPERH, I., SANCHEZ, C., CORTES, M.L., DEL PULGAR, T.G., IZQUIERDO, M. & GUZMAN, M. (2000). Anti-tumoral action of cannabinoids: involvement of sustained ceramide accumulation and extracellular signal-regulated kinase activation. *Nat Med*, **6,** 313-9.

GARCIA-ARENCIBIA, M., GONZALEZ, S., DE LAGO, E., RAMOS, J.A., MECHOULAM, R. & FERNANDEZ-RUIZ, J. (2007). Evaluation of the neuroprotective effect of cannabinoids in a rat model of Parkinson's disease: importance of antioxidant and cannabinoid receptor-independent properties. *Brain Res*, **1134,** 162-70.

GARCIA-CALVO, M., PETERSON, E.P., LEITING, B., RUEL, R., NICHOLSON, D.W. & THORNBERRY, N.A. (1998). Inhibition of human caspases by peptide-based and macromolecular inhibitors. *J Biol Chem*, **273,** 32608-13.

GARNOVSKAYA, M.N., GETTYS, T.W., VAN BIESEN, T., PRPIC, V., CHUPRUN, J.K. & RAYMOND, J.R. (1997). 5-HT1A receptor activates Na+/H+ exchange in CHO-K1 cells through Gialpha2 and Gialpha3. *J Biol Chem*, **272,** 7770-6.

GATLEY, S.J., GIFFORD, A.N., VOLKOW, N.D., LAN, R. & MAKRIYANNIS, A. (1996). 123I-labeled AM251: a radioiodinated ligand which binds in vivo to mouse brain

cannabinoid CB1 receptors. *Eur J Pharmacol*, **307,** 331-8.

GEISOW, M. (1982). Lysosome proton pump identified. *Nature*, **298,** 515-6.

GERARD, C., MOLLEREAU, C., VASSART, G. & PARMENTIER, M. (1990). Nucleotide sequence of a human cannabinoid receptor cDNA. *Nucleic Acids Res*, **18,** 7142.

GERARD, C.M., MOLLEREAU, C., VASSART, G. & PARMENTIER, M. (1991). Molecular cloning of a human cannabinoid receptor which is also expressed in testis. *Biochem J*, **279 (Pt 1),** 129-34.

GIACCIA, A.J. & KASTAN, M.B. (1998). The complexity of p53 modulation: emerging patterns from divergent signals. *Genes Dev*, **12,** 2973-83.

GIBB, S.L., BOSTON-HOWES, W., LAVINA, S.Z., GUSTINCICH, S., BROWN, R.H., JR., PASINELLI, P. & TROTTI, D. (2007). A caspase-3 cleaved fragment of the glial glutamate transporter EAAT2 is sumoylated and targeted to promyelocytic leukemia nuclear bodies in mutant SOD1 linked ALS. *J Biol Chem*.

GILBERT, G.L., KIM, H.J., WAATAJA, J.J. & THAYER, S.A. (2007). Delta9-tetrahydrocannabinol protects hippocampal neurons from excitotoxicity. *Brain Res*, **1128,** 61-9.

GLASS, M., DRAGUNOW, M. & FAULL, R.L. (1997). Cannabinoid receptors in the human brain: a detailed anatomical and quantitative autoradiographic study in the fetal, neonatal and adult human brain. *Neuroscience*, **77,** 299-318.

GOCHEVA, V. & JOYCE, J.A. (2007). Cysteine cathepsins and the cutting edge of cancer invasion. *Cell Cycle*, **6,** 60-4.

GODLEWSKI, G., GOTHERT, M. & MALINOWSKA, B. (2003). Cannabinoid receptor-independent inhibition by cannabinoid agonists of the peripheral 5-HT3 receptor-mediated von Bezold-Jarisch reflex. *Br J Pharmacol*, **138,** 767-74.

GOMEZ DEL PULGAR, T., DE CEBALLOS, M.L., GUZMAN, M. & VELASCO, G. (2002). Cannabinoids protect astrocytes from ceramide-induced apoptosis through the phosphatidylinositol 3-kinase/protein kinase B pathway. *J Biol Chem*, **277,** 36527-33.

GONG, J.P., ONAIVI, E.S., ISHIGURO, H., LIU, Q.R., TAGLIAFERRO, P.A., BRUSCO, A. & UHL, G.R. (2006). Cannabinoid CB2 receptors: immunohistochemical localization in rat brain. *Brain Res*, **1071,** 10-23.

GOPARAJU, S.K., UEDA, N., TANIGUCHI, K. & YAMAMOTO, S. (1999). Enzymes of porcine brain hydrolyzing 2-arachidonoylglycerol, an endogenous ligand of cannabinoid receptors. *Biochem Pharmacol*, **57,** 417-23.

GOPARAJU, S.K., UEDA, N., YAMAGUCHI, H. & YAMAMOTO, S. (1998). Anandamide amidohydrolase reacting with 2-arachidonoylglycerol, another cannabinoid receptor ligand. *FEBS Lett*, **422,** 69-73.

GOSTISSA, M., HENGSTERMANN, A., FOGAL, V., SANDY, P., SCHWARZ, S.E., SCHEFFNER, M. & DEL SAL, G. (1999). Activation of p53 by conjugation to the ubiquitin-like protein SUMO-1. *Embo J*, **18,** 6462-71.

GOTHERT, M., BRUSS, M., BONISCH, H. & MOLDERINGS, G.J. (1999). Presynaptic imidazoline receptors. New developments in characterization and classification. *Ann N Y Acad Sci*, **881,** 171-84.

GRAMPP, T., SAUTER, K., MARKOVIC, B. & BENKE, D. (2007). Gamma-aminobutyric acid type B receptors are constitutively internalized via the clathrin-dependent pathway and targeted to lysosomes for degradation. *J Biol Chem*, **282,** 24157-65.

GREEN, D.R. & CHIPUK, J.E. (2006). p53 and metabolism: Inside the TIGAR. *Cell*, **126,** 30-2.

GROTE, H.E. & HANNAN, A.J. (2007). Regulators of adult neurogenesis in the healthy and diseased brain. *Clin Exp Pharmacol Physiol*, **34,** 533-45.

GUBENSEK, F., BARSTOW, L., KREGAR, I. & TURK, V. (1976). Rapid isolation of cathepsin D by affinity chromatography on the immobilized synthetic inhibitor. *FEBS Lett*, **72,** 42-4.

GUICCIARDI, M.E., DEUSSING, J., MIYOSHI, H., BRONK, S.F., SVINGEN, P.A., PETERS, C., KAUFMANN, S.H. & GORES, G.J. (2000). Cathepsin B contributes to TNF-alpha-mediated hepatocyte apoptosis by promoting mitochondrial release of cytochrome c. *J Clin Invest*, **106,** 1127-37.

GUICCIARDI, M.E., LEIST, M. & GORES, G.J. (2004). Lysosomes in cell death. *Oncogene*, **23,** 2881-90.

GULYAS, A.I., CRAVATT, B.F., BRACEY, M.H., DINH, T.P., PIOMELLI, D., BOSCIA, F. & FREUND, T.F. (2004). Segregation of two endocannabinoid-hydrolyzing enzymes

into pre- and postsynaptic compartments in the rat hippocampus, cerebellum and amygdala. *Eur J Neurosci*, **20,** 441-58.

GUO, J. & IKEDA, S.R. (2004). Endocannabinoids modulate N-type calcium channels and G-protein-coupled inwardly rectifying potassium channels via CB1 cannabinoid receptors heterologously expressed in mammalian neurons. *Mol Pharmacol*, **65,** 665-74.

GUZMAN, M., SANCHEZ, C. & GALVE-ROPERH, I. (2002). Cannabinoids and cell fate. *Pharmacol Ther*, **95,** 175-84.

HAJOS, N., KATHURIA, S., DINH, T., PIOMELLI, D. & FREUND, T.F. (2004). Endocannabinoid transport tightly controls 2-arachidonoyl glycerol actions in the hippocampus: effects of low temperature and the transport inhibitor AM404. *Eur J Neurosci*, **19,** 2991-6.

HAMPSON, A.J., BORNHEIM, L.M., SCANZIANI, M., YOST, C.S., GRAY, A.T., HANSEN, B.M., LEONOUDAKIS, D.J. & BICKLER, P.E. (1998). Dual effects of anandamide on NMDA receptor-mediated responses and neurotransmission. *J Neurochem*, **70,** 671-6.

HAMPSON, A.J., GRIMALDI, M., AXELROD, J. & WINK, D. (1998). Cannabidiol and (-)Delta9-tetrahydrocannabinol are neuroprotective antioxidants. *Proc Natl Acad Sci U S A*, **95,** 8268-73.

HAMPSON, R.E., MU, J. & DEADWYLER, S.A. (2000). Cannabinoid and kappa opioid receptors reduce potassium K current via activation of G(s) proteins in cultured hippocampal neurons. *J Neurophysiol*, **84,** 2356-64.

HANSEN, H.H., SCHMID, P.C., BITTIGAU, P., LASTRES-BECKER, I., BERRENDERO, F., MANZANARES, J., IKONOMIDOU, C., SCHMID, H.H., FERNANDEZ-RUIZ, J.J. & HANSEN, H.S. (2001). Anandamide, but not 2-arachidonoylglycerol, accumulates during in vivo neurodegeneration. *J Neurochem*, **78,** 1415-27.

HANUS, L., ABU-LAFI, S., FRIDE, E., BREUER, A., VOGEL, Z., SHALEV, D.E., KUSTANOVICH, I. & MECHOULAM, R. (2001). 2-arachidonyl glyceryl ether, an endogenous agonist of the cannabinoid CB1 receptor. *Proc Natl Acad Sci U S A*, **98,** 3662-5.

HARDELAND, U., STEINACHER, R., JIRICNY, J. & SCHAR, P. (2002). Modification of the human thymine-DNA glycosylase by ubiquitin-like proteins facilitates

enzymatic turnover. *Embo J*, **21,** 1456-64.

HARDWICK, J.S. & SEFTON, B.M. (1995). Activation of the Lck tyrosine protein kinase by hydrogen peroxide requires the phosphorylation of Tyr-394. *Proc Natl Acad Sci U S A*, **92,** 4527-31.

HARKANY, T., GUZMAN, M., GALVE-ROPERH, I., BERGHUIS, P., DEVI, L.A. & MACKIE, K. (2007). The emerging functions of endocannabinoid signaling during CNS development. *Trends Pharmacol Sci*, **28,** 83-92.

HARRIS, L.W., SHARP, T., GARTLON, J., JONES, D.N. & HARRISON, P.J. (2003). Long-term behavioural, molecular and morphological effects of neonatal NMDA receptor antagonism. *Eur J Neurosci*, **18,** 1706-10.

HATTORI, N. & MIZUNO, Y. (2004). Pathogenetic mechanisms of parkin in Parkinson's disease. *Lancet*, **364,** 722-4.

HAY, R.T. (2005). SUMO: a history of modification. *Mol Cell*, **18,** 1-12.

HAY, R.T. (2007). SUMO-specific proteases: a twist in the tail. *Trends Cell Biol*, **17,** 370-6.

HE, J., TOHYAMA, Y., YAMAMOTO, K., KOBAYASHI, M., SHI, Y., TAKANO, T., NODA, C., TOHYAMA, K. & YAMAMURA, H. (2005). Lysosome is a primary organelle in B cell receptor-mediated apoptosis: an indispensable role of Syk in lysosomal function. *Genes Cells*, **10,** 23-35.

HE, J.C., GOMES, I., NGUYEN, T., JAYARAM, G., RAM, P.T., DEVI, L.A. & IYENGAR, R. (2005). The G alpha(o/i)-coupled cannabinoid receptor-mediated neurite outgrowth involves Rap regulation of Src and Stat3. *J Biol Chem*, **280,** 33426-34.

HE, L.M., CHEN, L.Y., LOU, X.L., QU, A.L., ZHOU, Z. & XU, T. (2002). Evaluation of beta-amyloid peptide 25-35 on calcium homeostasis in cultured rat dorsal root ganglion neurons. *Brain Res*, **939,** 65-75.

HECHT, D. & ZICK, Y. (1992). Selective inhibition of protein tyrosine phosphatase activities by H2O2 and vanadate in vitro. *Biochem Biophys Res Commun*, **188,** 773-9.

HEINRICH, M., NEUMEYER, J., JAKOB, M., HALLAS, C., TCHIKOV, V., WINOTO-MORBACH, S., WICKEL, M., SCHNEIDER-BRACHERT, W., TRAUZOLD, A., HETHKE, A. & SCHUTZE, S.

(2004). Cathepsin D links TNF-induced acid sphingomyelinase to Bid-mediated caspase-9 and -3 activation. *Cell Death Differ*, **11,** 550-63.

HEISHMAN, S.J., ARASTEH, K. & STITZER, M.L. (1997). Comparative effects of alcohol and marijuana on mood, memory, and performance. *Pharmacol Biochem Behav*, **58,** 93-101.

HEISHMAN, S.J., HUESTIS, M.A., HENNINGFIELD, J.E. & CONE, E.J. (1990). Acute and residual effects of marijuana: profiles of plasma THC levels, physiological, subjective, and performance measures. *Pharmacol Biochem Behav*, **37,** 561-5.

HEJAZI, N., ZHOU, C., OZ, M., SUN, H., YE, J.H. & ZHANG, L. (2006). Delta9-tetrahydrocannabinol and endogenous cannabinoid anandamide directly potentiate the function of glycine receptors. *Mol Pharmacol*, **69,** 991-7.

HERKENHAM, M., LYNN, A.B., JOHNSON, M.R., MELVIN, L.S., DE COSTA, B.R. & RICE, K.C. (1991). Characterization and localization of cannabinoid receptors in rat brain: a quantitative in vitro autoradiographic study. *J Neurosci*, **11,** 563-83.

HERKENHAM, M., LYNN, A.B., LITTLE, M.D., JOHNSON, M.R., MELVIN, L.S., DE COSTA, B.R. & RICE, K.C. (1990). Cannabinoid receptor localization in brain. *Proc Natl Acad Sci U S A*, **87,** 1932-6.

HERR, I. & DEBATIN, K.M. (2001). Cellular stress response and apoptosis in cancer therapy. *Blood*, **98,** 2603-14.

HILGARTH, K.S.R. (2005). *Detection of Sumoylated proteins from Ubiquitin-Proteasome protocols* New York: Humana Press Inc.,.

HILLARD, C.J., EDGEMOND, W.S., JARRAHIAN, A. & CAMPBELL, W.B. (1997). Accumulation of N-arachidonoylethanolamine (anandamide) into cerebellar granule cells occurs via facilitated diffusion. *J Neurochem*, **69,** 631-8.

HILLARD, C.J. & JARRAHIAN, A. (2000). The movement of N-arachidonoylethanolamine (anandamide) across cellular membranes. *Chem Phys Lipids*, **108,** 123-34.

HILLARD, C.J., WILKISON, D.M., EDGEMOND, W.S. & CAMPBELL, W.B. (1995). Characterization of the kinetics and distribution of N-arachidonylethanolamine (anandamide) hydrolysis by rat brain. *Biochim Biophys Acta*, **1257,** 249-56.

HIROSE, M., KITANO, J., NAKAJIMA, Y., MORIYOSHI, K., YANAGI, S., YAMAMURA, H., MUTO, T., JINGAMI, H. & NAKANISHI, S. (2004). Phosphorylation and recruitment

of Syk by immunoreceptor tyrosine-based activation motif-based phosphorylation of tamalin. *J Biol Chem*, **279,** 32308-15.

HOEGE, C., PFANDER, B., MOLDOVAN, G.L., PYROWOLAKIS, G. & JENTSCH, S. (2002). RAD6-dependent DNA repair is linked to modification of PCNA by ubiquitin and SUMO. *Nature*, **419,** 135-41.

HOELLER, C., THALLINGER, C., PRATSCHER, B., BISTER, M.D., SCHICHER, N., LOEWE, R., HEERE-RESS, E., ROKA, F., SEXL, V. & PEHAMBERGER, H. (2005). The non-receptor-associated tyrosine kinase Syk is a regulator of metastatic behavior in human melanoma cells. *J Invest Dermatol*, **124,** 1293-9.

HOENICKA, J., PONCE, G., JIMENEZ-ARRIERO, M.A., AMPUERO, I., RODRIGUEZ-JIMENEZ, R., RUBIO, G., ARAGUES, M., RAMOS, J.A. & PALOMO, T. (2007). Association in alcoholic patients between psychopathic traits and the additive effect of allelic forms of the CNR1 and FAAH endocannabinoid genes, and the 3' region of the DRD2 gene. *Neurotox Res*, **11,** 51-60.

HONDA, R. & YASUDA, H. (2000). Activity of MDM2, a ubiquitin ligase, toward p53 or itself is dependent on the RING finger domain of the ligase. *Oncogene*, **19,** 1473-6.

HOWLETT, A.C., BREIVOGEL, C.S., CHILDERS, S.R., DEADWYLER, S.A., HAMPSON, R.E. & PORRINO, L.J. (2004). Cannabinoid physiology and pharmacology: 30 years of progress. *Neuropharmacology*, **47 Suppl 1,** 345-58.

HOWLETT, A.C. & FLEMING, R.M. (1984). Cannabinoid inhibition of adenylate cyclase. Pharmacology of the response in neuroblastoma cell membranes. *Mol Pharmacol*, **26,** 532-8.

HOWLETT, A.C., QUALY, J.M. & KHACHATRIAN, L.L. (1986). Involvement of Gi in the inhibition of adenylate cyclase by cannabimimetic drugs. *Mol Pharmacol*, **29,** 307-13.

HOWLETT, A.C., SCOTT, D.K. & WILKEN, G.H. (1989). Regulation of adenylate cyclase by cannabinoid drugs. Insights based on thermodynamic studies. *Biochem Pharmacol*, **38,** 3297-304.

HSU, S.S., HUANG, C.J., CHENG, H.H., CHOU, C.T., LEE, H.Y., WANG, J.L., CHEN, I.S., LIU, S.I., LU, Y.C., CHANG, H.T., HUANG, J.K., CHEN, J.S. & JAN, C.R. (2007).

Anandamide-induced Ca2+ elevation leading to p38 MAPK phosphorylation and subsequent cell death via apoptosis in human osteosarcoma cells. *Toxicology*, **231,** 21-9.

HUANG, H.M., OU, H.C. & HSIEH, S.J. (2000). Antioxidants prevent amyloid peptide-induced apoptosis and alteration of calcium homeostasis in cultured cortical neurons. *Life Sci*, **66,** 1879-92.

HUANG, S.M., BISOGNO, T., TREVISANI, M., AL-HAYANI, A., DE PETROCELLIS, L., FEZZA, F., TOGNETTO, M., PETROS, T.J., KREY, J.F., CHU, C.J., MILLER, J.D., DAVIES, S.N., GEPPETTI, P., WALKER, J.M. & DI MARZO, V. (2002). An endogenous capsaicin-like substance with high potency at recombinant and native vanilloid VR1 receptors. *Proc Natl Acad Sci U S A*, **99,** 8400-5.

HUGHES, P.E., ALEXI, T., WALTON, M., WILLIAMS, C.E., DRAGUNOW, M., CLARK, R.G. & GLUCKMAN, P.D. (1999). Activity and injury-dependent expression of inducible transcription factors, growth factors and apoptosis-related genes within the central nervous system. *Prog Neurobiol*, **57,** 421-50.

HUIZINK, A.C. & MULDER, E.J. (2006). Maternal smoking, drinking or cannabis use during pregnancy and neurobehavioral and cognitive functioning in human offspring. *Neurosci Biobehav Rev*, **30,** 24-41.

HURD, Y.L., WANG, X., ANDERSON, V., BECK, O., MINKOFF, H. & DOW-EDWARDS, D. (2005). Marijuana impairs growth in mid-gestation fetuses. *Neurotoxicol Teratol*, **27,** 221-9.

HUTCHINGS, D.E., BRAKE, S., MORGAN, B., LASALLE, E. & SHI, T.M. (1987). Developmental toxicity of prenatal delta-9-tetrahydrocannabinol: effects of maternal nutrition, offspring growth, and behavior. *NIDA Res Monogr*, **76,** 363-9.

HUTCHINGS, D.E., MARTIN, B.R., GAMAGARIS, Z., MILLER, N. & FICO, T. (1989). Plasma concentrations of delta-9-tetrahydrocannabinol in dams and fetuses following acute or multiple prenatal dosing in rats. *Life Sci*, **44,** 697-701.

HWANG, S.W., CHO, H., KWAK, J., LEE, S.Y., KANG, C.J., JUNG, J., CHO, S., MIN, K.H., SUH, Y.G., KIM, D. & OH, U. (2000). Direct activation of capsaicin receptors by products of lipoxygenases: endogenous capsaicin-like substances. *Proc Natl*

Acad Sci U S A, **97,** 6155-60.

IRVIN, J.E. & MELLORS, A. (1975). Delta9-tetrahydrocannabinol-uptake by rat liver lysosomes. *Biochem Pharmacol*, **24,** 305-7.

ISHAC, E.J., JIANG, L., LAKE, K.D., VARGA, K., ABOOD, M.E. & KUNOS, G. (1996). Inhibition of exocytotic noradrenaline release by presynaptic cannabinoid CB1 receptors on peripheral sympathetic nerves. *Br J Pharmacol*, **118,** 2023-8.

ISHISAKA, R., UTSUMI, T., KANNO, T., ARITA, K., KATUNUMA, N., AKIYAMA, J. & UTSUMI, K. (1999). Participation of a cathepsin L-type protease in the activation of caspase-3. *Cell Struct Funct*, **24,** 465-70.

ISHISAKA, R., UTSUMI, T., KANNO, T., ARITA, K., KATUNUMA, N., AKIYAMA, J. & UTSUMI, K. (1999). Participation of a cathepsin L-type protease in the activation of caspase-3. *Cell Struct Funct*, **24,** 465-70.

ISLEKEL, H., ISLEKEL, S., GUNER, G. & OZDAMAR, N. (1999). Evaluation of lipid peroxidation, cathepsin L and acid phosphatase activities in experimental brain ischemia-reperfusion. *Brain Res*, **843,** 18-24.

IUVONE, T., ESPOSITO, G., ESPOSITO, R., SANTAMARIA, R., DI ROSA, M. & IZZO, A.A. (2004). Neuroprotective effect of cannabidiol, a non-psychoactive component from Cannabis sativa, on beta-amyloid-induced toxicity in PC12 cells. *J Neurochem*, **89,** 134-41.

IVERSEN, L. (2000). *The science of marijuana*. New York: Oxford University Press.

IWAKUMA, T. & LOZANO, G. (2003). MDM2, an introduction. *Mol Cancer Res*, **1,** 993-1000.

JACOBSSON, S.O., WALLIN, T. & FOWLER, C.J. (2001). Inhibition of rat C6 glioma cell proliferation by endogenous and synthetic cannabinoids. Relative involvement of cannabinoid and vanilloid receptors. *J Pharmacol Exp Ther*, **299,** 951-9.

JAGER, G., KAHN, R.S., VAN DEN BRINK, W., VAN REE, J.M. & RAMSEY, N.F. (2006). Long-term effects of frequent cannabis use on working memory and attention: an fMRI study. *Psychopharmacology (Berl)*, **185,** 358-68.

JANICKE, R.U., SPRENGART, M.L., WATI, M.R. & PORTER, A.G. (1998). Caspase-3 is required for DNA fragmentation and morphological changes associated with apoptosis. *J Biol Chem*, **273,** 9357-60.

JARRAHIAN, A., WATTS, V.J. & BARKER, E.L. (2004). D2 dopamine receptors modulate Galpha-subunit coupling of the CB1 cannabinoid receptor. *J Pharmacol Exp Ther*, **308,** 880-6.

JEFFERS, J.R., PARGANAS, E., LEE, Y., YANG, C., WANG, J., BRENNAN, J., MACLEAN, K.H., HAN, J., CHITTENDEN, T., IHLE, J.N., MCKINNON, P.J., CLEVELAND, J.L. & ZAMBETTI, G.P. (2003). Puma is an essential mediator of p53-dependent and -independent apoptotic pathways. *Cancer Cell*, **4,** 321-8.

JENTSCH, J.D., ANDRUSIAK, E., TRAN, A., BOWERS, M.B., JR. & ROTH, R.H. (1997). Delta 9-tetrahydrocannabinol increases prefrontal cortical catecholaminergic utilization and impairs spatial working memory in the rat: blockade of dopaminergic effects with HA966. *Neuropsychopharmacology*, **16,** 426-32.

JHAVERI, M.D., RICHARDSON, D., KENDALL, D.A., BARRETT, D.A. & CHAPMAN, V. (2006). Analgesic effects of fatty acid amide hydrolase inhibition in a rat model of neuropathic pain. *J Neurosci*, **26,** 13318-27.

JIANG, W., ZHANG, Y., XIAO, L., VAN CLEEMPUT, J., JI, S.P., BAI, G. & ZHANG, X. (2005). Cannabinoids promote embryonic and adult hippocampus neurogenesis and produce anxiolytic- and antidepressant-like effects. *J Clin Invest*, **115,** 3104-16.

JIN, K., XIE, L., KIM, S.H., PARMENTIER-BATTEUR, S., SUN, Y., MAO, X.O., CHILDS, J. & GREENBERG, D.A. (2004). Defective adult neurogenesis in CB1 cannabinoid receptor knockout mice. *Mol Pharmacol*, **66,** 204-8.

JOHANSSON, A.C., STEEN, H., OLLINGER, K. & ROBERG, K. (2003). Cathepsin D mediates cytochrome c release and caspase activation in human fibroblast apoptosis induced by staurosporine. *Cell Death Differ*, **10,** 1253-9.

JOHANSSON, E.M., KANNIUS-JANSON, M., BJURSELL, G. & NILSSON, J. (2003). The p53 tumor suppressor gene is regulated in vivo by nuclear factor 1-C2 in the mouse mammary gland during pregnancy. *Oncogene*, **22,** 6061-70.

JOHNSON, E.S. (2004). Protein modification by SUMO. *Annu Rev Biochem*, **73,** 355-82.

JOHNSON, E.S. & BLOBEL, G. (1999). Cell cycle-regulated attachment of the ubiquitin-related protein SUMO to the yeast septins. *J Cell Biol*, **147,** 981-94.

JONES, S.N., ROE, A.E., DONEHOWER, L.A. & BRADLEY, A. (1995). Rescue of embryonic lethality in Mdm2-deficient mice by absence of p53. *Nature*, **378,** 206-8.

JORGENSEN, R. (1990). Altered gene expression in plants due to trans interactions between homologous genes. *Trends Biotechnol*, **8,** 340-4.

KAGEDAL, K., JOHANSSON, A.C., JOHANSSON, U., HEIMLICH, G., ROBERG, K., WANG, N.S., JURGENSMEIER, J.M. & OLLINGER, K. (2005). Lysosomal membrane permeabilization during apoptosis--involvement of Bax? *Int J Exp Pathol*, **86,** 309-21.

KAGEDAL, K., JOHANSSON, U. & OLLINGER, K. (2001). The lysosomal protease cathepsin D mediates apoptosis induced by oxidative stress. *Faseb J*, **15,** 1592-4.

KAGEDAL, K., ZHAO, M., SVENSSON, I. & BRUNK, U.T. (2001). Sphingosine-induced apoptosis is dependent on lysosomal proteases. *Biochem J*, **359,** 335-43.

KAMBOJ, R.C., PAL, S., RAGHAV, N. & SINGH, H. (1993). A selective colorimetric assay for cathepsin L using Z-Phe-Arg-4-methoxy-beta-naphthylamide. *Biochimie*, **75,** 873-8.

KAMINSKI, N.E., KOH, W.S., YANG, K.H., LEE, M. & KESSLER, F.K. (1994). Suppression of the humoral immune response by cannabinoids is partially mediated through inhibition of adenylate cyclase by a pertussis toxin-sensitive G-protein coupled mechanism. *Biochem Pharmacol*, **48,** 1899-908.

KANAYAMA, G., ROGOWSKA, J., POPE, H.G., GRUBER, S.A. & YURGELUN-TODD, D.A. (2004). Spatial working memory in heavy cannabis users: a functional magnetic resonance imaging study. *Psychopharmacology (Berl)*, **176,** 239-47.

KANTHASAMY, A., ANANTHARAM, V., ALI, S.F. & KANTHASAMY, A.G. (2006). Methamphetamine induces autophagy and apoptosis in a mesencephalic dopaminergic neuronal culture model: role of cathepsin-D in methamphetamine-induced apoptotic cell death. *Ann N Y Acad Sci*, **1074,** 234-44.

KARSAK, M., COHEN-SOLAL, M., FREUDENBERG, J., OSTERTAG, A., MORIEUX, C., KORNAK, U., ESSIG, J., ERXLEBE, E., BAB, I., KUBISCH, C., DE VERNEJOUL, M.C. & ZIMMER, A. (2005). Cannabinoid receptor type 2 gene is associated with human osteoporosis. *Hum Mol Genet*, **14,** 3389-96.

KATONA, I., RANCZ, E.A., ACSADY, L., LEDENT, C., MACKIE, K., HAJOS, N. & FREUND, T.F. (2001). Distribution of CB1 cannabinoid receptors in the amygdala and their role in the control of GABAergic transmission. *J Neurosci*, **21,** 9506-18.

KEARN, C.S., BLAKE-PALMER, K., DANIEL, E., MACKIE, K. & GLASS, M. (2005). Concurrent stimulation of cannabinoid CB1 and dopamine D2 receptors enhances heterodimer formation: a mechanism for receptor cross-talk? *Mol Pharmacol*, **67,** 1697-704.

KERR, J.F. (2002). History of the events leading to the formulation of the apoptosis concept. *Toxicology*, **181-182,** 471-4.

KERR, J.F., WYLLIE, A.H. & CURRIE, A.R. (1972). Apoptosis: a basic biological phenomenon with wide-ranging implications in tissue kinetics. *Br J Cancer*, **26,** 239-57.

KHARBANDA, S., YUAN, Z.M., RUBIN, E., WEICHSELBAUM, R. & KUFE, D. (1994). Activation of Src-like p56/p53lyn tyrosine kinase by ionizing radiation. *J Biol Chem*, **269,** 20739-43.

KIM, S.H., WON, S.J., MAO, X.O., JIN, K. & GREENBERG, D.A. (2006). Molecular mechanisms of cannabinoid protection from neuronal excitotoxicity. *Mol Pharmacol*, **69,** 691-6.

KIM, S.R., LEE, D.Y., CHUNG, E.S., OH, U.T., KIM, S.U. & JIN, B.K. (2005). Transient receptor potential vanilloid subtype 1 mediates cell death of mesencephalic dopaminergic neurons in vivo and in vitro. *J Neurosci*, **25,** 662-71.

KITANO, J., KIMURA, K., YAMAZAKI, Y., SODA, T., SHIGEMOTO, R., NAKAJIMA, Y. & NAKANISHI, S. (2002). Tamalin, a PDZ domain-containing protein, links a protein complex formation of group 1 metabotropic glutamate receptors and the guanine nucleotide exchange factor cytohesins. *J Neurosci*, **22,** 1280-9.

KOBAYASHI, Y., ARAI, S., WAKU, K. & SUGIURA, T. (2001). Activation by 2-arachidonoylglycerol, an endogenous cannabinoid receptor ligand, of p42/44 mitogen-activated protein kinase in HL-60 cells. *J Biochem (Tokyo)*, **129,** 665-9.

KONDO, S., KONDO, H., NAKANE, S., KODAKA, T., TOKUMURA, A., WAKU, K. & SUGIURA, T. (1998). 2-Arachidonoylglycerol, an endogenous cannabinoid receptor agonist: identification as one of the major species of monoacylglycerols in various rat tissues, and evidence for its generation through CA2+-dependent and -independent mechanisms. *FEBS Lett*, **429,** 152-6.

KOZAK, K.R., GUPTA, R.A., MOODY, J.S., JI, C., BOEGLIN, W.E., DUBOIS, R.N., BRASH, A.R.

& MARNETT, L.J. (2002). 15-Lipoxygenase metabolism of 2-arachidonylglycerol. Generation of a peroxisome proliferator-activated receptor alpha agonist. *J Biol Chem*, **277,** 23278-86.

KOZAK, K.R. & MARNETT, L.J. (2002). Oxidative metabolism of endocannabinoids. *Prostaglandins Leukot Essent Fatty Acids*, **66,** 211-20.

KRAMMER, P.H. (1999). CD95(APO-1/Fas)-mediated apoptosis: live and let die. *Adv Immunol*, **71,** 163-210.

KREUTZ, S., KOCH, M., GHADBAN, C., KORF, H.W. & DEHGHANI, F. (2007). Cannabinoids and neuronal damage: differential effects of THC, AEA and 2-AG on activated microglial cells and degenerating neurons in excitotoxically lesioned rat organotypic hippocampal slice cultures. *Exp Neurol*, **203,** 246-57.

KWEK, S.S., DERRY, J., TYNER, A.L., SHEN, Z. & GUDKOV, A.V. (2001). Functional analysis and intracellular localization of p53 modified by SUMO-1. *Oncogene*, **20,** 2587-99.

LAI, J.Y., COX, P.J., PATEL, R., SADIQ, S., ALDOUS, D.J., THURAIRATNAM, S., SMITH, K., WHEELER, D., JAGPAL, S., PARVEEN, S., FENTON, G., HARRISON, T.K., MCCARTHY, C. & BAMBOROUGH, P. (2003). Potent small molecule inhibitors of spleen tyrosine kinase (Syk). *Bioorg Med Chem Lett*, **13,** 3111-4.

LAI, Z., FERRY, K.V., DIAMOND, M.A., WEE, K.E., KIM, Y.B., MA, J., YANG, T., BENFIELD, P.A., COPELAND, R.A. & AUGER, K.R. (2001). Human mdm2 mediates multiple mono-ubiquitination of p53 by a mechanism requiring enzyme isomerization. *J Biol Chem*, **276,** 31357-67.

LAKKARAJU, A., DUBINSKY, J.M., LOW, W.C. & RAHMAN, Y.E. (2001). Neurons are protected from excitotoxic death by p53 antisense oligonucleotides delivered in anionic liposomes. *J Biol Chem*, **276,** 32000-7.

LAN, R., LIU, Q., FAN, P., LIN, S., FERNANDO, S.R., MCCALLION, D., PERTWEE, R. & MAKRIYANNIS, A. (1999). Structure-activity relationships of pyrazole derivatives as cannabinoid receptor antagonists. *J Med Chem*, **42,** 769-76.

LANE, D.P. (1992). Cancer. p53, guardian of the genome. *Nature*, **358,** 15-6.

LASTRES-BECKER, I., MOLINA-HOLGADO, F., RAMOS, J.A., MECHOULAM, R. & FERNANDEZ-RUIZ, J. (2005). Cannabinoids provide neuroprotection against 6-

hydroxydopamine toxicity in vivo and in vitro: relevance to Parkinson's disease. *Neurobiol Dis*, **19,** 96-107.

LAUCKNER, J.E., HILLE, B. & MACKIE, K. (2005). The cannabinoid agonist WIN55,212-2 increases intracellular calcium via CB1 receptor coupling to Gq/11 G proteins. *Proc Natl Acad Sci U S A*, **102,** 19144-9.

LAURENT-MATHA, V., MARUANI-HERRMANN, S., PREBOIS, C., BEAUJOUIN, M., GLONDU, M., NOEL, A., ALVAREZ-GONZALEZ, M.L., BLACHER, S., COOPMAN, P., BAGHDIGUIAN, S., GILLES, C., LONCAREK, J., FREISS, G., VIGNON, F. & LIAUDET-COOPMAN, E. (2005). Catalytically inactive human cathepsin D triggers fibroblast invasive growth. *J Cell Biol*, **168,** 489-99.

LAVIN, M.F. & GUEVEN, N. (2006). The complexity of p53 stabilization and activation. *Cell Death Differ*, **13,** 941-50.

LAWSTON, J., BORELLA, A., ROBINSON, J.K. & WHITAKER-AZMITIA, P.M. (2000). Changes in hippocampal morphology following chronic treatment with the synthetic cannabinoid WIN 55,212-2. *Brain Res*, **877,** 407-10.

LE BRAS, M., ROUY, I. & BRENNER, C. (2006). The modulation of inter-organelle cross-talk to control apoptosis. *Med Chem*, **2,** 1-12.

LEE, D.C., WOMBLE, T.A., MASON, C.W., JACKSON, I.M., LAMANGO, N.S., SEVERS, W.B. & PALM, D.E. (2007). 6-Hydroxydopamine induces cystatin C-mediated cysteine protease suppression and cathepsin D activation. *Neurochem Int*, **50,** 607-18.

LEE, J., DI MARZO, V. & BROTCHIE, J.M. (2006). A role for vanilloid receptor 1 (TRPV1) and endocannabinnoid signalling in the regulation of spontaneous and L-DOPA induced locomotion in normal and reserpine-treated rats. *Neuropharmacology*, **51,** 557-65.

LEE, J., DUAN, W., LONG, J.M., INGRAM, D.K. & MATTSON, M.P. (2000). Dietary restriction increases the number of newly generated neural cells, and induces BDNF expression, in the dentate gyrus of rats. *J Mol Neurosci*, **15,** 99-108.

LEE, J.C. & PETER, M.E. (2003). Regulation of apoptosis by ubiquitination. *Immunol Rev*, **193,** 39-47.

LEE, M.C., SMITH, F.L., STEVENS, D.L. & WELCH, S.P. (2003). The role of several kinases in mice tolerant to delta 9-tetrahydrocannabinol. *J Pharmacol Exp Ther*, **305,**

593-9.

LEE, M.H., LEE, S.W., LEE, E.J., CHOI, S.J., CHUNG, S.S., LEE, J.I., CHO, J.M., SEOL, J.H., BAEK, S.H., KIM, K.I., CHIBA, T., TANAKA, K., BANG, O.S. & CHUNG, C.H. (2006). SUMO-specific protease SUSP4 positively regulates p53 by promoting Mdm2 self-ubiquitination. *Nat Cell Biol*, **8,** 1424-31.

LEIST, M. & JAATTELA, M. (2001). Triggering of apoptosis by cathepsins. *Cell Death Differ*, **8,** 324-6.

LEKER, R.R., AHARONOWIZ, M., GREIG, N.H. & OVADIA, H. (2004). The role of p53-induced apoptosis in cerebral ischemia: effects of the p53 inhibitor pifithrin alpha. *Exp Neurol*, **187,** 478-86.

LEVINE, A.J. (1997). p53, the cellular gatekeeper for growth and division. *Cell*, **88,** 323-31.

LI, J. & SIDELL, N. (2005). Growth-related oncogene produced in human breast cancer cells and regulated by Syk protein-tyrosine kinase. *Int J Cancer*, **117,** 14-20.

LI, S.J. & HOCHSTRASSER, M. (1999). A new protease required for cell-cycle progression in yeast. *Nature*, **398,** 246-51.

LI, W., YUAN, X., NORDGREN, G., DALEN, H., DUBOWCHIK, G.M., FIRESTONE, R.A. & BRUNK, U.T. (2000). Induction of cell death by the lysosomotropic detergent MSDH. *FEBS Lett*, **470,** 35-9.

LI, W., YUAN, X.M., IVANOVA, S., TRACEY, K.J., EATON, J.W. & BRUNK, U.T. (2003). 3-Aminopropanal, formed during cerebral ischaemia, is a potent lysosomotropic neurotoxin. *Biochem J*, **371,** 429-36.

LI, Y., SCHLAMP, C.L., POULSEN, G.L., JACKSON, M.W., GRIEP, A.E. & NICKELLS, R.W. (2002). p53 regulates apoptotic retinal ganglion cell death induced by N-methyl-D-aspartate. *Mol Vis*, **8,** 341-50.

LIEBERMAN, A.P. (2004). SUMO, a ubiquitin-like modifier implicated in neurodegeneration. *Exp Neurol*, **185,** 204-7.

LIN, J.Y., OHSHIMA, T. & SHIMOTOHNO, K. (2004). Association of Ubc9, an E2 ligase for SUMO conjugation, with p53 is regulated by phosphorylation of p53. *FEBS Lett*, **573,** 15-8.

LIU, J., WANG, L., HARVEY-WHITE, J., OSEI-HYIAMAN, D., RAZDAN, R., GONG, Q., CHAN,

A.C., Zhou, Z., Huang, B.X., Kim, H.Y. & Kunos, G. (2006). A biosynthetic pathway for anandamide. *Proc Natl Acad Sci U S A*, **103,** 13345-50.

Lo, A.C., Houenou, L.J. & Oppenheim, R.W. (1995). Apoptosis in the nervous system: morphological features, methods, pathology, and prevention. *Arch Histol Cytol*, **58,** 139-49.

Lord, S.J., Rajotte, R.V., Korbutt, G.S. & Bleackley, R.C. (2003). Granzyme B: a natural born killer. *Immunol Rev*, **193,** 31-8.

Ludlow, F. (1857). *The hasheesh eater: Being passages from the life of a pyathagorean*. New York: Harper bros.

Maccarrone, M., Bisogno, T., Valensise, H., Lazzarin, N., Fezza, F., Manna, C., Di Marzo, V. & Finazzi-Agro, A. (2002). Low fatty acid amide hydrolase and high anandamide levels are associated with failure to achieve an ongoing pregnancy after IVF and embryo transfer. *Mol Hum Reprod*, **8,** 188-95.

Maccarrone, M., Cecconi, S., Rossi, G., Battista, N., Pauselli, R. & Finazzi-Agro, A. (2003). Anandamide activity and degradation are regulated by early postnatal aging and follicle-stimulating hormone in mouse Sertoli cells. *Endocrinology*, **144,** 20-8.

Maccarrone, M. & Finazzi-Agro, A. (2003). The endocannabinoid system, anandamide and the regulation of mammalian cell apoptosis. *Cell Death Differ*, **10,** 946-55.

Maccarrone, M., Lorenzon, T., Bari, M., Melino, G. & Finazzi-Agro, A. (2000). Anandamide induces apoptosis in human cells via vanilloid receptors. Evidence for a protective role of cannabinoid receptors. *J Biol Chem*, **275,** 31938-45.

MacCoun, R. & Reuter, P. (1997). Interpreting Dutch cannabis policy: reasoning by analogy in the legalization debate. *Science*, **278,** 47-52.

MacCoun, R. & Reuter, P. (2001). Evaluating alternative cannabis regimes. *Br J Psychiatry*, **178,** 123-8.

Mackie, K. (2005). Cannabinoid receptor homo- and heterodimerization. *Life Sci*, **77,** 1667-73.

Mackie, K., Devane, W.A. & Hille, B. (1993). Anandamide, an endogenous cannabinoid, inhibits calcium currents as a partial agonist in N18 neuroblastoma

cells. *Mol Pharmacol*, **44,** 498-503.

MACKIE, K. & STELLA, N. (2006). Cannabinoid receptors and endocannabinoids: evidence for new players. *Aaps J*, **8,** E298-306.

MACKOWIAK, M., CHOCYK, A., MARKOWICZ-KULA, K. & WEDZONY, K. (2004). Neurogenesis in the adult brain. *Pol J Pharmacol*, **56,** 673-87.

MACKOWIAK, M., CHOCYK, A., MARKOWICZ-KULA, K. & WEDZONY, K. (2004). Neurogenesis in the adult brain. *Pol J Pharmacol*, **56,** 673-87.

MAHABELESHWAR, G.H. & KUNDU, G.C. (2003). Syk, a protein-tyrosine kinase, suppresses the cell motility and nuclear factor kappa B-mediated secretion of urokinase type plasminogen activator by inhibiting the phosphatidylinositol 3'-kinase activity in breast cancer cells. *J Biol Chem*, **278,** 6209-21.

MAINGRET, F., PATEL, A.J., LAZDUNSKI, M. & HONORE, E. (2001). The endocannabinoid anandamide is a direct and selective blocker of the background K(+) channel TASK-1. *Embo J*, **20,** 47-54.

MAIONE, S., BISOGNO, T., DE NOVELLIS, V., PALAZZO, E., CRISTINO, L., VALENTI, M., PETROSINO, S., GUGLIELMOTTI, V., ROSSI, F. & DI MARZO, V. (2006). Elevation of endocannabinoid levels in the ventrolateral periaqueductal grey through inhibition of fatty acid amide hydrolase affects descending nociceptive pathways via both cannabinoid receptor type 1 and transient receptor potential vanilloid type-1 receptors. *J Pharmacol Exp Ther*, **316,** 969-82.

MANZA, L.L., CODREANU, S.G., STAMER, S.L., SMITH, D.L., WELLS, K.S., ROBERTS, R.L. & LIEBLER, D.C. (2004). Global shifts in protein sumoylation in response to electrophile and oxidative stress. *Chem Res Toxicol*, **17,** 1706-15.

MARCHENKO, N.D., ZAIKA, A. & MOLL, U.M. (2000). Death signal-induced localization of p53 protein to mitochondria. A potential role in apoptotic signaling. *J Biol Chem*, **275,** 16202-12.

MARSICANO, G., GOODENOUGH, S., MONORY, K., HERMANN, H., EDER, M., CANNICH, A., AZAD, S.C., CASCIO, M.G., GUTIERREZ, S.O., VAN DER STELT, M., LOPEZ-RODRIGUEZ, M.L., CASANOVA, E., SCHUTZ, G., ZIEGLGANSBERGER, W., DI MARZO, V., BEHL, C. & LUTZ, B. (2003). CB1 cannabinoid receptors and on-demand defense against excitotoxicity. *Science*, **302,** 84-8.

MARSICANO, G., MOOSMANN, B., HERMANN, H., LUTZ, B. & BEHL, C. (2002). Neuroprotective properties of cannabinoids against oxidative stress: role of the cannabinoid receptor CB1. *J Neurochem*, **80,** 448-56.

MARTIN, S., NISHIMUNE, A., MELLOR, J.R. & HENLEY, J.M. (2007). SUMOylation regulates kainate-receptor-mediated synaptic transmission. *Nature*, **447,** 321-5.

MARX, J. (2005). Cell biology. SUMO wrestles its way to prominence in the cell. *Science*, **307,** 836-9.

MASON, R. (1996). *Biology of the lysosome*. New York Plenum Press.

MATHEW, R.J., WILSON, W.H., COLEMAN, R.E., TURKINGTON, T.G. & DEGRADO, T.R. (1997). Marijuana intoxication and brain activation in marijuana smokers. *Life Sci*, **60,** 2075-89.

MATOCHIK, J.A., ELDRETH, D.A., CADET, J.L. & BOLLA, K.I. (2005). Altered brain tissue composition in heavy marijuana users. *Drug Alcohol Depend*, **77,** 23-30.

MATSUDA, L.A., LOLAIT, S.J., BROWNSTEIN, M.J., YOUNG, A.C. & BONNER, T.I. (1990). Structure of a cannabinoid receptor and functional expression of the cloned cDNA. *Nature*, **346,** 561-4.

MATTSON, M.P. (2000). Apoptosis in neurodegenerative disorders. *Nat Rev Mol Cell Biol*, **1,** 120-9.

MATUNIS, M.J., COUTAVAS, E. & BLOBEL, G. (1996). A novel ubiquitin-like modification modulates the partitioning of the Ran-GTPase-activating protein RanGAP1 between the cytosol and the nuclear pore complex. *J Cell Biol*, **135,** 1457-70.

MATVEYEVA, M., HARTMANN, C.B., HARRISON, M.T., CABRAL, G.A. & MCCOY, K.L. (2000). Delta(9)-tetrahydrocannabinol selectively increases aspartyl cathepsin D proteolytic activity and impairs lysozyme processing by macrophages. *Int J Immunopharmacol*, **22,** 373-81.

MAYKUT, M.O. (1985). Health consequences of acute and chronic marihuana use. *Prog Neuropsychopharmacol Biol Psychiatry*, **9,** 209-38.

MCALLISTER, S.D. & GLASS, M. (2002). CB(1) and CB(2) receptor-mediated signalling: a focus on endocannabinoids. *Prostaglandins Leukot Essent Fatty Acids*, **66,** 161-71.

MCGUINNESS, L., BARDO, S.J. & EMPTAGE, N.J. (2007). The lysosome or lysosome-

related organelle may serve as a Ca2+ store in the boutons of hippocampal pyramidal cells. *Neuropharmacology*, **52,** 126-35.

McIsaac, W., Fritchie, G.E., Idanpaan-Heikkila, J.E., Ho, B.T. & Englert, L.F. (1971). Distribution of marihuana in monkey brain and concomitant behavioural effects. *Nature*, **230,** 593-4.

Mechoulam, R., Ben-Shabat, S., Hanus, L., Ligumsky, M., Kaminski, N.E., Schatz, A.R., Gopher, A., Almog, S., Martin, B.R., Compton, D.R. & et al. (1995). Identification of an endogenous 2-monoglyceride, present in canine gut, that binds to cannabinoid receptors. *Biochem Pharmacol*, **50,** 83-90.

Mechoulam, R., Feigenbaum, J.J., Lander, N., Segal, M., Jarbe, T.U., Hiltunen, A.J. & Consroe, P. (1988). Enantiomeric cannabinoids: stereospecificity of psychotropic activity. *Experientia*, **44,** 762-4.

Mechoulam, R. & Gaoni, Y. (1965). A Total Synthesis of Dl-Delta-1-Tetrahydrocannabinol, the Active Constituent of Hashish. *J Am Chem Soc*, **87,** 3273-5.

Mechoulam, R., Lander, N., Srebnik, M., Breuer, A., Segal, M., Feigenbaum, J.J., Jarbe, T.U. & Consroe, P. (1987). Stereochemical requirements for cannabimimetic activity. *NIDA Res Monogr*, **79,** 15-30.

Mechoulam, R., Panikashvili, D. & Shohami, E. (2002). Cannabinoids and brain injury: therapeutic implications. *Trends Mol Med*, **8,** 58-61.

Melchior, F. (2000). SUMO--nonclassical ubiquitin. *Annu Rev Cell Dev Biol*, **16,** 591-626.

Melchior, F. & Hengst, L. (2002). SUMO-1 and p53. *Cell Cycle*, **1,** 245-9.

Melck, D., De Petrocellis, L., Orlando, P., Bisogno, T., Laezza, C., Bifulco, M. & Di Marzo, V. (2000). Suppression of nerve growth factor Trk receptors and prolactin receptors by endocannabinoids leads to inhibition of human breast and prostate cancer cell proliferation. *Endocrinology*, **141,** 118-26.

Melvin, L.S. & Johnson, M.R. (1987). Structure-activity relationships of tricyclic and nonclassical bicyclic cannabinoids. *NIDA Res Monogr*, **79,** 31-47.

Mereu, G., Fa, M., Ferraro, L., Cagiano, R., Antonelli, T., Tattoli, M., Ghiglieri, V., Tanganelli, S., Gessa, G.L. & Cuomo, V. (2003). Prenatal exposure to a

cannabinoid agonist produces memory deficits linked to dysfunction in hippocampal long-term potentiation and glutamate release. *Proc Natl Acad Sci U S A*, **100,** 4915-20.

MESTRE, L., CORREA, F., DOCAGNE, F., CLEMENTE, D., ORTEGA-GUTIERREZ, S., AREVALO-MARTIN, A., MOLINA-HOLGADO, E., BORRELL, J. & GUAZA, C. (2006). [Cannabinoid system and neuroinflammation:therapeutic perspectives in multiple sclerosis]. *Rev Neurol*, **43,** 541-8.

MICALE, V., MAZZOLA, C. & DRAGO, F. (2007). Endocannabinoids and neurodegenerative diseases. *Pharmacol Res.*

MICHIUE, H., TOMIZAWA, K., MATSUSHITA, M., TAMIYA, T., LU, Y.F., ICHIKAWA, T., DATE, I. & MATSUI, H. (2005). Ubiquitination-resistant p53 protein transduction therapy facilitates anti-cancer effect on the growth of human malignant glioma cells. *FEBS Lett*, **579,** 3965-9.

MILMAN, G., MAOR, Y., ABU-LAFI, S., HOROWITZ, M., GALLILY, R., BATKAI, S., MO, F.M., OFFERTALER, L., PACHER, P., KUNOS, G. & MECHOULAM, R. (2006). N-arachidonoyl L-serine, an endocannabinoid-like brain constituent with vasodilatory properties. *Proc Natl Acad Sci U S A*, **103,** 2428-33.

MILTON, N.G. (2002). Anandamide and noladin ether prevent neurotoxicity of the human amyloid-beta peptide. *Neurosci Lett*, **332,** 127-30.

MIYASHITA, T. & REED, J.C. (1995). Tumor suppressor p53 is a direct transcriptional activator of the human bax gene. *Cell*, **80,** 293-9.

MOLDERINGS, G.J., LIKUNGU, J. & GOTHERT, M. (1999). Presynaptic cannabinoid and imidazoline receptors in the human heart and their potential relationship. *Naunyn Schmiedebergs Arch Pharmacol*, **360,** 157-64.

MOLINA-HOLGADO, F., PINTEAUX, E., MOORE, J.D., MOLINA-HOLGADO, E., GUAZA, C., GIBSON, R.M. & ROTHWELL, N.J. (2003). Endogenous interleukin-1 receptor antagonist mediates anti-inflammatory and neuroprotective actions of cannabinoids in neurons and glia. *J Neurosci*, **23,** 6470-4.

MOMAND, J., WU, H.H. & DASGUPTA, G. (2000). MDM2--master regulator of the p53 tumor suppressor protein. *Gene*, **242,** 15-29.

MOMAND, J., ZAMBETTI, G.P., OLSON, D.C., GEORGE, D. & LEVINE, A.J. (1992). The mdm-

2 oncogene product forms a complex with the p53 protein and inhibits p53-mediated transactivation. *Cell*, **69,** 1237-45.

MONTES DE OCA LUNA, R., WAGNER, D.S. & LOZANO, G. (1995). Rescue of early embryonic lethality in mdm2-deficient mice by deletion of p53. *Nature*, **378,** 203-6.

MOORE, T.H., ZAMMIT, S., LINGFORD-HUGHES, A., BARNES, T.R., JONES, P.B., BURKE, M. & LEWIS, G. (2007). Cannabis use and risk of psychotic or affective mental health outcomes: a systematic review. *Lancet*, **370,** 319-28.

MORAN, M. & MICELI, M.C. (1998). Engagement of GPI-linked CD48 contributes to TCR signals and cytoskeletal reorganization: a role for lipid rafts in T cell activation. *Immunity*, **9,** 787-96.

MOROY, M.Z.T. (1996). Regulators of life and death: the bcl-2 gene family. *Cell Physiol Biochem* **6,** 312-336.

MORRISON, J.H. & HOF, P.R. (2007). Life and death of neurons in the aging cerebral cortex. *Int Rev Neurobiol*, **81,** 41-57.

MORRISON, R.S., KINOSHITA, Y., JOHNSON, M.D., GUO, W. & GARDEN, G.A. (2003). p53-dependent cell death signaling in neurons. *Neurochem Res*, **28,** 15-27.

MOVSESYAN, V.A., STOICA, B.A., YAKOVLEV, A.G., KNOBLACH, S.M., LEA, P.M.T., CERNAK, I., VINK, R. & FADEN, A.I. (2004). Anandamide-induced cell death in primary neuronal cultures: role of calpain and caspase pathways. *Cell Death Differ*, **11,** 1121-32.

MULLER, S., BERGER, M., LEHEMBRE, F., SEELER, J.S., HAUPT, Y. & DEJEAN, A. (2000). c-Jun and p53 activity is modulated by SUMO-1 modification. *J Biol Chem*, **275,** 13321-9.

MUNRO, S., THOMAS, K.L. & ABU-SHAAR, M. (1993). Molecular characterization of a peripheral receptor for cannabinoids. *Nature*, **365,** 61-5.

NACD, N.A.C.O.D.A.D.A.A.I.A.R.U.D.A. (2005). Drug use in Ireland and Northern Ireland from the 2002/2003 drug prevalence survey: Cannabis results.

NACERDDINE, K., LEHEMBRE, F., BHAUMIK, M., ARTUS, J., COHEN-TANNOUDJI, M., BABINET, C., PANDOLFI, P.P. & DEJEAN, A. (2005). The SUMO pathway is essential for nuclear integrity and chromosome segregation in mice. *Dev Cell*, **9,**

769-79.

NADLER, V., MECHOULAM, R. & SOKOLOVSKY, M. (1993). Blockade of 45Ca2+ influx through the N-methyl-D-aspartate receptor ion channel by the non-psychoactive cannabinoid HU-211. *Brain Res*, **622,** 79-85.

NAGAYAMA, T., SINOR, A.D., SIMON, R.P., CHEN, J., GRAHAM, S.H., JIN, K. & GREENBERG, D.A. (1999). Cannabinoids and neuroprotection in global and focal cerebral ischemia and in neuronal cultures. *J Neurosci*, **19,** 2987-95.

NAKAI, M., QIN, Z.H., CHEN, J.F., WANG, Y. & CHASE, T.N. (2000). Kainic acid-induced apoptosis in rat striatum is associated with nuclear factor-kappaB activation. *J Neurochem*, **74,** 647-58.

NAKANE, S., OKA, S., ARAI, S., WAKU, K., ISHIMA, Y., TOKUMURA, A. & SUGIURA, T. (2002). 2-Arachidonoyl-sn-glycero-3-phosphate, an arachidonic acid-containing lysophosphatidic acid: occurrence and rapid enzymatic conversion to 2-arachidonoyl-sn-glycerol, a cannabinoid receptor ligand, in rat brain. *Arch Biochem Biophys*, **402,** 51-8.

NETZEBAND, J.G., CONROY, S.M., PARSONS, K.L. & GRUOL, D.L. (1999). Cannabinoids enhance NMDA-elicited Ca2+ signals in cerebellar granule neurons in culture. *J Neurosci*, **19,** 8765-77.

NICHOLSON, R.A., LIAO, C., ZHENG, J., DAVID, L.S., COYNE, L., ERRINGTON, A.C., SINGH, G. & LEES, G. (2003). Sodium channel inhibition by anandamide and synthetic cannabimimetics in brain. *Brain Res*, **978,** 194-204.

NIE, J. & LEWIS, D.L. (2001). The proximal and distal C-terminal tail domains of the CB1 cannabinoid receptor mediate G protein coupling. *Neuroscience*, **107,** 161-7.

NIJHAWAN, D., HONARPOUR, N. & WANG, X. (2000). Apoptosis in neural development and disease. *Annu Rev Neurosci*, **23,** 73-87.

NILSSON, E., GHASSEMIFAR, R. & BRUNK, U.T. (1997). Lysosomal heterogeneity between and within cells with respect to resistance against oxidative stress. *Histochem J*, **29,** 857-65.

NIRODI, C.S., CREWS, B.C., KOZAK, K.R., MORROW, J.D. & MARNETT, L.J. (2004). The glyceryl ester of prostaglandin E2 mobilizes calcium and activates signal

transduction in RAW264.7 cells. *Proc Natl Acad Sci U S A*, **101,** 1840-5.

NOEL, J. & POUYSSEGUR, J. (1995). *Am. J. Physiol.*, **268,** C283-C296.

NUNEZ, E., BENITO, C., PAZOS, M.R., BARBACHANO, A., FAJARDO, O., GONZALEZ, S., TOLON, R.M. & ROMERO, J. (2004). Cannabinoid CB2 receptors are expressed by perivascular microglial cells in the human brain: an immunohistochemical study. *Synapse*, **53,** 208-13.

NUNEZ, G., BENEDICT, M.A., HU, Y. & INOHARA, N. (1998). Caspases: the proteases of the apoptotic pathway. *Oncogene*, **17,** 3237-45.

NYLANDSTED, J., GYRD-HANSEN, M., DANIELEWICZ, A., FEHRENBACHER, N., LADEMANN, U., HOYER-HANSEN, M., WEBER, E., MULTHOFF, G., ROHDE, M. & JAATTELA, M. (2004). Heat shock protein 70 promotes cell survival by inhibiting lysosomal membrane permeabilization. *J Exp Med*, **200,** 425-35.

O'KANE, C.J., TUTT, D.C. & BAUER, L.A. (2002). Cannabis and driving: a new perspective. *Emerg Med (Fremantle)*, **14,** 296-303.

O'SHAUGNESSEY, W. (1842). On the preparation of the Indian hemp, or gunjah (*cannabis indica)* and their effects on the animal system in health and their uility in the treatmetn of tetanus and other convulsive disorders. *Trans Med Phys Soc Calcutta* **8,** 421-461.

ODA, E., OHKI, R., MURASAWA, H., NEMOTO, J., SHIBUE, T., YAMASHITA, T., TOKINO, T., TANIGUCHI, T. & TANAKA, N. (2000). Noxa, a BH3-only member of the Bcl-2 family and candidate mediator of p53-induced apoptosis. *Science*, **288,** 1053-8.

OKA, S., ARAI, S., WAKU, K., TOKUMURA, A. & SUGIURA, T. (2007). Depolarization-induced rapid generation of 2-arachidonoylglycerol, an endogenous cannabinoid receptor ligand, in rat brain synaptosomes. *J Biochem (Tokyo)*, **141,** 687-97.

OKURA, T., GONG, L., KAMITANI, T., WADA, T., OKURA, I., WEI, C.F., CHANG, H.M. & YEH, E.T. (1996). Protection against Fas/APO-1- and tumor necrosis factor-mediated cell death by a novel protein, sentrin. *J Immunol*, **157,** 4277-81.

ONAIVI, E.S., ISHIGURO, H., GONG, J.P., PATEL, S., PERCHUK, A., MEOZZI, P.A., MYERS, L., MORA, Z., TAGLIAFERRO, P., GARDNER, E., BRUSCO, A., AKINSHOLA, B.E., LIU, Q.R., HOPE, B., IWASAKI, S., ARINAMI, T., TEASENFITZ, L. & UHL, G.R. (2006). Discovery of the presence and functional expression of cannabinoid CB2

receptors in brain. *Ann N Y Acad Sci*, **1074,** 514-36.

ONAIVI, E.S., LEONARD, C.M., ISHIGURO, H., ZHANG, P.W., LIN, Z., AKINSHOLA, B.E. & UHL, G.R. (2002). Endocannabinoids and cannabinoid receptor genetics. *Prog Neurobiol*, **66,** 307-44.

OREN, M. (1999). Regulation of the p53 tumor suppressor protein. *J Biol Chem*, **274,** 36031-4.

OZ, M., ZHANG, L., RAVINDRAN, A., MORALES, M. & LUPICA, C.R. (2004). Differential effects of endogenous and synthetic cannabinoids on alpha7-nicotinic acetylcholine receptor-mediated responses in Xenopus Oocytes. *J Pharmacol Exp Ther*, **310,** 1152-60.

PACHER, P., BATKAI, S., OSEI-HYIAMAN, D., OFFERTALER, L., LIU, J., HARVEY-WHITE, J., BRASSAI, A., JARAI, Z., CRAVATT, B.F. & KUNOS, G. (2005). Hemodynamic profile, responsiveness to anandamide, and baroreflex sensitivity of mice lacking fatty acid amide hydrolase. *Am J Physiol Heart Circ Physiol*, **289,** H533-41.

PAGOTTO, U. & PASQUALI, R. (2006). Endocannabinoids and energy metabolism. *J Endocrinol Invest*, **29,** 66-76.

PALAZUELOS, J., AGUADO, T., EGIA, A., MECHOULAM, R., GUZMAN, M. & GALVE-ROPERH, I. (2006). Non-psychoactive CB2 cannabinoid agonists stimulate neural progenitor proliferation. *Faseb J*, **20,** 2405-7.

PANIKASHVILI, D., MECHOULAM, R., BENI, S.M., ALEXANDROVICH, A. & SHOHAMI, E. (2005). CB1 cannabinoid receptors are involved in neuroprotection via NF-kappa B inhibition. *J Cereb Blood Flow Metab*, **25,** 477-84.

PANIKASHVILI, D., SIMEONIDOU, C., BEN-SHABAT, S., HANUS, L., BREUER, A., MECHOULAM, R. & SHOHAMI, E. (2001). An endogenous cannabinoid (2-AG) is neuroprotective after brain injury. *Nature*, **413,** 527-31.

PARK, C.K., NEHLS, D.G., GRAHAM, D.I., TEASDALE, G.M. & MCCULLOCH, J. (1988). The glutamate antagonist MK-801 reduces focal ischemic brain damage in the rat. *Ann Neurol*, **24,** 543-51.

PATEL, N.A., MOLDOW, R.L., PATEL, J.A., WU, G. & CHANG, S.L. (1998). Arachidonylethanolamide (AEA) activation of FOS proto-oncogene protein

immunoreactivity in the rat brain. *Brain Res*, **797,** 225-33.

PATON, W.D. & PERTWEE, R.G. (1972). Effect of cannabis and certain of its constituents on pentobarbitone sleeping time and phenazone metabolism. *Br J Pharmacol*, **44,** 250-61.

PEREZ-REYES, M., HICKS, R.E., BUMBERRY, J., JEFFCOAT, A.R. & COOK, C.E. (1988). Interaction between marihuana and ethanol: effects on psychomotor performance. *Alcohol Clin Exp Res*, **12,** 268-76.

PERRY, M.E. (2004). Mdm2 in the response to radiation. *Mol Cancer Res*, **2,** 9-19.

PERRY, M.E., MENDRYSA, S.M., SAUCEDO, L.J., TANNOUS, P. & HOLUBAR, M. (2000). p76(MDM2) inhibits the ability of p90(MDM2) to destabilize p53. *J Biol Chem*, **275,** 5733-8.

PERTWEE, R.G. (2001). Cannabinoid receptors and pain. *Prog Neurobiol*, **63,** 569-611.

PERTWEE, R.G. (2005). Pharmacological actions of cannabinoids. *Handb Exp Pharmacol*, 1-51.

PERTWEE, R.G. (2006). Cannabinoid pharmacology: the first 66 years. *Br J Pharmacol*, **147 Suppl 1,** S163-71.

PERTWEE, R.G. (2007). GPR55: a new member of the cannabinoid receptor clan? *Br J Pharmacol*, **152,** 984-6.

PESTONJAMASP, V.K. & BURSTEIN, S.H. (1998). Anandamide synthesis is induced by arachidonate mobilizing agonists in cells of the immune system. *Biochim Biophys Acta*, **1394,** 249-60.

PITT, D., WERNER, P. & RAINE, C.S. (2000). Glutamate excitotoxicity in a model of multiple sclerosis. *Nat Med*, **6,** 67-70.

POCHAMPALLY, R., FODERA, B., CHEN, L., LU, W. & CHEN, J. (1999). Activation of an MDM2-specific caspase by p53 in the absence of apoptosis. *J Biol Chem*, **274,** 15271-7.

POCHAMPALLY, R., FODERA, B., CHEN, L., SHAO, W., LEVINE, E.A. & CHEN, J. (1998). A 60 kd MDM2 isoform is produced by caspase cleavage in non-apoptotic tumor cells. *Oncogene*, **17,** 2629-36.

PORTER, A.C. & FELDER, C.C. (2001). The endocannabinoid nervous system: unique opportunities for therapeutic intervention. *Pharmacol Ther*, **90,** 45-60.

PORTER, A.C., SAUER, J.M., KNIERMAN, M.D., BECKER, G.W., BERNA, M.J., BAO, J., NOMIKOS, G.G., CARTER, P., BYMASTER, F.P., LEESE, A.B. & FELDER, C.C. (2002). Characterization of a novel endocannabinoid, virodhamine, with antagonist activity at the CB1 receptor. *J Pharmacol Exp Ther*, **301,** 1020-4.

PRYCE, G. & BAKER, D. (2007). Control of spasticity in a multiple sclerosis model is mediated by CB1, not CB2, cannabinoid receptors. *Br J Pharmacol*, **150,** 519-25.

QIN, S., MINAMI, Y., HIBI, M., KUROSAKI, T. & YAMAMURA, H. (1997). Syk-dependent and -independent signaling cascades in B cells elicited by osmotic and oxidative stress. *J Biol Chem*, **272,** 2098-103.

QIN, Z.H., CHEN, R.W., WANG, Y., NAKAI, M., CHUANG, D.M. & CHASE, T.N. (1999). Nuclear factor kappaB nuclear translocation upregulates c-Myc and p53 expression during NMDA receptor-mediated apoptosis in rat striatum. *J Neurosci*, **19,** 4023-33.

QUINN, R. (2005). *Comparing rat's age to human's age: How old is my rat in people years?*: Elsevier.

RAFFRAY, M. & COHEN, G.M. (1997). Apoptosis and necrosis in toxicology: a continuum or distinct modes of cell death? *Pharmacol Ther*, **75,** 153-77.

RAIVICH, G., BOHATSCHEK, M., DA COSTA, C., IWATA, O., GALIANO, M., HRISTOVA, M., NATERI, A.S., MAKWANA, M., RIERA-SANS, L., WOLFER, D.P., LIPP, H.P., AGUZZI, A., WAGNER, E.F. & BEHRENS, A. (2004). The AP-1 transcription factor c-Jun is required for efficient axonal regeneration. *Neuron*, **43,** 57-67.

RAMAEKERS, J.G., BERGHAUS, G., VAN LAAR, M. & DRUMMER, O.H. (2004). Dose related risk of motor vehicle crashes after cannabis use. *Drug Alcohol Depend*, **73,** 109-19.

RAMIREZ, B.G., BLAZQUEZ, C., GOMEZ DEL PULGAR, T., GUZMAN, M. & DE CEBALLOS, M.L. (2005). Prevention of Alzheimer's disease pathology by cannabinoids: neuroprotection mediated by blockade of microglial activation. *J Neurosci*, **25,** 1904-13.

RAVANKO, K., JARVINEN, K., HELIN, J., KALKKINEN, N. & HOLTTA, E. (2004). Cysteine cathepsins are central contributors of invasion by cultured adenosylmethionine

decarboxylase-transformed rodent fibroblasts. *Cancer Res*, **64,** 8831-8.

RAZ, A., SCHURR, A., LIVNE, A. & GOLDMAN, R. (1973). Effect of hashish compounds on rat liver lysosomes in vitro. *Biochem Pharmacol*, **22,** 3129-31.

REED, J.C. (1997). Cytochrome c: can't live with it--can't live without it. *Cell*, **91,** 559-62.

RICE, A.S., FARQUHAR-SMITH, W.P. & NAGY, I. (2002). Endocannabinoids and pain: spinal and peripheral analgesia in inflammation and neuropathy. *Prostaglandins Leukot Essent Fatty Acids*, **66,** 243-56.

RINALDI-CARMONA, M., BARTH, F., HEAULME, M., SHIRE, D., CALANDRA, B., CONGY, C., MARTINEZ, S., MARUANI, J., NELIAT, G., CAPUT, D. & ET AL. (1994). SR141716A, a potent and selective antagonist of the brain cannabinoid receptor. *FEBS Lett*, **350,** 240-4.

ROBERG, K. & OLLINGER, K. (1998). Oxidative stress causes relocation of the lysosomal enzyme cathepsin D with ensuing apoptosis in neonatal rat cardiomyocytes. *Am J Pathol*, **152,** 1151-6.

ROBERTSON, J.R., MILLER, P. & ANDERSON, R. (1996). Cannabis use in the community. *Br J Gen Pract*, **46,** 671-4.

ROBINSON, R. (1996). *The great book of hemp.*: Park street press.

RODRIGUEZ DE FONSECA, F., DEL ARCO, I., BERMUDEZ-SILVA, F.J., BILBAO, A., CIPPITELLI, A. & NAVARRO, M. (2005). The endocannabinoid system: physiology and pharmacology. *Alcohol Alcohol*, **40,** 2-14.

RODRIGUEZ DE FONSECA, F., RAMOS, J.A., BONNIN, A. & FERNANDEZ-RUIZ, J.J. (1993). Presence of cannabinoid binding sites in the brain from early postnatal ages. *Neuroreport*, **4,** 135-8.

RODRIGUEZ, M.S., DESTERRO, J.M., LAIN, S., MIDGLEY, C.A., LANE, D.P. & HAY, R.T. (1999). SUMO-1 modification activates the transcriptional response of p53. *Embo J*, **18,** 6455-61.

ROGEL, A., POPLIKER, M., WEBB, C.G. & OREN, M. (1985). p53 cellular tumor antigen: analysis of mRNA levels in normal adult tissues, embryos, and tumors. *Mol Cell Biol*, **5,** 2851-5.

ROTH, J., DOBBELSTEIN, M., FREEDMAN, D.A., SHENK, T. & LEVINE, A.J. (1998). Nucleo-

cytoplasmic shuttling of the hdm2 oncoprotein regulates the levels of the p53 protein via a pathway used by the human immunodeficiency virus rev protein. *Embo J*, **17,** 554-64.

RUBINO, T., FORLANI, G., VIGANO, D., ZIPPEL, R. & PAROLARO, D. (2004). Modulation of extracellular signal-regulated kinases cascade by chronic delta 9-tetrahydrocannabinol treatment. *Mol Cell Neurosci*, **25,** 355-62.

RUEDA, D., GALVE-ROPERH, I., HARO, A. & GUZMAN, M. (2000). The CB(1) cannabinoid receptor is coupled to the activation of c-Jun N-terminal kinase. *Mol Pharmacol*, **58,** 814-20.

RUI, H.L., FAN, E., ZHOU, H.M., XU, Z., ZHANG, Y. & LIN, S.C. (2002). SUMO-1 modification of the C-terminal KVEKVD of Axin is required for JNK activation but has no effect on Wnt signaling. *J Biol Chem*, **277,** 42981-6.

RUSSO, E. & GUY, G.W. (2006). A tale of two cannabinoids: the therapeutic rationale for combining tetrahydrocannabinol and cannabidiol. *Med Hypotheses*, **66,** 234-46.

RUSSO, P., STRAZZULLO, P., CAPPUCCIO, F.P., TREGOUET, D.A., LAURIA, F., LOGUERCIO, M., BARBA, G., VERSIERO, M. & SIANI, A. (2007). Genetic variations at the endocannabinoid type 1 receptor gene (CNR1) are associated with obesity phenotypes in men. *J Clin Endocrinol Metab*, **92,** 2382-6.

RYBERG, E., LARSSON, N., SJOGREN, S., HJORTH, S., HERMANSSON, N.O., LEONOVA, J., ELEBRING, T., NILSSON, K., DRMOTA, T. & GREASLEY, P.J. (2007). The orphan receptor GPR55 is a novel cannabinoid receptor. *Br J Pharmacol*, **152,** 1092-101.

RYBERG, E., VU, H.K., LARSSON, N., GROBLEWSKI, T., HJORTH, S., ELEBRING, T., SJOGREN, S. & GREASLEY, P.J. (2005). Identification and characterisation of a novel splice variant of the human CB1 receptor. *FEBS Lett*, **579,** 259-64.

SADA, K., TAKANO, T., YANAGI, S. & YAMAMURA, H. (2001). Structure and function of Syk protein-tyrosine kinase. *J Biochem (Tokyo)*, **130,** 177-86.

SAELENS, X., FESTJENS, N., VANDE WALLE, L., VAN GURP, M., VAN LOO, G. & VANDENABEELE, P. (2004). Toxic proteins released from mitochondria in cell death. *Oncogene*, **23,** 2861-74.

SAITOH, H. & HINCHEY, J. (2000). Functional heterogeneity of small ubiquitin-related

protein modifiers SUMO-1 versus SUMO-2/3. *J Biol Chem*, **275,** 6252-8.

SAITOH, H. & HINCHEY, J. (2000). Functional heterogeneity of small ubiquitin-related protein modifiers SUMO-1 versus SUMO-2/3. *J Biol Chem*, **275,** 6252-8.

SANCHEZ, A.J., GONZALEZ-PEREZ, P., GALVE-ROPERH, I. & GARCIA-MERINO, A. (2006). R-(+)-[2,3-Dihydro-5-methyl-3-(4-morpholinylmethyl)-pyrrolo-[1,2,3-de]-1,4 -benzoxazin-6-yl]-1-naphtalenylmethanone (WIN-2) ameliorates experimental autoimmune encephalomyelitis and induces encephalitogenic T cell apoptosis: partial involvement of the CB(2) receptor. *Biochem Pharmacol*, **72,** 1697-706.

SANCHEZ, C., GALVE-ROPERH, I., CANOVA, C., BRACHET, P. & GUZMAN, M. (1998). Delta9-tetrahydrocannabinol induces apoptosis in C6 glioma cells. *FEBS Lett*, **436,** 6-10.

SANCHEZ, C., GALVE-ROPERH, I., RUEDA, D. & GUZMAN, M. (1998). Involvement of sphingomyelin hydrolysis and the mitogen-activated protein kinase cascade in the Delta9-tetrahydrocannabinol-induced stimulation of glucose metabolism in primary astrocytes. *Mol Pharmacol*, **54,** 834-43.

SANCHO, R., CALZADO, M.A., DI MARZO, V., APPENDINO, G. & MUNOZ, E. (2003). Anandamide inhibits nuclear factor-kappaB activation through a cannabinoid receptor-independent pathway. *Mol Pharmacol*, **63,** 429-38.

SANG, N., ZHANG, J. & CHEN, C. (2007). COX-2 oxidative metabolite of endocannabinoid 2-AG enhances excitatory glutamatergic synaptic transmission and induces neurotoxicity. *J Neurochem*, **102,** 1966-77.

SARKER, K.P. & MARUYAMA, I. (2003). Anandamide induces cell death independently of cannabinoid receptors or vanilloid receptor 1: possible involvement of lipid rafts. *Cell Mol Life Sci*, **60,** 1200-8.

SARKER, K.P., OBARA, S., NAKATA, M., KITAJIMA, I. & MARUYAMA, I. (2000). Anandamide induces apoptosis of PC-12 cells: involvement of superoxide and caspase-3. *FEBS Lett*, **472,** 39-44.

SARNATARO, D., GRIMALDI, C., PISANTI, S., GAZZERRO, P., LAEZZA, C., ZURZOLO, C. & BIFULCO, M. (2005). Plasma membrane and lysosomal localization of CB1 cannabinoid receptor are dependent on lipid rafts and regulated by anandamide in human breast cancer cells. *FEBS Lett*, **579,** 6343-9.

SARNE, Y. & KEREN, O. (2004). Are cannabinoid drugs neurotoxic or neuroprotective? *Med Hypotheses*, **63,** 187-92.

SARNE, Y. & MECHOULAM, R. (2005). Cannabinoids: between neuroprotection and neurotoxicity. *Curr Drug Targets CNS Neurol Disord*, **4,** 677-84.

SAVINAINEN, J.R., SAARIO, S.M., NIEMI, R., JARVINEN, T. & LAITINEN, J.T. (2003). An optimized approach to study endocannabinoid signaling: evidence against constitutive activity of rat brain adenosine A1 and cannabinoid CB1 receptors. *Br J Pharmacol*, **140,** 1451-9.

SCALLET, A.C. (1991). Neurotoxicology of cannabis and THC: a review of chronic exposure studies in animals. *Pharmacol Biochem Behav*, **40,** 671-6.

SCALLET, A.C., UEMURA, E., ANDREWS, A., ALI, S.F., MCMILLAN, D.E., PAULE, M.G., BROWN, R.M. & SLIKKER, W., JR. (1987). Morphometric studies of the rat hippocampus following chronic delta-9-tetrahydrocannabinol (THC). *Brain Res*, **436,** 193-8.

SCHATZ, A.R., LEE, M., CONDIE, R.B., PULASKI, J.T. & KAMINSKI, N.E. (1997). Cannabinoid receptors CB1 and CB2: a characterization of expression and adenylate cyclase modulation within the immune system. *Toxicol Appl Pharmacol*, **142,** 278-87.

SCHESTKOWA, O., GEISEL, D., JACOB, R. & HASILIK, A. (2007). The catalytically inactive precursor of cathepsin D induces apoptosis in human fibroblasts and HeLa cells. *J Cell Biochem*, **101,** 1558-66.

SCHESTKOWA, O., GEISEL, D., JACOB, R. & HASILIK, A. (2007). The catalytically inactive precursor of cathepsin D induces apoptosis in human fibroblasts and HeLa cells. *J Cell Biochem*, **101,** 1558-66.

SCHLAEPFER, T.E., LANCASTER, E., HEIDBREDER, R., STRAIN, E.C., KOSEL, M., FISCH, H.U. & PEARLSON, G.D. (2006). Decreased frontal white-matter volume in chronic substance abuse. *Int J Neuropsychopharmacol*, **9,** 147-53.

SCHMID, H.H., SCHMID, P.C. & NATARAJAN, V. (1996). The N-acylation-phosphodiesterase pathway and cell signalling. *Chem Phys Lipids*, **80,** 133-42.

SCHMIDT, D. & MULLER, S. (2002). Members of the PIAS family act as SUMO ligases for c-Jun and p53 and repress p53 activity. *Proc Natl Acad Sci U S A*, **99,** 2872-

7.

SCHMITZ, I., KIRCHHOFF, S. & KRAMMER, P.H. (2000). Regulation of death receptor-mediated apoptosis pathways. *Int J Biochem Cell Biol*, **32,** 1123-36.

SCHUEL, H., BURKMAN, L.J., LIPPES, J., CRICKARD, K., MAHONY, M.C., GIUFFRIDA, A., PICONE, R.P. & MAKRIYANNIS, A. (2002). Evidence that anandamide-signaling regulates human sperm functions required for fertilization. *Mol Reprod Dev*, **63,** 376-87.

SCHWEITZER, P. (2000). Cannabinoids decrease the K(+) M-current in hippocampal CA1 neurons. *J Neurosci*, **20,** 51-8.

SHEN, M. & THAYER, S.A. (1998). The cannabinoid agonist Win55,212-2 inhibits calcium channels by receptor-mediated and direct pathways in cultured rat hippocampal neurons. *Brain Res*, **783,** 77-84.

SHEN, Z., PARDINGTON-PURTYMUN, P.E., COMEAUX, J.C., MOYZIS, R.K. & CHEN, D.J. (1996). Associations of UBE2I with RAD52, UBL1, p53, and RAD51 proteins in a yeast two-hybrid system. *Genomics*, **37,** 183-6.

SHESKIN, T., HANUS, L., SLAGER, J., VOGEL, Z. & MECHOULAM, R. (1997). Structural requirements for binding of anandamide-type compounds to the brain cannabinoid receptor. *J Med Chem*, **40,** 659-67.

SHIAH, S.G., CHUANG, S.E. & KUO, M.L. (2001). Involvement of Asp-Glu-Val-Asp-directed, caspase-mediated mitogen-activated protein kinase kinase 1 Cleavage, c-Jun N-terminal kinase activation, and subsequent Bcl-2 phosphorylation for paclitaxel-induced apoptosis in HL-60 cells. *Mol Pharmacol*, **59,** 254-62.

SHIBATA, T., IIO, K., KAWAI, Y., SHIBATA, N., KAWAGUCHI, M., TOI, S., KOBAYASHI, M., KOBAYASHI, M., YAMAMOTO, K. & UCHIDA, K. (2006). Identification of a lipid peroxidation product as a potential trigger of the p53 pathway. *J Biol Chem*, **281,** 1196-204.

SHIEH, S.Y., IKEDA, M., TAYA, Y. & PRIVES, C. (1997). DNA damage-induced phosphorylation of p53 alleviates inhibition by MDM2. *Cell*, **91,** 325-34.

SHIMASUE, K., URUSHIDANI, T., HAGIWARA, M. & NAGAO, T. (1996). Effects of anandamide and arachidonic acid on specific binding of (+) -PN200-110, diltiazem and (-) -desmethoxyverapamil to L-type Ca2+ channel. *Eur J*

Pharmacol, **296,** 347-50.

SHIN, C.Y., SHIN, J., KIM, B.M., WANG, M.H., JANG, J.H., SURH, Y.J. & OH, U. (2003). Essential role of mitochondrial permeability transition in vanilloid receptor 1-dependent cell death of sensory neurons. *Mol Cell Neurosci*, **24,** 57-68.

SHIRE, D., CARILLON, C., KAGHAD, M., CALANDRA, B., RINALDI-CARMONA, M., LE FUR, G., CAPUT, D. & FERRARA, P. (1995). An amino-terminal variant of the central cannabinoid receptor resulting from alternative splicing. *J Biol Chem*, **270,** 3726-31.

SIDORENKO, S.P., LAW, C.L., CHANDRAN, K.A. & CLARK, E.A. (1995). Human spleen tyrosine kinase p72Syk associates with the Src-family kinase p53/56Lyn and a 120-kDa phosphoprotein. *Proc Natl Acad Sci U S A*, **92,** 359-63.

SIEGMUND, S.V. & BRENNER, D.A. (2005). Molecular pathogenesis of alcohol-induced hepatic fibrosis. *Alcohol Clin Exp Res*, **29,** 102S-109S.

SIEGMUND, S.V., QIAN, T., DE MINICIS, S., HARVEY-WHITE, J., KUNOS, G., VINOD, K.Y., HUNGUND, B. & SCHWABE, R.F. (2007). The endocannabinoid 2-arachidonoyl glycerol induces death of hepatic stellate cells via mitochondrial reactive oxygen species. *Faseb J*, **21,** 2798-806.

SIM, L.J., HAMPSON, R.E., DEADWYLER, S.A. & CHILDERS, S.R. (1996). Effects of chronic treatment with delta9-tetrahydrocannabinol on cannabinoid-stimulated [35S]GTPgammaS autoradiography in rat brain. *J Neurosci*, **16,** 8057-66.

SIMON, G.M. & CRAVATT, B.F. (2006). Endocannabinoid biosynthesis proceeding through glycerophospho-N-acyl ethanolamine and a role for alpha/beta-hydrolase 4 in this pathway. *J Biol Chem*, **281,** 26465-72.

SIMONS, K. & IKONEN, E. (1997). Functional rafts in cell membranes. *Nature*, **387,** 569-72.

SINGH TAHIM, A., SANTHA, P. & NAGY, I. (2005). Inflammatory mediators convert anandamide into a potent activator of the vanilloid type 1 transient receptor potential receptor in nociceptive primary sensory neurons. *Neuroscience*, **136,** 539-48.

SINOR, A.D., IRVIN, S.M. & GREENBERG, D.A. (2000). Endocannabinoids protect cerebral cortical neurons from in vitro ischemia in rats. *Neurosci Lett*, **278,** 157-60.

SIPE, J.C., ARBOUR, N., GERBER, A. & BEUTLER, E. (2005). Reduced endocannabinoid immune modulation by a common cannabinoid 2 (CB2) receptor gene polymorphism: possible risk for autoimmune disorders. *J Leukoc Biol*, **78,** 231-8.

SJöGREN S, RYBERG E, LINDBLOM A, N, L., ASTRAND A, S, H. & ET AL. (2005). A new receptor for cannabinoid ligands. . In *Symposium on the cannabinoids*. pp. p 106. Burlington, Vermont, USA: International Cannabinoid Reasearch Society.

SLEE, E.A., HARTE, M.T., KLUCK, R.M., WOLF, B.B., CASIANO, C.A., NEWMEYER, D.D., WANG, H.G., REED, J.C., NICHOLSON, D.W., ALNEMRI, E.S., GREEN, D.R. & MARTIN, S.J. (1999). Ordering the cytochrome c-initiated caspase cascade: hierarchical activation of caspases-2, -3, -6, -7, -8, and -10 in a caspase-9-dependent manner. *J Cell Biol*, **144,** 281-92.

SMITH, F.L., CICHEWICZ, D., MARTIN, Z.L. & WELCH, S.P. (1998). The enhancement of morphine antinociception in mice by delta9-tetrahydrocannabinol. *Pharmacol Biochem Behav*, **60,** 559-66.

SMITH, I.F., GREEN, K.N. & LAFERLA, F.M. (2005). Calcium dysregulation in Alzheimer's disease: recent advances gained from genetically modified animals. *Cell Calcium*, **38,** 427-37.

SMITH, L.M., LAGASSE, L.L., DERAUF, C., GRANT, P., SHAH, R., ARRIA, A., HUESTIS, M., HANING, W., STRAUSS, A., DELLA GROTTA, S., LIU, J. & LESTER, B.M. (2006). The infant development, environment, and lifestyle study: effects of prenatal methamphetamine exposure, polydrug exposure, and poverty on intrauterine growth. *Pediatrics*, **118,** 1149-56.

SMITH, T., GROOM, A., ZHU, B. & TURSKI, L. (2000). Autoimmune encephalomyelitis ameliorated by AMPA antagonists. *Nat Med*, **6,** 62-6.

SONG, X., TANAKA, S., COX, D. & LEE, S.C. (2004). Fcgamma receptor signaling in primary human microglia: differential roles of PI-3K and Ras/ERK MAPK pathways in phagocytosis and chemokine induction. *J Leukoc Biol*, **75,** 1147-55.

SONKUSARE, S.K., KAUL, C.L. & RAMARAO, P. (2005). Dementia of Alzheimer's disease and other neurodegenerative disorders--memantine, a new hope. *Pharmacol Res*, **51,** 1-17.

STAROWICZ, K., NIGAM, S. & DI MARZO, V. (2007). Biochemistry and pharmacology of endovanilloids. *Pharmacol Ther*, **114,** 13-33.

STELLA, N. & PIOMELLI, D. (2001). Receptor-dependent formation of endogenous cannabinoids in cortical neurons. *Eur J Pharmacol*, **425,** 189-96.

STELLA, N. & PIOMELLI, D. (2001). Receptor-dependent formation of endogenous cannabinoids in cortical neurons. *Eur J Pharmacol*, **425,** 189-96.

STELLA, N., SCHWEITZER, P. & PIOMELLI, D. (1997). A second endogenous cannabinoid that modulates long-term potentiation. *Nature*, **388,** 773-8.

STRINDBERG, A. (1909). *The son of a servant: The story of the evolution of a human being*: Doubleday.

SUAREZ, I., BODEGA, G., FERNANDEZ-RUIZ, J., RAMOS, J.A., RUBIO, M. & FERNANDEZ, B. (2004). Down-regulation of the AMPA glutamate receptor subunits GluR1 and GluR2/3 in the rat cerebellum following pre- and perinatal delta9-tetrahydrocannabinol exposure. *Cerebellum*, **3,** 66-74.

SUAREZ, I., BODEGA, G., FERNANDEZ-RUIZ, J.J., RAMOS, J.A., RUBIO, M. & FERNANDEZ, B. (2002). Reduced glial fibrillary acidic protein and glutamine synthetase expression in astrocytes and Bergmann glial cells in the rat cerebellum caused by delta(9)-tetrahydrocannabinol administration during development. *Dev Neurosci*, **24,** 300-12.

SUAREZ, I., BODEGA, G., RUBIO, M., FERNANDEZ-RUIZ, J.J., RAMOS, J.A. & FERNANDEZ, B. (2004). Prenatal cannabinoid exposure down- regulates glutamate transporter expressions (GLAST and EAAC1) in the rat cerebellum. *Dev Neurosci*, **26,** 45-53.

SUGIURA, T. (2007). Biosynthesis of anandamide and 2-arachidonoylglycerol. In *Cannabinoids and the brain*. ed. Kofalvi, A.: Springer-Verlag.

SUGIURA, T., KISHIMOTO, S., OKA, S. & GOKOH, M. (2006). Biochemistry, pharmacology and physiology of 2-arachidonoylglycerol, an endogenous cannabinoid receptor ligand. *Prog Lipid Res*, **45,** 405-46.

SUGIURA, T., KOBAYASHI, Y., OKA, S. & WAKU, K. (2002). Biosynthesis and degradation of anandamide and 2-arachidonoylglycerol and their possible physiological significance. *Prostaglandins Leukot Essent Fatty Acids*, **66,** 173-92.

SUGIURA, T., KODAKA, T., KONDO, S., TONEGAWA, T., NAKANE, S., KISHIMOTO, S., YAMASHITA, A. & WAKU, K. (1996). 2-Arachidonoylglycerol, a putative endogenous cannabinoid receptor ligand, induces rapid, transient elevation of intracellular free Ca2+ in neuroblastoma x glioma hybrid NG108-15 cells. *Biochem Biophys Res Commun*, **229,** 58-64.

SUGIURA, T., KONDO, S., SUKAGAWA, A., NAKANE, S., SHINODA, A., ITOH, K., YAMASHITA, A. & WAKU, K. (1995). 2-Arachidonoylglycerol: a possible endogenous cannabinoid receptor ligand in brain. *Biochem Biophys Res Commun*, **215,** 89-97.

SZOKE, E., CZEH, G., SZOLCSANYI, J. & SERESS, L. (2002). Neonatal anandamide treatment results in prolonged mitochondrial damage in the vanilloid receptor type 1-immunoreactive B-type neurons of the rat trigeminal ganglion. *Neuroscience*, **115,** 805-14.

TAKAHASHI-FUJIGASAKI, J., ARAI, K., FUNATA, N. & FUJIGASAKI, H. (2006). SUMOylation substrates in neuronal intranuclear inclusion disease. *Neuropathol Appl Neurobiol*, **32,** 92-100.

TAN, Z., SANKAR, R., TU, W., SHIN, D., LIU, H., WASTERLAIN, C.G. & SCHREIBER, S.S. (2002). Immunohistochemical study of p53-associated proteins in rat brain following lithium-pilocarpine status epilepticus. *Brain Res*, **929,** 129-38.

TANIGUCHI, T., KOBAYASHI, T., KONDO, J., TAKAHASHI, K., NAKAMURA, H., SUZUKI, J., NAGAI, K., YAMADA, T., NAKAMURA, S. & YAMAMURA, H. (1991). Molecular cloning of a porcine gene syk that encodes a 72-kDa protein-tyrosine kinase showing high susceptibility to proteolysis. *J Biol Chem*, **266,** 15790-6.

TARDY, C., CODOGNO, P., AUTEFAGE, H., LEVADE, T. & ANDRIEU-ABADIE, N. (2006). Lysosomes and lysosomal proteins in cancer cell death (new players of an old struggle). *Biochim Biophys Acta*, **1765,** 101-25.

TELEK, A., BIRO, T., BODO, E., TOTH, B.I., BORBIRO, I., KUNOS, G. & PAUS, R. (2007). Inhibition of human hair follicle growth by endo- and exocannabinoids. *Faseb J.*

TERMAN, A., GUSTAFSSON, B. & BRUNK, U.T. (2006). The lysosomal-mitochondrial axis theory of postmitotic aging and cell death. *Chem Biol Interact*, **163,** 29-37.

TERRANOVA, J.P., MICHAUD, J.C., LE FUR, G. & SOUBRIE, P. (1995). Inhibition of long-

term potentiation in rat hippocampal slices by anandamide and WIN55212-2: reversal by SR141716 A, a selective antagonist of CB1 cannabinoid receptors. *Naunyn Schmiedebergs Arch Pharmacol*, **352,** 576-9.

TOKUMOTO, Y.M., TANG, D.G. & RAFF, M.C. (2001). Two molecularly distinct intracellular pathways to oligodendrocyte differentiation: role of a p53 family protein. *Embo J*, **20,** 5261-8.

TSELNICKER, I., KEREN, O., HEFETZ, A., PICK, C.G. & SARNE, Y. (2007). A single low dose of tetrahydrocannabinol induces long-term cognitive deficits. *Neurosci Lett*, **411,** 108-11.

TSOU, K., NOGUERON, M.I., MUTHIAN, S., SANUDO-PENA, M.C., HILLARD, C.J., DEUTSCH, D.G. & WALKER, J.M. (1998). Fatty acid amide hydrolase is located preferentially in large neurons in the rat central nervous system as revealed by immunohistochemistry. *Neurosci Lett*, **254,** 137-40.

TSUJIMURA, T., YANAGI, S., INATOME, R., TAKANO, T., ISHIHARA, I., MITSUI, N., TAKAHASHI, S. & YAMAMURA, H. (2001). Syk protein-tyrosine kinase is involved in neuron-like differentiation of embryonal carcinoma P19 cells. *FEBS Lett*, **489,** 129-33.

TSUTSUMI, T., KOBAYASHI, T., UEDA, H., YAMAUCHI, E., WATANABE, S. & OKUYAMA, H. (1994). Lysophosphoinositide-specific phospholipase C in rat brain synaptic plasma membranes. *Neurochem Res*, **19,** 399-406.

TURK, B., STOKA, V., ROZMAN-PUNGERCAR, J., CIRMAN, T., DROGA-MAZOVEC, G., ORESIC, K. & TURK, V. (2002). Apoptotic pathways: involvement of lysosomal proteases. *Biol Chem*, **383,** 1035-44.

TURK, B., TURK, V. & TURK, D. (1997). Structural and functional aspects of papain-like cysteine proteinases and their protein inhibitors. *Biol Chem*, **378,** 141-50.

TURNER, M., SCHWEIGHOFFER, E., COLUCCI, F., DI SANTO, J.P. & TYBULEWICZ, V.L. (2000). Tyrosine kinase SYK: essential functions for immunoreceptor signalling. *Immunol Today*, **21,** 148-54.

TZILOS, G.K., CINTRON, C.B., WOOD, J.B., SIMPSON, N.S., YOUNG, A.D., POPE, H.G., JR. & YURGELUN-TODD, D.A. (2005). Lack of hippocampal volume change in long-term heavy cannabis users. *Am J Addict*, **14,** 64-72.

UEDA, N., KURAHASHI, Y., YAMAMOTO, S. & TOKUNAGA, T. (1995). Partial purification and characterization of the porcine brain enzyme hydrolyzing and synthesizing anandamide. *J Biol Chem*, **270,** 23823-7.

UNGER, T., JUVEN-GERSHON, T., MOALLEM, E., BERGER, M., VOGT SIONOV, R., LOZANO, G., OREN, M. & HAUPT, Y. (1999). Critical role for Ser20 of human p53 in the negative regulation of p53 by Mdm2. *Embo J*, **18,** 1805-14.

VALJENT, E., PAGES, C., ROGARD, M., BESSON, M.J., MALDONADO, R. & CABOCHE, J. (2001). Delta 9-tetrahydrocannabinol-induced MAPK/ERK and Elk-1 activation in vivo depends on dopaminergic transmission. *Eur J Neurosci*, **14,** 342-52.

VAN DER STELT, M., HANSEN, H.H., VELDHUIS, W.B., BAR, P.R., NICOLAY, K., VELDINK, G.A., VLIEGENTHART, J.F. & HANSEN, H.S. (2003). Biosynthesis of endocannabinoids and their modes of action in neurodegenerative diseases. *Neurotox Res*, **5,** 183-200.

VAN DER STELT, M., MAZZOLA, C., ESPOSITO, G., MATIAS, I., PETROSINO, S., DE FILIPPIS, D., MICALE, V., STEARDO, L., DRAGO, F., IUVONE, T. & DI MARZO, V. (2006). Endocannabinoids and beta-amyloid-induced neurotoxicity in vivo: effect of pharmacological elevation of endocannabinoid levels. *Cell Mol Life Sci*, **63,** 1410-24.

VAN DER STELT, M., VELDHUIS, W.B., VAN HAAFTEN, G.W., FEZZA, F., BISOGNO, T., BAR, P.R., VELDINK, G.A., VLIEGENTHART, J.F., DI MARZO, V. & NICOLAY, K. (2001). Exogenous anandamide protects rat brain against acute neuronal injury in vivo. *J Neurosci*, **21,** 8765-71.

VAN SICKLE, M.D., DUNCAN, M., KINGSLEY, P.J., MOUIHATE, A., URBANI, P., MACKIE, K., STELLA, N., MAKRIYANNIS, A., PIOMELLI, D., DAVISON, J.S., MARNETT, L.J., DI MARZO, V., PITTMAN, Q.J., PATEL, K.D. & SHARKEY, K.A. (2005). Identification and functional characterization of brainstem cannabinoid CB2 receptors. *Science*, **310,** 329-32.

VANCOMPERNOLLE, K., VAN HERREWEGHE, F., PYNAERT, G., VAN DE CRAEN, M., DE VOS, K., TOTTY, N., STERLING, A., FIERS, W., VANDENABEELE, P. & GROOTEN, J. (1998). Atractyloside-induced release of cathepsin B, a protease with caspase-processing activity. *FEBS Lett*, **438,** 150-8.

VENANCE, L., PIOMELLI, D., GLOWINSKI, J. & GIAUME, C. (1995). Inhibition by anandamide of gap junctions and intercellular calcium signalling in striatal astrocytes. *Nature*, **376,** 590-4.

VIJAY-KUMAR, S., BUGG, C.E. & COOK, W.J. (1987). Structure of ubiquitin refined at 1.8 A resolution. *J Mol Biol*, **194,** 531-44.

VOGEL, Z., BARG, J., LEVY, R., SAYA, D., HELDMAN, E. & MECHOULAM, R. (1993). Anandamide, a brain endogenous compound, interacts specifically with cannabinoid receptors and inhibits adenylate cyclase. *J Neurochem*, **61,** 352-5.

VON LINNE, C. (1753). *Species Plantarum*. Uppsala.

WAGER-MILLER, J., WESTENBROEK, R. & MACKIE, K. (2002). Dimerization of G protein-coupled receptors: CB1 cannabinoid receptors as an example. *Chem Phys Lipids*, **121,** 83-9.

WANG, H., XIE, H. & DEY, S.K. (2006). Endocannabinoid signaling directs periimplantation events. *Aaps J*, **8,** E425-32.

WATSON, I.R. & IRWIN, M.S. (2006). Ubiquitin and ubiquitin-like modifications of the p53 family. *Neoplasia*, **8,** 655-66.

WESIERSKA-GADEK, J., GUEORGUIEVA, M. & HORKY, M. (2005). Roscovitine-induced up-regulation of p53AIP1 protein precedes the onset of apoptosis in human MCF-7 breast cancer cells. *Mol Cancer Ther*, **4,** 113-24.

WILLIAMS, E.J., WALSH, F.S. & DOHERTY, P. (2003). The FGF receptor uses the endocannabinoid signaling system to couple to an axonal growth response. *J Cell Biol*, **160,** 481-6.

WILSON, P.D., FIRESTONE, R.A. & LENARD, J. (1987). The role of lysosomal enzymes in killing of mammalian cells by the lysosomotropic detergent N-dodecylimidazole. *J Cell Biol*, **104,** 1223-9.

WILSON, R.I. & NICOLL, R.A. (2001). Endogenous cannabinoids mediate retrograde signalling at hippocampal synapses. *Nature*, **410,** 588-92.

WILSON, R.I. & NICOLL, R.A. (2002). Endocannabinoid signaling in the brain. *Science*, **296,** 678-82.

WU, G.S. (2004). The functional interactions between the p53 and MAPK signaling pathways. *Cancer Biol Ther*, **3,** 156-61.

WYLLIE, A.H. (1987). Apoptosis: cell death under homeostatic control. *Arch Toxicol Suppl*, **11,** 3-10.

XIANG, H., HOCHMAN, D.W., SAYA, H., FUJIWARA, T., SCHWARTZKROIN, P.A. & MORRISON, R.S. (1996). Evidence for p53-mediated modulation of neuronal viability. *J Neurosci*, **16,** 6753-65.

YAMASHIMA, T., KOHDA, Y., TSUCHIYA, K., UENO, T., YAMASHITA, J., YOSHIOKA, T. & KOMINAMI, E. (1998). Inhibition of ischaemic hippocampal neuronal death in primates with cathepsin B inhibitor CA-074: a novel strategy for neuroprotection based on 'calpain-cathepsin hypothesis'. *Eur J Neurosci*, **10,** 1723-33.

YANAGI, S., INATOME, R., TAKANO, T. & YAMAMURA, H. (2001). Syk expression and novel function in a wide variety of tissues. *Biochem Biophys Res Commun*, **288,** 495-8.

YESAVAGE, J.A., LEIRER, V.O., DENARI, M. & HOLLISTER, L.E. (1985). Carry-over effects of marijuana intoxication on aircraft pilot performance: a preliminary report. *Am J Psychiatry*, **142,** 1325-9.

YUAN, J., SHAHAM, S., LEDOUX, S., ELLIS, H.M. & HORVITZ, H.R. (1993). The C. elegans cell death gene ced-3 encodes a protein similar to mammalian interleukin-1 beta-converting enzyme. *Cell*, **75,** 641-52.

YUAN, X.M., LI, W., DALEN, H., LOTEM, J., KAMA, R., SACHS, L. & BRUNK, U.T. (2002). Lysosomal destabilization in p53-induced apoptosis. *Proc Natl Acad Sci U S A*, **99,** 6286-91.

ZDOLSEK, J., ZHANG, H., ROBERG, K. & BRUNK, U. (1993). H2O2-mediated damage to lysosomal membranes of J-774 cells. *Free Radic Res Commun*, **18,** 71-85.

ZDOLSEK, J.M. & SVENSSON, I. (1993). Effect of reactive oxygen species on lysosomal membrane integrity. A study on a lysosomal fraction. *Virchows Arch B Cell Pathol Incl Mol Pathol*, **64,** 401-6.

ZERBINI, L.F., WANG, Y., CORREA, R.G., CHO, J.Y. & LIBERMANN, T.A. (2005). Blockage of NF-kappaB induces serine 15 phosphorylation of mutant p53 by JNK kinase in prostate cancer cells. *Cell Cycle*, **4,** 1247-53.

ZHANG, P.W., ISHIGURO, H., OHTSUKI, T., HESS, J., CARILLO, F., WALTHER, D., ONAIVI,

E.S., Arinami, T. & Uhl, G.R. (2004). Human cannabinoid receptor 1: 5' exons, candidate regulatory regions, polymorphisms, haplotypes and association with polysubstance abuse. *Mol Psychiatry*, **9,** 916-31.

Zhang, T. & Prives, C. (2001). Cyclin a-CDK phosphorylation regulates MDM2 protein interactions. *J Biol Chem*, **276,** 29702-10.

Zhao, M., Antunes, F., Eaton, J.W. & Brunk, U.T. (2003). Lysosomal enzymes promote mitochondrial oxidant production, cytochrome c release and apoptosis. *Eur J Biochem*, **270,** 3778-86.

Zhao, M., Brunk, U.T. & Eaton, J.W. (2001). Delayed oxidant-induced cell death involves activation of phospholipase A2. *FEBS Lett*, **509,** 399-404.

Zhou, F., Hu, J., Ma, H., Harrison, M.L. & Geahlen, R.L. (2006). Nucleocytoplasmic trafficking of the Syk protein tyrosine kinase. *Mol Cell Biol*, **26,** 3478-91.

Zhou, W., Ryan, J.J. & Zhou, H. (2004). Global analyses of sumoylated proteins in Saccharomyces cerevisiae. Induction of protein sumoylation by cellular stresses. *J Biol Chem*, **279,** 32262-8.

Zhu, X., Yu, Q.S., Cutler, R.G., Culmsee, C.W., Holloway, H.W., Lahiri, D.K., Mattson, M.P. & Greig, N.H. (2002). Novel p53 inactivators with neuroprotective action: syntheses and pharmacological evaluation of 2-imino-2,3,4,5,6,7-hexahydrobenzothiazole and 2-imino-2,3,4,5,6,7-hexahydrobenzoxazole derivatives. *J Med Chem*, **45,** 5090-7.

Zhuang, S., Kittler, J., Grigorenko, E.V., Kirby, M.T., Sim, L.J., Hampson, R.E., Childers, S.R. & Deadwyler, S.A. (1998). Effects of long-term exposure to delta9-THC on expression of cannabinoid receptor (CB1) mRNA in different rat brain regions. *Brain Res Mol Brain Res*, **62,** 141-9.

Ziemssen, T. & Ziemssen, F. (2005). The role of the humoral immune system in multiple sclerosis (MS) and its animal model experimental autoimmune encephalomyelitis (EAE). *Autoimmun Rev*, **4,** 460-7.

Zioncheck, T.F., Harrison, M.L., Isaacson, C.C. & Geahlen, R.L. (1988). Generation of an active protein-tyrosine kinase from lymphocytes by proteolysis. *J Biol Chem*, **263,** 19195-202.

Zornig, M., Hueber, A., Baum, W. & Evan, G. (2001). Apoptosis regulators and their

role in tumorigenesis. *Biochim Biophys Acta*, **1551,** F1-37.

ZOU, L., SATO, N. & KONE, B.C. (2004). Alpha-melanocyte stimulating hormone protects against H2O2-induced inhibition of wound restitution in IEC-6 cells via a Syk kinase- and NF-kappabeta-dependent mechanism. *Shock*, **22,** 453-9.

ZUZARTE-LUIS, V., MONTERO, J.A., TORRE-PEREZ, N., GARCIA-PORRERO, J.A. & HURLE, J.M. (2007). Cathepsin D gene expression outlines the areas of physiological cell death during embryonic development. *Dev Dyn*, **236,** 880-5.

VIII Appendix I - solutions

Cell culture solutions

70% EtOH (1 litre)

700 ml EtOH

300 ml dH_2O

1XPBS (1 litre)

100 ml Dulbecco's modified phosphate buffered saline

900 ml ddH_2O

Trypsin inhibitor solution

Soyabean trypsin inhibitor (0.03 mg/ml)

DNase (0.02 mg/ml)

$MgSO_4$ (0.1 M)

10 ml 1XPBS

Supplemented neurobasal solution (day of neuronal prep; 500 ml final volume)

Heat inactivated horse serum (50 ml)

Penicillin/streptomycin (100 U/ml)

Glutamax (2 mM)

B27 (1%)

Neurobasal medium (440 ml)

Supplemented neurobasal solution (day 3-antimitotic)

Heat inactivated horse serum (50 ml)

Penicillin/streptomycin (100 U/ml)

Glutamax (2 mM)

ARA-C (5 ng/ml)

Neurobasal medium (440 ml)

Cell harvesting solutions

Lysis buffer, pH 7.4 (harvesting total protein)

HEPES (25 mM)

$MgCl_2$ (5 mM)

Dithiothreitol (5 mM)

EDTA (5 mM)

PMSF (2 mM)

Leupeptin (10 μg/ml)

Pepstatin (6.25 μg/ml)

Aprotinin (10 μg/ml)

Immunoprecipitation harvesting buffer pH 6.7

Tris-HCl (0.15 M)

SDS (5%)

Glycerol (30%)

Nonidet P-40 (0.5%)

Complete protease inhibitor cocktail

Immunoprecipitation wash buffer pH 8.0

Tris-HCl (50 mM)

NaCl (150 mM)

NP-40 (1%)

SDS-PAGE solutions

Tris buffered saline-Tween (TBS-Tween), pH 7.4

Tris-HCl (20 mM)

NaCl (150 mM)

Tween 20 (0.1%)

Sample Buffer, pH 6.8

Tris-HCl

Glycerol

SDS (10%)

β-Mercaptoethnanol

Bromophenol blue

Immunoprecipitation reducing buffer pH 6.5

Tris-Base (25 mM)

DTT (50 mM)

SDS (6%)

Glycerol (10%)

Bromophenol blue (0.05%)

Stacking gel (4% pH 6.8)

Acrylamide/bis-acrylamide (30% stock, 13% (v/v))

dH_2O 60%

Tris-NaCl (0.5 mM)

SDS (2% (w/v))

APS (0.5% (w/v))

TEMED (0.5% (v/v))

Separating gel (10% pH 8.8)

Acrylamide/bis-acrylamide (30% stock, 13% (v/v))

dH_2O 40%

Tris-NaCl (0.5 mM)

SDS (2% (w/v))

APS (0.5% (w/v))

TEMED (0.5% (v/v))

Stacking gel (12% pH 8.8)

Acrylamide/bis-acrylamide (30% stock, 13% (v/v))

dH_2O 33%

Tris-NaCl (0.5 mM)

SDS (2% (w/v))

APS (0.5% (w/v))

TEMED (0.5% (v/v))

Electrode running buffer

Tris-Base (25 mM)

Glycine (200 mM)

SDS (0.1 %)

Transfer buffer

Tris-Base (25 mM)

Glycine (192 mM)

SDS (0.05%)

MeOH (20%)

Immunoprecipitation nitrocellulose membrane wash buffer pH 7.3

Tris-HCl (25 mM)

NaCl (0.15 M)

Tween-20 (0.1%)

Fluorogenic assay solution

Lysis buffer (cathepsin-L assay, pH 5)

NaOAc (20 mM)

EDTA (4 mM)

DTT (8 mM)

Urea (4 M)

Incubation buffer (cathepsin-L assay, pH 5)

HEPES (100 mM)

DTT (5 mM)

Lysis buffer (caspase-3 assay, pH 7.4)

HEPES (25 mM)

$MgCl_2$ (5 mM)

Dithiothreitol (5 mM)

EDTA (5 mM)

PMSF (2 mM)

Leupeptin (10 μg/ml)

Pepstatin (6.25 μg/ml)

Aprotinin (10 μg/ml)

Incubation buffer (caspase-3 assay, pH 7.4)

HEPES (50 mM)

Dithiothreitol (10 mM)

Glycerol (20% (v/v))

IX Publications

Abstracts

Henstridge C., Gowran A., Campbell V.A., Irving A., Pro-apoptotic actions of CB_1 receptor antagonist AM 251 in cultured cerebellar granule cells (2007), 17th Symposium on the Cannabinoids, Cannada, The International Cannabinoid Research Society.

Gowran A., Downer E.J., Campbell V.A., The role of p53 in Δ^9-Tetrahydrocannabinol-induced neuronal apoptosis, 2007, 19th National meeting of The British Neuroscience Association, England.

Gowran A., Campbell V.A., Lysosomal dynamics in Δ^9-Tetrahydrocannabinol-induced apoptosis in rat cortical neurons (2006), 16th Symposium on the Cannabinoids-Hungary, The International Cannabinoid Research Society.

Gowran A., Downer E.J., Campbell V.A., Molecular mechanisms of cannabinoid-induced neurotoxicity in rat cortical neurons (2006), The Journal of the European College of Neuropsychopharmacology, France, Volume 16, supplement 1, S26.

Papers

Gowran A, Campbell VA, (2008), A role for p53 in the regulation of lysosomal permeability by Delta(9)-tetrahydrocannabinol in rat cortical neurones: implications for neurodegeneration, J Neurochem, **105**, 1513-1524.

Campbell VA, Gowran A, (2007), Alzheimer's disease; taking the edge off with cannabinoids? *Br J Pharmacol,* **152,** 655-662.

Downer E.J, Gowran A, Campbell VA, (2007), A comparison of the apoptotic effect of Delta(9)-tetrahydrocannabinol in the neonatal and adult rat cerebral cortex. *Brain Res*, **1175,** 39-47.

Downer EJ, Gowran A, Murphy AC, Campbell VA, (2007), The tumour suppressor protein, p53, is involved in the activation of the apoptotic cascade by Delta(9)-tetrahydrocannabinol in cultured cortical neurons. Eur J Pharmacol, **564,** 57-65.

JOURNAL OF NEUROCHEMISTRY | 2008 | 105 | 1513–1524 doi: 10.1111/j.1471-4159.2008.05278.x

A role for p53 in the regulation of lysosomal permeability by Δ^9-tetrahydrocannabinol in rat cortical neurones: implications for neurodegeneration

Aoife Gowran and Veronica A. Campbell

Department of Physiology and Trinity College Institute of Neuroscience, Trinity College, Dublin, Ireland

Abstract

The psychoactive ingredient of marijuana, Δ^9-tetrahydrocannabinol (Δ^9-THC), can evoke apoptosis in cultured cortical neurones. Whilst the intracellular mechanisms responsible for this apoptotic pathway remain to be fully elucidated, we have recently identified a role for the CB_1 type of cannabinoid (CB) receptor and the tumour suppressor protein, p53. In the current study, we demonstrate the Δ^9-THC promotes a significant increase in lysosomal permeability in a dose- and time-dependent manner. The increase in lysosomal permeability was blocked by the CB_1 receptor antagonist, AM251. Δ^9-THC increased the localization of phospho-p53Ser15 at the lysosome and stimulated the release of the lysosomal cathepsin enzyme, cathepsin-D, into the cytosol. The p53 inhibitor, pifithrin-α and small interfering RNA-mediated knockdown of p53 prevented the Δ^9-THC-mediated increase in lysosomal permeability. Furthermore, the Δ^9-THC -mediated induction of apoptosis was abrogated by a cell-permeable cathepsin-D inhibitor (10 μM). Thus, the study demonstrates that Δ^9-THC impacts on the lysosomal system, via p53, to evoke lysosomal instability as an early event in the apoptotic cascade. This provides evidence for a novel link between the CB_1 receptor and the lysosomal branch of the apoptotic pathway which is crucial in regulating neuronal viability following exposure to Δ^9-THC.

Keywords: Δ^9-tetrahydrocannabinol, lysosomes, neuron, p53, apoptosis.

J. Neurochem. (2008) **105**, 1513–1524.

Δ^9-Tetrahydrocannabinol (Δ^9-THC) is the psychoactive ingredient of the cannabis plant, *Cannabis sativa* (marijuana). Δ^9-THC exerts its effect on the CNS by activating the G protein-coupled cannabinoid (CB_1) receptor, which is widely distributed in the brain (Herkenham *et al.* 1991), and is linked to activation of a number of signal transduction pathways including extracellular-regulated protein kinase (Derkinderen *et al.* 2003), stress-activated protein kinases (Downer *et al.* 2003) and sphingomyelinase (Blázquez *et al.* 2003). CB_1 receptor activation is involved in the physiological control of synaptic activity (Carlson *et al.* 2002), motor function (Kishimoto and Kano 2006), as well as feeding, appetite and pain perception (Fride 2005).

Marijuana is a commonly used drug of abuse that induces euphoria (Ameri 1999), although the detrimental effects of the drug include memory impairments (Ranganathan and De Souza 2006) and an increased risk of psychosis (Moore *et al.* 2007). Although the potential neurotoxicity of marijuana is poorly defined, chronic recreational use has been linked with morphological changes in brain structures that are indicative of toxicity (Scallet 1991; Lawston *et al.* 2000). Functional magnetic resonance imaging studies have shown a reduction in frontal white-matter volume in cannabis abusers (Schlaepfer *et al.* 2006) and heavy marijuana users are found to have reduced grey matter in the parahippocampal gyrus and reduced white matter in the left parietal lobe (Matochik *et al.* 2005). Some of the deleterious effects of marijuana may be related to alterations in pathways associated with neurogenesis, synaptogenesis and wiring (Harkany *et al.* 2007), impaired myelination (Schlaepfer *et al.* 2006) or possibly aberrant neuronal death. The impact of CBs on neuronal viability is controversial with both neuroprotective and neurotoxic effects having been reported. Thus, in cultured

Received November 8, 2007; revised manuscript received January 21, 2008; accepted January 21, 2008.

Address correspondence and reprint requests to Professor Veronica A. Campbell, Department of Physiology & Trinity College Institute of Neuroscience, Trinity College Dublin, Dublin 2, Ireland.
E-mail: vacmpbll@tcd.ie

Abbreviations used: Δ^9-THC, Δ^9-tetrahydrocannabinol; AM251, 1-(2,4-dichlorophenyl)-5-(4-iodophenyl]])-4-methyl-*N*-(1-piperidyl)pyrazole-3-carboxamide; AO, acridine orange; CB, cannabinoid; DTT, dithiothreitol; PBS, phosphate-buffered saline; siRNA, small interfering RNA; TdT, terminal deoxynucleotidyl transferase.

neurones (Chan *et al.* 1998; Campbell 2001; Downer *et al.* 2003) and glioma cells (Galve-Roperh *et al.* 2000), Δ^9-THC evokes apoptosis via activation of c-jun N terminal kinase and formation of ceramide respectively. However, Δ^9-THC also protects neurones against excitotoxicity both *in vitro* (Gilbert *et al.* 2007) and *in vivo* (Raman *et al.* 2004) and has antioxidant (Hampson *et al.* 1998) and anti-inflammatory (Lyman *et al.* 1989) actions in the brain which may mediate neuroprotection (Campbell and Gowran 2007). The impact of CBs on neuronal fate is possibly determined by the stage of neuronal development as the neonatal brain is more vulnerable than the adult brain to the neurotoxic actions of Δ^9-THC (Downer *et al.* 2007a) and such toxicity may contribute to the deficits in neuronal function that are observed following prenatal exposure to cannabis (Fried and Smith 2001).

Apoptosis is a programmed form of cell death which is essential for brain development, although excessive apoptosis is a feature of neurodegenerative disease (Blomgren *et al.* 2007). The apoptotic pathway involves the translocation of mitochondrial cytochrome *c* into the cytosol with a subsequent activation of a caspase protease cascade (Slee *et al.* 1999). Indeed, we have previously shown that exposure of cultured cortical neurones to Δ^9-THC causes cytochrome *c* release and caspase 3 activation with a subsequent demise of the cell (Campbell 2001). Modulation of intracellular organelles is a common phenomenum during apoptosis but, whilst most studies focus on the mitochondrial regulation of apoptosis, several reports have indicated a role for lysosomes in early apoptotic events (Kågedal *et al.* 2001; Mathiasen and Jäättelä 2002; Stoka *et al.* 2007). Destabilization of the lysosomal membrane and translocation of lysosomal cathepsin enzymes from the lysosomal compartment to the cytosol have been reported as upstream apoptotic events induced by various stimuli such as synthetic retinoids (Zang *et al.* 2001), oxidative stress (Roberg and Ollinger 1998; Antunes *et al.* 2001), staurosporine (Kågedal *et al.* 2001), and over-expression of the tumour suppressor protein, p53 (Yuan *et al.* 2002). The mechanisms that control lysosomal permeability during apoptosis are ill-defined but over-expression of Bcl-2 can inhibit lysosomal-dependent apoptosis by stabilizing the lysosome (Zhao *et al.* 2001) and the pro-apoptotic member of the Bcl-family protein member, Bax, can insert into the lysosomal membrane to promote the release of lysosomal enzymes during staurosporine-induced apoptosis (Kågedal *et al.* 2001). Thus, members of the Bcl-family of proteins, classically associated with regulating the mitochondrial branch of apoptosis, also appear to influence lysosomal events associated with apoptosis. The reports that p53 induces lysosomal destabilization (Yuan *et al.* 2002) is of particular interest given that we have recently reported that p53 is instrumental in inducing Δ^9-THC-mediated apoptosis in cultured neurones (Downer *et al.* 2007b). In the current study, we examined the influence of Δ^9-THC on lysosomal membrane permeability and the association of p53 with lysosomes, as well as the role of lysosomal cathepsin proteases in mediating Δ^9-THC-induced apoptosis. The findings demonstrate that the neuronal lysosomal system is a novel target for modulation by CBs and that this interaction is pertinent in the CB-mediated induction of neuronal apoptosis.

Materials and methods

Culture of cortical neurones

Primary cortical neurones were established as we have previously described (MacManus *et al.* 2000). Rats were decapitated in accordance with Institutional and National Ethical Guidelines and cerebral cortices were removed. The dissected cortices were incubated in phosphate-buffered saline (PBS) containing trypsin (0.3%) for 25 min at 37°C. The tissue was then triturated (5×) in PBS containing soyabean trypsin inhibitor (0.1%) and Dnase (0.2 mg/mL) and gently filtered through a sterile mesh filter. Following centrifugation, 2000 *g* for 3 min at 20°C, the pellet was resuspended in neurobasal medium, supplemented with heat-inactivated horse serum (10%), penicillin (100 U/mL), streptomycin (100 U/mL) and glutamax (2 mM). Suspended cells were plated out at a density of 0.25×10^6 cells on circular 10 mm diameter coverslips, coated with poly-L-lysine (60 μg/mL) and incubated in a humidified atmosphere containing 5% CO_2 : 95% air at 37°C. After 48 h, 5 ng/mL cytosine-arabino-furanoside was included in the culture medium to prevent proliferation of non-neuronal cells. Culture media were exchanged every 3 days and cells were grown in culture for 7 days prior to Δ^9-THC treatment.

Drug treatment

Δ^9-Tetrahydrocannabinol was obtained under license from Sigma-Aldrich Company Ltd. (St. Louis, MO, USA) and diluted to the required concentration with warmed culture media. Absolute alcohol was used as vehicle control. In some experiments, cells were incubated with the CB_1 receptor antagonist, AM251 (1-(2,4-dichlorophenyl)-5-(4-iodophenyl]])-4-methyl-*N*-(1-piperidyl)pyrazole-3-carboxamide; 10 μM) for 30 min prior to Δ^9-THC treatment as previously described (Downer *et al.* 2003). The p53 inhibitor, pifithrin-α (Calbiochem, Darmstadt, Germany) was made up as a 1 mM stock in dimethylsulphoxide and diluted to a final concentration of 100 nM in culture medium. Cells were exposed to pifithrin-α for 60 min prior to Δ^9-THC treatment. Pifithrin-α is a cell permeable highly lipophilic molecule that efficiently inhibits p53 phosphorylation (Chua *et al.* 2006) and p53-dependent transactivation of p53-responsive genes (Culmsee *et al.* 2001). The cell-permeable cathepsin-D inhibitor octapeptide, H-Gly-Glu-Gly-Phe-Leu-Gly-D-Phe-Leu-OH (Bachem, St. Helens, UK) was stored at −20°C as a 5 mM stock solution in dimethylsulphoxide, and was used at a final concentration of 10 μM. Cells were pre-treated with the cathepsin-D inhibitor for 30 min before exposure to Δ^9-THC.

RNA interference

Custom ON-TARGET plus smart pool small interfering RNA (siRNA) containing a mixture of four SMART selection designed siRNAs targeting rat p53 (GenBank™ accession number

NM_030989; p53 siRNA) was purchased from Dharmacon (Chicago, IL, USA). Primary cortical neurones were transfected with p53 siRNA (100 nM) using Dharmacon transfection lipid number 3. After 48 h of transfection, cells were treated with THC (5 μM) or vehicle (0.006% ethanol). A control siRNA duplex containing at least four mismatches to any rat gene (ON-TARGET Plus siControl Non-Targeting siRNA; Con siRNA) was used in parallel experiments. Optimal transfection efficiency and conditions were determined by using carboxyfluorescein-labelled non-specific siRNA (SiGlo green; Dharmacon). Effective p53 knockdown was analysed using immunocytochemistry and western immunoblot as we have previously described (Downer *et al.* 2007b).

Lysosomal localization of phospho-p53

The fluorescent probe, LysoTracker Red (Molecular Probes, Leiden, The Netherlands) was used to visualize lysosomes in intact cells. Cells were exposed to pre-warmed neurobasal medium containing LysoTracker Red (700 nM) for 25 min prior to exposure to Δ^9-THC. Cells were then fixed with *p*-formaldehyde (4%) for 30 min at 37°C, permeabilized with Triton X-100 (0.2%) and re-fixed with 4% *p*-formaldehyde for 10 min. Cells were incubated overnight at 4°C with a rabbit polyclonal antibody which recognizes p53 phosphorylated on serine 15 (p-p53Ser15; Cell Signalling Technologies, Beverly, MA, USA). Immunoreactivity was detected using a biotinylated goat anti-rabbit IgG. Cells were then incubated with Alexa Fluor 488 avidin-conjugate (1 : 600 dilution in 2.5% serum; Molecular Probes) and viewed under 63× magnification using a confocal microscope (Zeiss LSM 510 META; Carl Zeiss Jena GmgH, Jena, Germany). The multitrack FITC/Rhodamine channel configuration was selected, emission spectra for Alexa 488 (excitation 488 nm and emission 520 nm) and for LysoTracker probe (excitation 543 nm and emission 599 nm).

Lysosomal integrity assay: acridine orange relocation

The lysosomal integrity assay was carried out as described by Yuan *et al.* (2002). Cells were exposed to pre-warmed supplemented neurobasal medium containing acridine orange (AO; 5 μg/mL; Molecular Probes) for 15 min at 37°C. Cells were rinsed in neurobasal medium and exposed to THC (5 μM) for 5–60 min and viewed by confocal microscopy. Visualization of the fluorophore was achieved using the 488 nm argon laser in the lambda mode where emission over the 499–670 nm range was collected. The configuration parameters were as follows: (i) Filters: Ch3-BP 585–615, Ch2-BP 505–530, ChS1 499.3–670.7 nm; (ii) Beam Splitters: HFT 488; (iii) Scan zoom 1. For each digital image, 512 × 512 pixels were used. The leakage of AO from the lysosome produces a decrease in the 633 nm emission and this parameter was used as an index of lysosomal integrity, as previously reported (Antunes *et al.* 2001). The average cellular fluorescence at 633 nm was counted from at least 200 cells for each treatment, from at least four independent experiments.

Cathepsin-D localization

To assess the intracellular distribution of cathepsin-D, neurones were incubated with LysoTracker Red (700 nM; Invitrogen, Paisley, UK) for 25 min at 37°C to label lysosomes and BIODIPY FL-pepstatin A (1 μM; Molecular Probes) for 1 h at 37°C to label cathepsin-D. BODIPY FL-pepstatin A is Pepstatin A (isovaleryl-L-valyl-4-amino-3-hydroxy-6-methylheptanoyl-L-alanyl-4-amino-3-hydroxy-6-methlheptanoic acid), covalently conjugated with the Boron dipyrromethene difluoride fluorophore (BODIPY; Chen *et al.* 2000). Following treatment with Δ^9-THC, the cells were fixed with 4% *p*-formaldehyde and incorporated fluorophores were examined with a confocal microscope (Zeiss, LSM 510 META), as previously described (Chen *et al.* 2000).

Cathepsin-D activity

Cathepsin-D activity was measured using a fluorogenic assay. Cells were harvested in ice-cold buffer [25 mM HEPES, 5 mM $MgCl_2$, 5 mM EDTA, 8 mM dithiothreitol (DTT) and 2 μg/mL leupeptin, pH 7.5], centrifuged at 10 000 *g* for 10 min at 4°C to yield the cytosolic fraction. Cathepsin-D was purified from cytosolic fractions using a 96-well plate coated with monoclonal anti-cathepsin-D antibody. The cathepsin-D activity was then detected using an internally quenched fluorescent cathepsin-D substrate peptide, Mca-Gly-Lys-Pro-Ile-Leu-Phe-Arg-Leu-Lys-(Dnp)-D-Arg-NH_2. Release of the fluorescent product, Mca-Gly-Lys-Pro-Ile-Leu-Phe was determined fluorometrically at excitation 328 nm and emission 393 nm. Cathepsin-D activity was read from a standard curve of affinity purified cathepsin-D enzyme.

Caspase 3 analysis

Cleavage of the fluorogenic caspase 3 substrate (DEVD-aminofluorocoumarin; Alexis Corporation, San Diego, USA) to its fluorescent product was used to measure caspase 3 activity. Following treatment the cultured neurones were lysed in buffer (25 mM HEPES, 5 mM $MgCl_2$, 5 mM DTT, 5 mM EDTA, 2 mM phenylmethylsulphonyl fluoride, 10 μg/mL leupeptin and 10 μg/mL pepstatin, pH 7.4), sonicated for 2 s and centrifuged at 10 000 *g* for 10 min at 4°C. Samples of supernatant (90 μL) were incubated with the DEVD peptide (500 μM; 10 μL) for 1 h at 30°C. Incubation buffer (900 μL; 50 mM HEPES, pH 7.4, containing 2 mM EDTA, 20% glycerol and 10 mM DTT) was added and fluorescence was assessed (excitation 400 nm and emission 505 nm). Results are expressed as the fold-change in caspase 3 activity induced by Δ^9-THC.

Caspase 3 activity was also assessed by immunocytochemistry using an anti-active caspase 3 antibody (Promega Corporation, Madison, WI, USA). Cells were fixed with 4% *p*-formaldehyde, blocked with 30% goat serum in PBS overnight at 4°C. Following blocking the cells were incubated in rabbit anti-active caspase 3 (1 : 1000 in 30% blocking buffer; Promega Corporation) for 1 h at 20°C. The primary antibody was detected using a biotinylated goat anti-rabbit secondary antibody (1 : 1500 in 30% blocking buffer). The biotinylated secondary antibody was detected by the avidin conjugated fluorophore Alexa Fluor 488 (1 : 2000 in 30% blocking buffer). Cells were viewed under 40× magnification using a confocal microscope (Zeiss LSM 510 META; Carl Zeiss). The flurophore was visualized using the following scan configurations: excitation 488 nm, 5% argon laser transmission, beam splitters HFT 488, channel filters LP 505, detector gain 652, pinhole 66 μm and 16 scan averages.

Terminal deoxynucleotidyl transferase-mediated UTP-end nick labelling

Apoptotic cell death was assessed using the Dead End™ Fluorometric apoptosis detection system (Promega Corporation). Cells

were fixed with *p*-formaldehyde (4%), permeabilized with Triton X-100 (0.1%) and fluorescein nucleotide was incorporated at 3′-OH DNA ends using the enzyme terminal deoxynucleotidyl transferase (TdT). Fluorescein was visualized by fluorescent confocal microscopy (Zeiss LSM 510-META) using the 488 nm Argon/2 laser with the following scan configurations; laser output 50%, % transmission 5%, band pass filter 505–530, beam splitter 488/543, detector gain 719, amplifier gain 1, amplifier offset −0.14, pinhole 96 μm (1 Airy unit) and 16 scan averages. All cells were counterstained with propidium iodide.

Statistics

Data are reported as the mean ± SEM of the number of experiments indicated in each case. Statistical analysis was carried out using one-way ANOVA followed by the *post hoc* Student–Newman–Keuls test when significance (at the < 0.05 level) was indicated. When comparisons were being made between two treatments, an unpaired Student's *t*-test was performed and $p < 0.05$, $p < 0.01$, or $p < 0.001$ were considered significant.

Results

Δ^9-THC evokes a transient decrease in lysosomal membrane stability

Cortical neurones were loaded with AO and the mean fluorescence intensity at 633 nm emission was observed (Fig. 1). Δ^9-THC evoked a dose- and time-dependent reduction in 633 nm emission, reflective of leakage of AO from the lysosomal compartment. Thus, exposure of cells to Δ^9-THC at a concentration of 0.5, 5 and 50 μM evoked a

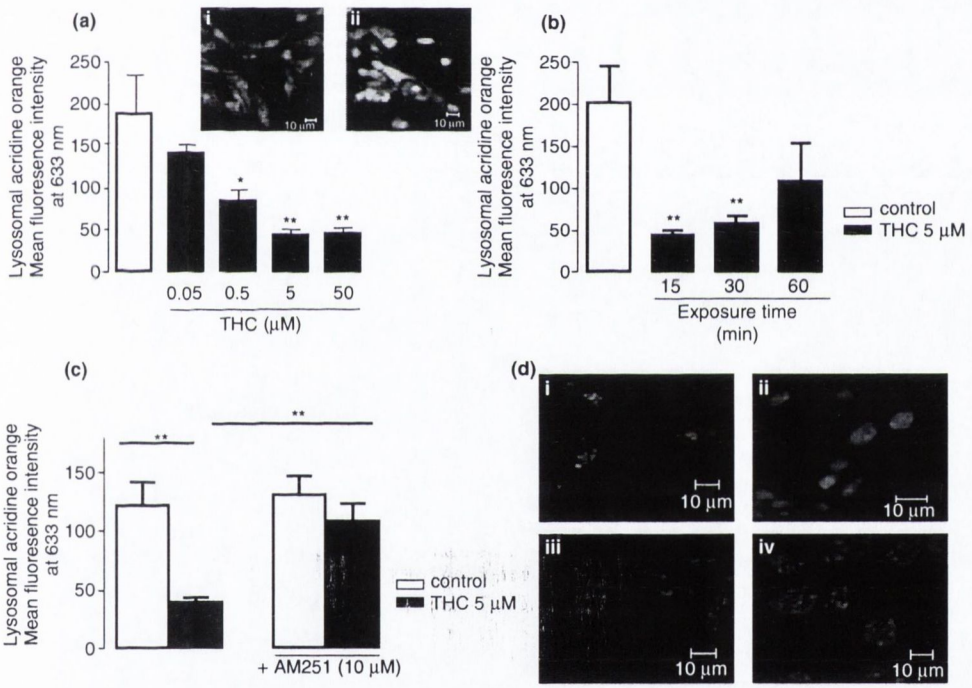

Fig. 1 Δ^9-THC causes lysosomal rupture in a CB_1-dependent manner. (a) Cultured neurones were loaded with acridine orange (AO), exposed to Δ^9-THC (0.05–50 μM) for 15 min and viewed by confocal microscopy. The fluorescence emission at 633 nm, representing intact lysosomes, was significantly decreased by 0.5, 5 and 50 μM Δ^9-THC. The lower concentration of Δ^9-THC, 0.05 μM, had no effect on AO distribution. Results are expressed as mean ± SEM for four independent experiments, $^*p < 0.05$ and $^{**}p < 0.01$. Inset: AO staining in (i) control cells and (ii) cells exposed to Δ^9-THC (5 μM, 15 min). The punctate distribution of orange fluorescence at 633 nm emission indicates a high proportion of cells with intact lysosomes. (b) cultured neurones were loaded with AO and exposed to Δ^9-THC (5 μM) for 15–60 min. The fluorescence emission at 633 nm, representing intact lysosomes, was significantly decreased following exposure to Δ^9-THC (5 μM) for 15 and 30 min. Results are expressed as mean ± SEM for four independent experiments, $^*p < 0.05$ and $^{**}p < 0.01$. (c) The Δ^9-THC-induced decrease in fluorescence emission at 633 nm (5 μM, 15 min) was reversed by the CB_1-receptor antagonist, AM251 (10 μM). Results are expressed as mean ± SEM for four independent experiments, $^{**}p < 0.01$. (d) sample confocal images of (i) control cells, (ii) cells exposed to Δ^9-THC (5 μM, 15 min), (iii) cells exposed to AM251 (10 μM) and (iv) cells exposed to Δ^9-THC in the presence of AM251. The punctate distribution of orange fluorescence (633 nm emission) indicates a high percentage of cells with intact lysosomes (i, iii and iv) that are able to retain AO, whilst the diffuse green fluorescence (ii) represents AO within the cytosol as a consequence of lysosomal rupture.

significant 70% decrease in the fluorescence signal within 15 min ($p < 0.01$, ANOVA, $n = 6$, Fig. 1a) indicating a loss in lysosomal membrane integrity. The inset image shows the pattern of AO staining in control and Δ^9-THC-treated cells where the orange punctate staining reflects AO accumulation in the lysosome which emits at 633 nm, while the green diffuse staining represents cytosolic AO. The reduction in 633 nm emission occurred within 15 min of exposure to Δ^9-THC (5 μM) and was retained up until 30 min ($p < 0.01$, ANOVA, $n = 6$, Fig. 1b). However, by 60 min the fluorescence signal was approaching that of control cells. These data demonstrate that Δ^9-THC evokes a rapid, but transient, decrease in lysosomal membrane integrity, which is reflected by an inability of AO to accummulate in the acidic organelles and produce a fluorescence signal at 633 nm.

Figure 1c demonstrates that the impact of Δ^9-THC on lysosomal membrane integrity is mediated through the CB_1 receptor as AM251 (10 μM) abrogated the Δ^9-THC-mediated reduction in mean fluorescence intensity at 633 nm. Thus in control cells, mean fluorescence intensity was 122 ± 19 (mean arbitrary units ± SEM) and was significantly decreased to 39 ± 3 in cells exposed to Δ^9-THC (5 μM) for 15 min ($p < 0.01$, ANOVA compared with control cells, $n = 6$). AM251 alone had no effect on mean fluorescence intensity at 633 nm, but it significantly reversed the Δ^9-THC-induced reduction in mean fluorescence intensity ($p < 0.01$, ANOVA compared with cells exposed to THC, $n = 6$). Figure 1d illustrates sample AO staining demonstrating the CB_1-dependent relocalization of AO to the cytosol following exposure to Δ^9-THC (5 μM) for 15 min.

THC increases the association of phospho-p53 at the lysosome

Figure 2 demonstrates that Δ^9-THC increases the association of phospho-p53Ser15 with lysosomes. Thus, in control cells phospho-p53Ser15 immunoreactivity was undetectable, and the staining of florescence produced by LysoTracker Red was punctate, indicative of intact lysosomes. However, when cells were exposed to Δ^9-THC (5 μM, 15 min) phospho-p53Ser15 immunoreactivity was observed in punctate regions of the cell, some of which was found to co-localize with the lysosomal marker, LysoTracker red. Although we found that by 15 min Δ^9-THC had caused the release of AO (Fig. 1b), indicative of increased lysosomal permeability, the LysoTracker red staining was still apparent in Δ^9-THC-treated neurons. However, under those conditions the

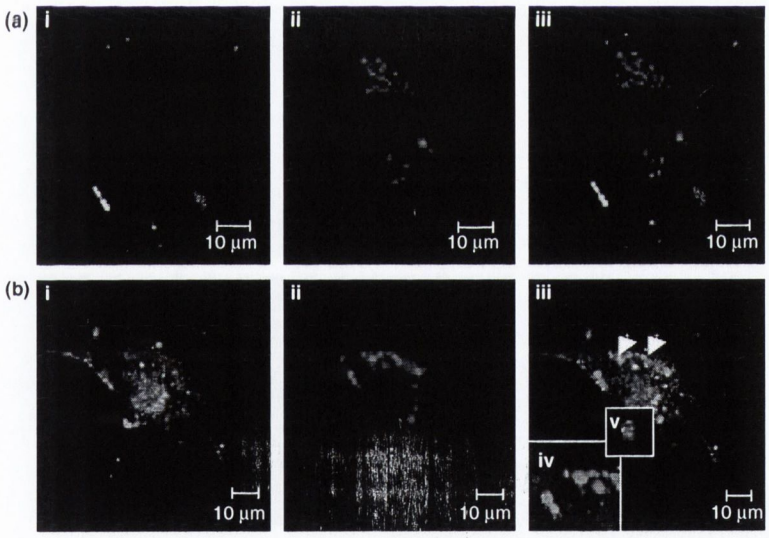

Fig. 2 Δ^9-THC promotes the association of phospho-p53 with lysosomes. Confocal microscopy was used to visualize the distribution of phospho-p53Ser15 within cortical neurones following treatment with Δ^9-THC (5 μM, 15 min). Cells were double labelled with (i) an Alexa-488-conjugated phospho-p53Ser15 antibody and (ii) the lysosomal-specific marker, LysoTracker Red; panel (iii) represents the overlay of phospho-p53Ser15 immunoreactivity with LysoTracker Red. In control cells (a) there was no evidence of phospho-p53Ser15 at the lysosomes. However, 15 min following exposure to Δ^9-THC (b) phospho-p53Ser15 immunoreactivity was increased and, in part, co-localized with the lysosomal marker, as indicated by purple staining (iii). In image (iv), phospho-p53Ser15 immunoreactivity at the lysosomes is indicated by purple. Panel (iv) in a zoomed image of lysosomes using 63× objective and scan zoom 6 and panel (v) is a zoomed image of a lysosome, with 63× objective and scan zoom 9, illustrating LysoTracker Red (red) co-localizing with phospho-p53Ser15 immunoreactivity (purple). Images are single 1 μm thick z-sections taken midway through the cell. Arrows indicate regions of co-localization. Scale bar: 10 μm.

lysosomes were larger [Fig. 2b(ii)] reflecting a change to the lysosomal system (He *et al.* 2005). The AO protocol is considered to be more sensitive to changes in lysosomal permeability and can monitor very fast granular alkalinization events in live cells (Yuan *et al.* 2002). In contrast, LysoTracker Red staining was performed in fixed cells and the probe is retained in lysosomal membranes through an as yet uncharacterized mechanism. Thus, LysoTracker Red is considered to be less sensitive to rapid changes in lysosomal permeability and often the loss of LysoTracker staining is not apparent until the very final stages of the apoptotic cascade (Kaasik *et al.* 2005). In Δ^9-THC-treated cells some p53 immunoreactivity was also detected within the nucleus, consistent with a role for p53 in governing transcriptional events (Green and Chipuk 2006). The observation that Δ^9-THC promotes the association of phospho-p53 with lysosomes prompted us to examine whether p53 was pertinent in the Δ^9-THC-mediated destabilization of the lysosomal membrane.

p53 plays a role in the THC-mediated destabilization of the lysosomes

Figure 3a demonstrates that the impact of THC on lysosomal membrane integrity is mediated through p53 as the p53 inhibitor, pifithrin-α (100 nM) abrogated the THC-mediated reduction in mean fluorescence intensity at 633 nm. Thus in control cells, mean fluorescence intensity was 118 ± 21 and this significantly decreased to 39 ± 3 in cells exposed to THC (5 μM) for 15 min ($p < 0.01$, ANOVA compared with control cells, $n = 6$). In the presence of pifithrin-α, the Δ^9-THC-induced reduction in mean fluorescence intensity was significantly attenuated ($p < 0.05$, ANOVA, $n = 6$). Sample AO staining demonstrating the p53-dependent relocalization of AO to the cytosol, and concomitant decrease in 633 nm emission, following exposure to THC (5 μM) for 15 min is shown in Fig. 3b. This result was confirmed with knockdown of p53 with siRNA (Fig. 3c) where the Δ^9-THC-induced increase in lysosomal membrane permeability, as reflected by

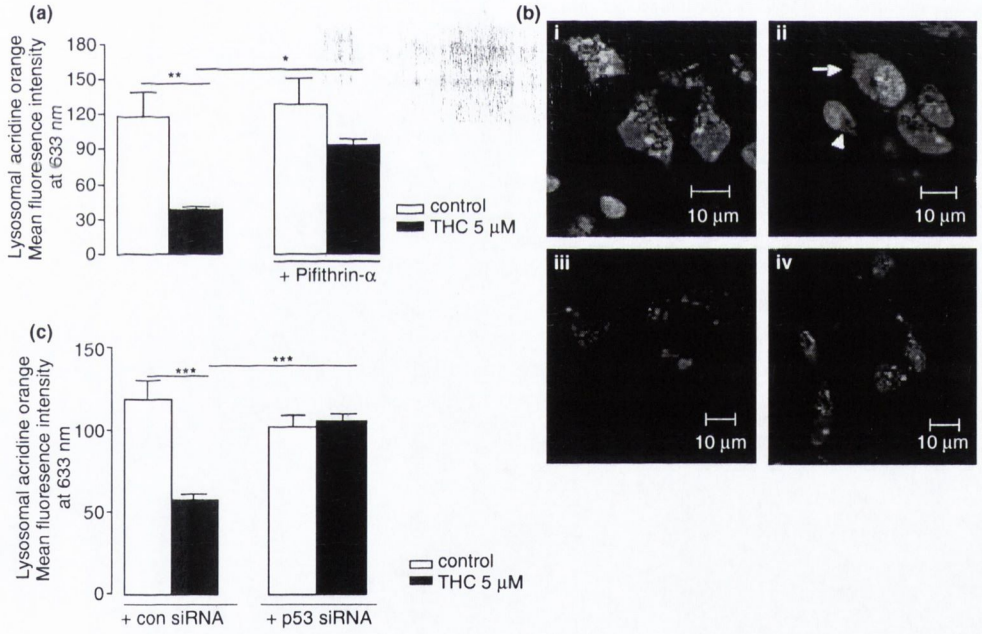

Fig. 3 Δ^9-THC evokes lysosomal destabilization in a p53-dependent manner. (a) Cells were loaded with acridine orange (AO), exposed to Δ^9-THC (5 μM, 15 min) and viewed by confocal microscopy. Δ^9-THC evoked a significant reduction in fluorescence at 633 nm emission which was abrogated by the p53 inhibitor, pifithrin-α (100 nM). Results are expressed as mean ± SEM for six independent experiments, $^*p < 0.05$ and $^{**}p < 0.01$. (b) Representative AO staining in (i) control cells, (ii) cells exposed to Δ^9-THC (5 μM, 15 min), (iii) cells exposed to pifithrin-α (100 nM) and (iv) cells exposed to Δ^9-THC in the presence of pifithrin-α. The punctate distribution of orange fluorescence (633 nm emission) indicates a high percentage of cells with intact lysosomes. In Δ^9-THC-treated cells (ii) the punctate distribution of orange fluorescence was reduced and increased diffuse green fluorescence was observed, which was abrogated by pifithrin-α (iv). Arrows indicate cells with reduced punctate orange staining and increased diffuse green fluorescence, indicative of lysosomal rupture and redistribution of AO to the cytosol. C, siRNA knockdown of p53 prevents the Δ^9-THC-induced decrease in lysosomal integrity. Exposure of neurones to Δ^9-THC (5 μM) for 15 min in the presence of control siRNA significantly decreased the fluorescence emission at 633 nm, indicative of lysosomal rupture. Treatment with p53 siRNA (100 nM; 48 h) prior to Δ^9-THC treatment prevented the THC-induced decrease in fluorescence emission at 633 nm. Results are expressed as mean ± SEM for six observations, $^{***}p < 0.001$.

a significant reduction in fluorescence emission at 633 nm, was not observed in cells pre-treated with p53 siRNA.

Δ^9-THC evokes a redistribution of cathepsin protease

A destabilization of the lysosomal membrane would be expected to promote the release of lysosomal constituents into the cytosol. Cultured neurones were incubated with BODIPY®-FL pepstatin-A to label cathepsin-D, and Lyso-Tracker Red to observe lysosomes. Figure 4a demonstrates that the BODIPY®-FL pepstatin-A co-localizes with lysosomes in untreated cells. When neurones were incubated with Δ^9-THC (5 μM, 15 min) the punctate distribution of BODIPY®-FL pepstatin-A, reflective of cathepsin-D localization within lysosomes, changed to a diffuse pattern of staining, representative of the presence of cathepsin-D in the cytosol (Fig. 4b). This result demonstrates that the increase in lysosomal permeability is associated with a redistribution of cathepsin-D from the lysosomal compartment into the cytosol. Furthermore, exposure of neurones to Δ^9-THC (5 μM, 15 min) evoked a significant increase in the activity of cathepsin-D ($p < 0.01$, ANOVA compared with vehicle-treated cells, $n = 6$) and this was significantly reduced by pifithrin-α (100 nM, $p < 0.01$, ANOVA compared with THC-treated cells, $n = 6$; Fig. 4c).

Δ^9-THC-induced apoptosis involves cathepsin-D

We have previously reported that Δ^9-THC induces the activation of pro-apoptotic caspase 3 (Campbell 2001). The Δ^9-THC-induced activation of caspase 3, as determined by expression of anti-active caspase 3 immunoreactivity (Fig. 5a) and fluorogenic assay (Fig. 5b) was prevented by the cathepsin-D inhibitor peptide (10 μM). Thus, exposure to Δ^9-THC (5 μM, 1 h) caused an increase in expression of active-caspase 3 immunoreactivity and evoked a 2.28 ± 0.27-fold increase in caspase 3 activity ($p < 0.05$, ANOVA, $n = 6$). In the presence of the cathepsin-D inhibitor, the Δ^9-THC-induced increase in active-caspase 3 immunoreactivity (Fig. 5a) and caspase 3 activity (Fig. 5b; $p < 0.01$, ANOVA, $n = 6$) was abolished. This result suggests that the impact of Δ^9-THC on the lysosomal system promotes a

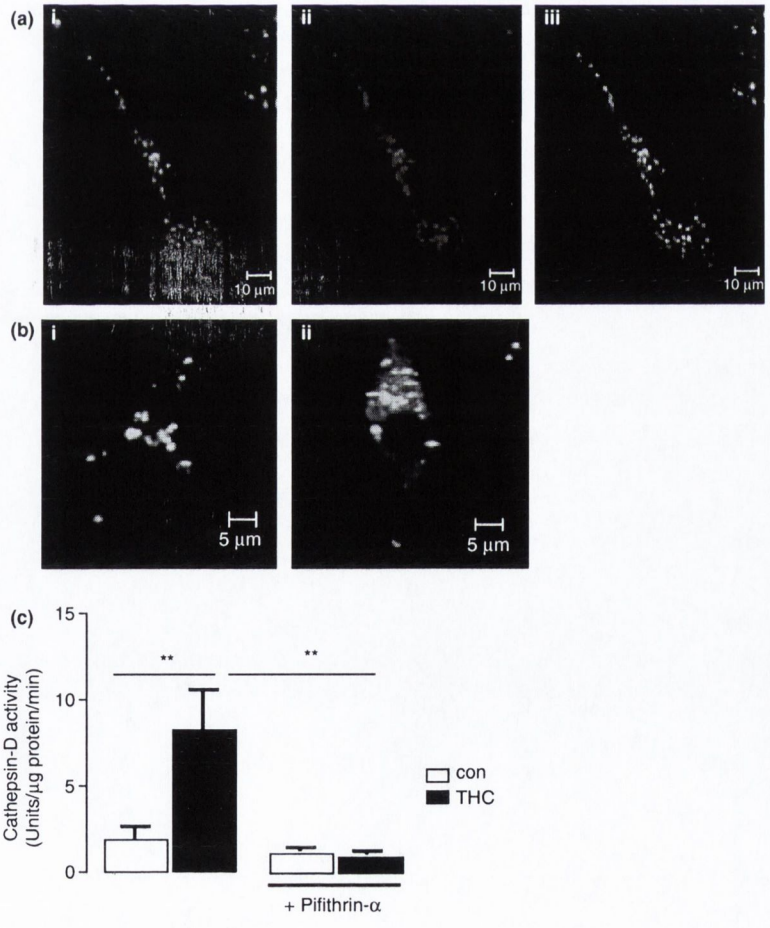

Fig. 4 Δ^9-THC increases the cytosolic expression and activity of cathepsin-D. BIODIPY FL-pepstatin-A fluorescence was used to label intracellular cathepsin-D localization. (a) BIODIPY FL-pepstatin-A co-localized with LysoTracker Red in untreated cells. (i) BIODIPY FL-pepstatin-A fluorescence, (ii) LysoTracker Red fluorescence and (iii) co-localization of BIODIPY FL-pepstatin-A and LysoTracker Red is indicated by yellow fluorescence. Scale bar: 10 μm. (b) Cells were exposed to (i) vehicle control or (ii) Δ^9-THC (5 μM) for 15 min and BIODIPY FL-pepstatin-A fluorescence was used to monitor intracellular cathepsin-D localization. In control cells, BIODIPY staining was punctate, indicative of compartmentalization within lysosomes. In Δ^9-THC-treated cells, BODIPY staining was present throughout the cytosol, reflecting the redistribution of cathepsin-D from the lysosomes to the cytosol. Scale bar: 5 μm. (c) Δ^9-THC (5 μM; 15 min) evoked a significant increase in cathepsin-D activity and this was abolished by pifithrin-α (100 nM). Results are expressed as mean ± SEM for six independent observations, $^{**}p < 0.01$.

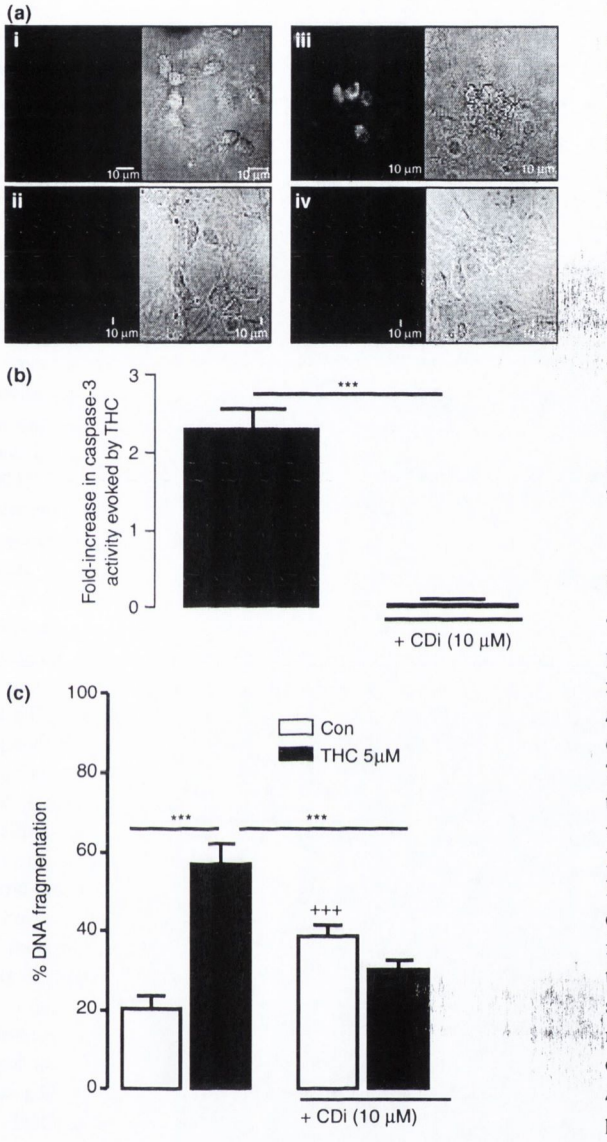

Fig. 5 The Δ^9-THC increase in caspase 3 activity and DNA fragmentation is dependant upon cathepsin-D. (a) Representative active-caspase 3 immunoreactivity in (i) control cells, (ii) cells exposed to Δ^9-THC (5 μM, 1 h), (iii) cells exposed to cathepsin-D inhibitor (10 μM) and (iv) cells exposed to Δ^9-THC in the presence of cathepsin-D inhibitor. THC evoked an increase in active-caspase 3 immunoreactivity (ii; indicated by arrows), and this was prevented in cells exposed to Δ^9-THC in the presence of the cathepsin-D inhibitor (iv). The left side of each image is active-caspase 3 immunofluorescence and the corresponding phase contrast image is shown on the right. Scale bar: 10 μm. (b) Δ^9-THC (5 μM, 1 h) evoked a twofold increase in caspase 3 activity and this was significantly reduced by the cathepsin-D inhibitor (10 μM). Results are expressed as mean fold-increase in caspase 3 activity evoked by Δ^9-THC ± SEM for six independent observations, $^{***}p < 0.001$. (c) Δ^9-THC (5 μM, 3 h) evoked a significant increase in DNA fragmentation and this was prevented by the cathepsin-D inhibitor (10 μM). Results are expressed as mean ± SEM for six independent observations, $^{***}p < 0.001$ and $^{+++}p < 0.001$ (compared with control cells, ANOVA, $n = 6$).

redistribution of cathepsin-D which in turn contributes to the activation of caspase 3. The Δ^9-THC-induced increase in apoptotic cell death, as assessed by TdT-mediated UTP-end nick labelling staining (Fig. 5c) was also prevented by the cathepsin-D inhibitor, further demonstrating that this lysosomal protease is involved in the apoptotic cell death evoked by Δ^9-THC. In neurones exposed to the cathepsin-D inhibitor alone, a significant increase in DNA fragmentation was observed and this indicates that cathepsin-D may have a pro-survival role in this cell type. However, the lack of any further increase in DNA fragmentation in cells exposed to Δ^9-THC in the presence of cathepsin-D inhibitor, would lend support of a role for cathepsin-D in Δ^9-THC-iduced neuronal apoptosis.

Discussion

The aim of this study was to examine the impact of the phytocannabinoid, Δ^9-THC, on lysosomal membrane permeability and to assess whether lysosomes play a role in the Δ^9-THC-induced activation of the apoptotic pathway previously reported (Campbell 2001; Downer *et al.* 2003, 2007a). The results demonstrate that Δ^9-THC causes a dose- and time-dependent destabilization of the lysosomal membrane via activation of the CB_1 receptor. Δ^9-THC evoked co-localization of p53, phosphorylated at Ser15, with the lysosome and this association is likely to contribute to the destabilization of the lysosomal membrane as both the p53 inhibitor, pifithrin-α and siRNA knockdown of p53 reversed the Δ^9-THC-induced loss in lysosomal integrity. The transient nature of this event suggests that lysosomal constituents may play a necessary role in orchestrating downstream cellular events associated with apoptosis. In support of this, Δ^9-THC caused an increase in expression of the aspartic protease, cathepsin-D, in the cytosol, and the cathepsin-D inhibitor abrogated that Δ^9-THC-induced activation of caspase 3 and DNA fragmentation. These data provide evidence for a lysosomal branch of the apoptotic programme induced by Δ^9-THC in neurones.

Lysosomes are emerging as important regulators of the cell death cascade. Originally thought to be stable organelles, only becoming destabilized during the end stages of cell death, there is a large body of evidence demonstrating that lysosomes occupy an upstream regulatory role in apoptosis (Li *et al.* 2000; Brunk *et al.* 2001). Early in apoptosis lysosomes become permeable causing the translocation of lysosomal cathepsin proteases into the cytosol (Werneburg *et al.* 2002; Kagedal *et al.* 2005). The redistribution of cathepsins is suspected to be an important initiating event in apoptosis (Reiners *et al.* 2002) and the release of lysosomal

enzymes may cause changes in mitochondrial permeability directly (Zhao *et al.* 2001) or indirectly (Stoka *et al.* 2001), followed by cytochrome *c* release, apoptosome formation with Apaf-1 and caspase activation. There may also be a direct activation of caspases by lysosomal cathepsins (Vancompernolle *et al.* 1998). Furthermore, cathepsin-D, both in its mature or inactive form, can impact on an as yet unidentified substrate to induce apoptosis (Schestkowa *et al.* 2007). In this study, the lysosomal destabilization occurred rapidly following exposure to Δ^9-THC. Furthermore, the destabilization of lysosomes observed at 15 min occurs prior to the onset of activation of caspase 3 and preceeds induction of morphological features of apoptosis, which we have previously found to occur at a later time point when neurones are exposed to the same concentration of Δ^9-THC to that used in the current study (Campbell 2001; Downer *et al.* 2001). The early lysosomal destabilization, coupled with the transient nature of this event, would suggest that the lysosomes have a role in orchestrating CB-mediated neuronal death. In neurones, the lysosomal permeabilization evoked by Δ^9-THC is likely mediated through the CB_1 receptor, although a role for CB_2 receptors cannot be completely excluded as in macrophages Matveyeva *et al.* (2000) have demonstrated that Δ^9-THC increases cathepsin-D activity via the CB_2 receptor which may contribute to deficits in antigen-dependent processing. Early reports in the literature describing the lytic effect of Δ^9-THC on isolated liver lysosomes and subsequent release of acid hydrolases (Britton and Mellors 1973) would indicate that Δ^9-THC, which is highly lipophilic, may directly influence lysosomal permeability in some cell types.

Following exposure to Δ^9-THC, an increase in expression of the phosphorylated form of the apoptotic effector, p53, was observed, which may reflect stabilization of the protein by c-jun N-terminal kinase (Downer *et al.* 2007b). Our previous studies have demonstrated that Δ^9-THC evokes a rapid increase in phospho-p53 expression in cell lysates and that p53 knockdown with siRNA protects neurones from Δ^9-THC-induced apoptosis (Downer *et al.* 2007b). In the current study, we found that Δ^9-THC promotes association of the p53 protein with the nucleus where it is likely to participate in the transcription of apoptotic genes (Green and Chipuk 2006). However, a substantial proportion of p53 immunoreactivity co-localized with the lysosomal marker, LysoTracker Red, indicating the association of p53 with the lysosomal compartment. To assess whether p53 regulates lysosomal integrity we used the reversible p53 inhibitor, pifithrin-α, which prevents p53 transactivation (Komarov *et al.* 1999; Culmsee *et al.* 2001) and p53 phosphorylation (Chua *et al.* 2006), as well as siRNA-mediated depletion of p53. Using both experimental approaches the THC-induced permeabilization of lysosomes was prevented, providing evidence of a role for p53 in controlling lysosomal permeability. To the authors' knowledge, this is the first demonstration that p53 directly associates with lysosomes during an apoptotic cascade, although the lysosomal targets that may be regulated by p53 to control lysosomal integrity remain to be elucidated. Indeed, there is currently no consensus on the mechanisms that are responsible for control of lysosomal membrane destabilization during apoptosis (Stoka *et al.* 2007). Cytoplasmic p53 can directly activate pro-apoptotic members of the Bcl family of proteins to cause mitochondrial permeabilization and apoptosis (Chipuk *et al.* 2005), and given that Bax can directly insert into the lysosomal membrane during staurosporine-induced apoptosis (Kagedal *et al.* 2005), it is interesting to speculate that functional crosstalk exists between p53 and Bax in relation to the control of lysosomal permeability. Other members of the Bcl family, such as Bcl-2, block oxidative stress-induced apoptosis by stabilizing lysosomes (Zhao *et al.* 2001). A number of other signalling molecules are pertinent in the regulation of lysosomal dynamics, such as intracellular sphingosine (Kagedal *et al.* 2005), and this is significant given that CBs couple to ceramide production to evoke apoptosis in glioma cells (Galve-Roperh *et al.* 2000). Another explanation for the triggering of lysosomal rupture implicates reactive oxygen species as oxidative stress can induce lysosomal destabilization very rapidly, resulting in the release of cathepsins, *in vitro* (Kalra *et al.* 1989) and *in vivo* (Ollinger and Brunk 1995). Lysosomes are particularly vulnerable to oxidative stress as they contain the most important pool of reactive iron in the cell (Antunes *et al.* 2001), and again it is significant that CBs are coupled to the generation of reactive oxygen species in neurones (Chan *et al.* 1998) and glia (Massi *et al.* 2006).

Using a BODIPY-conjugated cathepsin-D inhibitor, we demonstrate that Δ^9-THC causes a redistribution of cathepsin-D from the lysosome to the cytosol, and this correlated with an increase in activity of cathepsin-D. The impact of Δ^9-THC on cathepsin-D was blocked by the CB_1 antagonist, AM251, as well as pifithrin-α. Lysosomal rupture and subsequent release of cathepsin-D have been reported to occur prior to changes in mitochondrial membrane potential (Turk *et al.* 2002) in a number of apoptotic pathways (Stoka *et al.* 2007). It is likely that the release of cathepsin-D is a regulated process and not a consequence of general lysosomal rupture because the increase in cytosolic cathepsin-D that we observe in Δ^9-THC-treated cells does not coincide with an increase in cytosolic activity of other cathepsins, such as cathepsin-L (data not shown). Our observation that the Δ^9-THC-induced increase in caspase 3 activity and DNA fragmentation was blocked by the cathepsin-D inhibitor peptide provides further support for a lysosomal involvement in this CB-induced apoptotic cascade. A link between cathepsin-D and caspase 3 has been reported in staurosporine-induced apoptosis in fibroblasts via a Bid-signalling pathway (Johansson *et al.* 2003), although pathways other than Bid are also likely to signal between cathepsin-D and

caspase 3 to evoke apoptosis (Houseweart *et al.* 2003). Our *in vivo* studies have recently demonstrated that administration of Δ^9-THC increases the cytosolic expression and activity of cathepsin-D in the cerebral cortex as part of an apoptotic cascade (Downer *et al.* 2007a) and the results presented herein would indicate that p53-mediated regulation of lysosomal integrity is a key factor in this neurotoxic event. Given that Δ^9-THC has been reported to evoke apoptosis in other cell types such as gliomas (Velasco *et al.* 2004), leukaemic cells (Jia *et al.* 2006) and airway epithelia (Sarafian *et al.* 2005), it is interesting to speculate that those CB-induced apoptotic pathways also involve a lysosomal component.

While the potential neurotoxicity associated with recreational use of cannabis is controversial, some imaging studies of chronic cannabis users have identified reductions in grey and white matter volume (Scallet 1991; Lawston *et al.* 2000; Tzilos *et al.* 2005; Schlaepfer *et al.* 2006). Δ^9-THC and other CBs have been shown to evoke apoptosis in neuronal (Chan *et al.* 1998; Downer *et al.* 2003) and glial (Galve-Roperh *et al.* 2000) cells. Potential mechanisms of apoptosis include formation of ceramide (Galve-Roperh *et al.* 2000), stress-activated protein kinase activity (Downer *et al.* 2003), calpain activation (Movsesyan *et al.* 2004), and engagement of the TRPV1 channel (Ligresti *et al.* 2006). The pro-apoptotic effect of the CB system is particularly robust in transformed cells and some studies have demonstrated that CBs do not induce apoptosis in healthy tissue (Carracedo *et al.* 2006; Massi *et al.* 2006); a property that may be harnessed in the development of a CB-based therapy for the selective eradication of tumour cells. It remains to be established whether the p53/lysosomal pathway is pertinent in the cannabinoid-induced apoptosis of transformed cells.

The current study demonstrates that in neurones Δ^9-THC causes lysosomal destabilization early in the apoptotic cascade in a manner that is dependent upon p53. This novel pathway may reflect a role of the endocannabinoid system in brain development (Harkany *et al.* 2007), in which physiological apoptosis is a feature. In this regard, it is notable that cathepsin-D gene expression outlines the regions of physiological cell death during embryonic development (Zuzarte-Luis *et al.* 2007). Also, the engagement of this apoptotic pathway by exogenous phytocannabinoids during cannabis abuse may contribute to the profound volumetric changes in the brain that have been reported (Schlaepfer *et al.* 2006). Neuronal apoptosis evoked by Δ^9-THC would also be expected to interfere with the physiological role of the presynaptic CB_1 receptor in controlling neurotransmitter release and this is likely to be of importance during brain development (Galve-Roperh *et al.* 2006).

In summary, this study identifies a novel lysosomal branch to the CB-mediated induction of apoptosis involving the tumour suppressor protein, p53. Given the interest in the ability of CBs to regulate cell fate (Guzman 2005), this pathway may be important for the anti-tumoural properties of CBs, as well as being involved in the control of neural cell viability.

Acknowledgement

This work was funded by Science Foundation Ireland.

References

Ameri A. (1999) The effects of cannabinoids on the brain. *Prog. Neurobiol.* **58**, 315–348.

Antunes F., Cadenas E. and Brunk U. T. (2001) Apoptosis induced by exposure to a low steady-state concentration of H_2O_2 is a consequence of lysosomal rupture. *Biochem. J.* **356**, 549–555.

Blázquez C., Sánchez C., Daza A., Galve-Roperh I. and Guzmán M. (2003) The stimulation of ketogenesis by cannabinoids in cultured astrocytes defines carnitine palmitoyltransferase 1 as a new ceramide-activated enzyme. *J. Neurochem.* **72**, 1759–1768.

Blomgren K., Leist M. and Groc L. (2007) Pathological apoptosis in the developing brain. *Apoptosis* **12**, 993–1010.

Britton R. S. and Mellors A. (1973) Lysis of rat liver lysosomes *in vitro* by tetrahydrocannabinol. *Biochem. Pharmacol.* **23**, 1342–1344.

Brunk U. T., Neuzil J. and Eaton J. W. (2001) Lysosomal involvement in apoptosis. *Redox Rep.* **6**, 91–97.

Campbell V. A. (2001) Tetrahydrocannabinol-induced apoptosis in cultured cortical neurones is associated with cytochrome *c* release and caspase-3 activation. *Neuropharmacology* **40**, 702–709.

Campbell V. and Gowran A. (2007) Alzheimer's disease' taking the edge off with cannabinoids? *Br. J. Pharmacol.* **152**, 655–662.

Carlson G., Wang Y. and Alger B. E. (2002) Endocannabinoids facilitate the induction of LTP in the hippocampus. *Nat. Neurosci.* **5**, 723–724.

Carracedo A., Gironella M., Lorente M., Garcia S., Guzman M., Velasco G. and Iovanna J. L. (2006) Cannabinoids induce apoptosis of pancreatic tumor cells via endoplasmic reticulum stress-related genes. *Cancer Res.* **66**, 6748–6755.

Chan G. C., Hinds T. R., Impey S. and Storm D. (1998) Hippocampal neurotoxicity of Δ^9-tetrahydrocannabinol. *J. Neurosci.*, **18**, 5322–5332.

Chen C. S., Chen W. N., Zhou M., Arttamangkul S. and Haugland R. P. (2000) Probing the cathepsin using a BODIPY FL-pepstatin A: applications in florescence p olarization and microscopy. *J. Biochem. Biophys. Methods* **42**, 137–151.

Chipuk J. E., Kuwana T., Bouchier-Hayes L., Droin N. M., Newmeyer D. D., Schuler M. and Green D. R. (2005) Direct activation of Bax by p53 mediates mitochondrial membrane permeabilization and apoptosis. *Science* **13**, 1010–1014.

Chua C. C., Liu X., Gao J., Hamdy R. C. and Chua B. H. L. (2006) Multiple actions of pifithrin-α on doxorubicin-induced apoptosis in rat myoblastic H9c2 cells. *Am. J. Physiol.* **290**, H2606–H2613.

Culmsee C., Zhu X., Yu Q. S., Chan S. L., Camandola S., Guo Z., Greig N. H. and Mattson M. (2001) A synthetic inhibitor of p53 protects neurones against death induced by ischemic and excitotoxic insults, and amyloid beta-peptide. *J. Neurochem.* **77**, 220–228.

Derkinderen P., Valjent E., Toutant M., Corvol J.-C., Enslen H., Ledent C., Trzaskos J., Caboche J., and Girault J.-A. (2003) Regulation of extracellular signal-regulated kinase by cannabinoids in hippocampus. *J. Neurosci.* **23**, 2371–2382.

Downer E., Boland B., Fogarty M. P., Campbell V. and (2001) Δ^9-Tetrahydrocannabinol induces the apoptotic pathway in cultured cortical neurones via activation of the CB_1 receptor. *Neuroreport* **12**, 3973–3978.

Downer E. J., Fogarty M. P. and Campbell V. A. (2003) Tetrahydrocannabinol-induced neurotoxicity depends on CB_1 receptor-mediated c-Jun N-terminal kinase activation in cultured cortical neurones. *Br. J. Pharm.* **140**, 547–557.

Downer E. J., Gowran A. and Campbell V. A. (2007a) A comparison of the apoptotic effect of Δ^9-tetrahydrocannabinol in the neonatal and adult rat cerebral cortex. *Brain Res.* **1175**, 39–47.

Downer E. J., Gowran A., Murphy A. C. and Campbell V. A. (2007b) The tumour suppressor protein, p53, is involved in the activation of the apoptotic cascade by Delta9-tetrahydrocannabinol in cultured cortical neurones. *Eur. J. Pharmacol.* **564**, 57–65.

Fride E. (2005) Endocannabinoids in the central nervous system, from neuronal networks to behavior. *Curr. Drug Targets CNS Neurol. Disord.* **4**, 633–642.

Fried P. A. and Smith A. M. (2001) A literature review of the consequences of prenatal marihuana exposure. An emerging theme of a deficiency in aspects of executive function. *Neurotoxicol. Teratol.* **23**, 1–11.

Galve-Roperh I., Sánchez C., Luisa Cortes M., Gómez del Pulgar T., Izquierdo M. and Guzmán M. (2000) Anti-tumoral action of cannabinoids: involvement of sustained ceramide accumulation and extracellular signal-regulated kinase activation. *Nat. Med.* **6**, 313–319.

Galve-Roperh I., Aquado T., Rueda D., Velasco G. and Guzman M. (2006) Endocannabinoids: a new family of lipid mediators involved in the regulation of neural cell development. *Curr. Pharm. Des.* **12**, 2319–2325.

Gilbert G. L., Kim H. J., Waataja J. J. and Thayer S. A. (2007) Delta9-tetrahydrocannabinol protects hippocampal neurones from excitotoxicity. *Brain Res.* **1128**, 61–69.

Green D. R. and Chipuk J. E. (2006) p53 and metabolism: inside the TIGAR. *Cell* **126**, 30–32.

Guzman M. (2005) Effects on cell viability. *Handb. Exp. Pharmacol.* **168**, 627–642.

Hampson A. J., Grimaldi M., Axelrod J. and Wink D. (1998) Cannabidiol and $(-)\Delta^9$-tetrahydrocannabinol are neuroprotective antioxidants. *Proc. Natl Acad. Sci. USA* **95**, 8268–8273.

Harkany T., Guzmán M., Galve-Roperh I., Berghuis P., Devi L. A. and Mackie K. (2007) The emerging functions of endocdannabinoid signalling during CNS development. *Trends Pharmacol. Sci.* **28**, 83–92.

He J., Tohyama Y., Yamamoto K., Kobavashi M., Shi Y., Takano T., Noda C., Tohyama K. and Yamamura H. (2005) Lysosome is a primary organelle in B cell receptor-mediated apoptosis: an indispensable role of Syk in lysosomal function. *Genes Cells* **10**, 23–35.

Herkenham M., Lynn A. B., Johnson M. R., Melvin L. S., de Costa B. R. and Rice K. C. (1991) Characterization and localization of cannabinoid receptors in rat brain: a quantitative in vitro autoradiographic study. *J. Neurosci.* **11**, 563–583.

Houseweart M. K., Vilaythong A., Yin X. M., Turk B., Noebels J. L. and Myers R. M. (2003) Apoptosis caused by cathepsins does not involve Bid signaling in an in vivo model of progressive myoclonus epilepsy (EPM1). *Cell Death Differ.* **10**, 1329–1335.

Jia W., Hegde V. L., Singh N. P., Sisco D., Grant S., Nagarkatti M. and Nagarkatti P. S. (2006) Delta9-tetrahydrocannabinol-induced apoptosis in Jurkat leukemia T cells is regulated by translocation of Bad to mitochondria. *Mol. Cancer Res.* **4**, 549–562.

Johansson A. C., Steen H., Ollinger K. and Roberg K. (2003) Cathepsin D mediates cytochrome c releaser and caspase activation in human fibroblast apoptosis induced by staraus porine. *Cell Death Differ.* **10**, 1253–1259.

Kaasik A., Rikk T., Piirsoo A., Zharkovsky T. and Zharkovsky A. (2005) Up-regulation of lysosomal cathepsin-L and autophagy during neuronal death induced by reduced serum and potassium. *Eur. J. Neurosci.* **22**, 1023–1031.

Kagedal K., Johansson A. C., Johansson U., Heimlich G., Roberg K., Wang N. S., Jurgensmeier J. M. and Ollinger K. (2005) Lysosomal membrane permeabilization during apoptosis: involvement of Bax? *Int. J. Exp. Pathol.* **86**, 309–321.

Kågedal K., Zhao M., Svensson I. and Brunk U. T. (2001) Sphingosine-induced apoptosis is dependent on lysosomal proteases. *Biochem. J.* **359**, 335–343.

Kalra J., Chaudhary A. K. and Prasad K. (1989) Role of oxygen free radicals and pH on the release of cardiac lysosomal enzymes. *Mol. Cell Cardiol.* **21**, 1125–1136.

Kishimoto Y. and Kano M. (2006) Endogenous cannabinoid signalling through the CB_1 receptor is essential for cerebellum-dependent discrete motor learning. *J. Neurosci.* **26**, 8829–8837.

Komarov P. G., Komarova E. A., Kondratov R. V., Christov-Tselkov K., Coon J. S., Chernov M. V. and Gudkov A. V. (1999) A chemical inhibitor of p53 that protects mice from the side effects of cancer. *Science* **285**, 1733–1737.

Lawston J., Borella A., Robinson J. K. and Whitaker-Azmitia P. M. (2000) Changes in hippocampal morphology following chronic treatment with the synthetic cannabinoid WIN 55212-2. *Brain Res.* **877**, 407–410.

Li W., Yuan X., Nordgren G., Dalen H., Dubowchik G. M., Firestone R. A. and Brunk U. T. (2000) Induction of cell death by the lysosomotropic detergent MSDH. *FEBS Lett.* **470**, 35–39.

Ligresti A., Moriello A. S., Starowicz K., Matias I., Pisanti S., De Petrocellis L., Laezza C., Portella G., Bifulco M. and Di Marzo V. (2006) Antitumor activity of plant cannabinoids with emphasis on the effect of cannabidiol on human breast carcinoma. *J. Pharmacol. Exp. Ther.* **318**, 1375–1387.

Lyman W. D., Sonett J. R., Brosnan C. F., Elkin R. and Bornstein M. B. (1989) Δ^9-tetrahydrocannabinol: a novel treatment for experimental autoimmune encephalomyelitis. *J. Neuroimmunol.* **23**, 73–81.

MacManus A., Ramsden M., Murray M., Pearson H. A. and Campbell V. (2000) Enhancement of $^{45}Ca^{2+}$ influx and voltage-dependent Ca^{2+} channel activity by β-amyloid$_{(1-40)}$ in rat cortical synaptosomes and cultured cortical neurones: modulation by the proinflammatory cytokine interleukin-1β. *J. Biol. Chem.* **275**, 4713–4718.

Massi P., Vaccani A., Bianchessi S., Costa B., Mcchi P. and Parolaro D. (2006) The non-psychoactive cannabidiol triggers caspase activation and oxidative stress in human glioma cells. *Cell Mol. Life Sci.* **63**, 2057–2066.

Mathiasen I. S. and Jäättelä M. (2002) Triggering caspase-independent cell death to combat cancer. *Trends Mol. Med.* **5**, 212–220.

Matochik J. A., Eldreth D. A., Cadet J. L. and Bolla K. I. (2005) Altered brain tissue composition in heavy marijuana users. *Drug Alcohol Depend.* **77**, 23–30.

Matveyeva M., Hartmann C. B., Harrison M. T., Cabral G. A. and McCoy K. L. (2000) Delta (9)-tetrahydrocannabinol selectively increases aspartyl cathepsin D proteolytic activity and impairs lysozyme processing by macrophages. *Int. J. Immunopharmacol.* **22**, 373–381.

Moore T. H., Zammit S., Lingford-Hughes A., Barnes T. R., Jones P. B., Burke M. and Lewis G. (2007) Cannabis use and risk of psychotic or affective mental health outcomes: a systematic review. *Lancet* **370**, 319–328.

Movsesyan V. A., Stoica B. A., Yakoviev A. G., Knoblach S. M., Lea P. M., Cernak I., Vink R. and Faden A. I. (2004) Anandamide-induced cell death in primary neuronal cultures: role of calpain and caspase pathways. *Cell Death Differ.* **11**, 1121–1132.

Ollinger K. and Brunk U. T. (1995) Cellular injury induced by oxidative stress is mediated through lysosomal damage. *Free Radic. Biol. Med.* **19**, 565–574.

Raman C., McAllister S. D., Rizvi G., Patel S. G., Moore D. H. and Abood M. E. (2004) Amyotrophic lateral sclerosis: delayed disease progression in mice by treatment with a cannabinoid. *Amyotroph. Lateral Scler. Other Motor Neuron Disord.* **5**, 33–39.

Ranganathan M. and De Souza D. C. (2006) The acute effects of cannabinoids on memory in humans: a review. *Psychopharmacology* **188**, 425–444.

Reiners J. J. Jr, Caruso J. A., Mathieu P., Chelladurai B., Yin X. M. and Kessel D. (2002) Release of cytochrome c and activation of pro-caspase-9 following lysosomal photodamage involves Bid cleavage. *Cell Death Differ.* **9**, 934–944.

Roberg K. and Ollinger K. (1998) Oxidative stress causes relocation of the lysosomal enzyme cathepsin D with ensuing apoptosis in neonatal rat cardiomyocytes. *Am. J. Pathol.* **152**, 1151–1156.

Sarafian T., Habib N., Mao J. T., Tsu I. H., Yamamoto M. L., Hsu E., Tashkin D. P. and Roth M. D. (2005) Gene expression changes in human small airway epithelial cells exposed to Δ^9-tetrahydrocannabinol. *Toxicol. Lett.* **158**, 95–107.

Scallet A. C. (1991) Neurotoxicology of cannabis and THC: a review of chronic exposure studies in animals. *Pharmacol. Biochem. Behav.* **40**, 671–676.

Schestkowa O., Geisel D., Jacob R. and Hasilik A. (2007) The catalytically inactive precursor of cathepsin D induces apoptosis in human fibroblasts and HeLa cells. *J. Cell. Biochem.* **101**, 1558–1566.

Schlaepfer T. E., Lancaster E., Heidbreder R., Strain E. C., Kosel M., Fisch H. U. and Pearlson G. D. (2006) Decreased frontal white-matter volume in chronic substance abuse. *Drug Alcohol Depend.* **77**, 23–30.

Slee E. A., Harte M. T., Kluck R. M. *et al.* (1999) Ordering the cytochrome c-initiated caspase cascade: hierarchical activation of caspases-2,-3,-6,-7,-8, and -10 in a caspase-9-dependent manner. *J. Cell Biol.* **144**, 281–292.

Stoka V., Turk B., Schendel S. L. *et al.* (2001) Lysosomal protease pathways to apoptosis. Cleavage of bid, not pro-caspases, is the most likely route. *J. Biol. Chem.* **276**, 3149–3157.

Stoka V., Turk V. and Turk B. (2007) Lysosomal cysteine cathepsins; signaling pathways in apoptosis. *Biol. Chem.* **388**, 555–560.

Turk B., Stoka V., Rozman-Pungercar J., Cirman T., Droga-Mazovec G., Oresic K. and Turk V. (2002) Apoptotic pathways; involvement of lysosomal proteases. *Biol. Chem.* **382**, 1035–1044.

Tzilos G. K., Cintron C. B., Wood J. B., Simpson N. S., Young A. D., Pope H. G. and Yurgelun-Todd D. A. (2005) Lack of hippocampal volume change in long-term heavy cannabis users. *Am. J. Addict.* **14**, 64–72.

Vancompernolle K., Van Herreweghe F., Pynaert G., Van de Craen M., De Vos K., Totty N., Sterling A., Fiers W., Vandenabeele P. and Grooten J. (1998) Atractyloside-induced release of cathepsin B, a protease with caspase-processing activity. *FEBS Lett.* **438**, 150–158.

Velasco G., Galve-Roperh I., Sánchez C., Blázquez C. and Guzmán M. (2004) Hypothesis: cannabinoid therapy for the treatment of gliomas? *Neuropharmacology* **47**, 315–323.

Werneburg N. W., Guicciardi M. E., Bronk S. F. and Gores G. J. (2002) Tumor necrosis factor-alpha-associated lysosomal permeabilization is cathepsin B dependent. *Am. J. Physiol.* **283**, G947–G956.

Yuan X.-M., Li W., Dalen H., Lotem J., Kama R., Sachs L. and Brunk U. T. (2002) Lysosomal destabilization in p53-induced apoptosis. *Proc. Natl. Acad. Sci. USA* **99**, 6286–6291.

Zang Y., Beard R. L., Chandraratna R. A. and Kang J. X. (2001) Evidence of a lysosomal pathway for apoptosis induced by the synthetic retinoid CD437 in human leukaemia HL-60 cells. *Cell Death Differ.* **8**, 477–485.

Zhao M., Eaton J. W. and Brunk U. T. (2001) Bcl-2 phosphorylation is required for inhibition of oxidative stress-induced lysosomal leak and ensuing apotosis. *FEBS Lett.* **14**, 405–412.

Zuzarte-Luis V., Montero J. A., Torre-Perez N., Garcia-Porrero J. A. and Hurle J. (2007) Cathepsin D gene expression outlines the areas of physiological cell death during embryonic development. *Dev. Dyn.* **236**, 330–335.

British Journal of Pharmacology (2007) 152, 655–662

0007–1188/07 $30.00
www.brjpharmacol.org

REVIEW

Alzheimer's disease; taking the edge off with cannabinoids?

VA Campbell and A Gowran

Department of Physiology and Trinity College Institute of Neuroscience, Trinity College Dublin, Dublin, Ireland

Alzheimer's disease is an age-related neurodegenerative condition associated with cognitive decline. The pathological hallmarks of the disease are the deposition of β-amyloid protein and hyperphosphorylation of tau, which evoke neuronal cell death and impair inter-neuronal communication. The disease is also associated with neuroinflammation, excitotoxicity and oxidative stress. In recent years the proclivity of cannabinoids to exert a neuroprotective influence has received substantial interest as a means to mitigate the symptoms of neurodegenerative conditions. In brains obtained from Alzheimer's patients alterations in components of the cannabinoid system have been reported, suggesting that the cannabinoid system either contributes to, or is altered by, the pathophysiology of the disease. Certain cannabinoids can protect neurons from the deleterious effects of β-amyloid and are capable of reducing tau phosphorylation. The propensity of cannabinoids to reduce β-amyloid-evoked oxidative stress and neurodegeneration, whilst stimulating neurotrophin expression neurogenesis, are interesting properties that may be beneficial in the treatment of Alzheimer's disease. Δ^9-tetrahydrocannabinol can also inhibit acetylcholinesterase activity and limit amyloidogenesis which may improve cholinergic transmission and delay disease progression. Targeting cannabinoid receptors on microglia may reduce the neuroinflammation that is a feature of Alzheimer's disease, without causing psychoactive effects. Thus, cannabinoids offer a multi-faceted approach for the treatment of Alzheimer's disease by providing neuroprotection and reducing neuroinflammation, whilst simultaneously supporting the brain's intrinsic repair mechanisms by augmenting neurotrophin expression and enhancing neurogenesis. The evidence supporting a potential role for the cannabinoid system as a therapeutic target for the treatment of Alzheimer's disease will be reviewed herewith.
British Journal of Pharmacology (2007) **152**, 655–662; doi:10.1038/sj.bjp.0707446; published online 10 September 2007

Keywords: Alzheimer's disease; cannabinoid; CB_1 receptor; CB_2 receptor; β-amyloid; neurodegeneration

Abbreviations: Aβ, β-amyloid; AD, Alzheimer's disease; CB, cannabinoid; CBD, cannabidiol; NMDA, *N*-methyl D-aspartate; Δ^9-THC, Δ^9-tetrahydrocannabinol

Pathophysiology of Alzheimer's disease

Alzheimer's disease (AD) is a chronic debilitating neurodegenerative condition that is associated with progressive cognitive decline and profound neuronal loss, and estimated to affect 10% of people over the age of 65 years and 25% of people over the age of 80 years (Herbert *et al.*, 2003). Western society is developing an increasingly aged population and this demographic shift is associated with a rise in the prevalence of age-related illnesses such as AD. The United Nations population projections estimate that 370 million people will be older than 80 years by 2050 and the associated increase in patients with AD will pose a substantial socio-economic burden. While a small proportion of AD cases have a genetic basis, the majority of cases are sporadic with unknown aetiology. A consistent feature of the AD brain is the presence of senile plaques composed of pathogenic extracellular deposits of β-amyloid (Aβ), a 1–42 amino acid peptide derived from aberrant processing of the transmembrane amyloid precursor protein (Walsh and Selkoe, 2007). Aβ fragments are proposed to play a central role in the genesis of the disease by evoking neuronal cell death (Boland and Campbell, 2003). The senile plaques are located within various brain regions but the hippocampus, cerebral cortex and amygdala are particularly vulnerable and plaques begin to form in these regions early in the disease process resulting in memory loss and behavioural changes (Ogomori *et al.*, 1989). A second pathological hallmark of the disease is the hyperphosphorylation of the microtubule-associated protein, tau, resulting in formation of the intracellular neurofibrillary tangles that impair inter-neuronal communication (Mi and Johnson, 2006). AD is also associated with neuroinflammatory events and oxidative stress that are likely to exacerbate the disease process. Epidemiological studies support an involvement of inflammatory

Correspondence: Dr VA Campbell, Department of Physiology and Trinity College Institute of Neuroscience, Trinity College Dublin, Dublin 2, Ireland.
E-mail: vacmpbll@tcd.ie
Received 29 May 2007; revised 3 July 2007; accepted 8 August 2007; published online 10 September 2007

mechanisms in AD since patients using non-steroidal anti-inflammatory drugs for a 2-year period have a 60–80% reduction in the risk for the disease, while long-term non-steroidal anti-inflammatory drug treatment attenuates disease onset and reduces the severity of symptoms (Rich *et al.*, 1995). Microglia are the Principal immune cells in the brain and in the AD brain they surround the senile plaques, possibly recruited to the plaque region in an attempt to clear the Aβ burden by phagocytosis (Wilkinson and Landreth, 2006). In AD, the Aβ deposition exceeds the phagocytic ability of the microglia and the persistent presence of activated microglia at the plaque results in a prolonged release of proinflammatory cytokines such as interleukin-1β (Bayer *et al.*, 1999; Heneka and O'Banion, 2007) which mediate local inflammation and have the proclivity to increase the processing of amyloid precursor protein to generate more Aβ fragments (Heneka and O'Banion, 2007), as well as having a direct neurotoxic influence (Vereker *et al.*, 2000). The association of activated microglia at the periphery of the senile plaque contributes to the generation of reactive oxygen species that mediate the oxidative damage found in the brains of patients with AD (Wilkinson and Landreth, 2006). Thus, inflammation and oxidative stress play a critical role in the disease process and anti-inflammatory and antioxidant strategies are likely to have enormous therapeutic potential for AD patients. Other factors that are thought to contribute to the pathophysiology of AD include dysregulation of intracellular calcium homeostasis and excitotoxicity (LaFerla, 2002). Cholinergic neurones are particularly vulnerable in AD and current therapeutics include acetylcholinesterase (AChE) inhibitors that aim to enhance acetylcholine (ACh) availability. However, such drugs are only suitable for the mild cognitive impairment that occurs early in the disease and no treatments are currently available to reverse the progression of the disease.

Cannabinoid system in the brain

The discovery of an endogenous cannabinoid (CB)-signalling system in the brain has prompted much research into understanding how this system regulates physiological and pathological events within the central nervous system. The endocannabinoid molecules, 2-arachidonoyl glycerol and anandamide, interact with the G-protein-coupled cannabinoid receptors, CB_1 and CB_2. These receptors are also activated by phytocannabinoids, such as Δ^9-tetrahydrocannabinol (Δ^9-THC), isolated from the *Cannabis sativa* plant. The action of endocannabinoids at their receptors is terminated by enzymatic degradation of the endocannabinoids, or by membrane transport (Piomelli, 2003). Early reports indicating a potential role for the cannabinoid system in the management of AD are based on the finding that Dronabinol, an oil-based solution of Δ^9-THC, improves the disturbed behaviour and stimulates appetite in AD patients (Volicer *et al.*, 1997), and alleviates nocturnal agitation in severely demented patients (Walther *et al.*, 2006). More recently, an increasing body of evidence has accumulated to suggest antioxidant, anti-inflammatory and neuroprotective roles of the cannabinoid system (Jackson *et al.*, 2005). Such properties may be harnessed to circumvent the neurodegenerative process and offer more effective approaches to treat AD (Pazos *et al.*, 2004). In this review the recent experimental evidence that highlights the potential of the cannabinoid system to alleviate some of the pathology and cognitive decline associated with AD will be discussed.

The cannabinoid system in the AD brain

The CB_1 receptor is abundant within the brain and associated with the cortex, hippocampus, cerebellum and basal ganglia (Herkenham *et al.*, 1991). CB_1 receptors in the hippocampus contribute to the effect of cannabinoids on learning and memory (Riedel and Davies, 2005); cognitive processes, which are disrupted early in the course of AD. CB_2 receptors have a more limited expression in the central nervous system, being largely confined to neurones within the brainstem (Van Sickle *et al.*, 2005), cerebellum (Ashton *et al.*, 2006) and microglia (Nunez *et al.*, 2004). Post-mortem studies of AD brains have detected increased expression of CB_1 and CB_2 receptors on microglia within the senile plaque, while CB_1 expression is reduced in neurones more remote from the plaque (Ramirez *et al.*, 2005). Also, cannabinoid receptors in the AD brain are nitrosylated, and this may contribute to the impaired coupling of these receptors to downstream effector signalling molecules (Ramirez *et al.*, 2005). Other studies have failed to establish a link between changes in CB_1 receptors in the AD brain and the specific pathological events that take place in this illness (Westlake *et al.* 1994), and report no changes in expression of CB_1 receptors in the vicinity of the senile plaque (Benito *et al.*, 2003). However, the endocannabinoid metabolizing enzyme, fatty acid amide hydrolase, is upregulated in the senile plaque (Benito *et al.*, 2003), and may contribute to the increase in expression of anandamide metabolites, such as arachidonic acid, in the vicinity of the senile plaque. Such a pathway may be involved in increasing the production of prostaglandins and related pro-inflammatory molecules that are pertinent to the inflammatory process of AD. The association of fatty acid amide hydrolase with astrocytes within the senile plaque may participate in the astrocytic events that culminate in the reactive gliosis that is observed in regions rich in Aβ deposits (Wyss-Coray, 2006).

Cannabinoids mediate neuroprotection

Neuronal damage can increase the production of endocannabinoids (Stella *et al.*, 1997; Marsicano *et al.*, 2003), and cells lacking CB_1 receptors are more vulnerable to damage (Marsicano *et al.*, 2003). Those studies indicate that neural cannabinoid tone influences neuronal survival and suggest that augmentation of the cannabinoid system may offer protection against the deleterious consequences of pathogenic molecules such as Aβ. Recently, Aβ has been demonstrated to induce hippocampal degeneration, gliosis and cognitive decline, with a concomitant increase in the production of the endocannabinoid, 2-arachidonoyl glycerol, and this may reflect an attempt of the endocannabinoid system to provide neuroprotection from Aβ-induced damage

(Van Der Stelt *et al.*, 2006). Furthermore, in that study, when endocannabinoid uptake was inhibited by VDM-11, the Aβ-induced neurotoxicity and memory impairment were reversed, although this was dependent upon early administration of the reuptake inhibitor. Those findings suggest that robust and early pharmacological enhancement of brain endocannabinoid levels may protect against the deleterious consequences of Aβ. Other endocannabinoids, such as anandamide and noladin ether, have been found to reduce Aβ neurotoxicity *in vitro* via activation of the CB_1 receptor and engagement the extracellular-regulated kinase pathway (Milton, 2002). Thus, endocannabinoids can reverse the negative consequences of exposure to Aβ, and such findings suggest that drugs designed to augment endocannabinoid tone, including inhibitors of membrane uptake and fatty acid amide hydrolase inhibitors, may have potential in the treatment of AD. However, the study by Van Der Stelt *et al.* (2006) cautions that the timing of endocannabinoid upregulation by pharmacological intervention in relation to the time-course of development of the disease pathology is crucial, since administration of VDM-11 later in the pathological cascade actually worsens memory retention in rodents. Also, the physiological role of the cannabinoid system in mnemonic processes should not be underestimated. In the hippocampus CB_1 receptor activation is negatively associated with the performance of rodents in memory tasks (Castellano *et al.*, 2003), possibly via a reduction in hippocampal ACh levels (Gifford *et al.*, 2000), while the CB_1 antagonist, SR141716A improves performance in memory tasks (Wolff and Leander, 2003). Furthermore, the impairment in memory evoked by Aβ in rodents is reversed by SR141716A (Mazzola *et al.*, 2003), suggesting that CB_1 receptor blockade may be beneficial in reversing the amnesia associated with AD. However, given the evidence for a neuroprotective role of the CB_1 receptor (Marsicano *et al.*, 2003; Alger, 2006), CB_1 antagonists pose the risk of exacerbating the neurodegenerative component of the disease, which may negate the beneficial effects of such drugs on amnesia.

Cannabinoids and excitotoxicity

The dysregulation of intracellular Ca^{2+} homeostasis (Smith *et al.*, 2005) and excessive activation of the *N*-methyl D-aspartate (NMDA) subtype of glutamate receptor, leading to excitotoxicity, are features of the AD brain (Sonkusare *et al.*, 2005). All of the clinical mutations in the presenilin genes (PS1/PS2) that have been linked with the inherited form of AD disrupt calcium signalling (Smith *et al.*, 2005), which may contribute to subsequent neurodegeneration and memory impairments (Rose and Konnerth, 2001). Also, Aβ can itself directly increase voltage-dependent Ca^{2+} channel activity (MacManus *et al.*, 2000), as well as forming Ca^{2+}-permeable pores in lipid bilayers (Arispe *et al.*, 1993), to increase intracellular Ca^{2+} concentration as part of the pathogenic mechanism. Aβ also reduces glutamate uptake by astrocytes and increases the activation of glutamate receptors to evoke excitotoxicity (Sonkusare *et al.*, 2005). Thus, strategies that reduce Ca^{2+} influx and limit excitotoxicity may confer neuroprotection in AD. The non-competitive NMDA receptor antagonist, memantine (Namenda, Ebixa) is used in the treatment of moderate to severe AD (Cosman *et al.*, 2007), and its beneficial properties are based on an ability to inhibit pathological, but not physiological, functions of NMDA receptors, as well as antioxidant action and a propensity to increase production of brain-derived neurotrophic factor in the brain (Sonkusare *et al.*, 2005). Manipulation of the cannabinoid system has several consequences that mirror those observed with memantine. Thus, the protective effects of some cannabinoids are related to the direct regulation of the NMDA receptor, since the non-psychotropic cannabinoid, HU-211, acts as a stereoselective inhibitor of the NMDA receptor and protects rat forebrain cultures (Nadler *et al.*, 1993) and cortical neuronal cultures (Eshhar *et al.*, 1993) from NMDA-induced neurotoxicity. Furthermore, activation of the CB_1 receptor protects mouse spinal neurons (Abood *et al.*, 2001) and cultured hippocampal neurones (Shen and Thayer, 1998) from excitotoxicity, possibly through inhibition of presynaptic Ca^{2+} entry (Mackie and Hille, 1992; Twitchell *et al.*, 1997) and the subsequent suppression of excessive glutamatergic synaptic activity (Shen and Thayer, 1998; Takahashi and Castillo, 2006). CB_1 receptor agonists also inhibit glutamate release, which may contribute to a reduction in excitotoxicity (Wang, 2003). The evidence for a Ca^{2+}-dependent synthesis of anandamide and 2-arachidonoyl glycerol (Di Marzo *et al.*, 1994; Stella *et al.*, 1997) would suggest that endocannabinoids are generated in response to an intracellular Ca^{2+} load in an attempt to provide feedback inhibition of excitotoxicity. In this regard it is notable that endocannabinoid upregulation is a feature of a number of neurotoxic paradigms that are associated with elevated intracellular Ca^{2+} concentration (Hansen *et al.*, 2001). Alternative mechanisms that are pivotal to cannabinoid-mediated protection include inhibition of $[Ca^{2+}]_i$ by reducing calcium release from ryanodine-sensitive stores (Zhuang *et al.*, 2005), inhibition of protein kinase A and reduced nitric oxide generation (Kim *et al.*, 2006). Like memantine, cannabinoids are also capable of increasing brain-derived neurotrophic factor to confer protection against excitotoxicity (Khaspekov *et al.*, 2004). In non-neuronal cells, the induction of nerve growth factor is also facilitated by cannabinoids, acting through the PI3K/PKB pathway (Sanchez *et al.*, 2003), and activation of the CB_1 receptor by the endocannabinoid, 2-arachidonoyl glycerol, can also couple to an axonal growth response, whereas CB_1 receptor antagonists inhibit axonal growth (Williams *et al.*, 2003). Thus, dampening excessive glutamatergic transmission and excitotoxicity, coupled with neurotrophic actions, may represent interesting actions of cannabinoids that could be exploited for the treatment of AD.

Cannabidiol prevents Aβ-mediated neurotoxicity

Cannabidiol (CBD) is the principal non-psychoactive component of *Cannabis sativa*, with potent antioxidant properties that offer neuroprotection against glutamate toxicity (Hampson *et al.*, 1998). In differentiated PC12 cells exposed to Aβ, CBD reduces the induction of inducible nitric oxide synthase (iNOS), nitric oxide production and activation of

the stress-activated protein kinase p38 and the inflammatory transcription factor, nuclear factor-κB (Esposito *et al.*, 2006a), providing evidence for a CBD-mediated downregulation of the inflammatory signalling events associated with exposure to Aβ. As well, CBD reduces Aβ-induced neuronal cell death by virtue of its ability to scavenge reactive oxygen species and reduce lipid peroxidation; antioxidant properties that occur independently of the CB_1 receptor (Iuvone *et al.*, 2004). CBD also reverses tau hyperphosphorylation, a key hallmark of AD, by reducing phosphorylation of glycogen synthase kinase-3β, a tau protein kinase responsible for the tau hyperphosphorylation in AD (Esposito *et al.*, 2006b). Moreover, since glycogen synthase kinase-3β also evokes amyloid precursor protein processing to increase Aβ production (Phiel *et al.*, 2003), the CBD-mediated inhibition of glycogen synthase kinase-3β is likely to be effective in reducing the amyloid burden. Thus, from such *in vitro* studies one can speculate that CBD may be therapeutically beneficial in AD, since it can prevent the deleterious effects of Aβ and ameliorate several features of AD pathology, including tau hyperphosphorylation, oxidative stress, neuroinflammation and apoptosis. Whether such actions of CBD are retained in the AD brain remains to be established, and experiments to test the effect of CBD in the various transgenic animal models of AD are eagerly awaited. In the meantime, reports that CBD is effective as an antioxidant and neuroprotectant in an animal model of Parkinson's disease (Lastres-Becker *et al.*, 2005), and orally effective in a rat model of chronic inflammation (Costa *et al.*, 2007), lend support to its potential therapeutic value in AD. There are a number of advantages of CBD as a therapeutic agent for AD; it is devoid of psychoactive activity and since CB receptors are nitrosylated in the AD brain, a feature that may hinder CB receptors coupling to their downstream effectors (Ramirez *et al.*, 2005), a therapy that does not depend on signalling through CB receptors may have a distinct advantage. Sativex is a cannabinoid-based oromucosal spray, containing CBD and THC, that is devoid of tolerance or withdrawal symptoms (Perez, 2006). This therapy is already available for the treatment of neuropathic pain and multiple sclerosis and may be exploited in the future for the treatment of AD.

CB_2 receptors and neuroinflammation

The CB_2 receptor is largely confined to glial cells in the brain (Nunez *et al.*, 2004), although some studies have reported CB_2 receptors in neuronal populations within the brainstem and cerebellum (van Sickle *et al.*, 2005; Ashton *et al.*, 2006). CB_2 receptors have been implicated in the control of neural survival (Fernandez-Ruiz *et al.*, 2007) and mediate neuroprotection through their anti-inflammatory actions (Ehrhart *et al.*, 2005). CB_2 receptors are upregulated in activated microglia and astrocytes, and this upregulation is proposed to control the local production of proinflammatory mediators such as interleukin-1β, reactive oxygen species and prostaglandins. In the AD brain and in animal models of AD-like pathology, CB_2 receptors are upregulated within the active microglia present in those brain regions where senile plaques are abundant (Benito *et al.*, 2003; Ramirez *et al.*, 2005). The upregulation of CB_2 in such pathological situations may be an attempt to reduce neuroinflammation since CB_2 receptor activation *in vitro* reduces the microglial production of pro-inflammatory molecules (Facchinetti *et al.*, 2003). Such control in the production of inflammatory mediators may be due to a direct impact on activity of transcription factors, such as nuclear factor κB (Panikashvili *et al.*, 2005; Esposito *et al.*, 2006a). Thus, the neuroprotective mechanisms of cannabinoids are likely to include a downregulation in activity of the transcription factors that are pertinent to induction of the pro-inflammatory cytokines that serve as key players in neurodegenerative disease, while also stimulating the production of anti-inflammatory species such as IL-1ra (Molina-Holgado *et al.*, 2003). The manipulation of such inflammatory pathways may be exploited for the treatment of AD. In support of this contention, Ramirez *et al.* (2005) have demonstrated that in rats treated with Aβ, the induction of AD-like pathology and cognitive impairment, is reversed by the CB_1/CB_2 agonist, WIN,55212–22 and the CB_2-selective agonist, JWH-133. Since the CB_2 receptor was only associated with activated microglia located within the plaque, those authors have suggested that the CB_2 receptor may be a promising target for AD by virtue of its ability to serve as a brake for the neuroinflammatory cascade that is a feature of AD. CB_2 agonists offer the advantage of being devoid of psychoactivity, although it is important to recognize that they may have other side effects such as immune suppression (Pertwee, 2005), which would be undesirable in an elderly population.

Cannabinoids and neurogenesis in the adult brain

Another exciting mechanism that could account for the ability of cannabinoids to confer neuroprotection may be related to their regulation of neurogenesis. Adult neurogenesis can occur in the dentate gyrus of the hippocampus and the subventricular zone (Grote and Hannan, 2007), resulting in the presence of newly generated neurones. In several mouse models of AD neurogenesis is reduced (Dong *et al.*, 2004), although it should be noted that in the post-mortem AD brain, neurogenesis is increased (Jin *et al.*, 2004). Factors that enhance neurogenesis, such as dietary restriction and upregulation of brain-derived neurotrophic factor, enhance neurogenesis and improve the memory performance in animal models of AD (Lee *et al.*, 2000). Thus, targeting adult neurogenesis is receiving interest as a means to mitigate the symptoms of AD. In this regard it is notable that the cannabinoid system also regulates neurogenesis (Galve-Roperh *et al.*, 2007). Adult neurogenesis is defective in mice lacking CB_1 receptors (Jin *et al.*, 2004), and the synthetic cannabinoid, WIN55212-2, stimulates adult neurogenesis by opposing the antineurogenic effect of nitric oxide (Kim *et al.*, 2006). Also, the CB_1 agonist HU-210 has anxiolytic and antidepressant effects, which may be a functional consequence of enhanced neurogenesis (Jiang *et al.*, 2005). CB_2 receptor activation also stimulates neural progenitor proliferation *in vitro* and *in vivo* (Palazuelos *et al.*, 2006), and targeting neurogenesis via the CB_2 receptor would avoid undesired psychoactive side effects. Thus, the neuroprotective

effects of cannabinoids may involve short-term adaptation to neuronal stress, such as limiting excitotoxicity, as well as longer-term adaptations, such as enhancing neurogenesis. It remains to be established whether or not the beneficial effects of cannabinoids on memory, neuroinflammation and neurodegeneration in animal models of AD are due to a functional consequence of an enhancement in neurogenesis.

Targeting acetylcholinesterase with cannabinoids

Currently there are four approved drugs (tacrine, Cognex; donepezil, Aricept; rivastigmine, Exelon; galantamine, Reminyl) that are used to alleviate the symptoms of early stage AD by inhibiting the active site of AChE, thus increasing the levels of ACh at the synaptic cleft and enhancing cholinergic transmission. In addition, AChE accelerates that assembly of Aβ peptides into fibrillar species by forming complexes with Aβ via the peripheral anionic site on AChE (Inestrosa *et al.*, 1996), an interaction that increases the neurotoxicity of the Aβ fibrils (Alvarez *et al.*, 1998). Thus, AChE inhibitors offer a two-pronged attack for the treatment of AD by virtue of their ability to enhance ACh availability, as well as reduce amyloidogenesis and subsequent neurotoxicity. A recent study has demonstrated that Δ^9-THC competitively inhibits AChE and prevents the AChE-induced aggregation of Aβ by virtue of Δ^9-THC binding to the peripheral anionic site on AChE (Eubanks *et al.*, 2006). Compared with tacrine and donepezil, Δ^9-THC was found to be more robust inhibitor of Aβ aggregation, suggesting that Δ^9-THC and its analogues warrant further investigation as AChE inhibitors for use in the treatment of AD.

Do cannabinoids have a role for the treatment of other neurodegenerative conditions?

It is also worth considering how the aforementioned properties of cannabinoids may be beneficial in ameliorating the symptoms of other diseases in which neuroinflammation, oxidative stress and neurodegeneration are key features, such as multiple sclerosis and Parkinson's disease. Benito *et al.* (2007) have reported that components of the cannabinoid system are upregulated in multiple sclerosis (MS) plaques, suggesting that endocannabinoids either have a role in the pathogenesis of MS or may be upregulated as a consequence of the pathology. MS is associated with excitotoxicity (Pitt *et al.*, 2000; Smith *et al.*, 2000) and neuroinflammation (Ziemssen, 2005), and these represent features of the disease that cannabinoids may be able to circumvent. In encephalomyelitis virus-induced demyelinating disease, an animal model of MS, the mixed cannabinoid agonist HU210 reduces axonal damage and improves motor function as a consequence of a concomitant activation of the CB_1 receptor in neurones and CB_2 in astrocytes (Docagne *et al.*, 2007). Other studies in animal models of MS have demonstrated a role for the CB_2 receptor in enhancing T-cell apoptosis (Sanchez *et al.*, 2006) and suppressing microglial activation (Ehrhart *et al.*, 2005), while the CB_1 receptor is associated with neuroprotection (Pryce and Baker, 2007). Such neuroprotective and antioxidant properties of cannabinoids also underlie their ability to reverse the motor deficits in animal models of Parkinson's disease (Lastres-Becker *et al.*, 2005; Garcia-Arencibia *et al.*, 2007), and lend support of a potential role for cannabinoid-based therapies to mitigate the symptoms of a range of neurodegenerative conditions.

Conclusion

Alzheimer's disease is a devastating illness for which there is no cure. Current AD drugs, which serve as AChE inhibitors, have a number of unpleasant side effects such as hepatotoxicity and gastrointestinal disturbances. While the NMDA receptor antagonist, memantine, can modify the disease, it cannot reverse the process of neurodegeneration.

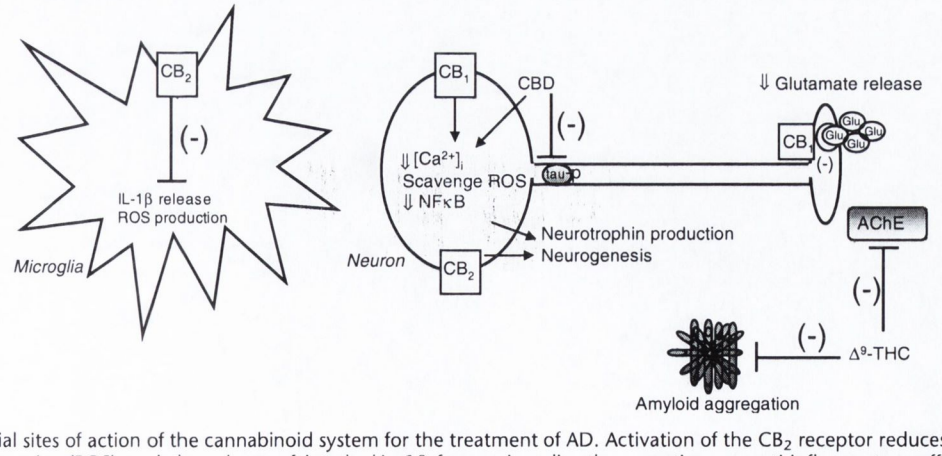

Figure 1 Potential sites of action of the cannabinoid system for the treatment of AD. Activation of the CB_2 receptor reduces the formation of reactive oxygen species (ROS) and the release of interleukin-1β from microglia, thus exerting an anti-inflammatory effect. In neurones, activation of the CB_1 receptor reduces intracellular Ca^{2+} concentration ($[Ca^{2+}]_i$), protects against oxidative stress and reduces inflammatory signalling by inhibition of nuclear factor κB. CB_1 activation also inhibits glutamate release to reduce excitotoxicity, and enhances neurotrophin expression and neurogenesis. CBD is neuroprotective and anti-inflammatory in a CB receptor-independent manner, and also reduces tau phosphorylation. Δ^9-THC inhibits AChE, resulting in enhanced cholinergic transmission and reduced amyloidogenesis. AD, Alzheimer' disease; AChE, acetylcholinesterase; CB, cannabinoid; CBD, cannabinoid; Δ^9-THC, Δ^9-tetrahydrocannabinol.

Manipulation of the cannabinoid pathway offers a novel pharmacological approach for the treatment of AD that may be more efficacious than current treatment regimes. Cannabinoids can reduce the oxidative stress, neuroinflammation and apoptosis that is evoked by Aβ, while promoting the brain's intrinsic repair mechanisms. Certain cannabinoids, such as Δ^9-THC, may also increase ACh availability and reduce amyloidogenesis, although potential psychoactive side effects may hinder its clinical usefulness. Cannabinoids clearly offer a multifaceted approach for the treatment of AD and future studies should focus on examining the efficacy of cannabinoids in the array of animal models that exhibit AD-like pathology and cognitive decline. Targeting the CB_2 receptor to reduce neuroinflammation while stimulating neurogenesis is likely to be of particular interest, given the reduced risk of psychoactive activity and the close association of the CB_2 receptor with the senile plaque, thus limiting drug effects to the region of pathology and sparing the potential for widespread effects on normal neurophysiological processes. In conclusion, manipulation of the cannabinoid system offers the potential to upregulate neuroprotective mechanisms while dampening neuroinflammation. Whether these properties will be beneficial in the treatment of AD in the future is an exciting topic that undoubtedly warrants further investigation (Figure 1).

Conflict of interest

The authors state no conflict of interest.

References

Abood ME, Rizvi G, Sallapudi N, McAllister S (2001). Activation of the CB_1 cannabinoid receptor protects cultured mouse spinal neurons against excitotoxicity. *Neuroscience Lett* **309**: 197–201.

Alger BE (2006). Not too excited? Thank your endocannabinoids. *Neuron* **51**: 393–395.

Alvarez A, Alarcon A, Opazo C, Campos EO, Munoz F, Calderon FH *et al.* (1998). Stable complexes involving acetylcholinesterase and amyloid-β-fibrils change the biochemical properties of the enzyme and increase the neurotoxicity of Alzheimer's fibrils. *J Neurosci* **18**: 407–416.

Arispe N, Pollard HB, Rojas E (1993). Giant multilevel cation channels formed by Alzheimer's disease Aβ1-40 in bilayer membranes. *Proc Natl Acad Sci USA* **90**: 10573–10577.

Ashton JC, Friberg D, Darlington CL, Smith PF (2006). Expression of the cannabinoid CB2 receptor in the rat cerebellum: an immunohistochemical study. *Neurosci Lett* **396**: 113–116.

Bayer TA, Buslei R, Havas L, Falkai P (1999). Evidence for activation of microglia in patients with psychiatric illnesses. *Neurosci Lett* **271**: 126–128.

Benito C, Nunez E, Tolon RM, Carrier EJ, Rabano A, Hillard CJ *et al.* (2003). Cannabinoid CB_2 receptors and fatty acid amide hydrolase are selectively overexpressed in neuritic plaque-associated glia in Alzheimer's disease brains. *J Neurosci* **23**: 11136–11141.

Benito C, Romero JP, Tolon RM, Clemente D, Docagne F, Hillard CJ *et al.* (2007). Cannabinoid CB_1 and CB_2 receptors and fatty acid amide hydrolase are specific markers of plaque cell subtypes in human multiple sclerosis. *J Neurosci* **27**: 2396–2402.

Boland B, Campbell V (2003). Amyloid-induced apoptosis of cultured cortical neurones involves calpain-mediated cleavage of poly-ADP ribose polymerase. *Neurobiol Aging* **24**: 179–186.

Castellano C, Rossi-Arnaud C, Cestari V, Costanzi M (2003). Cannabinoids and memory: animal studies. *Curr Drug Targets CNS Neurol Disord* **2**: 389–402.

Cosman KM, Boyle LL, Porsteinsso AP (2007). Memantine in the treatment of mild-to-moderate Alzheimer's disease. *Expert Opin Pharmacother* **8**: 203–214.

Costa B, Trovato AE, Comelli F, Giagnoni G, Colleoni M (2007). The non-psychoactive cannabis constituent cannabidiol is an orally effective therapeutic agent in rat chronic inflammatory and neuropathic pain. *Eur J Pharmacol* **556**: 75–83.

Di Marzo V, Fontana A, Cadas H, Schinell S, Clmlno G, Schwartz J *et al.* (1994). Formation and inactivation of endogenous cannabinoid anandamide in central neurones. *Nature* **372**: 686–691.

Docagne F, Muñetón V, Clemente D, Ali C, Loría F, Correa F *et al.* (2007). Excitotoxicity in a chronic model of multiple sclerosis: neuroprotective effects of cannabinoids through CB_1 and CB_2 receptor activation. *Mol Cell Neurosci* **34**: 551–561.

Dong H, Goico B, Martin M, Csernansky CA, Bertchume A, Csernansky JG (2004). Modulation of hippocampal cell proliferation, memory and amyloid plaque deposition in APPsw (Tg2576) mutant mice by isolation stress. *Neuroscience* **127**: 601–609.

Ehrhart J, Obergon D, Mri T, Hou H, Sun N, Bai Y *et al.* (2005). Stimulation of CB_2 suppresses microglial activation. *J Neuroinflamm* **12**: 22–29.

Eshhar N, Streim S, Biegon A (1993). HU-211, a non-psychotropic cannabinoid, rescues cortical neurones from excitatory amino acid toxicity in culture. *Neuroreport* **5**: 237–240.

Esposito G, De Filippis D, Carnuccio R, Izzo AG, Iuvone T (2006b). The marijuana component, cannabidiol, inhibits β-amyloid-induced tau protein hyperphosphorylation through Wnt/β-catenin pathway rescue in PC12 cells. *J Mol Med* **84**: 253–258.

Esposito G, De Filippis D, Maiuri MC, De Stefano D, Carnuccio R, Iuvone T (2006a). Cannabidiol inhibits inducible NOS expression and NO production in β-amyloid-stimulated PC12 neurons through p38 MAP kinase and NFκB involvement. *Neurosci Lett* **399**: 91–95.

Eubanks LM, Rogers CJ, Beuscher AE, Koob GF, Olson AJ, Dickerson TJ *et al.* (2006). A molecular link between the active component of marijuana and Alzheimer's disease pathology. *Mol Pharm* **3**: 773–777.

Facchinetti F, Del Giudice E, Furegato S, Passarotto M, Leon A (2003). Cannabinoids ablate release of TNFα in rat microglial cells stimulated with lipopolysaccharide. *Glia* **41**: 161–168.

Fernandez-Ruiz J, Romero J, Velasco G, Tolon RM, Ramos JA, Guzman M (2007). Cannabinoid CB_2 receptor: a new target for controlling neural cell survival? *Trends Pharm Sci* **28**: 39–45.

Galve-Roperh I, Aguada T, Palazuelos J, Guzman M (2007). The endocannabinoid system and neurogenesis in health and disease. *Neuroscientist* **13**: 109–114.

Garcia-Arencibia M, Gonzalez S, deLago E, Ramos JA, Mechoulam R, Fernandez-Ruiz J (2007). Evaluation of the neuroprotective effect of cannabinoids in a rat model of Parkinson's disease: importance of antioxidant and cannabinoid receptor-independent properties. *Brain Res* **1134**: 162–170.

Gifford AN, Bruneus M, Gatley SJ, Volkow ND (2000). Cannabinoid receptor-mediated inhibition of acetylcholine release from hippocampal and cortical synaptosomes. *Br J Pharmacol* **131**: 645–650.

Grote HE, Hannan AJ (2007). Regulators of adult neurogenesis in the healthy and diseased brain. *Clin Exp Pharm Phys* **34**: 533–545.

Hampson AJ, Grimaldi M, Axelrod J, Wink D (1998). Cannabidiol and $(-)\Delta^9$-tetrahydrocannabinol are neuroprotective antioxidants. *Proc Natl Acad Sci USA* **95**: 8268–8273.

Hansen HH, Ikonomidou C, Bittigau P, Hansen SH, Hansen HS (2001). Accumulation of the anandamide precursor and other *N*-acylethanolamine phospholipids in infant rat models of *in vivo* necrotic and apoptotic neuronal death. *J Neurochem* **76**: 39–46.

Heneka MT, O'Banion MK (2007). Inflammatory processes in Alzheimer's disease. *J Neuroimmunol* **184**: 69–91.

Herbert LE, Scherr PA, Bienias JL, Bennett DA, Evans DA (2003). Alzheimer's disease in the US population: prevalence estimates using the 2000 census. *Archiv Neurol* **60**: 1119–1122.

Herkenham M, Lynn AB, Johnson MR, Melvin LS, de Costa BR, Rice KC (1991). Characterization and localization of cannabinoid receptors in rat brain: a quantitative *in vitro* autoradiographic study. *J Neurosci* **11**: 563–583.

Inestrosa NC, Alvarez A, Pecez CA, Moreno RD, Vicente M, Linker C *et al.* (1996). Acetylcholinesterase accelerates assembly

of amyloid-β-peptides into Alzheimer's fibrils: possible role of the peripheral site of the enzyme. *Neuron* **16**: 881–891.

Iuvone T, Esposito G, Esposito R, Santamaria R, Di Rosa M, Izzo AA (2004). Neuroprotective effect of cannabidiol, a non-psychoactive component from *Cannabis sativa*, on β-amyloid-induced toxicity in PC12 cells. *J Neurochem* **89**: 134–141.

Jackson SJ, Diemel LT, Pryce G, Baker D (2005). Cannabinoids and neuroprotection in CNS inflammatory disease. *J Neurol Sci* **233**: 21–25.

Jiang W, Zhang Y, Xiao L, Van Cleemput J, Ji S, Bai G (2005). Cannabinoids promote embryonic and adult hippocampal neurogenesis and produce anxiolytic and anti-depressant-like effects. *J Clin Invest* **115**: 3104–3116.

Jin K, Peel AL, Mao XL, Xie L, Cottrell B, Henshall DC *et al.* (2004). Increased hippocampal neurogenesis in Alzheimer's disease. *Proc Natl Acad Sci USA* **101**: 343–347.

Khaspekov LG, Brenz Verca MS, Frumkina LE, Hermann H, Marsicano G, Lutz B (2004). Involvement of brain-derived neurotrophic factor in cannabinoid receptor-dependent protection against excitotoxicity. *Eur J Neurosci* **19**: 1691–1698.

Kim SH, Won SJ, Mao A, Ledent C, Jin K, Greenberg DA (2006). Role for neuronal nitric-oxide synthase in cannabinoid-induced neurogenesis. *J Pharmacol Exp Ther* **319**: 150–154.

LaFerla FM (2002). Calcium dyshomeostasis and intracellular signaling in Alzheimer's disease. *Nat Rev Neurosci* **3**: 862–872.

Lastres-Becker I, Molina-Holgado F, Ramos JA, Mechoulam R, Fernandez-Ruiz J (2005). Cannabinoids provide neuroprotection against 6-hydroxydopamine toxicity *in vivo* and *in vitro*: relevance to Parkinson's disease. *Neurobiol Dis* **19**: 96–107.

Lee J, Duan W, Long JM, Ingram GK, Mattson MP (2000). Dietary restriction increases the number of newly generated neural cells and induced BDNF expression in the dentate gyrus of rats. *J Mol Neurosci* **15**: 99–108.

Mackie K, Hille B (1992). Cannabinoids inhibit N-type calcium channels in neuroblastoma–glioma cell lines. *Proc Natl Acad Sci USA* **89**: 3825–3829.

MacManus A, Ramsden M, Murray M, Pearson HA, Campbell V (2000). Enhancement of $^{45}Ca^{2+}$ influx and voltage-dependent Ca^{2+} channel activity by β-amyloid$_{(1-40)}$ in rat cortical synaptosomes and cultured cortical neurones: modulation by the proinflammatory cytokine interleukin-1β. *J Biol Chem* **275**: 4713–4718.

Marsicano G, Goodenough S, Monory K, Hermann H, Eder M, Cannich A *et al.* (2003). CB_1 receptors and on-demand defense against excitotoxicity. *Science* **302**: 84–88.

Mazzola C, Micale V, Drago F (2003). Amnesia induced by β-amyloid fragments in counteracted by cannabinoid CB_1 receptor blockade. *Eur J Pharmacol* **477**: 219–225.

Mi K, Johnson GV (2006). The role of tau phosphorylation in the pathogenesis of Alzheimer's disease. *Curr Alzheimer Res* **3**: 449–463.

Milton NGN (2002). Anandamide and noladin ether prevent excitotoxicity of the human amyloid-β-peptide. *Neurosci Lett* **332**: 127–130.

Molina-Holgado F, Pinteaux E, Moore JD, Molina-Holgado E, Guaza C, Gibson RM *et al.* (2003). Endogenous interleukin-1 receptor antagonist mediates anti-inflammatory and neuroprotective actions of cannabinoids in neurons and glia. *J Neurosci* **12**: 6470–6474.

Nadler V, Mechoulam R, Sokolovsky M (1993). The non-psychotropic cannabinoid (+)-3S,4S)-7-hydroxy-Δ^6-tetrahydrocannabinol 1,1-dimethylheptyl (HU-211) attenuates *N*-methyl-D-aspartate receptor-mediated neurotoxicity in primary cultures of rat forebrain. *Neurosci Lett* **162**: 43–45.

Nunez E, Benito C, Pazos MR, Barbachano A, Fajardo O, Gonzalez S *et al.* (2004). Cannabinoid CB_2 receptors are expressed by perivascular microglial cells in the human brain: an immunohistochemical study. *Synapse* **53**: 208–213.

Ogomori K, Kitamoto T, Tateishi J, Sato Y, Suetsugu M, Abe M (1989). Protein amyloid is widely distributed in the central nervous system of patients with Alzheimer's disease. *Am J Pathol* **134**: 243–251.

Palazuelos J, Aguado T, Egia A, Mechoulam R, Guzman M, Galve-Roperh I (2006). Non-psychoactive CB_2 cannabinoid agonists stimulate neural progenitor proliferation. *FASEB J* **20**: 2405–2407.

Panikashvili D, Mechoulam R, Beni SM, Alexandrovich A, Shohami E (2005). CB_1 cannabinoid receptors are involved in neuroprotection via NFκB. *Blood Flow Metab* **25**: 477–484.

Pazos MR, Nunez E, Benito C, Tolon RM, Romero J (2004). Role of the endocannabinoid system in Alzheimer's disease: new perspectives. *Life Sci* **75**: 1907–1915.

Perez J (2006). Combined cannabinoid therapy via oromucosal spray. *Drugs Today* **42**: 495–503.

Pertwee RG (2005). Pharmacological actions of cannabinoids. *Handb Exp Pharmacol* **168**: 1–51.

Phiel CJ, Wilson CA, Lee VM, Klein PS (2003). GSK3 regulates production of Alzheimer's disease β-amyloid peptides. *Nature* **423**: 435–439.

Piomelli D (2003). The molecular logic of endocannabinoid signalling. *Nat Rev Neurosci* **4**: 873–884.

Pitt D, Werner P, Raine CS (2000). Glutamate excitotoxicity in a model of multiple sclerosis. *Nat Med* **6**: 67–70.

Pryce G, Baker D (2007). Control of spasticity in a multiple sclerosis model is mediated by CB_1, not CB_2, cannabinoid receptors. *Br J Pharmacol* **150**: 519–525.

Ramirez BG, Blazquez C, Gomez del Pulgar T, Guzman M, de Caballos ML (2005). Prevention of Alzheimer's disease pathology by cannabinoids: neuroprotection mediated by blockade of microglial activation. *J Neurosci* **25**: 1904–1913.

Rich JB, Rasmusson DX, Folstein MF, Carson KA, Kawas C, Brandt J (1995). Nonsteroidal anti-inflammatory drugs in Alzheimer's disease. *Neurology* **45**: 51–55.

Riedel G, Davies SN (2005). Cannabinoid function in learning, memory and plasticity. *Handb Exp Pharmacol* **168**: 445–477.

Rose CR, Konnerth A (2001). Stores not just for storage, intracellular calcium release and synaptic plasticity. *Neuron* **31**: 519–522.

Sanchez AJ, Gonzalez-Perez P, Galve-Roperh I, Garcia-Merino A (2006). R-(+)-[2,3-dihydro-5-methyl-3-(4-morpholinylmethyl)-pyrrolo-[1,2,3-de]-1,4-benzoxazin-6-yl]-1-naphtalenylmethanone (WIN-2) ameliorates experimental autoimmune encephalomyelitis and induces encephalitogenic T cell apoptosis: partial involvement of the CB(2) receptor. *Biochem Pharmacol* **72**: 1697–1706.

Sanchez MG, Ruiz-Llorente L, Sanchez AM, Diaz-Laviada I (2003). Activation of phosphoinositol 3-kinase/PKB pathway by CB_1 and CB_2 cannabinoid receptors expressed in prostate PC-3 cells. Involvement in Raf-1 stimulation and NGF induction. *Cell Signal* **15**: 851–859.

Shen M, Thayer SA (1998). Cannabinoid receptor agonists protect cultured mouse hippocampal neurons from excitotoxicity. *Brain Res* **783**: 77–84.

Smith IF, Green KN, LaFerla FM (2005). Calcium dysregulation in Alzheimer's disease: recent advances gained from genetically modified animals. *Cell Calcium* **38**: 427–437.

Smith T, Groom A, Zhu B, Turski L (2000). Autoimmune encephalomyelitis ameliorated by AMPA antagonists. *Nat Med* **6**: 62–66.

Sonkusare SK, Kaul CL, Ramarao P (2005). Dementia of Alzheimer's disease and other neurodegenerative disorders—memantine, a new hope. *Pharmacol Res* **51**: 1–17.

Stella N, Schweitzer P, Piomelli D (1997). A second endogenous cannabinoid that modulates long-term potentiation. *Nature* **388**: 773–778.

Takahashi KA, Castillo PE (2006). CB_1 cannabinoid receptor mediates glutamatergic synaptic suppression in the hippocampus. *Neuroscience* **139**: 795–802.

Twitchell W, Brown S, Mackie K (1997). Cannabinoids inhibit N- and P/Q-type calcium channels in cultured rat hippocampal neurons. *J Neurophysiol* **78**: 43–50.

Van Der Stelt M, Mazzola C, Espositp G, Mathias I, Petrosino S, De Filippis D *et al.* (2006). Endocannabinoids and β-amyloid-induced neurotoxicity *in vivo*: effect of pharmacological elevation of endocannabinoid levels. *Cell Mol Life Sci* **63**: 1410–1424.

Van Sickle MD, Duncan M, Kingsley PJ, Mouihate A, Urbani P, Mackie K *et al.* (2005). Identification and functional characterization of brainstem cannabinoid CB_2 receptors. *Science* **310**: 329–332.

Vereker E, Campbell V, Roche E, McEntee E, Lynch MA (2000). Lipopolysaccharide inhibits long-term potentiation in the rat dentate gyrus by activation of caspase-1. *J Biol Chem* **275**: 26252–26258.

Volicer L, Stelly M, Morris J, McLaughlin J, Volicer BJ (1997). Effects of Dronabinol on anorexia and disturbed behaviour in patients with Alzheimer's disease. *Int J Geriatr Psych* **12**: 913–919.

Walsh DM, Selkoe DJ (2007). Aβ oligomers—a decade of discovery. *J Neurochem* **101**: 1172–1184.

Walther S, Mahlberg R, Eichmann U, Kunz D (2006). Δ^9-Tetrahydrocannabinol for nighttime agitation in severe dementia. *Psychopharmacology* **185**: 524–528.

Wang SJ (2003). Cannabinoid CB1 receptor-mediated inhibition of glutamate release from rat hippocampal synaptosomes. *Eur J Pharmacol* **469**: 47–55.

Westlake TM, Howlett AC, Bonner TI, Matsuda LA, Herkenham M (1994). Cannabinoid receptor binding and mRNA expression in human brain: an *in vitro* receptor autoradiography and *in situ* hybridization histochemistry of normal aged and Alzheimer's brains. *Neuroscience* **63**: 637–652.

Wilkinson BL, Landreth GE (2006). The microglial NADPH oxidase complex as a source of oxidative stress in Alzheimer's disease. *J Neuroinflamm* **3**: 30–42.

Williams EJ, Walsh FS, Doherty P (2003). The FGF receptor uses the endocannabinoid signalling system to couple to an axonal growth response. *J Cell Biol* **160**: 448–481.

Wolff MC, Leander JD (2003). SR141716A, a cannabinoid CB_1 receptor antagonist, improves memory in a delayed radial maze task. *Eur J Pharmacol* **477**: 213–217.

Wyss-Coray T (2006). Inflammation in Alzheimer's disease: driving force, bystander or beneficial response? *Nat Med* **12**: 1005–1015.

Zhuang S-Y, Bridges D, Grigoenko E, McCloud S, Boon A, Hampson RE *et al.* (2005). Cannabinoids produce neuroprotection by reducing intracellular calcium release from ryanodine-sensitive stores. *Neuropharmacology* **28**: 1086–1096.

Ziemssen T (2005). Modulating processes within the central nervous system is central to therapeutic control of multiple sclerosis. *J Neurol* **252**: 38–45.

BRAIN RESEARCH 1175 (2007) 39–47

available at www.sciencedirect.com

ScienceDirect

www.elsevier.com/locate/brainres

BRAIN RESEARCH

Research Report

A comparison of the apoptotic effect of Δ^9-tetrahydrocannabinol in the neonatal and adult rat cerebral cortex

*Eric J. Downer, Aoife Gowran, Veronica A. Campbell**

Department of Physiology and Trinity College Institute of Neuroscience, Trinity College Dublin, Dublin 2, Ireland

ARTICLE INFO

Article history:
Accepted 30 July 2007
Available online 16 August 2007

Keywords:
Δ^9-Tetrahydrocannabinol
Apoptosis
Caspase-3
Cathepsin
Development

ABSTRACT

The maternal use of cannabis during pregnancy results in a number of cognitive deficits in the offspring that persist into adulthood. The endocannabinoid system has a role to play in neurodevelopmental processes such as neurogenesis, migration and synaptogenesis. However, exposure to phytocannabinoids, such as Δ^9-tetrahydrocannabinol, during gestation may interfere with these events to cause abnormal patterns of neuronal wiring and subsequent cognitive impairments. Aberrant cell death evoked by Δ^9-tetrahydrocannabinol may also contribute to cognitive deficits and in cultured neurones Δ^9-tetrahydrocannabinol induces apoptosis via the CB_1 cannabinoid receptor. In this study we report that Δ^9-tetrahydrocannabinol (5–50 μM) activates the stress-activated protein kinase, c-jun N-terminal kinase, and the pro-apoptotic protease, caspase-3, in *in vitro* cerebral cortical slices obtained from the neonatal rat brain. The proclivity of Δ^9-tetrahydrocannabinol to impact on these pro-apoptotic signalling molecules was not observed in *in vitro* cortical slices obtained from the adult rat brain. *In vivo*, subcutaneous administration of Δ^9-tetrahydrocannabinol (1–30 mg/kg) activated c-jun N-terminal kinase, caspase-3 and cathepsin-D, and induced DNA fragmentation in the cerebral cortex of neonatal rats. In contrast, *in vivo* administration of Δ^9-tetrahydrocannabinol to adult rats was not associated with the apoptotic pathway in the cerebral cortex. The data provide evidence which supports the hypothesis that the neonatal rat brain is more vulnerable to the neurotoxic influence of Δ^9-tetrahydrocannabinol, suggesting that the cognitive deficits that are observed in humans exposed to marijuana during gestation may be due, in part, to abnormal engagement of the apoptotic cascade during brain development.

1. Introduction

Δ^9-Tetrahydrocannabinol (Δ^9-THC) is the principal psychoactive cannabinoid moiety in the Indian hemp plant *Cannabis sativa* (marijuana). Δ^9-THC exerts its psychoactive effects through activation of the central cannabinoid (CB) receptor subtype CB_1, which is located in several brain regions including the cerebral cortex (Herkenham et al., 1991; Mailleux and Vanderhaeghen, 1992). The CB_1 receptor is expressed in the fetal and early postnatal brain (Berrendero et al., 1999; Rodriguez de Fonseca et al., 1993) but its expression pattern varies during development (Fernández-Ruiz et al., 2000; Berrendero et al., 1999) and this is consistent with a role for the cannabinoid system in controlling events pertinent in neural development (Harkany et al., 2007). Prenatal exposure to marijuana in humans is associated with deficits in executive function and

* *Corresponding author.* Fax: +353 1 6793545.
E-mail address: vacmpbll@tcd.ie (V.A. Campbell).

0006-8993/$ – see front matter © 2007 Elsevier B.V. All rights reserved.
doi:10.1016/j.brainres.2007.07.076

visuospatial working memory that persist into adulthood (Fried and Smith, 2001; Smith et al., 2006). Also, in animal studies, exposure to CB_1 receptor agonists during gestation reduces glutamatergic transmission (Mereu et al., 2003) and causes deficits in learning and emotional reactivity in adulthood (Antonelli et al., 2005). Thus, whilst a neurodevelopmental role for endocannabinoids is becoming clear, aberrant activation of such pathways by exogenous phytocannabinoids may have undesired consequences on the developing brain leading to cognitive impairments in later life. Marijuana is a commonly used drug of abuse although the potential of the drug to elicit neurotoxicity is controversial (Sarne and Mechoulam, 2005). In adults, chronic recreational use of marijuana has been linked with morphological changes in brain structures that are indicative of toxicity (Lawston et al., 2000; Scallet, 1991). fMRI studies have shown a reduction in frontal whitematter volume in cannabis abusers (Schiaepfer et al., 2006) and heavy marijuana users were found to have reduced grey matter in the parahippocampal gyrus and reduced white matter in the left parietal lobe, as well as other structural changes (Matochik et al., 2005). Some of those deleterious effects of marijuana may be related to alterations in pathways involved in the control of neurogenesis, synaptogenesis and wiring (Harkany et al., 2007), impaired myelination (Schiaepfer et al., 2006) or possibly aberrant neuronal death. We have previously reported that Δ^9-THC evokes programmed cell death (apoptosis) in cultured cortical neurones via activation of the stress-activated protein kinase, c-jun N-terminal kinase (JNK) and caspase-3 (Campbell, 2001; Downer et al., 2003, 2007). In spite of the aforementioned deleterious effects of Δ^9-THC, neuroprotective properties of cannabinoids have also been reported. Thus, Δ^9-THC protects neurones against excitotoxicity both *in vitro* (Gilbert et al., 2007) and *in vivo* (Raman et al., 2004) and has anti-oxidant (Hampson et al., 1998) and anti-inflammatory actions (Lyman et al., 1989) in the brain which lend support for cannabinoid-based approaches to treat adult neurodegenerative disorders.

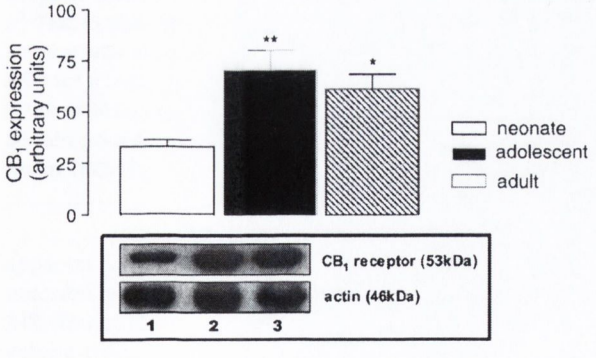

Fig. 1 – Developmental changes in CB_1 receptor expression in rat cerebral cortex. (A) A significant increase in CB_1 receptor expression was observed in the cortices of adolescent and adult rats compared to the cortices of neonatal rats. Results are expressed as mean ± SEM for 6 observations, **$P<0.01$, *$P<0.05$, ANOVA and post hoc Student–Newman–Keuls test. (B) Sample Western immunoblot demonstrating CB_1 receptor expression in cortices obtained from neonatal (lane 1), adolescent (lane 2) and adult (lane 3) rats. Actin immunoblots confirm equal protein loading.

Given the dichotomy in the literature of neuroprotective versus neurotoxic effects of Δ^9-THC, the aim of this study was to compare the proclivity of Δ^9-THC to couple to the biochemical hallmarks of apoptosis, namely activation of the stress-activated protein kinase, c-jun N terminal kinase (JNK), caspase-3 and DNA fragmentation, in the neonatal and adult rat cerebral cortex.

2. Results

2.1. CB_1 receptor expression

Fig. 1 demonstrates that the CB_1 cannabinoid receptor is expressed in the neonatal rat cerebral cortex and that its expression level is significantly increased in the cerebral cortex of adolescent and adult rats ($P<0.01$, ANOVA, $n=6$). This result is in accordance with Mato et al. (2003), who reported a progressive increase in neuronal CB_1 receptors from prenatal stages to adulthood.

2.2. Δ^9-THC couples to activation of JNK and caspase-3 in cerebral cortices prepared from neonatal, but not adult, rat brain

When cerebral cortical slices from the neonatal rat were incubated with Δ^9-THC for 2 h *in vitro* a dose-dependent increase in activation of JNK (Fig. 2A) and caspase-3 (Fig. 2C) was observed. Thus, exposure to 5 μM and 50 μM Δ^9-THC evoked a significant increase in expression of phospho-JNK compared to vehicle ($P<0.01$, ANOVA, $n=5$) and this was abrogated by the CB_1 antagonist AM251 (10 μM; Fig. 2B). Similarly, Δ^9-THC, at 5 and 50 μM, significantly increased caspase-3 activity from 277 ± 99 pmol AFC produced/mg/min (mean ± SEM) to 1417 ± 161 pmol AFC produced/mg/min ($P<0.05$, ANOVA, $n=5$) and 1756 ± 490 ($P<0.01$, ANOVA, $n=5$), respectively. The increase in caspase-3 activity evoked by Δ^9-THC (5 μM) was abolished by the CB_1 antagonist AM251 (Fig. 2D). The activation of this apoptotic pathway in *in vitro* slices from the neonatal cerebral cortex is consistent with our previous cell culture studies in which we have demonstrated that Δ^9-THC activates JNK and caspase-3 in cultured cortical neurones (Campbell, 2001; Downer et al., 2003, 2007).

In contrast to Δ^9-THC evoking activation of JNK and caspase-3 in the cortical slices prepared from neonatal rats, cortical slices prepared from the adult rat were less susceptible to the Δ^9-THC-induced activation of JNK (Fig. 3A) and caspase-3 (Fig. 3B). Only at the highest concentration of Δ^9-THC (50 μM) was a significant increase in phospho-JNK expression observed ($P<0.01$, ANOVA, $n=5$) and no induction of caspase-3 activity was observed at any of the concentrations of Δ^9-THC examined.

2.3. *In vivo*, Δ^9-THC couples to JNK and caspase-3 activation, and DNA fragmentation in the neonatal, but not adult, cerebral cortex

We also sought to examine whether the increased ability of Δ^9-THC to couple to the biochemical pathways associated with apoptosis in the neonatal, but not adult, cerebral cortex was

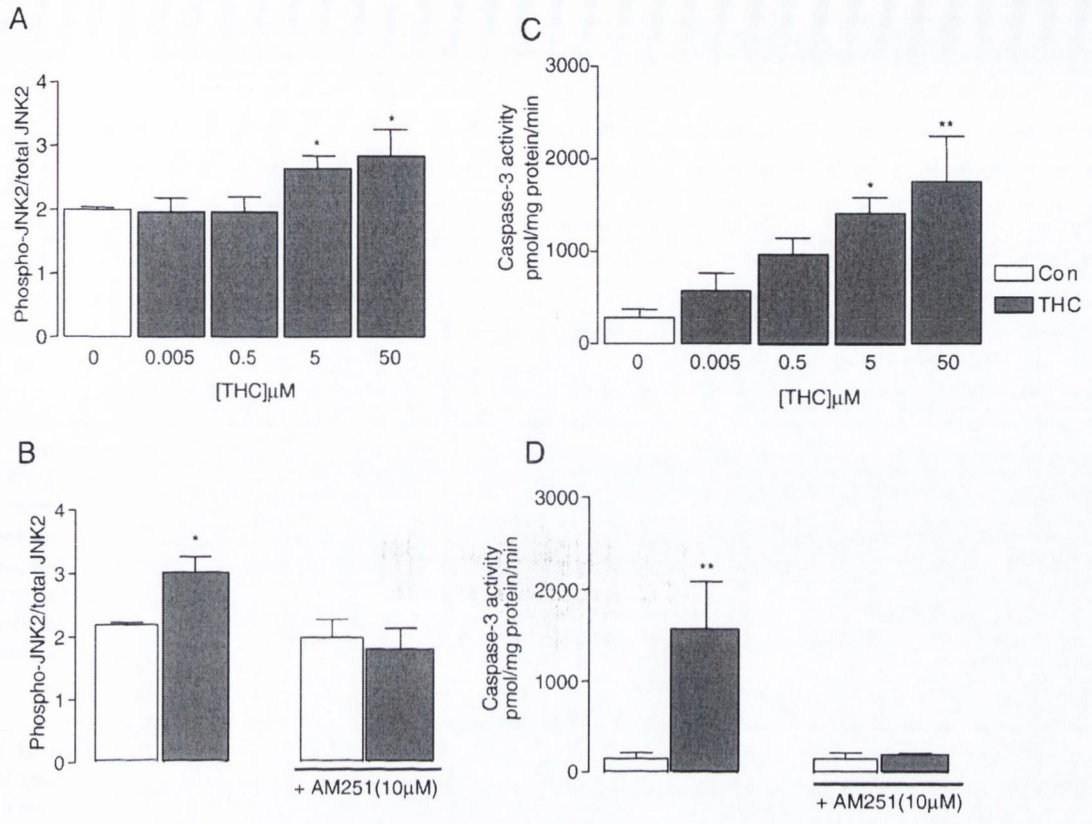

Fig. 2 – Δ^9-THC couples to activation of JNK and capase-3 via CB_1 receptor in neonatal rat cerebral cortex *in vitro*. (A) Cortical slices obtained from neonatal rat pups were treated with increasing concentrations of Δ^9-THC (5 nM–50 μM) for 2 h and JNK phosphorylation was assessed by Western immunoblot. A significant increase in phospho-JNK expression was observed following treatment with Δ^9-THC at concentrations of 5 μM and 50 μM. Exposure of slices to 5 nM and 0.5 μM Δ^9-THC had no effect on phospho-JNK expression. Results are expressed as mean ± SEM for 5 independent observations, *P < 0.05, compared to vehicle control, ANOVA and post hoc Student–Newman–Keuls test. (B) When cortical slices obtained from neonatal rats were pre-incubated with AM 251 (10 μM) for 30 min prior to Δ^9-THC (5 μM, 2 h) the Δ^9-THC-induced increase in phospho-JNK expression was abolished. Results are expressed as mean ± SEM for 5 observations, *P < 0.05, ANOVA and post hoc Student–Newman–Keuls test. (C) Cortical slices obtained from neonatal rat pups were treated with increasing concentrations of Δ^9-THC (5 nM–50 μM) for 2 h and caspase-3 activity assessed by fluorogenic assay. A significant increase in caspase-3 activity was observed following treatment with Δ^9-THC at concentrations of 5 μM and 50 μM. Results are expressed as mean ± SEM for 6 independent observations, *P < 0.05, **P < 0.01, compared to vehicle control, ANOVA and post hoc Student–Newman–Keuls test. (D) When cortical slices obtained from neonatal rats were pre-incubated with AM 251 (10 μM) for 30 min prior to Δ^9-THC (5 μM, 2 h) the Δ^9-THC-induced increase in caspase-3 activity was abolished. Results are expressed as mean ± SEM for 6 observations, **P < 0.01, ANOVA and post hoc Student–Newman–Keuls test.

apparent following administration of Δ^9-THC *in vivo* (Fig. 4). In neonatal rat pups, Δ^9-THC (10 mg/kg, s.c.) increased phospho-JNK immunoreactivity in the cerebral cortex compared to vehicle-treated controls (Fig. 4A) and significantly increased caspase-3 activity from 396 ± 55 pmol AFC produced/mg/min to 818 ± 97 pmol AFC produced/mg/min ($P < 0.01$, Student's unpaired *t*-test, $n = 9$; Fig. 4B). Also, Δ^9-THC (1-30 mg/kg, s.c.) significantly increased the activity of cathepsin-D from 0.31 ± 0.06 U/mg protein/min (mean ± SEM) to 0.77 ± 0.16 U/mg protein/min ($P < 0.05$, ANOVA, $n = 4$; Δ^9-THC 1 mg/kg) and 1.45 ± 0.21 U/mg protein/min ($P < 0.01$, ANOVA, $n = 4$; Δ^9-THC 30 mg/kg; Fig. 4C) and enhanced the cytosolic expression of cathepsin-D (Fig. 4C inset). Thus *in vivo*, peripheral administration of Δ^9-THC couples to the activation of biochemical pathways associated with cell death in the neonatal rat cerebral cortex. In contrast, when adult rats were administered Δ^9-THC peripherally (1–30 mg/kg, s.c.) no activation of JNK, caspase-3 or cathepsin-D was observed (Figs. 4D–F). Together, these data provide evidence that acute peripheral administration of Δ^9-THC activates a biochemical pathway associated with cellular stress in neonatal, but not adult, rat cortices *in vivo*.

In order to evaluate the influence of Δ^9-THC on viability of cells within the cerebral cortex of neonatal and adult rats, the slices were analysed for DNA fragmentation, a hallmark of apoptosis (Fig. 5). In the cerebral cortex of neonatal rats, Δ^9-THC (10 mg/kg s.c.) substantially increased DNA fragmentation (Fig. 5A, iv) compared to animals treated with vehicle

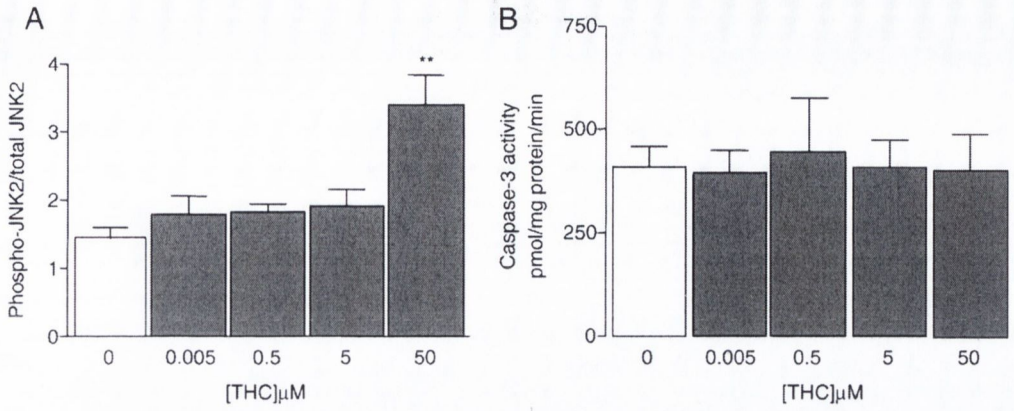

Fig. 3 – Δ^9-THC does not affect caspase-3 activity in the adult rat cerebral cortex *in vitro*. (A) Cortical slices obtained from adult rats were incubated with increasing concentrations of Δ^9-THC (5 nM-50 μM) for 2 h and JNK phosphorylation was assessed by Western immunoblot. A significant increase in phospho-JNK expression was observed only following treatment with THC at the highest concentration of 50 μM. Exposure of slices to 5 nM, 0.5 μM and 5 μM Δ^9-THC had no effect on phospho-JNK expression. Results are expressed as mean ± SEM for 5 independent observations, $^{**}P<0.01$, compared to vehicle control, ANOVA and post hoc Student–Newman–Keuls test. (B) Exposure of cortical slices obtained from the adult rat to increasing concentrations of Δ^9-THC (5 nM–50 μM) for 2 h had no affect on caspase-3 activity. Results are expressed as mean ± SEM for 6 independent observations.

(Fig. 5A, i). However, Δ^9-THC only had a modest effect on the amount of DNA fragmentation observed in adult rat cortices (Fig. 5B). This observation supports the contention that the neonatal brain is more vulnerable to the neurotoxic influence of Δ^9-THC.

3. Discussion

The aim of this study was to examine the relationship between the stage of brain development and the potential for Δ^9-THC to couple to activation of a stress response, namely activation of JNK and caspase-3; enzymes that have previously been found to be involved in mediating the pro-apoptotic effect of Δ^9-THC in cultured neurones (Campbell, 2001; Downer et al., 2003, 2007). In our *in vitro* studies, Δ^9-THC induced the activation of JNK and caspase-3 in the cerebral cortex isolated from the neonatal rat, via activation of the CB_1 receptor. In contrast, cortical slices obtained from the adult rat brain were less susceptible to the Δ^9-THC-induced activation of JNK and caspase-3. A similar profile was observed in the *in vivo* study, in which neonatal rat cortices were more vulnerable than adult rat cortices to the activation of JNK, caspase-3, cathepsin-D, and DNA fragmentation following an acute peripheral administration of Δ^9-THC. Thus, in spite of the increase in CB_1 receptor expression in the adult cerebral cortex compared to the neonatal cerebral cortex, the activation of the apoptotic pathway by Δ^9-THC is less robust in the adult rat cerebral cortex. These data therefore indicate that the neonatal cerebral cortex is more vulnerable to the neurotoxic profile of Δ^9-THC, at least within the 2-h timeframe investigated in this study. In humans, one third of the plasma Δ^9-THC is estimated to cross the placental barrier and if one considers that the neonatal rat brain is a model of the developing human brain during the third trimester of pregnancy, our data suggest that the immature cerebral cortex *in utero* may be vulnerable to Δ^9-THC-induced neurotoxicity at this critical phase in brain development. It is also important to note that chronic exposure of the adult brain to Δ^9-THC causes structural changes (Matochik et al., 2005) that may relate to degenerative events. Thus, we cannot exclude the possibility that the reduced coupling of Δ^9-THC to the apoptotic cascade observed in the adult cerebral cortex may relate to a slower induction of apoptosis which would not have been apparent within the 2-h exposure time used in this study.

The central CB_1 cannabinoid receptor is one of the most abundantly expressed neuronal receptors and is localised in brain regions most likely involved in the psychoactive effects of Δ^9-THC, including the cerebral cortex (Tsou et al., 1998; Mailleux and Vanderhaeghen, 1992). The CB_1 receptor is expressed in the fetal and early postnatal brain (Berrendero et al., 1999; Rodriguez de Fonseca et al., 1993) but its expression pattern varies during development (Fernández-Ruiz et al., 2000; Berrendero et al., 1999). Although this may have important implications in terms of a modulatory role of the cannabinoid system in neurobiological processes, in particular neural development, overstimulation of cannabinoid receptors at critical stages of development may have damaging consequences on nervous system functioning. Indeed, several studies have shown that prenatal and early postnatal exposure to Δ^9-THC produces long-term abnormalities in brain function and behaviour (Garcia et al., 1996; Navarro et al., 1995). Some of these long-term consequences of early exposure to Δ^9-THC may be related to deleterious effects on astroglial maturation which contribute to fetal brain growth retardation (Suarez et al., 2004) or changes in the development of certain neurological pathways (Rodríquez de Fonseca et al., 1992). Chronic exposure to Δ^9-THC or marijuana extracts as well as to synthetic cannabinoids (Lawston et al., 2000), alter the structure of the rat hippocampus. Although apoptotic

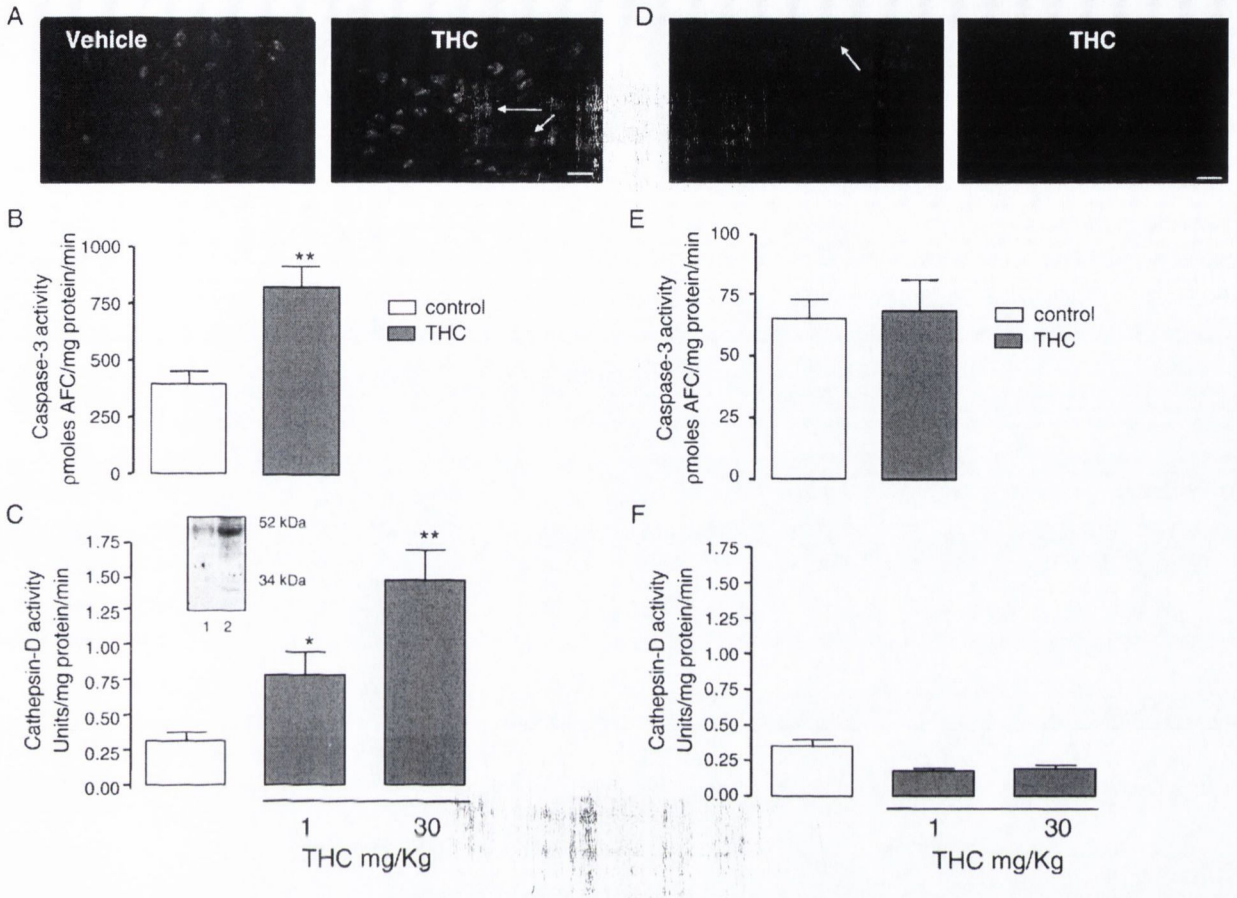

Fig. 4 – Peripheral administration of Δ^9-THC increases JNK and caspase-3 activity in the neonatal, but not adult, cerebral cortex. Neonatal (A–C) or adult (D–F) rats received subcutaneous (s.c.) injections of Δ^9-THC (10 mg/kg). (A) Phospho-JNK expression in the cerebral cortex was assessed as an index of JNK activity in cryostat sections using fluorescence microscopy. Images of phospho-JNK expression in (i) cerebral cortex of vehicle-treated neonatal rats compared to (ii) cerebral cortex of Δ^9-THC-treated neonatal rats which shows intense phospho-JNK immunoreactivity. Arrows indicate phospho-JNK immunoreactive cells. Scale bar is 25 μm. (B) In neonatal rats administered Δ^9-THC (10 mg/kg, s.c.) a significant increase in caspase-3 activity in the cerebral cortex was observed. Results are expressed as the mean ± SEM for 9 observations, $^{**}P<0.01$, Student's t-test. (C) In neonatal rats administered Δ^9-THC (1-30 mg/kg, s.c.) a significant increase in cytosolic cathepsin-D activity in the cerebral cortex was observed. Results are expressed as the mean ± SEM for 4 observations, $^{*}P<0.05$, $^{**}P<0.01$, ANOVA and post hoc Student–Newman–Keuls test. Inset: a sample immunoblot demonstrating the increase in cytosolic expression of the 52-kDa and 34-kDa forms of cathepsin-D in the cerebral cortex following administration of Δ^9-THC (30 mg/kg, s.c.) to neonatal rat (lane 2), compared to vehicle-treated animals (lane 1). (D) Phospho-JNK expression in the cerebral cortex was unaffected following subcutaneous administration of Δ^9-THC (10 mg/kg) to adult rats. Fluorescence images of phospho-JNK expression in (i) cerebral cortex of vehicle-treated adult rats and (ii) cerebral cortex of Δ^9-THC-treated adult rats. Scale bar is 25 μm. (E) In adult rats administered Δ^9-THC (10 mg/kg, s.c.) no change in caspase-3 activity in the cerebral cortex was observed. Results are expressed as the mean ± SEM for 9 observations. (F) In adult rats administered Δ^9-THC (1-30 mg/kg, s.c.) no change in cytosolic cathepsin-D activity in the cerebral cortex was observed. Results are expressed as the mean ± SEM for 4 observations.

parameters were not identified in those studies, the authors conclude that the morphological changes in the hippocampus are indicative of cannabinoid neurotoxicity. Szoke et al. (2002) have also shown that neonatal rats injected with anandamide show evidence of mitochondrial damage, which may reflect cannabinoid toxicity. CB_1 receptor antagonists protect against NMDA-induced excitotoxicity *in vivo* providing further evidence that the cannabinoid system has the proclivity to contribute to neuronal damage (Hansen et al., 2002).

The JNK and caspase-3 signalling pathways activated by Δ^9-THC in the neonatal brain *in vivo* reported herewith are consistent with the cannabinoid-induced apoptotic signalling mechanisms that we have previously described in cultured neurones (Downer et al., 2003). In this study we have also identified that peripheral administration of Δ^9-THC increases the cytosolic expression and activity of the lysosomal protease, cathepsin-D in the neonatal rat cerebral cortex. Lysosomal permeabilisation is an upstream event in apoptosis (Kågedal

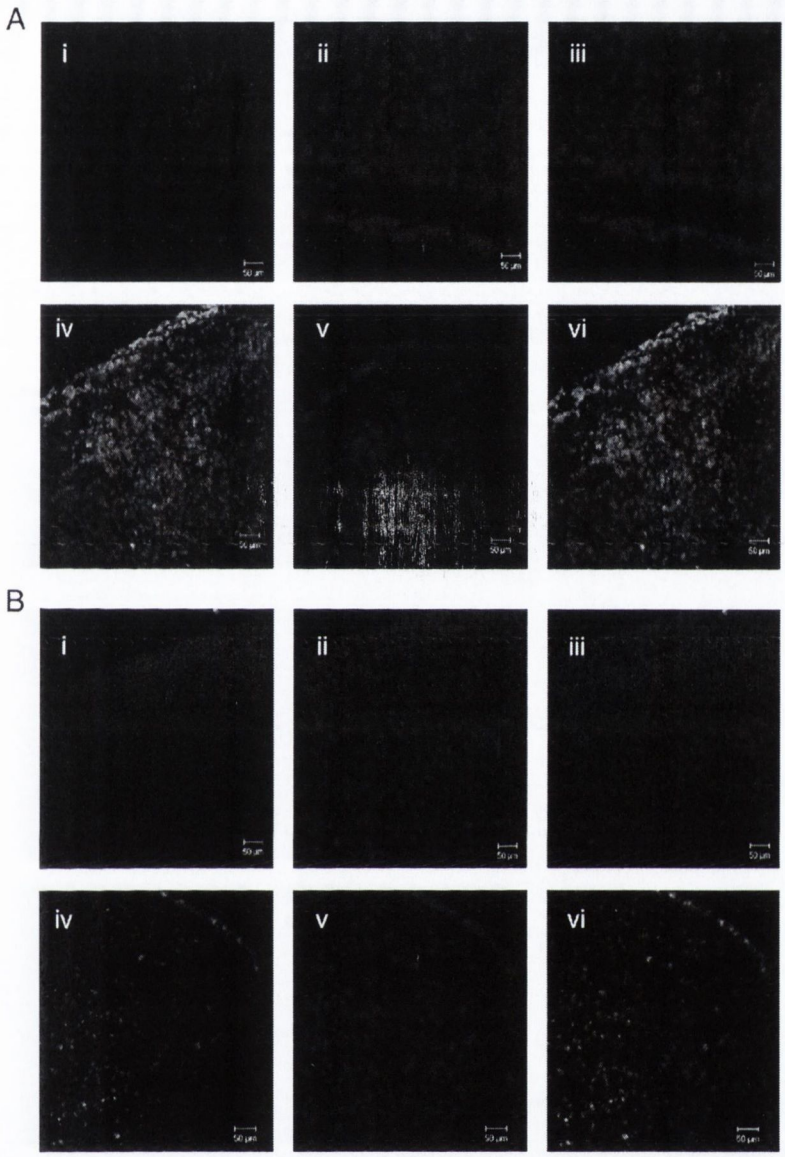

Fig. 5 – Peripheral administration of Δ^9-THC increases DNA fragmentation in the neonatal, but not adult, cerebral cortex. Neonatal (A) or adult (B) rats received subcutaneous (s.c.) injections of Δ^9-THC (10 mg/kg) and after 2 h cryostat sections of the cerebral cortex were prepared and stained for DNA fragmentation using by TUNEL. Cells with fragmented DNA stained green and the Hoescht stain labelled nuclei blue. (A) In the neonatal rats administered Δ^9-THC an increase in DNA fragmentation was observed in the cerebral cortex (iv) compared to vehicle-treated rats (i). Panels ii and v represent Hoescht staining in the cerebral cortex of vehicle-treated and Δ^9-THC-treated neonatal rats, respectively. Panels iii and vi represent double labelling of DNA fragmentation (green) and Hoescht staining (blue) in the cerebral cortex of vehicle-treated and Δ^9-THC-treated neonatal rats, respectively. (B) In the adult rats administered Δ^9-THC, DNA fragmentation in the cerebral cortex (iv) was comparable to vehicle-treated rats (i). Panels ii and v represent Hoescht staining in the cerebral cortex of vehicle-treated and Δ^9-THC-treated adult rats, respectively. Panels iii and vi represent double labelling of DNA fragmentation (green) and Hoescht staining (blue) in the cerebral cortex of vehicle-treated and Δ^9-THC-treated adult rats, respectively.

et al., 2005) and leads to the release of lysosomal cathepsin enzymes into the cytosol which in turn participate in the apoptotic cascade (Schestkowa et al., 2007). This pathway is implicated in the physiological cell death that occurs during embryonic development (Zuzarte-Luis et al., 2007). Interestingly in macrophages, Δ^9-THC has been reported to increase cathepsin activity via the CB_2 receptor (Matveyeva et al., 2000). The data presented herein provide evidence for Δ^9-THC coupling to the lysosomal/cathepsin system in the brain *in vivo*. It is interesting to speculate that when the immature brain is exposed to Δ^9-THC following maternal use of marijuana, aberrant activation of the cathepsin pathway may evoke

excessive neuronal apoptosis that may contribute, in part, to the cognitive deficits observed in adulthood.

A number of *in vitro* and *in vivo* experiments have described differential effects of cannabinoids on cell viability (Chan et al., 1998; Downer et al., 2007; Galve-Roperh et al., 2000; Sinor et al., 2000; Van der Stelt et al., 2001). This study has demonstrated that the proclivity of Δ^9-THC to couple to the apoptotic pathway is more robust in the neonatal rat cerebral cortex, compared to the adult cerebral cortex. The finding that the immature rat brain is more vulnerable to the toxicity of Δ^9-THC may underlie the cognitive deficits that occur following gestational exposure to cannabis in humans (Fried and Smith, 2001; Smith et al., 2006) and the data inform the growing debate about the teratogenic potential of cannabis.

4. Experimental procedure

All animals used were an inbred strain of male Wistar rat supplied by the Bio Resources Unit, Trinity College, Dublin. Four- to seven-day-old rat pups (8–13 g), 20- to 25-day-old adolescent rats (70 g) and 3- to 4-month-old adult rats (180–250 g) were maintained under a 12-h light–dark cycle with food (normal laboratory chow) and water available *ad libitum*. Ambient temperature was controlled between 22 and 23 °C. All animal experimentation was performed under a licence granted by the Minister for Health and Children (Ireland) under the Cruelty to Animals Act, 1876 and the European Community Directive, 86/609/EC. In the *in vivo* experiments rats were anaesthetised by intraperitoneal (i.p) injection of urethane (1.5 g/kg). The absence of a pedal reflex was used to confirm deep anaesthesia. The Δ^9-THC group received subcutaneous injections (0.05 ml/10 g body weight) of 1 mg/kg, 10 mg/kg or 30 mg/kg Δ^9-THC in vehicle (5% absolute alcohol, 5% Cremophor EL and 90% sterile saline) and the control group received injections of vehicle alone. Rats were killed by decapitation 2 h post treatment and the right cerebral cortex removed for analysis of caspase-3, cathepsin-D and JNK activity. Cryostat sections (50 μm) of the left cerebral cortex were prepared for immunocytochemical staining of phospho-JNK and analysis of DNA fragmentation.

For the *in vitro* experiments, rats (4- to 7-day-old pups or 3-month-old adults) were killed by decapitation and the cerebral cortex was sliced (350 μm) and placed in microfuge tubes containing HEPES-buffered saline (145 mM NaCl, 5 mM KCl, 1 mM $MgCl_2$, 2 mM $CaCl_2$, 1 mM Mg_2SO_4, 1 mM KH_2PO_4, 10 mM glucose, 30 mM HEPES, pH 7.4) and Δ^9-THC (5 nM-50 μM) or vehicle (0.007% methanol (v/v)). Slices were incubated for 2 h at 37 °C with agitation. In some experiments cortical slices were pre-incubated with the CB_1 receptor antagonist, AM 251 (1-(2,4-dichlorophenyl)-5-(4-iodophenyl]])-4-methyl-*N*-(1-piperidyl) pyrazole-3-carboxamide) 30 min before treating with Δ^9-THC.

4.1. *Protein quantification using the Bradford assay*

Protein standards were prepared from stock solution of 1000 μg/ml bovine serum albumin (BSA; Sigma-Aldrich, Dorset, UK). Samples (10 μl) and standards (10 μl) were added to a 96-well plate (Sarstedt, Wexford, Ireland) in duplicate and Bio-Rad dye reagent concentrate (1:5 dilution in dH_2O, 200 μl; Bio-Rad, Hertfordshire, UK) was added to both and absorbance was assessed at 600 nm using a 96-well plate reader (Labsystems Multiskan RC). The concentration of protein in samples was calculated from the regression line plotted (Instat 2.03) from the absorbance of the BSA standards.

4.2. *Western immunoblot for analysis of CB_1 receptor, phospho-JNK and cathepsin-D*

Cortices were lysed in buffer (25 mM HEPES, 5 mM $MgCl_2$, 5 mM EDTA, 5 mM dithiothreitol, 0.1 mM PMSF, 5 μg/ml pepstatin A, 2 μg/ml leupeptin, 2 μg/ml aprotinin, pH 7.4). The tissue was centrifuged (15,000×*g* for 20 min at 4 °C) and the supernatant diluted to 50 μg protein/ml with sample buffer (150 mM Tris–HCl pH 6.8, 10% v/v glycerol, 4% w/v SDS, 5% v/v β-mercaptoethanol, 0.002% w/v Bromophenol Blue). Samples were then heated to 100 °C for 3 min. Proteins (10 μg per lane) were separated by electrophoresis on a 10% polyacrylamide minigel, transferred to nitrocellulose membrane and immunoblotted with a goat polyclonal CB_1 receptor antibody (Santa Cruz Biotechnology Inc., Santa Cruz, CA, USA) and secondary antibody (anti-goat IgG) conjugated to horseradish peroxidase; or an anti-active JNK monoclonal antibody (1:1000, Santa Cruz Biotechnology Inc., California) purified from mouse serum, which recognises the active forms of JNK following phosphorylation on Thr-183 and Tyr-185 and secondary antibody (anti-mouse IgG) conjugated to horseradish peroxidase; or an anti-cathepsin-D polyclonal antibody raised in rabbit (Calbiochem, Darmstadt, Germany) which recognises the 52-kDa pro-form and the 34-kDa active subunit of cathepsin-D and secondary (anti-rabbit IgG) conjugated to horse radish peroxidase. Bands were visualised by chemiluminescence (Supersignal, Pierce, Leiden, Netherlands). Blots were stripped and re-probed for actin or total JNK, where appropriate, to normalise protein loading and band widths were quantified by densitometry (D-Scan PC software).

4.3. *Cathepsin-D activity*

Cathepsin-D was purified from cytosolic fractions of neonatal and adult cortical tissue using a 96-well plate coated with monoclonal anti-cathepsin-D antibody. The cathepsin-D activity was then detected using an internally quenched fluorescent cathepsin-D substrate peptide, Mca-Gly-Lys-Pro-Ile-Leu-Phe-Arg-Leu-Lys-(Dnp)-D-Arg-NH_2. Release of the fluorescent product, Mca-Gly-Lys-Pro-Ile-Leu-Phe was determined fluorometrically at excitation of 328 nm and emission of 393 nm. Cathepsin-D activity was read from a standard curve of affinity purified cathepsin-D enzyme.

4.4. *Caspase-3 analysis*

Cleavage of the fluorogenic caspase-3 substrate (DEVD-aminofluorocoumarin (AFC); Alexis Corporation, USA) to its fluorescent product was also used to measure caspase-3 activity. Following treatment with THC, cortices were lysed in buffer (25 mM HEPES, 5 mM $MgCl_2$, 5 mM DTT, 5 mM EDTA, 2 mM PMSF, 10 μg/ml leupeptin, 10 μg/ml pepstatin; pH 7.4), subjected to 3 freeze–thaw cycles and centrifuged at 10,000 rpm for 10 min at 4 °C. Samples of supernatant (90 μl)

were incubated with the DEVD peptide (500 μM; 10 μl) for 1 h at 30 °C. Incubation buffer (900 μl; 100 mM HEPES containing 10 mM DTT; pH 7.4) was added and fluorescence was assessed (excitation, 400 nm; emission, 505 nm).

4.5. *TdT-mediated UTP-end nick labelling (TUNEL)*

Apoptotic cell death was assessed using the Dead End™ Fluorometric apoptosis detection system (Promega Corporation, Madison, USA). Tissue sections were fixed with paraformaldehyde (4%), permeabilised with triton-X100 (0.1%), and biotinylated nucleotide was incorporated at 3′-OH DNA ends using the enzyme Terminal deoxynucleotidyl Transferase (TdT). Fluorescein-labelled streptavidin then bound to the biotinylated nucleotide and this was visualised by fluorescent confocal microscopy (Zeiss LSM 510-META) using the 488-nm argon/2 laser with the following scan configurations; laser output 50%, transmission 5%, band pass filter 505–530, beam splitter 488/543, detector gain 719, amplifier gain 1, amplifier offset −0.14, pinhole 96 μm (1 Airy unit) and 16 scan averages. Hoescht staining of nuclei was visualised using the 543-nm helium neon laser.

4.6. *Statistics*

Data are reported as the mean ± SEM of the number of experiments indicated in each case. Statistical analysis was carried out using one-way analysis of variance (ANOVA) followed by the post hoc Student–Newman–Keuls test when significance (at the 0.05 level) was indicated. When comparisons were being made between two treatments, an unpaired Student's t-test was performed and $P<0.05$ or $P<0.01$ was considered significant.

Acknowledgments

The authors acknowledge financial support from the Health Research Board and Science Foundation Ireland.

REFERENCES

Antonelli, T., Tomasini, M.C., Tattoli, M., Cassano, T., Tanganelli, S., Finetti, S., Mazzoni, E., 2005. Prenatal exposure to the CB1 receptor agonist WIN 55,212-2 causes leaning disruption associated with impaired cortical NMDA receptor function and emotional reactivity changes in rat offspring. Cereb. Cerebral cortex 15, 2013–2020.

Berrendero, F., Sepe, N., Ramos, J.A., Di Marzo, V., Fernández-Ruiz, J.J., 1999. Analysis of cannabinoid receptor binding and mRNA expression and endogenous cannabinoid contents in the developing rat brain during late gestation and early postnatal period. Synapse 33 (3), 181–191.

Campbell, V.A., 2001. Tetrahydrocannabinol-induced apoptosis in cultured cortical neurones is associated with cytochrome c release and caspase-3 activation. Neuropharmacology 40, 702–709.

Chan, G.C., Hinds, T.R., Impey, S., Storm, D.R., 1998. Hippocampal neurotoxicity of Δ^9-tetrahydrocannabinol. J. Neurosci. 18 (14), 5322–5332.

Downer, E.J., Fogarty, M.P., Campbell, V.A., 2003. Tetrahydrocannabinol-induced neurotoxicity depends on CB_1 receptor-mediated c-Jun N-terminal kinase activation in cultured cortical neurons. Br. J. Pharm. 140, 547–557.

Downer, E.J., Gowran, A., Murphy, A.C., Campbell, V.A., 2007. The tumour suppressor protein, p53, is involved in the activation of the apoptotic cascade by Delta9-tetrahydrocannabinol in cultured cortical neurons. Eur. J. Pharmacol. 564, 57–65.

Fernández-Ruiz, J., Berrendero, F., Hernandez, M.L., Ramos, J.A., 2000. The endogenous cannabinoid system and brain development. Trends Neurosci. 23, 14–20.

Fried, P.A., Smith, A.M., 2001. A literature review of the consequences of prenatal marihuana exposure. An emerging theme of a deficiency in aspects of executive function. Neurotoxicol. Teratol. 23, 1–11.

Galve-Roperh, I., Sánchez, C., Luisa Cortes, M., Gómez del Pulgar, T., Izquierdo, M., Guzmán, M., 2000. Anti-tumoral action of cannabinoids: involvement of sustained ceramide accumulation and extracellular signal-regulated kinase activation. Nat. Med. 6, 313–319.

Garcia, L., de Miguel, R., Ramos, J.A., Fernandez-Ruiz, J.J., 1996. Perinatal Δ^9-tetrahydrocannabinol exposure in rats modifies the responsiveness of midbrain dopaminergic neurons in adulthood to a variety of challenges with dopaminergic drugs. Drug Alcohol Depend. 42, 155–166.

Gilbert, G.L., Kim, H.J., Waataja, J.J., Thayer, S.A., 2007. Δ^9-Tetrahydrocannabinol protects hippocampal neurons from excitotoxicity. Brain Res. 1128, 61–69.

Hampson, A.J., Grimaldi, M., Axelrod, J., Wink, D., 1998. Cannabidiol and (−)Δ^9-tetrahydrocannabinol are neuroprotective antioxidants. Proc. Natl. Acad. Sci. U. S. A. 95, 8268–8273.

Hansen, H.H., Azcoitia, I., Pons, S., Romero, J., Garcia-Sequra, L.M., Ramos, J.A., Hansen, H.S., Fernandez-Ruiz, J., 2002. Blockade of cannabinoid CB_1 receptor function protects against *in vivo* disseminating brain damage following NMDA-induced excitotoxicity. J. Neurochem. 82, 154–158.

Harkany, T., Guzmán, M., Galve-Roperh, I., Berghuis, P., Devi, L.A., Mackie, K., 2007. The emerging functions of endocdannabinoid signalling during CNS development. Trends Pharmacol. Sci. 28, 83–92.

Herkenham, M., Lynn, A.B., Johnson, M.R., Melvin, L.S., de Costa, B.R., Rice, K.C., 1991. Characterization and localization of cannabinoid receptors in rat brain: a quantitative *in vitro* autoradiographic study. J. Neurosci. 11, 563–583.

Kågedal, K., Johansson, A.C., Johansson, U., Heinmlich, G., Roberg, K., Wang, N.S., Jürgensmeier, J.M., Ollinger, K., 2005. Lysosomal membrane permeabilization during apoptosis-involvement of Bax? Int. J. Exp. Pathol. 86, 309–321.

Lawston, J., Borella, A., Robinson, J.K., Whitaker-Azmitia, P.M., 2000. Changes in hippocampal morphology following chronic treatment with the synthetic cannabinoid WIN 55,212-2. Brain Res. 877, 407–410.

Lyman, W.D., Sonett, J.R., Brosnan, C.F., Elkin, R., Bornstein, M.B., 1989. Delta 9-tetrahydrocannabinol: a novel treatment for experimental autoimmune encephalomyelitis. Neuroimmunology 23, 73–81.

Mailleux, P., Vanderhaeghen, J.-J., 1992. Distribution of neuronal cannabinoid receptor in the adult rat brain: a comparative receptor binding radioautography and *in situ* hybridization histochemistry. Neuroscience 48, 655–668.

Mato, S., Del Olmo, E., Pazos, A., 2003. Ontogenetic development of cannabinoid receptor expression and signal transduction functionality in the human brain. Eur. J. Neurosci. 17, 1747–1754.

Matochik, J.A., Eldreth, D.A., Cadet, J.L., Bolla, K.I., 2005. Altered brain tissue composition in heavy marijuana users. Drug Alcohol Depend. 77, 23–30.

Matveyeva, M., Hartmann, C.B., Harrison, M.T., Cabral, G.A., McCoy, K.L., 2000. Delta (9)-tetrahydrocannabinol selectively increases aspartyl cathepsin D proteolytic activity and impairs lysozyme processing by macrophages. Int. J. Immunopharmacol. 22, 373–381.

Mereu, G., Fa, M., Ferraro, L., Cagiano, R., Antonelli, T., Tattoli, M., Ghiglieri, V., Tanganelli, S., Gesssa, G.L., Cuomo, V., 2003. Prenatal exposure to a cannabinoid agonist produces memory deficits linked to dysfunction in hippocampal long-term potentiation and glutamate release. Proc. Natl. Acad. Sci. USA 100, 4915–4920.

Navarro, M., Rubio, P., de Fonseca, F.R., 1995. Behavioural consequences of maternal exposure to natural cannabinoids in rats. Psychopharmacology 122, 1–14.

Raman, C., McAllister, S.D., Rizvi, G., Patel, S.G., Moore, D.H., Abood, M.E., 2004. Amyotrophic lateral sclerosis: delayed disease progression in mice by treatment with a cannabinoid. Amyotroph. Lateral Scler. Other Mot. Neuron Disord. 5, 33–39.

Rodriguez de Fonseca, F., Ramos, J.A., Bonnin, A., Fernández-Ruiz, J.J., 1993. Presence of cannabinoid binding sites in the brain from early postnatal ages. Neuroreport 4, 135–138.

Rodríquez de Fonseca, F., Hernández, M.L., de Miguel, R., Fernández-Ruiz, J.J., Ramos, J.A., 1992. Early changes in the development of dopaminergic neurotransmission after maternal exposure to cannabinoids. Pharmacol. Biochem. Behav. 41, 469–474.

Sarne, Y., Mechoulam, R., 2005. Cannabinoids: between neuroprotection and neurotoxicity. Curr. Drug Targets CNS Neurol. Disord. 4, 677–684.

Scallet, A.C., 1991. Neurotoxicology of cannabis and THC: a review of chronic exposure studies in animals. Pharmacol. Biochem. Behav. 40, 671–676.

Schestkowa O, Geisel D, Jacob R, Hasilik A., 2007. The catalytically inactive precursor of cathepsin D induces apoptosis in human fibroblasts and HeLa cells. J. Cell Biochem. 101, 1558–1566.

Schiaepfer, T.E., Lancaster, E., Heidbreder, R., Strain, E.C., Kosel, M., Fisch, H.U., Pearlson, G.D., 2006. Decreased frontal white-matter volume in chronic substance abuse. Drug Alcohol Depend. 77, 23–30.

Sinor, A.D., Irvin, S.M., Greenberg, D.A., 2000. Endocannabinoids protect cerebral cortical neurons from *in vitro* ischemia in rats. Neurosci. Lett. 278, 157–160.

Smith, A.M., Fried, P.A., Hogan, M.J., Cameron, I., 2006. Effects of prenatal marijuana on visuospatial working memory: an fMRI study in young adults. Neurotoxicol. Teratol. 28, 286–295.

Suarez, I., Bodega, G., Rubio, M., Fernandez-Ruiz, J.J., Ramos, J.A., Fernandez, B., 2004. Prenatal cannabinoid exposure down-regulates glutamate transporter expressions (GLAST and EAAC1) in the rat cerebellum. Dev. Neurosci. 26, 45–53.

Szoke, E., Czéh, G., Szolcsányi, J., Seress, L., 2002. Neonatal anandamide treatment in prolonged mitochondrial damage in the vanilloid receptor type 1-immunoreactive B-type neurons of the rat trigeminal ganglion. Neuroscience 115, 805–814.

Tsou, K., Brown, S., Sanudo-Pena, M.C., Mackie, K., Walker, J.M., 1998. Immunohistochemical distribution of cannabinoid CB_1 receptors in the rat central nervous system. Neuroscience 83, 393–411.

Van der Stelt, M., Veldeheis, W.B., Bar, P.R., Veldink, G.A., Vliegenthart, J.F.G., Nicolay, K., 2001. Neuroprotection by Δ^9-tetrahydrocannabinol, the main active compound in marijuana, against ouabain-induced *in vivo* excitotoxicity. J. Neurosci. 21, 6475–6479.

Zuzarte-Luis, V., Montero, J.A., Torre-Perez, N., Garcia-Porrero, J.A., Hurle, J., 2007. Cathepsin D gene expression outlines the areas of physiological cell death during embryonic development. Dev. Dyn. 236, 330–335.

Available online at www.sciencedirect.com
ScienceDirect
ELSEVIER
European Journal of Pharmacology 564 (2007) 57–65
ejp
www.elsevier.com/locate/ejphar

The tumour suppressor protein, p53, is involved in the activation of the apoptotic cascade by Δ^9-tetrahydrocannabinol in cultured cortical neurons

Eric J. Downer, Aoife Gowran, Áine C. Murphy, Veronica A. Campbell *

Department of Physiology and Trinity College Institute of Neuroscience, Trinity College, Dublin 2, Ireland

Received 19 July 2006; received in revised form 30 January 2007; accepted 1 February 2007
Available online 22 February 2007

Abstract

Cannabis is the most commonly used illegal drug of abuse in Western society. Δ^9-tetrahydrocannabinol, the psychoactive ingredient of marijuana, regulates a variety of neuronal processes including neurotransmitter release and synaptic transmission. An increasing body of evidence suggests that cannabinoids play a key role in the regulation of neuronal viability. In cortical neurons tetrahydrocannabinol has a neurodegenerative effect, the mechanisms of which are poorly understood, but involve the cannabinoid receptor subtype, CB_1. In this study we report that tetrahydrocannabinol (5 μM) evokes a rapid phosphorylation, and thus activation, of the tumour suppressor protein, p53, in a manner involving the cannabinoid CB_1 receptor, and the stress-activated protein kinase, c-jun N-terminal kinase, in cultured cortical neurons. Tetrahydrocannabinol increased expression of the p53-transcriptional target, Bax and promoted Bcl phosphorylation. These events were abolished by the p53 inhibitor, pifithrin-α (100 nM). The tetrahydrocannabinol-induced activation of the pro-apoptotic cysteine protease, caspase-3, and DNA fragmentation was also blocked by pifithrin-α. A siRNA knockdown of p53 further verified the role of p53 in tetrahydrocannabinol-induced apoptosis. This study demonstrates a novel cannabinoid signalling pathway involving p53 that culminates in neuronal apoptosis.

Keywords: Tetrahydrocannabinol; p53; Apoptosis

1. Introduction

Δ^9-tetrahydrocannabinol (THC) is the principal psychoactive ingredient of the Indian hemp plant, *Cannabis sativa*, and can evoke a variety of central effects such as memory impairments, analgesia, and changes in locomotor activity (Iversen, 2003), via activation of the cannabinoid CB_1 receptor which is widely distributed in the brain (Herkenham et al., 1991). The cannabinoid CB_1 receptor is G protein-coupled and linked to the regulation of Ca^{2+} and K^+ ion channels, the mitogen-activated protein kinase pathway and regulation of adenylyl cyclase (Howlett et al., 2004). THC has been reported to induce cell death in glioma cells (Galve-Roperh et al., 2000) and neurons (Downer et al., 2003) via generation of ceramide and activation of c-jun N-terminal kinase, respectively, however the exact molecular basis for THC-induced apoptosis in the brain remains to be fully elucidated. p53 is a nuclear phospho-protein that acts as a tumour suppressor providing a protective effect against tumour growth (Zörnig et al., 2001). A range of stress stimuli such as cytotoxic drugs, metabolite deprivation, physiological damage, and heat shock leads to p53 activation (Blatt and Glick, 2001) which in turn plays an important role in the regulation of stress-mediated G1 cell cycle arrest in order to enable DNA repair, or alternatively to induce apoptosis (Levine, 1997). However, as most neurons are in a post-mitotic state (Miller et al., 2000), the cell cycle regulatory function of p53 is absent. Hence, in post-mitotic neurons exposed to a toxic insult, the regulation of p53 expression is largely associated with mechanisms underlying cellular apoptosis rather than recovery from the insult (Enokido et al., 1996; Jordan et al., 1997). A role for p53 has been demonstrated for neuronal apoptosis induced by Aβ (Fogarty et al., 2003), excitotoxicity (Culmsee et al., 2001), and oxidative stress (Shibata et al., 2006).

Normal cellular p53 concentrations are low due to its short half-life and metabolic instability when inactivated (Evan and Littlewood, 1998). Although it is still largely unknown how p53 regulates growth arrest and apoptosis, it has been shown that phosphorylation plays an important role in regulating the biological activities of p53 (Herr and Debatin, 2001). The

* Corresponding author. Tel.: +353 1 608 1192; fax: +353 1 6793545.
E-mail address: vacmpbll@tcd.ie (V.A. Campbell).

0014-2999/$ - see front matter © 2007 Elsevier B.V. All rights reserved.
doi:10.1016/j.ejphar.2007.02.025

phosphorylation state of p53 is controlled by a large number of proteins including c-jun N-terminal kinase (JNK; Blatt and Glick, 2001), a kinase we have previously shown to be pertinent in THC-induced apoptosis (Downer et al., 2003). Once phosphorylated, the stability of the p53 protein is increased, allowing it to act as a transcription factor to upregulate the gene encoding the pro-apoptotic Bcl-2 family member, Bax, and repress the anti-apoptotic Bcl-2 gene (Miyashita and Reed, 1995). Bax is an integral membrane protein bound to organelles or a soluble protein found in the cytoplasm (Wolter et al., 1997). Following cell damage, Bax can translocate to the mitochondrial membrane (Wolter et al., 1997) to regulate cytochrome *c* translocation to the cytosol (Kim et al., 2001) and subsequent activation of the executioner cysteine protease, caspase-3. In contrast to Bax, Bcl-2 is an anti-apoptotic mitochondrial-associated protein that prevents Bax-induced cytochrome *c* translocation and resultant cell death by inhibiting Bax redistribution from the cytoplasm to the mitochondria (Murphy et al., 2000).

The aim of this study was to determine if THC impacts on p53 signalling in cultured cortical neurons and to determine the contribution of p53 to THC-induced apoptosis. Specifically, the role of p53 in THC-induced Bax expression, caspase-3 activation and DNA fragmentation was assessed. To address this question we used the reversible p53 inhibitor, pifithrin-α, which has been shown to have anti-apoptotic effects in a number of systems (Gudkov, 2005) by preventing p53 transactivation (Komarov et al., 1999) and inhibiting Bax expression (Culmsee et al., 2001). More recently, pifithrin-α has been demonstrated to inhibit p53 phosphorylation and subsequent apoptosis (Chua et al., 2006). Further evaluation of the role of p53 in THC-induced apoptosis was assessed by employing a siRNA knockdown approach.

2. Materials and methods

2.1. Culture of cortical neurons

Primary rat cortical neurons were established as described previously (MacManus et al., 2000) and maintained in neurobasal medium (Gibco BRL, Paisley, Scotland). Rats were decapitated in accordance with institutional and national ethical guidelines and cerebral cortices removed. The dissected cortices were incubated in phosphate-buffered saline (PBS) containing trypsin (0.25%) for 2 min at 37 °C. The tissue was then triturated (×5) in PBS containing soyabean trypsin inhibitor (0.1%) and DNAse (0.2 mg/ml) and gently filtered through a sterile mesh filter. Following centrifugation, 2000 ×*g* for 3 min at 20 °C, the pellet was resuspended in neurobasal medium, supplemented with heat inactivated horse serum (10%), penicillin (100 U/ml), streptomycin (100 U/ml) and glutamax (2 mM). Suspended cells were plated out at a density of 0.25×10^6 cells on circular 10 mm diameter coverslips, coated with poly-L-lysine (60 μg/ml), and incubated in a humidified atmosphere containing 5% CO_2: 95% air at 37 °C. After 48 h 5 ng/ml cytosine-arabino-furanoside was included in the culture medium to prevent proliferation of non-neuronal cells. Culture media were exchanged every 3 days and cells were grown in culture for 12 days prior to THC treatment. All protocols concerning animal use were approved by the institutional ethics committee.

2.2. Drug treatment

THC was obtained under licence from Sigma-Aldrich Company Ltd and diluted to the required concentration with warmed culture media. Absolute alcohol was used as vehicle control (vcon) for THC. Cells were incubated with the cannabinoid CB_1 receptor antagonist, AM 251 (1-(2,4-dichlorophenyl)-5-(4-iodophenyl]])-4-methyl-*N*-(1-piperidyl)pyrazole-3-carboxamide; 1 μM) for 30 min prior to THC treatment. The p53 inhibitor, pifithrin-α (Calbiochem, Germany) was made up as a 1 mM stock in dimethylsulphoxide and diluted to a final concentration of 50 nM in culture medium. Cells were exposed to pifithrin-α for 60 min prior to THC treatment. Pifithrin-α is a cell permeable highly lipophilic molecule that efficiently inhibits p53-dependent transactivation of p53-responsive genes and reversibly blocks p53-mediated apoptosis (Culmsee et al., 2001). The cell permeable D-JNK inhibitor 1 (Alexis Biochemicals, Switzerland) was stored as a 1 mM stock in sterile PBS and diluted to a final concentration of 1 μM in warm culture media. Neurons were pre-incubated with D-JNK inhibitor 1 for 30 min before treating with THC.

2.3. Western immunoblot for analysis of p53, phospho-p53, Bax, p-Bcl-2 expression

Following incubation with THC, cortical neurons were harvested in lysis buffer (20 mM HEPES, 10 mM KCl, 1.5 mM $MgCl_2$, 1 mM EGTA, 1 mM EDTA, 1 mM dithiothreitol, 0.1 mM PMSF, 5 μg/ml pepstatin A, 2 μg/ml leupeptin, 2 μg/ml aprotinin, pH 7.4) and left on ice for 20 min. The cells were centrifuged (15,000 ×*g* for 20 min at 4 °C) and the supernatant was diluted to 50 μg protein/ml with sample buffer (150 mM Tris–HCl pH 6.8, 10% v/v glycerol, 4% w/v SDS, 5% v/v β-mercaptoethanol, 0.002% w/v Bromophenol Blue). Samples were then heated to 100 °C for 3 min. Proteins (1 μg per lane) were separated by electrophoresis on a 10% polyacrylamide minigel, transferred to nitrocellulose membrane and immunoblotted with an the appropriate primary antibody.

For Bax, membranes were incubated with a rabbit polyclonal Bax antibody (DAKO Corporation, Carpinteria, CA, USA) that recognises amino acids 43–61 of Bax (1:200 dilution in TBS containing 0.1% tween, 0.1% BSA; w/v) followed by a horse radish peroxidase-conjugated anti-rabbit IgG (1:2000 dilution in Tris-buffered saline containing 0.1% Tween X100 (TBS-T) and 0.1% BSA (w/v); Sigma, Dorset, UK). Bcl-2 phosphorylation (p-Bcl) was assessed using a rabbit polyclonal anti-phospho-Bcl-2 antibody (Oncogene, Boston, MA, USA) that recognises a peptide corresponding to amino acids 81–94 of *bcl-2* (1:250 dilution in TBS-T containing 0.1% BSA; w/v), followed by horse radish peroxidase-conjugated goat anti-rabbit IgG (1:1000 dilution in TBS containing 0.1% tween, 0.1% BSA (w/v); Santa Cruz Biotechnology Inc, Santa Cruz, CA, USA). To monitor total p53 expression (t-p53) and p53 phosphorylation (p-p53), anti-p53 polyclonal antibody (Santa Cruz Biotechnology Inc,

California) and anti-phospho^{ser15} p53 (1: 1000, Cell Signaling Technology, Inc.) polyclonal antibodies purified from rabbit serum were used. Immunoreactive bands were detected using the horseradish peroxidase-conjugated anti-rabbit IgG and enhanced chemiluminescence. The chemiluminescent detection chemical (SuperSignal Ultra; Pierce, Leiden, Netherlands) was added and the blotting paper exposed photographic film (Hyperfilm, Amersham, Buckinghamshire, United Kingdom) and developed using a Fuji X-ray processor. In all cases quantification of protein bands exposed onto photographic film was achieved by densitometric analysis using ZERO-Dscan Image Analysis system (Scanalytics, Massachusetts, USA). Values are expressed as arbitrary units. Blots were stripped with an antibody stripping solution (Reblot Plus Strong antibody stripping solution; Chemicon, California, USA) and reprobed for actin, total p53 or total-Bcl expression, where appropriate, in order to confirm equal loading of protein. Levels of phospho-p53 and phospho-Bcl were normalised to t-p53 and t-Bcl, respectively. Bax expression was normalised to actin.

2.4. Immunocytochemistry

Following treatment the cells were fixed with 4% paraformaldehyde, permeabilised with 0.2% Triton X-100 and non-reactive sites were blocked with 10% goat serum, 4% bovine serum albumin in TBS. To determine the expression of phosphorylated p53, the cells were incubated overnight with an anti-p53 antibody, which recognises the phosphorylated form of p53 (p53^{ser15}; Cell Signalling Technology) purified from rabbit serum. For analysis of Bax expression, cells were incubated overnight with a monoclonal primary antibody raised against amino acids 1–171 of Bax of mouse origin (1:500 dilution in TBS containing 10% blocking buffer (v/v); Santa Cruz Biotechnology Inc, Santa Cruz, CA, USA). The cells were then washed in TBS and incubated in the dark with horse biotinylated anti-mouse IgG (1:50 in 10% blocking buffer (v/v); Vector Laboratories Inc., CA, USA) or goat biotinylated anti-rabbit IgG (Vector Laboratories) for 1 h at room temperature. Cells were subsequently incubated with ExtrAvidin® FITC (Sigma-Aldrich). Cover slips were mounted using Vectashield® fluorescent mounting media (Vector Laboratories). For Bax, mounted coverslips were viewed under ×40 magnification by fluorescence microscopy (Leitz Orthoplan Microscope, Leica Microsystems AG, Wetzlar, Germany) using Improvision software (Improvision, Coventry, UK). Cells were observed under excitation, 490 nm; emission, 520 nm for FITC labelled antibodies. For p53, confocal fluorescence microscopy imaging was performed using Zeiss 510 Meta confocal laser scanning microscope (LSM 510 META). The FITC fluorophore was detected using the 488–514 nm Argon laser.

2.5. Protein quantification using the Bradford assay

Protein standards were prepared from stock solution of 1000 μg/ml bovine serum albumin (BSA; Sigma-Aldrich, Dorset, UK). Samples (10 μl) and standards (10 μl) were added to a 96-well plate (Sarstedt, Wexford, Ireland) in duplicate and Bio-Rad dye reagent concentrate (1:5 dilution in dH_2O, 200 μl; Bio-Rad, Hertfordshire, UK) was added to both and absorbance was assessed at 600 nm using a 96-well plate reader (Labsystems Multiskan RC). The concentration of protein in samples was calculated from the regression line plotted (Instat 2.03) from the absorbance of the BSA standards.

2.6. Measurement of caspase-3 activity

Cleavage of the fluorogenic caspase-3 substrate (DEVD-aminofluorocoumarin (AFC); Alexis Corporation, USA) to its fluorescent product was used as a measure of caspase-3 activity. Cortical neurons were harvested in lysis buffer (25 mM HEPES, 5 mM $MgCl_2$, 5 mM DTT, 5 mM EDTA, 2 mM PMSF, 10 μg/ml leupeptin, 10 μg/ml pepstatin; pH 7.4), subjected to 3 freeze–thaw cycles and centrifuged at 10,000 rpm for 10 min at 4 °C. Samples of supernatant (90 μl) were incubated with the DEVD peptide (500 μM; 10 μl) for 1 h at 30 °C. Incubation buffer (900 μl; 100 mM HEPES containing 10 mM DTT; pH 7.4) was added and fluorescence was assessed (excitation, 400 nm; emission, 505 nm).

2.7. RNA interference

Custom ON-TARGET Plus Smart pool small interfering RNA (siRNA) containing a mixture of 4 SMART selection designed siRNAs targeting rat p53 (Gen Bank™ accession number NM_030989; p53 siRNA) was purchased from Dharmacon (Lafayette, CO., U.S.A.). Primary cortical neurons were transfected with p53 siRNA (100 nM) using Dharmacon transfection lipid number 3. After 48 h of transfection, cells were treated with THC (5 μM) or vehicle (0.006% ethanol) for 2 h. A control siRNA duplex containing at least 4 mismatches to any rat gene (ON-TARGET Plus siControl Non-Targeting siRNA; Con siRNA) was used in parallel experiments. Optimal transfection efficiency and conditions were determined by using FAM labelled non-specific siRNA (SiGlo green; Dharmacon, Lafayette, CO, U.S.A.). Effective p53 knockdown was analysed using immunohistochemistry.

2.8. TdT-mediated-UTP-end nick labelling (TUNEL)

Apoptotic cell death was assessed using the DeadEnd colorimetric apoptosis detection system (Promega Corporation, Madison, USA). Cells were then fixed with paraformaldehyde (4%), permeabilised with Triton X-100 (0.1%), and biotinylated nucleotide was incorporated at 3′-OH DNA ends using the enzyme Terminal deoxynucleotidyl Transferase (TdT). Horseradish-peroxidase-labelled streptavidin then bound to the biotinylated nucleotide and this was detected using the peroxidase substrate H_2O_2 and the chromogen diaminobenzidine. Cells were then viewed under light microscopy at ×40 magnification, where the nuclei of TUNEL-positive cells stained brown. In some experiments the Dead End™ Fluorometric Tunel assay was employed. TUNEL-positive cells with incorporated fluorescein-12-dUTP-labelled fragmented DNA was visualised by fluorescent confocal microscopy (Zeiss LSM 510-META) using

the 488 nm Argon/2 laser with the following scan configurations; laser output 50%, % transmission 5%, band pass filter 505–530, beam splitter 488/543, detector gain 719, amplifier gain 1, amplifier offset −0.14, pinhole 96 μm (1 Airy unit) and 16 scan averages. Propidium iodide (stains all cells apoptotic and non-apoptotic) was visualised using the 543 nm Helium Neon laser with the following scan configurations; laser output 50%, % transmission 100%, band pass filter 560–615, beam splitter 488/543, detector gain 622, amplifier gain 1, amplifier offset 0, pinhole 108 μm (1 Airy unit) and 16 scan averages. Apoptotic cells (TUNEL positive) were counted and expressed as a percentage of the total number of cells examined. To exclude the possibility that the number of living cells present on the coverslip had an affect on the TUNEL-positive ratio the same number of cells (~400) was counted for each treatment.

2.9. Statistics

Statistical analysis was carried out using one-way analysis of variance (ANOVA) followed by the post-hoc Student–Newman–Keuls test when significance (at the 0.05 level) was indicated. When comparisons were being made between two treatments, a paired Student's *t*-test was performed and $P<0.05$ or $P<0.01$ was considered significant.

3. Results

3.1. THC induces an increase in p53 protein expression in cultured cortical neurons

Phosphorylation plays an important role in regulating the biological activities of p53 (Herr and Debatin, 2001). Once phosphorylated the stability of the p53 protein is increased allowing it to act as a transcription factor to enhance and repress genes involved in the apoptotic process (Miyashita and Reed, 1995). Phosphorylation of p53 at residue serine-15, a key site for p53 activation (Appella and Anderson, 2001), was assessed following treatment with THC (5 μM) using an antibody that detects endogenous levels of p53 only when phosphorylated at residue serine-15 (Fig. 1A). Following THC treatment for 5 min,

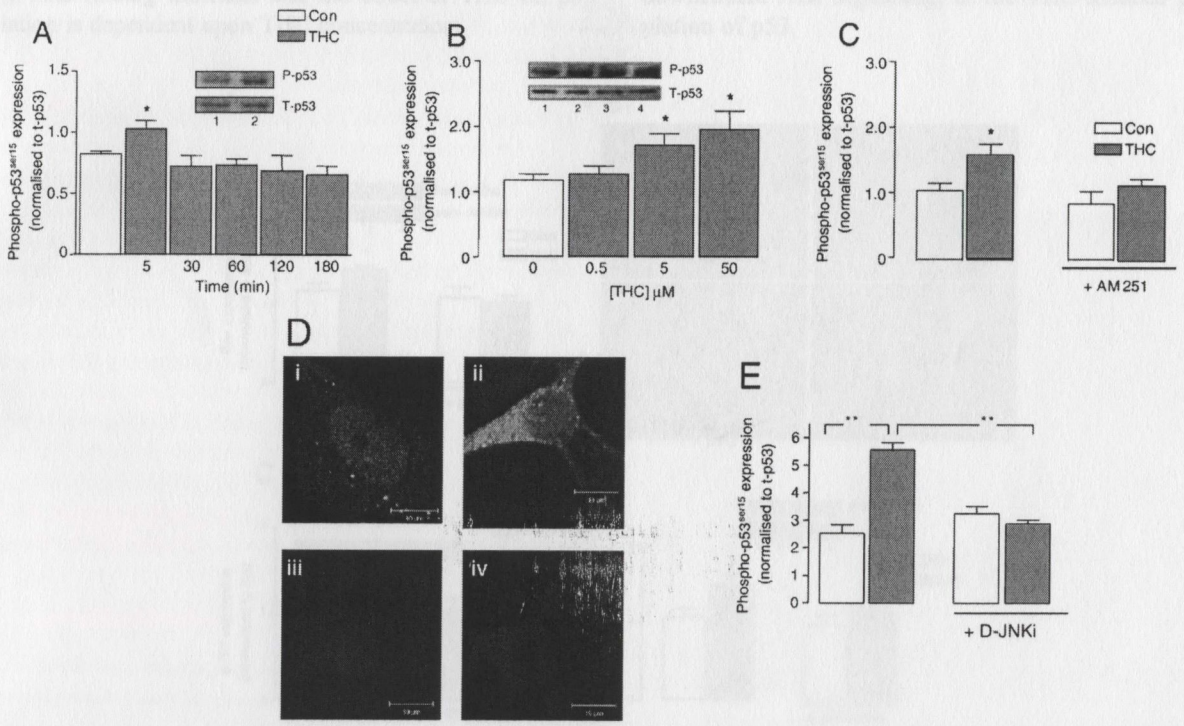

Fig. 1. THC increases p53 protein expression in a time-dependent manner. A, cultured cortical neurons were treated with THC (5 μM) for 5–180 min, cell protein was harvested and analysed for the expression levels of phospho-p53 using western immunoblot. THC significantly increased phospho-p53^{ser15} expression at 5 min but not at subsequent time-points (30–180 min). Results are expressed as mean±S.E.M for 5 observations, *$P<0.05$. Inset; a sample western immunoblot demonstrating the increase in phospho-p53^{ser15} expression at 5 min of THC treatment (lane 2) compared to untreated neurons (lane 1), neurons treated with THC for 30 min (lane 3), 60 min (lane 4), 120 min (lane 5) and 180 min (lane 6). T-p53 expression was monitored to ensure equal protein loading. B, a significant increase in phospho-p53^{ser15} protein expression was found following treatment with THC at concentrations of 5 μM and 50 μM. Exposure to THC at a concentration of 0.5 μM had no effect on the expression levels of phospho-p53^{ser15}. Results are expressed as mean±S.E.M for 5 observations, *$P<0.05$. inset; a sample western immunoblot demonstrating that a 5 min treatment with THC at doses of 5 μM (lane 3) and 50 μM (lane 4) significantly increased phospho-p53^{ser15} expression as compared to vehicle-treated neurons (lane 1). Data were normalised to t-p53 and actin expression was monitored to ensure equal protein loading. C, pre-incubation of cortical neurons with AM 251 (1 μM) prior to THC exposure abolished the THC-induced increase in phospho-p53^{ser15} expression observed at 5 min. Results are expressed as mean±S.E.M for 6 observations, *$P<0.05$. D, confocal images of phospho-p53^{ser15} immunostaining in (i) vehicle-treated neurons, (ii) THC-treated neurons (5 μM, 5 min), (iii) D-JNK1 (1 μM)-treated cultures and (iv) cultures treated with THC in the presence of D-JNKI (1 μM). Scale bar is 10 μm. E, pre-incubation of cortical neurons with D-JNKI (1 μM). prior to THC (5 μM) exposure abolished the THC-induced increase in phospho-p53^{ser15} expression observed at 5 min. Results are expressed as mean±S.E.M for 6 observations, **$P<0.01$.

mean phospho-p53^{ser15} expression was significantly increased ($P<0.05$, ANOVA; $n=5$ observations). Phospho-p53^{ser15} expression was unaltered in neurons exposed to THC for 30 min, 60 min, 120 min and 180 min. This finding indicates that THC evokes the early and transient increase in p53 phosphorylation at residue serine-15. A sample immunoblot demonstrating the increase in phospho-p53^{ser15} expression at 5 min following THC exposure is shown as an inset in Fig. 1A. The phosphorylation at this residue did not cause a sustained increase in expression of p53 (60–180 min) suggesting that this p53 phosphorylation event was not involved in the long-term stabilisation of p53.

A dose–response analysis of the effects of THC on phospho-p53 protein expression at 5 min was performed (Fig. 1B). Neuronal cell cultures treated with vehicle for 5 min showed a level of phospho-p53 expression comparable to that found in cells treated with 0.5 μM THC for 5 min. However, phospho-p53 protein expression was significantly increased in neurons treated with 5 μM THC for 5 min ($P<0.05$, ANOVA, $n=5$ observations). Similarly, a 50 μM THC dose significantly increased p53 protein expression at 5 min ($P<0.05$, ANOVA, $n=5$). This finding indicates that the effect of THC on p53 regulation is dependent upon THC concentration.

To assess the role of the cannabinoid CB_1 receptor in coupling THC to p53 signalling, cultured cortical neurons were pre-treated with the selective cannabinoid CB_1 receptor antagonist AM 251 (1 μM) for 30 min prior to THC (5 μM) exposure for 5 min. AM 251 prevented the THC-induced increase in p53 protein expression at 5 min (Fig. 1C). In vehicle-treated control neurons phospho-p53^{ser15} expression was significantly increased following treatment with THC (5 μM) for 5 min ($P<0.05$, ANOVA, $n=6$ observations). Exposure to AM 251 alone had no effect on phospho-p53^{ser15} expression, but prevented the THC-induced increase in phospho-p53^{ser15} expression. Furthermore, the THC-induced increase in phospho-p53 immunoreactivity was abrogated by the JNK inhibitor, D-JNKI (1 μM), indicating that JNK regulates p53 phosphorylation in this system. A sample confocal image demonstrating the JNK-dependent increase in phospho-p53 immunostaining is shown in Fig. 1D. Similarly, Fig. 1E demonstrates that the THC-induced increase in expression of phospho-p53 is abrogated by D-JNKI. These data demonstrate a role for the cannabinoid CB_1 receptor, and downstream JNK signalling, in the THC-induced phosphorylation of p53.

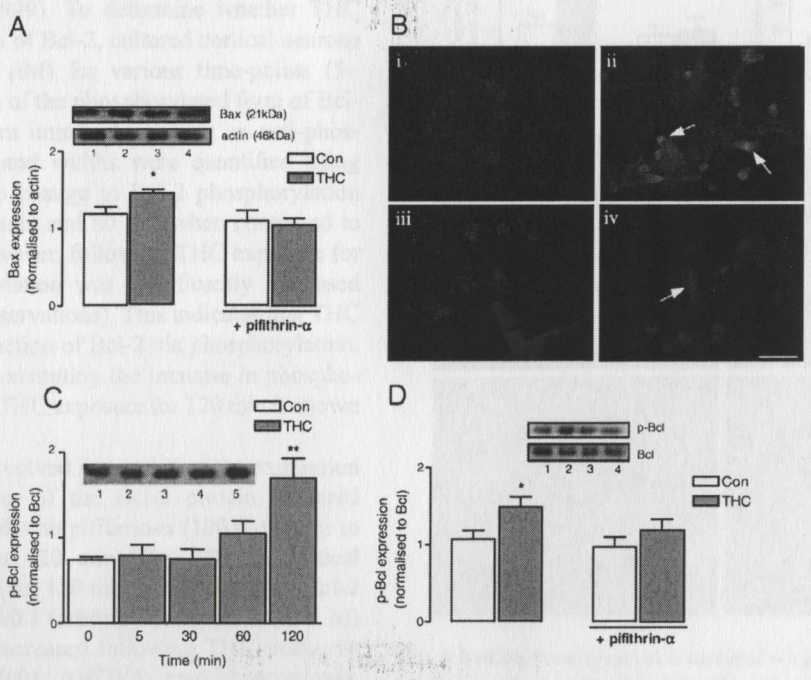

Fig. 2. THC-induced increase in Bax is reliant on p53. A, cultured cortical neurons were treated with THC (5 μM) for 120 min, cell protein was harvested and analysed for the expression levels of Bax using western immunoblot. THC evoked a significant increase in Bax protein expression, and this was abolished by pre-treatment with the p53 inhibitor, pifithrin-α (100 nM). Results are expressed as mean±S.E.M for 5 observations, *$P<0.05$. Inset; a sample western immunoblot demonstrating the increase in Bax protein expression following THC treatment (lane 2). Lane 1 represents vehicle-treated neurons, pifithrin-α-treated neurons (lane 3), neurons treated with THC in the presence of pifithrin-α (lane 4). An actin immunoblot confirms equal protein loading. B, images of Bax immunostaining in (i) vehicle-treated neurons, (ii) THC-treated neurons (5 μM, 2 h), (iii) pifithrin-α-treated neurons and (iv) neurons treated with THC in the presence of pifithrin-α. Arrows indicate cells with intense Bax immunoreactivity. Scale bar is 25 μm. C, THC significantly increased phospho-Bcl (p-Bcl) expression at 120 min but not at earlier time-points (5–60 min). Results are expressed as mean±SEM for 6 observations, normalised to total-Bcl expression, **$P<0.01$. Inset; a sample western immunoblot demonstrating the increase in phospho-Bcl expression at 120 min of THC treatment (lane 5) compared to vehicle-treated neurons (lane 1), neurons treated with THC for 5 min (lane 2), 30 min (lane 3), 60 min (lane 4). D, neurons were pre-incubated with pifithrin-α (100 nM), treated with THC (5 μM) for 120 min and analysed for the expression levels of phospho-Bcl protein using western immunoblotting. Exposure to pifithrin-α abolished the THC-induced increase in Bax expression. Results are expressed as mean±S.E.M for 5 observations, normalised to total-Bcl expression, *$P<0.05$. Inset: a sample western immunoblot demonstrating phospho-Bcl (p-Bcl) and total-Bcl protein expression in cells treated with vehicle control (lane 1), THC (lane 2), pifithrin-α (lane 3) and THC+pifithrin-α (lane 4).

3.2. THC increases cytosolic Bax protein expression in cultured neurons

p53 induces apoptosis by altering the expression of the Bcl family of mitochondrial-associated proteins (Marchenko et al., 2000; Miyashita and Reed, 1995). To determine if p53 is involved in THC-induced apoptosis by regulating the expression of the pro-apoptotic protein, Bax, cultured neurons were treated with the p53 inhibitor, pifithrin-α (100 nM) prior to exposure to THC (5 μM) for 120 min (Fig. 2A), a time-point at which we have previously reported a THC-induced increase in Bax protein expression (Downer et al., 2003). A significant increase in Bax expression was observed following treatment with THC for 120 min (control, 1.2±0.1 versus THC treatment, 1.4±0.1, mean band width±S.E.M.; $P<0.05$, ANOVA, $n=5$ observations). Exposure to pifithrin-α alone had no effect on Bax expression but it prevented the THC-induced increase in Bax expression. Similarly, Fig. 2B demonstrates that the THC-induced increase in Bax immunoreactivity is abolished by pifithrin-α.

In contrast to Bax, the anti-apoptotic protein, Bcl-2, represses cell death (Korsmeyer, 1999). However, phosphorylation of Bcl-2 inhibits its pro-survival function (Pucci et al., 1999; Yamamoto et al., 1999). To determine whether THC induces the phosphorylation of Bcl-2, cultured cortical neurons were exposed to THC (5 μM) for various time-points (5–120 min). Expression levels of the phosphorylated form of Bcl-2 were measured by western immunoblot using an anti-phospho-Bcl-2 antibody, and band widths were quantified using densitometry (Fig. 2C). No change in Bcl-2 phosphorylation was observed at 5 min, 30 min and 60 min when compared to untreated cortical cells. However, following THC exposure for 120 min, Bcl-2 phosphorylation was significantly increased ($P<0.05$, ANOVA; $n=6$ observations). This indicates that THC inhibits the pro-survival function of Bcl-2 via phosphorylation. A sample immunoblot demonstrating the increase in phospho-Bcl-2 expression following THC exposure for 120 min is shown in Fig. 2C.

To determine if p53 is involved in regulating the expression of the phosphorylated form of the Bcl-2 protein, cultured cortical neurons were treated with pifithrin-α (100 nM) prior to THC (5 μM) exposure for 120 min (Fig. 2D). In cortical neurons treated with vehicle for 120 min, phosphorylated Bcl-2 protein expression was 1.1±0.1 (arbitrary units; mean±S.E.M) and this was significantly increased following THC treatment (120 min) to 1.5±0.1 ($P<0.01$, ANOVA, $n=6$ observations). Whilst pre-treatment with pifithrin-α alone had no effect on the level of phosphorylated Bcl-2 protein expression, it prevented the THC-induced increase in p53 expression, indicating that the modulation of Bcl-2 phosphorylation by THC is p53-dependent.

3.3. THC induces caspase-3 activation via p53

Since caspase-3 has a central role in the cell death pathway triggered by THC in the rat cortex (Downer et al., 2003), it was determined if p53 signalling was involved in regulating caspase-3 activity. Following the inhibition of p53 by exposing cultured cortical neurons to pifithrin-α, caspase-3 activity was assessed following THC exposure by monitoring the cleavage of the fluorescently labelled caspase-3 substrate, DEVD, to its fluorescent product (Fig. 3A). Neurons were pre-treated with pifithrin-α (100 nM) for 60 min prior to THC (5 μM; 120 min) treatment. In control conditions, caspase-3 activity was 5.5±0.9 nmol AFC produced/mg protein/min (mean±S.E.M) and this was significantly increased to 9.4±1.2 nmol AFC produced/mg protein/min when neurons were incubated with THC for 120 min ($P<0.05$, ANOVA, $n=6$ observations). Caspase-3 activity in neurons treated with pifithrin-α alone for 120 min was comparable to control levels of caspase-3 activity. However, the THC-induced increase in caspase-3 activity was significantly reduced in neurons treated with THC in the presence of pifithrin-α ($P<0.05$, ANOVA compared to cells treated with THC, $n=6$ observations) indicating that the THC-induced activation of caspase-3 is p53-dependent.

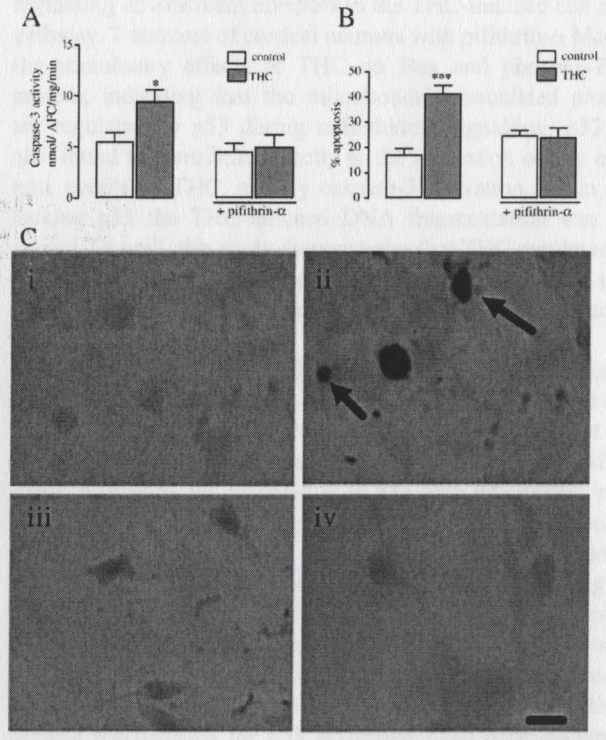

Fig. 3. THC-induced apoptosis is mediated via p53. A, treatment of primary cortical neurons with THC (5 μM; 120 min) significantly increased caspase-3 activity as assessed by the cleavage of the fluorogenic DEVD substrate. The stimulatory effect of THC on caspase-3 activity was prevented by pifithrin-α (100 nM). Exposure of cells to pifithrin-α had no effect on caspase-3 activity. Results are expressed as the mean±S.E.M for 4 observations, $*P<0.05$. B, cultured cortical neurons were treated with THC (5 μM; 120 min) in the presence or absence of pifithrin-α (100 nM) and cell viability was assessed by TUNEL staining. THC significantly increased DNA fragmentation and this was prevented by pifithrin-α. Results are expressed as mean±SEM for 4 observations, $***P<0.001$. C, images of TUNEL staining in (i) vehicle-treated neurons, (ii) THC-treated neurons, (iii) pifithrin-α-treated cultures and (iv) cultures treated with THC in the presence of pifithrin-α. Arrows indicate apoptotic neurons displaying DNA fragmentation following exposure to THC. Scale bar is 25 μm.

3.4. THC-induced DNA fragmentation is reliant on p53

THC causes a maximal increase in DNA fragmentation 2–3 h post-treatment (Downer et al., 2003), therefore this time-point was used to determine if p53 was involved directly in mediating THC-induced DNA fragmentation. Following p53 inhibition by exposing cultured cortical neurons to pifithrin-α (100 nM), the TUNEL technique was used to assess the levels of THC-induced DNA fragmentation at 120 min (Fig. 3B). In vehicle-treated control cells, 16.9±2.7% (mean±S.E.M) of cells displayed fragmented DNA in the nucleus (TUNEL positive). This was significantly increased to 41.3±3.4% in cells treated with THC for 120 min ($P<0.001$, ANOVA, $n=4$ observations). Whilst treatment of cells with pifithrin-α alone for 120 min had no effect on neuronal viability (22.6±2.3% neurons with fragmented DNA), it prevented the THC-induced increase in DNA fragmentation (23.8±4.1% TUNEL-positive neurons). This finding suggests that p53 is directly involved in THC-induced DNA fragmentation. Representative TUNEL images of neurons are shown in Fig. 3C.

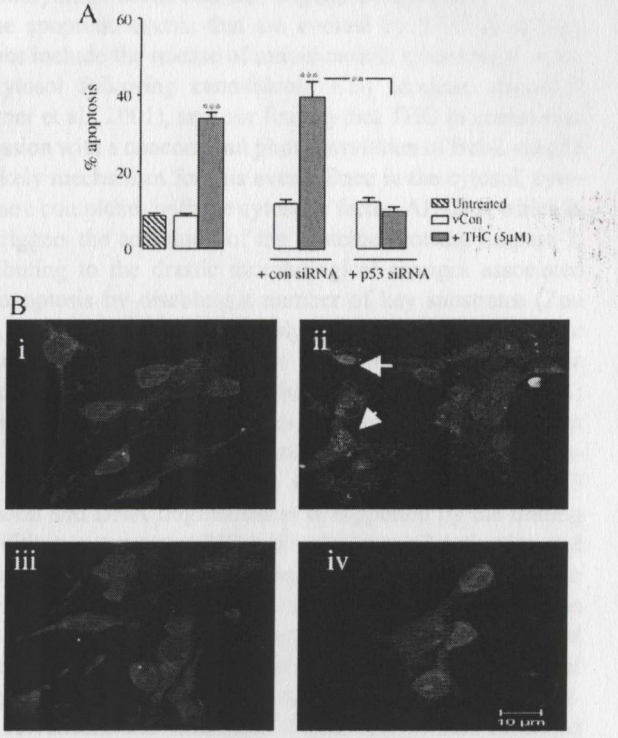

Fig. 4. siRNA knockdown of p53 prevents THC-induced DNA fragmentation. A, exposure of neurons to THC (5 μM) for 2 h significantly increased the percentage of cells with DNA fragmentation. Treatment with p53 siRNA (100 nM; 48 h) prior to THC treatment prevented the THC-induced increase in DNA fragmentation. Results are expressed as mean±S.E.M for 6 observations, ***$P<0.001$ versus vCon; ** versus p53 siRNA transfected cells exposed to THC. B, Representative confocal images of TUNEL stained neurons in (i) cells exposed to vehicle control, (ii) cells exposed to THC (5 μM, 2 h), (iii) cells pre-treated with p53 siRNA and (iv) cells exposed to THC (5 μM, 2 h) following p53 siRNA pre-treatment. Arrows indicate TUNEL-positive apoptotic cells.

The role of p53 in THC-induced apoptosis was verified using p53 siRNA (Fig. 4). Transfection of the cells with p53 siRNA (100 nM) for 48 h significantly abolished the induction of apoptosis evoked by THC (5 μM; $P<0.01$, ANOVA, $n=6$), whilst THC retained its neurotoxic profile in cells transfected with the control RNA which has no target sequence.

4. Discussion

In this study we examined the ability of THC to couple to the nuclear phospho-protein p53, and to determine if p53 signalling contributes to the apoptotic actions of THC in cultured cortical neurons. THC was found to induce a transient and dose-dependent increase in p53 phosphorylation via the central cannabinoid CB_1 receptor and the JNK signalling pathway. THC increased the phosphorylation of p53 on residue serine-15 within 5 min, a modification which increases its transcriptional activity. The p53 inhibitor, pifithrin-α, and siRNA-mediated knockdown of p53 were used to determine the role of p53 in regulating downstream effectors in the THC-induced cell death pathway. Treatment of cortical neurons with pifithrin-α blocked the stimulatory effects of THC on Bax and phospho-Bcl-2 protein, indicating that the mitochondrial-associated proteins are regulated by p53 during cannabinoid signalling. p53 was also found to contribute directly to the regulation of key apoptotic events by THC, namely caspase-3 activation and in cells lacking p53 the THC-induced DNA fragmentation was prevented. Overall, this study demonstrates that THC regulates p53 signal transduction in cultured cortical cells and that this pathway contributes to the apoptotic effects of THC in this neuronal system.

The level of p53 is kept low in normal healthy cells due its short half-life, but increases in response to cellular stress (Levine, 1997; Miller et al., 2000). There is evidence that p53 becomes phosphorylated on residue serine-15 following cellular stress, disrupting the association of p53 with its negative regulator, Mdm-2, which in turn prevents the degradation of the p53 protein (Shieh et al., 1997) and allows it to translocate to the nucleus to regulate pro-apoptotic genes. Hence, the finding that THC rapidly phosphorylates p53 on serine-15 provides a mechanism for p53 activation. A rapid and transient phosphorylation of p53 has been reported in other preparations exposed to neurotoxic stimuli (Chua et al., 2006; Fogarty et al., 2003). Several mechanisms for p53 activation have been suggested, including phosphorylation by ERK, casein kinases and JNK (Blatt and Glick, 2001). We have previously reported that THC induces activation of JNK1 (Downer et al., 2003) within a similar timeframe to the THC-induced increase in p53 phosphorylation observed in the current study, whilst JNK2 is activated at the later time-point of 2 h. Since the THC-induced increase in p53 phosphorylation was blocked with the JNK inhibitor, D-JNK1, we propose that the upstream activation of the JNK1 signalling pathway couples THC to p53 in this neuronal system.

The mechanism of p53-induced apoptosis has been extensively studied and involves the activation of the mitochondrial/caspase pathway (Marchenko et al., 2000; Bonini et al., 2004),

regulation of the Fas receptor (Bennet et al., 1998) and the transcription of genes involved in regulating the redox state of the cell (Polyak et al., 1997). A growing and diverse list of genes are involved in the apoptotic actions of p53, including the *bax* gene (Miyashita and Reed, 1995; Cregan et al., 1999). Bax is involved in apoptotic cascades utilising the mitochondria-dependent pathway (Reed, 2006) and is pro-apoptotic by virtue of its ability to promote cytochrome *c* release from the mitochondria. THC was found to increase cytosolic Bax expression in a p53-dependent manner. In addition to the evidence suggesting that p53 induces apoptosis by up-regulating the transcription of Bax, there is also evidence that p53 can regulate the expression of the anti-apoptotic protein, Bcl-2 (Mielke and Herdegen, 2000). In contrast to Bax, Bcl-2 represses cell death (Korsmeyer, 1999) since it prevents cytochrome *c* release from the mitochondria (Shimizu et al., 1999) by blocking the redistribution of Bax to the mitochondria (Gross et al., 1998). However, the pro-survival function of Bcl-2 is inhibited following phosphorylation of the Bcl-2 protein (Yamamoto et al., 1999) and there is evidence that Bcl-2 phosphorylation can be regulated by p53 (Pucci et al., 1999). Evidence presented herein demonstrate that THC induces the phosphorylation of Bcl-2 protein within the same timeframe of Bax induction, and this phosphorylation event was also dependent upon p53.

The apoptotic events that are evoked by THC in cortical neurons include the release of mitochondrial cytochrome *c* into the cytosol following cannabinoid CB_1 receptor activation (Downer et al., 2001), and our finding that THC increases Bax expression with a concomitant phosphorylation of Bcl-2 via p53 is a likely mechanism for this event. Once in the cytosol, cytochrome *c* complexes with the cytosolic factor, APAF-1, which in turn triggers the activation of the cysteine protease caspase-3, contributing to the drastic morphological changes associated with apoptosis by disabling a number of key substrates (Zou et al., 1997). We have previously shown that cytochrome *c* release and caspase-3 activation is central to the apoptotic cascade triggered by THC in cortical neurons (Campbell, 2001; Downer et al., 2001) and caspase-3 induction is dependent on JNK1 and JNK2 signalling (Downer et al., 2003). The involvement of p53 in the regulation of THC-induced caspase-3 activation and DNA fragmentation is supported by the finding that pifithrin-α prevents THC-induced caspase-3 activation and the fragmentation of DNA. Cannabinoids have been shown to evoke apoptosis in a variety of cell types including glioma (Velasco et al., 2004), leukemic cells (Powles et al., 2005) and colorectal carcinomas (Patsos et al., 2005) and manipulation of this apoptotic cascade may have therapeutic value in the treatment of cancers and leukemia. Whilst cannabinoid-mediated apoptosis of leukemic cells is p53-independent (Powles et al., 2005), the role of p53 in the anti-tumoural role of cannabinoids remains to be established. Cannabinoids can also evoke apoptosis in neurons (Movsesyan et al., 2004; Campbell, 2001), and this may contribute to the role of cannabinoids in brain development (Fernandez-Ruiz et al., 2004). The p53-dependent apoptotic pathway reported here may provide the molecular mechanism for the cannabinoid-mediated physiological cell death that is necessary for appropriate development of the brain.

In summary, the results demonstrate that THC impacts on the tumour suppressor protein, p53 in the brain, via cannabinoid CB_1 receptor and JNK activation. Downstream consequences of p53 activation include an increase in pro-apoptotic Bax expression and phosphorylation of Bcl-2, caspase-3 activation and DNA fragmentation. These results demonstrate that THC regulates p53 in cultured cortical cells and that p53 is critically involved in regulating the neurotoxic actions of THC.

Acknowledgements

The authors acknowledge financial support from the Science Foundation Ireland and the Health Research Board, Ireland.

References

Appella, E., Anderson, C.W., 2001. Post-translational modifications and activation of p53 by genotoxic stresses. Eur. J. Biochem. 268, 2764–2772.

Bennet, M., Macdonald, K., Chan, S.W., Luzio, J.P., Simari, P., Weissberg, P., 1998. Cell surface trafficking of Fas: a rapid mechanism of p53-mediated apoptosis. Science 282, 290–293.

Blatt, N.B., Glick, G.D., 2001. Signaling pathways and effector mechanisms pre-programmed cell death. Bioorg. Med. Chem. 9, 1371–1384.

Bonini, P., Cicconi, S., Cardinale, A., Vitale, C., Serafino, A.L., Ciotti, M.T., Marlier, L.N., 2004. Oxidative stress induces p53-mediated apoptosis in glia: p53 transcription-independent way to die. J. Neurosci. Res. 75, 83–95.

Campbell, V.A., 2001. Tetrahydrocannabinol-induced apoptosis in cultured cortical neurones is associated with cytochrome c release and caspase-3 activation. Neuropharmacology 40, 702–709.

Chua, C.C., Liu, X., Gao, J., Hamdy, R.C., Chua, B.H.L., 2006. Multiple actions of pifithrin-α on doxorubicin-induced apoptosis in rat myoblastic H9c2 cells. Am. J. Physiol. Heart Circ. Physiol. 290, H2606–H2613.

Cregan, S.P., MacLaurin, J.G., Craig, C.G., Robertson, G.S., Nicholson, D.W., Park, D.S., Slack, R.S., 1999. Bax-dependent caspase-3 activation is a key determinant in p53-induced apoptosis in neurons. J. Neurosci. 19, 7860–7869.

Culmsee, C., Zhu, X., Yu, Q.S., Chan, S.L., Camandola, S., Guo, Z., Greig, N.H., Mattson, M., 2001. A synthetic inhibitor of p53 protects neurons against death induced by ischemic and excitotoxic insults, and amyloid beta-peptide. J. Neurochem. 77, 220–228.

Downer, E., Boland, B., Fogarty, M., Campbell, V., 2001. Δ^9-Tetrahydrocannabinol induces the apoptotic pathway in cultured cortical neurones via activation of the cannabinoid CB1 receptor. NeuroReport 12, 3973–3978.

Downer, E.J., Fogarty, M.P., Campbell, V.A., 2003. Tetrahydrocannabinol-induced neurotoxicity depends on cannabinoid CB1 receptor-mediated c-Jun N-terminal kinase activation in cultured cortical neurons. Br. J. Pharmacol. 140, 547–557.

Enokido, Y., Araki, T., Tanaka, K., Aizawa, S., Hatanaka, H., 1996. Involvement of p53 in DNA strand break-induced apoptosis in postmitotic CNS neurons. Eur. J. Neurosci. 8, 1812–1821.

Evan, G., Littlewood, T., 1998. A matter of life and cell death. Science 281, 1317–1322.

Fernandez-Ruiz, J., Gomez, M., Hernandez, M., de Miguel, R., Ramos, J.A., 2004. Cannabinoids and gene expression during brain development. Neurotox. Res. 6, 389–401.

Fogarty, M.P., Downer, E.J., Campbell, V., 2003. A role for c-Jun N-terminal kinase 1 (JNK1), but not JNK2, in the β-amyloid-mediated stabilization of protein p53 and induction of the apoptotic cascade in cultured cortical neurons. Biochem J. 371, 789–798.

Galve-Roperh, I., Sánchez, C., Luisa Cortes, M., Gómez del Pulgar, T., Izquierdo, M., Guzmán, M., 2000. Anti-tumoral action of cannabinoids: involvement of sustained ceramide accumulation and extracellular signal-regulated kinase activation. Nat. Med. 6, 313–319.

Gross, A., Jockel, J., Wei, M.C., Korsmeyer, S.J., 1998. Enforced dimerization of BAX results in its translocation, mitochondrial dysfunction and apoptosis. EMBO J. 17, 3878–3885.

Gudkov, A.V., Komarova, E.A., 2005. Prospective therapeutic applications of p53 inhibitors. Biochem. Biophys Res. Commun. 331, 726–736.

Herkenham, M., Lynn, A.B., Johnson, M.R., Melvin, L.S., de Costa, B.R., Rice, K.C., 1991. Characterization and localization of cannabinoid receptors in rat brain: a quantitative in vitro autoradiographic study. J. Neurosci. 11, 563–583.

Herr, I., Debatin, K.M., 2001. Cellular stress response and apoptosis in cancer therapy. Blood 98, 2603–2614.

Howlett, A.C., Breivogel, C.S., Childers, S.R., Deadwyler, S.A., Hampson, R.E., Porrino, L.J., 2004. Cannabinoid physiology and pharmacology: 30 years of progress. Neuropharmacology 47, 345–358.

Iversen, L., 2003. Cannabis and the brain. Brain 126, 1252–1270.

Jordan, J., Galindo, M.F., Prehn, J.H., Weichselbaum, R.R., Beckett, M., Ghadge, G.D., Roos, R.P., Leiden, J.M., Miller, R.J., 1997. p53 expression induces apoptosis in hippocampal pyramidal neuron cultures. J. Neurosci. 17, 1397–1405.

Kim, H.J., Mun, J.Y., Chun, Y.J., Choi, K.H., Kim, M.Y., 2001. Bax-dependent apoptosis induced by ceramide in HL-60 cells. FEBS Lett. 505, 264–268.

Komarov, P.G., Komarova, E.A., Kondratov, R.V., Christov-Tselkov, K., Coon, J.S., Chernov, M.V., Gudkov, A.V., 1999. A chemical inhibitor of p53 that protects mice from the side effects of cancer. Science 285, 1733–1737.

Korsmeyer, S., 1999. BCL-2 gene family and the regulation of programmed cell death. J. Cancer Res. 59, 1693–1700.

Levine, A., 1997. p53 the cellular gatekeeper for growth and division. Cell 88, 323–331.

Marchenko, N., Zaika, A., Moll, U.M., 2000. Death signal-induced localization of p53 protein to mitochondria. A potential role in apoptotic signaling. J. Biol. Chem. 275, 16202–16212.

MacManus, A., Ramsden, M., Murray, M., Pearson, H.A., Campbell, V., 2000. Enhancement of $^{45}Ca^{2+}$influx and voltage-dependent Ca^{2+} channel activity by β-amyloid$_{(1-40)}$ in rat cortical synaptosomes and cultured cortical neurones: modulation by the proinflammatory cytokine interleukin-1β. J. Biol. Chem. 275, 4713–4718.

Mielke, K., Herdegen, T., 2000. JNK and p38 stress kinases-degenerative effectors of signal-transduction-cascades in the nervous system. Prog. Neurobiol. 61, 45–60.

Miller, F.D., Pozniak, C.D., Walsh, G.S., 2000. Neuronal life and death: an essential role for the p53 family. Cell Death Differ. 7, 880–888.

Miyashita, T., Reed, J.C., 1995. Tumour suppressor p53 is a direct transcriptional activator of the human Bax gene. Cell 80, 293–299.

Movsesyan, V.A., Stoica, B.A., Yakovlev, A.G., Knoblach, S.M., Lea, P.M., Cernak, I., Vink, R., Faden, A.I., 2004. Anandamide-induced cell death in primary neuronal cultures: role of calpain and caspase pathways. Cell Death Differ. 11, 1121–1132.

Murphy, K.M., Streips, U.N., Lock, R.B., 2000. Bcl-2 inhibits a Fas-induced conformational change in the Bax N-terminus and Bax mitochondrial translocation. J. Biol. Chem. 275, 17225–17228.

Patsos, H.A., Hicks, D.J., Dobson, R.R., Greenhough, A., Woodman, N., Lane, J.D., Williams, A.C., Paraskeva, C., 2005. The endogenous cannabinoid, anandamide, iduces cell death in colorectal carcinoma cells: a possible role for cyclooxygenase 2. Gut 54, 1741–1750.

Polyak, K., Xia, Y., Zweler, J.L., Kinzler, K.W., Vogelstein, B., 1997. A model for p53-induced apoptosis. Nature 389, 300–305.

Powles, T., te Poele, R., Shamash, J., Chaplin, T., Proper, D., Joel, S., Oliver, T., Liu, W.M., 2005. Cannabis-induced cytotoxicity in leukemic cell lines: the role of the cannabinoid receptors and the MAPK pathway. Blood 105, 1214–1221.

Pucci, B., Bellincampi, L., Tafani, M., Masciullo, V., Melino, G., Giordano, A., 1999. Paclitaxel induces apoptosis in Saos-2 cells with CD95L upregulation and Bcl-2 phosphorylation. Exp. Cell Res. 252, 134–143.

Reed, J.C., 2006. Proapoptotic multidomain Bcl-2/Bax-family proteins: mechanisms, physiological roles, and therapeutic opportunities. Cell Death Differ. 13, 1378–1386.

Shibata, T., Iio, K., Kawai, Y., Shibata, N., Kawaguchi, M., Toi, S., Kobayashi, M., Kobayashi, M., Yamamoto, K., Uchida, K., 2006. Identification of a lipid peroxidation product as a potential trigger of the p53 pathway. J. Biol. Chem. 281, 1196–1204.

Velasco, G., Galve-Roperh, I., Sanchez, C., Blazquez, C., Guzman, M., 2004. Hypothesis: cannabinoid therapy for the treatment of gliomas. Neuropharmacology 47, 315–323.

Yamamoto, K., Ichijo, I.L., Korsmeyer, S.J., 1999. Bcl-2 is phosphorylated and inactivated by an ASK1/Jun N-terminal protein kinase pathway normally activated at G(2)/M. Mol. Cell. Biol. 19, 8469–8478.

Wolter, K.G., Hsu, Y.T., Smith, C.L., Nechustan, A., Xi, X.G., Youle, R.J., 1997. Movement of Bax from the cytosol to mitochondria during apoptosis. J. Cell Biol. 139, 1281–1292.

Shieh, S.Y., Ikeda, M., Taya, Y., Prives, C., 1997. DNA damage-induced phosphorylation of p53 alleviates inhibition of Mdm2. Cell 91, 325–334.

Shimizu, S., Narita, M., Tsujimoto, Y., 1999. Bcl-2 family proteins regulate the release of apoptogenic cytochrome c by the mitochondrial channel VDAC. Nature 399, 483–487.

Zörnig, M., Hueber, A., Baum, W., Evan, G., 2001. Apoptosis regulators and their role in tumorigenesis. Biochim. Biophys. Acta 1551, F1–F37.

Zou, H., Henzel, W.J., Liu, X., Lutschg, A., Wang, X., 1997. Apaf-1, a human protein homologous *C. elegans* CED-4, participates in cytochrome c-dependent activation of caspase-3. Cell 90, 405–413.